Proceedings of the I·R·E

A Journal of Communications and Electronic Engineering

January, 1952

Volume 40 Number 1

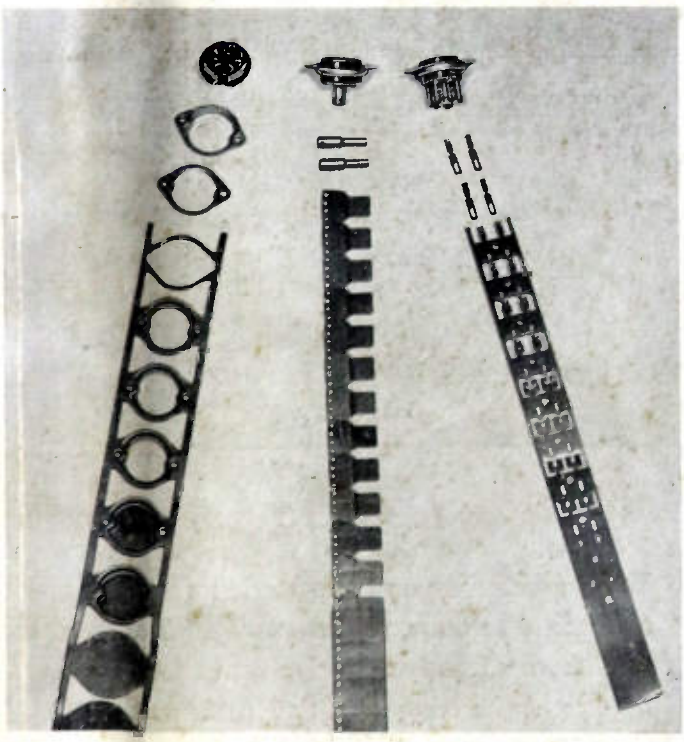

Sylvania Electric Products, Inc.

MINIATURE-TUBE SOCKET PRODUCTION

The various production steps are readily followed in the above. Crimping or staking then attaches the metal parts to a plastic body.

PROCEEDINGS OF THE I.R.E.

Table of Contents, Indicated by Black-and-White Margin, Follows Page 32A

1952 IRE National Convention, March 3-6, New York, N.Y.

The Institute of Radio Engineers

magnetrons?

PULSE • TUNABLE • CW

you can depend upon

AMPEREX

Specialists in the design and construction of all types of electron tubes for civilian and military applications . . . and recognized as one of the oldest, largest and finest organizations in the whole world.

With laboratory and production facilities tha are second to none, we draw a wealth of experi ence from extensive development files compilec by our engineering staff and their predecessor since 1896.

May we serve you?

AMPEREX ELECTRONIC CORP.

Our Newest Plant
Hicksville, New York

25 WASHINGTON STREET, BROOKLYN 1, N. Y.
In Canada and Newfoundland: Canadian Radio & Mfg. Co.
11-19 Brentcliffe Road, Leaside, Toronto, Ontario, Canada
Cable: "AMPRONICS"

AMPEREX

Come Again!

March 3-6 starts the big rush, once again to the 1952 IRE Convention and Radio Engineering Show at Grand Central Palace and the Waldorf-Astoria Hotel, in New York City. Here in four great days you will hear the latest technical information on all phases of radio from radar to television—guided missiles to instrumentation. Send in your hotel reservation if you do not choose to sleep in the park! Be sure to sign up for the ladies' program for your wife, and make reservations for the Banquet, President's Luncheon, and Cocktail Party. "Forty Years—Sets the Pace" (IRE 1912-1952) for the biggest of all Conventions and Shows. 347 Exhibits on four floors at the Palace. Remember the date, March 3-6, New York.

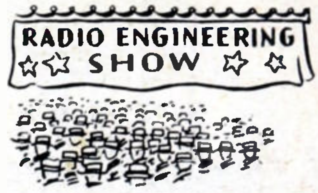

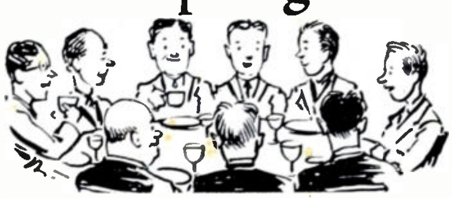

The Radio Engineering Show of The Institute of Radio Engineers

Proceedings of the I.R.E. January, 1952, Vol. 40, No. 1. Published monthly by the Institute of Radio Engineers, Inc., at 1 East 79 Street, New York 21, N.Y. Price per copy: members of the Institute of Radio Engineers $1.00; non-members $2.25. Yearly subscription price: to members $9.00; to non-members in United States, Canada and U.S. Possessions $18.00; to non-members in foreign countries $19.00. Entered as second class matter, October 26, 1927, at the post office at Menasha, Wisconsin, under the act of March 3, 1879. Acceptance for mailing at a special rate of postage is provided for in the act of February 28, 1925, embodied in Paragraph 4, Section 412, P.L. and R., authorized October 26, 1927.

Table of Contents will be found following page 32A

FLUOROFLEX-T® *gives you "Teflon"* with optimum chemical, electrical, thermal and physical properties, in rod, sheet, and machined parts*

You can't do better than Teflon for severe applications involving corrosive chemicals, solvents and heat. And for Teflon, you won't do better than availing yourself of Fluoroflex-T.

Here is Teflon produced under rigid control, in new equipment expressly designed by Resistoflex to bring out utmost inertness and stability in this material. You get Teflon with maximum tensile strength, "plastic memory," flexibility. Sheets are flat—easier to handle. Rods are uniform—machine properly. Parts are free from internal strains, cracks or porosity.

Fluoroflex-T withstands −90°F to +500°F continuous service. Chemically, it's essentially inert. It is non-adhesive and has little friction. Electrically, it is virtually the perfect insulator for ultra high frequencies.

We'll gladly consult with you on *your* application. Fluoroflex-T rods are available from ¼" to 2" diameter; sheets 21" x 21" in 1/16" to 1½" thicknesses; machined parts to specification. RESISTOFLEX CORPORATION, Belleville 9, N. J.

®Reg. trade mark of Resistoflex Corp. for products manufactured from fluorocarbon resins.
** Du Pont's trade mark for its tetrafluoroethylene resin.*

For out of the ordinary engineering with synthetics

RESISTOFLEX
CORPORATION
Belleville 9, New Jersey

Meetings with Exhibits

● As a service both to Members and the industry, we will endeavor to record in this column each month those meetings of IRE, its sections and professional groups, and some closely related groups *which include exhibits.*

Δ

IRE National Convention &
Radio Engineering Show
March 3-6, 1952
Waldorf-Astoria Hotel and
Grand Central Palace
New York City

Spring Technical Conference
on Television
April 19, 1952
Cincinnati Engineering Society
Building, Cincinnati, Ohio
Adv. & Exhibits: Wynne W. Gulden
3272 Dayton Avenue
Cincinnati 11, Ohio

Δ

NEREM, Saturday, May 10, 1952
Copley Plaza Hotel, Boston, Mass.
New England Radio
Engineering Meeting
Gen. Chairman: Alfred J. Pote
71 West Squantum St.
N. Quincy, Mass.

Δ

National Conference on
Airborne Electronics
May 12, 13 & 14, 1952
Hotel Biltmore, Dayton, Ohio
Exhibits: Paul D. Hauser
1430 Gascho Drive, Dayton 3

Δ

4th Southwestern IRE Conference
May 16, 17, 1952
Rice Hotel, Houston, Texas
Exhibits: Gerald L. K. Miller
1622 W. Alabama
Houston 6, Texas

Δ

Radio Parts Show
Chicago
May 19-24, 1952

Δ

Western Electronic Show and
IRE Regional Convention
August 27, 28 & 29, 1952
Municipal Auditorium
Exhibits: Heckert Parker
215 American Avenue
Long Beach, Calif.

Δ

National Electronic Conference
Sept. 29, 30, Oct. 1, 1952
Hotel Sherman, Chicago, Ill.

... JUST OFF PRESS comes this Sprague Catalog 21 with complete details on paper dielectric capacitors designed to meet Joint Army-Navy Specification JAN-C-25. Comprehensive data on sizes, characteristics, ratings, performance and other factors makes the new catalog invaluable to users of JAN paper capacitor types. Copies are available on letterhead request.

JAN (MIL) and SUPER-JAN (MIL)

Over and beyond JAN specifications, Sprague has developed many new ways to reduce size and weight and to improve the high-temperature performance of capacitors and other electronic components. In effect, these are "Super-JAN" components—fully approved via JAN deviations to equipment manufacturers and widely used in critical military applications. At the right are four examples of units that Sprague can supply where equipment engineering progress calls for components that *exceed* JAN requirements.

SPRAGUE SUBMINIATURE PAPER CAPACITORS

Hermetically-sealed, metal-encased and far smaller than equivalent JAN styles. Available in types for 85° C. and 125° C. operation. Sprague Bulletin 213-B gives full technical data.

COMPARISON—TYPICAL SUPER-JAN VERSUS JAN UNITS

Metal-Cased Tubular Paper Capacitor, Both Leads Insulated from Case

	Sprague Type 196P47492S1	Nearest JAN-C-25 Equivalent CP25A1EC504K
Capacitance (Mfd., ± 10%)	0.47	0.50
Voltage, DCW	200	200
Insulation Resistance: at 25°C	30,000 M Ω*	6000 M Ω
at 85°C	700*	600 M Ω
at 125°C	20*	**
Capacitance Change (%) From 25°C to −55°C	−4*	−15
Operating Ambient (°C) Max.	+125*	+85
Minimum	−55	−55
Dielectric Test	Twice Rated Volts for 2 Min.	Twice Rated Volts for 1 Min.
Life Test: at 85°C	250 hrs., 1.5 X rated DCWV	250 hrs., 1.5 X rated DCWV
Life Test: at 125°C	250 hrs., 1.4 X rated DCWV*	**
Moisture Resistance	Hermetically Sealed	Hermetically Sealed
Length	1-9/16*	2-1/8
Diameter	9/16*	3/4
Volume (cu. in.)	0.39*	.94

* Ahead of and Beyond JAN

** Above Temperature Limit of JAN-C-25

SPRAGUE

PIONEERS IN ELECTRIC AND ELECTRONIC DEVELOPMENT

SPRAGUE ELECTRIC COMPANY • NORTH ADAMS, MASSACHUSETTS

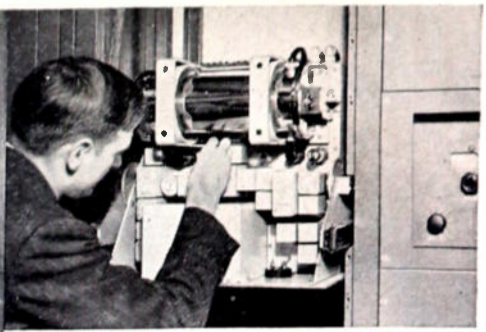

Each crystal is enclosed in a cylindrical oven which holds the crystal temperature to within 1/100 of a degree.

At the A. T. & T. building at 195 Broadway, New York, passersby set watches by the world's most accurate public clock, which is controlled by the master standard.

↑ Front of the new frequency-time standard at Bell Telephone Laboratories. In the rear there are 600 electron tubes and 25,000 soldered connections. Room temperature is maintained within two degrees.

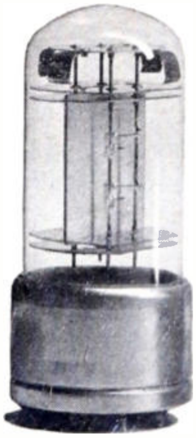

The controlling quartz crystal vibrates in vacuum at 100,000 cycles per second. The standard is powered by storage batteries, with steam turbo-generator standing by, just in case of emergency.

A vibrating crystal keeps master time

Ever since Galileo watched a lamp swinging in the Cathedral of Pisa three centuries ago, steady vibration has provided the practical measure of time. In the 1920s Bell Laboratories physicists proved that the quartz crystal oscillators they had developed to control electrical vibration frequency in your telephone system could pace out time more accurately than ever before.

The Laboratories' latest master standard keeps an electric current vibrating at a frequency that varies only one part in a billion, keeping time to one ten-thousandth second a day.

Through secondary standards, a master oscillator governs the carrier frequencies of the Bell System's ship-to-shore, overseas and mobile radiotelephone services, the coaxial and *Radio-Relay* systems which transmit hundreds of simultaneous conversations, or television. In the northeastern states, it keeps electric clocks on time through check signals supplied to electric light and power companies.

The new standard also provides an independent reference for time measurements made by the U. S. Naval Observatory and the National Bureau of Standards. Thus, world science benefits from a Laboratories development originally aimed at producing more and better telephone service.

BELL TELEPHONE LABORATORIES

AMERICAN TELEPHONE & TELEGRAPH CO. BELL SYSTEM AND ASSOCIATED COMPANIES

Improving telephone service for America provides careers for creative men in scientific and technical fields.

Let Bendix Solve Your Problems

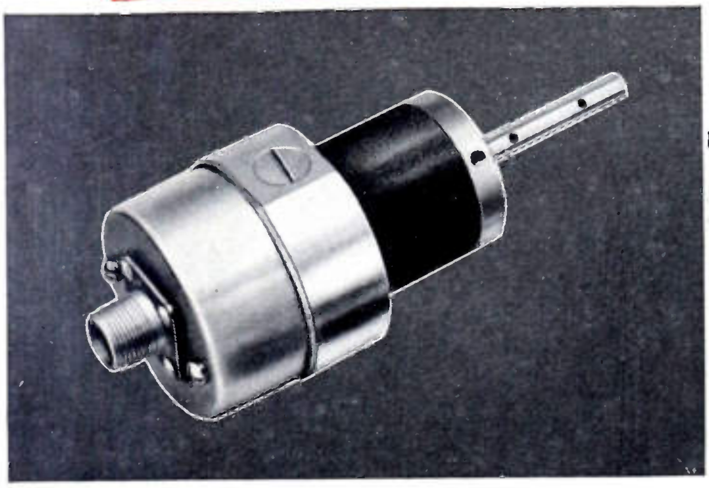

WITH

SPECIALIZED DYNAMOTORS

AND

DC MOTORS

When you are faced with specifications that place impossible requirements on dynamotors or small DC motors, according to World War II standards, take advantage of recently developed improvements in high temperature and high altitude techniques by simply outlining your requirements to Bendix. Model units *exactly* meeting your performance specifications will be developed and tested for pre-production use—production units will then follow in accordance with your manufacturing schedule.

DYNAMOTORS
Regular • Multiple output • Special purpose
DC MOTORS
1/100 hp—1/2 hp • Continuous and Intermittent Duty
DC Servos and special motors

RED BANK DIVISION OF BENDIX AVIATION CORPORATION
RED BANK, NEW JERSEY
Export Sales: Bendix International Division, 72 Fifth Avenue, New York 11, N.Y.

Write for this colorful and informative book—it's free. You'll find it loaded with facts and figures about all types of dynamotors.

RED BANK DIVISION
Bendix
AVIATION CORPORATION

Another Masterpiece of Truscon Engineering Skill

TRUSCON "G-W"

UNIFORM CROSS SECTION GUYED RADIO TOWER

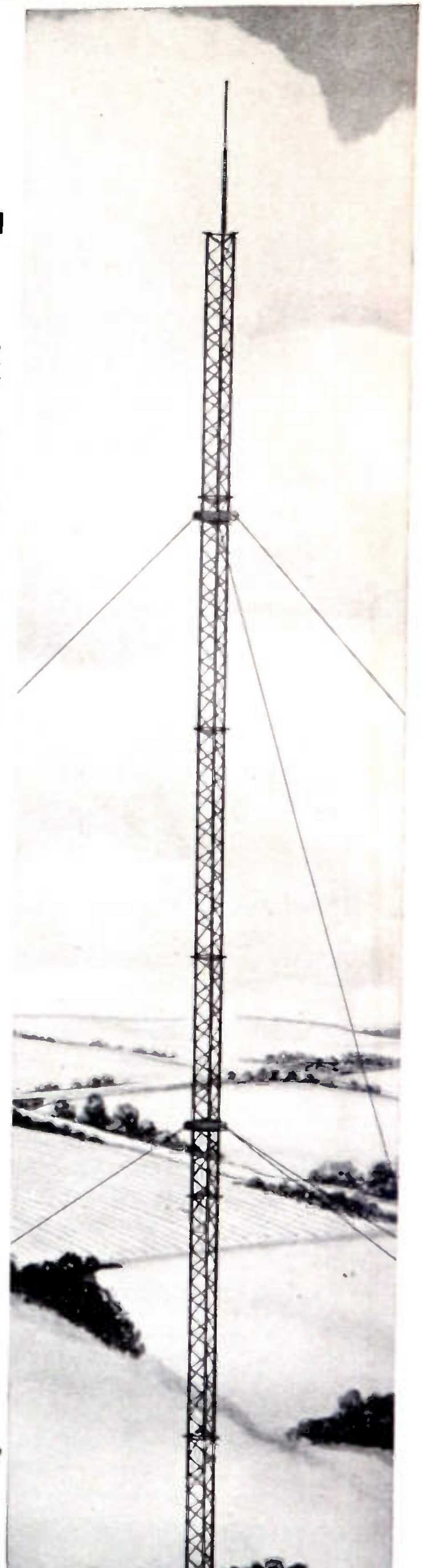

HERE again is another example of Truscon leadership in antenna design—another example of skill gained by nearly a half-century of experience in the fabrication of structural steel products.

Truscon Type "G-W" Radio Towers are of particular interest to the buyer who is desirous of obtaining the utmost in antenna quality and strength at a cost representing only a nominal premium above the cost of secondary types of construction. These guyed towers are available in shop-welded unit lengths for tower heights up to 528 feet, and include these features:

TRIANGULAR—because this design resists distortion with greater efficiency than any other form and is so recognized by the engineering profession.

UNIFORM IN CROSS SECTION—because radio engineers proclaim this feature a distinct asset in broadcasting.

STRONG—because these towers and all component parts are designed to resist a minimum wind load of 30 lbs. per square foot which is accepted as a design adequate for most geographical areas not subject to frequent cyclone visitation.

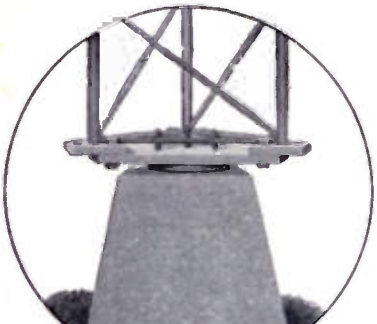

Typical central pier arrangement for non-insulated tower. Other arrangements are possible to meet specific conditions.

The Type "G-W" guyed tower can be adapted to a number of services. When base and guy insulated, it is an ideal antenna tower. It can also simultaneously support one or more cables or co-axial transmission lines having 3⅛" aggregate diameter and one or more whip-type UHF antennas or a side-mounted FM antenna, with some applications requiring nominal height reduction.

Although the Type "G-W" tower is rated to resist 30 pound per square foot minimum wind pressure, under certain conditions, such as an AM radiator not supporting superstructure for other services, it may be capable of safely resisting 40 or more pounds per square foot of wind pressure.

Base insulated central pier showing "Mast-Base" or "Pivot" type base insulator with Spark-Gap.

When non-insulated, the Type "G-W" tower is suitable for a number of services, such as an FM or UHF Antenna Support for Railroads; Public Utilities; Industry; Municipal, County, and State Police; and Communications Networks.

FREE CATALOG

Write for illustrated literature giving complete description, mechanical details, installation photos, and other important information on the new Truscon "G-W" Guyed Radio Towers.

TRUSCON SELF-SUPPORTING AND UNIFORM CROSS SECTION GUYED TOWERS

TRUSCON COPPER MESH GROUND SCREEN

TRUSCON STEEL COMPANY

YOUNGSTOWN 1, OHIO

Subsidiary of Republic Steel Corporation

LEADING TV MANUFACTURERS REPORT—

G.E.'s ELECTROSTATIC-FOCUS TUBES GIVE THE *Sharpest* FOCUS OF ALL!

17RP4/17HP4
17VP4
20HP4-A
21LP4
21LP4-A

Comparative tests proved General Electric tubes far superior in needle-sharp distinctness!

FOUR large builders of TV receivers ran their own detailed tests of new G-E zero-focus types against other makes of electrostatic tubes. In every case, General Electric tubes gave pictures with *greater sharpness and definition over the entire viewing area!*

● Improved gun design, precision manufacture, share the credit for this G-E contribution to a TV industry that continues to move ahead despite metal shortages and a heavy defense load.

● Saving precious cobalt, nickel, and copper—needing no receiver focus control, which means simpler TV operation—General Electric's new zero-focus tubes have this third big advantage: they produce outstandingly clear, vivid pictures!

● Five types in popular sizes are listed above. Wire or write for complete facts about the tubes in which you are interested as TV designer or manufacturer! *Electronics Division, General Electric Company, Schenectady 5, New York.*

You can put your confidence in—

GENERAL ELECTRIC

162-1A1

ARNOLD

Anything You May Need in TAPE-WOUND CORES

RANGE OF MATERIALS

Depending upon the specific properties required by the application, Arnold Tape-Wound Cores are available made of DELTAMAX . . . 4-79 MO-PERMALLOY . . . SUPERMALLOY . . . MUMETAL . . . 4750 ELECTRICAL METAL . . . or SELECTRON (grain-oriented silicon steel).

RANGE OF SIZES

Practically any size Tape-Wound Core can be supplied, from a fraction of a gram to several hundred pounds in weight. Toroidal cores are available in fifteen standard sizes with protective nylon cases. Special sizes of toroidal cores—and all cut cores, square or rectangular cores—are manufactured to meet your individual requirements.

RANGE OF TYPES

In each of the magnetic materials named, Arnold Tape-Wound Cores are produced in the following standard tape thicknesses: .012", .008", .004", .002", .001", .0005", or .00025", as required.

Applications

MAGNETIC AMPLIFIERS
PULSE TRANSFORMERS
CURRENT TRANSFORMERS
WIDE-BAND TRANSFORMERS
NON-LINEAR RETARD COILS
PEAKING STRIPS . . . REACTORS.

W&D 3963

THE ARNOLD ENGINEERING COMPANY

SUBSIDIARY OF ALLEGHENY LUDLUM STEEL CORPORATION
General Office & Plant: Marengo, Illinois

IN QUALITY PRODUCTS EVERYWHERE . . .

GUARDIAN *Controls*

As real as rockets, guided missiles and supersonic jets are the Guardian Controls that set them off and direct their flight. Guardian relays—stepping switches—contactor units—solenoids—multi-contact switches are the basic components of communications, bombing and firing equipment, of control stick switches, control wheels and myriad Guardian developments for the military. Certain basic Guardian control components are still available for peacetime products. Write.

Series 345 D.C. Relay
Hermetically Sealed or
with Open-Type Mounting

A.N. Connector Plug
Hermetic Seal Container

AN-3320-1 D.C.

AN-3324-1 D.C.

Series 595 D.C.

Series 610 A.C.—615 D.C.

Series 695 D.C.

Get Guardian's New HERMETICALLY SEALED RELAY CATALOG Now!

GUARDIAN ELECTRIC

1628-A W. WALNUT STREET CHICAGO 12, ILLINOIS

A COMPLETE LINE OF RELAYS SERVING AMERICAN INDUSTRY

SPECIFY Simpson

for Accurate, Dependable Electrical Measurements

BECAUSE—Simpson has developed quality control to a new modern high with *this* successful production policy. Design everything that goes into an instrument—make everything that goes into an instrument—keep designing for the future—keep quality steadily higher—keep prices consistent with material and labor costs without exploitation. This quality control is evident in every Simpson instrument whether panel or switchboard, custom-built or stock. The instruments illustrated in panel below are only a few of the wide variety of instruments in the complete Simpson line. Let Simpson engineers help you solve your panel instrument problems—and for your standard instrument requirements take advantage of our large stock.

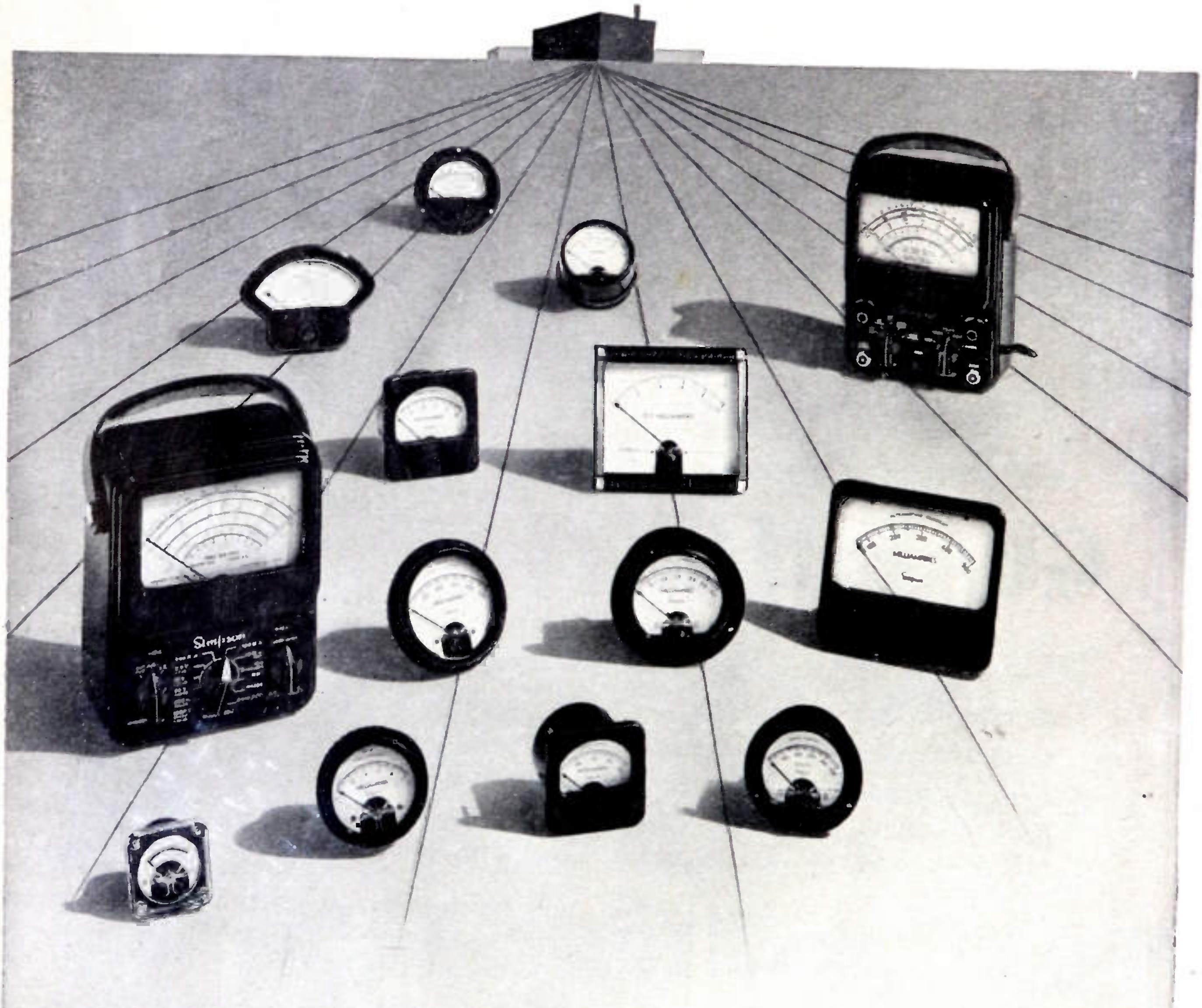

CONSERVE CRITICAL MATERIALS

Simpson ELECTRIC COMPANY

5200 W. KINZIE ST., CHICAGO 44 • COlumbus 1-1221 • In Canada: BACH-SIMPSON, LTD., LONDON, ONT.

Now in **MASS PRODUCTION...**

PYRAMID ULTRA-COMPACT

metallized paper capacitors

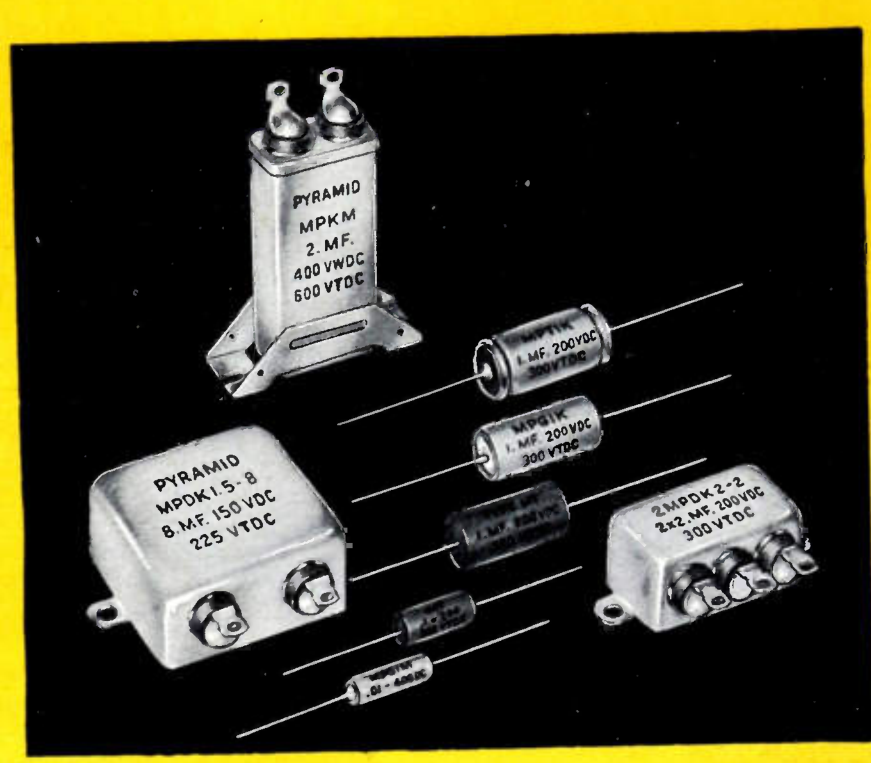

PYRAMID Series M CAPACITORS use a specially-prepared metallized paper, providing all-important savings in size and weight....Pyramid now produces large quantities of these capacitors in a wide variety of cardboard or hermetically sealed metal containers.

Your letterhead inquiries are invited

PYRAMID ELECTRIC COMPANY • 1445 HUDSON BLVD., North Bergen, N. J.

LITTON INDUSTRIES NEWS

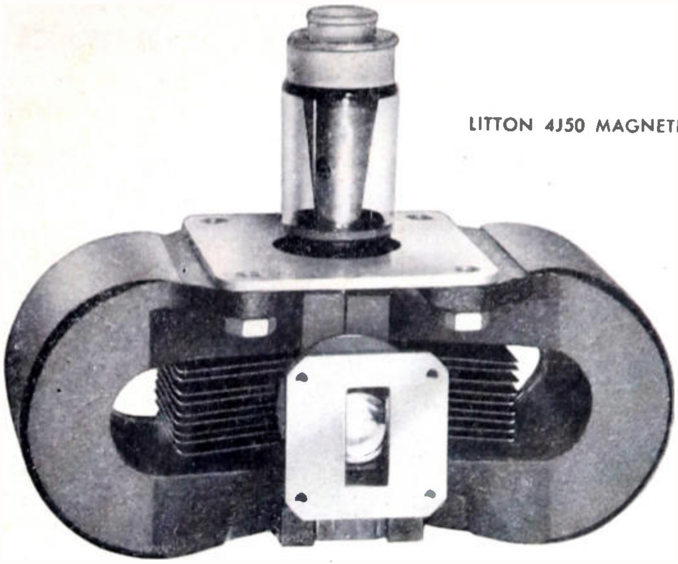

LITTON 4J50 MAGNETRON

SNAP-ON OPERATION, LONG SHELF LIFE WITH LITTON X BAND MAGNETRONS

Two high-quality pulse magnetrons in the 9345 to 9405 mc/sec range are now being manufactured by Litton Industries. Designated 4J50 and 4J52, these magnetrons require no aging or seasoning. Special design and processing have resulted in tubes with long shelf life and snap-on operation to full power immediately after completion of the cathode warm-up period.

These tubes offer either high or medium power outputs. Litton 4J50 is a high-power magnetron providing 225 kw minimum peak at .001 duty. 4J52 is a medium power magnetron offering 65 kw minimum peak at .001 duty. Both operate at or beyond ratings.

MOLECULAR LUBRICANT PRODUCTS

Litton Molecular Lubricant "C" has a vapor pressure of approximately 10^{-7} mm. Hg. at room temperature. In the presence of ionization it will give an indicated pressure of 10^{-6} mm. Hg. Its principal use is in vapor pumps and as a lubricant for bearing operation in vacuum.

Great care has been exercised in its refinement, and the product has a very narrow boiling range. The color and fluorescence are inherent to the material.

This oil has excellent lubricating qualities at temperatures below 100° C. and is suitable for use with anti-friction bearings operating within dynamic vacuum systems.

OIL VAPOR VACUUM PUMPS

The Litton Oil Vapor Vacuum Pumps are of all-steel construction which obviates the possibility of glass breakage and substantially increases the length of service of the equipment.

Boiler and charcoal baffles are easily demountable for cleaning purposes. Litton pumps feature replaceable external heaters, special cooling coils and demountable baffles. These pumps can be obtained in various combinations with high vacuum valve, with charcoal baffle for straight-through operation or side opening.

The Litton pump with charcoal baffle (straight-through operation) has an ultimate vacuum of 5×10^{-8} mm. of mercury. The speed (measured at 10^{-5} mm. of mercury) is 75 to 100 liters.

NEW LITTON PLANT ADDITION

Litton Industries has added a new building to its plant at San Carlos, California. 40,000 square feet of space is now used for research, manufacturing and general offices. The new building is windowless concrete-and-glass-block construction, completely air conditioned. The interior is light engineered for optimum working conditions.

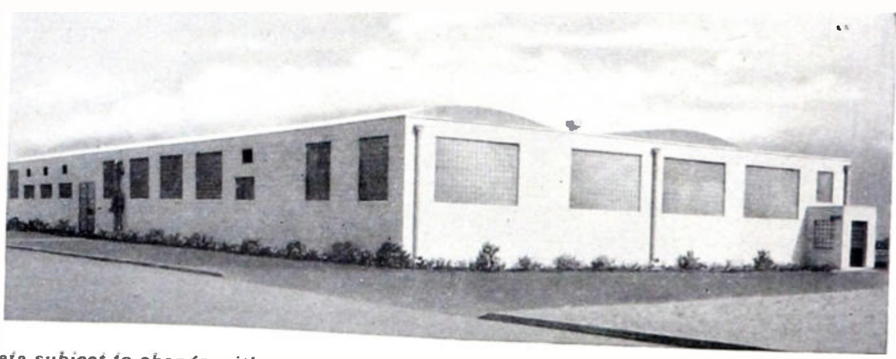

Write for price and delivery information. Data subject to change without notice.

LITTON INDUSTRIES

SAN CARLOS, CALIFORNIA, U.S.A.

2370

DESIGNERS AND MANUFACTURERS of

Glassworking Lathes and Accessories, Vertical Sealing Machines, Burner Equipment, Precision Spotwelders, Oil Vapor Vacuum Pumps, Glass Baking Ovens, Vacuum Tubes and Tube Components, Magnetrons, High Vacuum Molube Oil, Microwave Equipment.

Only One Source gives you Double Duty TV!

Highest Quality Studio Programming Resources—plus

GENERAL PRECISION LABORATORY INCORPORATED — GPL

Portable Packaging for Maximum Studio-Field Flexibility!

When you invest in GPL TV *studio* equipment, you're buying *field* equipment as well. Every GPL unit provides unparalleled flexibility, light weight, easy handling, precise control. Let GPL engineer *your* station, from camera to antenna. Have *The Industry's Leading Line*—in *quality*, in *design*.

Camera Unit

Precision-built, lightweight, fast-handling. Push-button turret, remote iris control, remote focus and range selection. Easiest to service.

Camera Control Unit

Touch-identified controls. 8½" monitor tube. Split or single headphone intercom system. CRO views horizontal, vertical, and vertical sync block. Iris control.

Camera Power Unit

Rugged, dependable, compact. Matched to other units in GPL chain. Standard relay panels swing out for maintenance.

Synchronizing Generator

Affords maximum circuit reliability without operator adjustment. Binary counters and delay lines, stable master oscillator. Built-in power supply.

Complete TV Station Installations from Camera to Antenna

Video Switcher

Full studio flexibility anywhere. Control can view, preview, fade, dissolve, etc. Views any of 5 inputs, 2 remotes, outgoing line. Twin fade levers.

3-2 Projector

Portable sync unit. No need for special phasing facilities. Projects rear-screen or "direct in." Ideal for remote origination of film. Relieves load on Telecine.

Professional TV Projector

Highest quality 16-mm projector designed specifically for TV. Delivers 100 foot-candles to tube. Sharp, steady pictures from 4000-foot film magazine.

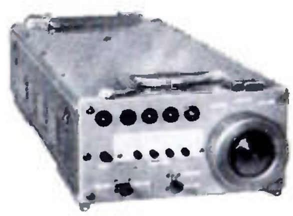

Remote Control Box

Provides revolutionary remote control of camera focus, lens change, pan, tilt. Styled to match other components in the GPL TV line.

WRITE WIRE OR PHONE FOR DETAILS

GENERAL PRECISION LABORATORY INCORPORATED — GPL

General Precision Laboratory

INCORPORATED

PLEASANTVILLE NEW YORK

TV Camera Chains • TV Film Chains • TV Field and Studio Equipment • Theatre TV Equipment

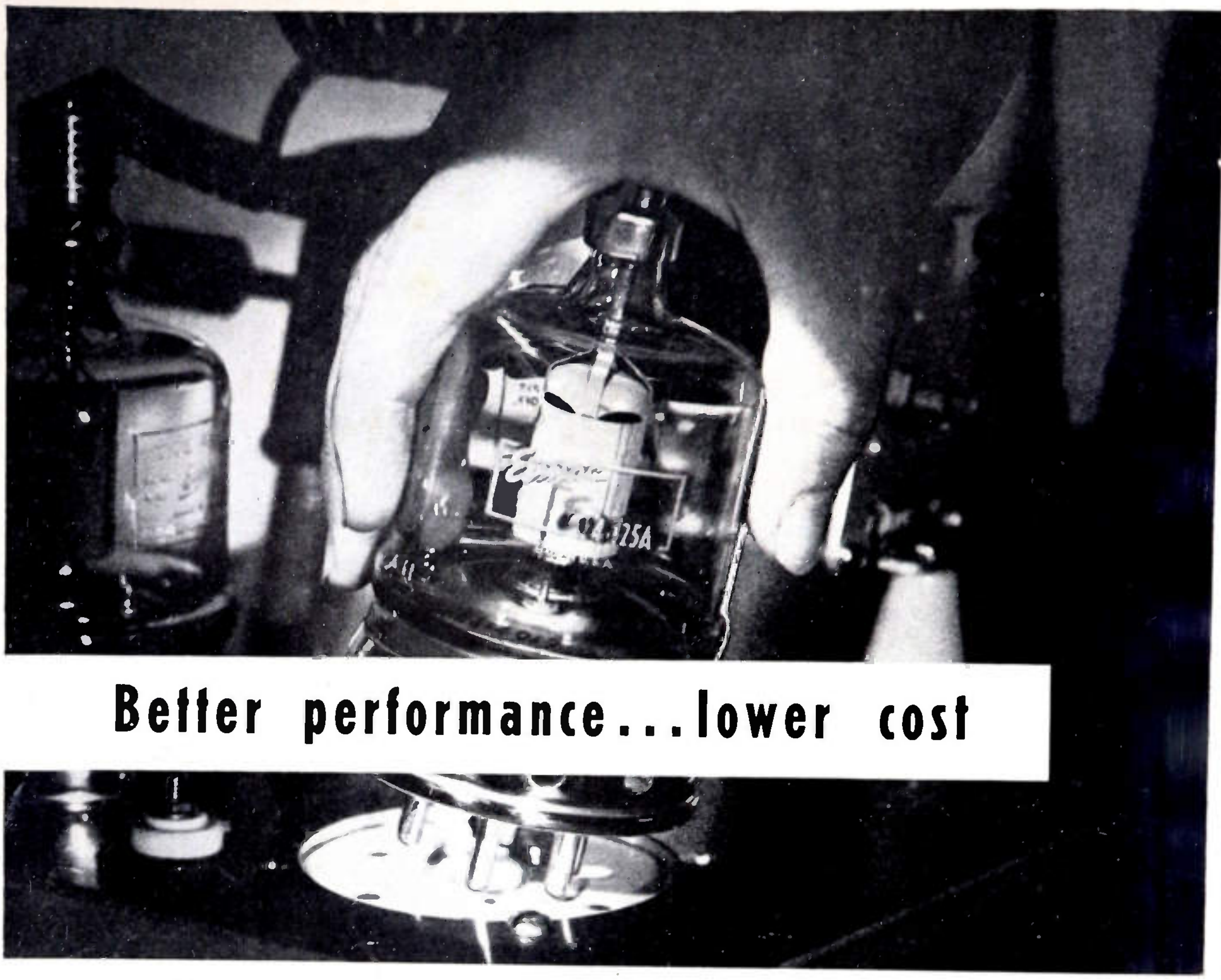

Better performance...lower cost

Transmitter performance goes up—costs go down . . . the inevitable result of specifying Eimac tetrodes to fill key sockets. Costs will stay down because the service life of these time-proved tubes is long, replacement costs are low, and the circuit simplicity they allow keeps power bills down.

Eimac tetrodes are made for a wide range of power from 65 watts plate dissipation to 20,000 watts dissipation. They are unexcelled for amplifier, oscillator, and modulator service. All are backed by the experience and know-how of America's foremost transmitting tube manufacturer.

Take the advice of countless users and equipment manufacturers who consistently not only recommend but rely on . . . Eimac tetrodes for unvarying performance, exceptional service life, and compatibility to modern circuit techniques.

Write For The Free Eimac Quick Reference Tube Catalog

Follow the Leaders to
Eimac
TUBES
The Power for R-F

302

EITEL-McCULLOUGH, INC.
San Bruno, California
Export Agents: Frazar & Hansen, 301 Clay St., San Francisco, California

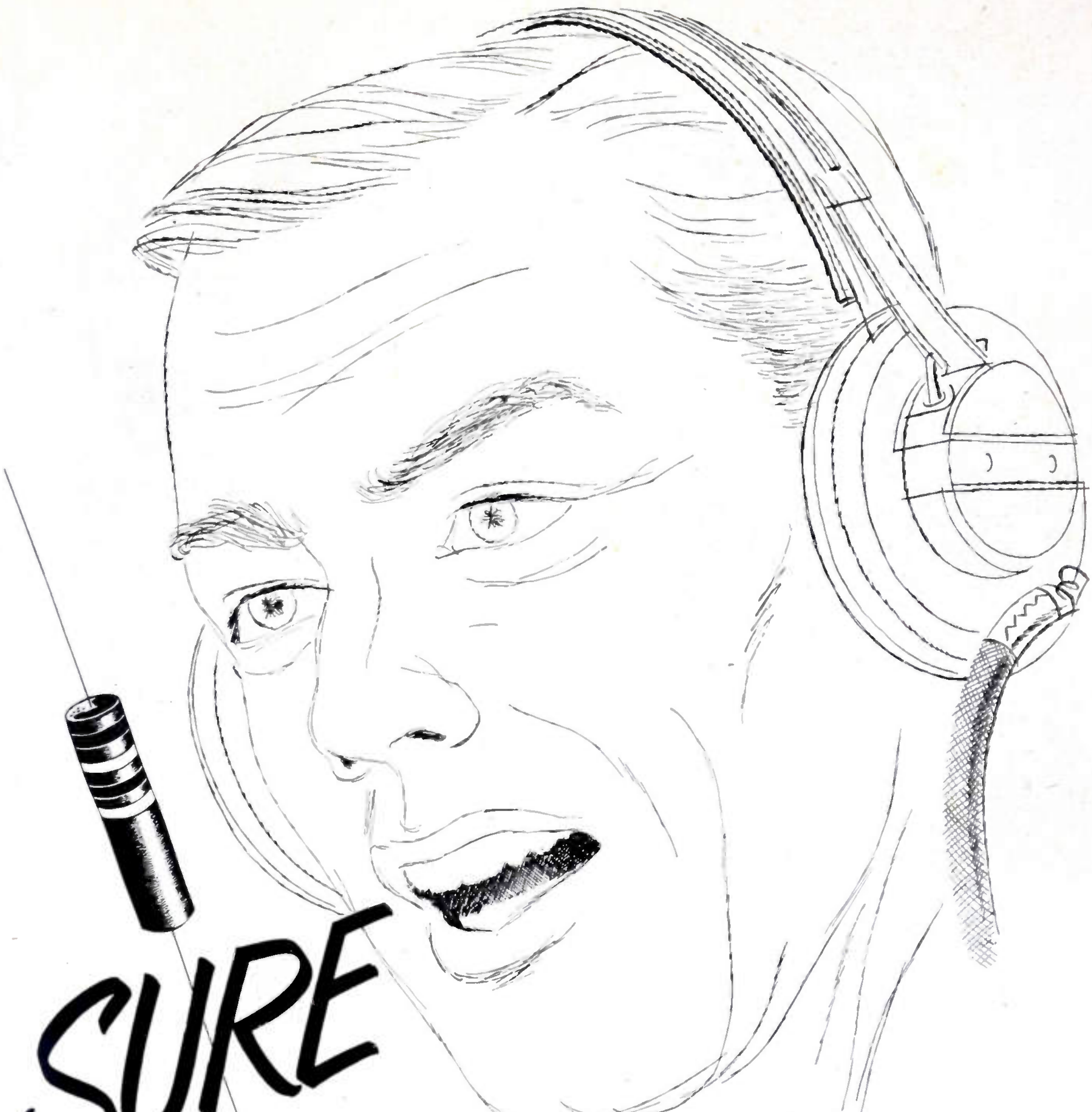

buy SPEER
when you buy RESISTORS

...for consistent resistance values

Complete your circuits with R. F. coils...chokes...tubular and disc capacitors...high voltage condensers...capristors by
JEFFERS ELECTRONICS, INC.
DU BOIS, PA.
Another Speer Carbon Co. Subsidiary

SPEER Resistor CORP.
A SPEER CARBON COMPANY SUBSIDIARY
ST. MARYS, PENNSYLVANIA

7570

International

Selenium Rectifiers

for unsurpassed performance

TYPE W-HS-SERIES

60 Milliamperes DC

In 1¼" Phenolic Tube with stud mounting at each end. Circuit-Half-Wave. Overall length varies to 14", depending on DC Output Voltage rating. For many applications for heavier duty and inverse peak suppressor circuits.

PARTIAL LISTING
W-HS SERIES

DC Output Voltage	Rectifier Part No.
20	W1HS
60	W3HS
100	W5HS
400	W20HS
800	W40HS
1500	W75HS
2500	W125HS
3500	W175HS
4500	W225HS
6000	W300HS

Over 500 other types

Type W248HS
4960 Volts DC Output
60 ma. Overall
length, 13"

Over 3,000,000 various types produced and in service during the past 4 years. Designed and built to meet Government Specifications. Manufactured for temperatures up to 100° C ambient —100% humidity. A recent month's production included Rectifiers to supply 40 microamperes, 1 volt and Rectifiers with a capacity of 140,000 amperes, 14 volts. Owned and managed by Engineers who are specialists in the design and manufacture of Selenium Rectifiers. Submit your problems for analysis and we will be glad to offer our recommendations.

Hermetically sealed Cartridge Type Rectifiers

Power Rectifiers — Ratings to 250 KW

High Voltage Rectifiers — Cartridge Type

Miniature Rectifiers — from 65 to 1,000 ma.

GENERAL OFFICES:
1521 E. Grand Ave.
El Segundo, Calif.
Phone El Segundo 1890

CHICAGO BRANCH OFFICE:
205 W. Wacker Dr.
Franklin 2-3889


RAYTHEON
RELIABLE
cathode type
SUBMINIATURE
TUBES
here are more RAYTHEON SUBMINIATURES
in world-wide use than all other makes combined

For Tubes You Can Trust To Meet Your Requirements And More

Specify

RAYTHEON RELIABLE

Cathode Type

SUBMINIATURE TUBES

These new Raytheon Reliable Subminiature tubes resulting from five years of continuous production of their prototypes are designed to meet the stringent requirements of vital military equipments. In addition to the rigid ratings for shock, fatigue, centrifugal acceleration, 5000 hour life, and heater cycle life, particular attention has been paid in the design and manufacture of these tubes to permit 200°C ambient temperature operation and lower noise output ratings as indicated under each type.

Write Today!

For complete mechanical and electrical data on these new RAYTHEON types, ask for the new Raytheon RELIABLE Subminiature Tube Catalog I.

CK6148
R. F. Pentode
$E_f = 6.3V.$ $I_f = 200$ mA.
Noise output 50 mV. max.
$E_b = 200$ V. max.
$E_{c2} = 150$ V. max.

CK6149
Medium Mu Triode
$E_f = 6.3V.$ $I_f = 200$ mA
Noise output 25 mV. max.
$E_b = 275$ V. max.

CK6150
R. F. Pentode – Mixer
$E_f = 6.3V.$ $I_f = 200$ mA
Noise output 100 mV. max.
$E_b = 200$ V. max.
$E_{c2} = 155$ V. max.

CK6151
High Mu Triode
$E_f = 6.3V.$ $I_f = 200$ mA
Noise output 25 mV. max.
$E_b = 275$ V. max.

CK6152
Low Mu Triode
$E_f = 6.3V.$ $I_f = 200$ mA
Noise output 25 mV. max.
$E_b = 250$ V. max.

RAYTHEON MANUFACTURING COMPANY
RECEIVING TUBE DIVISION • NEWTON 58, MASSACHUSETTS
Reliable Subminiature and Miniature Tubes • Germanium Diodes and Transistors
Radiac Tubes • Receiving and Picture Tubes • Microwave Tubes

RAYTHEON
Excellence in Electronics

FERRAMIC *cores*

by

GENERAL CERAMICS

Ferramics are soft magnetic materials featuring:

HIGH PERMEABILITY
HIGH VOLUME RESISTIVITY
HIGH EFFICIENCY
LIGHT WEIGHT
ELIMINATE LAMINATIONS

TYPE OF FERRAMIC MATERIAL

PROPERTY	UNIT	A 34	B 90	C 159	D 216	E 174	G 254	H 419	I 141	J 472
Initial permeability at 1mc/sec	—	15	95	220	410	750	410	850	600	330
Maximum permeability	—	97	183	710	1030	1710	3300	4300	1010	750
Saturation flux density	Gauss	840	1900	3800	3100	3800	3200	3400	1540	2900
Residual magnetism	Gauss	615	830	2700	1320	1950	1050	1470	660	1600
Coercive force	Oersted	3.7	3.0	2.1	1.0	0.65	0.25	0.18	0.40	.80
Temperature coefficient of initial permeability	%/°C.	0.65	0.04	0.4	0.3	0.25	1.3	0.66	0.3	0.22
Curie point	°C.	280	260	330	165	160	160	150	70	180
Volume resistivity	Ohm-cm	1×10^9	2×10^5	2×10^3	3×10^7	4×10^5	1.5×10^8	1×10^4	2×10^5	—
Loss Factor: at 1 mc/sec	—	—	.00016	.00007	.00005	.00008	.00008	.00030	.0003	.000055
at 5 mc/sec	—	.0004	.0011	.0008	.0012	.002	.00075	.00155	.005	—
at 10 mc/sec	—	.0005	—	—	—	—	.0017	.00275	—	—

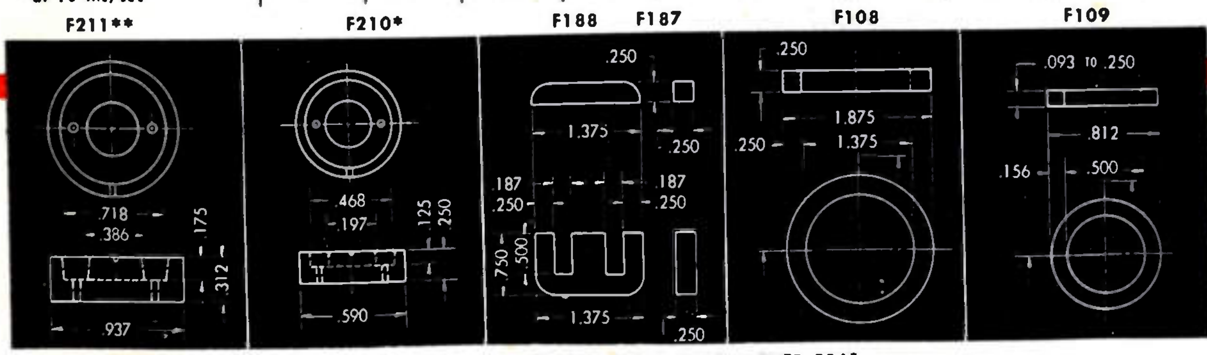

* FOR .145" HOLE, ORDER F260 ** FOR .096" HOLE, ORDER F261

General CERAMICS AND STEATITE CORP.

GENERAL OFFICES and PLANT: KEASBEY, NEW JERSEY

AKERS OF STEATITE, TITANATES, ZIRCON PORCELAIN, FERRAMICS, LIGHT DUTY REFRACTORIES, CHEMICAL STONEWARE, IMPERVIOUS GRAPHITE

Leading the Quality Field for more than 25 Years

KENYON
TRANSFORMERS
for all ARMY–NAVY specifications

built for durability
• engineered for trouble-free operation
• designed for standard and special applications

use KENYON TRANSFORMERS for

RADAR • BROADCAST • SPECIAL MACHINERY
JAN APPLICATIONS • ATOMIC ENERGY
EQUIPMENT • AUTOMATIC CONTROLS
EXPERIMENTAL WORK

Write for details **KENYON TRANSFORMER CO., Inc.**
840 BARRY STREET • NEW YORK 59, N. Y.

Announcing

The new RCA WV-87A *Master* VoltOhmyst*

$112.50 Suggested User Price

Measures . . . (Full-scale ranges)

DC VOLTAGE: 0 to 1.5, 5, 15, 50, 150, 500, 1500 volts
PEAK-TO-PEAK VOLTAGE: 0 to 4, 14, 42, 140, 420, 1400, 4200 volts
RMS VOLTAGE: 0 to 1.5, 5, 15, 50, 150, 500, 1500 volts
RESISTANCE: 0 to 1000 megohms in seven overlapping ranges
DC CURRENT: 0 to 0.5, 1.5, 5, 15, 50, 150, 500 milliamperes; 0 to 1.5, 15 amperes

Sold Complete—with the following Probes and Cables

- Direct Probe and Cable
- DC Probe
- Ohms Cable and Probe
- + Current Cable (Red)
- — Current Cable (Black)
- Ground (Case) Cable

Accessory Probes Available on Separate Order

✓ WG-264 Crystal-Diode Probe for measuring ac voltages at frequencies up to 250 Mc.

✓ WG-289 High-Voltage Probe, with WG-206 Multiplier Resistor, for increasing dc-voltage range to 50,000 volts and input resistance to 1100 megohms.

FEATURING an 8½" meter, the new WV-87A Master VoltOhmyst is really the master of every testing application. Its peak-to-peak scales are particularly useful for television, radar, and other types of pulse work.

The WV-87A measures dc voltages accurately in high-impedance circuits, even with ac present. It also reads rms values of sine waves and the peak-to-peak values of complex waves or recurrent pulses, even in the presence of dc.

Like all RCA VoltOhmysts, the WV-87A features ±1% multiplier and shunt resistors, a ±2% meter movement, high-input resistance, zero-center scale adjustment for discriminator alignment, dc polarity-reversing switch, and a sturdy metal case for good rf shielding.

On direct-current measurements, extremely low-meter resistance gives an average voltage drop of only 0.3 volt for full-scale readings on all ranges. Nine overlapping ranges provide dc readings from 10 microamperes to 15 amperes.

An outstanding feature is its usefulness as a television signal tracer . . . made possible by its high ac input resistance, wide frequency range, and direct reading of peak-to-peak voltages.

The RCA WV-87A *Master* VoltOhmyst has the accuracy and stability for laboratory work. Its large, easy-to-read meter also makes it especially desirable as a permanently mounted instrument in the factory and repair shop.

For complete information on the WV-87A, see your RCA Test Equipment Distributor or write RCA, Commercial Engineering, Section AX47, Harrison, New Jersey.

*Reg. U. S. Pat. Off.

Get complete details today from your RCA Test Equipment Distributor.

RADIO CORPORATION of AMERICA
TEST EQUIPMENT — **HARRISON, N. J.**

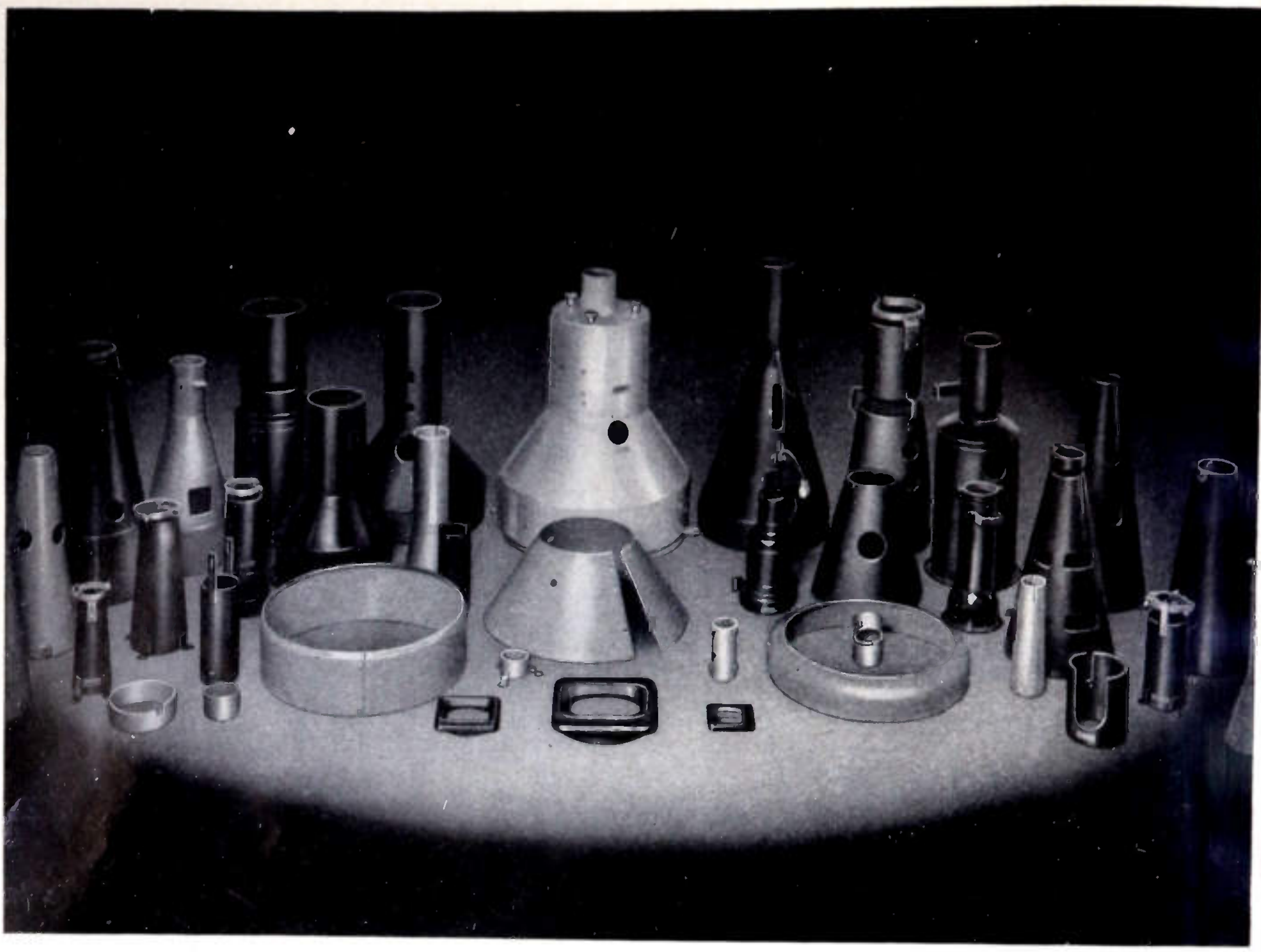

Designed for Application

Mu Metal Shields

The James Millen Mfg. Co. Inc. has for many years specialized in the production of magnetic metal cathode ray tube shields for the entire electronics industry, supplying magnetic metal shields to manufacturing companies, laboratories and research organizations. Stock shields are immediately available for all of the more popular sizes and types of cathode ray tubes as well as bezels for 2", 3" and 5" size tubes.

Many production problems, however, make desirable special shields designed in conjunction with the specialized requirement of the basic apparatus. Herewith, are illustrated a number of such custom built shields. Our custom design and fabrication department is at the service of our customers for the development and manufacture of magnetic metal shields of either nicoloi or mumetal for such specialized applications.

JAMES MILLEN MFG. CO., INC.

MAIN OFFICE AND FACTORY

MALDEN, MASSACHUSETTS, U.S.A.

NEW from HI-Q*

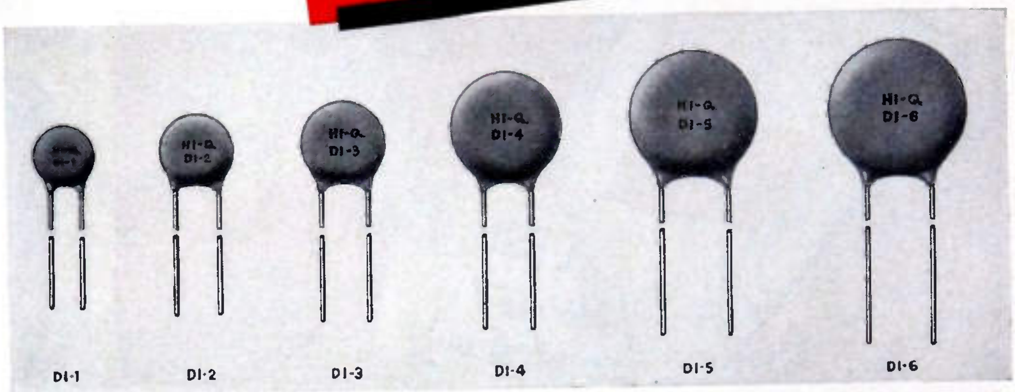

Illustrations approximately actual size.

Temperature Compensating DISK Capacitors

Capacity range from 475 mmf on the DI-6 N1400 material down to .3 mmf on the DI-1 size with tolerances of $\pm$ 5% or greater. Conservatively rated for working voltage at 500 volts DC and flash tested at 1500 volts DC. Insulation resistance at 100 volts is well over 10,000 megohms. Electrodes are fired directly to the low loss dielectric and are coated with a non-hydroscopic phenolic for protection against moisture and high humidities. Conform to RTMA Class 1 ceramic capacitors.

Extended Temperature Compensating DISK Capacitors

Produced from a recently developed group of extended coefficient ceramics, this type of **Hi-Q** Disk permits a much wider temperature compensating range than was possible on the formerly available normal linear temperature coefficient ceramics. Specifically developed for applications requiring a very large gradient of capacity versus temperature. These new **Hi-Q** Disks exhibit relatively higher dielectric constants permitting capacities in the range intermediate between the high K and linear or normal group of ceramics. The Q (a minimum of 250 at 1 megacycle) is somewhat lower than the Class 1 ceramics. It has, therefore, not been classified by RTMA as Class 1. However, characteristics are superior to by-pass Class 2 ceramics.

ALL HI-Q DISK CAPACITORS COME IN THESE SIX SIZES

Type	Diameter	Lead Width	Thickness
DI-1	5/16" Max.	3/16" $\pm$ 1/16"	5/32" Max.
DI-2	3/8" Max.	1/4" $\pm$ 1/16"	5/32" Max.
DI-3	7/16" Max.	1/4" $^{+1/8"}_{-0"}$	5/32" Max.
DI-4	19/32" Max.	1/4" $^{+1/8"}_{-0"}$	5/32" Max.
DI-5	11/16" Max.	3/8" $\pm$ 1/8"	5/32" Max.
DI-6	3/4" Max.	3/8" $\pm$ 1/8"	5/32" Max.

Companion Lines to the Popular HI-Q By-pass DISK Capacitors

The widely used **Hi-Q** By-pass Disks are fixed ceramic dielectric capacitors which meet RTMA Class 2 specifications. They are available in the complete capacity range of from .3 mmf to 30,000 mmf. Standard tolerances of 5% thru 20% where applicable can be furnished.

Write for Engineering Bulletin Giving Details of all HI-Q DISK Capacitors

**Trade Mark Registered, U. S. Patent Office*

HI-Q*

Electrical Reactance Corp.
OLEAN, N. Y.

SALES OFFICES: New York, Philadelphia, Detroit, Chicago, Los Angeles

PLANTS: Olean, N. Y., Franklinville, N. Y. Jessup, Pa., Myrtle Beach, S. C.

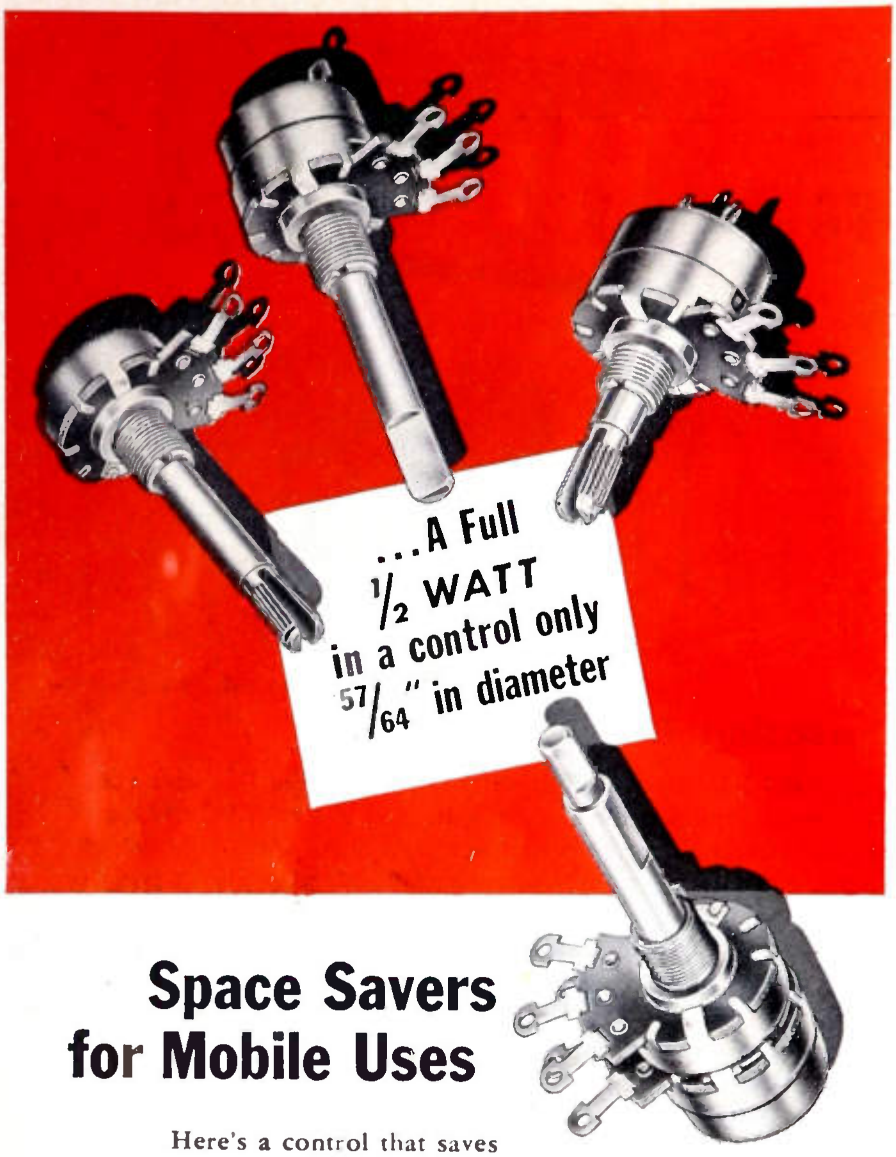

Space Savers for Mobile Uses

Here's a control that saves both space and weight—yet handles plenty of wattage for television receivers as well as for most mobile and aircraft radio uses.

You can get Stackpole LR controls with or without SP-ST or DP-ST line switches and in dual concentric arrangements. The wattage rating is conservative and these sturdy little units have proved their dependability on dozens of jobs formerly handled by materially larger controls.

Data bulletin covering the complete line of Stackpole controls on request.

Electronic Components Division

STACKPOLE CARBON COMPANY

St. Marys, Pa.

STACKPOLE

FIXED AND VARIABLE CARBON RESISTORS • IRON CORES • CERAMAG® NON-METALLIC CORES • MOLDED COIL FORMS • MOLDED CAPACITORS INEXPENSIVE LINE AND SLIDE SWITCHES

News—New Products

These manufacturers have invited PROCEEDINGS readers to write for literature and further technical information. Please mention your I.R.E. affiliation.

Air Line Lubricator

To provide automatic lubrication for tools using 10–60 cfm, **Keller Tool Co.**, Grand Haven, Mich., announces a recently developed Air Line Lubricator in two sizes, the larger of which is illustrated here.

With this new larger size, where a minimum of 10 cfm is used by one tool and a maximum of 60 cfm by all tools taking air through the lubricator, lubrication of one or more tools is accomplished automatically.

A transparent Plexene bowl, designed to hold 6 ounces of light oil, provides oil feed through a porous bronze wick. When used with a 35 cfm tool, the bowl holds enough oil for 8 to 10 weeks of lubrication under normal usage. No regulation of the oil flow is necessary.

Each tool, the manufacturer states, will receive the proper amount of lubricant. The quantity of oil dispensed into the air stream is dependent upon the amount of air passing the wick. Several tools operating from one lubricator will automatically draw more oil than just a single tool. Under normal conditions, pressure drop through the lubricator will not exceed 1 lb per square inch.

Installation of new Air Line Lubricator is made by screwing the device into a ½-inch air line ahead of the tool to be lubricated. A removable hex nut with holding chain permits refilling.

(Continued on page 74A)

This issue of *PROCEEDINGS OF THE I.R.E.* carries a summary of the advertising survey of preferences of members of the Institute. Many have been following the monthly findings as they were determined. The final analysis should be of interest to all persons engaged in writing and composing advertising promotion. The final monthly survey, based on the September issue, appeared in the December issue.

(Continued on page 106A)

WRITE FOR THIS CATALOG OF STOCK MAGNETS FOR YOUR EXPERIMENTAL NEEDS

Here's a handy reference, chock full of detailed permanent magnet information. If you are designing new products, or wish to improve present ones, this catalog will be of great value!

16% GREATER ENERGY

And, remember, all INDIANA permanent magnets described are available in INDIANA HYFLUX Alnico V—the permanent magnet material that offers an energy product averaging 5½ million BH max or more, with 5¼ million guaranteed!

Even though INDIANA HYFLUX Alnico V offers 16% greater energy product than regular Alnico V, it costs not a penny more!

INDIANA is the only manufacturer furnishing all commercial grades of permanent magnet alloys. You have a choice of cast, sintered, formed or ductile materials.

INDIANA
HYFLUX
ALNICO V

INDIANA engineers, with more than 30,000 successful permanent magnet applications to their credit, will be happy to help you with every permanent magnet problem.

Write—or phone—INDIANA today!
Ask for Catalog No. 11G-2

INDIANA PERMANENT MAGNETS

THE INDIANA STEEL PRODUCTS COMPANY

VALPARAISO, INDIANA • • • Sales Offices Coast to Coast

SPECIALISTS IN "PACKAGED ENERGY" SINCE 1908

Announcing a GERMANIUM

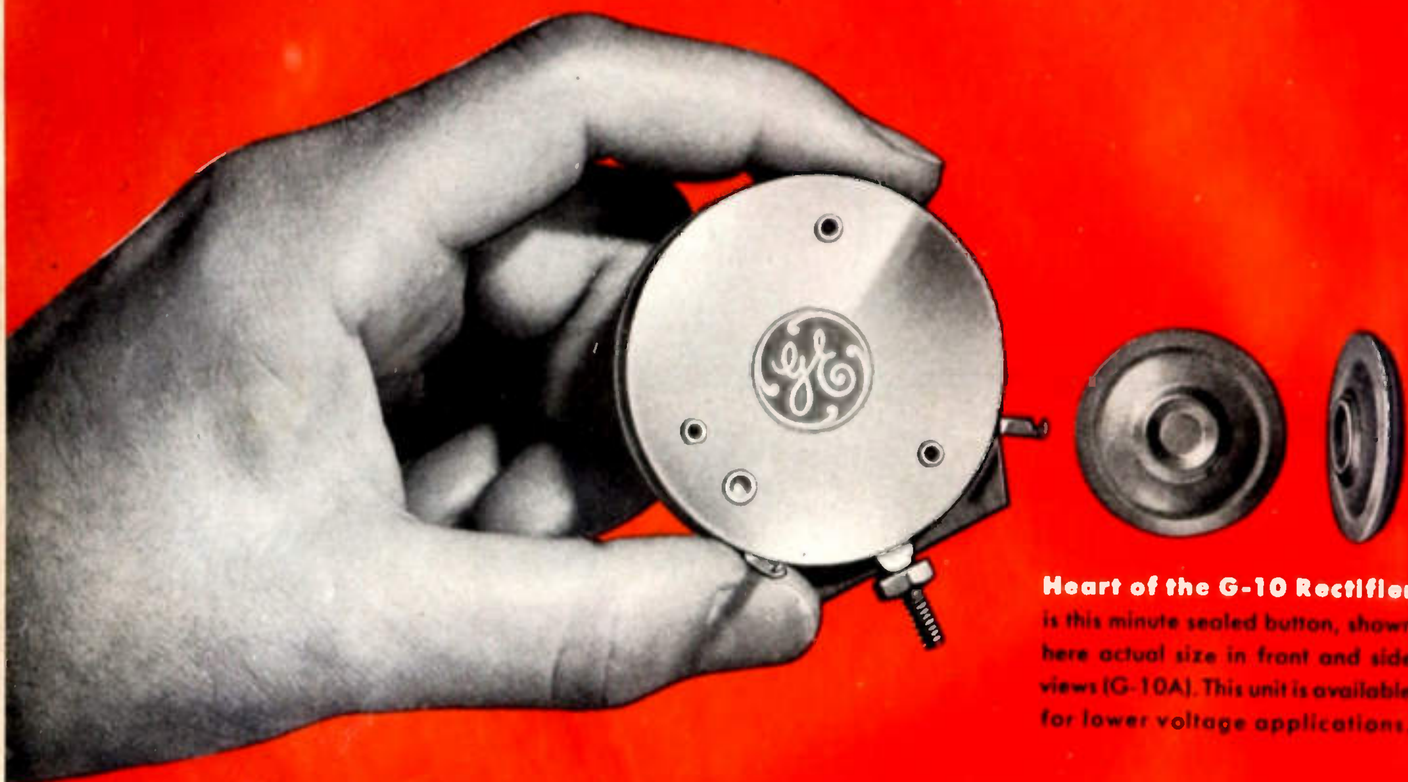

Heart of the G-10 Rectifier is this minute sealed button, shown here actual size in front and side views (G-10A). This unit is available for lower voltage applications.

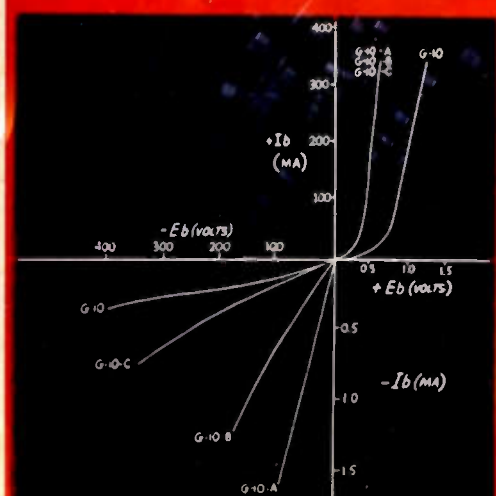

Typical Current-Voltage Characteristics

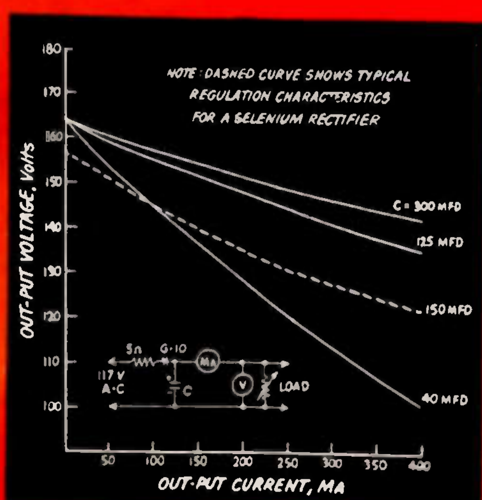

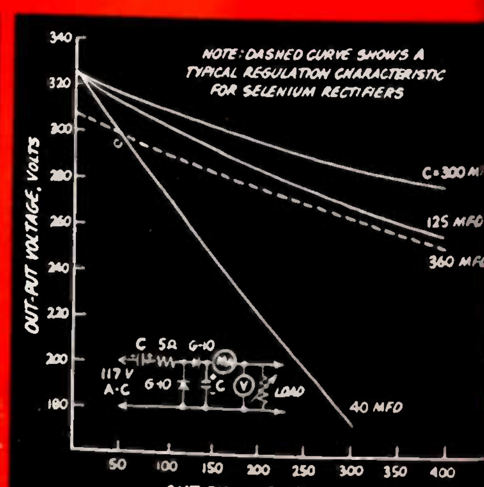

Regulation Characteristics

Revolutionary NEW POWER RECTIFIER!

G-E Research Advances New Principle of Area Rectification . . . Usage with Large Currents and Exceptionally Low Losses Now Possible

Can You Use These Outstanding Features?

- **Higher Output Voltage**—15 volts more B+ in typical TV power supply due to rectification efficiency up to 98%
- **Longer Life**—Moisture and fume resistant...gasket-sealed units
- **Lower Forward Resistance**—Approx. 3.5 ohms forward resistance at 350 ma
- **Higher Current Capacity**—400 ma average dc current
- **Higher Peak Inverse Voltage**—400 volts
- **Higher Back Resistance**—approx. 1 megohm at 350v
- **Smaller Size**—smaller than comparably rated dry rectifiers of other types

Specifications

Description and Maximum Ratings
Type G-10

Ambient Temperature	40°C	55°C	65°C
RMS Input Voltage (Max.)	130	130	130 Volts
RMS Current (Max.)	1.2	1.2	.2 Amps
D-C Output Current (Max.)	400	350	50 Ma
D-C Surge Current (Max.)	25	20	2.5 Amps
Peak Forward Current (Max.)	3	3	.5 Amps
Peak Inverse Voltage (Max.)	400	400	400 Volts
Full Load Voltage Drop (Max.)	1.5	1.4	1.3 Volts
Operating Frequency (Max.)	50	50	50 Kc

Single Rectifier Types		G-10A	G-10B	G-10C
RMS Input Voltage (Max.)	25°C	32	50	65 Volts
	40°C	32	50	65 Volts
RMS Current (Max.)	25°C	.6	.6	.6 Amps
	40°C	.5	.5	.5 Amps
D-C Output Current (Max.)	25°C	200	200	200 Ma
	40°C	150	150	150 Ma
D-C Surge Current (Max.)	25°C	10	10	10 Amps
	40°C	8	8	8 Amps
Peak Forward Current (Max.)	25°C	1.5	1.5	1.5 Amps
	40°C	1.2	1.2	1.2 Amps
Peak Inverse Voltage (Max.)	25°C	100	150	200 Volts
	40°C	100	150	200 Volts
Full Load Voltage Drop (Max.)	25°C	.8	.8	.8 Volts
	40°C	.7	.7	.7 Volts
Operating Frequency (Max.)	25°C	50	50	50 Kc
	40°C	50	50	50 Kc

● These rectifiers are now in pilot production. To purchase sample quantities, call the G-E Electronics Division Tube Dept. office near you or wire us: *Commercial and Government Equipment Dept., Electronics Park, Syracuse, N. Y.*

● *A newly printed bulletin on the G-10 Germanium Power Rectifier will be sent to you on request.* General Electric Company, Section 5212, Electronics Park, Syracuse, New York.

You can put your confidence in—

GENERAL ELECTRIC

Where mechanical precision means electrical accuracy

There's more to a precision potentiometer than accurate windings. In order that the required high *electrical* tolerances be held, it is absolutely essential that such parts as the shaft, mounting plate, and housing be designed and built for highest *mechanical* accuracy.

At Fairchild, we've concentrated on building precision equipment of all kinds for more than thirty years. Our engineers and craftsmen eat, drink, and sleep precision. Since our first potentiometer was produced, we've made it a practice to carefully control every phase of manufacture by building in our own plant every part that affects accuracy.

The example below is but one case of how this extra mechanical precision assures highest electrical accuracy.

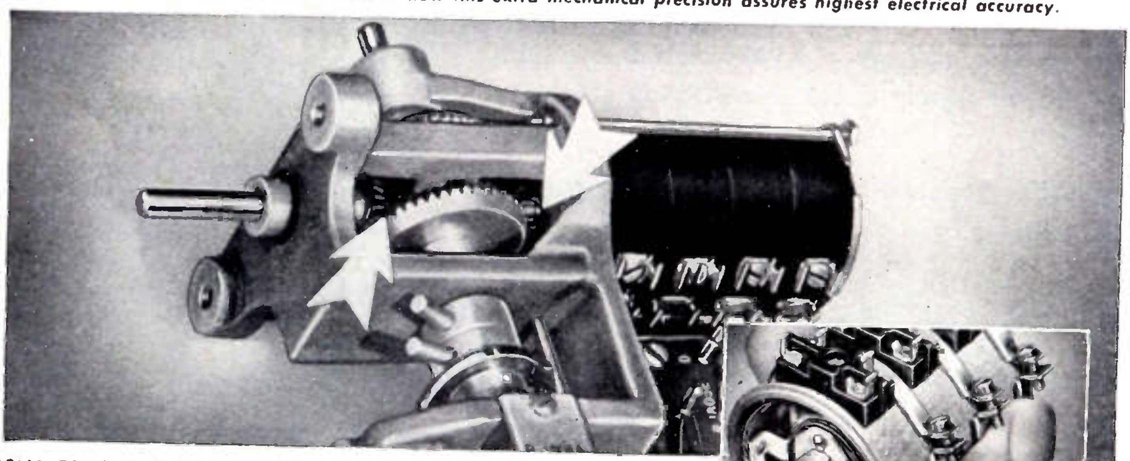

CRUCIAL PRECISION IN A RADAR CONTROL ASSEMBLY The gears on this radar control assembly were precision cut to eliminate backlash and binding, but the care that went into their manufacture could have been completely nullified if the potentiometer coupled to them was not mechanically precise. In this case, overall accuracy is assured by using a Fairchild precision unit.

Like all Fairchild potentiometers, this one has a shaft that is centerless ground from stainless steel to a tolerance of +.0000, −.0005 inch. Its radial shaft play is held to .0015 inch F.I.R. or better and concentricity of shaft to pilot bushing is .0025 inch F.I.R. or better, depending on type. Shaft to mounting-plate squareness is held to .001 inch per inch.

The windings of all Fairchild potentiometers are custom-made on special Fairchild-designed machines. Guaranteed functional tolerances are ±0.5% for linear windings, ±1.0% for non-linear windings—even better in some cases.

A COMPLETE LINE EXPERTLY DESIGNED AND BUILT TO INDIVIDUAL SPECIFICATIONS

PROMPT ATTENTION TO SAMPLE ORDERS. Prompt, expert attention to special potentiometer problems is yours by merely dropping us a line. Our Potentiometer Sample Laboratory is set up explicitly to fill such needs. Where sample orders are requested, quick delivery is assured. Write today, giving complete details to *Fairchild Camera and Instrument Corporation, 88-06 Van Wyck Boulevard, Jamaica 1, N. Y. Dept. 140-20H1.*

FAIRCHILD
PRECISION POTENTIOMETERS

New CBS-HYTRON 12B4

New 9-pin miniature; high-perveance, low-mu triode with 6/12-volt heater for parallel or series connection. 12B4 is designed specifically for vertical amplifiers with limited primary B supply voltages. Delivers adequate vertical sweep power in proper circuit to sweep any 70° rectangular picture tube. Characteristics of 12B4 are similar to those of 6W6GT, but 12B4 . . . for same input . . . supplies substantially more sweep power. 12B4, because of special design and processing, is also virtually free from grid emission.

New CBS-HYTRON 12BY7

New 9-pin miniature; very-high-transconductance pentode amplifier. As video amplifier in high-quality receivers, gives extended gray scale. In low-cost receivers, 12BY7 provides adequate voltage amplification for wide-band video amplifiers with primary B voltages as low as 135 volts.

Within its power capabilities, 12BY7 gives gains equal to those of 6AG7. High ratio of transconductance to interelectrode capacitances makes 12BY7 useful as video i-f or pulse amplifier for radar. High grid-to-screen transconductance suits 12BY7 (within its power handling capabilities) for class C harmonic oscillators.

Which of these CBS-HYTRON ORIGINALS can you use?

New CBS-HYTRON 5Y3WGT

New "ruggedized," full-wave filamentary-type rectifier with electrical characteristics equivalent to those of 5Y3GT . . . but 5Y3WGT is specially designed for equipment subject to high impact and shock.

New CBS-HYTRON 12A4

New high-perveance, medium-mu, 9-pin miniature triode for use as vertical amplifier, class C oscillator, or low-distortion audio output amplifier in push pull.

New CBS-HYTRON 12BZ7

New high-mu, 9-pin miniature dual triode for high-gain audio amplifiers, gating circuits, synch separators and amplifiers.

Write for Complete Data Today

CBS HYTRON RADIO TUBES

MANUFACTURERS OF RECEIVING TUBES SINCE 1921
HYTRON RADIO AND ELECTRONICS CO.
A DIVISION OF COLUMBIA BROADCASTING SYSTEM, INC.

MAIN OFFICE: SALEM, MASSACHUSETTS

HYTRON RADIO & ELECTRONICS CO.
Salem, Massachusetts

Please rush me full specifications for the new CBS-Hytron types I have checked:

12B4 .... 12BY7 .... 5Y3WGT ....

12A4 .... 12BZ7 ....

Name ....
(please print)

Street ....

City and State ....

DU MONT

SPECIAL cathode-ray tubes

The line of Du Mont cathode-ray tubes is carefully engineered to provide the broadest possible coverage of the entire range of standard applications. In some instances, however, the requirements of highly specialized applications are beyond the capabilities of RTMA Registered cathode-ray tube types. For such cases, Du Mont SPECIAL CATHODE-RAY TUBES offer the answer. Typical examples of these special tubes are shown below.

TYPE K1101P — 5-inch flat-faced tube designed for ultra-high-speed oscillography. Will provide spot writing speeds as high as 1000 in./μsec. Overall maximum accelerating potential of 37,000 volts, with good deflection sensitivity.

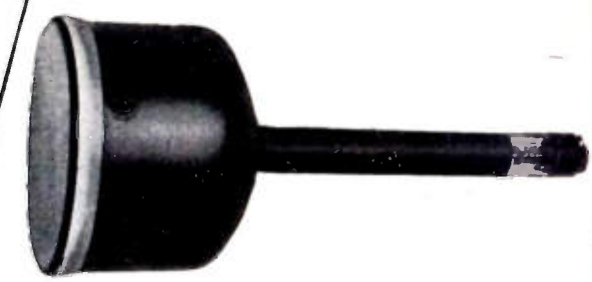

TYPE K1080P — 7-inch magnetically focused and deflected tube operating at accelerating potentials up to 30,000 volts, providing high light output with excellent resolution. Face-plate manufactured to conform to uniform standard of curvature and thickness.

TYPE K1065P — 3-inch flat-faced tube with high deflection sensitivity. Deflection-electrode connections through neck enable high-frequency applications.

TYPE K1052P — 7-inch tube containing 5 wholly independent electron-gun and deflection-electrode structures in a single envelope. Auxilliary ring-socket for easy connection to all deflection electrodes.

If you have a problem beyond the range of RTMA Registered cathode-ray tube types, the facilities of Du Mont, the skill of the most experienced designers of cathode-ray tubes in the industry, are at your disposal for consultation.

The above tubes are representative of the Du Mont line of SPECIAL CATHODE-RAY TUBES. For detailed information on these, and other Du Mont SPECIAL TUBES, write to Department G at the address below.

TUBE DEVELOPMENT LABORATORY, ALLEN B. DU MONT LABORATORIES INC., 100 MAIN AVENUE, CLIFTON, N. J.

NOW in Production

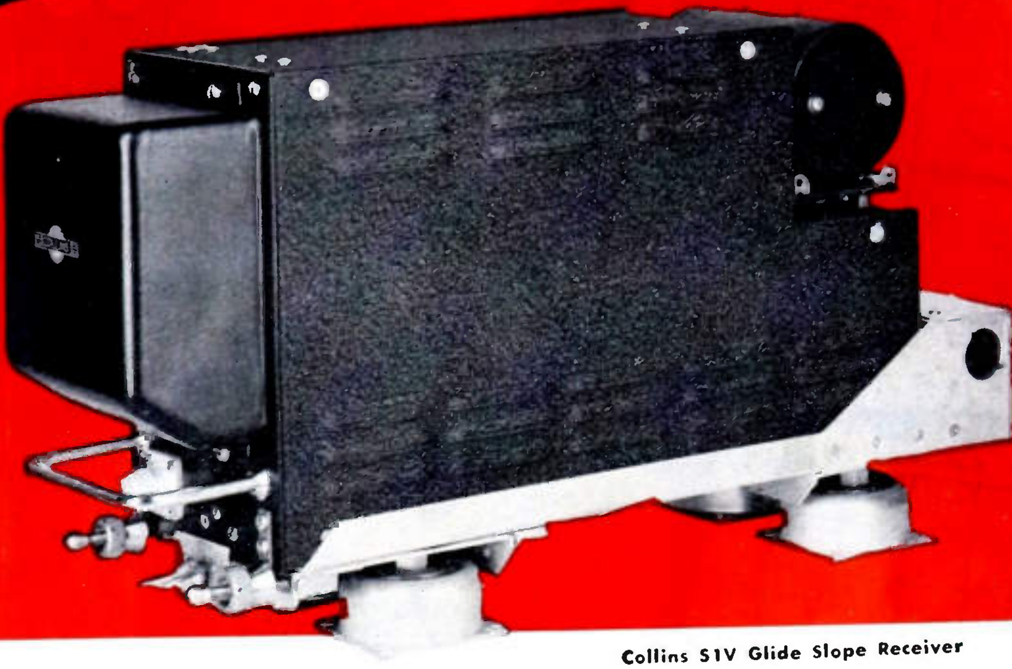

Collins 51V Glide Slope Receiver

The design of the Collins 51V-1 receiver, now on the assembly line, is based on "Glide Slope Receiver Characteristics" issued by Aeronautical Radio, Inc.

This receiver, together with the Collins 51R navigation equipment, will fulfill ILS receiving requirements for commercial and private as well as military aircraft.

The 51V is designed for reception of 90/150 cps tone modulated glide slope signals on all ten present and ten planned channels in the UHF range of 329-335 megacycles. It utilizes crystals identical with those employed in R-89B receivers and is electrically and mechanically interchangeable with modified ten channel R-89B's, greatly simplifying installation in present aircraft.

The 51V receiver control circuits are integrated with the standardized R/theta channeling system, with channel selection provided by a Collins type 314U remote control unit.

Choice may be had of a dynamotor for 12 or 24 volt d-c operation or an a-c power unit for operation from 115 volt 400 cycle supply.

If you are not thoroughly acquainted with this new glide slope receiver from previous contact or correspondence, write us for the 51V illustrated descriptive bulletin.

FOR PROGRESS IN INSTRUMENT LANDING SYSTEMS, IT'S . . . COLLINS

COLLINS RADIO COMPANY, Cedar Rapids, Iowa

11 W. 42nd St., NEW YORK 18 — 1937 Irving Blvd., DALLAS 2 — 2700 W. Olive Ave., BURBANK

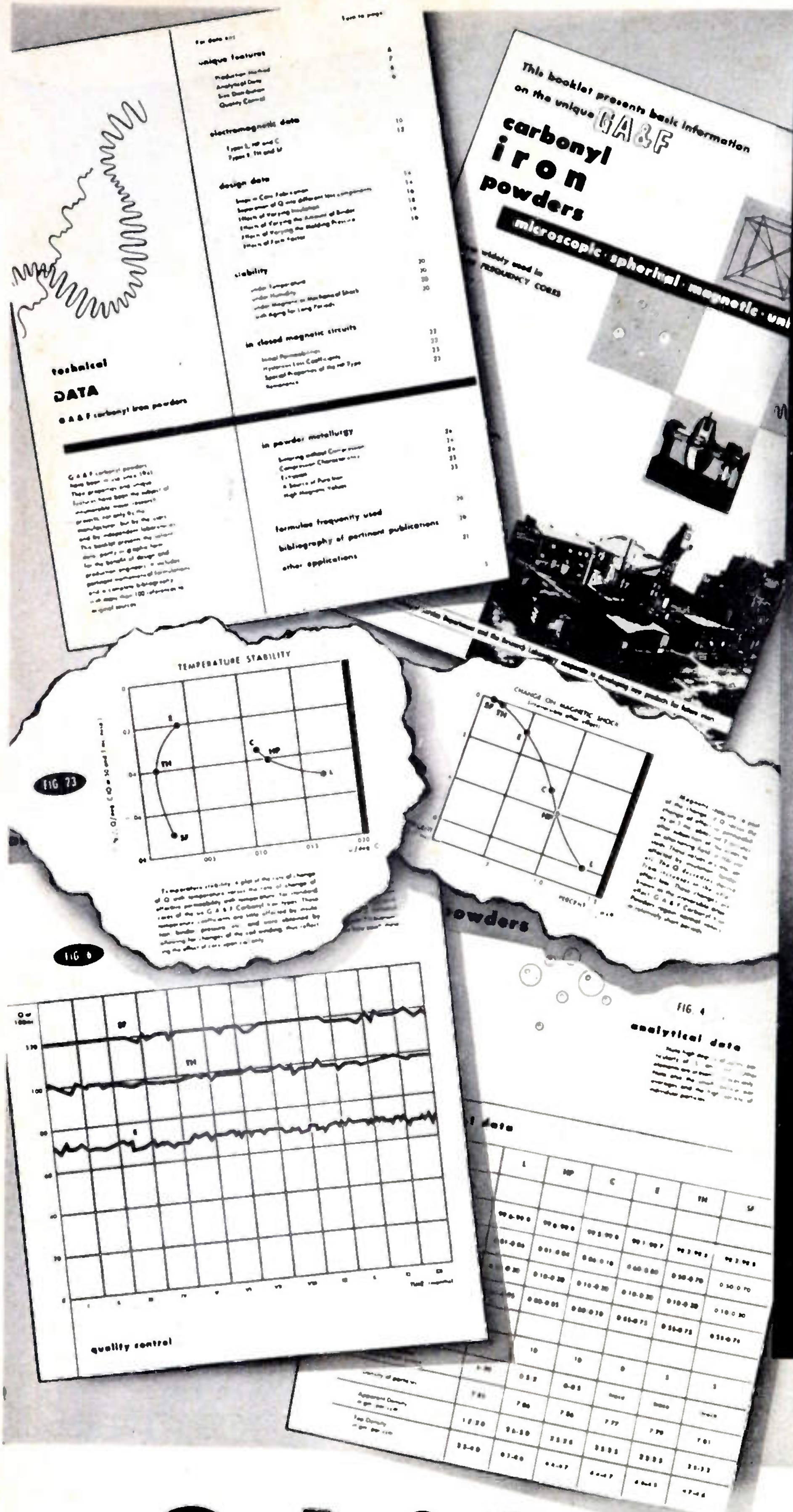

YOUR COPY

of this new book

awaits your request

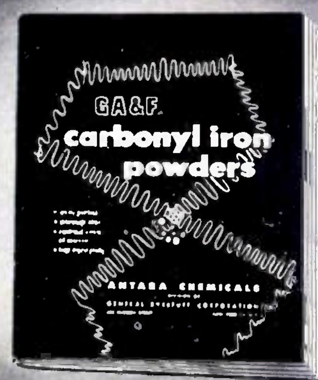

...the technical portrait of an unusual product

G A & F® Carbonyl

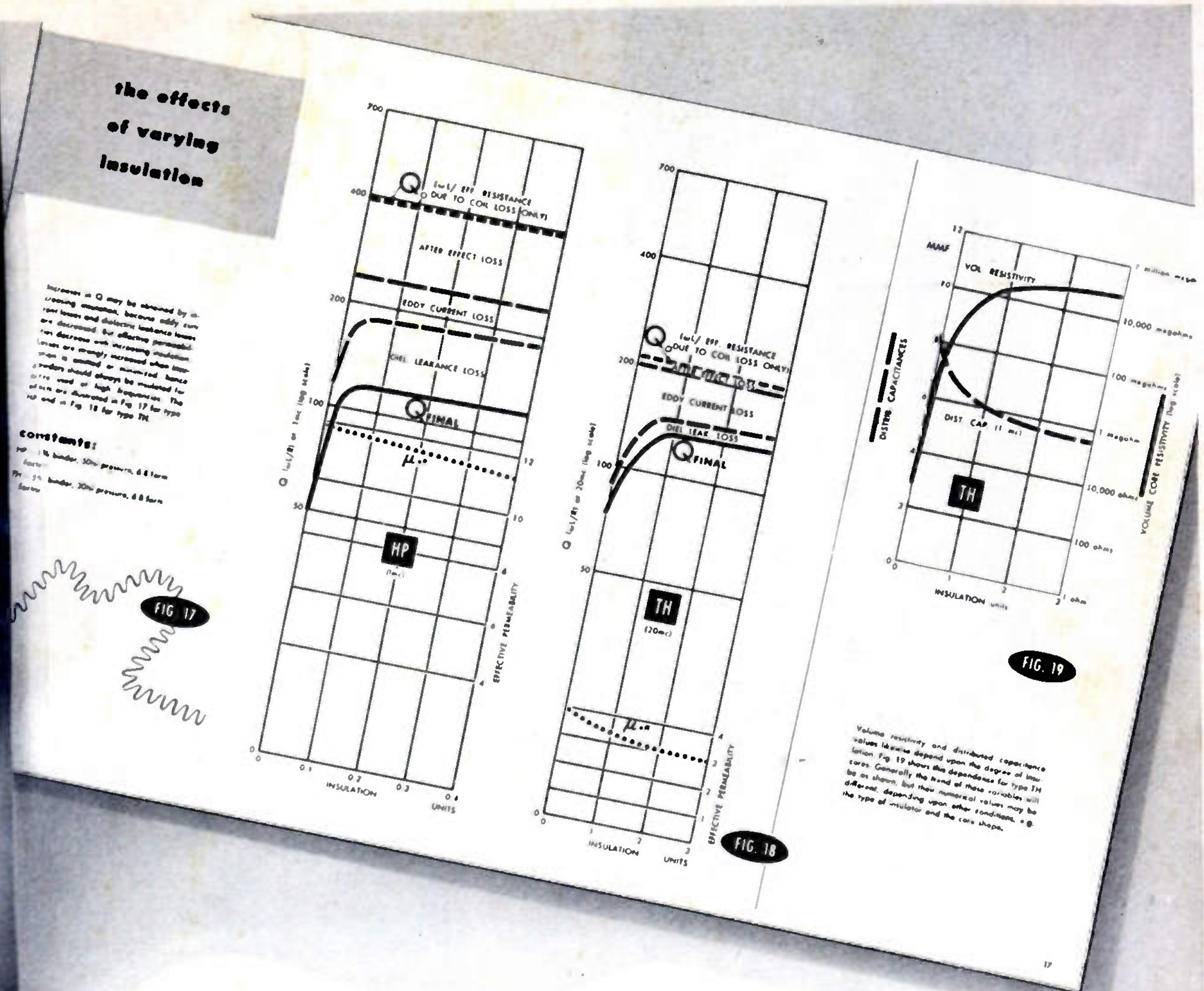

G A & F Carbonyl Iron Powders are unique . . . This new book is unique . . . Here is the most comprehensive treatment ever given to the characteristics and applications of Carbonyl Iron Powders. (The 3-page bibliography alone is a valuable addition to your reference library.)

This book was written for the manufacturer or engineer who wants a maximum of facts with a minimum of verbiage. 80% of the story is told with photomicrographs, diagrams, performance charts and tables. Established applications are fully covered; new applications are suggested. Ask your core maker, your coil winder, your industrial designer, how G A & F Carbonyl Iron Powders can improve the performance and reduce the cost of the equipment you manufacture. Write us — without obligation — for your copy of this new book. Kindly address your inquiry to Dept. 14.

ANTARA

ANTARA® CHEMICALS

DIVISION OF

GENERAL DYESTUFF CORPORATION

435 HUDSON STREET • NEW YORK 14, N. Y.

Iron Powders . . .

MEMBER mpa METAL POWDER ASSOCIATION

TYPICAL ICAS* OPERATING CONDITIONS
Class C Telegraphy and FM Telephony

Heater Voltage			6.3 volts
Heater Current			1.25 amps
	Below 60 Mc.		At 175 Mc.
DC Plate Voltage	600	750	400 volts
DC Grid-No. 2 Voltage	180	160	200 volts
DC Grid-No. 1 Voltage	−85	−85	−54 volts
DC Plate Current	150	120	150 ma
Power Output (Approx.)	69	69	35 watts

*Intermittent Commercial and Amateur Service.

Another RCA First...the RCA-6146

New beam power tube for VHF transmitters

Specifically designed for VHF transmitter applications, the new RCA-6146 features low cost, small size, unusual ruggedness, and high power sensitivity. It can deliver an output of 35 watts at 175 Mc under ICAS conditions, with a plate voltage of 400V., and a plate current of 150 ma. Adequate driving power can be obtained from a 5763, 2E26, or another 6146, depending upon the circuit design requirements.

The RCA-6146 employs a rugged button-stem construction with short internal leads, and an octal base with short metal sleeve which shields the input to the tube so completely that no other external shielding is required. Input and output circuits are well separated by bringing the plate lead out at the top of the bulb. Base pin connections permit three connections to the cathode, to provide good rf grounding.

For complete technical data on the RCA-6146 and RCA-6159, write RCA, Commercial Engineering, Section 47AR, Harrison, N. J., or your nearest RCA field office.

FIELD OFFICES: (East) Humboldt 5-3900, 415 S. 5th St., Harrison, N. J. (Midwest) Whitehall 4-2900, 589 E. Illinois St., Chicago, Ill. (West) Madison 9-3671, 420 S. San Pedro St., Los Angeles, Calif.

Another **new RCA tube**

The RCA 6159, identical with the 6146 except for its heater rating of 26.5 volts, 0.3 amperes, is designed for VHF service in aircraft application.

The Fountainhead of Modern Tube Development is RCA

RADIO CORPORATION of AMERICA
ELECTRON TUBES
HARRISON, N. J.

PROCEEDINGS OF THE I.R.E.

Published Monthly by

The Institute of Radio Engineers, Inc.

VOLUME 40 — *January, 1952* — NUMBER 1

BOARD OF
RECTORS, 1951*

I. S. Coggeshall
President

Jorgen Rybner
Vice-President

W. R. G. Baker
Treasurer

Haraden Pratt
Secretary

fred N. Goldsmith
Editor

S. L. Bailey
nior Past President

R. F. Guy
nior Past President

1951

. V. Eastman (7)
W. L. Everitt
D. G. Fink
. Hamburger (3)
E. R. Piore
H. J. Reich (1)
J. D. Reid (5)
D. B. Sinclair
J. A. Stratton

1951–1952

H. F. Dart (2)
W. R. Hewlett
P. L. Hoover (4)
J. W. McRae
W. M. Rust (6)
A. B. Oxley (8)

1951–1953

W. H. Doherty
G. R. Town

•

larold R. Zeamans
General Counsel

•

George W. Bailey
Executive Secretary

urence G. Cumming
Technical Secretary

•

Changes of address th advance notice of een days) and communications regarding scriptions and paynts should be mailed the Secretary of the titute, at 450 Ahnaip Menasha, Wiscon- , or 1 East 79 Street, w York 21, N. Y.

All rights of republican including translan into foreign languages, are reserved by Institute. Abstracts papers with mention their source may be inted. Requests for ublication privileges ould be addressed to e Institute of Radio gineers.

* Numerals in parentheses owing Directors' names ignate Region number.

PROCEEDINGS OF THE I.R.E.

INSTITUTE NEWS AND RADIO NOTES

EDITORIAL DEPARTMENT

Alfred N. Goldsmith
Editor

E. K. Gannett
Technical Editor

Marita D. Sands
Assistant Editor

•

ADVERTISING DEPARTMENT

William C. Copp
Advertising Manager

Lillian Petranek
Assistant Advertising Manager

•

BOARD OF EDITORS

Alfred N. Goldsmith
Chairman

PAPERS REVIEW COMMITTEE

George F. Metcalf
Chairman

ADMINISTRATIVE COMMITTEE OF THE BOARD OF EDITORS

Alfred N. Goldsmith
Chairman

Responsibility for the contents of papers published in the PROCEEDINGS OF THE I.R.E. rests upon the authors. Statements made in papers are not binding on the Institute or its members.

MEMBER AUDIT BUREAU OF CIRCULATIONS

Copyright, 1952, by The Institute of Radio Engineers, Inc.

Donald B. Sinclair

President, 1952

Donald B. Sinclair, who resides at Crescent Road, Concord, Mass., was born in Winnipeg, Manitoba, Canada, on May 23, 1910. He was educated at the University of Manitoba, in 1926–1929, and then transferred to the Massachusetts Institute of Technology, where he received the degree of S.B. in 1931, the S.M. in 1932, and the Sc.D. in 1935

Dr. Sinclair has been associated with the Bell Telephone Laboratories and the New York Telephone Company in New York, and with the Western Electric Company at Hawthorne. In 1927 he was associated with the Western Canada Airways as a radio operator.

He joined the General Radio engineering staff in 1936, becoming the assistant chief engineer in 1944. In 1950 he was appointed to the position of chief engineer in that company. His work has been mainly on the general development and design of high-frequency measuring instruments for which he received the IRE Fellow Award in 1943.

During World War II, Dr. Sinclair worked in the Countermeasures Division and Guided Missiles Division of NDRC, receiving the President's Certificate of Merit for outstanding services.

Dr. Sinclair has been a member of the Board of the Institute of Radio Engineers since 1945, and has been active on a number of its committees such as: Antennas, Awards, Executive, Papers, Planning, Radio Transmitters, and Television. In 1945–1946, he was the Institute Representative on the Radio Technical Planning Board, and in 1949–1950 he was the IRE Treasurer. Dr. Sinclair is a Fellow of the American Institute of Electrical Engineers, a member of the American Association for the Advancement of Science, and Sigma Xi.

Guided Missiles—A New Field for the Radio Engineer

Simon Ramo

During recent decades, it has become evident that communications and electronic engineers contribute substantially to the public welfare in peacetime, and also that they are an indispensable factor in the national defense and a strong bulwark for their country in wartime.

In the following guest editorial by a Fellow of the Institute, who is the Director of Operations of the Hughes Aircraft Company, there is presented an analytical study of the technical problems facing the designer of guided missiles, and the extent to which the solutions draw upon civilian communications techniques and on the field of advanced mechanical engineering.—*The Editor.*

Anticipating a continuation, if not a worsening, of the present world situation, it may be expected that the bulk of the electronics industry will soon be devoted to military needs. An even larger fraction of the electronics profession, and therefore of the membership of the IRE will be needed for the development, design, and production of new and complex devices and systems for military use. Among the new fields for the radio engineer, one which is second to none in its demands upon the technical staff and in its probable ultimate effect on the broad development of electronics, is the guided-missile field. In view of its coming importance to the IRE membership, a short description of the nature of this new engineering field appears in order at this time.

To the pure scientist, a guided missile may be said to represent nothing new, since most of what has been done and probably will be done during the next decade requires no basic discoveries. However, to the engineer and applied physicist, radical advances are possible by utilizing essentially the existing body of fundamental knowledge. In this sense, guided-missile engineering represents the reduction to practice of highly novel ideas in which intimate knowledge of a number of different engineering fields is combined to develop one consistent system. Other more specific factors which characterize guided-missile engineering are found in the following:

(a) Reliability and ruggedness; ability to withstand shock, vibration, wide temperature fluctuations, and humidity—the requirement here is often higher by several orders of magnitude in guided-missile engineering than in the general electronic engineering field.

(b) In basic theory of operation and design, the overall system considerations are complex. Ordinary information theory, for example, as applied to a relatively simple voice-communication system may already be regarded properly as a difficult, theoretical, frontier field; but in guided-missile engineering, added to the ordinary information-theory aspects, are the matters of stability and precision, often on a nonstationary or changing-noise base. In addition to a communication link, complex as that might be, there are computing and servo systems, and couplings to aerodynamics, target conditions, and to intricate observation devices.

(c) The precision aspect of guided-missile engineering is worth a special comment. Small effects usually ignored in most electronic devices are often all important in the electronics package of a guided missile. Also important is the fact that guided-missile systems usually require a highly co-ordinated design consisting equally of precision electronic circuits and precision mechanical components. This kind of mechanical engineering, the precision instrument kind, is actually more often the bottleneck in the engineering of a missile than the electronics. Because the electronics physicists and engineers are more accustomed to dealing with feedback, system considerations, noise, and the physics of the problem in general, a conjunction of the talents of the electronics expert and the unusual mechanical engineer must be effected. In this joining, considerable weight falls on the electronics partner who must be a broad engineer in fields other than his specialty. If nothing else, the guided missile may once and for all bring a firm understanding of the mechanical engineering aspects of electronic equipment to the electronics engineer (who has so often in the past lacked a true appreciation of the importance of that associated field).

(d) In general, in the guided-missile field, it is found that all of the engineering techniques, whether they are in electronics, mechanics, aerodynamics, or metallurgy, are being forced simultaneously well beyond the current state of the art. In the design of a new line of devices it is not often that for each and every component thereof, the designer is called upon to make an important advance. That kind of development can be handled only by unusually broad and able physicists and engineers.

(e) As always, when a new and complex set of electronic applications is investigated, new electron tubes need to be invented and are invented. Generally, electronics will benefit as new and important applications for these new tubes then follow in nonmissile fields.

It is often said that during a period of military preparedness great advances are made in applied science. This statement is sometimes only a hope and a rationalization in an attempt to find something good about wars. In the case of guided-missile development, this is more than a rationalization, at least from the standpoint of electronics science. In the field of synthetic electronic intelligence lies an enormous potential aid to mankind. It has been predicted that some day more such electronic devices will be manufactured to aid business, industry, and transportation than television sets for entertainment. If so, the guided missile, developed through military necessity, will be credited with playing a leading role in bringing about this result.

Robert H. Marriott

1879–1951

Robert H. Marriott, a founder and the first President of The Institute of Radio Engineers, died on October 31, at his home in Brooklyn, New York.

Known to his associates for his vigor, vision, and co-operativeness, tenacity of purpose, and broad knowledge, he was widely regarded as one of the leading contributors to the advancement of radio communication and to the growth and success of The Institute of Radio Engineers.

Mr. Marriott's pioneering efforts to form a radio engineering society materialized in 1909 with the founding of the Wireless Institute. He served as its President until 1912 when, through the efforts of Alfred N. Goldsmith, John V. L. Hogan, and himself, the Wireless Institute merged with the Society of Wireless Telegraph Engineers to form The Institute of Radio Engineers. He became the first IRE President in 1912, and served as Vice-President in 1913 and on the Board of Directors in 1914–1916, 1920–1922, and 1926–1932. Mr. Marriott was instrumental in forming the Seattle Section of the IRE, and became the first Chairman of that Section in 1915–1919.

Born on February 19, 1879 at Richwood, Ohio, Mr. Marriott started his radio experimental work in 1897, at the Ohio State University, where he graduated with the Bachelor of Science degree in 1901. He was the first man to put into use in America the telephone and detector method of radio reception, a system that was a forerunner of the vacuum tube. He completed the first Pacific Coast commercial broadcasting station operative between Avalon, Catalina Island, and the California mainland. Mr. Marriott did experimental work for a number of early radio concerns, was a radio aide of the U. S. Navy in 1915–1925, and was a consulting engineer of the Federal Radio Commission in 1928–1929. He continued in private practice as a consultant until his retirement in 1943. Mr. Marriott was responsible for a number of patents and was the author of many papers and articles on radio which included a series of articles in the New York Herald Tribune in 1927 and 1928.

Mr. Marriott became a Fellow of the IRE in 1915 and a Life Member in 1949. He was a Fellow of the American Institute of Electrical Engineers, and an Honorary Member of the Radio Club of America, and of the Veterans Wireless Operators Association.

Mr. Marriott's last illness prevented the formal presentation to him of an engrossed testimonial volume, signed by all of the members of the IRE Board of Directors, attesting to its full recognition and deep appreciation of the great worth of his work in the foundation, administration, and upbuilding of The Institute of Radio Engineers.

The Board at its meeting on November 7, 1951, adopted a resolution on the death of Robert H Marriott which contained the following excerpt from that testimonial volume:

> His foresight in discerning the need for a society of radio engineers was a powerful stimulus to the foundation of the Institute.
>
> His unselfish, skilled, and unlimited devotion to the conduct of the activities of the Institute in its earlier years contributed substantially to the creation of the firm foundation upon which the Institute has grown.

After the Freeze*

W. R. G. BAKER†, FELLOW, IRE

By authorization of the Board of Directors, there is included in these PROCEEDINGS from time to time a limited number of papers dealing with the industrial and merchandising aspects of the communications and electronics field. It is thought that these papers will be instructive enlightening, and helpful to the membership.

Included in this series is the following analytic (and pleasantly informal) study of present-day commercial trends in the television-manufacturing and television-broadcasting fields. It was made available by its author, who is a past president of the Institute, its present treasurer, and chairman of its Professional Groups Committee, as well as vice-president of the General Electric Company.—*The Editor.*

WHEN the subject "After the Freeze," was selected I had in mind the freeze on construction of new television stations which will have been in effect three years at the close of this past September. Actually, the electronics industry has been confronted with two freezes. From last May up to the present it has experienced what might be called a freeze on consumer buying. The relation between the consumer freeze and the FCC freeze is not only important, but in fact may indicate what can be expected after the FCC freeze has thawed out.

The television industry has blamed many of its ills upon the construction freeze to the extent that many persons look upon the lifting of this freeze as the palliative, if not the cure all, of all the ills of the industry.

First, let us take a short look at what did happen during the three years of the freeze. As more and more of the 107 television transmissions now operating in the United States went on the air, some 92 set manufacturers began manufacturing television receivers as fast as they could, and set dealers in the broadcast areas were beset by more customers than they could accommodate.

But then, from May of 1951, this supposedly never-ending stream of set customers began to dry up, and this last summer, almost disappeared entirely. This was the consumer freeze.

At this point we have a rather strange situation. The television-set owner has no privacy. Opinion researchers and survey experts have dissected him, examined him, analyzed, him, reported on him. They know how many hours he watches television each week, what he eats for breakfast, how he parts his hair, and, if he has hair. They know how many packages of cigarettes he smokes each week, how old his children are, whether he uses cream in his coffee, and a thousand other things about him. Knowing all of these things about the TV owner, it would be more normal to expect that someone would be able to answer the question as to why the prospective TV owner stopped buying TV sets, and perhaps more important, how to get him started buying TV sets again?

It would be interesting to examine some of the figures about the owners of television sets. Here is what one study says about the average set owner: he makes $644 a year more than the man who doesn't own a television receiver. He bought nearly 75 per cent of the new cars sold in the past six months. He buys more beer and orange juice, uses more hair tonic and shampoos, has more children, and spends two and a quarter hours a day watching television programs.

But, no one seemed to know why more television sets weren't being purchased in the areas where television reception existed.

Let us take a look at the major effect of the construction freeze and then at the consumer freeze.

First we must recognize one fundamental marketing principle. When a market has changed from a sellers to a buyers market, there are generally only three correctives: The market can be broadened to bring in new consumers who will buy at the then existing price levels; the market can be deepened, which means that at new and lower price levels customers can be brought in who either could not afford or who just would not buy at the prior price levels, or the selling campaign may be stepped up. The last alternative is very difficult if the market is under the influence of political, economic, or technological factors peculiar to a particular set of conditions.

Certainly the construction freeze very effectively prevented the broadening of the market for television receivers. This meant that at the existing price levels a certain percentage of the public would buy. The rate at which they would buy could be and was influenced by certain factors which were probably nonrecurring. When this phenomenon began to taper off, the industry began to talk about saturation and other fairly plausible reasons for the beginning of the consumer freeze.

Let us try to examine the factors bearing on the consumer freeze.

The initial surge of television-receiver sales need not be explored since the reasons are well known.

If the curves showing the sale of consumer hard goods for the period 1950–1951, to date are examined it will be noted that starting with January, 1950 the volume trend was distinctly upward. A small peak occurred in March, 1950 when a decrease took place which was indicative of the normal cyclical trend of this business. In July, 1950 there occurred a major peak in sales volume. From this first major peak the volume tapered off until, in February, 1951, a second major peak developed. Since this February 1951 peak, volume has tapered off until, in July, 1951, the volume had receded to the January, 1950 level.

It is interesting to note that the sales trends for soft goods show the same variation characteristics as hard goods, except that the peaks were smaller than for hard goods. Incidentally, the soft goods sales curve started an upward trend in July, 1951.

What these curves say is that the recent subnormal buying of consumer hard goods is a compensating action for the panic spending of the summer of 1950 and of last winter.

In the case of soft goods the upturn in July of this year presumably indicates that the compensating action has run its course.

What about consumer hard goods and, in particular, television receivers? Has the consumer overbuying been compensated?

We should examine this question in more detail. For example, what were the causes for the overbuying, what was the play of the corrective or compensating actions, and what are the possibilities for a distinct uptrend in that section of the hard goods represented by television receivers?

With respect to television receivers, the sales trend during the summer of 1950 and last winter was to a considerable extent influenced by

1. The acceptance by the public of television as a major form of entertainment, information, and education.
2. The Korean war.
3. Purchasing in anticipation of taxes.
4. The threat of production restrictions due to the shortage of material.

Perhaps no one of these factors were controlling in all phases of the uptrend, but taken collectively the result was the establishment of two major and one minor buying swings.

What stopped buying? Certainly no one specific thing. In all probability a combination of the following factors:

1. The inability of the market to broaden due to the construction freeze resulted in the saturation of the buying levels which were open to buy at the then existing price levels.
2. The failure of any "shot in the arm" to compensate for the normal cyclical sales trend in television receivers. By this I mean the normal decline in sales due to warm weather, daylight saving, and the relatively unattractive summer programs.

* Decimal classification: R583. Original manuscript received by the Institute, September 12, 1951. This paper was taken from a speech given by Dr. W. R. G. Baker before the National Electronic Distributors Association at Cleveland, Ohio on September 10, 1951.

† General Electric Co., Syracuse, N. Y.

3. The impact of credit restrictions, the increase in taxes of all types, and the upward trend in cost of living was beginning to be felt by the consumer.
4. To some extent the color controversy and the talk about uhf.
5. Perhaps the consumer began to believe that rollbacks would become a reality.
6. The definite and continued trend in the increase in savings which started early in 1951.

This brings us to the very important question of whether the over-buying has been compensated, and if so what were the correctives, that is, why do we think the compensating action has been completed?

In our opinion the compensating actions are

1. The market has been deepened through reduction in list prices; hence new consumer buying levels have been opened up.
2. The recent authorized increase in power of present television transmitters.
3. Reduction in credit restrictions and the fact that savings are available for the purchase of goods.
4. Unless there is another major controversy on color and uhf, it is believed that the consumer has discounted these technological questions.
5. The return of high-grade programs.
6. The resolution, at least in part, regarding sports programs.
7. The opening of the transcontinental relay, making possible (a) the addition of perhaps 6,000,000 families to network service and (b) the great potentiality for new and outstanding programs and events (such as the signing of the treaty with Japan).

Perhaps some of us have forgotten the traditional sales cycle of the radio-receiver business. Television receivers should have the same cyclical characteristics. During the past two years these cyclical trends have been masked by factors which are probably not of a recurring nature.

So far, the real threat of material shortages has not been mentioned. From the viewpoint of the consumer these shortages never materialized. But with steel cut to 58 per cent, copper to 54 per cent, aluminum to 46 per cent, and with nickel a major unknown factor, the ingenuity of our industry will be really put to work to compensate for these cutbacks.

From the viewpoint of the consumer, I think they will have to be shown real physical shortages of merchandise before they can be again stampeded into a buying splurge.

Is the consumer freeze over? My answer is that it is well on the way to thawing out provided the industry recognizes that selling and not order-taking is the real order of the day.

Now, let us examine the freeze on the construction of television stations. When this freeze thaws out, will there be another gold rush?

It is about time we look at some of the facts, and then perhaps decide on what the end of the freeze can and cannot do for the electronics industry.

These facts can be divided into four major classifications: (1) economic, (2) political, (3) production, and (4) scientific. Let us take them up one by one.

First, what are the economic facts concerning early 1952 when, according to the chairman of the Federal Communications Commission, the freeze will be lifted? We shall still be in the middle of an expanding economy, with our national gross product reaching a new high of some 310 or more billion dollars a year, due in part to the heavy federal military expenditures, to the government's deficit spending and to a dropping, but still fairly adequate, supply of consummer products, and a high level of disposable income.

Secondly, the political fact that concerns us most is that we are, and barring an all-out war, that we will be living, in 1952, in a garrison state, a controlled economy, with definite limitations on the amount of civilian production and with controls on profits, wages, and prices.

And that leads us to the third classification—production. If the present pattern of mobilization is followed, there will not be available for television manufacture enough critical materials for industry to produce more than five million sets in 1952. It may even be four million or less if proposed restrictions on critical materials are adhered to rigidly. It might even be fewer sets if nickel is unavailable for receiving tubes. It takes a long time for many of the military contracts to build up to any volume, and that is particularly true for complicated military electronic equipment requiring a large amount of engineering. The major drain on the supply of critical basic materials may fall most heavily in 1952 and in early 1953.

The last of the four classifications which we must consider before we make any predictions as to the future of television after the spring thaw is the scientific; in other words, the state of the advancement of television. Improved black-and-white receivers for uhf as well as vhf will be available. Picture tube sizes are still increasing. No compatible color receiver of an all-electronic type will have been developed to the point that it will be in quantity production by the time the freeze is unfrozen.

These are the basic facts, the principal factors affecting the growth of television within the United States once the artificial restrictions of the freeze are lifted. Some are limiting factors, others will work for more rapid expansion.

According to the allocation plan set forth by the Federal Communications Commission, there could be at some indefinite time in the future, approximately 2,000 TV transmitters established in some 1,400 cities. At the present time there are approximately 440 applications pending, many of these from cities which do not have television stations at present, and many of which are not within broadcast reception areas.

For example, some of these cities that are presently without a transmitter are Mobile, Alabama; Tucson, Arizona; Sacramento, California; Denver, Colorado; Augusta, Georgia; Peoria, Illinois; Ft. Wayne, Indiana; Des Moines, Iowa; Wichita, Kansas; Shreveport, Louisiana; Portland, Maine; Flint, Michigan; Akron, Ohio; Allentown, Pennsylvania; Columbia, South Carolina; to name a few.

When the thawing comes, how soon will transmitters go on the air in these cities? Some of the areas they will cover are now receiving television signals from adjoining areas. Present coverage ranges from Allentown, Pennsylvania, which is already 47 per cent saturated with TV receivers, to Denver, Colorado, where there are none.

In other words, how soon will these areas become gold mines, and to what extent? There is one rule of thumb that can be used, but that would only indicate probabilities. If a city is a good market area; if it is on the coaxial cable, or relay network, or within one microwave link of the cable; if it has only one applicant for permission to construct and operate the station, then, according to our market research experts, it has a pretty good chance of getting on the air in the next two years. If any one of these items is missing, it may be five years.

If five years is a little too long in your way of thinking, let's take a look at what we probably will have two years after the end of the freeze.

There are now 107 vhf stations operating. At the end of two years we can expect to see 141 more vhf stations on the air for a total of 248 vhf transmitters. There are now no uhf stations operating, with the exception of some experimental transmitters like our own at Electronics Park. At the end of two years after the freeze is lifted, we can expect a minimum of 36 uhf stations to be on the air.

At the end of five years I think we can look forward to a minimum of 343 vhf stations and 166 uhf stations or more than 500 stations in the United States. This doesn't agree with many predictions ranging as high as 1,500 transmitters in five years, and admittedly the estimates are conservative. If materials, including construction materials, should be in free supply, then these estimates could be quite low.

It has been said that any area large enough to support a daily newspaper can support a television station. The proposed allocation plan would place several transmitters in areas that have only one newspaper.

In cities not within any reception area today, and where establishing a station provides a new service to the community, the building up of the audience in the area will, of course, follow the pattern established in other cities. The audience build-up may be sharper and quicker because people nationwide are pretty much "preconditioned" to the advantages of television.

These forecasts may be considered to be pessimistic by some. On the contrary, they are realistic, not based alone on what industry members think can be produced, as many surveys are. Perhaps the other side of the picture may be a little happier. We also believe there will be 44.5 million wired homes in 1955, or 14 per cent more than in 1950. We believe that by the end of 1955, nearly 80 per cent of these homes, or approximately 35 and one half million families, will be within range of a television station. And, there is a possibility that nine out of ten of these 35.5 million families will own at least one television receiver.

In addition, obsolescence will be operating, occasioned by technological and other factors. For example, there are now in use about 5,000,000 sets of the 10- and 12-inch variety. They are ripe for replacement.

What does all this mean to the distributors? The best figures available indicate electronic parts and components distributors did a gross business, not including net sales, of approximately 320 million dollars in 1950. In 1951, this will jump to 475 million dollars. But by 1955, distributors' gross business on an annual basis is expected to be in the neighborhood of one billion dollars, or more than triple the 1950 figure.

This discussion should not be closed without some mention of industrial electronics. It is hard to look at the electronics picture without being blinded by the reflected glare of television. Manufacturers see the untapped market for receivers. Distributors consider the untapped market for components and parts. Advertisers think of the tremendous impact upon the public. Educators see television as the instrument for raising the intellectual level of the entire country. Propagandists see TV as the most effective instrument ever devised for influencing the lives and opinions of the masses.

Television may be many things to many people, in addition to being the most dazzling development of present-day electronic science. But when some historian of science, a few centuries from now, weighs the various developments in the light of their contributions to the advancement of human society, television may have had the greatest impact, yet industrial electronics may far outshadow TV in its effect upon the standard of living and way of life.

I would like to quote two brief statements. The first is from an article by Harold G. Moulton, president of the Brookings Institute. He said, "without continuing and progressive increases in productive efficiency we cannot hope to realize our basic national objectives—military security, relatively stable prices, greater social security, and higher standards of living."

The second quotation is from an article on Economic Affairs written by Lawrence Fertig for the *New York World-Telegram and Sun*. "First of all," he says, "it is important to note what is the cause of mounting production for each man-hour of work. Basically, of course, it is more high-speed tools of production—the man with the bulldozer produces more than the man with the shovel. During the past fifty years investment in tools per worker increased about $2,000 to approximately $12,000 and, as a result, real wages have increased more than threefold. But more machines and increased horsepower are only part of the story. Important also are new technical developments, greater skill in management and more efficient plant operation. Then, too, there is the great increase in working capital which permits corporations to carry the large inventories necessary for efficient production and the free flow of materials in finished goods."

What have these quotations to do with television? Little perhaps with television, but a great deal with electronics. If we are to advance not only our standard of living but the general level of our civilization we must maintain continuing and progressive increases in productive efficiency.

This is not a one-man job, nor is success dependent upon any one factor. Certainly many things can be done to increase our national productivity, and neither more efficient management nor better labor-management relations are at the bottom of the list. But the most important is the continual strengthening of the arm of the worker by creating machines that place more and more horsepower at his command and that perform the repetitive tasks of manufacturing, assembling, and inspection. This electronics can do through the magic of its ability to perform amazingly co-ordinated feats of control, analysis, and memory.

There is no freeze on human ability, even though there does seem, at some times and in certain circles, a freeze on our willingness to apply that ability intelligently. Frozen human resources can be thawed by applying the warmth of understanding, and of intelligence, to the problems we face in our daily lives.

Unless we can match the advances we are making in electronics with an equal advance in the human sciences we are not making real progress. Contributions to better living, health, and comfort can be stolen away through human greed, moral laxity, and intolerance. Against these thieves of the fruits of human endeavor we must wage an unceasing battle, whether it be at home, in business, in government, or in international affairs.

A Single-Ended Push-Pull Audio Amplifier*

ARNOLD PETERSON†, SENIOR MEMBER, IRE AND DONALD B. SINCLAIR†, FELLOW, IRE

This paper was procured, and is here presented, through the co-operation of the IRE Professional Group on Audio—*The Editor*

***Summary*—An amplifier circuit for push-pull operation of two output tubes that provides a direct output to a grounded load is described. This circuit avoids any necessity for close magnetic coupling between halves of a split primary of an output transformer; it does not use any interstage coupling transformer; and its simplifies the application of feedback from the output stage to preceding single-ended stages. Methods for using this circuit with triode and beam-power output tubes are given, and the ultimate possibility of eliminating the output transformer for driving a loudspeaker is discussed.**

* Decimal classification: R363.222. Original manuscript received by the Institute, July 30, 1951. A condensed version of this paper was presented at the 1951 IRE National Convention, New York, N. Y., March 22, 1951, and was published and distributed to its members by the IRE Professional Group on Audio.

† General Radio Co., Cambridge, Mass

Introduction

Among the various goals set out for the communications engineer, surely one of the most eagerly sought since the discovery of electronic amplification has been faithful reproduction, after the amplification process, of the input signal. Electronic devices are notoriously nonlinear, and nonlinearity has been the constant enemy of faithful reproduction. The two most potent weapons so far developed to combat nonlinearity in power amplifiers have been push-pull operation and negative feedback.[1] Push-pull operation,

[1] H. S. Black, "Stabilized feedback amplifiers," *Bell Sys. Tech. Jour.*, vol. 13, pp. 1–18; January, 1934.

by making the input-output relation symmetrical about the operating point, eliminates harmonics and combination frequencies produced by even-order distortion. Feedback improves faithfulness of reproduction by feeding a portion of the output wave back to the input in such a manner as to reduce the effects of nonlinearity.

A combination of the two systems has been found, generally, to produce an amplifier of the highest performance. Various difficulties, however, have plagued designers, and over the years continuous development has been carried on to overcome them. One of the most serious problems has been the tendency of even the best amplifiers to develop increasing distortion at the highest frequencies. This increase in distortion has been caused, in many cases, by phase shift which reduces the effectiveness of the negative feedback. General improvements in frequency characteristic and in phase-shift compensation have been found effective in reducing trouble from this source to manageable proportions.

Another serious source of trouble in high-efficiency amplifiers has been emphasized recently. This trouble arises from imperfections of the output transformer necessary to couple the high-impedance balanced output of a push-pull amplifier to a low-impedance single-ended load. The most important imperfection has been found to be insufficient coupling between the two halves of the primary in the plate circuit of the push-pull tubes. At the higher audio frequencies, leakage reactance arising from lack of complete coupling between these windings introduces distortion that may be thought of as switching transients, particularly in class-B operation.[2] In order to eliminate these transients, considerable effort has gone into methods of improving the coupling coefficient between the primary halves.

An ingenious solution has been worked out by McIntosh and Gow.[3] They use a bifilarly wound primary and a circuit that overcomes the problem of capacitance between windings by combined excitation of the primary halves from cathode and plate feed. Through the use of this specialized transformer, one can obtain extremely high coupling coefficients and concomitant low distortion at high frequencies.

Another solution, outlined in this paper, consists of entirely eliminating primary-to-primary leakage reactance by using the same primary for both tubes, thereby obtaining the equivalent of unity coupling. Other advantages accrue from the circuit to be described, not the least of which is the fact that no special components are required, the output transformer becoming basically a device for impedance matching and requiring no special characteristics other than adequate frequency characteristic and power handling capacity.

[2] A. Pen-Tung Sah, "Quasi transients in class-B audio-frequency push-pull amplifiers," Proc. I.R.E., vol. 24, pp. 1522–1541; November, 1936.

[3] F. H. McIntosh and G. J. Gow, "Description and analysis of a new 50-watt amplifier circuit," *Audio Eng.*, vol. 33, pp. 9–11; December, 1949.

The Output System

The basic plan of the output system is shown in Fig. 1, where two triode-amplifier stages are shown. The lower one is a simple amplifier supplying a resistance load in the plate circuit, and the upper one is similar except

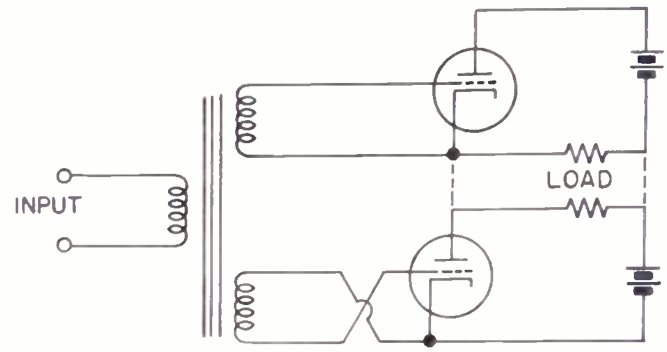

Fig. 1—Circuit to illustrate principle of operation of the push-pull output system. The grids are driven out of phase, and the ac load currents add while the dc load currents subtract.

that the load and the dc plate supply have been interchanged. It is important to notice that this amplifier is not a cathode follower, since the ac grid voltage is applied between the grid and cathode. If the two tubes are identical in characteristics and the supply voltages and loads are the same, the dc plate currents in the two loads will be identical. Then, if the connections shown by the dotted lines are made, the two currents will cancel because they are in opposite directions. When equal ac signals are applied to the two circuits, the ac components in the loads are equal. These two components would also cancel, when the connections are made, if the grid driving voltages were in phase. But, with oppositely phased voltages on the grids, the ac plate currents add in the load so that the tubes are in series for the dc plate supply and in parallel for ac signals.[4] However, this first circuit has the serious disadvantage of requiring a driving transformer with its associated expense and difficulties in maintaining proper balance at high frequencies.

Phase-Inverter Driver

In order to avoid a driving transformer, it is necessary to devise a phase-inverter stage that will supply the voltages in the correct phase and at the proper electrodes. One such phase inverter is shown in Fig. 2. This driver stage receives its plate-supply voltage from the midpoint of the two series-connected output stages. It has equal resistors in the plate and the cathode. Then a change in its plate current, produced by a signal on the grid, will result in equal voltages being developed across these resistors. The voltage in the cathode circuit is developed between the cathode and grid of the lower tube, and an equal and oppositely phased voltage is developed between the cathode and grid of the upper

[4] In connection with this circuit, we should like to note that when this paper was in preparation, our attention was called to the work of R. E. Rawlins, presented before the Los Angeles section of the IRE on December 19, 1944.

tube. It is important to notice that this upper grid is not driven with respect to ground. If it were, the upper tube would act as a cathode follower, and the balance of the two tubes would be destroyed.

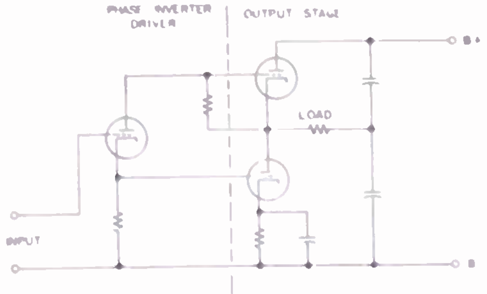

Fig. 2—Method of driving output stage by a phase inverter. Each of the output tubes is driven from grid to cathode.

This driver is shown direct coupled to the ouput stages. This direct coupling is frequently desirable, even though it is not essential except for a dc amplifier. The dc voltage drop across the resistor in the driver plate develops a negative bias for the upper output tube. The voltage drop in the lower resistor is in the wrong direction for supplying negative bias. In the circuit shown, the proper bias is obtained by the voltage drop in the cathode resistor of the lower output tube, which supplies a voltage equal to twice the bias required for a single tube.

Driving Voice Coil Directly

The amplifier circuit shown here uses no transformers at the output or between stages for class-A or class-AB operation of push-pull triodes. By using some of the newer low-impedance tubes, the optimum output load resistance can be made quite low because the tubes drive the load in parallel. As an extreme example, the use of the two halves of a single type 6AS7-G would lead to an optimum load impedance of about 280 ohms. While this value is still far from the usual 8- or 16-ohm impedance of a loudspeaker voice coil, voice coils can be built with appreciably higher impedances so that they can be driven directly without a matching transformer. To a first approximation, the voice-coil impedance can be increased without affecting the loudspeaker efficiency. As a practical matter, the limit of increase is determined by the smallest aluminum or copper wire that can be handled in a production set up and the maximum allowable mass for the voice coil.

For example, one particular standard 12-inch dynamic loudspeaker uses number 33 wire for its 3.2-ohm voice coil. One of these has been rewound for 100 ohms with number 40 wire, and its efficiency is within 1/2 db of the standard one. Another of these has been rewound for 500 ohms with number 44 wire.[5] While this latter wire is too small in diameter to be readily handled in production, the number 40 wire is entirely reasonable.

[5] We are indebted to Dr. Harry F. Olson of the RCA Laboratories, Princeton, New Jersey, for the information on this standard, 12-inch loudspeaker and the higher impedance versions.

The loudspeaker cited does not have an unusually heavy voice coil, and therefore it seems reasonable that the voice coils of moderate-size to large loudspeakers can be wound to the level required in order to dispense with a matching transformer. Furthermore, it is entirely possible that a suitable ring-armature drive[6] for small speakers can be developed. Then there should be no difficulty in winding this type for an impedance of almost any desired level.

In order to determine to what extent one should go to eliminate coupling transformers, it is useful to review some of their characteristics. Audio power transformers are generally expensive, heavy, and bulky. They usually limit the low-frequency capabilities of an amplifier by increasing the distortion and reducing the output at low frequencies. Furthermore, because the output transformers are only moderately efficient, they absorb an appreciable fraction of the available power. These disadvantages are sufficiently important that considerable effort toward eliminating coupling transformers is justified.

Circuit Limitations and Requirements

Two characteristics of the circuit of Fig. 2 limit its range of operation. One is the inherent negative feedback, and the other is the effect of capacitance from the plate of the driver stage to ground. Since the plate voltage of the driver tube is taken from the output, the output voltage is fed back to this stage. This feedback is negative, and it can be considered useful for reducing distortion. However, when it is desired to avoid the associated loss in gain, the feedback can be minimized by using a pentode driver.

The impedance level at the plate of the driver stage is, in effect, multiplied by the gain of the output stage. That is, the frequency characteristic of the drive for the upper tube is determined by the RC combination of the total capacitance from the plate to ground and the plate resistor multiplied in value by one more than the gain of the output stage. For the audio-frequency range, the resulting drop in output can be kept very small. But, if an attempt is made to use an amplifier of this type over the video range, this effect will be serious.

The load is shown in Fig. 2 connected in a balanced fashion to the output stages to make it easier to see the principle of operation. Actually, it is usually more useful to have one end of the load grounded to the negative side of the plate supply and to feed the other end from the midpoint through a series blocking capacitor.

When the output tubes are to be operated over the wide ranges required for full output in class-AB_1 operation, these circuits must be designed, just as any other, to meet the requirements of that operation. For example, the circuit should be arranged to provide constant bias for the output tubes even with large plate-current swings. Another requirement is that adequate driving voltage must be available from the phase inverter. In

[6] E. E. Mott and R. C. Miner, "The ring armature telephone receiver," *Bell Sys. Tech. Jour.*, vol. 30, pp. 110–140; January, 1951.

the simple connection of Fig. 2, the plate voltage for the driver is only one-half the total plate voltage, and the resulting output from the phase inverter is usually inadequate for class-AB_1 operation. By using a resistance-capacitance coupling for the driver and by taking advantage of the bias supply as added plate voltage for the driver, this output can be increased. A pentode driver stage is also a suitable alternative in some cases. When an output matching transformer is used, the available plate swing from the driver can also be increased by a connection of a form shown later in Fig. 3.

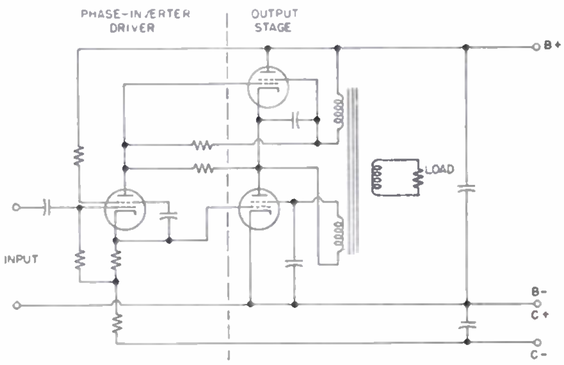

Fig. 3—Method of supplying proper screen voltages for beam-power tubes. The dc screen currents flow through the two windings in the opposite sense so that there is no net dc flux from the screen currents.

There additional current is supplied to the phase-inverter stage by the resistor connected from the one transformer primary to the plate of the phase inverter.

One objection that might be raised to the basic series circuit is that the required plate voltage for the output stage is twice normal. The development of the high-voltage selenium rectifier, with voltage-doubler circuits, has made this point less objectionable at the present time. Another factor is the development of the low-impedance or high-perveance tubes for television use. Their use in this circuit permits the production of relatively high powers with moderate total plate voltage.

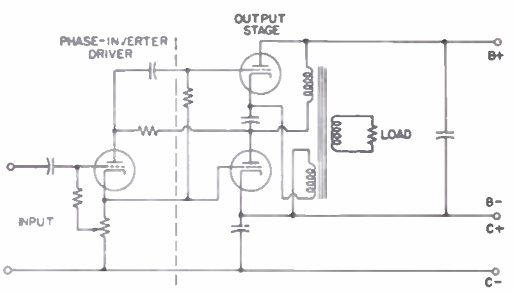

Fig. 4—Method of using the load matching transformer to put the output tubes in parallel for the dc supply.

If a transformer is to be used in the output as a matching device, it is possible to set up the single-ended output circuit with normal plate voltage in several ways. One method is shown in Fig. 4. Here the plate currents of the two tubes flow through the two halves of the primary winding, and the two halves are connected in parallel for signal currents by the by-pass capacitors. It is important to notice here that the driving voltages for the two output tubes are again developed between cathode and grid in each case. The capacitor in the cathode-to-plate connection must be large enough to avoid a degenerative effect in the cathode circuit.

Amplifiers Using Beam-Power Tubes

These amplifiers show triodes in the output stages. But many designers of audio amplifiers are interested in using beam-power tubes with their possibilities of high gain and high efficiency. It is obvious that the proper connections for the screen voltages can readily be made in the circuit of Fig. 4, but the connections for the basic series circuit are not so simple.

The main problem in using these beam tubes is in the method of supplying the proper voltage for the screen of the upper tube. The dc voltage of the screen is normally near that of the plate, and the screen should be at cathode potential for the signal voltage. If the screen of the upper tube is supplied through a dropping resistor from the plate supply, then the by-pass to the cathode puts the dropping resistor in parallel with the load, and some signal power is lost. In some cases this loss in power can be made small. In other applications, the voltage for the upper screen can be fed through the load so that no signal power is lost.

Since loudspeakers with high-impedance voice coils are not available at present, an output transformer is still needed for driving a speaker. How this transformer can be used for supplying the screen voltages is shown in Fig. 3. The primary is in two sections. One section is connected from the plate supply to the upper screen, which is by-passed to its cathode at the midpoint where the plate and cathode of the two output tubes are connected together. The other section is connected from the screen of the lower tube, which is by-passed to ground, to the midpoint. The dc screen currents flow through the windings in the opposite sense, so that there is no net dc flux from the screen currents in the windings.

By following the transformer connections, it can be seen that the two sections of the primary are connected in parallel, for signal voltages, by the by-pass capacitors. Because of this parallel connection, the two halves of a standard push-pull transformer can be used to obtain the required impedance level for this single-ended circuit. Furthermore, because these windings are connected in parallel by capacitors, the circuit does not depend on close magnetic coupling between the two sections of the primary. This point is important, since in class-AB operation the usual push-pull connection does have serious switching transients unless the coupling between the two halves of the primary is very good. In order to verify this point experimentally, the circuit shown was set up, using a type 6AK6 pentode to drive a pair of type 6L6 beam-power tubes. The operation was with fixed bias as shown, class AB_1, and with no feedback. An output of 50 watts was obtained with a plate efficiency of 59 per cent. The output waveform was independent of the magnetic coupling between the halves of the primary. To illustrate this independence,

Fig. 5 shows a photograph of some pertinent waveforms. For tnis case, two separate chokes were used in place of the transformer so that the magnetic coupling was essentially zero. The operating frequency shown here is 20 kc, and the power level is 50 watts. The upper trace is the output voltage and the lower trace is the cathode current in the lower tube. It is clear that current is flowing in each tube for only slightly longer than one-half cycle, and there is no sign of a switching transient. Thus the general behavior of the circuit is verified.

This output of 50 watts was obtained within the plate dissipation ratings of the Type 6L6 of 38 watts for two tubes. But the screen ratings were exceeded to obtain this output with class-AB_1 operation. However, this output can be obtained within the ICAS ratings of the type 1614, the transmitting version of the type 6L6. Using two type 1614's with two cascaded stages of type 6AK6's in this circuit and with negative feedback, we have obtained at 1 kc less than 0.1 per cent harmonic distortion for all output levels up to 50 watts. To obtain this low level of distortion, careful adjustment of operating conditions and feedback of 25 to 30 db are necessary, and the method of obtaining stable operation with this feedback will now be discussed.

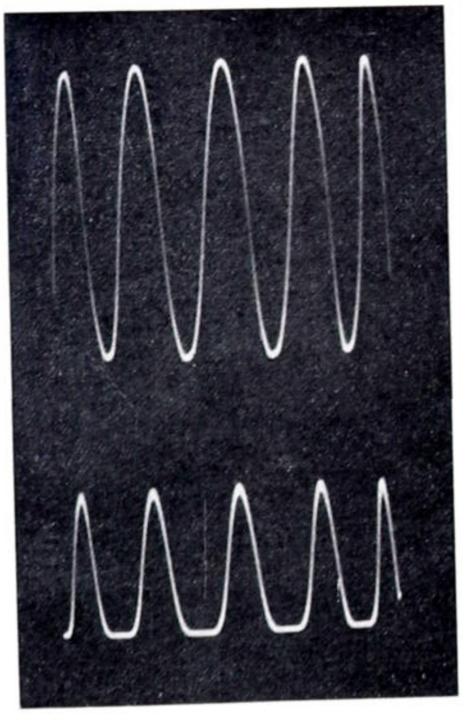

Fig. 5—Upper trace is the wave form of the output voltage for the circuit of Fig. 4, and the lower trace is the cathode current in the lower tube. Both traces were obtained at a 50-watt power level and at 20 kc.

Use of Negative Feedback

One method for applying negative feedback to an amplifier of this type is shown in Fig. 6. Since the output is single ended, the feedback can be made directly from the midpoint of the output stage to a preceding single-ended stage. In the three-stage amplifier shown, the feedback is applied to the cathode of the first stage. Because of the direct coupling of the phase-inverter driver, there is little danger of low-frequency motorboating with feedback. Furthermore, since the feedback does not have to be taken from the secondary of the output transformer, there is less danger than usual of

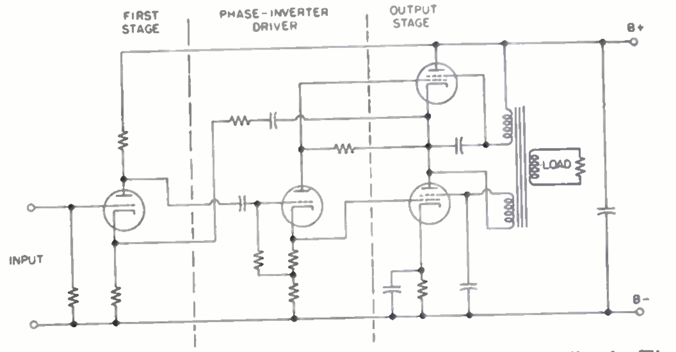

Fig. 6—Circuit to illustrate one method of applying feedback. The feedback is taken from the junction of the two output tubes to the cathode of the first stage.

high-frequency oscillations. Or, expressed differently, greater amounts of negative feedback can be used, when applied as shown, with stable operation, than can be used with feedback from the secondary of the usual output transformer.

The usual feedback from the secondary tends to correct for the drop in response at the high-frequency end by the feedback system. This feedback forces the output system to operate at higher levels than normal at high frequencies to produce the uniform output desired. Unless the transformer is very good, with feedback from the secondary, the result may be high distortion at high frequencies. This distortion is usually exhibited as intermodulation of high-frequency signals, and serious distortion of this type is more easily avoided with feedback from the primary as shown here.

The feedback shown in this circuit puts the secondary of the transformer outside the feedback loop. Then corrective networks can be used, if necessary, at the secondary without introducing serious phase shift in the feedback loop.

Conclusion

The circuits shown here should be useful in many applications. The series circuit using the phase-inverter driver has the advantage of requiring no coupling transformers for obtaining push-pull operation. The circuits have other advantages, principally for amplifiers that must have very low distortion. In addition, the developments described should serve to show possible new lines of approach for improving audio reproduction. These further developments might include high-impedance loudspeakers, loudspeakers of different fundamental design, low-impedance twin output tubes with 117-volt heaters, and the elimination or simplification of output transformers.

Acknowledgment

We appreciate the helpful suggestions made by William F. Byers and Carlton A. Woodward, Jr. in the course of this development, and acknowledge particularly Mr. Woodward's help in the experimental work.

The Binac*

A. A. AUERBACH‡, ASSOCIATE, IRE, J. P. ECKERT, JR.†, ASSOCIATE, IRE, R. F. SHAW‡, SENIOR MEMBER, IRE, J. R. WEINER†, ASSOCIATE, IRE, AND L. D. WILSON†, MEMBER, IRE

Summary—**The Binac was the first high-speed electronic digital computer of its type to be completed. It consists of a main computing section, input-output equipment, and a mercury delay-line memory of 512-word capacity. Although designed for a specific purpose, the Binac is well adapted to any type of general mathematical computation.**

While the number of tubes is comparatively large, the Binac is a combination of a few basic circuits. Extensive use is made of crystal diodes in switching or gating circuits. These circuits fall into three basic classifications: function tables or diode matrices, used for converting coded groups of signals such as instructions into corresponding but differently coded groups of signals to operate switching circuits; switching gates, which control the flow of information in accordance with signals received from function tables or similar sources; and reshaping gates, which, as their name implies, reshape signals that have become distorted in electric delay lines or other circuits. The use of reshaping gates, together with suitable shaping networks, makes possible the use of a "pulse envelope" or "non-return-to-zero" system of representing information, thus effectively doubling the bandwidth of circuits.

Crystal gates are used with electric delay lines to form a serial binary adder. A one-word register is formed by combining an electric delay line with appropriate reshaping gates, input and output gates, and amplifiers, all connected to form a closed loop. Insertion of the adder in the loop results in an accumulator. By temporarily inserting or removing a one-pulse delay in the loop, information can be made to precess, which is equivalent to multiplication by positive or negative powers of two.

Input data are supplied to the memory from a keyboard or magnetic tape through the use of a synchronizer which reconciles the randomly timed input signals with the accurately timed internal memory. The same synchronizer is also used for transferring data from the memory to magnetic tape, or to paper by means of an electric typewriter.

Extensive tests have demonstrated the usefulness of the Binac in the solution of mathematical problems. Some striking results have been obtained in connection with the solution of Poisson's equation for various boundary conditions. An example is given of the coding for a square-root routine (see Table I).

I. Introduction

THE BINAC, first computer of its type to be completed successfully in the United States and successor, historically, to the electronic numerical integrator and computer (ENIAC), is a high-speed, automatic digital computer, operating in serial fashion on numbers expressed in binary form. The digits occur at a repetition rate of four million per second, considerably faster than any computer yet built. Thus, it may truly be called "high speed." The computer is automatic in the sense that, properly instructed, it will perform a complicated series of computations by itself. This is in contrast to a desk calculator, for instance, which assists the human operator by performing individual elementary operations, but must be separately manipulated for each such operation.

The major instructions which the Binac can follow are the four basic arithmetic operations, instructions involving the moving of data from one storage register to another, and the so-called "conditional and unconditional transfers of control" which contribute largely to the automaton characteristic of the computer. Normally, the Binac follows instructions in their originally given sequence. A transfer of control instruction, however, may tell the computer to proceed to another instruction that does not follow sequentially (i.e., either

TABLE I

Square-Root Routine for Binac

000	25000		Skip
		U 024	Transfer to 024 to start computation
001 to	023 inclusive		μ's (radicands)
024	*A* (001)		
		H 057	μ to storage register 057
025	23000		Shift right (divide by 2)
		A 046	$Z_i = 1/2\ (\mu+1)$
026	*C* 055		Z_i to storage register 055; clear *A*
		25000	Skip
027	*A* 057		μ to *A*
		D 055	μ/Z_i
030	*S* 055		$\mu/Z_i - Z_i$
		23000	Shift right (divide by 2)
031	*A* 055		$1/2\ (\mu/Z_i + Z_i) = Z_i+1$
		C 056	Z_i+1 to storage register 056
032	*A* 055		Z_i to *A*
		S 056	$Z_i - Z_i+1$
033	*S* 054		$Z_i - Z_i+1-2^{-14}$
		T 036	Test sign of $Z_i - Z_i+1-2^{-14}$
034	*A* 056		Z_i+1 to *A*
		C 055	Z_i+1 to Z_i
035	25000		Skip
		U 027	Start next iteration
036	*A* 056		$Z_i+1 = \sqrt{\mu}$
		C(755)	$\sqrt{\mu}$ to output
037	*A* 024		Instruction in 024 to *A* for modification
		A 052	Modify to pick up next μ in series
040	*C* 024		Modified instruction back to 024
		A 036	
041	*A* 053		Modification of instruction in 036
		H 036	
042	*S* 051		Subtract 051 from 036
		T 024	Test
043	*A* 047		Reset 024 to original value
		C 024	
044	*A* 050		Reset 036 to original value
		C 036	
045	25000		Skip
		U 754	Transfer control to 754 to stop process
046	40000	00000	1/2
047	*A* 001	*H* 057	Original setting of 024
050	*A* 056	*C* 755	Original setting of 036
051	*A* 056	*A* 000	Test word
052	00001	00000	2^{-16}
053	00000	00001	2^{-30}
054	00002	00000	2^{-14}
055			Storage register for Z_i
056			Storage register for Z_i+1
057			Storage register for μ
754	25000		Skip
		01000	Stop
755 to	777, inclusive		Storage for computed roots

* Decimal classification: 621.375.2. Original manuscript received by the Institute, December 15, 1950; revised manuscript received July 16, 1951.

† Eckert-Mauchly Computer Corp., Division of Remington Rand, Inc., 3747 Ridge Ave., Philadelphia 32, Pa.

‡ Formerly with the Eckert-Mauchly Computer Corp. Now with the Electronic Computer Corp., 265 Butler St., Brooklyn 16, N. Y.

an instruction that occurred previously in the sequence, or one that lies somewhere ahead). An instruction which insists that this be done, unconditionally, is known as an "unconditional transfer." On the other hand, there may be a "conditional transfer" of control, whereupon *if* an equality condition is met, and only if it is met, will the computer deviate from the original sequence of instructions.

By virtue of the first transfer possibility, the Binac is capable of circling around (i.e., repeating a sequence of instructions or calculations). By virtue of its ability to transfer control conditionally, it can decide when a particular calculation is complete, and proceed to a new set of instructions. In this manner, by means of a "built-in" logic and power of decision, the Binac will perform a computation automatically.

The memory is the Binac component which stores the sequence of instructions as well as the numerical data that constitute the raw material of a given calculation, and also stores intermediate results and final data. As distinct from this, there is the computer proper, which, utilizing the instructions called from the memory, operates upon the numerical data. The device initially used to insert both data and instructions into the memory, as well as to inform the operator of the results of a calculation by printing them in visible form, is known as the "converter."

The Binac actually consists of one converter, or input-output unit, *two* computing units, and *two* memories. The memories are filled with identical programs (instructions and data), and the two units are run together and checked against each other. Any difference (which of course indicates an error) between information being handled by the duplicate units stops operation immediately. The existence within one computer of identical parallel units greatly simplifies the problem of finding the source of error, and also serves as an almost perfect checking device on the operation of the computer because of the extreme improbability of identical faults being present simultaneously in both units. (This has been proved true in practice. Many self-checking problems were run through the Binac, and identical faults never appeared.)

Although built to solve a specific problem, the Binac contains all the necessary elements for solving a great variety of problems. This will be treated further in Section IV of this paper.

II. System Considerations

A. Representation of Information

1. Electrical Representation of Numerical Data

As mentioned earlier in the paper, the Binac utilizes the binary system of notation rather than the more familiar decimal system. One advantage of the binary system is its use of only two states: 0, 1; +, −; on, off; and so on. This system is particularly well adapted to the representation of information by the use of relays, flip-flops, binary counters, and other circuits having only two stable states. To this list may be added vacuum tubes, in general, which are either fully conducting or completely cut off. This, of course, reduces the problem of amplitude discrimination to an absolute minimum. A "one" is then represented in the computer by the presence of a pulse at some instant, the setting of a flip-flop or counter to the "one" position, or possibly by the energizing of a relay.

2. Word Structure

A "word" is the basic unit for both instructions (or orders) and numerical quantities. Words are represented in the Binac as groups of pulses that occur at a basic repetition rate of four million per second. The pulse width is, therefore, one quarter of a μsec. A word consists of 42 pulse positions; the time required for its transmission (10.5 μsec) is known as a minor cycle. Thirty-one pulse positions contain information; the others, referred to collectively as the "space between words" (although they should be considered a part of the word), provide time for switching between the significant part of one word and that of the next.

For convenient reference, the pulse positions of a word are numbered from $p0$ to $p41$, inclusive. Positions $p0$ to $p6$, inclusive, are always unfilled.

The digits of a number, as shown in Fig. 1, are labeled $p7$ to $p36$, inclusive. The $p7$ digit is least significant, and represents the binary quantity 2^{-30}. The $p36$ digit

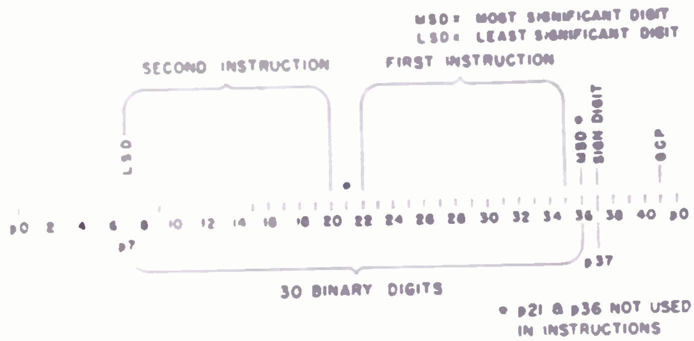

Fig. 1—Word structure.

is most significant, and represents 2^{-1}, or $\frac{1}{2}$; similarly, the $p35$ pulse represents $\frac{1}{4}$, and so on. The least significant digit occurs first in time so that Fig. 1 indicates a number as it would appear on an oscilloscope, which is contrary to the usual positional notation used in mathematics. The $p37$ pulse indicates the sign of the number. Presence of a pulse in that position indicates that the number is negative; conversely, its absence indicates that the number is positive. The $p41$ pulse is referred to as a "gain control pulse." It has no numerical significance, existing only to stabilize the gain of the memory circuits (see Section III C4). Thus, nothing of significance exists between $p37$ and $p7$, and this area is the "space between words" referred to above.

Negative numbers exist in the Binac as complements with respect to two; in this connection, the $p37$ position may be considered as corresponding to 2^0. It follows, then, that negative numbers will have a 1 in the $p37$ position. To represent $-\frac{5}{8}$, the sum $(2-\frac{5}{8})$ or $1\frac{3}{8}$ would be formed. The 1 exists to the left of the binary point and corresponds to a $p37$; $\frac{3}{8}$ is simply $\frac{1}{4}$ plus $\frac{1}{8}$ (i.e., a $p35$ and a $p34$). Thus, $-\frac{5}{8}$ could be written as 1.011.

The structure of instructions is shown in Fig. 1. Two general classes of instructions exist. There are those which involve transferring a word to or from the memory, and those which do not. The instruction itself may be specified by, at most, 5 binary digits. *If* the instruction involves a memory transfer, a memory position is associated with it. Since the memory holds 512 or 2^9 words (in positions 0 to 511), 9 pulse positions are required to specify that memory position. Thus, a single instruction may consist of 14 pulse positions. On the other hand, if the instruction does not involve the memory, it will consist of, at most, 5 pulses, the other 9 positions being unfilled. The Binac uses only twenty of the possible thirty-two instructions that could be formed from the 5 digits available, and these combinations were chosen so as to minimize the number of pulses in the order group.

An instruction, then, is completely specified by, at most, a 14-pulse group. On the other hand, 31 pulse positions are available in a word. For this reason, instructions are paired, controls being arranged to execute the first and then the second instruction in the order in which they are typed.

Since instructions are stored in the memory together with numbers, the necessary gain control pulse must also be included in the $p41$ position. Since only 14 digits, at most, specify an instruction, they are separated slightly, with the first instruction occurring from $p22$ to $p35$, inclusive, the second from $p7$ to $p20$, inclusive.

3. *Basic Computer Cycle*

Starting with the existence of two instructions within one word, it follows directly that one step of the computer cycle must be the execution of the first instruction and the following cycle the execution of the second instruction. These cycles are referred to as γ and δ. On the other hand, since the instructions which have been stored in the memory are executed sequentially by the Binac, there are the further requirements: (a) that the pairs of instructions be called from the memory; and (b) that a count be kept, the numerical position in the sequence to be increased by one for each computer cycle.

Thus, on the alpha (α) cycle, the numerical position of the pair of instructions *to be selected* from the memory is determined. On beta (β), the selected word is called from the memory, while the number in the memory-position counter or "control counter" increases by one. At the end of β, the first instruction in the word sets up the controls which permit its execution. On gamma (γ), this first instruction is executed, while the second instruction of the pair is set up at the end of γ. On delta (δ), this second instruction is executed, the next number in the sequence being set up at the end of δ in preparation for the execution of the next alpha cycle.

This process may be modified when an instruction calls for an executed "transfer of control," conditional or unconditional. Its effect is to change the number in the memory sequence to the memory position indicated by the transfer instruction. From that point on, however, the instructions will again be taken from the memory sequentially, unless again interrupted by another transfer of control instruction. The over-all effect of this ability to "transfer control" is to add greater flexibility to the Binac, as already discussed.

B. *Arithmetic Processes*[1]

1. *Addition and Subtraction*

The basic operation of binary addition utilizes the following rather simple rules:

Addends	*Sum*	*Carry*
0 and 0	0	0
0 and 1	1	0
1 and 1	0	1

In the Binac adder, the carry is fed back as an additional adder input; thus the rule is modified as follows:

Addends	*Sum*	*Carry*
0, 0, and 0	0	0
0, 0, and 1	1	0
0, 1, and 1	0	1
1, 1, and 1	1	1

As previously stated, negative numbers are represented as complements with respect to 2. To form the complement of a number, it suffices to replace its zeros by ones, and its ones by zeros, and to add a unit in the least significant position. (This is demonstrated in the appendix.)

The Binac must, of course, be capable of adding both positive and negative numbers (the latter in complement form) whose absolute value lies in the range between 0 and 1. If digits that may carry beyond the sign position are disregarded, both positive and negative numbers can be treated in the same manner. The accumulator is designed to do precisely this, carries beyond the sign digit being eliminated at the delete gate in the accumulator (A). For proof of the validity of this process, see the appendix.

2. *Multiplication*

Any multiplication is basically a series of additions separated by shifts. Multiplication in the binary system

[1] R. F. Shaw, "Arithmetic operations in a binary computer," *Rev. Sci. Instr.*, vol. 21, pp. 687–693; August, 1950.

is somewhat simplified by the fact that the multiplier digit can be only 0 or 1. Thus, additions and shifts alternate. The basic multiplication process then consists of examining successively the digits of the multiplier, starting with the least significant; of adding the multiplicand into the partial product if the digit is one; and of adding 0 if the digit is zero. After each such addition but the last (corresponding to the sign digit), the multiplicand must be added into a position more significant by one digit. This can be done by shifting the multiplicand left or the partial product right. Actually, the latter course is taken.

Since the accumulator capacity is limited to one word, this implies that of the 60 digits which would result from the multiplication of two 30-digit binary numbers, 30 digits are lost. Again, the delete gate serves the function of removing these 30 least significant digits.

Since the computer must be capable of forming correct products regardless of sign, the multiplication process must be generalized to include the cases where one or both factors are in complement form. It can be shown that two relatively simple correction steps will accomplish this; if either factor is negative, the complement of the other must be added to the result. For reasons which will become clear later (see discussion of arithmetic circuits, Section III B 4 a), the multiplier is lost during the building up of the product. The correction for a negative multiplicand is, therefore, made piecemeal as the product is built up, while the correction for a negative multiplier is made by adding the complement of the multiplicand to the product.

3. *Division*

To perform a division, the Binac utilizes a variation of the familiar nonrestoring method, which can be shown to be valid regardless of the signs of the operands. The method basically consists of comparing the $p37$ (sign) digit of the divisor with that of the remainder (which is the dividend in the case of the first comparison). If these digits are alike, a 1 is placed in the quotient register and the divisor is subtracted from the left-shifted remainder. If they are not alike, a 0 is put in the quotient and the divisor is added to the left-shifted remainder. This procedure is then repeated.

The consequence of this scheme is to build up a quotient of the form

$$\sum_{k=1}^{n} 2^{-(k-1)} p_k,$$

where p_k is the quotient digit (0 or 1) and k represents its significance; n, of course, is 30. It can be demonstrated that the true quotient differs from this expression referred to as the "pseudo-quotient" by the amount $(2^{-n}-1)$. Thus, the procedure in division resolves into performing 30 steps as described and making the required correction. 2^{-n} is then 2^{-30}, or a digit in the least significant position. (-1) can be added by simply adding a unit in the most significant, or sign, position since $p37$ acts as -1 in the Binac. This, incidentally, is equivalent to reversing the sign of the pseudo-quotient. As in the other arithmetic processes, any carry beyond the sign position is deleted.

4. *Round-off Procedure*

The procedure adopted for round-off consists of "stuffing" a unit into the least significant (or 2^{-30}) position. That is, this digit is always made 1 by superposition beyond the adder so that no carries can occur.

This method has the advantage of not requiring the retention of the $(n+1)$st digit, which is necessary in some round-off schemes. It yields approximately the same bias as the retention method and no carries. In multiplication, it can be carried out concurrently with the correction step required where the multiplicand is negative. In division, it coincides with part of the general correction required to transform the pseudo-quotient into a true quotient.

C. *Generalized Block Diagram of the Binac*

Sufficient introductory material has been given so that a simplified block diagram of the Binac (Fig. 2) can be presented at this point. The arithmetic units proper

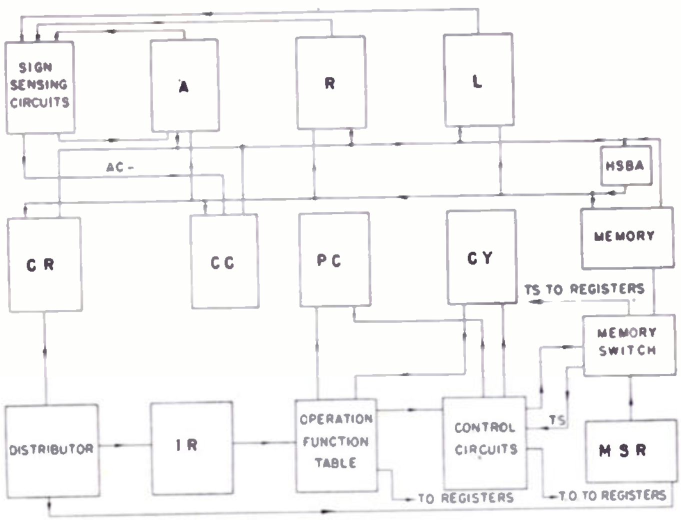

Fig. 2—Simplified block diagram of the Binac.

(by which is meant the blocks most directly involved in addition, multiplication, and the like) are the A, R, and L registers. The A, denoting accumulator, contains an adder, and is used to compute and hold sums, differences, products in multiplication (M), and the dividend (subsequently the remainder) in division (D). The R register holds the multiplier on M and a "pseudo-quotient" on D. (The pseudo-quotient is the quotient preceding a final correction step, the correction being made in A.) The L register contains the multiplicand on M and the divisor on D. The memory (My) is also shown, and it is from this unit that the numbers operated on by the arithmetic registers are taken.

Although the memory has been treated as a single unit thus far, it actually consists of 16 separate "tanks," or channels, each channel capable of holding 32 words. A "memory switch" is used to select a desired position in the memory; it consists of two parts—a "channel selector" to select one of the 16 channels, and a "time selector" to select one of the 32 words in that channel.

The problem of selecting the next word in the memory in a sequence of instructions is handled by the control counter, previously referred to as a memory position counter. Instructions taken from the memory are converted into form suitable for controlling other circuits by means of the control register, the instruction register, the memory switch registers 1 and 2, and the memory switch tank selector, the program counter, a comparator, and the time selector counter. Also involved are the clock, the cycling unit, the cycle counter, and the high-speed bus amplifier.

The clock generates basic timing pulses at a 4-mc/s rate. The clock frequency is set by a temperature-controlled crystal, the entire computer depending on the accuracy of the clock. The cycling unit is essentially a frequency divider, generating pulses at word frequency, that is, every 10.5 μsecs. These pulses occur at various points in the word. Thus, the cycling unit generates $p7$'s, $p37$'s, and the like; these are used as required throughout the computer.

The cycle counter is a two-stage binary counter whose four possible states are used to indicate whether the machine is on alpha, beta, gamma, or delta. It is assumed that a number indicating a particular memory position exists in the control counter. On alpha, this number, indicating the memory position of the next pair of instructions to be called from the memory, is transferred from the control counter to the control register and then to memory switch registers 1 and 2. As has been already indicated, this number will contain, at most, 9 digits or pulse positions. Combinations of the first 4 digits are sufficient to specify the tank called for (since there are only 16 tanks), and combinations of the last 5 digits specify the position within the tank, or time (there being 32 times or positions).

The transfer from control counter to control register is made by way of a bus or signal trunk, hereafter referred to as the "high-speed bus," which includes an amplifier (high-speed bus amplifier). Indeed, all transfers to and from the memory as well as interregister transfers proceed by this path. The existence of such a single transfer path simplifies the design of the Binac considerably. Furthermore, it provides an ideal point at which to check the operation of the two halves of the Binac. Comparison circuits, not shown in the block diagram, are connected to the outputs of the two high-speed bus amplifiers. As has been indicated, any differences between the pulse groups passing this point stop the computer immediately.

Continuing now with the problem of selecting a word from the memory, the contents of the control counter have been transferred through the control register to the memory switch registers 1 and 2. The latter consist simply of 4 and 5 "flip-flop" circuits, respectively. The first 4 digits of the number transferred then set up memory switch register 1. The term "set up" here means that a diode matrix or function table (the tank selector) is activated by memory switch register 1, with the consequence that an output, corresponding to the chosen tank, is selected. The second group of 5 digits sets up memory switch register 2. This similarly delivers an output to the comparator, the output corresponding to the position or time in the tank. With these steps completed, the alpha cycle is finished, the computer then entering into the beta cycle. This is done through the operation of the control circuits upon the cycle counter.

The beta cycle consists mainly of waiting for the selected time to arrive. The time finally selected is determined by the coincidence of the time selector counter and memory switch register 2. The former is a 5-stage continuously running binary counter whose 32 possible states correspond to the 32 words in each tank. Meanwhile, memory switch register 1 also has been delivering its output to the tank selector. Thus, the proper tank and time within that tank are chosen, and the output gate of the chosen tank opens, permitting the word to emerge from the memory. The word then passes through the high-speed bus amplifier. It feeds back through an "input gate" to the same memory position, and proceeds through the control register, setting up the instruction register and memory switch registers 1 and 2, this time in preparation for the gamma cycle. (The word is still retained in the control register, however, this being necessary for the execution of the delta cycle.) The beta cycle is now complete, the selected word having been taken from the memory.

Referring now to Fig. 1, it may be pointed out that the most significant part of the instruction pair (between $p35$ and $p22$) is first used. It is this portion of the word, then, that controls the gamma cycle. Like memory switch registers 1 and 2, the instruction register consists simply of 5 flip-flop circuits, there being one flip-flop for each digit of the instruction. The entire set of flip-flops, 14 in all, is sometimes referred to as the "static register."

On gamma, then, the instruction register sets up in a manner corresponding to the instruction itself. The function table is activated, and it selects, in turn, the various control signals required to execute the order. The control signals go to the registers involved in carrying out the instruction (see Fig. 2). One such signal is necessarily an "instruction-ending" signal, which goes to the main control unit. This signal indicates that all the required steps have been performed in executing the given instruction. The control then cycles the cycle counter from gamma to delta, initiating the next computer cycle.

It will be recalled that, at the conclusion of beta, the word selected from the memory was retained in the control register, the first instruction of the pair being

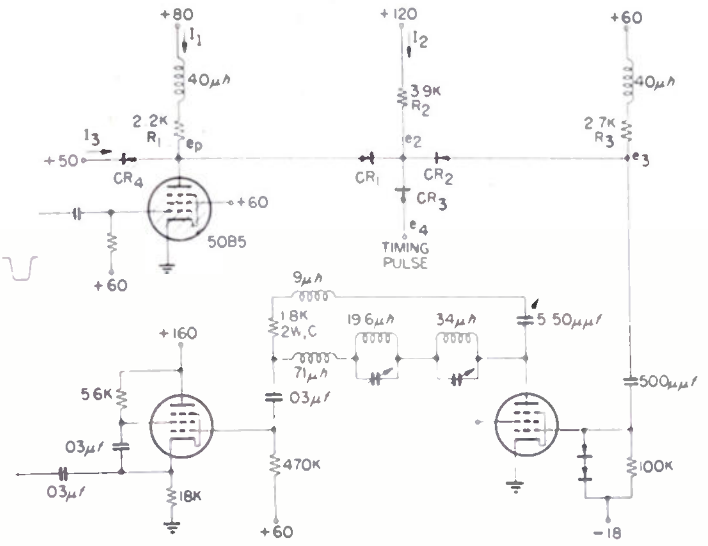

Fig. 3—Pulse former and reshaper (PFR).

executed on gamma. On delta, the second instruction of the pair is executed in exactly the same way that the gamma step was performed. The function table again delivers an instruction-ending signal so that the next alpha cycle is initiated. The basic computer cycle is thus complete. It should be noted that only on γ and δ proper can the contents of the memory be modified. One type of "memory instruction" simply reads out the contents of a memory location, and it is retained there by being fed back through the input gate. Another type, however, inhibits this path, permitting new data to enter that location.

In the course of this discussion of the block diagram, all of the basic units, except the program counter, the synchronizing register, and the converter, have been dealt with briefly. The program counter is important only during multiplication and division. Its function, as will be seen in greater detail later, is to control the four basic steps of M and the three steps of D. The converter and synchronizing register are used to bring original data and instructions into the memory and to remove results of a computation from the memory. Together they serve as the input-output mechanism of the Binac. It may be noted that both a typewriter and a magnetic tape are available as original sources of data as well as devices by which the contents of the memory may be recorded.

III. Engineering Design

A. Basic Circuits

1. *Clock Gate and PF*

The purpose of the timing pulse gate, or "clock gate," and pulse-forming network used at numerous points in the computer is to reshape signals which have degenerated in respect to rise time and signal-to-noise ratio as a result of passing through delay lines and other circuits. The signal to be reshaped is timed (by inserting a small compensating delay, if necessary) so that the timing pulses at the clock gate fall in the center of the pulse-envelope pulses; this adjustment assures maximum gating tolerances. The output of the clock gate will be a signal having a timing pulse wherever there was a pulse-envelope pulse in the original signal. These pulses are amplified by the following tube, whose plate load is a Guillemin line. The latter is adjusted to convert each timing pulse into a flat-topped pulse having a half-amplitude width of approximately 0.25 µsec; the output of the network is, therefore, a pulse-envelope signal equivalent to the original input signal but with improved rise time and signal-to-noise ratio. Since the leading edge of an output signal corresponds to a timing pulse which was, in turn, centered with respect to the input signal, it follows that the network introduces a time delay of approximately half a pulse time. A cathode follower, to minimize capacitive loading of the network, completes the reshaping circuit. The entire circuit of Fig. 3 is represented by a block labeled "pulse former and reshaper" on the block diagrams.

2. *Gates and Buffers*

The gates used for switching purposes in the Binac are, in general, crystal diode gates designed to handle negative signals and to use the circuit in Fig. 4 (a).

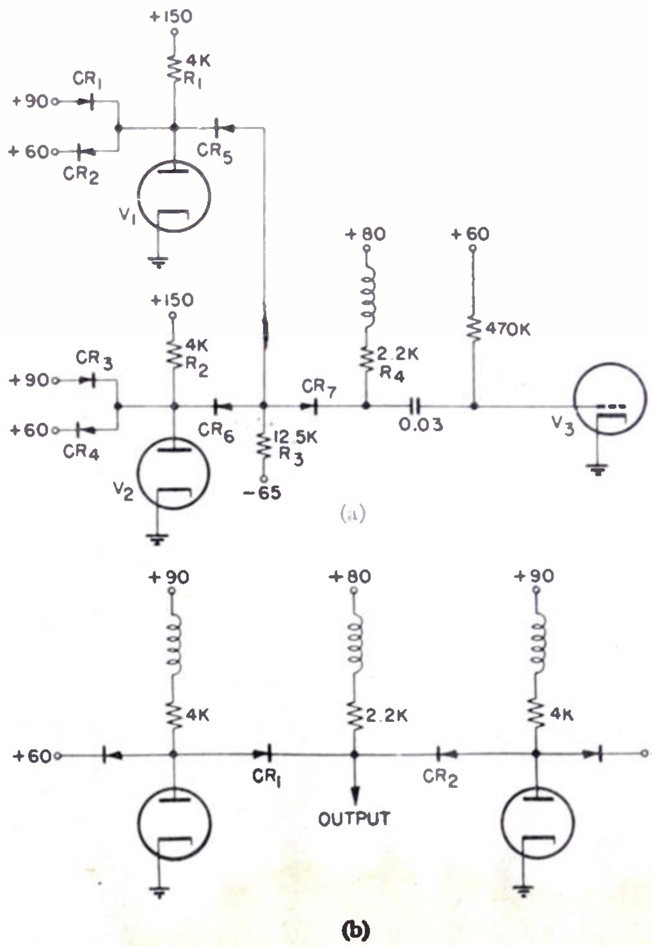

Fig. 4—Gate (a) and buffer (b) circuits.

In many cases it is necessary to supply signals to a point from various sources without having the latter react on each other. A "buffer" circuit of this sort, responsive to negative pulses, is shown in Fig. 4(b).

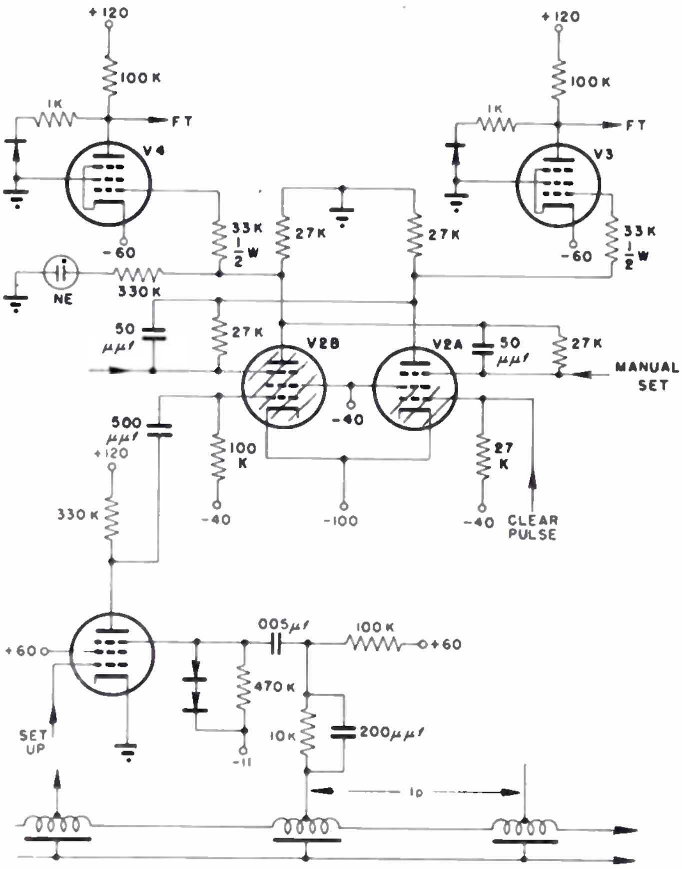

Fig. 5—Distributor and static register stage.

3. *Flip-flops, Counters*

The flip-flops used in the Binac for memory and switching purposes are, in many cases, essentially similar to those used in the ENIAC.[2] They require little comment, except to note that the static-register flip-flops (see Fig. 5 at left) use multigrid tubes, permitting the use of separate grids for internal coupling and for triggering or clearing.

Multistage binary counters are used in several places, but these also require little comment as they differ only slightly from those previously described in the literature.[3] A circuit of one of these, the cycle counter, is shown in Fig. 6.

4. *Distributor*

The distributor circuit, together with a group of flip-flops which constitute a static register, provides the means for converting information consisting of pulse patterns circulating in a delay line into patterns of steady (dc) signals more suitable for performing switching operations. A typical distributor stage is shown in Fig. 5.

Positive pulse-envelope signals are fed to an electric delay line through a pulse former and line driver. The line is tapped at points one pulse time apart. Therefore, at some particular instant the entire pattern of pulses (or unfilled pulse positions, as the case may be) will exist in such a position along the line that the voltage at each tap will be relatively positive or negative, according to whether the corresponding pulse position in the pattern

[2] A. W. Burks, "Electronic computing circuits of the E.N.I.A.C.," Proc. I.R.E., vol. 35, pp. 756–767; August, 1947.

[3] Staff of Engineering Research Associates, "High-Speed Computing Devices," McGraw-Hill Book Co., New York, N. Y.; 1950.

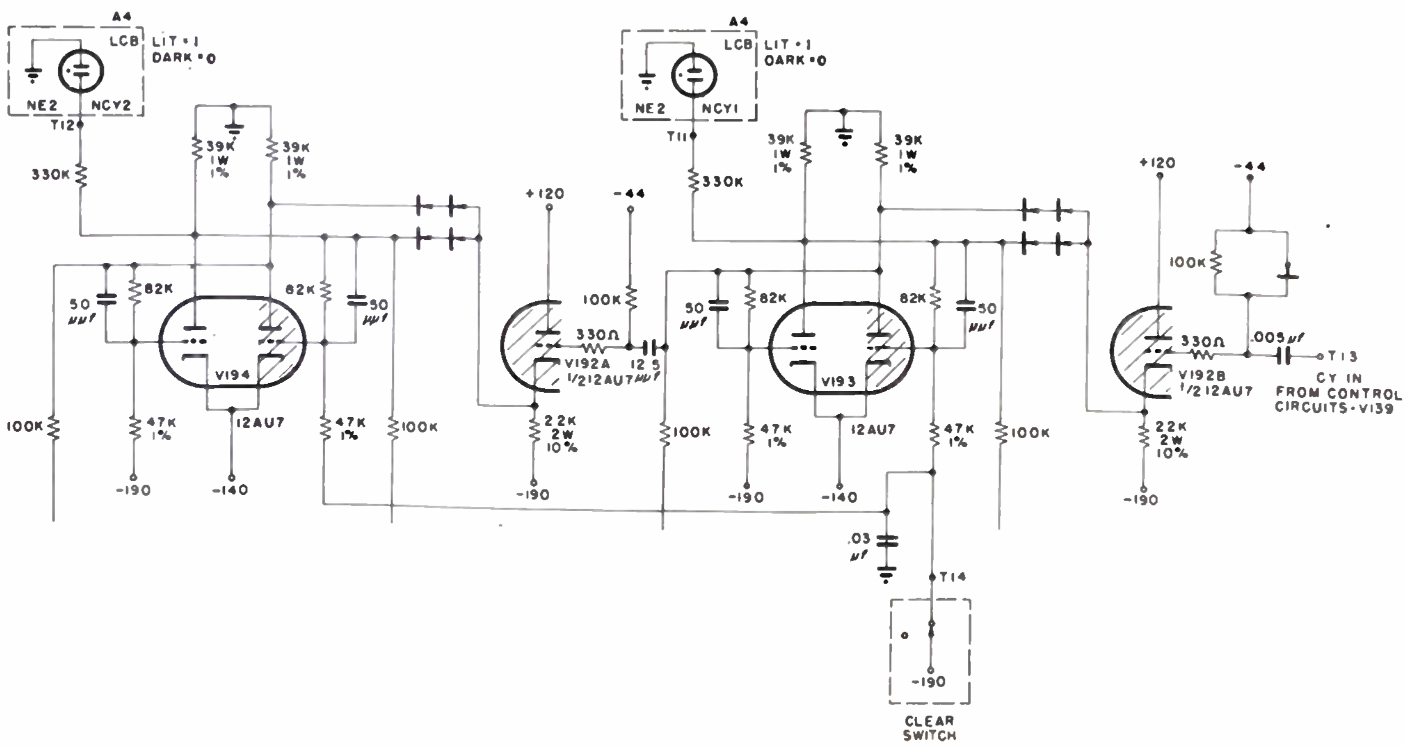

Fig. 6—Cycle counter (CY), typical of the binary counters used in the Binac.

contains a one or a zero. If the first grids of all the distributor gates are now simultaneously pulsed, those corresponding to *ones* will give output signals to set their respective flip-flops; others, receiving no signal from their respective line taps, will produce no outputs and will leave their flip-flops in the cleared position. As a result of the application of the set-up pulse to the gates, therefore, the pulse pattern is converted into a corresponding set of dc voltages. These are ordinarily amplified and applied to function tables although in the case of the time selector (see Section III B 3) they are applied to comparator gates directly (that is, without amplification).

5. *Asynchronous to Synchronous Devices*

Any transfer of information into the computer from the outside, whether it be numerical or program information from magnetic tape or keyboard, or simply the signal to start computing, must be timed to enter the machine in synchronism with the basic pulse rate of the computer and also at the correct time with respect to the information circulating in the delay-line registers and memory.

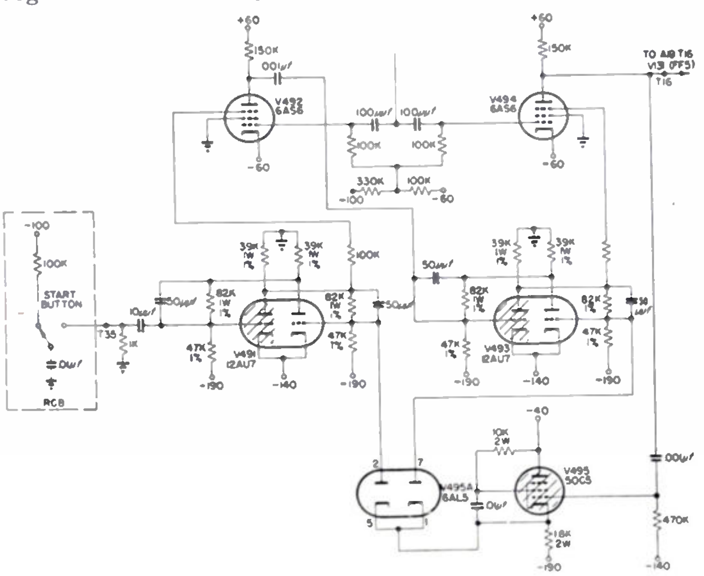

Fig. 7—Single pulse device (start circuit).

The start circuit, shown in Fig. 7, is an example of the method used to go from the asynchronous to the synchronous system.

6. *Shift Circuits*

It is necessary in multiplication and division to shift the data in a one-word register to the right or left, respectively. In a timed-pulse system this is equivalent to causing the pulse pattern to lag behind or advance ahead of its previous position relative to the minor cycle. A lag of one-pulse time can be produced by introducing an extra one pulse delay for a period of one minor cycle, while a lead can be produced by shortening the loop by a corresponding amount for the same period of time. A register capable of producing one-digit shifts in either direction, therefore, has a circuit like that shown in Fig. 8.

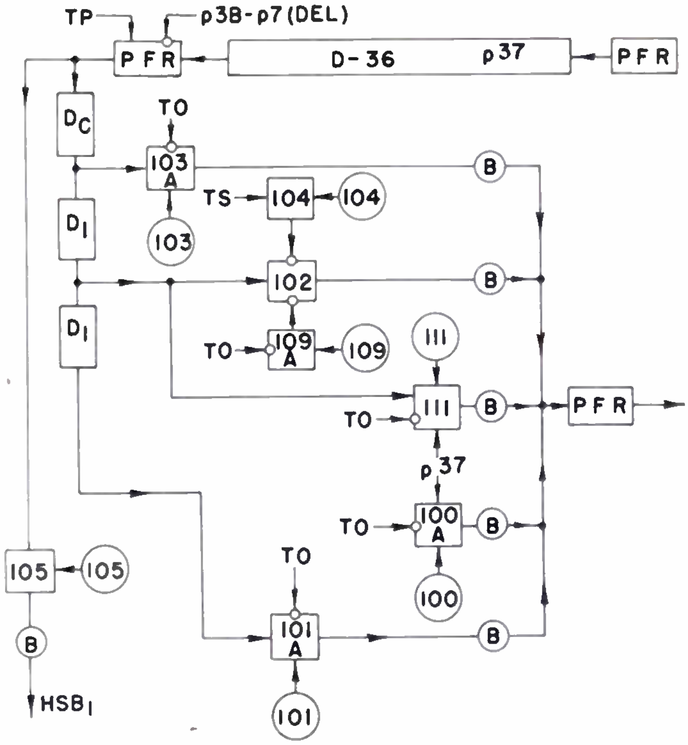

Fig. 8—Shift circuit.

7. *Half Adder and Adder*

In block form, a half adder may be represented as at (a) in Fig. 9 and a full or binary adder as at (b). A combination of two half adders may also be used to form

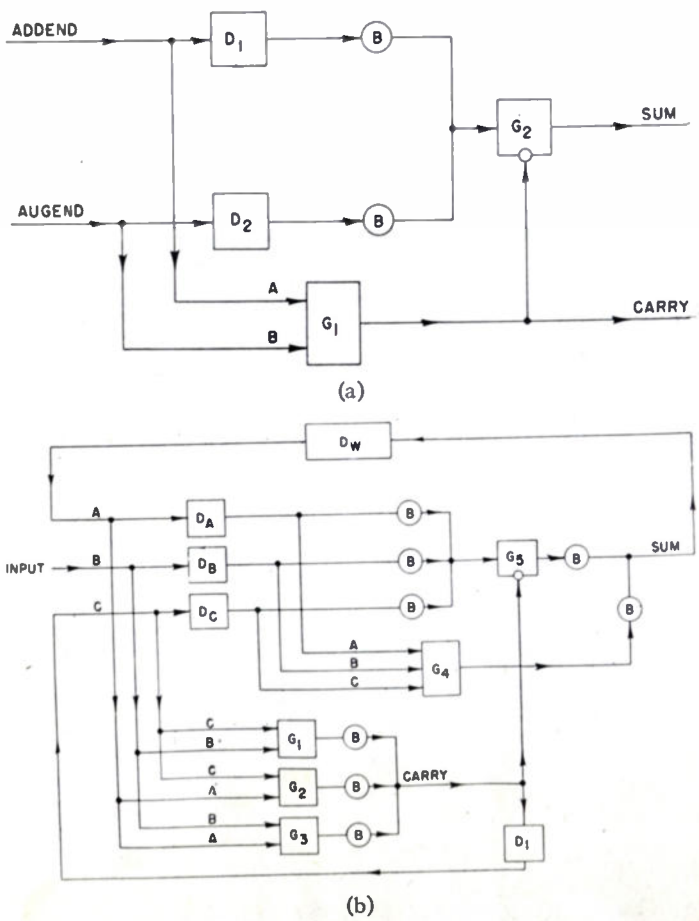

Fig. 9—Block diagram of half adder (a) and full adder (b).

an adder, but it is somewhat more economical to use the form shown. The corresponding schematics of the half adder and adder are shown in Figs. 10(a) and 10(b), respectively.

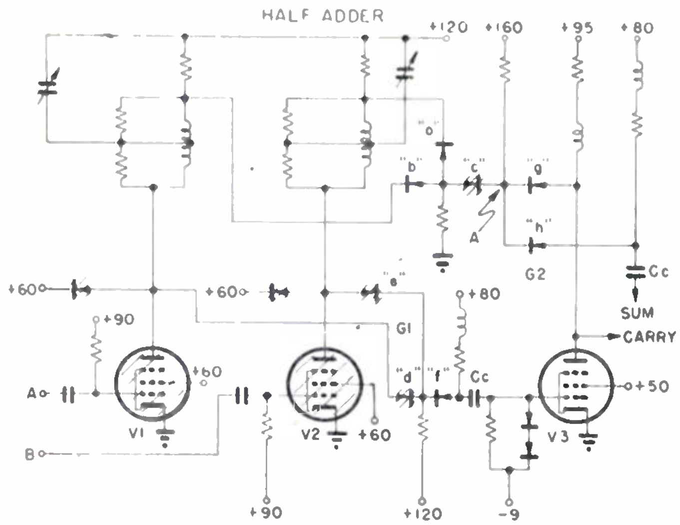

(a)

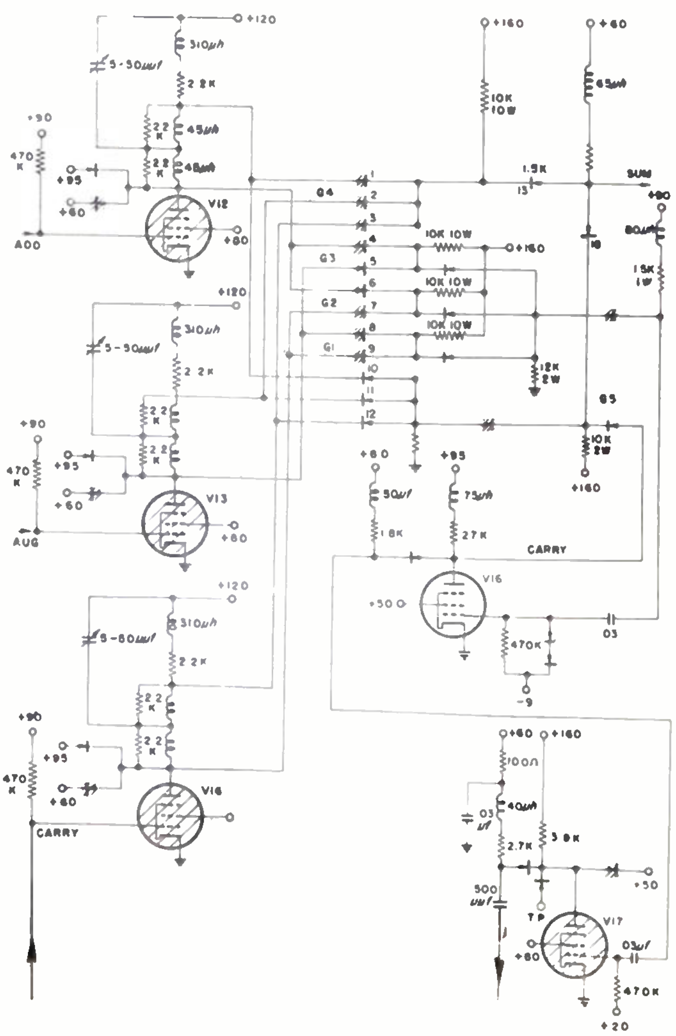

(b)

Fig. 10—Schematic diagram of half adder (a) and adder (b).

The properties required of a half adder were summarized in Section II B (1). Thus, in Fig. 9(a), if one input is present, it is buffed into $G2$, and appears on the sum line since no carry is present to inhibit this gate. If both inputs are present, the carry pulse from $G1$ inhibits $G2$. Thus, the carry line is operated while no sum appears. The half adder can be used as a complementer (reversing zeros and ones) if, for the duration of the word to be complemented (which enters one input), the other input is continuously *one*. The output is then taken off the sum line. As can be readily seen, for a zero in the word entering, a 1 appears as the sum output; and for a one entering, a zero appears as the sum output.

B. System Considerations

1. Synthesis of a One-Word Register

In dealing with numbers or words, it is clear that the first requirement is a means by which the numbers may be held while manipulating them. This is done in the Binac by means of one-word registers. The general principle used is that of a recirculation loop and regeneration and retiming gate. The loop itself must contain a delay element that, together with the remainder of the loop, is sufficiently long to permit the word to exist within it. Since words are temporal sequences of pulses that appear within a 42-pulse or 10.5-μsec interval, the recirculation loop is made the same length. Any duration other than 10.5 μsec, or an exact multiple of 10.5 μsec, would result in the word precessing around the register, a fact which is employed in designing shift circuits, as previously described. Fig. 11 represents in block form a one-word register. $D38$ is the major delay element. The delay found in the complete loop, plus D38, of course, must equal 10.5 μsec.

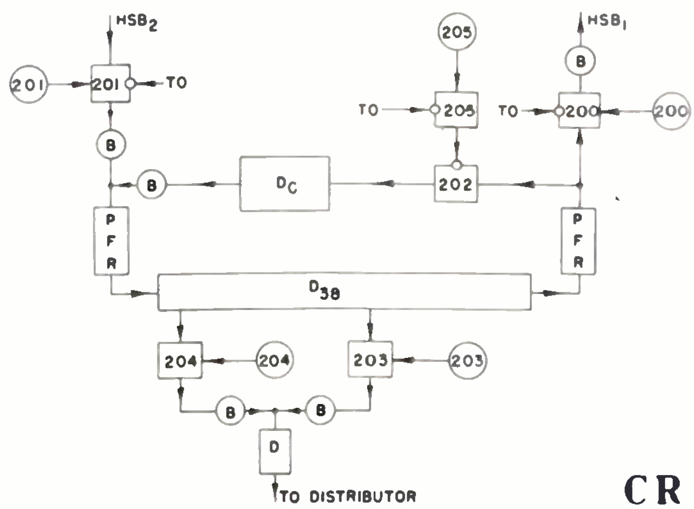

Fig. 11—Control register (CR), a typical one-word register.

To maintain this delay exactly and, also, to maintain the word in usable form is manifestly impossible using $D38$ alone. In the first place, the one-word delay element (which in the Binac is a lumped constant electric delay line using some mutual coupling between sections) is subject to temperature drift. Even with temperature control of the lines, over a period of several hours precession of the word would be unavoidable. In the second place, the delay line both attenuates and distorts the signals. Thus, after a few circulations, the information would have deteriorated in both amplitude and shape to the point of unusability.

To eliminate the amplitude loss, the gain around the loop must be made to equal unity. Any other value means loss of the information—either because it deteriorates into random noise when the gain is less than 1, or builds up into unusable oscillation when the gain is greater than 1. The maintenance of unity gain must then be accomplished by adding precisely the required energy to the circuit by means of amplifiers and associated circuits external to $D38$. These elements are represented by the pulse former and reshaper (PFR).

Were achieving unity gain the only consideration, the block pulse former and reshaper could assume quite a variety of forms (e.g., amplifiers with swings limited on both sides). The deterioration of wave shape could be avoided by a variety of reshaping circuits. However, these alone would not prevent precession of the word; retiming as well as amplification and reshaping must be provided. The pulse former and reshaper is a clock gate and pulse former of the type previously described. The timing pulses are generated by a highly accurate "clock" whose frequency deviation is less than 20 parts per million. Since timing pulses are common to the entire computer, the effect of making timing pulses one of the gate inputs is to keep the signals in synchronism with those in other parts of the computer. The signal, in short, may be somewhat out of step at the input to the gate, but will be precisely in synchronism with the basic clock at the output.

In this paper a buffer circuit will be denoted by the symbol shown in Fig. 12(a). A gate will be denoted by the symbol of Fig. 12(b), with either the letter G or a gate number in the square.

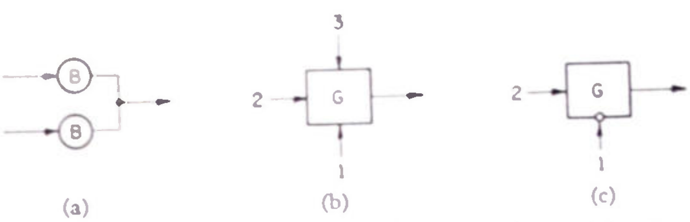

Fig. 12—Block-diagram symbols: (a) buffer; (b) gate; (c) gate with inhibitory input.

Further extending the gate symbology, an inhibitory input to a gate will be denoted by a circle (see input No. 1 of Fig. 12(c)). Signal (2) normally passes through G, but when (1) is present, it inhibits the passage of (2). Actually, there is no real difference between the inhibiting gate and the normal gate. It is still an "and" circuit. The symbol indicates that when signal (2) *and* the lack of signal (1) exist simultaneously, an output is produced.

It is possible to combine gates and buffers to serve as a means of getting information into the one-word register. The inputs to the gate $G201$ are the desired information and a control signal (201), which is applied when it is desired to put the information into the register. The original information appears at the output of $G201$, and is read in through the buffer, whereupon the control signal (201) is removed. Thereafter, it continues along the recirculation loop, meets the second buffer, but continues around again through $D38$, the path through the original buffer being closed. The information is thus trapped in the register.

To take information out of the register, a similar device is used. Signal (200) must now be applied when information is to be read out of the register. In the case of reading out, if it is desired at the same time to retain the information, the pulse former and reshaper circuit must include an amplifier capable of driving both the output gate and the next stage of the normal recirculation path.

Actually, the above is still an incomplete description of a one-word register since an essential timing detail has not yet been considered. All information moves between registers by way of the high-speed bus amplifier. The high-speed bus amplifier circuits have finite delays since they are required to reshape and retime. Thus, information coming out of the high-speed bus amplifier will lag behind the information coming in. It follows from this that were information to be transferred from one register to another without compensating for this delay it would be displaced correspondingly in the transfer process. For this reason a delay D_e equal to that of the high-speed bus amplifier system is placed between the input and output gates. Outgoing information is then read out at a point in time earlier than that at which information is read in. Thus, after reading from some Register I to an identical Register II, at corresponding points in these registers identical pulse patterns are observed that are not displaced in time relative to each other. Mathematically, this means that the significance of the digits has not been changed—the sign pulse, for example is still retained in the sign position. Since the over-all loop delay must still be one minor cycle, D is correspondingly shorter by the amount D_e or $D38+D_e+$circuit delay$\,=1$ minor cycle.

Other possibilities remain. Thus, it is ordinarily necessary to erase the old information in the register when new information is entered. In this case an inhibitory gate, $G202$, would be put in series with the recirculation loop. In the case considered, then, signals (201) and (205) operate together. The information into $G202$ is lost and information arriving at $G201$ is gated into the loop. If, simultaneously, $G200$ is operated, the original information would be read out. This, therefore, cannot be done if the information arriving at $G201$ is coming from another register since the two signals would be superimposed on the high-speed bus. In the case of the memory, signals corresponding to (201), (200), and (205) are all operated together in order that the tube driving $G200$ and $G202$ may never have to drive both simultaneously; thus, when reading out of the memory, the high-speed bus amplifier forms part of the recirculation path. In this case, the one-word register receiving the signals from the memory has only gates corresponding to $G201$ and $G205$ operated. When reading *into* the memory, a gate between the memory output and the high-speed bus amplifier is inhibited in order to clear out the previous contents of the memory.

A variety of circuits are used to operate gates and buffers, drive the delay lines, and do other jobs. These, and in particular the delay D_c, make necessary another retiming operation. A typical register will, therefore, have more than one pulse former and reshaper. The main delay line D may be tapped to provide output signals shifted in time with respect to the usual reference point (which, in the Binac, is the clock gate of the high-speed bus amplifier).

2. *Clock and Cycling Unit*

The timing pulses used at the clock gates are positive pulses of approximately 28-volts amplitude and 0.06-μsec duration at a 4-mc per second repetition rate. They are generated by a crystal oscillator using a type 807 tube and employing a temperature controlled 4-mc quartz crystal. The oscillator output is coupled to the grid of a Class C amplifier, also using a type 807 tube. The plate current pulses are coupled through a pulse transformer to a load consisting of the parallel inputs of eight resistance-terminated 93-ohm coaxial cables which carry the signals to all parts of the computer.

The cycling unit (Fig. 13) has several features which differ from those of the sample register just discussed.

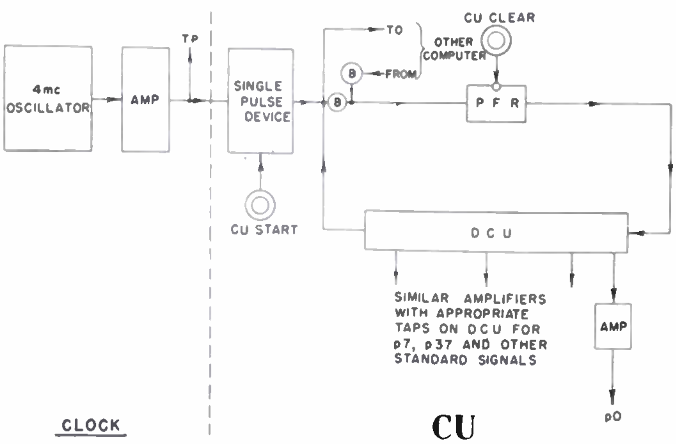

Fig. 13—Clock and cycling unit.

The only input to the register is a single pulse introduced by operation of the cycling-unit start button. Depressing the start button causes one of the clock pulses to trigger a flip-flop whose output is differentiated and shaped by means of a line-pulse former to produce an accurately timed signal input pulse for the loop. This pulse continues to circulate until interrupted by operation of the cycling-unit clear switch.

To obtain control pulses at various times during the minor cycle, signals are taken from taps along the cycling unit delay line. These signals are, in most cases, used to gate timing pulses which are fed into pulse formers, followed by amplifiers as shown. In two cases, the error gate and the delete gate, signals of several digits duration, are needed. For these signals, two taps on the register line are used, the two timing pulses gated being used to set and reset a flip-flop. The signal from the flip-flop plate provides the desired gating signal. For those cases where the timing of the desired signal is less critical, the output of the register delay-line tap was used without gating of a timing pulse. An example of such a signal is the $p0$ signal used for oscilloscope synchronization during test and maintenance operations.

3. *Control Circuits*

The basic operation cycle of the Binac was outlined in Section II A 3. A two-stage binary counter, the cycle counter (see Fig. 17), controls the four basic cycles; its decoded outputs are used to excite lines in the encoding function table which actuate the gates necessary for the required operations.

The control register has already been mentioned as an example of a one-word register. Its purpose is to hold the second instruction of a pair until the first has been completed; although it would be possible to return to the memory to bring out the second instruction directly into the static register, as is done with the first, the necessity for setting up the memory location of the instruction in the static register and the latency delay make this a time-consuming operation. Therefore, on the β cycle the pair of instructions is brought into the control register, and the first instruction set up in the static register after passing through $G204$; meanwhile, the entire word continues to circulate in the control register until cleared out at the time the next pair of instructions is brought in.

Pairs of instructions are ordinarily taken from the memory in numerical order; to accomplish this, a one-word register, the control counter, containing a unit adder (see Fig. 9(c)), is used to keep a record of the location from which the next pair of instructions is to be taken. As the word is read out of the specified location on the β cycle, a unit is added to the number in the control counter so that on the next β cycle the pair of instructions in the next memory location will be read out. Instructions from the control register are converted into static form by means of a distributor and static register.

For convenience in testing, push buttons are provided for setting up manually any desired combination in the static register flip-flops. Another push button can clear all flip-flops, while a different button can clear only the nine representing the memory location. All 14 flip-flops are cleared automatically by the ending pulse, which occurs at the completion of every instruction.

Of the 14 binary digits in an instruction, 9 are necessary to specify the memory location with which the instruction is concerned, leaving only 5 for the instruction proper. Since the number of gates employed by various instructions is much larger than 5, it is impossible to have a one-to-one correspondence between instruction digits and gates. The instruction must first be decoded into one of the 32 possible combinations represented by the 5 pulses (actually, not all the 32 combinations are used); this signal can then be used to operate the proper combination of gates. Electrical function tables are used for the decoding and encoding. Fig. 14(a) shows the decoding table, each dot representing a crystal diode. The output lines, which in turn form the inputs of the encoding table, are labeled at the top with their numerical equivalents, expressed in octal form, and at the bottom with alphabetic symbols, which are used for convenience in programming. Thus, for example, the instruction calling for addition is actually typed into the computer as the combination 05 followed by the memory location of the addend; in

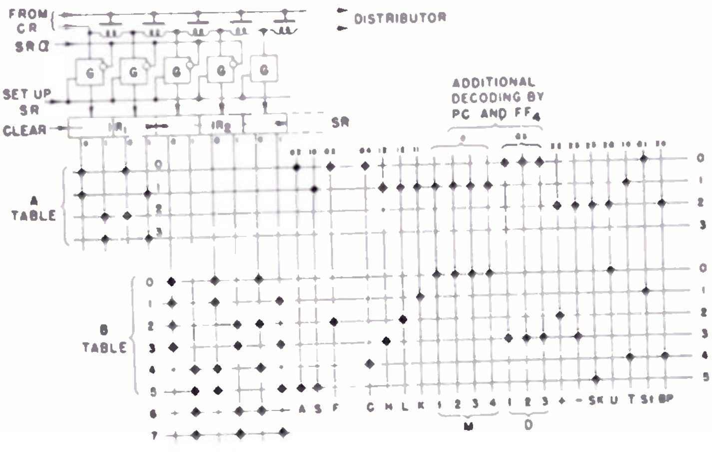

(a)

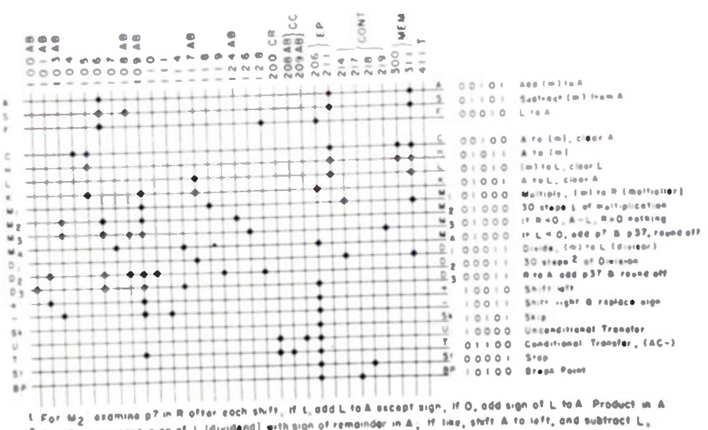

(b)

Fig. 14—Function tables: (a) decoding; (b) encoding.

programming, however, it is more convenient to designate this operation by A, subtraction (15) by S, division (03) by D, and so on.

Fig. 14(b) shows the encoding table which converts each output signal from the table of Fig. 14(a) into a combination of gate signals. Again, each dot represents a crystal diode; when an input wire is excited by being made relatively more positive, it pulls up any output lines to which it is connected, turning on the normally off gate driver tubes connected to those outputs.

The function table is so extensive that its wiring capacitances, and those of its output circuits, result in time constants considerably longer than the space between words. It can be shown that in a computer of the Binac type, where the latency time of the memory has an important bearing on the over-all speed, it is more economical to allow a full minor cycle for switching operations between instructions than to increase the space between words, and consequently the length of the minor cycle. A so-called "time-out" period is, therefore, introduced at the beginning of each operation requiring a change in the function-table signals. Some type of fast switching circuit, capable of operating in the space between words, is still needed to prevent gating of parts of words during the time the function-table signals are changing; but the "time-out" principle permits the burden of fast switching to be shifted from the numerous function-table signals to a single flip-flop which can furnish inhibitory signals to any gates which require them.

This "time-out" flip-flop (see Fig. 17) is set by the same $p0$ pulse which clears the static register in preparation for setting up a new instruction. It is also set by certain pulses into the program counter, as described later. Since "time out" is normally required for only one minor cycle, the "time-out" flip-flop resets itself by gating the next $p0$ pulse into its reset input.

Selection of one of 16 tanks in the memory is accomplished by means of a small function table which decodes the four most significant digits of the memory location specified in an instruction set up in the static register.

The 5 remaining binary digits in the memory location number specify one of the 32 words stored in the tank. Fig. 15 shows the time-selector circuit which selects the desired word. A 5-stage binary counter, the time-selector counter is driven by $p0$ pulses from the cycling unit. Since this is a scale-of-32 counter driven by minor cycle pulses, there will always be a one-to-one correspondence between the reading of the counter and the word appearing at the gates of the memory tank. Thus, if the time-selector counter, by comparison with the memory location set up in the static register, is used to control the storing of a given word in the memory, it will always be possible to extract that same word by setting up the same number in the static register and comparing it with the time-selector counter to control the operation of the output gate of the memory.

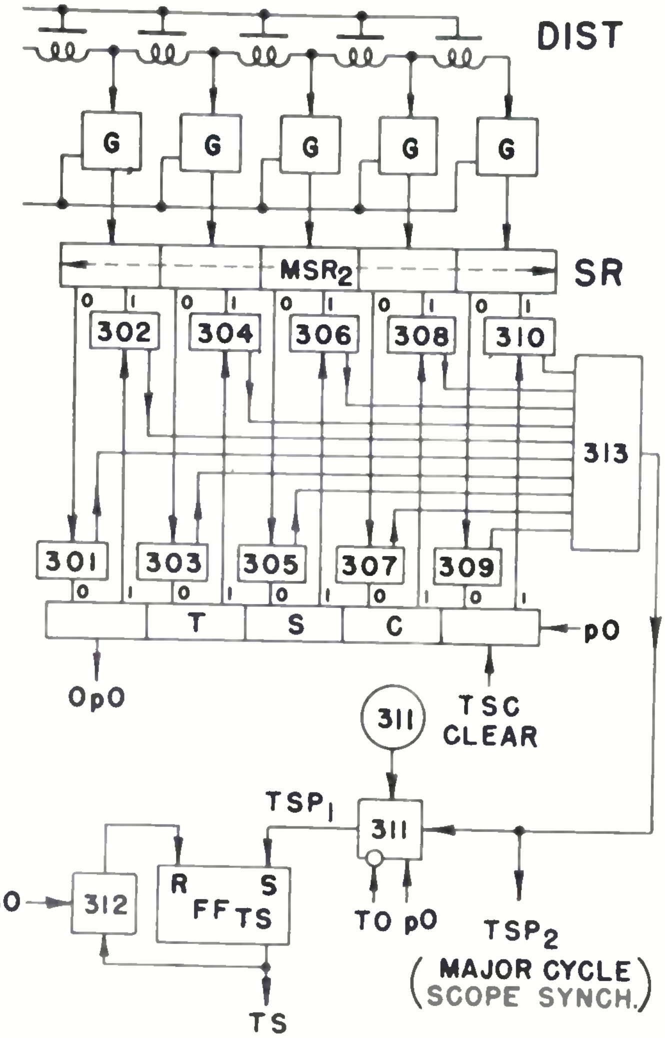

Fig. 15—Time selector (TS) circuits.

4. *Arithmetic Equipment*

Section II B discussed the general arithmetic processes. Multiplication and division involved a series of repetitive additions (or subtractions) and shifts, followed by required corrections. In analyzing these operations, it is convenient to divide multiplication into four steps (designated $M1$, $M2$, $M3$, and $M4$) and division into three ($D1$, $D2$, and $D3$). The steps of multiplication are discussed individually with reference to the block diagram, Fig. 16.

a. Multiplication: The $M(m)$ instruction, together with another order, is transferred from the memory on the β cycle. It sets up in the IR on γ_{TO} or δ_{TO}, depending on whether it is the first or second order in the order pair. The multiplicand is assumed to be stored in the L register as a result of some previous operation.

The program counter (PC) is used to subdivide M and D into their individual steps (see Fig. 17, the following page). It is a 6-stage (scale of 64) binary counter with its own decoding function table. The outputs of this table are connected into the main function table in such a way that when the M line, for example, is excited by SR, PC will determine whether $M1$, $M3$, or $M4$ is excited. Since $M2$ lasts for 30 cycles, it is more economical to allow a flip-flop ($FF4$) to take over the controlling function rather than to decode all 30 combinations of PC and buff them together. With this arrangement, $FF4$ is set at the end of $M1$, and it is then only necessary to decode PC's output on the 29th of the 30 repetitive steps to get a reset signal for $FF4$. A similar procedure is used on $D2$.

It will be noted that position 1 of PC corresponds to the binary combination 111111 (decimal 63). By clearing PC to this state rather than to 000000, carry-overs are not produced by the clearing operation, and a narrower clear pulse (a gated $p0$) can be used. Thus, $M1$ corresponds to PC 63, and $M2$ starts on $PC0$ and ends on $PC29$; $M3$ and $M4$ correspond to $PC30$ and $PC31$, respectively.

The $M1$ step is used to select the multiplier and transfer it from the memory to the R register. The product is to be built up in A. At this point, then, it is convenient to clear both A and R. Clearing of A and R takes place on the first minor cycle following γ_{TO} or δ_{TO}, as the case may be. $M1$ selects FT signals 109A and 109B, which inhibit G102 in A and G115 in R, respectively, when the machine goes off time out. FT signal 311 is also selected to cause reading out from the memory of the word selected by the memory location part of the multiplication instruction. Since FT signal 118 is activated on $M1$, the multiplier enters R through G118. G214 is also energized on $M1$ during the TS period. Thus, the same $p0$ that resets FF_{TS} passes through G214 to set $FF4$ and FF_{TO}, and step PC to $PC0$. This puts a TO between $M1$ and the $M2$ step to follow. $FF4$ is used

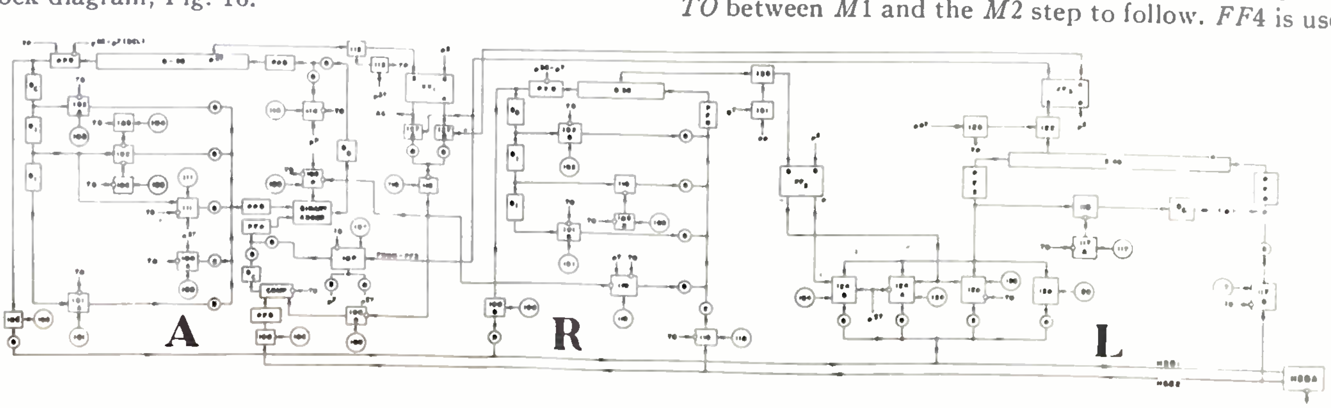

Fig. 16—Arithmetic circuits (A, R, and L registers).

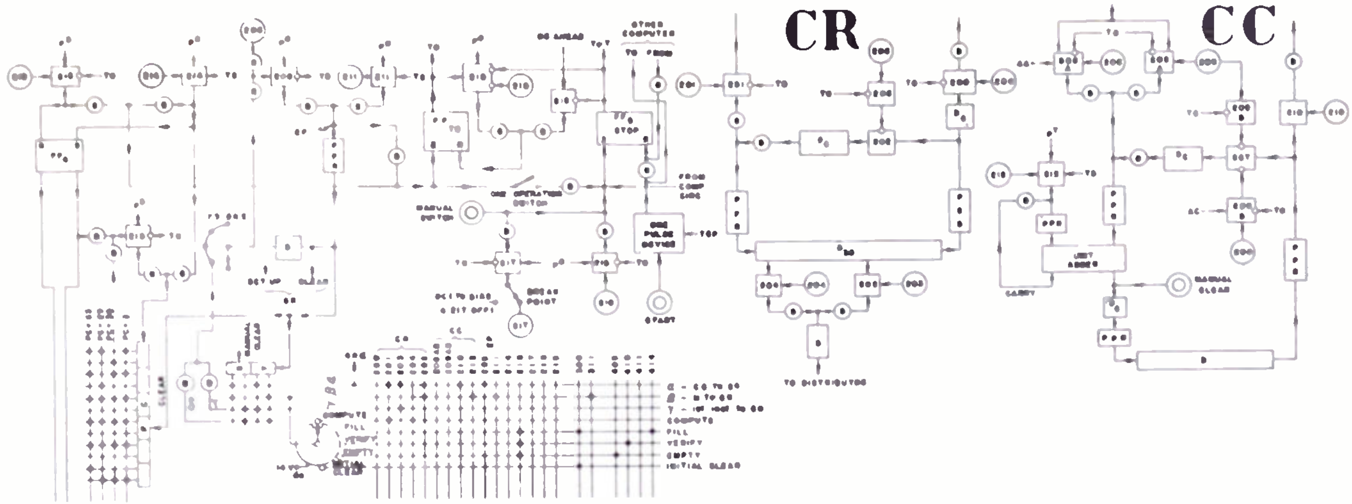

Fig. 17—Control circuits.

to control the next 30 minor cycles of $M2$. During $M2$, PC must keep track of the operation by counting, which it now can do by way of $G213$ (which permits $P0$'s to pass, under the control of $FF4$, as soon as the TO inhibition is removed).

With the multiplicand and multiplier in L and R, respectively, the 30 repetitive steps are begun. In accordance with the mathematical requirements discussed in Section II B, the digits of the multiplier are examined, starting with the least significant. For a zero, only the sign digit of the multiplicand is transferred to A; for a 1, the multiplicand, without its sign, is transferred to A. A right shift in both A and R follows each transfer, permitting examination of the next multiplier digit and proper positioning for the next addition of the multiplicand. At the conclusion of 30 steps, PC is in position 29. The $PC29$ signal excites $G219$, which gates a $p0$ to reset $FF4$ and set FF_{TO}, conclude the $M2$ cycle, and initiate the TO before $M3$.

Examination of the block diagram shows that on $M2$ the FT signals 103A, 103B, 106, 109A, 109B, 124A, and 124B are activated. These, in turn, activate G103A and G103B (opening the right shift paths in A and R); $G106$ (permitting the transfer into A); G109A, and G109B (which inhibit the normal recirculation paths in A and R); and G124A and G124B (permitting read out of the multiplicand from L under the control of $FF2$ and $p37$). $FF2$ is set only if the $p7$ digit in R is a 1, in which case G124A operates, the $p37$ which may be in L being inhibited. Reset pulses are fed to $FF2$ every minor cycle, but the tap on the R line is so adjusted that $FF2$ is immediately set again if a pulse is present in the $p7$ position. If $FF2$ remains reset (i.e., if the R digit is 0), G124B is operated and only the $p37$ or sign is added into A.

On $M3$, a correction is made if the multiplier is negative. In this case, the multiplicand is subtracted from the uncorrected product in A. Note that the $M3$ line produces FT signals 103A, 103B, 106, 108A, 108B, 109A, 109B, 126, and 219; 108B operates G108B, activating the complementer. Thus, the correction term from L has its ones replaced by zeros and its zeros by ones. In conjunction with this operation, 108A simultaneously operates G108A, which adds in the $p7$ required to complete the subtraction of the multiplicand. The multiplicand itself leaves L via $G126$. The remaining gates operate as described before. Note that $G126$ is under the control of $FF2$. Thus, *only* if R is negative (its sign digit has finally been shifted into the $p7$ position and can, therefore, control $FF2$) does $G120$ pass a signal which sets $FF2$ and permits $G126$ to open. $G219$ sets FF_{TO} and steps PC, permitting the $M4$ step to be initiated.

The $M4$ cycle is used to correct the partial product if the multiplicand is negative. A partial correction has already been made in this case during $M2$ since for multiplier digits equal to 0 the negative sign of the multiplicand (if present) was added into the partial product via transfers through G124B. The remaining step then is to add in a $p7$ and $p37$ to A. Simultaneously, it is convenient to round off the partial product by stuffing in a $p7$, as described in Section II B 4.

The $M4$ line activates FT signals 107, 114, and 206, these signals in turn operating gates 107, 114, and 206. $G107$ operates under the additional control of $FF3$. This, in turn, is set through $G122$, which receives its input from a tap on the line of L in such a position as to sense there the presence of a $p37$. Thus, the $p7$ and $p37$ correction in A is made only if the multiplicand is negative. $G114$ performs the round-off operation by superimposing a $p7$ on the partial product in A. With the completion of the round-off step, the final product is now held in A. Since $G206$ is operated, an ending pulse is passed which sets FF_{TO}, clears the static register, and advances CY to the next cycle (δ if $M(m)$ were performed on γ, and α if it were performed on δ). At the conclusion of the M operation, then, the final product is in A, the multiplicand is still in L, but by reason of the continuous right shift in R, the multiplier has been cleared out.

b. Miscellaneous Operations: Although the Binac ordinarily obtains instructions from successive memory locations, as controlled by the control counter, it is frequently necessary to depart from the normal sequence and obtain a pair of instructions from a location specified in a "transfer of control instruction." This is accomplished by reading the contents of the control register into the control counter. If the transfer instruction is placed in the right-hand position of the word, its memory position falls into the same place in the control counter as the number which was being built up there. On the next α step, the new location can be read back into the control register and the static register, and the desired pair of instructions brought out of the memory on β. Furthermore, the new number remains in the control counter, having a unit added to it on each β step, and thus a new sequence of operations is started, continuing until another transfer of control instruction again changes the number in the control counter.

The transfer can be unconditional (the *Um* instruction), replacing the number in the control counter, as described above, or it may be made conditional on some situation in the computer (the *Tm* instruction). The conditional transfer allows the choice of two courses of computation to be made, dependent on the result of a previous computation. The sign of the quantity in A was chosen as the determining factor in the *Tm* instruction. If the quantity in A is positive, the sign sensing flip-flop prevents the reading of the new number from the control register into the control counter, and permits the original contents of CC to remain; but if the quantity in A is negative, the operation is the same as that of a *Um* instruction.

Several instructions transfer data from one register to another; these include *Cm*, *Fm*, *Hm*, *Km*, and *Lm* (see Appendix E). The skip is generally used to fill in the left-hand position ahead of a T or U instruction where the last preceding instruction does not fall in this position. The break-point instruction can be inserted at strategic points in a program; it causes the computer to stop at each of these points if the break-point switch is set—an aid in checking new programs. With the break-point switch set to "continuous," break-point instructions are treated as skips. The stop instruction, as its names implies, stops computation by setting $FF5$, which in turn blocks $G216$ and prevents FF_{TO} from being reset.

For testing and maintenance, and for checking new programs, it is essential to be able to cause the computer to perform a single operation and stop, continuing with the next operation only after manual operation of a start button. The "time-out" feature furnishes a convenient means for achieving this. Since all significant gating operations, including, in particular, the gating of the ending pulse, are inhibited during "time out," interrupted operation can be achieved by inhibiting the automatic resetting of the time-out flip-flop (through $G216$) and by providing a circuit which produces a single $p0$ pulse to reset the flip-flop when the start button is pushed. A "stop" flip-flop ($FF5$) is used to inhibit $G216$, and is set by the same pulse which sets the time-out flip-flop. But this occurs only if an operation control switch is set to "one operation," if a stop instruction is encountered, or if a break-point instruction with the break-point switch is set to "break" position. The start button is used to reset the stop flip-flop.

The discussion up to this point has referred to the Binac as if it were a single computer. Actually, the entire computer, with the exception of the input-output converter, is duplicated. The two computers are started in synchronism, and computations proceed in parallel, with a half adder in each computer making a continuous comparison of signals on the high-speed buses. Any discrepancy will produce a signal at the "sum" outputs of the half-adders; these signals are used to set the stop flip-flops of both computers. An additional check is provided by a gate circuit supplied by a cycling unit signal which corresponds to the space between words; if any signals in these pulse positions appear on the high-speed bus, the gate produces an output which sets the stop flip-flop.

5. *Input-Output Equipment*

Since the Binac is designed for mathematical operations in which a relatively small amount of input data forms the basis of extensive computations, which, in turn, produce a relatively small volume of output data, very simple input and output facilities are sufficient. These consist of a keyboard, a printer, a manually controlled magnetic-tape reading and recording device, and a converter for transferring data between the Binac memory and the other units.

The keyboard has eight keys representing the octal digits 0 to 7, inclusive; numbers (including instructions, which are in numerical form as previously described) typed on the keyboard are recorded by the printer as they are typed, forming a visible record for checking. A word is not transferred to the memory until its last character is typed, giving the operator an opportunity to proofread. If it is necessary to retype a word before transferring to the memory, an erase key clears it out. It is also possible to print out the contents of the memory.

A one-word synchronizing register forms the link between the converter and the main Binac memory. In typing in from the keyboard, each key stroke produces a signal corresponding to three binary digits; this signal sets up the corresponding combination in a group of three flip-flops. A transfer pulse, generated by a pulse circulating in another one-word line having a shifter network, transfers the signal from the flip-flops to the synchronizing register. Each successive group of three pulses is inserted in its proper place in the word because the pulse in the timing register, which generates the transfer pulse, is shifted three pulse times after each transfer. When the word in the synchronizing register is completed (by typing its last octal digit), it is transferred to the main memory; the control counter controls the transfers to consecutive memory locations.

The above procedure is reversed when printing the contents of the memory; in this case words from consecutive locations are transferred to the synchronizing register, and from there are transferred one octal digit at a time to flip-flops which control the printer magnets.

The printer is an electric typewriter whose keyboard has been removed. It has been fitted with solenoid actuators for the characters 0 to 7, inclusive. An automatic carriage return is provided to operate after an integral number of words; once the "emptying" operation is initiated, the entire contents of the memory are printed out automatically.

Because most problems require a considerable amount of data (instructions and initial or boundary values) in the memory, the typing operation can become laborious. An accident, such as power failure, can destroy an hour's work in a moment; furthermore, it is frequently found that numerous computer runs of a particular problem require the same input data, with only very minor modifications which can be easily made after a standardized routine has been entered in the memory. For these reasons it is customary, after typing in a set of data, to record the latter on tape. The process is similar to that of printing out the contents of the memory, except that the recording heads on the tape equipment are connected in place of the printer magnets. The data so recorded can then be read back into the memory at any time, again using the converter, but setting up the synchronizing flip-flops with signals from the head amplifiers rather than from the keyboard.

6. *Memory*

The Binac memory is of the mercury delay-line type, and was described in a previous article.[4] It consists of sixteen channels, each storing 32 words. An additional channel is used for the temperature-control circuit. A memory-channel recirculation circuit is quite similar to an electric delay-line register, with the line amplifier replaced by a wide-band amplifier and detector, and the line driver operating directly out of the clock gate without the use of a pulse former (since the mercury delay line and following amplifier broaden the pulses into a pulse-envelope signal).

IV. Applications

The Binac is suitable, within the limitations imposed by the size of its memory and the nature of its input and output operations, for the solution of a wide variety of mathematical problems. These must, of course, first be reduced to suitable form for solution by numerical methods. Solutions of Poisson's equation in two dimensions for various boundary shapes and load conditions were obtained during the testing period, and results indicated that the Binac can effect a very substantial saving in time for the solution of such problems as compared to solutions by hand computation using desk-type calculators.

The program in Table I,[5] showing the computation of the square roots of a series of 20 numbers, is presented here to illustrate the method of coding problems for the Binac. All numbers are expressed in octal form. The first column shows the memory location in which each pair of instructions is stored; the next two contain, respectively, the first and second instructions in the word. A brief description of the operation appears in the fourth column. Before typing the program into the computer, the letters in columns 2 and 3 are replaced by numerical equivalents ($05=A$, $04=C$, and so on). After clearing the memory and clearing the control counter to zero, the program is typed in, after which the control counter is again cleared to zero. Computation is now started, and will stop automatically when the 20 roots have been computed. At this time the control counter will read 754. The computer can then be switched to "empty" so that it will start printing with memory location 755, the first root. Printing will continue until all 20 roots have been printed, after which the operation stops.

In the program shown, 000 contains a skip followed by an unconditional transfer to the first instruction in 024. The parentheses around 001 indicate that this portion of the instruction is modified in the course of computation. The Newton-Raphson method of computing roots is used here.

$$Z_{i+1} = 1/2(\mu/Z_i + Z_i),$$

where the Z_i are successive approximations and μ is the radicand. Z_0 is taken as 1. In line 024, μ is brought in; Z_1 is computed in lines 025 to 026. Lines 027 to 031 constitute the iterated process. In lines 032 to 033 the new approximation is compared with the previous one; if the difference is not sufficiently small, Z_{i+1} is substituted for Z_i, and another iteration is performed. If the difference is small enough, however, the latest Z_i is placed in one of the registers 755 to 777, inclusive, to be printed later.

Having computed the root of the first μ, the computer must obtain the next μ; it does this by modifying the first instruction in 024, adding 1 to its memory location. The second instruction of 036 must be similarly modified so that the next computed root will be placed in a different register for printing. These modifications are made in lines 037 to 041.

[4] I. L. Auerbach, J. P. Eckert, Jr., R. F. Shaw, and C. B. Sheppard, "Mercury delay-line memory using a pulse rate of several megacycles," Proc. I.R.E., vol. 37, pp. 855–861; August, 1949.

[5] J. J. Bartik, "Square-Root Routine," Computational Analysis Laboratory, Eckert-Mauchly Computer Corp., Division Remington Rand, Inc., Philadelphia, Pa.

Since it is necessary to know when all 20 roots have been computed, a test is made in line 042. When the last modification of 036 takes place, an overflow occurs, changing $C777$ to $A000$ (the A has no significance here; actually $C777 = 04777$, which on addition of 1 becomes 05000, which happens to be $A000$). Thus, subtraction of $A056A000$ will cause a sign reversal on each iteration, except the last, and the absence of the sign reversal on the last one causes the T to be ineffective. Lines 043–044 are a "patch-up" routine to restore 024 and 036 to their original settings; line 045 contains a transfer of control to 754, where a stop instruction is placed. By putting the stop in 754 rather than in 045, the control counter is left with the proper setting, and the results, which are stored in locations starting with 755, may be printed.

While the foregoing example is a relatively simple routine, it illustrates several of the principles of programming. In particular, it shows the manner in which instructions are modified (by adding constants to their memory locations) and the use of tests (employing conditional transfer instructions) to determine whether an iterative process has been completed. It is of interest to point out that, although there are 20 lines of coding (excluding constants, storage registers, and the like), only 5 (025–031) are concerned with the actual computation. This is characteristic of computers of the class to which the Binac belongs.

Acknowledgment

The authors wish to acknowledge the contributions of their associates in the Eckert-Mauchly Computer Corporation to the work described in this paper. Appreciation is also due several others for assistance in preparing the manuscript and illustrations.

Appendix A

Proof of Rule for Complementing

To form the complement of any m-digit number n $(2 > n \geqq 0)$ with respect to 2, replace all zeros of n by ones, and all ones by zeros; then add a unit in the extreme right-hand position.

Let $n = \sum_{-m}^{0} a_i 2^i$ and let the number n^1 formed by reversing zeros and ones in n be $\Sigma\, b_i 2^i$. Now, for any given i, if $a_i = 0$, $b_i = 1$; if $a_i = 1$, $b_i = 0$. It then follows that for any i, $a_i + b_i = 1$, and, therefore, $n + n^1 = \Sigma(a_i + b_i)2^i = 1.111 \cdots$. Adding 2^{-m}, $n + n^1 + 2^{-m} = 10.0$, and, therefore, (since 10.0 is the binary equivalent of 2) $n^1 + 2^{-m}$ is the complement of n with respect to 2.

If the convention is now adopted that numbers lying in the range $1 > n \geqq 0$ are positive, it follows that negative numbers in the range $0 \geqq n \geqq -1$, if represented by the complements of their absolute values with respect to 2, must lie in the range $2 > n \geqq 1$. They will, therefore, always have a 1 in the position to the left of the binary point (i.e., in the $p37$ position). The notation used can, therefore, represent numbers in the range $1 > n \geqq -1$. It also follows that the complementing method is reversible as, of course, it must be if it is to be of any value.

Appendix B

Addition of Complements

In the following discussion it is assumed that all original numbers are within range of the computer (i.e. $1 > n \geqq -1$) and negative numbers are represented by their complements, as previously described. A simple binary addition should then give the correct result regardless of whether one or both addends may be negative.

If n_1 is positive and n_2 negative, the quantities added will be $|n_1|$ and $2 - |n_2|$. Their sum will then be $2 + |n_1| - |n_2|$. Now $\big||n_1| - |n_2|\big|$ must be less than 1 since $|n_1|$ and $|n_2|$ are each less than 1; therefore, if $|n_1| - |n_2|$ is positive, the $p37$ position must contain a zero. The 2 would normally occupy the $p38$ position, but it is deleted by the delete gate so that the actual result is $|n_1| - |n_2|$, which is correct. If $|n_1| - |n_2|$ is negative, it can be written $-\big||n_1| - |n_2|\big|$, and the result of the addition is $2 - \big||n_1| - |n_2|\big|$, which is the complement of $|n_1| - |n_2|$; again this is correct since negative results should be expressed in complement form.

If n_1 and n_2 are both negative, they will be represented by $2 - |n_1|$ and $2 - |n_2|$, respectively, and the sum will be $4 - |n_1| - |n_2|$. Since all pulses beyond $p37$ are deleted, it follows (since $2 = p38$) that the addition of $2p$ to any number where p is any positive integer greater than zero, leaves the number unchanged. Therefore, as far as the computer is concerned, $4 - |n_1| - |n_2| = 2 - |n_1| - |n_2|$. Since $2 - |n_1| - |n_2| = 2 - \big(|n_1| + |n_2|\big)$, the result of the addition is the complement of the sum of n_1 and n_2, and is therefore correct.

It should be noted that if the addition of two positive numbers causes a carry-over into the sign ($p37$) position this implies that the sum exceeded 1, and is therefore outside the range of the computer; such a result must be distinguished from the negative number, which it superficially resembles. Similarly, the addition of two negative numbers must be considered improper if the result does *not* contain a 1 in the $p37$ position.

Appendix C

Illustrative Example of Multiplication

1. $0.110 \times 0.101 = 0.01111$ $(3/4 \times 5/8 = 15/32)$

A	R	Explanation
0.000	0.101	*LSD* in *R* is found to be 1.
0.000+0.110=0.110	0.101	*L* is added to *A*.
0.0110	0.010	*A* and *R* are shifted; *LSD* of *R* is 0.
0.00110	0.001	There is no addition, but another shift; *LSD* of *R* is 1 again.
0.0011+0.110=0.1111	0.001	*L* is added to *A*.
0.01111	0.000	*A* and *R* are shifted; *LSD* of *R* (originally sign) is 0. No correction is needed, and the process is complete.

Note: Digits to the right of 0.011 are actually deleted in the Binac.

2. $1.010 \times 1.011 = 0.01111$ $(-3/4 \times -5/8 = 15/32)$

A	R	Explanation
0.000	1.011	*LSD* of *R* is 1.
0.010	1.011	Add *L* (without sign) to *A*.
0.001	0.101	Shift *A* and *R*; *LSD* again 1.
0.001+0.010=0.011	0.101	Add *L* again and shift.
0.0011	0.010	*LSD* of *R* now 0.
1.0011	0.010	Add only the sign digit of *L* and shift.
0.10011	0.001	*LSD* of *R* (formerly sign) is 1.
0.10011+0.110=1.01011		Add $-L$ (0.110) to *A*; sign of *L* is also 1.
1.01011+1.001=0.01111		Add 1.001 to *A* to get final result.

APPENDIX D

INSTRUCTION CODE

In the following list, m is a 3-digit octal number representing a memory location, (m) means "contents of m."

Am	Add (m) to (A), result in A.
Cm	Transfer (A) to m and clear A.
Dm	Divide (A) by (L), quotient in A.
Fm‡	Add (L) to (A), result in A.
Hm	Transfer (A) to m without clearing A.
Km‡	Clear L, transfer (A) to L and clear A.
Mm	Multiply (L) by (m), product (rounded off) in A.
Sm	Subtract (m) from (A), result in A.
Tm	Transfer control to m (i.e., replace the number in the control counter by the number "m") if sign of (A) is negative.
Um	Transfer control to m unconditionally.
01*m*‡	Stop computation, leaving computer on "time out."
22*m*‡	Shift (A)** one binary digit to left, i.e., multiply (A) by 2.
23*m*‡	Shift (A) one binary digit to right, i.e., divide (A) by 2 without rounding off.
24*m*‡	Stop computation if "break point" switch is set; otherwise proceed to next instruction.
25*m*‡	Proceed to next instruction (skip).

‡ In these instructions m is not significant, and 000 is customarily used.

** The shift instructions also operate on R, but this is not significant except when the shift forms a part of the multiplication or division process.

Bibliography

1. H. H. Goldstine and A. Goldstine, "The electronic numerical integrator and computer (ENIAC)," pp. 97–110. July, 1946.
2. D. R. Brown and N. Rochester, "Rectifier networks for multiposition switching," Proc. I.R.E., vol. 37, pp. 139–147; February, 1949.
3. University of Pennsylvania, Staff of the Moore School of Electrical Engineering, "Progress Report on the EDVAC," University of Pennsylvania, Philadelphia, June 30, 1946.

Logical Description of Some Digital-Computer Adders and Counters*

HARRY J. GRAY, JR.†, ASSOCIATE, IRE

Summary—A number of adding and counting circuits which have a high degree of reliability are presented. Most of them have been used in a digital computer. A high-speed binary counter is described which can be cycled either forwards or backwards.

Introduction

When the ENIAC[1] was nearing completion, it became apparent that a reconsideration of the logic would make possible a much smaller and more flexible digital computer. In the course of a development program for such a machine, a large number of computer circuits and techniques were conceived, many of which found their way into the EDVAC.[2–4] A few of these circuits are described below. They are adding and counting circuits which, with one exception, do not use Eccles-Jordan-type trigger circuits. The one circuit which uses an Eccles-Jordan-type trigger circuit does so in an unconventional manner.

Representation of Information[3,4]

In the EDVAC there are two types of information, numbers, and orders. The orders tell the EDVAC what to do with the numbers. These two types of information can be represented by "words." A word consists of 44 binary digits,[5] where the binary digit "1" is represented by a voltage pulse and the binary digit "0" is represented by the absence of a pulse. For example, a string of forty-four "1"'s would be represented by a temporal array of pulses about 0.3 microsecond wide (standard width) and spaced one microsecond apart. Since the numerical value assigned to a pulse or a "no pulse" or blank depends on its position in time, a time reference is provided by a crystal-controlled timing unit called the "Timer,"[6] which divides machine time into periodically recurring intervals of 48 microseconds duration called "minor cycles." Each minor cycle is further divided into 48 equally spaced-in-time positions called pulse positions, 44 of which can be occupied by the pulses or

* Decimal classification: 621.375.2. Original manuscript received by the Institute, December 4, 1950; revised manuscript received, April 24, 1951.

† Moore School of Electrical Engineering, University of Pennsylvania, Philadelphia, Pa.

[1] ENIAC: Electronic Numerical Integrator and Computer, designed and constructed by the University of Pennsylvania, Moore School of Electrical Engineering, for the Ordnance Department, Department of the Army, under Contract No. W-670-ORD-4926.

[2] EDVAC: Electronic Discrete Variable Computer, designed and constructed by the University of Pennsylvania, Moore School of Electrical Engineering, for the Ordnance Department, Department of the Army, under Contract No. W36-034-ORD-7593.

[3] G. W. Patterson, R. L. Snyder, L. P. Tabor, and I. Travis, "The EDVAC—A Preliminary Report on Logic and Design," University of Pennsylvania, Moore School of Electrical Engineering, Research Division Report 48-2; February 16, 1948.

[4] EDVAC Staff, "A Functional Description of the EDVAC," vols. I, II, University of Pennsylvania, Moore School of Electrical Engineering, Research Division Report 50-9; November 1, 1949.

[5] H. E. Buchanan and L. C. Emmons, "A Brief Course in Advanced Algebra," Houghton Mifflin Co., Boston, Mass., pp. 169–179; 1937. This book contains a lucid explanation of number bases, conversion from one base to another, and so on.

[6] R. M. Goodman, "A digital computer timing unit" (completed manuscript to be submitted for publication in the near future).

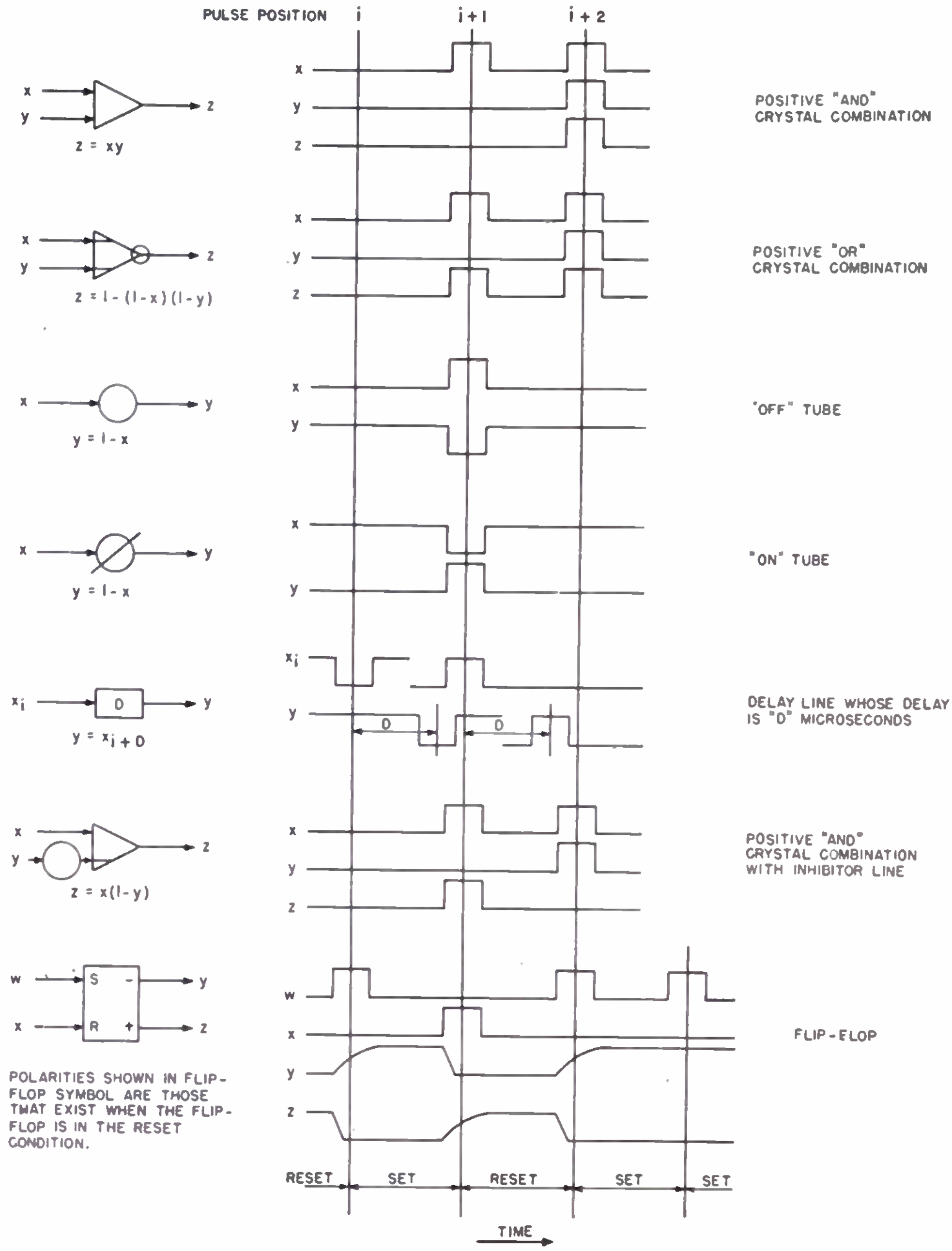

Fig. 1—Standard symbols for block diagrams.

blanks of a word. The computing circuits of the EDVAC should know the algebraic sign of a number as soon as possible. Consequently, the sign pulse occupies the earliest pulse position of a word. Since the addition and subtraction processes begin with the least significant digits and carries are propagated to the more significant digits, the circuits to be described require that the least significant digits of the word occupy the earliest pulse positions after the sign.[7]

[7] In the EDVAC, numbers are represented by their absolute magnitudes and the algebraic sign. It is believed that the EDVAC was once unique in this respect. In the ENIAC, for example, negative numbers are represented by their complements (with respect to 10^{10}) and the sign.

Standard Symbols for Block Diagrams[4]

A device as complex as the EDVAC (3,563 tubes) would present a formidable task in design, or to one trying to understand its functions, if the circuit schematics were the only graphical aids available. For this reason it is simpler to refer to block or logical diagrams using symbols such as those in Fig. 1. The first column of Fig. 1 shows the symbols for circuit components which perform certain fundamental operations. Under each symbol there is an equation, obtained from Boolean algebra,[8] which provides essentially the same

[8] A form of Boolean algebra known as the propositional (or statement) calculus is appropriate here. Numerous notations have been

information as shown in the second column of Fig. 1. The variables in these equations obey all the laws of ordinary algebra, but take on only the values zero and one, from which it follows that $x^2 = x$ and that $(1-x)^2 = (1-x)$.

Half Adder-Subtracter

The half adder-subtracter performs the operations of addition and subtraction of binary digits. The rules of binary addition and subtraction are shown in Table I. The symbols m, s, u, c, and b are defined on Fig. 2. A simplified block diagram of a half adder-subtracter is shown in Fig. 2, and is built up from the standard symbols in Fig. 1. The CP (Clock Pulses) are pulses of standard width with a repetition frequency of one mc and are one of the outputs of the Timer. They are used here to "clock," that is, to retime and reshape, and can be represented by "1" in our equations. Application of the Boolean algebra to Fig. 2 shows that

$$c = ms \tag{1}$$

$$u = m + s - 2ms \tag{2}$$

$$b = s(1 - ms) = s(1 - m). \tag{3}$$

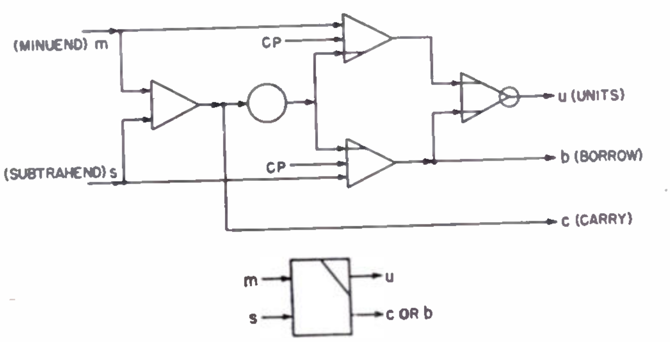

Fig. 2—Half adder-subtracter and its symbol.

Substitution of the appropriate values of m and s in the above equations shows that they present the same information as contained in Table I. This demonstrates that the half adder-subtracter actually does the operation of adding or subtracting the digits represented by the pulses in corresponding pulse positions. However, the half adder-subtractor cannot be used alone to perform the operations of adding and subtracting words, but two of them can be connected as in Fig. 3 to perform these operations. The EDVAC computers are built around such an adder-subtracter. The half adder-subtracter has also been used for other purposes, e.g., to test for equality of two words. One way of doing this is to perform a subtraction and see whether or not the answer is zero. However, the same function can be performed by the half adder-subtracter. Two words are equal if the information in all corresponding pulse positions is the same. Equation (2) says that if m and s are always the same, u is always zero. The EDVAC has two identical computers, and half adder-subtracters are used to compare words continuously at corresponding points in the two computers. If a disagreement is noted, the output of the half adder-subtracter detecting the disagreement is used to notify the operator.

TABLE I

m	s	u	c	b
0	0	0	0	0
0	1	1	0	1
1	0	1	0	0
1	1	0	1	0

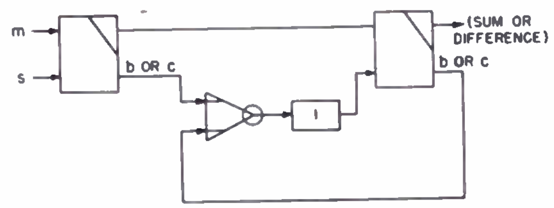

Fig. 3—Binary adder or subtracter.

The half adder-subtractor can also be used for complementing digits. Suppose a CP is applied to m. After substitution of 1 for m in (2), $u = 1 - s$. Thus, if s is 1, u is zero, and vice versa. However, it should be pointed out that if the half adder-subtracter were replaced by an off tube or an on tube, the digits of s would not be complemented, even though this form of Boolean algebra implies that they are.

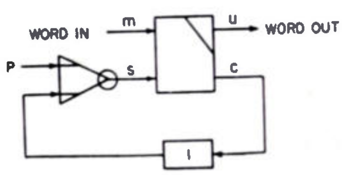

Fig. 4—Computer round-off adder.

Computer Round-Off Adder

The half adder-subtracter as shown in Fig. 4 is being used to add one to a word (which may be a number

---

used, e.g., George Boole, "The Mathematical Analysis of Logic," MacMillan, Barclay, and MacMillan, Cambridge; 1847. George Bell, London; 1847. Philosophical Library reprint, New York; 1948.

Claude E. Shannon, "A symbolic analysis of relay and switching circuits," *Trans. AIEE*, vol. 57, 713–723; 1938.

Harvard Computation Laboratory Progress Reports 1–5, "Investigations for Design of Digital Calculating Machinery;" May 10, 1948–August 10, 1949.

Alfred Tarski, "Introduction to Logic," Oxford University Press; 1941.

W. V. Quine, "Mathematical Logic," (Ed. 2), Harvard University Press, Cambridge, Mass.; 1947.

A markedly different approach to the algebra of computing devices and numerous other systems has been developed by the author's colleague Professor George W. Patterson. No description has been published as yet, but an outline appears in G. W. Patterson's, "Logical Syntax and Transformation Rules," University of Pennsylvania, Moore School of Electrical Engineering, Research Division Report 50-8; October 10, 1949.

represented as an absolute value) entering at m. This circuit has been used in the EDVAC to perform round-off. It is instructive to consider an example. The pulse P occurs at the same time as the first pulse position of the word at m. Using subscripts to identify the variables for different pulse positions,

$$P_i = 1 \quad \text{if } i = 1$$

$$P_i = 0 \quad \text{if } i \neq 1$$

$$m_i = s_i = 0 \quad \text{if } i \text{ is less than } 1.$$

Now from (2)

$$u_i = m_i + s_i - 2m_is_i$$

and

$$c_i = m_is_i \quad \text{for all } i.$$

But

$$s_i = P_i + c_{i-1} - P_ic_{i-1}.$$

Therefore,

$$s_i = 1 \quad \text{if } i \text{ equals } 1,$$

and

$$s_i = c_{i-1} = m_{i-1}s_{i-1} \quad i > 1.$$

Consider the word at m to be 111011;

$$m_1 = 1,\ m_2 = 1,\ m_3 = 0,\ m_4 = 1,\ m_5 = 1,\ m_6 = 1.$$

Then

$$s_1 = 1,\quad s_2 = 1,\quad s_3 = 1,\quad s_4 = 0,\quad s_5 = 0,\quad s_6 = 0$$

and

$$u_1 = 0,\quad u_2 = 0,\quad u_3 = 1,\quad u_4 = 1,\quad u_5 = 1,\quad u_6 = 1.$$

Therefore the word at u is 111100, which is 111011 plus 1.

An Operation Counter

A counter contains a device to remember a total and an adder to add one to the total when it is desired to do so. Thus, if the above adder which adds one to a word

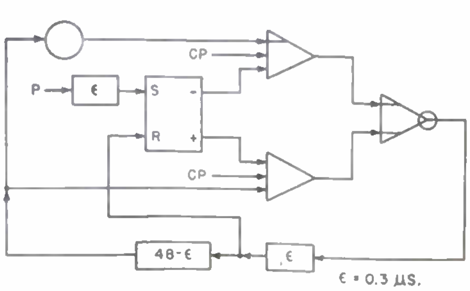

Fig. 5—Operation counter.

is made to remember the word by connecting its u output through a suitable delay to its m input, it becomes a counter. The mechanism of adding one to a word, such as in the example above, can be phrased in another way: A one is replaced by a zero beginning with the least significant digit; when the first zero is reached, it is replaced by a one; the remaining digits are not disturbed. Fig. 5 shows a counter using this principle. It has performed in the EDVAC at least a million operations without failure.

A Binary Counter

The half adder-subtracter can be used to make a single stage binary counter which is shown in Fig. 6. It has two stable states, one of them being the state in which there is no pulse in the one microsecond memory loop and which is called the "zero" state and the other

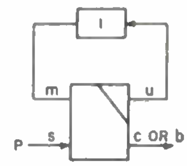

Fig. 6—Binary counter.

being the state in which there is a pulse in this loop (the "one" state). It will be shown below that the counter will remain in a given state until a pulse is applied at s, at which time it will change to the other state. When it returns to the "zero" state, a pulse is emitted at c; when it goes to the "one" state, a pulse is emitted at b. Using subscripts referring to the clock-pulse times on the Boolean variables, from (1), (2), and (3) it follows that

$$c_i = m_is_i$$

$$u_i = m_i + s_i - 2m_is_i$$

$$b_i = s_i(1 - m_is_i).$$

But

$$m_{i+1} = u_i \quad \text{for all } i.$$

Now if

$$s_i = 0 \quad \text{for all } i,$$

then

$$c_i = 0, \quad u_i = m_i = m_{i+1}.$$

Thus, if m_i is zero for any i, m_i is zero for all i; and if m_i is one for any i, m_i is one for all i showing the existence of two stable states. Now if the counter is in the "zero" state, $m_i = 0$.
Then

$$c_i = 0, \qquad u_i = s_i = m_{i+1}, \qquad b_i = s_i.$$

If s is pulsed at time j,

$$s_j = 1, \qquad (s_i = 0 \text{ for } i \neq j).$$

Then

$$c_j = 0, \qquad u_j = 1, \qquad m_{j+1} = 1, \qquad b_j = 1,$$

and the counter is in the "one" state at time $j+1$. Now if the counter is in the "one" state, then

$$c_i = s_i, \qquad u_i = 1 - s_i = m_{i+1}, \qquad b_i = s_i(1 - s_i);$$

and if s is pulsed at time j, $s_j = 1$ ($s_i = 0$ for $i \neq j$). Then

$$c_j = 1, \qquad u_j = 0, \qquad m_{j+1} = 0, \qquad b_j = 0,$$

and the counter is in the "zero" state at time $j+1$.

Now if the c output is connected to the s input of another single-stage binary counter of this type, and the c output of this second stage is connected to the s input of a third stage, and so on, there results a multi-stage binary counter which can be triggered at the clock-pulse frequency and at any submultiple of it. On the other hand, if the b output is connected to the s input of a second stage and so forth, there results a very unusual type of multistage binary counter which cycles backwards, that is, every time it is pulsed, one is subtracted from its contents. The two last possibilities are illustrated in Fig. 7.

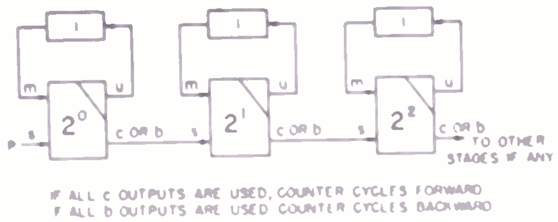

Fig. 7—Multistage binary counter.

Conclusion

Circuits using the principles of operation of the half adder-subtracter can be used for many of the adding and counting operations performed in a digital computer. All of the circuits described have been tested and put into operation in the EDVAC except for the single-stage binary counter and its descendants which are to be used in another computer under development.[9] These circuits have been reduced to their simplest logical terms in order to clarify the presentation. Vacuum-tube pulse amplifiers, additional delay lines required for proper timing and inhibiting, and similar paraphernalia have been omitted.

Acknowledgments

The material reported in this paper represents the efforts of many individuals whose work is inextricably mixed in the final results. It is unfortunate that it has been impossible to delineate the contributions of various present and former associates, and the author hopes this note will compensate for a lack of more direct acknowledgement.

[9] This counter and its descendants have been developed by the University of Pennsylvania, Moore School of Electrical Engineering, for the Signal Corps, United States Army, under Contract No. DA36-039-sc 14.

CORRECTION

Seymour B. Cohn, author of the paper, "Determination of Aperture Parameters by Electrolytic-Tank Measurements," which appeared on pages 1416-1421 of the November, 1951 issue of the Proceedings of the I.R.E., has brought to the attention of the editors errors in Table 1 of that paper. The corrected table appears in its entirety.

TABLE 1

Values of M/l^3

	$\frac{w}{l} = 0.1$	0.15	0.2	0.25	0.3	0.35	0.5	0.75	1.0
Rectangle	0.0645	0.0780	0.0906		0.1139		0.1575	0.2096	0.2590
Rounded slot	0.0610	0.0711	0.0801		0.0964		0.1222	0.1455	0.1667
Cross	0.0611	0.0728	0.0832	0.0930		0.1093			0.1667
Rosette	0.1028	0.1172	0.1282	0.1368	0.1434				0.1667
Dumbbell*	0.0610	0.0675	0.0757	0.0848	0.0932	0.1012	0.1208		0.1667
H-shape	0.1358	0.1426	0.1442	0.1418			0.1222		

* Width of bar = $0.1l$.

Reduction of Interference in FM Receiver by Feedback Across the Limiter*

R. M. WILMOTTE†, FELLOW, IRE

Summary—Described in this paper is the theory of a feedback circuit around a limiter of an FM receiver, which has the effect of reducing the interference caused by an undesired signal of nearly equal intensity to the desired signal.

Theory of Operation

When two FM signals, covering the same frequency band, or at least having overlapping frequency bands but different amplitudes, are passed through a limiter, the radio-frequency output comprises principally the stronger signal with an amount of distortion dependent on a number of factors which include the ratio of the intensities of the two signals. If this signal output is fed back at some point of the system on the input side of the limiter, its effect will therefore be quite different from the well-known effects of applying feedback in an AM amplifier.

It was found that a suitable feedback across a limiter has the capability of reducing the amount of distortion in the output of the limiter, or alternatively, of permitting the ratio of the desired to the interfering signal to be decreased. Signals as close to each other as 1 or 2 db have been substantially separated. The explanation of this result is as follows:

A typical vector diagram is shown in Fig. 1. In this diagram OA is the stronger of the two FM signals. AB is the vector for the weaker. If OA is represented as stationary, then the vector AB rotates at a frequency equal to the difference in frequency between the two FM signals. If this corresponds to q radians per second, then

$$q = d\theta/dt. \tag{1}$$

The signal which is fed back from an ideal limiter is constant in amplitude. It is represented in Fig. 1 by the vector $C'O$, the point C' lying on the circumference of a circle of radius x and center O. This vector referred to as X' must terminate on the circumference of a circle because its amplitude is constant. The input to the limiter is the resultant R' of the vectors a, b, and X', and is therefore represented by $C'B$. The output of the limiter is in phase with R'.

The feedback vector X' is related to the input vector to the limiter R' solely by the characteristics of the feedback circuit. If this phase difference is zero, the vector diagram is $COABC$, with CB (representing R) in line with CO (representing X). If the phase of R' lags an angle α behind X', the vector diagram is $C'OABC'$, X becoming X' and R' making an angle α with X'.

ϕ_R and ϕ_x are the angles that R' and X' make with the vector for the larger of the two signals represented by OA. The angle between the vector OB and OA is

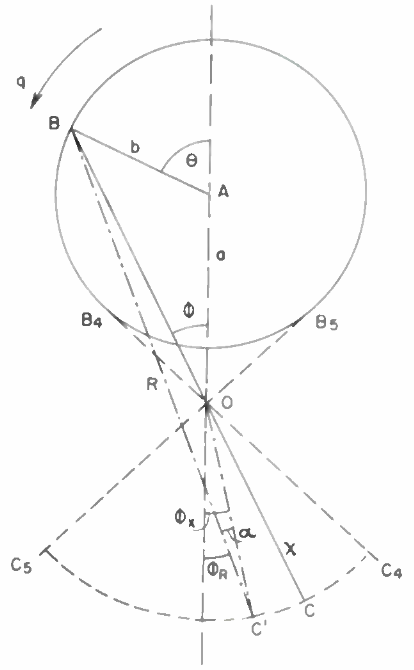

Fig. 1—Vector diagram of feedback operation.

ϕ. Either R' or X' may be applied to the discriminator as the designer may decide, although X' is preferred.

ϕ_R or ϕ_x, as the case may be, is the phase shift of the input of the discriminator relative to that of the desired signal. The differential of that phase shift with respect to time is therefore the distortion produced by the interfering signal when the amplitude variations are eliminated by the limiter.

Taking the more general case of R' and X' being out of phase by an angle α, it can readily be shown, if a is made unity that

$$\frac{1}{q}\frac{d\phi_R}{dt} = \frac{b\cos(\theta-\phi_R) - x\cos\alpha\dfrac{d\alpha}{d\theta}}{\cos\phi_R + b\cos(\theta-\phi_R)} \tag{2}$$

and

$$\frac{1}{q}\frac{d\phi_x}{dt}$$

$$= \frac{b\cos(\theta-\phi_R) - \left[\cos\phi_R + b\cos(\theta-\phi_R) + x\cos\alpha\right]\dfrac{d\alpha}{d\theta}}{\cos\phi_R + b\cos(\theta-\phi_R)}. \tag{3}$$

* Decimal classification: R361.111. Original manuscript received by the Institute, September 15, 1950; revised manuscript received May 21, 1950.

† 1469 Church St., N. W., Washington 5, D. C.

If the vector diagram repeats itself every revolution of the vector b as it must do when a steady state has been reached, then

$$\int_0^{2\pi} \frac{d\phi_R}{dt} d\theta = 0 \quad \text{and} \quad \int_0^{2\pi} \frac{d\phi_x}{dt} d\theta = 0. \tag{4}$$

This means that if the whole of $d\phi_R/dt$ or $d\phi_x/dt$ is accepted by the discriminator circuit the average distortion due to the presence of the weaker FM signal b is zero over each complete rotation of the vector AB. In practice, when the weaker signal b is nearly equal to the strong signal a, $d\phi_R/dt$ will reach higher peaks than $d\phi_x/dt$. It is therefore preferable to apply the vector X' rather than the vector R' to the discriminator.

If the discriminator can accept the whole of $d\phi_x/dt$ without appreciable distortion or cutting off, then the audio output will be substantially free from distortion from the weaker signal b. With perfect operation the remaining distortion would then be due only to the distortion occurring within a single revolution of the vector AB, and will therefore comprise only harmonics of the beat frequency. There may also be a distortion due to the initial stage before a steady state is reached. Since the amplitudes are relatively small with the feedback circuit and the frequencies are frequently beyond the acceptance of our senses, this remaining distortion will in general be small, and certainly much reduced as compared with the distortion obtained without the feedback circuit.

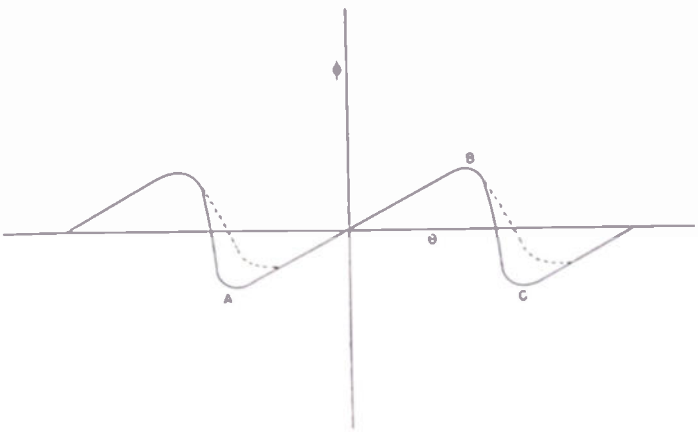

Fig. 2—Relation of phase of weaker signal to resultant of input to system, with and without feedback.

A typical curve of the relationship between ϕ and θ is shown in Fig. 2. During the period A to B, ϕ varies relatively slowly. This corresponds to the point B in Fig. 1 moving from position B_5 around the greater part of the circle to position B_4. But as B moves from B_4 to B_5 through the smaller arc, the change of ϕ is much more rapid, as shown by the steep part BC of the curve. The steepness of this part increases rapidly as the ratio of the intensity approaches unity. In fact, the maximum gradient increases in proportion to $a/(a-b)$.

If a feedback circuit is inserted around the limiter and that circuit contains a band-pass filter wide enough to carry the intelligence contained in Signal A, but not much more, the circuit will follow the changes in the phase ϕ quite closely over the portion AB while ϕ is changing only slowly; but when ϕ changes rapidly during the portion BC, it may not be able to do so. Instead it will follow a value, shown by a dotted curve, which corresponds to ϕ_x instead of ϕ.

This means that the angle α between R' and X' changes in value while the value of ϕ changes rapidly. The change in that value is represented by the difference between the dotted line and the solid line in Fig. 2.

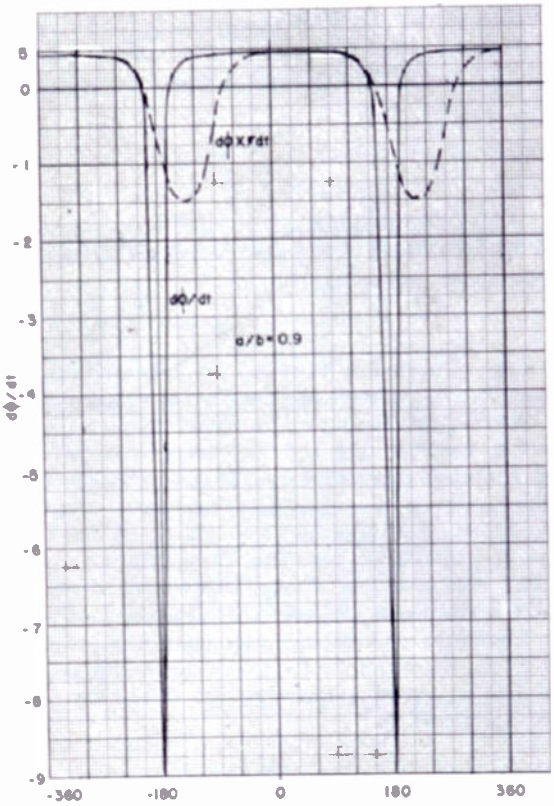

Fig. 3—Rate of change of phase, with and without feedback.

The important feature of this feedback system is that the vector X' cannot contain frequencies or large values of $d\phi/dt$ that fall outside of the band-pass of the filter of the feedback circuit. Therefore, the phase angle ϕ_x cannot change very rapidly, even during those short periods that ϕ changes rapidly as it does around the condition $\theta=\pi$ and particularly when the ratio of the signal vectors (b/a) is nearly equal to unity. Fig. 3 shows the curve for the variation of $d\phi/dt$ with θ when the ratio of b/a is 0.9. The tremendous spike that is produced near $\theta=\pi$ cannot be carried without distortion by a normal discriminator, for the spike corresponds to frequencies far beyond the linear portion of the discriminator characteristics. Distortion will therefore occur in an ordinary circuit since it is only if the full spike is carried that condition (4) will hold. Arguimbau[1] has

[1] L. B. Arguimbau and J. Granlund, *Electronics*, vol. 22, pp. 101–103; December, 1949.

proven this practically by using very wide-band discriminator characteristics.

If, however, an inverse feedback circuit is used with a limited frequency response and if the voltage corresponding to the vector X' is applied to the discriminator, condition (4) still holds when a steady state has been reached. The frequency limitation of the filter has the effect of blunting the spike and at the same time spreading it out. The filter circuit is designed to reduce the amplitude of the transient inherent in the spike and to attenuate its effect as rapidly as possible.

A block diagram of the circuit is shown in Fig. 4, on which the corresponding vector of Fig. 1 is indicated at each point of the circuit.

It is believed that this circuit may prove particularly useful when dealing with wide-band transmission.

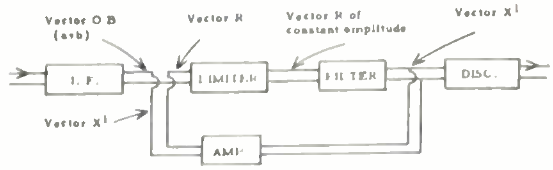

Fig. 4—Block diagram of circuit.

Acknowledgments

Mr. Gregory Harmon assembled some circuits which produced results indicated by the above theory. He was able to separate adequately FM signals which had a ratio of amplitude of less than 2 db. Closer ratios could probably have been used if flatter IF amplifiers had been available.

Quartz-Crystal Measurement at 10 to 180 Megacycles*

E. A. GERBER†, ASSOCIATE, IRE

Summary—**A method is described for measuring the equivalent parameters of both the main and spurious modes of very high-frequency crystal units. The crystal is placed between the plate and cathode of an amplifier tube, and the voltage developed across it is recorded as a function of frequency. The series resistance R_s can be obtained by comparing the resulting voltage peaks with the voltage developed across a pure capacitive load. The series capacitance C_s is measured by recording the resonance curve with the crystal unit in circuit, and then recording a second resonance curve when the capacitance across the crystal unit has been increased by a known amount. The frequency difference between the two curves gives a measure for C_s. Correction functions are derived for evaluating the recorded data for crystal units having high R_s and low reactance of the static capacitance C_0.**

I. Introduction

As Van Dyke[1] has shown, the electrical behavior of a piezoelectric crystal can be described by its equivalent circuit, consisting of the series connection of an inductance L_s, capacitance C_s, and resistance R_s in parallel with the static capacitance C_0. This circuit corresponds to the main resonance frequency of the crystal. At very high frequencies, the frequency spectrum of a crystal is rather complicated. It shows, besides the main resonance frequency, a multitude of other resonance frequencies which would be represented by similar networks more or less coupled together, as well as to the network representing the main response.

The most important task in producing crystals for very high frequencies is to eliminate, or at least to reduce, the spurious responses. To be able to perform this task, measuring equipment is necessary which not only surveys the crystal spectrum but allows simultaneous measurements of the equivalent parameters of the main and spurious responses.

This paper discusses such equipment, and gives a brief description of a unit developed and built at the Signal Corps Engineering Laboratories for the 10-mc to 180-mc frequency range.

II. Principles of Operation

A. Measurement of the Series Resistance R_s

Because voltages, if not too small, may be measured without great difficulties even at high frequencies, an antiresonance arrangement is used, as shown in Fig. 1. The crystal is placed between the plate and cathode of an amplifier tube, and the voltage e_p is measured. As the frequency of the signal generator is changed, the recording of the plate voltage e_p will appear as in Fig. 6.

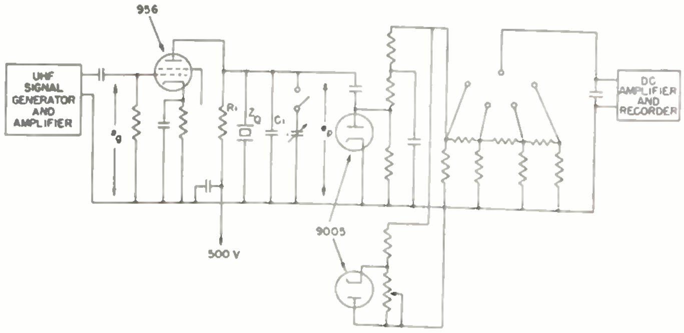

Fig. 1—Principal circuit diagram of the unit.

If the resistance R_1 and the reactance of C_1 are both larger than the series resistance R_s at the operating fre-

* Decimal classification: R214.211. Original manuscript received by the Institute, June 8, 1950; revised manuscript received May 10, 1951.

† Signal Corps Engineering Laboratories, Fort Monmouth, N. J.

[1] K. S. Van Dyke, "The electric network equivalent of a piezoelectric resonator," *Phys. Rev.*, vol. 25, p. 895; 1925.

quency $\omega/2\pi$ of the crystal, as is usually the case, then the antiresonance impedance of the crystal unit is very close to the "performance index"[2]

$$PI = (\omega^2 C_1^2 R_s)^{-1}. \quad (1)$$

R_1 may include the plate resistance of the tube and the input resistance of the receiver, and C_1 may include all capacitances of the circuit and the static capacity C_0 of the crystal. By measuring e_p and e_g, it is possible to obtain PI if R_1 and the transconductance of the tube are known.[3]

To avoid determining the transductance, however, it is preferable to compare the antiresonance peak of the plate voltage e_{p_1} with the plate voltage e_{p_2} away from any resonance point (see Fig. 6). The latter voltage is developed across a pure capacitive load because the internal resistance R_1 of the circuit is very much larger than the reactance of the capacitance C_1. We then have

$$\frac{e_{p_1}}{e_{p_2}} = \omega C_2\left(\frac{1}{PI} + \frac{1}{R_1}\right)^{-1}. \quad (2)$$

The capacitance is now called C_2 because it may in general be different from the capacitance C_1. To make e_{p_2} large, C_2 should be made small, such as by removing the crystal unit from its socket; then C_2 is the circuit capacitance as seen from the crystal socket. From (2), PI and R_s may be obtained.

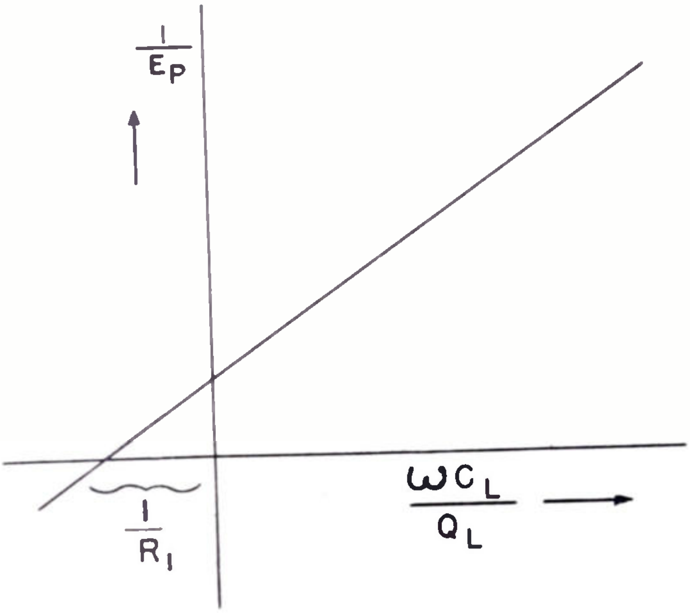

Fig. 2—Method for measuring internal resistance R_1.

For determining R_1 the following method is satisfactory. The crystal unit is replaced by one of several coils chosen so as to obtain for one given frequency at least three different readings, corresponding to resonance, on the dial of a tunable condenser in parallel with the crystal unit. In this case, the formula for the amplification is

$$g_m \frac{e_g}{e_p} = \frac{\omega C_L}{Q_L} + \frac{1}{R_1}. \quad (3)$$

Q_L is the quality factor of the coil measured in a bridge or in a Q-meter at the frequency $\omega/2\pi$, and C_L is the capacitance which resonates with the coil at the same frequency. If we plot $\omega C_L/Q_L$ for the different values of C_L/Q_L against $1/e_p$ (g_m and e_g are constant), we obtain a straight line (see Fig. 2) whose intersection with the abscissa gives $1/R_1$. This measurement needs to be done at different frequencies to obtain values of R_1 over the frequency range.

B. Frequency Calibration on Recording Tape

For determining the distance between the resonance frequencies of a crystal, it is necessary to have a frequency calibration of the recording. That is easily done by amplitude modulating the signal generator by means of a known audio frequency. The distance between one sideband and the main response furnishes a frequency mark which can be used for the calibration of the whole recording, provided that the generator sweep is linear.

C. Measurement of the Quality Factor Q and Series Capacitance C_s

The quality factor $Q = 1/\omega C_s R_s$ and, therewith, C_s may be measured by determining the width $\Delta\omega$ of the resonance curve between two points whose ordinates are $1/\sqrt{2}$ times the value of the maximum ordinate. The magnitude of Q is that of the ratio $\omega/\Delta\omega$. The quality factor is effectively that of the crystal unit if $R_1 \gg (\omega^2 C_1^2 R_s)^{-1}$.

In many cases, however, the resonance curves are too narrow for obtaining an exact measurement of Q. The following method, which does not require that the value of R_s be known, is preferable in these cases for the measurement of C_s. The resonance curve of the crystal unit is recorded; C_1 is then increased by ΔC_1, making the resulting antiresonance frequency of the circuit, including the crystal unit, lower than the first antiresonance frequency. This resonance curve is then recorded. The frequency difference $(\omega - \omega_1)/2\pi = \Delta\omega/2\pi$, between the two curves taken from the recording, is a measure of the value of C_s according to the equation

$$C_s = 2\frac{\Delta\omega}{\omega}\frac{C_1}{\Delta C_1}(C_1 + \Delta C_1). \quad (4)$$

III. Correction Functions

For the validity of (2) and (4), the same restrictions are in force as for (1). If these conditions are not fulfilled, i.e., if

$$\left.\begin{matrix} R_1 \\ \dfrac{1}{\omega C_1} \end{matrix}\right\} \gg R_s$$

[2] C. W. Harrison, "The measurement of the performance index of quartz plates," *Bell Sys. Tech. Jour.*, vol. 24, pp. 217–252; April, 1945.
R. A. Heising, "Quartz Crystals for Electrical Circuits," D. Van Nostrand Co., New York, N. Y., pp. 458–492; 1945.

[3] This method for measuring R_s of high-frequency crystals was first used by H. Heinzmann in his unpublished dissertation, Jena, Germany, 1938.

does not hold true, more complicated expressions must replace the above-mentioned equations. In order to make the above method applicable to high frequencies where $1/\omega C_1$ is small, correction functions have been derived by means of conformal representation which give the correct results when incorporated into (2) and (4).

$$\frac{e_{p1}}{e_{p2}} = \frac{\omega C_2}{\omega^2 C_1^2 R_s + \frac{1}{R_1}}(1 + f_1) \tag{5}$$

$$C_s = 2\frac{\Delta\omega}{\omega}\frac{C_1}{\Delta C_1}(C_1 + \Delta C_1)(1 + f_3). \tag{6}$$

$(1+f_1)/(\omega^2 C_1^2 R_s + 1/R_1)$ is none other than the absolute peak value of the total impedance, $|W_m|$, as measured. Therefore, we have for R_s

$$R_s = \frac{1}{\omega^2 C_1^2}\left(\frac{1 + f_1}{|W_m|} - \frac{1}{R_1}\right). \tag{7}$$

R_1 can be included in the correction function f_1 to give another correction function f_2.

$$R_s = \frac{1}{\omega^2 C_1^2}\frac{1 + f_2}{|W_m|}. \tag{8}$$

f_1, f_2, and f_3 are functions of the relations: $k = R_s\omega C_1$ and $A = R_s/R_1$. Their exact derivation is given in the appendix. f_1 and f_3 are plotted in Figs. 3 and 4 as a function of k^2 for different values of A. In Fig. 4 the curves also are plotted for three different values of $C_1/\Delta C_1$. Looking at Fig. 3, we see that the error in measuring R_s is approximately 10 per cent for a value of k as large as $\sqrt{0.1}$. That means, for instance, that in the case of a 100-mc crystal with a C_1 of 15 $\mu\mu$f, we must apply corrections if R_s is expected to be larger than 35 ohms. If R_1 still remains larger than R_s (see Section IV c), the correction is simple because (7) or (8) gives us the following:

$$R_s = \frac{1}{\omega^2 C_1^2 |W_m|}\cdot\frac{1}{1 - 1/(\omega^2 C_1^2 |W_m|^2)}. \tag{9}$$

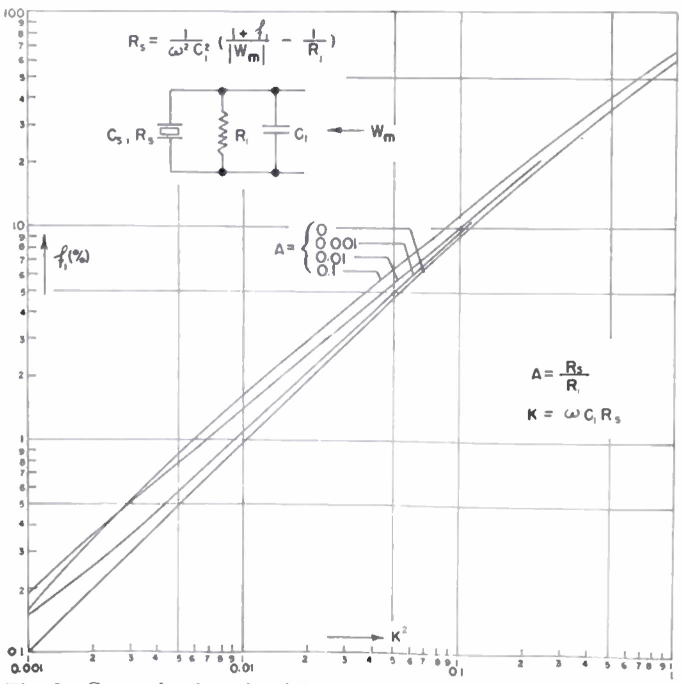

Fig. 3—Correction function f_1 for the purpose of correcting the result for the series resistance R_s if $\left.\begin{matrix}R_1\\1/\omega C_1\end{matrix}\right\} \gg R_s$ is not fulfilled. R_1 is not included in the correction function.

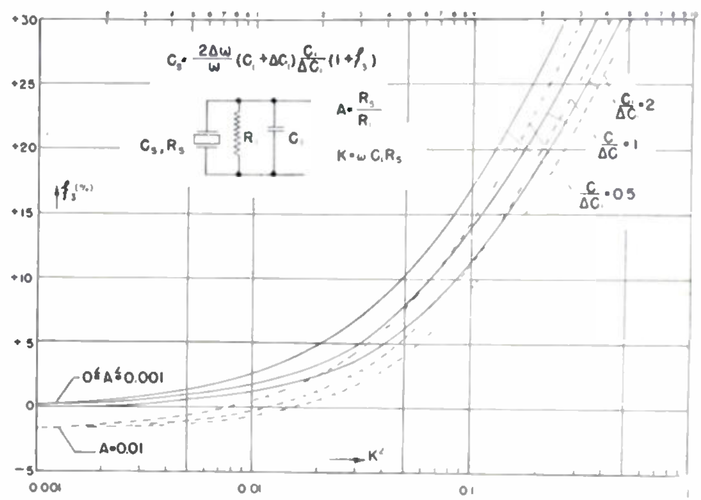

Fig. 4—Correction function f_3 for the purpose of correcting the result for the series capacitance C_s.

IV. Description of the Circuit

As mentioned in Section III, R_1 and $1/\omega C_1$ should be large in comparison with the series resistance R_s of the crystal in order to have the advantage of a very simple evaluation of the recordings. The following provisions were made for this purpose:

a. To achieve a high plate resistance, even at higher frequencies, the acorn tube type 956 was chosen. This tube has a satisfactory value of transconductance and a small grid-plate capacitance. It is important to keep the latter as small as possible for the Miller effect can change the rf grid voltage during measurement to a great extent.

b. A 100,000-ohm Ohmite "brown-devil" wire wound resistor was selected as the plate-coupling resistor. Its resistive value, as a function of frequency, is shown in Fig. 5. In order to have the proper value of dc voltage, a supply voltage of 500 volts was chosen.

c. To keep the input resistance of the rectifier high, and its input capacity low, the diode tube type 9005 with a high load resistor was selected. This resistor consists of the input resistance of the dc amplifier. Since the 715-A General Radio dc amplifier has a large input capacity, a resistance network has to be used between the diode and dc amplifier to minimize the influence of the input capacity on the crystal circuit.

d. Regarding the above requirements, it was possible to keep the circuit capacity C_2 (less the static capacity C_0

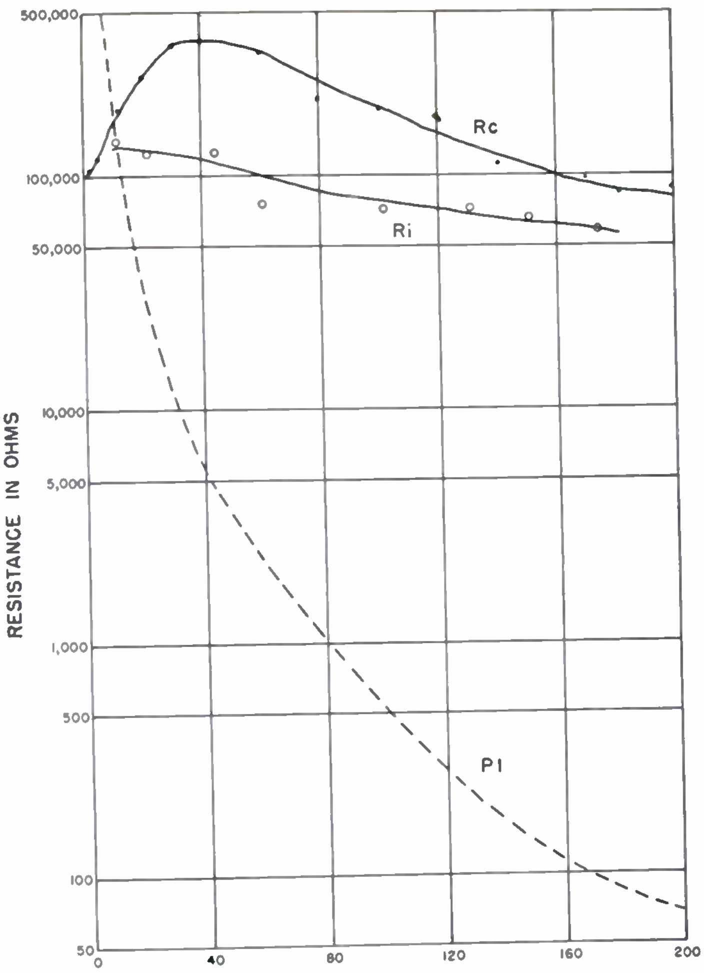

Fig. 5—Resistance of the plate coupling resistor R_c, internal resistance R_1, and maximum value of PI to be expected as a function of frequency.

of the crystal) down to 11 $\mu\mu$f, and the internal resistance R_1 larger than 50,000 ohms in the whole frequency range (see Fig. 5). R_1 was measured by using the method described in Section II A. For comparison, the maximum PI to be expected is also plotted in Fig. 5.

e. The principle of the measuring circuit is shown by the diagram of Fig. 1. A General Radio uhf Signal Generator, Type No. 804-B, is used as the source of driving voltage. A small two-plate tunable motor-driven capacitor is placed in parallel with the tuning capacitor.

The measuring unit itself consists of the following: a normal tuned uhf amplifier with a very broad resonance curve, the crystal stage with the diode for measuring e_p, an attenuation network for selecting the proper measuring range, the General Radio dc amplifier, Type No. 715-A, and an Esterline-Angus 5-ma recorder.

The residual current of the 9005 diode is compensated by another such diode; this was necessary because, when the measuring range is changed, the residual current alters the zero deflections. A constant-resistance attenuation network which is matched to the two diodes is used for selecting the correct measuring range. It is placed between the output of the diodes and the input of the dc amplifier. Thus, the output voltage of the diode can be divided by the factors, 2, 6, and 12. Together with the different measuring ranges of the dc amplifier a range of from 0.1 to 20 volts rf can be obtained.

V. Examples

Fig. 6 shows the recordings of the responses of three different polished AT-cut-crystal units. The following Table I gives the results for main and spurious modes calculated from the recordings with the aid of (5)

TABLE I

Frequency (mc)	C_0 $\mu\mu$f	$C_1=C_0+C_2$	ΔC_1 ($\mu\mu$f)	R_s (ohms)	C_s ($\mu\mu$f)	Q (from resonance curve)	Q (calculated from R_s and C_3)
32.18 (fundamental)	4.4	15.4	9.0	7.7	0.0080	75,000	80,000
30.20 (3rd harmonic)	28.5	39.5	22.5	14.0	0.0024	167,000	157,000
			Spurious modes	7.1	0.00415	185,000	180,000
				8.1	0.0040	150,000	160,000
157.7 (5th harmonic)	6.5	19.5	19.75	35	0.00093 (from Q)	31,000	
			Spurious mode	60			

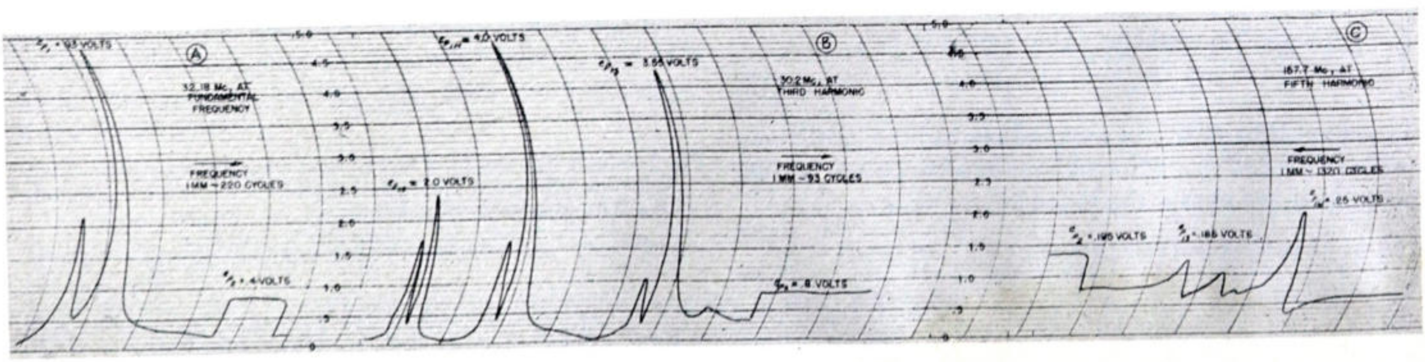

Fig. 6—Recordings of three crystals to illustrate the measuring method. The lines parallel to the frequency scale give the voltages e_{p_2} across a pure capacitive load. The peaks marked $e_{p_{1m}}$ are the main modes, and the peaks marked $e_{p_{1s}}$ are the spurious modes. The unmarked peaks in the recordings A and B are not spurious modes but resonance curves repeated with a larger parallel capacitance for measuring C_s (see Section II C).

and (6). The quality factor Q is first determined from the width of the resonance curve, and then it is calculated independently from R_s and C_s.

VI. Appendix: Calculation of the Correction Functions

Following Harrison,[2] conformal representation is felt to be a very convenient tool for circuit analysis involving crystals. The basis for this analysis is the equation of the linear fractional transformation,

$$W = \frac{\alpha + \beta Z}{\gamma + \delta Z}. \tag{10}$$

It can represent any impedance whose frequency of operation is controlled by a crystal. The terms α, β, γ, and δ are complex constants, and Z represents a complex variable whose value is a quadratic function of frequency. To obtain a linear relationship between Z and a frequency dependent x, not the frequency itself, but the detuning,

$$x = \frac{\omega^2}{\omega_s^2} - 1 \tag{11}$$

is introduced into the equation for the impedance W of the crystal unit plus R_1. Thus, we have the following for the different symbols of (10):

$$\alpha = R_s; \quad \beta = 1/\omega C_1; \quad \gamma = 1 + A + jk;$$
$$\delta = A/k + j; \quad Z = j\,x\,C_1/C_s. \tag{12}$$

$1/\omega C_1$ is assumed to be constant in the small frequency range under consideration.

W, the impedance variable, is a circle in the W-plane (see Fig. 7). $W_m = R + jX$ is the maximum impedance to be sought. Its absolute value amounts to

$$|W_m| = (\sigma^2 + \eta^2)^{1/2} + \rho. \tag{13}$$

Inserting into (13) the expressions for the center coordinates σ and η, and for the radius ρ whose calculation is omitted, we obtain the following for W_m:

$$|W_m| = \frac{1}{\omega^2 C_1^2 R_s + 1/R_1}\left[1 + \left(\frac{\sqrt{(1+2A)^2 + 4k^2} + 1}{2(1 + A^2/(k^2 + A))} - 1\right)\right] = \frac{1}{\omega^2 C_1^2 R_s + 1/R_1}\left[1 + f_1(A, k)\right]; \tag{14}$$

or, if we include R_1 in the error function f_1,

$$|W_m| = \frac{1}{\omega^2 C_1^2 R_s}\left[1 + \left(\frac{\sqrt{(1+2A)^2 + 4k^2} + 1}{2(1 + (A^2 + A)/k^2)} - 1\right)\right]$$
$$= \frac{1}{\omega^2 C_1^2 R_s}\left[1 + f_2(A, k)\right]. \tag{15}$$

For the purpose of finding an exact expression for C_s (see (6)) we calculate the detuning, x, corresponding to the maximum impedance, by transforming the maximum impedance point W_m into the Z-plane. Performing this operation yields

$$x = \frac{1}{2}\frac{C_s}{C_1}\left[(1 + 2A) + \{(1 + 2A)^2 + 4k^2\}^{1/2}\right]. \tag{16}$$

If C_1 is enlarged by the factor $a = 1 + \Delta C_1/C_1$, we have

$$x_2 = \frac{1}{2}\frac{C_s}{aC_1}\left[(1 + 2A) + \{(1 + 2A)^2 + 4a^2k^2\}^{1/2}\right]. \tag{17}$$

Subtracting (17) from (16), using the subscript 1 for (16), and solving for C_s finally yields

$$C_s = (x_1 - x_2)(C_1 + \Delta C_1)\frac{C_1}{\Delta C_1}\,2\left\{(1 + 2A)\left[\left(\frac{C_1}{\Delta C_1} + 1\right)\left(1 + \sqrt{1 + \frac{4k^2}{(1 + 2A)^2}}\right) - \frac{C_1}{\Delta C_1}\left(1 + \sqrt{1 + \frac{4k^2a^2}{(1 + 2A)^2}}\right)\right]\right\}^{-1}. \tag{18}$$

$x_1 - x_2$ may be approximated by $2\Delta\omega/\omega_s$, $\Delta\omega$ being the frequency difference between the two impedance maxima. Then we have the following for C_s:

$$C_s = 2\frac{\Delta\omega}{\omega_s}(C_1 + \Delta C_1)\frac{C_1}{\Delta C_1}\left[1 + f_3(A, k)\right]. \tag{19}$$

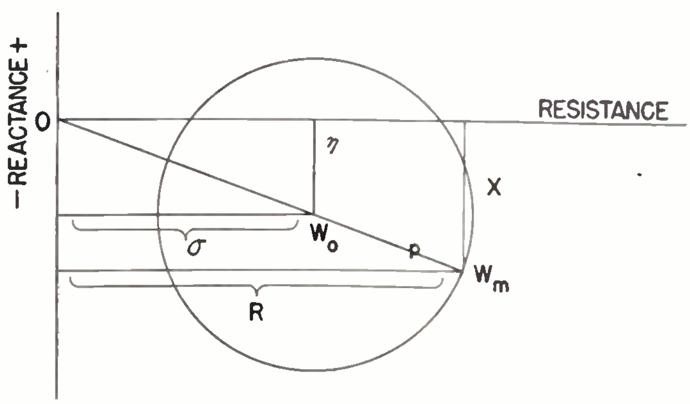

Fig. 7—Circle diagram for a crystal with a parallel resistance $1/\omega C_1$ is assumed to be constant; distance circle ordinate is exaggerated; W_m is the maximum impedance.

An Experimental High-Transconductance Tube Using Space-Charge Deflection of the Electron Beam*

J. T. WALLMARK†, ASSOCIATE, IRE

Summary—In the past, electron tubes have been built using either current density control or deflection control; the tube to be described uses a new principle combining both of these methods of operation, with control by a conventional grid. This grid controls the space charge in the usual manner, and the space charge produces a displacement of the electron beam from its space-charge-free path. By means of a fixed intercepting edge, this in turn can be converted into additional current variation at an anode. An analysis of this new principle has been made and demonstrates the possibility of an increase in both transconductance and the transconductance-to-plate-current ratio of the tube.

Experimental tubes of the orbital-beam type, utilizing this principle, have been built in nine-pin miniature envelopes. In the output structure, that portion of the beam which passes an intercepting edge enters a single-stage secondary-emission dynode and collector system. Transconductances of 25,000 micromhos have been obtained with only 3 ma output current. These values, particularly the transconductance-to-current ratio, are many times better than those obtained from an ordinary grid-controlled tube, and no increase in capacitances is involved. The measured equivalent noise resistance is about 900 ohms, and the gain-bandwidth product is 320 mc. Because of its mode of operation, the tube requires stable voltages and good mechanical alignment. However, neither of these requirements appears to be severe, and the high transconductance with low current and small capacitance should make this type of tube quite valuable for broad-band amplifier applications.

I. Introduction

Since World War II broad-band amplification has become increasingly important because of the growth of applications, such as navigational systems, radar, pulse communication, television, and so forth. This has led to some serious problems, caused by the shortcomings of present-day tubes. To meet the requirements for higher gain per stage and broader bandwidths, tubes are needed with high transconductance combined with small input and output capacitances. The figure of merit for an amplifying stage,[1] gain times bandwidth, requires that the tube have high transconductance-to-capacitance ratio. At the same time, it is always desirable to reduce tube noise so as to handle extremely small signals efficiently, and this additional requirement has also been more stringent since World War II.

The transconductance-to-capacitance ratio for a triode or screen-grid tube is, to a first approximation, proportional to $V_a^{1/2}/d$, where V_a is the anode (or screen-grid) potential and d is the cathode-to-control-grid distance.[2] Modern close-spaced tubes, however, are frequently operated under conditions where the space-charge laws are modified by considerable "island formation"[3] on the cathode and, in that case, the exponent for V_a is increased. For a given anode voltage, nevertheless, the transconductance-to-capacitance ratio can be improved only by reducing d. Practical economic considerations put a limit to d of the order of 0.004 inch $=0.1$ mm, as in the 6AK5,[4] although tubes have been built with still smaller d.[5] (Western Electric type 416A, $d=0.0006$ inch $=0.015$ mm).

One approach to the problem of constructing tubes with still higher transconductance-to-capacitance ratios has been the addition of one or more stages of secondary-electron multiplication to a grid-controlled tube.[6,7] In this manner, the transconductance is increased in proportion to the multiplication factor, while the capacitance remains substantially the same. Until recently,[8] this has led to several difficulties because the tubes required were more complicated and the change of secondary-emitting surface during life sometimes introduced a drift in the characteristics. Considerable improvement has now been made, and one may now consider, with less trepidation, the use of an electron multiplier. However, the introduction of the secondary-emission multiplier does not improve the signal-to-noise ratio. On the contrary, additional noise is caused by the multiplier section, and the signal-to-noise ratio is, therefore, slightly inferior to that of the grid-controlled tube, prior to introduction of the multiplier. Furthermore, the bleeder for the secondary-emitting electrode has to have a rather low ohmic resistance in order to

* Decimal classification: R339. Original manuscript received by the Institute, January 2, 1951; revised manuscript received, May 16, 1951. Presented, National IRE Convention, New York, N. Y., March 8, 1950.

† Formerly, Fellow of American-Scandinavian Foundation at RCA Laboratories Division, Radio Corporation of America, Princeton, N. J.; now, Royal Institute of Technology, Stockholm, Sweden.

[1] G. E. Vailey and H. Wallman, "Vacuum Tube Amplifiers," McGraw-Hill Book Co., New York, N.Y.; 1948 (especially chapters IV and the following).

[2] H. Rothe and W. Kleen, "Grundlagen und Kennlinien der Elektronenrohren," Leipzig, 1943 (especially chapters XVIII:3 and XXXVI:3).

[3] See chapter XXI:1 of footnote reference 2.

[4] G. T. Ford, "Characteristics of vacuum tubes for radar intermediate frequency amplifiers," *Bell Sys. Tech. Jour.*, vol. 25, p. 385; July, 1946.

[5] J. A. Morton, "A microwave triode for radio relay," *Bell Lab. Rec.*, p. 166; May, 1949.

[6] B. J. Thompson, "Voltage controlled multipliers," Proc. I.R.E., vol. 29, pp. 583–587; November, 1941.

[7] H. H. Wagner and W. R. Ferris, "The orbital-beam secondary-electron multiplier for u-h-f amplification," Proc. I.R.E., vol. 29, pp. 598–602; November, 1941.

[8] C. W. Mueller, "Receiving tubes employing secondary electron emitting surfaces exposed to the evaporation from oxide cathodes," Proc. I.R.E., vol. 38, pp. 159–164; February, 1950.

keep the voltage sufficiently stable; consequently, it has a large power consumption.

In the previous use of an electron multiplier with grid control, it is also soon found that limitations are encountered because of the low ratio of transconductance to current that can be achieved. This low ratio, at the same time, also contributes to the noise since the noise output is often related to the current. Within the past few years, it has been shown[9,10] that a high transconductance-to-current ratio and a low noise can be achieved by use of beam-deflection control. Straightforward beam deflection principles, however, require unusual tube-manufacturing techniques, and beam-deflection tubes have not yet been commercially produced. Even more complex beam-deflection methods have been devised[11] which also allow a high transconductance-to-current ratio, but these lead to fairly complicated structures and practicable tubes utilizing such ideas have not yet been made.

The following article describes a new principle for an amplifier tube which combines the advantages of both the control-grid type of tube and the deflection type of tube and, at the same time, is well suited for use with an electron multiplier. The new method, therefore, leads to high transconductance-to-capacitance ratios and excellent signal-to-noise ratio performance and uses a structure adaptable to mass-production techniques. The new solution uses an electron beam whose current (and hence its space charge) is controlled by a conventional grid. The controlled space charge, in turn, produces a displacement of the beam from its space-charge-free path. By means of a fixed intercepting edge, the beam displacement is converted into additional current variation at the anode. Thus, the ordinary transconductance of the control grid remains operative and an additional transconductance occurs because of the deflection by the space charge. For this reason the new principle has been called "space-charge beam deflection."

For those who are not interested in the mathematical details, the essential facts are concentrated in the next two sections.

II. The Principle of Operation

Let us assume a parallel-plane arrangement, as in Fig. 1. From the plane A, which has a positive potential, electrons are projected towards the other plane R, which has a potential low enough to reflect the electrons back to A. If the current density is so low that the space charge can be neglected, the electron path describes a parabola and the electrons return to A after having traveled a distance x_I parallel to the emitting plane.

On the other hand, if the current is increased, the space charge causes a distortion of the electric field be-

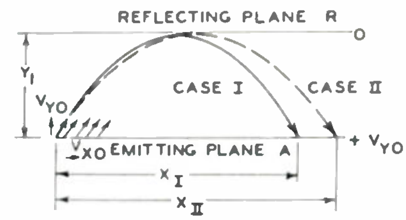

Fig. 1—Electron paths in the parallel-plane case.

tween A and R from the space-charge-free condition. A consequence of this is a corresponding distortion of the electron path; the electrons will return to A after having traveled a distance x_{II}, which is a function of the space-charge conditions.

This is analogous to the well-known increase in transit time in diodes with increasing space charge. Thus the increase in transit time allows the electrons to travel a longer distance.

Fig. 2 gives a simple technical realization of the principle described. Here a conventional tetrode structure, consisting of a cathode, a control grid, and a screen grid, sends a beam of electrons towards a reflecting plane.

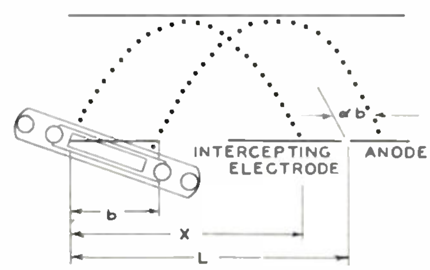

Fig. 2—Principle for practical application.

After reflection, the beam is collected by two electrodes, an intercepting electrode, and an anode. An increase of the beam current causes the beam path to shift, in the manner just described, so that a larger fraction of the beam is collected by the anode. A positive signal on the grid, therefore, causes the anode current to increase, both because the over-all current increases and because the anode fraction of the beam increases.

III. An Experimental Tube

Figs. 3 and 4 show the design of a practical tube to utilize this effect. The tube uses a combination of space-charge beam deflection and secondary-electron multiplication; this has several advantages. The input structure consists of a flat, indirectly heated oxide cathode, surrounded by the usual control and screen grids. The output structure consists of an intercepting electrode that also protects the anode from primary electrons. Those electrons not intercepted pass on to a secondary-emit-

[9] G. R. Kilgore, "Beam deflection control for amplifier tubes," *RCA Rev.*, vol. 8, pp. 480–505; September, 1947.

[10] E. W. Herold and C. W. Mueller, "Beam deflection mixer tubes for u-h-f," *Electronics*, vol. 22, pp. 76–80; May, 1949.

[11] J. L. H. Jonker and A. J. W. M. VanOverbeek, "Control of a beam of electrons by an intercepting electron beam," *Nature* (London), vol. 164, pp. 276–277; August 13, 1949.

ting electrode (dynode), and after multiplication, the secondary electrons are taken up by the anode. Between the input and output there is, for experimental purposes, an inner focusing electrode with which the focus of the beam and the main electric field can be somewhat influenced. The reflector has the shape of a cylinder surrounding the other electrodes. The over-all diameter of the internal tube structure is $\frac{5}{8}$ of an inch, and the tube is mounted in a 9-pin miniature envelope with a T-6$\frac{1}{2}$ bulb, as shown in Fig. 4.

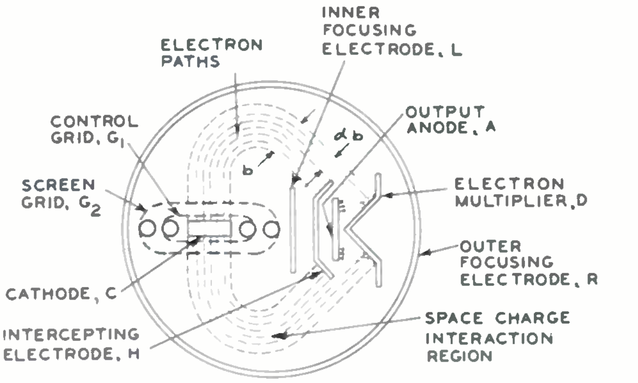

Fig. 3—Experimental tube utilizing space-charge beam deflection.

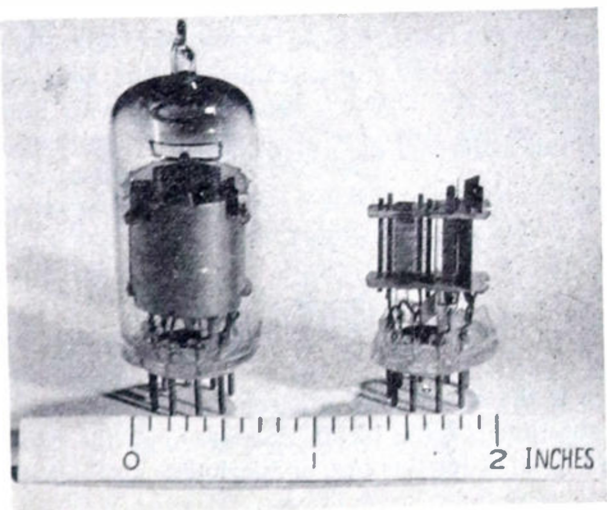

Fig. 4—Photo of the tube of Fig. 3.

The tube is, in some respects, similar to a multiplier type of tube known as the orbital-beam tube,[7] and it can be actually operated as such by a suitable choice of dimensions and voltages so that all the primary electrons hit the dynode. In that case, of course, the performance is that of a grid-controlled multiplier, only.

The space-charge beam-deflection tube presented here is not necessarily the best possible design for manufacture or use in circuits. Its construction was based on certain available parts with which the effect could conveniently be studied. However, the values, obtained from the measurements and given in Table I, are believed to be representative of what can be obtained in a practical tube.

The transconductance is 25 ma/v (25,000 micromhos) at an anode current of only 3 ma. The corresponding beam current is 2.8 ma, of which 1.7 ma are intercepted, and the remainder, multiplied by the secondary emission factor $\delta = 2.7$, constitutes the anode current. The improvement in transconductance is clear from a comparison of 25 ma/v with 15 ma/v, which could have been obtained under equal conditions in an ordinary multiplier (beam current 2.8 ma, $\delta = 2.7$, transconductance-to-current ratio of input structure = 2).

Along with the gain in transconductance comes the saving in current requirements, which leads to some secondary advantages. One is that the internal anode resistance can be made higher; another is a reduced current to the dynode, with improved life as a consequence.

Two more main advantages that will be described further in a later article are the low equivalent noise resistance, and some novel stabilizing circuits made possible by the low currents. The equivalent noise resistance is measured to be of the order of 900 ohms. The input capacity of the tube is 8.5 $\mu\mu$f, and the output capacity is 3.0 $\mu\mu$f.

The main disadvantages of the tube, at present, seem to be the sensitivity to voltage changes, intrinsic in all tubes with high transconductance-to-current ratios,[6] and the requirements of good mechanical alignment. Neither of these is believed to be severe.

[7] See footnote 6, p. 41.

TABLE I

COMPARISON OF HIGH-G_m TUBES

Tube Type	*Description*	*Transconductance* G_m *micromhos*	*Plate Current* I_p *ma*	*Ratio* $\frac{G_m}{I_p}$ $\frac{\text{Micromhos}}{\text{Milliampere}}$	*Equiv. Noise Res.* R_{eq} *ohms*	*Wide Band Sig./Noise* $\frac{1}{2\pi C_{in}R_{eq}}$ *megacycles*	*Wide Band Fig. M* $\frac{G_m}{2\pi C_T}$ *megacycles*	*Narrow Band Fig. M* $\frac{G_n}{(G_{in})^{1/2}}$ $(\mu mho)^{1/2}$
6AC7	TV amp pentode	9,000	10	900	700	16	68	200
6AG5	RF amp pentode	5,000	7	700	1,600	12	72	300
6AK5	RF amp pentode	5,000	8	700	1,700	17	90	450
WE404A	Close grid pentode	12,500	13	1,000	560	30	150	400
	Space charge Beam deflection	25,000	3	8,000	900	20	320	1,300

IV. Qualitative Analysis of the Transconductance

Let us consider a tube such as that in Fig. 3. Because of the symmetry we need examine only one half. Let us assume an electron beam of current I', whose transconductance is g_m', where the prime refers to the primary (input) section of the tube. When the beam reaches the output section, part of it is intercepted by H and only the fraction α is allowed to pass (see Fig. 2). There it is multiplied by the secondary-emission multiplication factor δ. Thus, the anode current is

$$I_p = I'\alpha\delta. \tag{1}$$

In calculating the transconductance, g_m, it has to be considered that α and I' are dependent upon V_g. If the secondary-emission factor δ is assumed to be a constant, differentiation gives the over-all transconductance

$$g_m = \frac{dI_p}{dV_g} = \alpha\delta\frac{dI'}{dV_g} + I'\delta\frac{d\alpha}{dV_g}, \tag{2}$$

$$= \alpha\delta g_m' + I'\delta\frac{\partial\alpha}{\partial I'}\frac{dI'}{dV_g},$$

$$= \alpha\delta g_m' + I'\delta\frac{\partial\alpha}{\partial I'}g_m'. \tag{3}$$

From (3) we find that the transconductance, g_m, differs from the conventional value $\delta g_m'$ by the factor α and the appearance of an additional second term. Here term 1 represents the normal transconductance obtainable with an ordinary multiplier ($=\delta g_m'$), slightly modified, and term 2 represents a component resulting from a shift of the terminal point of the path, as described in Fig. 1.

V. Quantitative Calculation of the Transconductance

Space charge, in calculations as well as in model tests, presents, in general, serious difficulties in a detailed analysis. In one-dimensional problems, however, it is possible to obtain exact solutions, and this has been done for a case, as described in Fig. 1. Calculations of somewhat the same nature have also been reported.[12–14] The results of the present calculations have been applied, with some approximations, to a simple tube structure, and expressions have been derived for transconductance and transconductance-to-current ratio. The expressions are further approximated to fit the tube structure of Fig. 3, and calculated values are compared with measurements.

[12] H. F. Ivey, "Cathode field in diodes under partial space-charge conditions," *Phys. Rev.*, vol. 76, pp. 554–558; August 15, 1949.
[13] R. Cockburn, "The variation of voltage-distribution and transit time with current in the planar diode," *Proc. Phys. Soc.* (London), vol. 47, pp. 810–817; 1935.
[14] G. Jaffe and J. E. Lilienfeld, "Theory of the high vacuum discharge," *Ann. der Phys.*, vol. 63, pp. 145–174; 1920.

A. Exact Solution of the Parallel-Plane Case

Assume two infinite planes A and R, parallel and separated by a distance y_1 (Fig. 1).

Assume that the plane A emits an evenly distributed, homogeneous flow of electrons towards R with a velocity V_0 and with an arbitrary angle of ejection.

Assume the potential of R to be such that the electrons just graze the plane and return to A.

Let $x-y$ be a coordinate system with the x axis in the plane A and the y axis perpendicular to it. Furthermore, let the initial electron velocity be parallel to the x-y plane. Then the velocity V_0 can be resolved into the components V_{x0} and V_{y0}.

The electron path may be calculated under different space-charge conditions. The electron paths and transit time can be found from the equations

$$\begin{cases} \dfrac{d^2x}{dt^2} = 0 \\[2ex] \dfrac{d^2y}{dt^2} = -\dfrac{e}{m}\cdot E, \end{cases} \tag{4}$$

where E is the electric field.

1. *Electron path when the space charge is negligible.* When the space charge is negligible, the field is a constant so that

$$E = \frac{V_{y0}}{y_1}.$$

From this is derived the usual solution,

$$x = \sqrt{\frac{2e}{m}}V_{x0}\cdot t$$

$$y = -\frac{e}{m}\cdot\frac{V_{y0}}{y_1}\cdot\frac{t^2}{2} + \sqrt{\frac{2e}{m}}V_{y0}\cdot t,$$

which is the equation of a parabola. The transit time, i.e., the time it takes for an electron to go the distance x_I in Fig. 1, is, for this case of "negligible space charge,"

$$t_I = \frac{4y_1}{\sqrt{\frac{2e}{m}}V_{y0}}.$$

2. *Electron path in the presence of space charge.* For the electron path in the presence of space charge E is no longer a constant, but varies with t. E can be computed from Poisson's equation, which since V is assumed to vary only in the direction of y, has the form

$$\frac{d^2V}{dy^2} = -\frac{\rho}{\mathcal{E}_0}, \tag{5}$$

where ρ is the space charge and $\mathcal{E}_0$ the dielectric constant ($=8.85\cdot10^{-12}$ farad/meter).

The current in the direction of y is zero at all points as the outgoing electrons at every point of an infinite plane are replaced by the same number returning. In order to get a relation between ρ and i, we consider the outgoing electrons, only. As the path is symmetrical with respect to the point of reflection, the returning part of the path is a mirror image of the outgoing part. Neglecting the returning part means that the space charge is cut in half. This is, however, a close approximation to the practical case, as shown later. Thus,

$$\rho = -\frac{i}{v_y} = -\frac{i}{\sqrt{\frac{2e}{m}V}}, \qquad (6)$$

where i is the current density of outgoing electrons in the direction of y. Combining (5) and (6) and integrating, we have

$$-\frac{dV}{dy} = E = \sqrt{Ki\sqrt{V} + E_0^2}, \qquad (7)$$

where

$$K = \frac{4}{\varepsilon_0\sqrt{\frac{2e}{m}}}$$

and E_0 = the electric field strength at R.

As E is not known at the boundaries, but is a function of i, E_0 cannot be computed directly. However, the potentials at the boundaries have fixed values, which should give the constants. Further integration leads, however, to complicated calculations, and will be considered under part 3, of Section A.

In the above expression V is still an unknown function of t. To find V the following expression is used:

$$-\frac{dV}{dt} = -\frac{\delta V}{\delta y}\frac{dy}{dt} = E\frac{dy}{dt}.$$

Substituting

$$\begin{cases} E = \sqrt{Ki\sqrt{V} + E_0^2} \\ \dfrac{dy}{dt} = \sqrt{\dfrac{2e}{m}V} \end{cases},$$

we have

$$-\frac{dV}{dt} = \sqrt{\frac{2e}{m}}V\sqrt{Ki\sqrt{V} + E_0^2}.$$

Integration with the boundary condition

$$\begin{cases} t = 0 \\ V = V_{y0} \end{cases}$$

gives

$$t = \frac{\varepsilon_0}{i}\left[\sqrt{Ki\sqrt{V_{y0}} + E_0^2} - \sqrt{Ki\sqrt{V} + E_0^2}\right] \qquad (8)$$

with

$$\sqrt{Ki\sqrt{V_{y0}} + E_0^2} = E_a. \qquad (9)$$

Where E_a represents the electric field strength at A,

$$E = E_a - \frac{i}{\varepsilon_0}\cdot t.$$

Now (4) can be solved, yielding

$$y = -\frac{e}{m}\left(E_a\frac{t^2}{2} - \frac{i}{\varepsilon_0}\frac{t^3}{6}\right) + \sqrt{\frac{2e}{m}V_{y0}}\cdot t. \qquad (10)$$

By comparison with Part 1 of Section A it is found that the space charge changes the path from a second-degree to a third-degree curve and the electrons describe a more extended arc, as shown by the dashed curve of Fig. 1. Equation (10) is only valid for the rising part of the arc. The falling part is a mirror image of the rising part.

The transit time in this case can be calculated from (8).

$$t_{II} = \frac{\varepsilon_0}{i}(E_a - E_0).$$

3. *Calculations of E_a and E_0*. In the foregoing section, E_a and E_0 are functions of i. To determine these, it is necessary, as mentioned earlier, to carry the integration of (4) one step further. Equation (7) can be integrated after substituting Z for $\sqrt{Ki\sqrt{V}+E_0^2}$.

This yields

$$\frac{4}{K^2i^2}\frac{Z^3}{3} - E_0^2\cdot Z = -y + \text{const.}$$

and

$$(2E_0^2 - Ki\sqrt{V})\sqrt{Ki\sqrt{V} + E_0^2} = \frac{3K^2i^2}{4}(y + C_1).$$

E_0 and C_1 can be computed from the boundary conditions

$$\begin{cases} y = 0 \\ V = V_{y0} \end{cases}$$

$$\begin{cases} y = y_1 \\ V = 0. \end{cases}$$

We introduce the relative values of E_0 and i to give simpler expressions

$$E_0 = \sigma\frac{V_{y0}}{y_1}$$

$$i = \eta\cdot\frac{16}{9}\cdot\frac{V_{y0}^{3/2}}{Ky_1^2} = \eta\cdot i_{max},$$

where the coefficients are chosen so that E_0 varies from $\frac{V_{y0}}{v_1}$ to 0, $(0 \leq \sigma \leq 1)$, and i varies from 0 to i_{max} $(0 \leq \eta \leq 1)$.

The latter represents the current density increasing from zero to the space-charge-limited value (virtual cathode). Then elimination of C_1 gives

$$\eta^2 - \eta - \frac{27}{16}\sigma^3 + \frac{27}{16}\sigma^2 = 0 \tag{11}$$

$$\eta = \frac{1}{2}\left[1 \pm \sqrt{1 - \frac{27}{4}(\sigma^2 - \sigma^3)}\right].$$

For different values of η, σ takes the values shown in Table II and Fig. 5. The corresponding values of i are

TABLE II

σ	η	κ	F
0	1	1.333	1.500
0.1	0.985	1.327	1.402
0.2	0.943	1.310	1.325
0.3	0.879	1.286	1.261
0.4	0.797	1.255	1.208
0.5	0.698	1.221	1.162
0.6	0.584	1.182	1.122
0.7	0.456	1.141	1.086
0.8	0.316	1.096	1.055
0.9	0.164	1.049	1.026
1	0	1	1

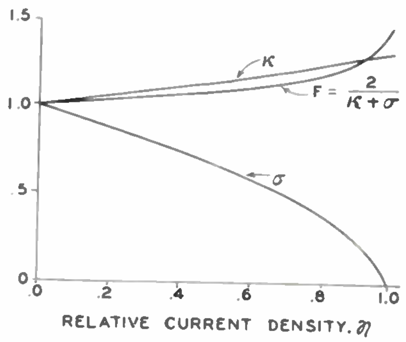

Fig. 5—Relative electric-field strength at R (σ) and at A (κ), and relative traveled distance (F) as function of current density (η). F is also relative transit time.

$$i = 1.166 \cdot 10^{-6} \cdot \frac{V_{y0}^{3/2}}{y_1^2}\left[1 \pm \sqrt{1 - \frac{27}{4}(\sigma^2 - \sigma^3)}\right].$$

E_a can be computed in a similar manner. By eliminating η between (9) and (11) and putting

$$\begin{cases} E_0 = \sigma \dfrac{V_{y0}}{y_1} \\ E_a = \kappa \dfrac{V_{y0}}{y_1}, \end{cases}$$

the following equation is obtained

$$\kappa^4 - \kappa^2\left(2\sigma^2 + \frac{16}{9}\right) + \sigma^4 - \frac{16}{3}\sigma^3 + \frac{64}{9}\sigma^2 = 0,$$

which gives the solution

$$\kappa = \sqrt{\sigma^2 + \frac{8}{9}\left[1 \pm \sqrt{1 - \frac{27}{4}(\sigma^2 - \sigma^3)}\right]}.$$

Table II and Fig. 5 give κ as a function of η.

4. *Comparison of the distance x in cases 1 and 2.* As the velocity in the x direction is constant, the distance x is proportional to the transit time in the two cases. We then get the relative value F as the ratio t_{II}/t_I.

$$F = \frac{x_{II}}{x_I} = \frac{t_{II}}{t_I} = \frac{\mathcal{E}_0(E_a - E_c)\sqrt{\dfrac{2e}{m}V_{y0}}}{4iy_1}.$$

To simplify this expression, we introduce the relative values as before. Then we obtain

$$F = \frac{2}{\sigma + \kappa}.$$

As σ and κ are known, we can calculate F for different values of η.

As can be seen from Table II and Fig. 5, the distance x increases 50 per cent when the current density is increased from zero until a virtual cathode is formed near the reflection plate. This increase is independent of the initial angle. F is also the change in transit time in a diode under partial space-charge conditions.

B. Exact Solution of a Beam-Type Tube Structure

In a practical application one has to consider a finite emitting area and an output structure, to convert the changes in electron path to changes in current. This leads to a beam-type structure, as shown in Fig. 2.

Assume two parallel equipotential planes A and R, infinite in a direction perpendicular to the plane of the paper. Assume part of the plane A emitting a homogeneous, parallel beam of electrons, which is reflected in the plane R and returns to A and is divided between two other parts of A, here called the "intercepting electrode" and the "anode."

Then

$$I_p = \alpha \cdot \eta \cdot I_{\max}',$$

where α = the fraction of I' that reaches the anode,

$I_{\max}'$ = maximum beam current before a virtual cathode forms at R

$$\eta = \frac{I'}{I_{\max}'}.$$

Assume

$$\begin{cases} \alpha = f(\eta) \\ I_{\max}' = \text{const.} \\ \eta = f(V_g) \end{cases}$$

Differentiation gives

$$\frac{dI_p}{dV_g} = \alpha \cdot I_{\max}' \cdot \frac{d\eta}{dV_g} + \eta \cdot I_{\max}' \cdot \frac{\delta\alpha}{\delta\eta} \cdot \frac{d\eta}{dV_g}.$$

Now

$$I_{\max}' \cdot \frac{d\eta}{dV_g} = g_m' = \text{the transconductance of the input}$$

section

$$\therefore \quad g_m = g_m'\left(\alpha + \eta\cdot\frac{\delta\alpha}{\delta\eta}\right).$$

With the symbols of Fig. 2 we have

$$b\alpha = x + b - L.$$

Differentiation gives

$$\frac{\delta\alpha}{\delta\eta} = \frac{1}{b}\cdot\frac{\delta x}{\delta\eta} = \frac{x_I}{b}\cdot\frac{\delta F}{\delta\eta} = \frac{x_{II}}{bF}\cdot\frac{\delta F}{\delta\eta}$$

$$\therefore \quad g_m = g_m'\left(\alpha + \frac{\eta x_{II}}{bF}\cdot\frac{\delta F}{\delta\eta}\right). \tag{12}$$

The condition for a gain in transconductance is

$$\alpha + \frac{\eta x_{II}}{bF}\cdot\frac{\delta F}{\delta\eta} > 1.$$

C. Approximate Solution for a Practical Tube

From the two solutions derived above, it is now possible to calculate approximately the transconductance of a practical tube. Suppose that the dimensions x_{II} and y_I are not too large, compared to b. Suppose that the dimensions perpendicular to the paper (i.e., the length of the cathode) are not too small compared to b.

Then one can, as a first approximation, substitute the values for $\delta F/\delta\eta$, F and η from the above solution into the expression (12).

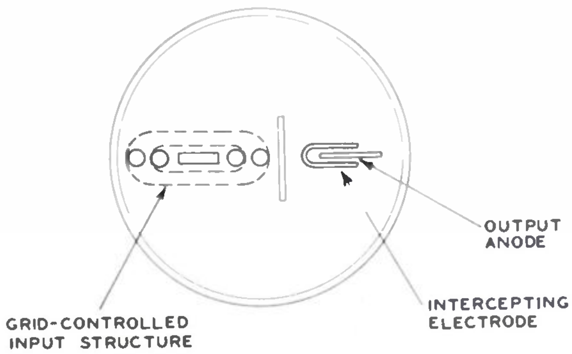

Fig. 6—Simple experimental tube.

Furthermore, in an approximate analysis, the results obtained can be applied to a tube structure such as Fig. 6. In the course of discovering, studying, and understanding the effect of space-charge beam deflection, however, most of the measurements have been carried out on a tube structure such as that in Fig. 3. A supporting factor for this choice was the extraordinary performance of this tube.

Fig. 7 shows an electric-field plot made on this tube structure and obtained from measurements in an electrolytic tank. As the tube contains a secondary emitter, the output voltages are rather high. In order to avoid excessive island formation on the cathode and heat dissipation in the grid, the screen-grid voltage, on the other hand, should not be chosen too high.

However, in the area where the space-charge action is strongest, i.e., near the turning point of the electrons, the field can be approximated by a parallel-plane field. Then an equivalent voltage V_{eq} can be determined, giving the same field strength in a parallel-plane arrangement of similar dimensions. This equivalent voltage is then used for the determination of $\delta F/\delta\eta$, F, and η.

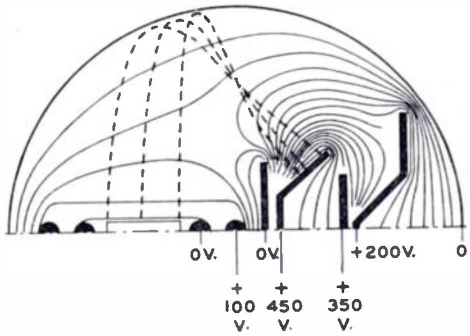

Fig. 7—Experimentally determined electric-field plot and electron paths.

Fig. 7 also shows some electron paths plotted from measurements on a rubber model. As the rubber model does not show the influence of space charge, all the paths end on the intercepting electrode. In the actual tube, the beam shifts over and part of the beam reaches the dynode anode.

Let us, for practical purposes, substitute x for x_{II}, where x is the distance from the center of the cathode to the intercepting edge.

With a secondary emitter in the tube, the expression for the transconductance changes to

$$g_m = g_m'\cdot\delta\cdot\left(\alpha + \frac{x\eta}{bF}\cdot\frac{\delta F}{\delta\eta}\right).$$

Here δ is the secondary-emission factor as measured in the tube

$$\delta = \frac{I_p}{I_p - |I_d|}.$$

D. Correlation with Measurements

Table III gives some values from measurements on three tubes under the same conditions. The transconductance for 1-ma anode current had the average value

TABLE III

	α	δ	g_m'	g_m for $I_a = 1$ ma
No. 204	0.20	4.0	3.3	10.0
205	0.08	4.5	3.2	7.2
226	0.11	4.5	4.0	10.1
Average	0.13	4.3	3.5	9.1

9.1 ma/v (9,100 μmhos). A calculation on the same tube gives 11.3 ma/v (11,300 μmhos). This good correlation is probably incidental, as the simplifications made should be expected to cause larger errors. The method of computing, however, seems to be a valuable tool for further work on the tube and the accuracy should, with reasonable care, be sufficient for engineering work.

VI. Conclusion

A new principle for the control of current in electron tubes has been presented. An analysis of the principle and the results from experimental tubes demonstrate that a high transconductance can be obtained at low current. This should be very useful in broad-band-amplification applications.

Work on calculation of noise, maximum performance, and the design of stabilizing circuits will be presented in a forthcoming paper.

VII. Acknowledgment

The discovery and experimental part of this work was done while the author was a trainee at the Radio Corporation of America, RCA Laboratories Division, Princeton, N. J., under the auspices of the American-Scandinavian Foundation The theoretical part was continued at the Royal Institute of Technology, Stockholm, Sweden. The author wishes to thank various persons in these organizations, but especially E. W. Herold, RCA Laboratories, and H. Alfvén, Royal Institute of Technology, for permanent encouragement and valuable advice, and C. W. Mueller and R. P. Stone, RCA Laboratories, for helpful suggestions. He also wishes to thank his wife for sharing the linguistic difficulties.

High-Frequency Characteristics of Resistance-Coupled Triode Amplifiers*

JAMES W. SAUBER†, MEMBER, IRE

Summary—This paper describes a semi-graphical method of calculating the steady-state high-frequency response of cascaded resistance-coupled triode amplifiers. Full allowance is made for the effects of interelectrode capacitances.

CONSIDER a stage of resistance-coupled triode amplification serving as an intermediate link in a chain of similar but not necessarily identical amplifiers, as shown in Fig. 1. Circuit components which contribute only to the degrading of the low-frequency response are omitted, as are power supply considerations. Primed quantities refer to the succeeding stage.

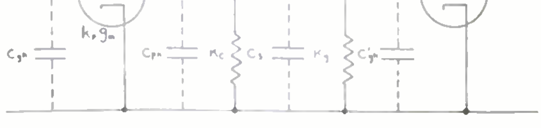

Fig. 1

Over the so-called middle audio-frequency range,

$$A_{\text{mid}} = \frac{-g_m}{K_0}, \tag{1}$$

where

$$K_0 = k_p + K_c + K_{gl}. \tag{2}$$

At higher frequencies the input admittance of the succeeding stage,

$$Y'_{\text{in}} = -\omega C'_{gp} A' \sin\theta' + j\omega(C'_{gk} + C'_{gp} + C'_{gp} A' \cos\theta'), \tag{3}$$

together with the other shunt capacities, determine the response. Grouping all the fixed capacities together as

$$C_0 = C_{pk} + C_{gp} + C_s + C'_{gk} + C'_{gp}, \tag{4}$$

the high-frequency amplification is

$$A = \frac{-g_m}{K_0 - \omega C'_{pg} A \sin\theta' + j\omega(C_0 + C'_{gp} A' \cos\theta')}. \tag{5}$$

Select the reference frequency

$$f_0 = \frac{K_0}{2\pi C_0}. \tag{6}$$

Then the normalized high-frequency response becomes

$$\frac{A}{A_{\text{mid}}} = \frac{1}{1 + \frac{f}{f_0}\left[-bA' \sin\theta' + j(1 + bA' \cos\theta')\right]}, \tag{7}$$

where

$$b = \frac{C'_{gp}}{C_0}. \tag{8}$$

* Decimal classification: R363.211. Original manuscript received by the Institute, January 26, 1951; revised manuscript received May 11, 1951. This paper is an extract from a thesis submitted in partial fulfillment of the requirements for the degree of M.S. in E.E. at the University of Tennessee.

† Ballantine Laboratories, Inc., Boonton, N. J.

The form of (7) is important, for by selecting the frequency ratio as the independent variable and bA' and θ' as independent parameters, the equation may be plotted as a set of universal normalized response curves for both magnitude and phase shift. The range of bA' is typically 0 to 20. The parameter θ' is divided into quadrants. The fourth quadrant, for which θ' is negative, corresponds to resistance-capacitance loading on the succeeding stage, and it is expected that the curves for this quadrant, Figs. 2 and 3, will be most useful.

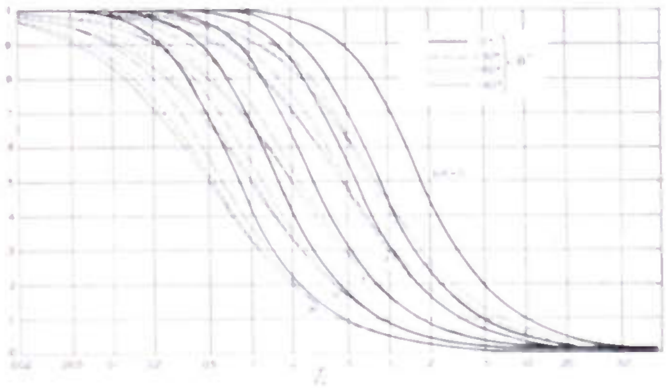

Fig. 2—A/A_{mid} Magnitude, fourth quadrant.

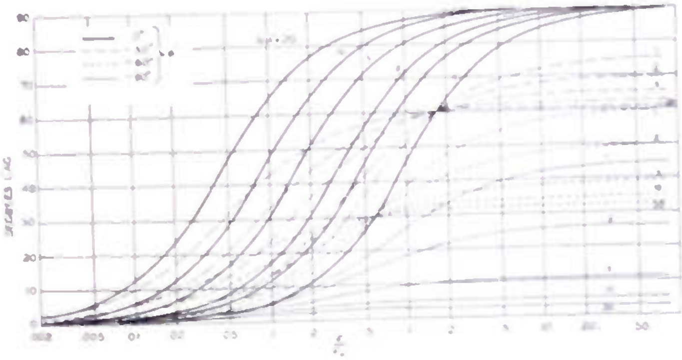

Fig. 3—A/A_{mid} Phase angle, fourth quadrant.

However, first and even third quadrant values of θ' are obtainable, depending upon the final stage loading, and curves for these quadrants are included as Figs. 4 through 7.

Obviously, the final stage (of any plate output type with shunt loading) must be analyzed first, and the analysis proceeds toward the first stage. For each intermediate stage the specification of bA' and θ' at each of several frequencies determines a series of points, which may be connected by a smooth curve. The absolute amplification depends on the scale factors, and the total amplification of the multistage amplifier requires the product of the magnitude responses and the sum of the phase shifts, with as many phase reversals as there are stages. A tabular method of analysis is recommended.

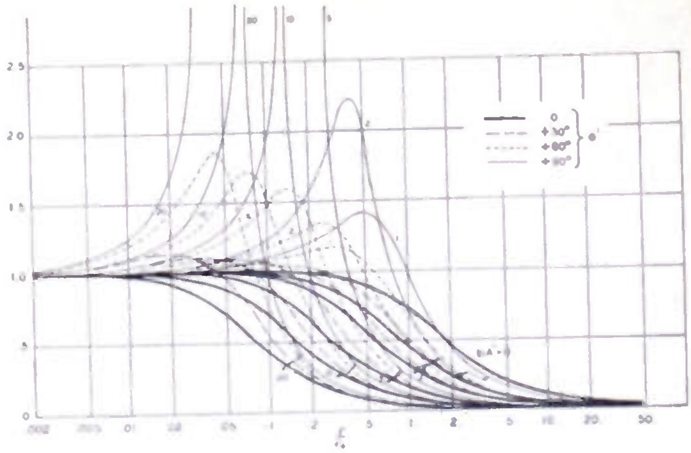

Fig. 4—A/A_{mid} Magnitude, first quadrant.

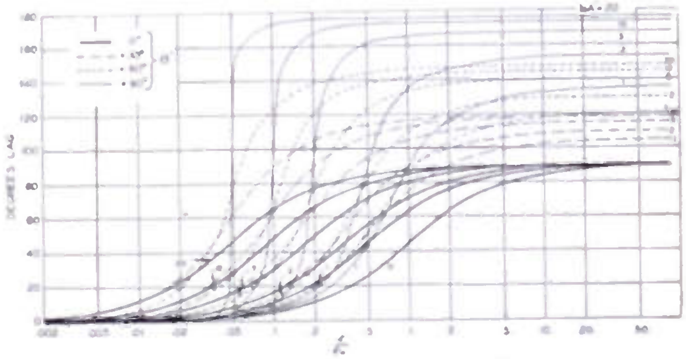

Fig. 5—A/A_{mid} Phase angle, first quadrant.

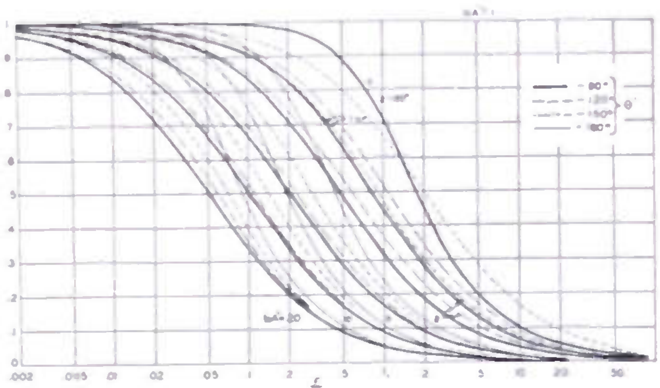

Fig. 6—A/A_{mid} Magnitude, third quadrant.

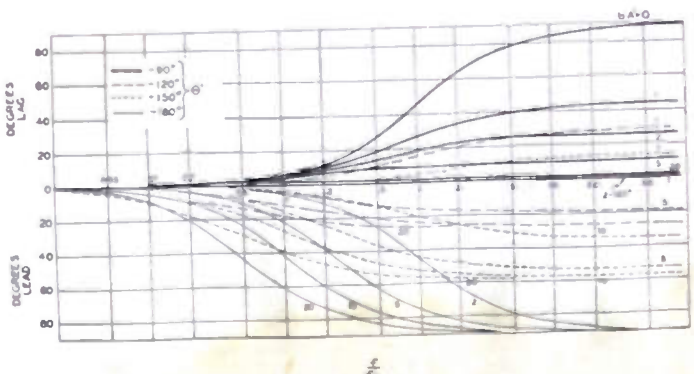

Fig. 7—A/A_{mid} Phase angle, third quadrant.

Measurements of the Parameters Involved in the Theory of Radio Scattering in the Troposphere*

C. M. CRAIN†, MEMBER, IRE, AND J. R. GERHARDT†

Summary—Booker and Gordon[1] have recently proposed a theory of radio scattering in the troposphere. Using atmospheric inhomogeneities in refractive index, the scattered power was shown to be a function of the intensity and scale of the existing turbulent variations. Lacking experimental data on the nature of the refractive index variations which may be present in the atmosphere, they predicted the magnitude of refractive index changes on the basis of limited temperature fluctuation measurements. Measurements have been made of refractive index and associated temperature fluctuations by the Electrical Engineering Research Laboratory of The University of Texas since 1948 with a somewhat detailed study being made from 10 inches to 50 feet above the ground since December, 1949. This paper includes a brief discussion of the recording refractometer and recording thermometer used for these studies, a meteorological analysis of the problem, and tracings of the refractive index and temperature fluctuations for several various conditions of the lower atmosphere.

INTRODUCTION

RECENT contributors to these pages[1] have applied the theory of scattering in a turbulent medium proposed by Peckeris to scattering of radio waves in the troposphere. The atmosphere is pictured as a turbulent medium in which random fluctuations of refractive index Δn occur in distances of a few centimeters to a few meters, depending on the stability of the atmosphere. The scale of turbulence l is considered to be the distance at which the cross correlation between two sets of simultaneous refractive index fluctuations falls to $1/e$ of the value obtained at zero separation.

Scattering theory was used to explain the fact that, in experiments made in the Caribbean Sea in 1945, the field strength decreased more slowly with distance for 9-cm wavelength radiation than could be explained by any existing theory.

Measurements made at the Electrical Engineering Research Laboratory of The University of Texas have also been in agreement with the scattering theory.[2] Studies made with directive antennas on the signal received from FM stations 72 to 183 miles distant have indicated that more signal was arriving from higher elevations above the horizon than could be explained except by the scattering theory.

In order to measure the quantities Δn and l, a recording refractometer has been used. As this instrument has been described elsewhere,[3] only a brief explanation will be added here.

INSTRUMENTATION

The refractometer uses two Pound stabilized oscillators and the beat frequency principle.[3] The frequency of these oscillators is controlled on a short-time basis (at least one minute) to a factor of the order of one part in 10^7 by the resonant frequency of associated cavity resonators. The beat frequency of the two oscillators is adjusted to 10.7 mc and applied to an amplifier and discriminator and finally to a zero-centered recording milliammeter. One cavity is sealed off; therefore, changes in the refractive index of the medium in the other cavity result in a deviation of the difference frequency from 10.7, and hence a proportional deflection from midscale of the milliammeter in the appropriate direction. A series of concentric circles drilled in the end plates of one of the cavity resonators has removed 24 per cent of the end plate area. A "blower" has been coupled to the cavity by means of a flexible piece of rubber hose so that air may be pulled through the cavity. The rate of flow has been such that a volume of air equal to that of the cavity is pulled through the cavity in 1/30 of a second. The actual flushing time of the cavity is obviously slightly longer. It may be easily shown that as long as the air speed is greater than about 3 miles per hour, the blower has negligible effect on the refractive index pattern of the medium being sampled by the cavity. During the measurements the cavity is always placed so that the end opposite the blower faces into the wind.

The temperature fluctuations were obtained using a bead-type thermistor of 0.5-second time constant in still air. The thermistor was used as one arm of a Wheatstone bridge. The bridge fed a differential type two-stage dc amplifier with the recording milliammeter being connected between plates in the second stage.

* Decimal classification: R113.308. Original manuscript received by the Institute, November 24, 1950; revised manuscript received, April 4, 1951.

The research reported in this document is being made possible through support extended The Electrical Engineering Research Laboratory, The University of Texas by the Office of Naval Research under contract N5ori-136 P. O. I.

† Electrical Engineering Research Laboratory, The University of Texas, Austin, Texas.

[1] H. G. Booker and W. E. Gordon: "A theory of radio scattering in the troposphere," Proc. I.R.E., vol. 38, pp. 401–412; April, 1950.

[2] A. W. Straiton, D. F. Metcalf, and C. W. Tolbert, "Scattering of radio frequency energy," to appear in Proc. I.R.E.

[3] C. M. Crain, "Apparatus for recording rapid fluctuations in the index of refraction of the atmosphere," *Rev. Sci. Instr.*, vol. 21, pp. 456–457; May, 1950.

The Index of Refraction at Microwave Frequencies as a Function of Meteorological Variables

Based on measurements made[4] at 3.2 cm for both dry air and water vapor, the index of refraction of atmospheric air is given approximately by

$$N \equiv (n - 1)10^6 = \frac{77.5}{T}\left[p + \frac{4860e}{T}\right], \qquad (1)$$

where n is the refractive index, T the temperature in degrees Kelvin, p the total atmospheric pressure in millibars, and e the partial pressure of water vapor in millibars. Since it has been shown[5] that the magnitude of the changes of air pressure are negligible under normal atmospheric conditions, (1) can be rewritten to obtain values of the changes or fluctuations of N for mean summer conditions. Thus

$$\Delta N = 4.2\Delta e - 1.4\Delta T. \qquad (2)$$

General Comments on Atmospheric Turbulence

It must first of all be recognized that turbulence results both from the frictional forces generated as result of surface drag and wind shear—mechanical turbulence—and the buoyancy forces derived from heat received at the earth's surface by solar radiation—thermal turbulence. During daytime heating the two forces act together in producing the resultant turbulent fluctuations, but during night hours the two forces are generally opposed and turbulence only results for a given degree of thermal stability if the wind shear exceeds certain critical values. In a typical model of turbulence, then, eddies set up as a result of mechanical or thermal forces produce the observed fluctuations at a point through mixing processes. Since, in general, horizontal gradients in the atmosphere are small, the observed fluctuations are primarily a result of vertical mixing in which air at a given height with average properties characteristic of the layer at that height is moved to another height with correspondingly different average properties. If we now recognize that in any turbulent process, a transfer of air properties occurs in the direction of the vertical gradient of this property, it is possible to correlate the magnitude of the observed fluctuations at a point with the magnitude of the corresponding vertical gradient. Thus, the larger the negative vertical gradients of temperature, the larger will be the observed fluctuations of air temperature. In general, then, as the vertical gradients of atmospheric properties are most apt to have their maximum values at or near the surface, it should be anticipated that the fluctuations of an air property near the surface should also in general reveal a decrease in intensity with height.

Very little is known concerning the variation of the scale of turbulence with height or meteorological conditions. It would seem probable, however, that atmospheric situations conducive to large values of the amplitude of fluctuations would also give rise to fluctuations of higher frequencies, although no conclusions can be made from the preliminary measurements to be presented here. Very long period fluctuations—of the order of 30 seconds or greater—are not believed caused by turbulence, but by large scale convective phenomena and by changes in local circulation patterns.

Presentation and Discussion of Data

The primary purpose of these observations lies in obtaining preliminary measures of the scale and intensity of turbulence through direct measurement of the variation of the index of refraction within the first 50 feet above the surface. In addition, the simultaneous measurement of air temperature variations shows that while the turbulent fluctuations of temperature, moisture, or refractive index are essentially random, the instantaneous correlation between any two of the above fluctuation patterns has a magnitude which is generally significantly greater than zero. Under these conditions, there can be little doubt as to the essential similarity of the turbulent transfer processes near the surface for the different air properties involved.

Simultaneous Observations of Temperature and Index of Refraction

A. The Effect of Turbulence Under Thermal Instability with Small Negative Humidity Gradients

The most frequently observed fluctuation pattern is that in which there is a significant positive correlation between index of refraction and air temperature variations. In this case, as in previously published examples,[6] having noted from (2) that temperature and index-of-refraction changes are negatively correlated, the deductions can be made that moisture fluctuations must be primarily responsible for the index-of-refraction variations, and that temperature and moisture fluctuations are also positively correlated. Under these conditions, the vertical gradients of temperature and air moisture must have the same sign, and as is normal under daytime heating with a moist or vegetation-covered surface, both gradients are negative. Thus, rising warm air also carries aloft air of greater moisture content and cooler descending air is dryer. For an example of this

[4] C. M. Crain, "Dielectric constants of several gases at a wave length of 3.2 centimeters," *Phys. Rev.*, vol. 74, pp. 691–693; September, 1948.

[5] R. D. M. Clark, "Atmospheric micro-oscillations," *Jour. Meteorology*, vol. 7, pp. 70–75; February, 1950.

[6] C. M. Crain and J. R. Gerhardt, "Some preliminary studies of the rapid variations in the index-of-refraction of atmospheric air at microwave frequencies," *Bull. of Amer. Meteorological Soc.*, vol. 31, pp. 330–335; November, 1950.

type of observation, reference should be made to Fig. 1 which shows the simultaneous recordings of index-of-refraction and air temperature made over a 90-second interval at two feet above the ground on July 6, 1950, at the grounds of the Off-Campus Research Center, The University of Texas. The mean air temperature and moisture at this level were 34.6°C and 25.4 mbs, respectively, with an average wind of 7 to 8 mph from the south. The peak-positive value of the cross correlation between the two traces is 0.62. With peak index-of-refraction variations between 8 and 9 N units and corresponding temperature changes of the order of 3.5°C, maximum moisture changes must have been of the order of 3 mbs.

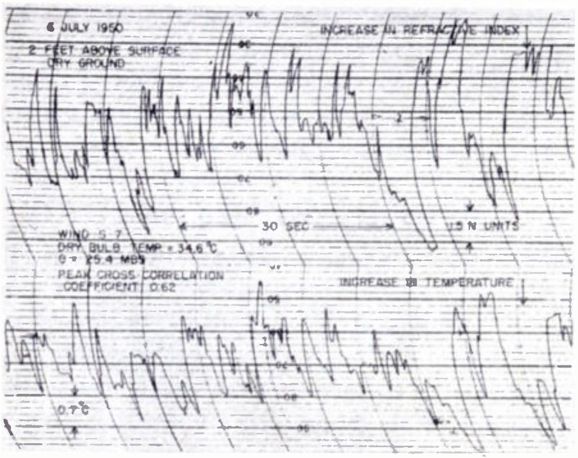

Fig. 1—Simultaneous recordings of changes in refractive index and air temperature at two feet above a relatively dry vegetation-covered surface under conditions of thermal instability.

B. The Effect of Turbulence under Thermal Instability with Essentially Zero Humidity Gradients

Although the positive correlation between index-of-refraction and air temperature is that most commonly observed, negative correlations are not unusual. It is apparent, under these conditions, that the effect of the temperature fluctuations on the resulting index-of-refraction variations is much larger than that of air moisture content fluctuations. Such conditions arise in dry air in which the possible changes in moisture are small or over surfaces which are not actively evaporating moisture into the air. In the latter case, then, with normal thermal turbulence, vertical mixing of the air produces an essentially zero vertical gradient of moisture. Fig. 2, for instance, illustrates a simultaneous recording of temperature and index-of-refraction taken on the afternoon of August 2, 1950, during a period of unobstructed sunshine. The equipment was located 10 inches above the surface in the center of a large asphalt-covered parking area where the air had an unobstructed flow of more than 100 yards over the asphalt before reaching the measuring elements. Surface wind was 6 mph from the SSE. The cross-correlation between the two traces has a peak value of -0.63. Maximum values of index-of-refraction and air temperature changes were about 4.5 N units and 2.0–3.0°C. Under these conditions, values of Δe are restricted to a few tenths of a millibar or less. In an extension of the above, it is seen from (2) that under conditions in which the vertical gradient of temperature in °C per unit height is approximately three times that of air moisture content in millibars per unit height, and is of the same sign, the normal positive correlation of temperature and moisture fluctuations will give rise to an essentially constant index-of-refraction recording. Under these conditions it is certainly obvious that estimates of ΔN cannot be made solely from measurements of ΔT.

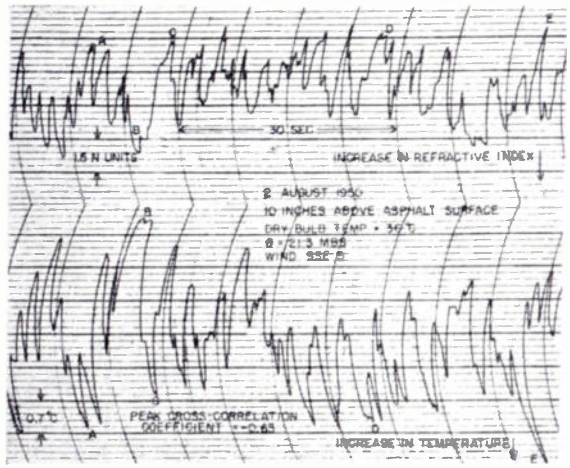

Fig. 2—Simultaneous recordings of changes in refractive index and air temperature at 10 inches above an asphalt surface under conditions of thermal instability.

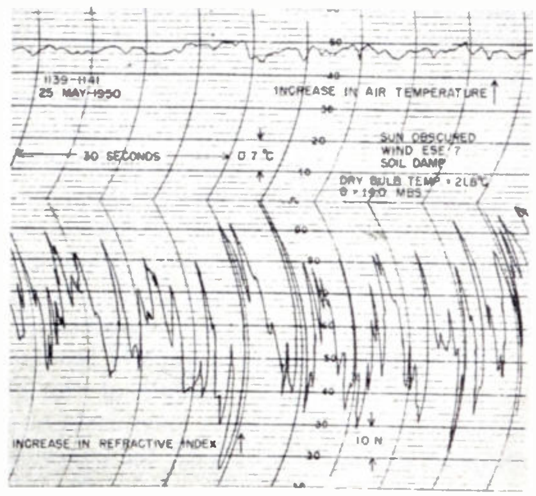

Fig. 3—Simultaneous recordings of changes in refractive index and air temperature at three feet above a damp desert type surface under conditions of neutral thermal stability.

C. The Effect of Turbulence Under Neutral Thermal Stability with Large Negative Humidity Gradients

An even more unusual pattern is demonstrated in Fig. 3 for a set of data taken over a desert-type surface at Seminole, Texas. Although the air was fairly dry (mean air moisture of 14 mbs), a light rain a few minutes earlier had produced a damp surface. With clouds obscuring the sun, the turbulence was essentially of the frictional variety. Under these conditions, the temperature lapse rate would be essentially adiabatic—giving rise to little if any temperature fluctuations—while with large values of the vertical gradient of air moisture near the surface as a result of evaporation into dry air from a moist surface, large values both of Δe and ΔN should be expected. Note instantaneous values of ΔN in excess of 7 to 8 N units in the order of 1 second. Corresponding values of ΔT were all less than a few tenths of a degree. Although the visual correlation between these two sets of data is low, it appears to be negative.

D. The Effect of Turbulence Under Thermal Stability with Small Negative Humidity Gradients

Only a few measurements have been made to date under nighttime conditions where the normal gradients of temperature and moisture would be such as to produce fluctuations of ΔT and Δe which would be negatively correlated. Under these conditions, i.e., a thermally stable vertical temperature gradient and a negative vertical gradient of moisture, ΔT and Δe would act together rather than in opposition in forming resultant values of ΔN. Such a set of data is illustrated in Fig. 4, where simultaneous traces of air temperature and refractive index were taken a few minutes after sunset over the desert-type soil at Seminole, Texas. The peak negative cross-correlation coefficient here was 0.80 with maximum variations of index of refraction and temperature of about 2 N units and 0.4°C, respectively. Computed values of Δe vary from 0.4 to 0.5 millibars.

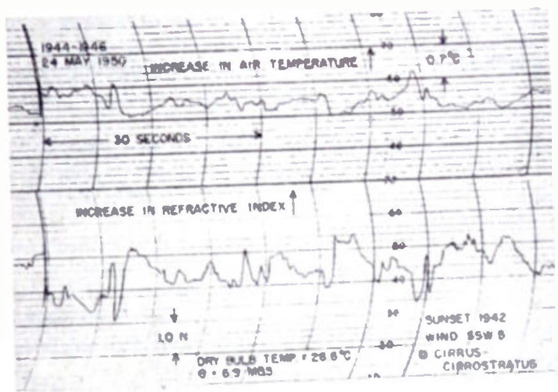

Fig. 4—Simultaneous recordings of changes in refractive index and air temperature at 3 feet above a dry desert-type surface under conditions of thermal stability.

E. The Effect of Increase in Height Above the Surface

A representative example of the effect of height on the observed turbulent fluctuations of N and T is given in Fig. 5. These measurements, taken at 32 feet above the ground, should be compared with those illustrated in Fig. 3 taken a few minutes earlier at two feet above the ground. Note the decrease in maximum amplitude and frequency of both index of refraction and air temperature. The effect of a reduction in thermal turbulence as a result of a cloud covering the sun is also well marked on the figure, and nearly constant values of ΔN and ΔT are observed for periods up to 15 seconds. Another effect of increasing height in the fluctuation patterns is normally a real loss in the correlation between any two parameters. While the loss of correlation is not too evident in Fig. 5, such has nearly always been the case in corresponding sets of data.

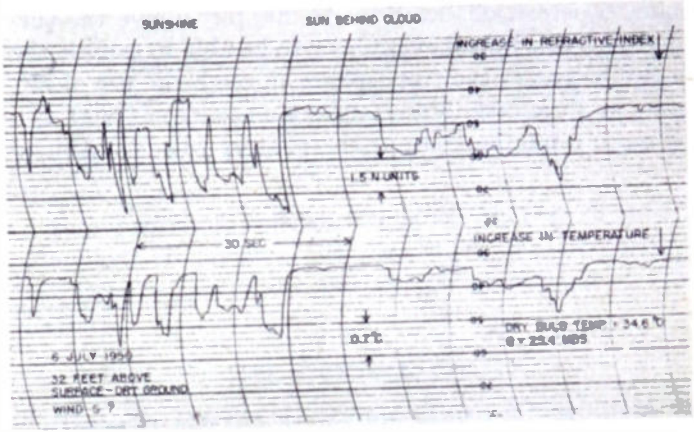

Fig. 5—Simultaneous recordings of changes in refractive index and air temperature at 32 feet above a relatively dry vegetation-covered surface under conditions of thermal instability.

Determination of Average Values of the Intensity and Scale of Turbulence

As is apparent from examining the recordings obtained from index-of-refraction fluctuations, an evaluation of the intensity Δn and scale l of turbulence must be of a statistical nature. Several methods are available for averaging these quantities. An autocorrelation analysis appears to be one of the most suitable methods of attack, and analysis of data on this basis is now being made at the Electrical Engineering Research Laboratory. There are, however, several difficulties involved in this system, among which are the effects of the length of sample on the derived autocorrelation function, and further study will be necessary before definite results can be published.

An auxiliary method of obtaining measures of Δn and l has, therefore, been used in this paper. This method, admittedly giving only rough approximations, involves the counting of all peaks and troughs and the determination of the total distance D of lateral pen travel over a certain time interval of the actual recording of index of refraction. If S changes in slope sign occur over a recording time Δt for a mean value $\bar{u}$ of wind speed, then

$$l \cong \frac{\bar{u}}{S/\Delta t}$$

and

$$10^6 (\Delta n) \cong \frac{1}{2} \frac{D}{S}.$$

In applying this method to the data, changes of the order of 0.1 N unit or less were not considered. It should again be noted that this system gives only approximate average peak as compared to mean-square values and the effect of variations in period of the fluctuations on Δn and l have been ignored. The values in Table I, taken only from the recordings presented here, are, however, among the first to be reported and are believed significant as to order of magnitude of Δn and l near the surface. An extension of these observations will be made soon to permit observations to 300 feet above the surface, and it is hoped eventually to be able to sample the entire height of the troposphere through the use of aircraft or dirigibles. Simultaneous measurements of two or more refractometers or thermistors will be taken to compare scales of turbulence computed from auto- and cross-correlation techniques.

TABLE I

AVERAGE VALUES OF Δn AND l FROM INDEX-OF-REFRACTION FLUCTUATIONS

Recording	Height	Av. Wind Feet/Seconds	Time Interval, Seconds	No. Changes Slope Sign	$(\Delta n)10^6$	l, Feet
Fig. 1	2 Feet	10	60	98	0.9	6
Fig. 2	10 Inches	8	60	91	0.7	6
Fig. 3	3 Feet	10	60	92	1.0	7
Fig. 4	3 Feet	7	60	51	0.2	8
Fig. 5 (Sunshine)	32 Feet	10	30	26	1.0	12
Fig. 5 (Cloudy)	32 Feet	10	30	20	0.2	15

Volume Integration of Scattered Radio Waves*

ALFRED H. LAGRONE†

THE GENERAL EQUATION for radio scattering developed by Booker and Gordon[1] is extended to a volume integral equation,[2] which gives the total scattered power density per unit cped at a receiver point relative to the power radiated per unit solid angle by an isotropic source.

The equation is expressed in terms of two power components, C_1 and C_2. The two components are at right angles to each other and normal to the direction of propagation. The C_1 component is in the plane containing the transmitter and receiver and the point at which scattering occurs. The C_2 component is normal to the plane containing C_1. The sum of the components is the power radiated per unit solid angle at the transmitter.

The equation is derived for these conditions: (a) Straight line propagation over a spherical earth; (b) Scattered power received by direct radiation from primary scattering of rays above the radio horizon at the transmitter; (c) Negligible loss of energy in the transmitted ray due to scattering;[3] (d) Scattering centers (blobs) are evenly distributed, of uniform size, and with the same average magnitude of index changes.

The total scattered power density per unit cped the receiver point is then P, where

$$P = \int_{\rho-\rho_m}^{\pi-\alpha} \int_{\alpha-\alpha_m}^{\pi-\rho_m} \int_{\beta=-\pi/2}^{\pi/2} \frac{\sigma(\theta, X)}{\sin^2 X} \left[\frac{C_1 \cos^2(\alpha+\rho) + C_2}{D}\right] d\alpha d\rho d\beta \quad (1)$$

and

$$\sigma(\theta, X) = \frac{\overline{(\Delta\epsilon/\epsilon)^2}(2\pi l/\lambda)^3 \sin^2 X}{\lambda[1 + \{(4\pi l/\lambda)\sin\frac{1}{2}(\alpha+\rho)\}^2]^2}.$$

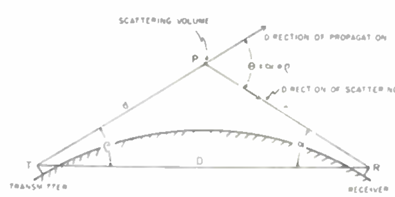

Fig. 1—Scattering geometry.

D = Distance from transmitter to receiver in same units used for λ. Fig. 1.

β = Angle made by plane containing the point of scattering and a vertical plane through the transmitter and receiver.

α = Elevation angle of scattering volume relative to line TR, Fig. 1, as measured at the receiver.

ρ = Elevation angle of scattering volume relative to line TR, Fig. 1, as measured at the transmitter.

α_m = Value of α when scattered ray grazes the receiver horizon, Fig. 1. α_m varies with β and D as shown in the literature.[2]

ρ_m = Value of ρ when transmitted ray grazes the transmitter horizon, Fig. 1. ρ_m varies with β and D as shown in the literature.[2]

Other symbols, not identified in the text, are identified in the literature.[1]

In setting up the integral expression for P, certain relations were found which considerably simplified the derivation.[2] They were as follows:

(1) The ray concept of the power radiated in an elementary solid angle permits considering the ray as a line of equal power.

(2) The increment of power, intercepted by a receiver scanning a given ray divided by the square of the distance from the intercepted portion of the ray to the receiver, is constant.

(3) The number of rays at a given elevation angle, ρ, is directly proportional to the perpendicular distance from the receiver to the rays.

(4) Any given polarization of the transmitted signal can be resolved into the components described earlier, and the scattered power received expressed as the sum of the power received from the two components.

Numerical application of Equation (1) in connection with the literature[2] shows, for the conditions assumed, that maximum scattered power intensity occurs in the direction of the transmitter and at the receiver horizon.

* Decimal classification: R113.242. Original manuscript received by the Institute, October 25, 1950; abstract received, May 14, 1951. Prepared under the Office of Naval Research Contract N5ori-136, T. O. I.

† Electrical Engineering Research Laboratory University of Texas, Austin, Tex.

[1] H. G. Booker and W. E. Gordon, "A theory of radio scattering in the troposphere," PROC. I.R.E., vol. 38, pp. 401–412; April, 1950.

[2] A. H. LaGrone, "Volume integration of scattered radio waves," Electrical Engineering Research Laboratory, The University of Texas, report no. 45; 1950.

[3] A. H. LaGrone, W. H. Benson, Jr., and A. W. Straiton, "Attenuation of radio signals caused by scattering," *Jour. Appl. Phys.*, vol. 22, pp. 672–674; May, 1951.

A General Theory for Frequency Discriminators Containing Null Networks*

JOHN L. STEWART†, ASSOCIATE, IRE

Summary—The characteristics of the ring demodulator and of null networks have suggested a generalized approach to the design of discriminators containing null networks. In the past, discriminators using null networks have been designed about various types of demodulators in which a carrier signal is necessary, the design fundamental being that the phase difference between the signal and carrier voltages applied to the demodulator should change by 180 degrees at the null frequency and be a multiple of pi radians immediately above and below the null frequency. However, since the phase difference has not been an even number of pi radians as the frequency departs from the null region, the output of the discriminator becomes sensitive to the amplitudes of both the signal and carrier voltages. The generalized theory presented in this paper permits the design of discriminators containing null networks where, neglecting second-order effects, coupling capacitors, and the like, the phase difference is maintained a multiple of pi radians at all frequencies.

The result is an inherently wide-band discriminator which can be constructed largely from unbalanced networks and which can be accurately calibrated. It is further possible to design discriminators of arbitrary sensitivities to the point where, neglecting noise, the discriminator behaves more as a frequency switch. The mechanization of the theory involves phase-equalizing networks in both the signal and carrier input systems to the demodulator. The general theory is concerned with admissible network functions consistent with the desire to maintain phase differences at a multiple of pi radians. One specific example is given.

I. Characteristics of the Ring Demodulator

THE OPERATING CHARACTERISTICS of the ring demodulator[1] of importance here (assuming linearity, zero reactance, and sinusoidal signal and carrier voltages of the same frequency) are as follows:

When the phase angle between the signal and carrier voltages is a multiple of pi radians and the ratio of the magnitudes of the carrier voltage to the signal voltage is at least two, the output will be proportional to only the signal voltage amplitude.

If the phase difference is not quite a multiple of pi radians, the output will be somewhat sensitive to the amplitude of the carrier voltage. This effect is proportional to the sine of the phase angle and inversely proportional to the ratio of the amplitudes, and can usually be made negligible.

II. Characteristics of Null Networks

Another type of circuit that will be used in the general class of discriminators is the null network. The classic example of a null network is the Wien bridge; however, there are many circuits, both balanced and unbalanced, that can be classified as null networks.[2] The unbalanced networks will be of most concern here.

It is useful to define a null network as one whose transfer function, when plotted on the complex frequency plane, has at least one pair of conjugate zeros on or near the real frequency axis. In this paper, it will be assumed that these zeros lie exactly on the real frequency axis.

It immediately follows, therefore, that at resonance (the null frequency) the amplitude of the transfer function becomes zero and the phase changes by 180 degrees.

III. General Theory

Consider the block diagram shown in Fig. 1. If the two networks are designed so that over the frequency range of interest

$$|E_s\underline{/\phi_1}| \leq \tfrac{1}{2}|E_c\underline{/\phi_2}|, \qquad \phi_1 - \phi_2 = n\pi \tag{1}$$

then, assuming the ideal ring demodulator, the dc output E_o will be directly proportional to E_s only. If dissipation and unbalance in the ring demodulator is neglected,

$$E_o = \pm 0.636 E_{sm}, \tag{2}$$

where E_{sm} is the peak value of E_s and the factor 0.636 relates the peak to the average value of E_s.

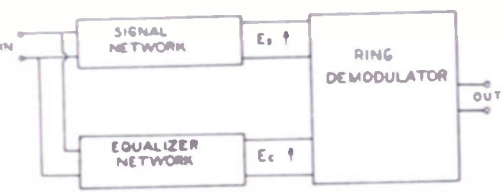

Fig. 1—General-system block diagram.

A little thought will show that if (1) is satisfied and if E_s shows a null-network behavior at some frequency ω_0, the output, E_o, will display the well-known discriminator characteristic about a center frequency of ω_0, assuming that the quasi steady-state method of analysis holds as usual.[3]

Hence the requirements on the two networks are specified. Note that the relative phase between E_c and

* Decimal classification: R361.217×R143. Original manuscript received by the Institute, December 4, 1950; revised manuscript received May 7, 1951.

This paper presents the results of research carried out at the Jet Propulsion Laboratory of the California Institute of Technology, under Contract DA-04-495-Ord-18, sponsored by the Department of the Army, Ordnance Corps.

† Stanford University, Stanford, Calif.

[1] V. Hughes, E. L. MacNichol, D. Sayre, and F. C. Williams, "Waveforms," Radiation Laboratory Series, McGraw-Hill Book Co., Inc., New York, N. Y., vol. 19, pp. 409–413; 1949.

[2] G. R. Harris, "Bridged reactance-resistance networks," Proc. I.R.E., vol. 37, pp. 882–887; August, 1949.

[3] J. R. Carson and T. C. Fry, "Variable electric circuit theory with applications to the theory of frequency modulation," *Bell Sys. Tech. Jour.*, vol. 16, p. 513; 1937.

E_s is all that is important, absolute phase angles (with respect to the source) being of only minor interest.

If the plots of the transfer functions of the signal and carrier networks on the complex frequency plane are identical, the relative phase will of course be zero. However, if they are identical except for the presence of a conjugate pair of zeros exactly on the real frequency axis, it can be seen that the relative phase angle will be either zero or 180 degrees. Continuing in this manner, three conditions can be deduced that the two networks must obey in order to obtain the desired end result.[4]

Condition 1: E_s and E_c will be in phase or in phase opposition at all frequencies only if the plots of the transfer functions of the signal and carrier networks on the complex frequency plane are identical. There are two exception, however: (1) The difference in the number of singular points (poles or zeros) at the origin of the plots of the signal and carrier networks must be an even number. (2) Any number of conjugate singularities may be present in either network if these singularities are purely imaginary.

Condition 2: If the first condition is satisfied and if the gain through the two networks is adjusted so that over the range of frequencies of interest $E_s \leqq \frac{1}{2}E_c$, then the output E_o will be directly proportional to only E_s.

Condition 3: If the first two conditions are satisfied and if a particular pair of conjugate zeros exists on the real frequency axis of the plot of the signal network at $j\omega_0$, but does not appear on the plot of the carrier network at the same point or may not appear at all, the entire system will be a discriminator whose center frequency is at ω_0.

The third condition, with the first two as necessary, is sufficient to permit the design of any discriminator covered by the theory of this paper.

IV. Methods for Obtaining Networks

The desired over-all discriminator transfer function can be obtained by means of two different methods or any combination thereof.

The first method is that of adding in the carrier system networks that give poles and zeros of the same type and at the same points as those appearing in the signal network. This method may be called "carrier equalization."

The second method is that of adding, in the signal network, networks designed to produce singularities of the opposite types but at the same points as those appearing in the same signal network in order to cancel undesirable poles or zeros. This method may be called "signal equalization."

It is also clear that any properly isolated filter amplifier, with any transfer function whatsoever, may be added in cascade with either the signal or carrier stages without violating the three conditions only if, for each stage added in one network, an identical stage is added to the other network.

[4] The inference to vectors given by a collection of poles and zeros on the complex frequency plane is highly useful here in visualizing the phase functions.

V. Example—A Low-Frequency Discriminator

The example shown in Fig. 2 neglects loading on the twin-T null network and stray capacitances; hence, the equations are valid only at low frequencies. The twin-T was chosen as its transfer function is simple when the T is not loaded, the function being given by

$$\frac{e_{out}}{e_{in}} = \frac{p^2 = \dfrac{G^2}{2C^2}}{\left(p + \dfrac{3+\sqrt{7}}{2}\dfrac{G}{C}\right)\left(p + \dfrac{3-\sqrt{7}}{2}\dfrac{G}{C}\right)}, \tag{3}$$

where the values in Fig. 2 are adjusted to give zeros on the real frequency axis so that the null frequency can be tuned, using a three-gang variable resistor where the three gangs are identical.

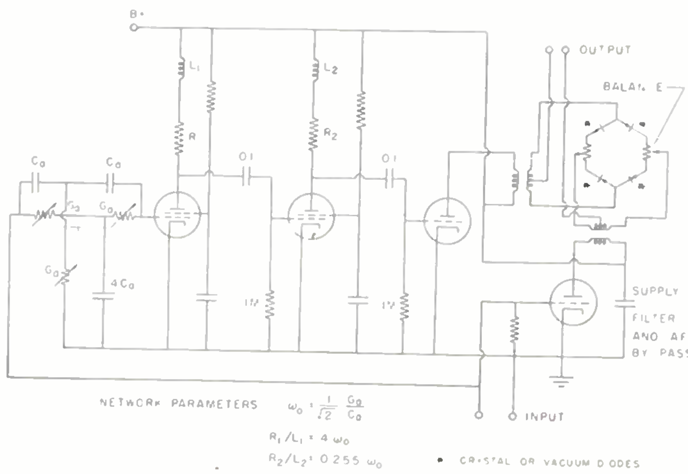

Fig. 2—A low-frequency discriminator.

Fig. 2 shows that pure signal equalization is used, there being no carrier network. As such, the two resistance-inductance series circuits can be made to cancel the two poles given by the twin-T. When cancellation occurs, the over-all discriminator transfer function can be written as

$$G_t = [g_{m_1}g_{m_2}L_1L_2(\omega_0^2 - \omega^2)]G_dG_rG_e, \tag{4}$$

where subscripts 1 and 2 refer to the first and second interstages, respectively, and where G_t is the over-all gain, G_d is the gain of the triode demodulator driver, G_r is the transfer gain of the ring demodulator, g_m is the vacuum-tube transconductance, and G_e is the gain of any further stages (not shown in Fig. 2) added in cascade with the signal-equalization networks. It is assumed that G_e is purely real.

It can be seen from (4) that the sensitivity of the discriminator can be increased to the noise level, 2 volts dc per cycle at 1,500 cycles being readily obtainable using the circuit of Fig. 2.

As an alternate to the circuit of Fig. 2, a discriminator was built utilizing pure carrier equalization. As such, a carrier network introducing two poles on the negative imaginary frequency axis of the complex plane at the same points as those introduced by the twin T is needed. Such a circuit can be constructed from a two-section resistance-capacitance ladder-type filter. Then, only purely real gain will exist in the signal network in cascade with the null network.

A note can be added regarding the tuning of the null network. A three-gang variable capacitor makes a good tuning arrangement, but is impractical at the lower frequencies if wide tuning excursions are desired. If resistance tuning is used in a resistance-capacitance null network, the null frequency will be inversely proportional to resistance. Quite acceptable resistance-inductance null networks at low frequencies can be built, in which case the null frequency is directly proportional to resistance.

For small tuning excursions only the null network need be tuned. Imperfect cancellation of the effects of the roots of the null network on the negative real axis will result, but the effect will be small. For wide tuning excursions, the equalizing networks should also be adjusted, but the tracking need not be excessively close as the relative phase error at the inputs to the ring demodulator will usually be small.

Input Admittance Characteristics of a Tuned Coupled Circuit*

ROY A. MARTIN,† MEMBER, IRE, AND R. D. TEASDALE,‡ MEMBER, IRE

Summary—A steady-state analysis is given of an important double-tuned coupled circuit to determine the input admittance when the primary Q is high and the secondary Q is low. Particular emphasis is placed on the phase variation of the admittance with frequency. Dimensionless curves of magnitude and phase illustrate the effect of varying the coefficient of coupling and the secondary Q. Mathematical expressions are obtained for the points where the phase passes through zero, and are used in a discussion of bandwidth. The effect of detuning is also considered.

I. Introduction

Tuned coupled circuits are widely used in amplifier, filter, and oscillator applications. They have been investigated from several points of view by Aiken,[1] Dishal,[2] Chang,[3] and others.[4-10] In almost every case, however, interest has centered upon the transfer functions, particularly when the secondary Q is high.[1,2] In contrast, this paper is concerned with a study of input admittance, particularly when the secondary Q is low.

This investigation provides information useful in solving two oscillator problems of current interest: (a) to synchronize an oscillator with a very small signal to secure performance equivalent to that of a high-gain limiter amplifier for frequency-modulated signals;[11,12,13] and (b) to produce a high-frequency crystal-controlled oscillator circuit to operate over a wide frequency range (60 ± 10 mc), the operating frequency to be selected merely by inserting a suitable crystal.

A requirement common to both these problems is that the magnitude of the input admittance should remain relatively constant, and the phase deviation small, over a wide frequency range. Typically, it is desirable to design a coupled circuit whose total phase deviation will be less than a specified amount over the widest practical frequency range. With certain restrictions it is possible to adjust the coupling coefficient and the secondary Q of the circuit of Fig. 1 to obtain the desired results. Practical coupled circuits for these applications are characterized by low values of secondary Q (below 10) and relatively high values of k (about 0.3).

* Decimal classification: R142.3. Original manuscript received by the Institute, November 30, 1950; revised manuscript received, May 22, 1951.

† Research Engineer, State Engineering Experiment Station, Georgia Institute of Technology, Atlanta, Ga.

‡ School of Electrical Engineering, Georgia Institute of Technology, Atlanta, Ga.

[1] C. B. Aiken, "Two mesh tuned coupled-circuit filters," Proc. I.R.E., vol. 25, pp. 230–272; February, 1937.

[2] M. Dishal, "Exact design and analysis of double- and triple-tuned band-pass amplifiers," Proc. I.R.E., vol. 35, pp. 606–626; June, 1947.

[3] S. H. Chang, "Parabolic loci for two tuned coupled circuits," Proc. I.R.E., vol. 36, pp. 1384–1388; November, 1948.

[4] A. E. Harrison and N. W. Mather, "Graphical analysis of tuned coupled circuits," Proc. I.R.E., vol. 37, pp. 1016–1020; September, 1949.

[5] V. C. Rideout, "A note on a parallel-tuned transformer design," *Bell Sys. Tech. Jour.*, vol. 27, pp. 96–108; January, 1948.

[6] F. L. Smith, "Radiotron Designers Handbook," Amalgamated Wireless Valve Company, Ltd., Sydney, Australia; 1940.

[7] E. S. Purrington, "Single and coupled-circuit systems," Proc. I.R.E., vol. 18, pp. 983–1016; June, 1930.

[8] J. E. Maynard, "Universal performance curves for tuned transformers," *Electronics*, vol. 10, pp. 15–18; February, 1937.

[9] N. I. Korman, "Coupled resonant circuits for transmitters," Proc. I.R.E., vol. 31, pp. 28–32; January, 1943.

[10] N. W. Mather, "An analysis of triple-tuned coupled circuits," Proc. I.R.E., vol. 38, pp. 813–822; July, 1950.

[11] G. L. Beers, "A frequency-dividing locked-in oscillator frequency-modulation receiver," Proc. I.R.E., vol. 22, pp. 730–737; December, 1944.

[12] W. E. Bradley, "Single-stage fm detector," *Electronics*, vol. 19, pp. 88–91; October, 1946.

[13] C. W. Carnahan and H. P. Halmus, "Synchronized oscillators as fm-receiver limiters," *Electronics*, vol. 17, pp. 108–111; August, 1944.

The notation used is shown in Fig. 1 and Table I.

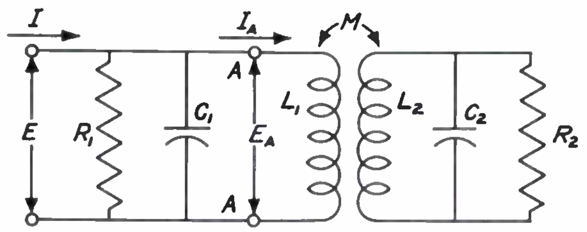

Fig. 1—Parallel form of tuned coupled circuit.

TABLE I

NOTATION

$k = M/\sqrt{L_1L_2}$ Coupling coefficient.
$\omega_1 = 1/\sqrt{L_1C_1}$ Resonant frequency of primary alone.
$\omega_2 = 1/\sqrt{L_2C_2}$ Resonant frequency of secondary alone.
$\omega_0 =$ Resonant frequency when $\omega_1 = \omega_2$.
$x = \omega/\omega_2$ Ratio of actual frequency to resonant frequency of secondary.
$y = \omega/\omega_1$ Ratio of actual frequency to resonant frequency of primary.
$\rho = x/y = \omega_1/\omega_2$ Detuning parameter.
$Q_1 = R_1/\omega_0L_1$ Primary Q.
$Q_2 = R_2/\omega_0L_2$ Secondary Q.
$m = 1 - k^2$ Useful dimensionless factor.
$Y_A = I_A/E_A = G_A + jB_A$ Input admittance at section AA.
$Y = I/E = G + jB =$ Input admittance of complete network.
$\phi = \tan^{-1} B/G =$ Phase angle of Y.
$x_1, x_2, x_3 =$ Roots of $\phi(x) = 0$ in ascending order.
$\Delta x_{13} = x_3 - x_1$ root separation; a value related to bandwidth.
$\Delta x, \Delta\phi =$ Bandwidth and associated total phase deviation.
$Q_{2c} =$ Critical Q_2.
$k_c =$ Critical k.

II. The Admittance Equation

The input admittance Y for the circuit of Fig. 1 may be determined by a straightforward application of Kirchhoff's Laws. If dimensionless qualities from Table I are introduced, this input admittance can be written in normalized form, as follows:

$$Y\omega_0L_1 = \frac{1 + \dfrac{Q_2}{Q_1(1 - x^2m)} - x^2m + j\left[Q_2x(1 - x^2m) + \dfrac{xm}{Q_1} + Q_2\left(x - \dfrac{1}{x}\right)\right]}{Q_2(1 - x^2m) + jxm}. \qquad (1)$$

In obtaining (1), use was made of the restriction $\omega_1 = \omega_2 = \omega_0$. The detuning case for which $\omega_1 \neq \omega_2$ is treated later in Section VI.

Although (1) is concisely written, it is unwieldly because of the many variables. Examination of (1) shows that before the input admittance can be plotted against x, three parameters must be specified, i.e., Q_1, Q_2, and m (or k). In many practical circuits the primary and secondary admittance levels are such that a relatively large value of Q_1 is required to obtain matching. In the present case, in particular, interest centers on high values of Q_1 (above 20) and low values of Q_2 (below 10). For this range of values of Q_2, the nature of the terms in (1) is such that the input admittance will change only slightly for values of Q_1 above 20. Thus, for practical purposes (1) with $Q_1 = 20$ adequately represents the situation for $Q_1 \gg 20$ as well. With Q_1 fixed at 20, (1) then represents a double family of curves. With Q_2 fixed, the parameter k defines one family; with k fixed, the parameter Q_2 defines a second family.

Attempts to obtain detailed information as to the shape of the admittance and phase curves solely from examination of (1) proved futile. Therefore, the study was continued on a numerical basis.

With $Q_1 = 20$, as discussed above, Q_2 was chosen as 5 on the basis of laboratory experience. With the Q values thus specified, preliminary computations indicated that values of k near 0.3 would produce a phase curve which deviated from zero by approximately ± 20 degrees throughout the entire bandwidth. This particular value was chosen as representative of a good oscillator design because most crystals will function satisfactorily within this 20-degree limit.

III. Computed Curves

The results of the computations with $Q_1 = 20$ throughout have been plotted. Figs. 2 and 3 show the variation of the magnitude and phase of the input admittance for k constant and Q_2 variable. Fig. 4 shows the variation of phase for Q_2 constant and k variable. Since Q_2 may be changed rather easily by varying R_2 and since k is more difficult to measure than Q_2, the curves of Figs. 2 and 3 appear to be of more practical interest than that of Fig. 4.

The magnitude of $Y\omega_0L_1$ versus x for constant k (Fig. 2) exhibits the familiar double hump, typical of an overcoupled circuit. These curves possess no exact symmetry. While they become somewhat more symmetrical in the region of the peak as Q_2 increases, the magnitude increases so much that the added symmetry is of minor importance. Actually, it is desirable to keep Q_2 at or below 5 to hold the peak value sufficiently low.

The problem of keeping the phase deviation small over a wide range of x places more exacting restrictions on Q_2. The phase curves of Fig. 3 show the transition from the shorted secondary condition ($Q_2 = 0$) through the complete range of Q_2 to the open secondary case ($Q_2 = \infty$). The shorted secondary condition gives the exact phase curve for the primary circuit alone and is in agreement with well-known theory. As Q_2 increases, the curves cross the $\phi = 0$ line once below Q_{2c} (the critical secondary Q) and three times above Q_{2c}. For the k and Q_1 of Fig. 3, $Q_{2c} = 2.63$. As shown later, the crossing at $x = 1.07$ remains fixed at $1/\sqrt{1-k^2}$ or $1/\sqrt{m}$ for all values of Q_1 and Q_2. There is a slight tendency toward symmetry for Q_2 above 10. Values of Q_2 somewhat larger than Q_{2c} yield curves which satisfy the specified ± 20-degree phase deviation requirements for crystal oscillators; however, for $Q_2 = 5$ the phase curve exceeds this

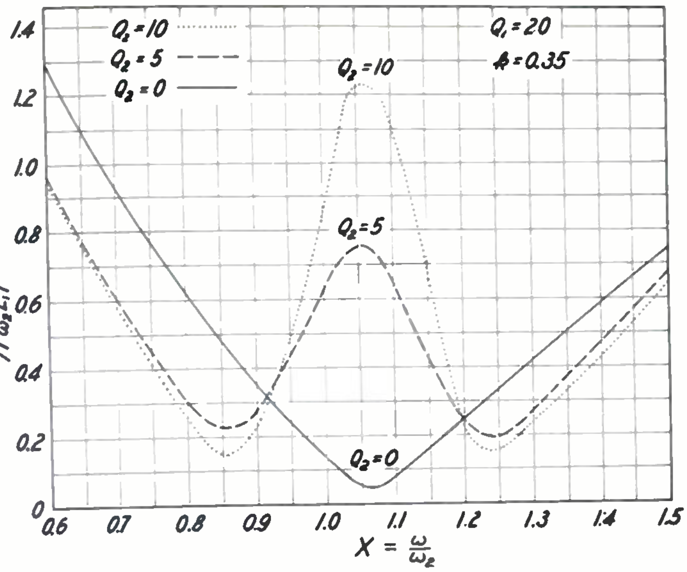

Fig. 2—Variation of the input admittance with secondary Q.

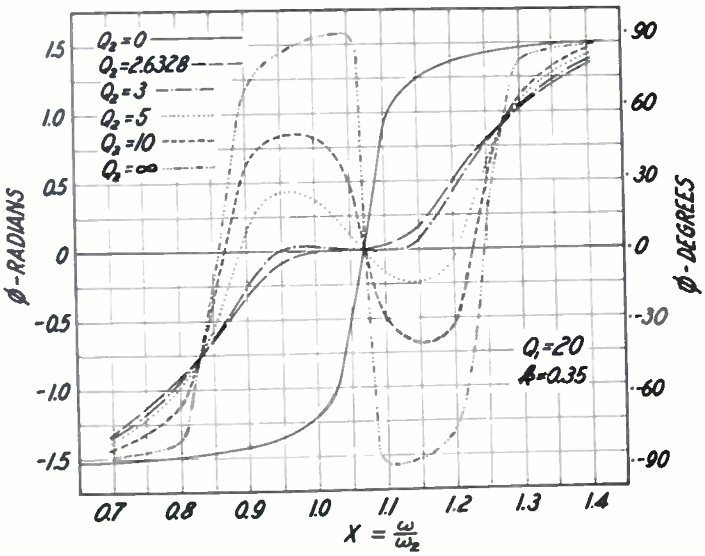

Fig. 3—Variation of the phase angle of the input admittance with secondary Q.

limit by 5 degrees on the low-frequency side.

A magnitude curve of $Y\omega_0L_1$ for constant Q_2 will also exhibit a double hump. Although these curves resemble those of Fig. 2, increasing k does not improve symmetry in the region of interest. As k is increased, the peak near $x=1$ shifts continually toward the right. As in Fig. 2, the changes in magnitude near the region of interest become larger as k increases.

The phase variation, as k is changed (Fig. 4), is of greater interest. As k increases, the left-hand intercept x_1 of the phase curves approaches the value $x=0.707$, as shown for the $k=1$ curve. For values of k near 0.3 the symmetry of the phase curves remains reasonably good. These curves show the transition from the condition of no coupling to that of maximum coupling. For the Q_1 and Q_2 of Fig. 4 the critical k is 0.19. Below critical k the curves cross the $\phi=0$ line only once; above k_c the curves cross three times. As k approaches unity, both the extreme right and center crossings move off an indefinite distance to the right.

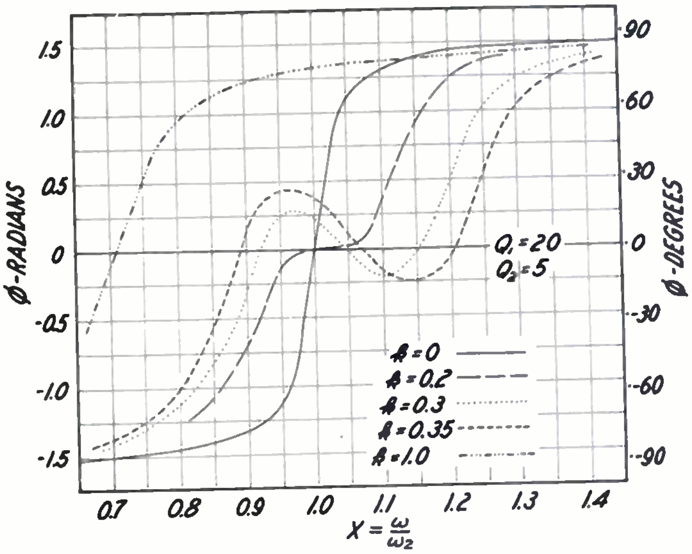

Fig. 4—Variation of the phase angle of the input admittance with coupling coefficient.

IV. Zero-Phase Intercepts

An examination of the $\phi=0$ intercepts is suggested by the behavior of the phase characteristics near $x=1$. A mathematical expression for $\phi(x)$ may be obtained by expressing ϕ from (1) in terms of the numerator phase angle θ_N and the denominator phase angle θ_D, i.e. $\phi(x)=\theta_N(x)-\theta_D(x)$. Algebraic manipulations then yield

$$\phi(x) = \tan^{-1}\frac{(x^2m-1)\left[Q_2mx^4+(m-2Q_2)x^2+Q_2^2\right]}{xQ_2+\dfrac{xQ_2^2(1-x^2m)}{Q_1}+\dfrac{x^2m^2}{Q_1}-xmQ_2}. \quad (2)$$

Inspection of the factors of (2) shows that $\phi(x)$ vanishes for

$$x = 1/\sqrt{m} \quad (3)$$

and for

$$x = +\left[1/m - 1/2Q_2^2 \pm \sqrt{(1/m - 1/2Q_2^2)^2 - 1/m}\right]^{1/2}. \quad (4)$$

Only the positive value of the outer radical is considered, for $x=\omega/\omega_0$ cannot be negative. Since x cannot be complex, (4) requires the condition that

$$(1/m - 1/2Q_2^2)^2 - 1/m \geq 0. \quad (5)$$

The positive root given by (3) is independent of both Q_1 and Q_2. The roots given by (4) are independent of Q_1. The real positive roots of $\phi(x)=0$ are, in ascending order,

$$x_1 = \left[1/m - 1/2Q_2^2 - \sqrt{(1/m - 1/2Q_2^2)^2 - 1/m}\right]^{1/2} \quad (6)$$

$$x_2 = 1/\sqrt{m} \quad (7)$$

$$x_3 = \left[1/m - 1/2Q_2^2 + \sqrt{(1/m - 1/2Q_2^2)^2 - 1/m}\right]^{1/2}. \quad (8)$$

The position of these roots is shown in Fig. 5. If condition (5) is not satisfied, x_1 and x_3 become complex and have no meaning. Thus, from (5), the equality

$$(1/m - 1/2Q_2^2)^2 - 1/m = 0 \tag{9}$$

defines a boundary or "critical" condition for which $x_1 = x_3$. Equation (9) has two variables, k and Q_2, and may be readily solved for either one in terms of the other. For the constant k characteristic of Fig. 3, (9) may be solved to yield the critical value of Q_2.

$$Q_{2c} = \sqrt{\frac{m}{2(1 - \sqrt{m})}}. \tag{10}$$

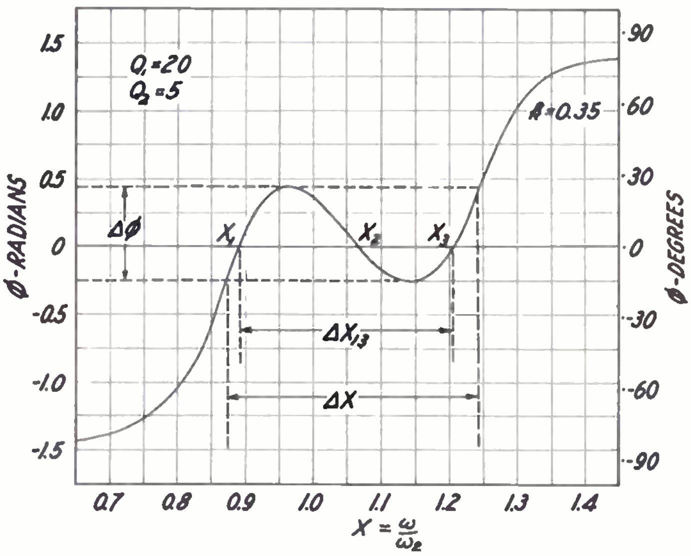

Fig. 5—Definition of the total phase deviation and bandwidth.

For the constant Q characteristic of Fig. 4, (9) may be solved to yield the critical value of k.

$$k_c = [1 - Q_2^4(\sqrt{1 + 2/Q_2^2} - 1)^2]^{1/2}. \tag{11}$$

As $Q_2 \to Q_{2c}$ or as $k \to k_c$, $x_1 \to x_3$; this critical condition represents the maximum value for x_1 and the minimum value for x_3.

Figs. 3 and 5 show that the separation of the roots, Δx_{13}, is closely associated with the bandwidth, Δx. Manipulation of (6), (8), and (10) yields a simple expression for Δx_{13} for the constant k case.

$$\Delta x_{13} = [1/Q_{2c}^2 - 1/Q_2^2]^{1/2}. \tag{12}$$

Since Δx_{13} is always less than Δx, (12) provides a pessimistic approximation of the exact bandwidth Δx. This simple approximation proves useful in adjusting circuit parameters to obtain a desired bandwidth when k is known and when Q_2 may be adjusted by loading.

V. Bandwidth

The phase characteristics and the oscillator problem are closely related. Accordingly, the bandwidth Δx and the total phase deviation $\Delta\phi$ are defined (Fig. 5).

Values of $\Delta\phi$ and Δx for k constant are read from Fig. 3, for Q_2 constant from Fig. 4. The resulting values are plotted in Figs. 6 and 7. These curves should be of considerable help in the selection of circuit parameters. The variation of $\Delta\phi$ in both cases is quite linear over the initial portion of the curves.

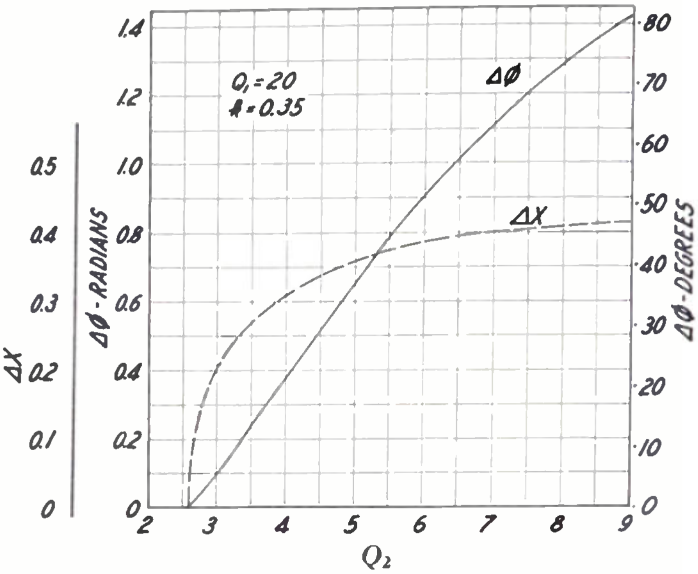

Fig. 6—Variation of total phase deviation and bandwidth with secondary Q.

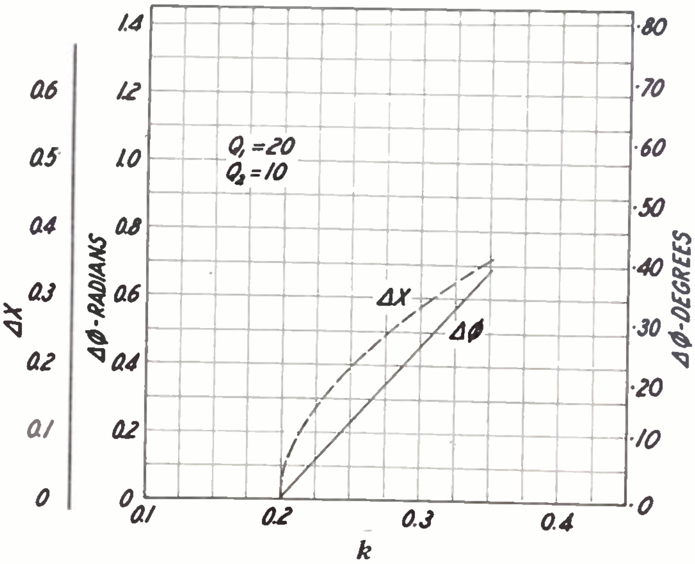

Fig. 7—Variation of total phase deviation and bandwidth with coupling coefficient.

VI. Effect of Detuning

Figs. 3 and 4 show that the phase deviations about $\phi = 0$ are not symmetrical when $\omega_1 = \omega_2$. In practice such symmetry is often desirable and may be obtained by a slight detuning. Accordingly, the situation when $\omega_1 \neq \omega_2$ has been investigated. The input admittance can be rewritten conveniently in component form,

$$Y = 1/R_1 + G_A + j(\omega C_1 + B_A), \tag{13}$$

where G_A and B_A are the conductance and susceptance as seen from section AA. Then introduction of a detuning parameter $\rho = x/y = \omega_1/\omega_2$ and substitution into (13) yields, after normalization,

$$Y\omega_1 L_1 = 1/Q_1 + \rho G_A \omega_2 L_1 + j(x/\rho + \rho B_A \omega_2 L_1). \quad (14)$$

In (14) x is still the dependent variable, but the admittance, Y, is now normalized to $\omega_1 L_1$, a constant only slightly different from $\omega_2 L_1$, provided ρ remains approximately 1.

Fig. 8 shows phase curves calculated from (14) for slight detuning. As ρ increases, the entire $\rho = 1$ curve rotates about the origin in a clockwise direction; as ρ decreases, the curve rotates in the opposite direction. For the particular case of Fig. 8 the $\rho = 1.025$ curve exhibits excellent symmetry, about $\phi = 0$. The slight detuning required to obtain $\rho = 1.025$ is best accomplished by varying C_1. Although ρ depends upon both ω_1 and ω_2, varying C_2 does not give a direct correction because C_2 acts on the primary by way of the coupling of L_1 and L_2. To obtain a clockwise rotation, ω_1 must be increased over ω_2 so that C_1 must be decreased.

An increase in ρ also gives a clockwise rotation to the magnitude curves, $Y\omega_1 L_1$ versus x; the effect is small compared to the effect on the phase curves of Fig. 8.

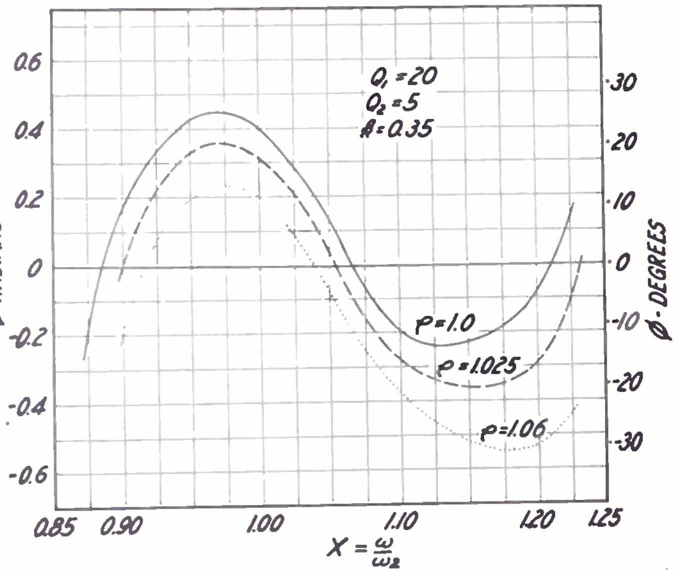

Fig. 8—Variation of the phase angle of the input admittance with the detuning parameter ρ.

VII. Conclusions

The analysis and curves presented herein show that the circuit of Fig. 1 may be used to obtain desirable input admittance characteristics. Specifically, small phase deviation and wide bandwidths may be achieved by using high values of Q_1, low values of Q_2, and intermediate values of k. Thus values of k and Q_2 may be chosen to obtain either a specified phase deviation $\Delta\phi$ or a specified bandwidth Δx. Use of the specific numerical curves should result in a considerable saving of time to the designer. Furthermore, (1) and (14) are general relations which permit computation of similar curves for any application requiring the circuit of Fig. 1.

Acknowledgment

The authors are pleased to acknowledge the helpful suggestions and constant encouragement of W. A. Edson of the School of Electrical Engineering, Georgia Institute of Technology.

Nullification of Space-Charge Effects in a Converging Electron Beam by a Magnetic Field*

M. E. HINES†, MEMBER, IRE

Summary—**This paper presents the conditions necessary for maintaining a uniformly converging conical electron beam in the presence of space charge. It is an extension of the Brillouin focusing condition to conical flow, requiring a converging rather than a uniform magnetic field. In this type of electron flow, the diverging effects of space charge are balanced against magnetic reaction forces for reasonably small cone angles of convergence. Though the balance of forces is exact only for infinitesimal angles, it is reasonably accurate for cones of half-angle as great as 10 degrees. The minimum beam size will be limited only by the effects of thermal velocities, by gun aberrations, and by the magnetic field obtainable.**

I. Introduction

THERE IS A NEED for electron guns and focusing methods to produce high-intensity electron beams of small diameter. In conventional electron guns of the Pierce type[1] the beam leaves the gun focused toward a point; however, space-charge repulsion prevents the beam from converging sharply, and instead it spreads outward again without achieving a true cross-over.

This paper presents a solution of the equations of motion for a uniformly converging conical electron beam in which the space-charge repulsion forces are nullified by means of a suitably shaped magnetic field The minimum beam diameter will be limited only by the magnetic field obtainable, by thermal electron velocities, and by focusing aberrations of the gun. The

* Decimal Classification: R138.1. Original manuscript received by the Institute, February 9, 1951; revised manuscript received May 21, 1951.

† Bell Telephone Laboratories, Murray Hill Laboratory, Murray Hill, N. J.

[1] J. R. Pierce, "Theory and Design of Electron Beams," D. Van Nostrand and Co., Inc., New York, N. Y., pp. 35–37, 152–155, and Chapt. X; 1949.

analysis given applies accurately only for cases of relatively small angles of convergence in which the cone half-angle is on the order of 0 to 10 degrees. The results reported here are theoretical and without experimental verification.

This conical-beam case is an extension of the uniform diameter-beam case treated by Brillouin,[2] Pierce,[1] and Samuel.[3] In that case, a beam of electrons travels along a uniform magnetic field. Each electron spirals about the axis at a uniform angular velocity and constant radius from the axis of the beam. The space-charge repulsion forces and the centrifugal forces of rotation are exactly cancelled by the magnetic reaction between the longitudinal magnetic field and the rotational velocity of the electrons.

In the conical-beam case described here similar cancellations occur. The beam spirals about the axis with an angular velocity inversely proportional to the beam diameter. The magnetic field converges so that it is also inversely proportional to the beam diameter, and the beam converges uniformly in this field with the beam assuming the shape of a cone. The two types of flow are shown in Fig. 1.

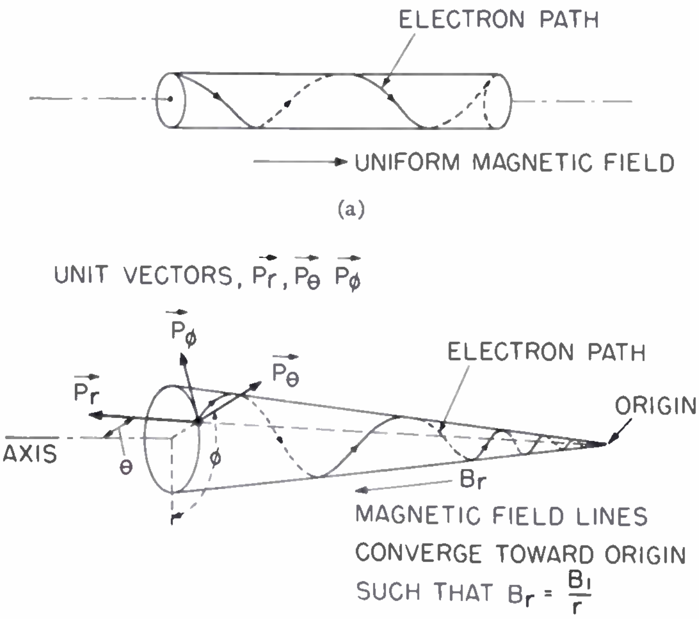

Fig. 1—(a) Uniform diameter beam flow of Brillouin. (b) Conical beam flow in a paraboloidal magnetic field.

II. Mathematical Analysis

Spherical polar co-ordinates will be used to describe the electron paths and the electric and magnetic fields. The orientation of the co-ordinates is shown in Fig. 1(b), and mks practical units will be used. Some of the symbols are defined in the following:

[2] L. Brillouin, "A theorem of Larmor and its importance for electrons in magnetic fields," *Phys. Rev.*, vol. 67, pp. 260–266; 1945.

[3] A. L. Samuel, "On the theory of axially symmetric electron beams in an axially symmetric magnetic field," Proc. I.R.E., vol. 11, pp. 1252–1258; November, 1949.

q = charge density expressed in coulombs per unit solid angle per meter along the radius

ρ = charge density in coulombs per cubic meter

η = charge to mass ratio of the electron 1.76×10^{11} coulombs per kg

ϵ = dielectric constant of vacuum $1/36\pi\times10^{-9}$ farads per meter

I = beam current in amperes

V_0 = axial potential in volts

V = space potential in volts

B = magnetic flux density in webers/m^2 (1 weber/m^2 = 10^4 gausses).

The "dot" notation signifies total time derivatives $\dot{r}$, indicating dr/dt, and $\ddot{r}$, indicating d^2r/dt^2, and so on.

The method of solution is indirect in that an assumed set of conditions is shown to satisfy the equations of motion for small angles of convergence. The first assumptions are that the radial velocity is constant and independent of θ and that there are no motions in the θ direction. A magnetic-field configuration, which roughly corresponds to the Brillouin condition at each point in the beam, is chosen. Such a field is described by the following equations:

$$B_r = \frac{B_1}{r}, \tag{1}$$

$$B_\theta = -\frac{B_1}{r}\tan\frac{\theta}{2}, \tag{2}$$

$$B_\phi = 0, \tag{3}$$

where B_1 is the magnitude of the radial component of the field at unity radius. This field has zero divergence and zero curl, and is physically realizable with appropriate boundary conditions. All magnetic equipotentials are paraboloids of revolution with a common focus at the origin.

It is also assumed that the cathode is shielded from the magnetic field and that all fields are axially symmetric. From Busch's theorem[4] we can deduce the angular velocity $\dot{\phi}$ for electrons at any point in the space. For this case the theorem specifies that

$$\dot{\phi} = \frac{\eta\Phi}{2\pi r^2\sin^2\theta},$$

where Φ is the total magnetic flux in the positive r direction which passes through a surface bounded by constant r and θ. For the magnetic field chosen,

$$\Phi = 4\pi r B_1\sin^2\frac{\theta}{2}$$

and

$$\dot{\phi} = \frac{\eta B_1}{2r\cos^2\frac{\theta}{2}}. \tag{4}$$

[4] A treatment of Busch's theorem is given by Pierce, Reference 2.

Our assumed velocity field is further specified by a constant r velocity and zero θ velocity, as summarized below.

$$\dot{r} = -\sqrt{2\eta V_0}, \tag{5}$$

$$\dot{\theta} = 0. \tag{6}$$

If we also assume a uniform radial-current density over the cone, we can find the electrostatic field configuration due to space charge. For a conical conducting boundary the field *within the beam* is given by

$$E_r = 0, \tag{7}$$

$$E_\theta = \frac{q}{\epsilon r}\tan\frac{\theta}{2}, \tag{8}$$

$$E_\phi = 0, \tag{9}$$

where q is the charge density expressed in coulombs per unit solid angle per unit radius. The total current carried within a cone bounded by an angle ψ is

$$I = 4\pi q\sqrt{2\eta V_0}\sin^2\frac{\psi}{2}\ \text{amperes}. \tag{10}$$

We now have a set of assumed conditions specifying the velocity distribution and the static fields. That these conditions satisfy the equations of electron motion remains to be demonstrated. These equations are

$$\ddot{r} - r\dot{\theta}^2 - (r\sin^2\theta)\dot{\phi}^2 = -\eta[E_r + r\dot{\theta}B_\phi - r\sin\theta\dot{\phi}B_\theta], \tag{11}$$

$$2\dot{r}\dot{\theta} + r\ddot{\theta} - (r\sin\theta\cos\theta)\dot{\phi}^2 = -\eta[E_\theta + r\sin\theta\dot{\phi}B_r - \dot{r}B_\phi], \tag{12}$$

$$(2\sin\theta)\dot{r}\dot{\phi} + (2r\cos\theta)\dot{\theta}\dot{\phi} + (r\sin\theta)\ddot{\phi} = -\eta[E_\phi + \dot{r}B_\theta - r\dot{\theta}B_r]. \tag{13}$$

Substitution of the assumed values for the velocities, fields, and accelerations into these equations yields exact identities for (11) and (13). With another substitution

$$q = -\frac{\eta\epsilon B_1^2}{2}, \tag{14}$$

(12) yields

$$-\frac{\eta^2 B_1^2\tan\frac{\theta}{2}}{2r}\left[\frac{\cos\theta}{\cos^2\frac{\theta}{2}}\right] \simeq \frac{-\eta^2 B_1^2\tan\frac{\theta}{2}}{2r}. \tag{12}$$

This approaches an identity for small θ, where the expression in the brackets may be considered equal to 1. It is very nearly an identity even for θ as large as 10 degrees where the ratio of cosines is 0.992. This discrepancy represents an unbalance of forces in the θ direction, which is practically negligible for reasonably small θ on the order of 0 to 10 degrees. This means that the assumed velocity distribution is not quite correct for the outer electrons in a wide-angle beam. Equation (14) specifies the magnetic field required for the proper balance of forces in the θ direction for any degree of space charge. In terms of current within a bounding angle ψ this expression becomes

$$\begin{aligned} I &= 2\sqrt{2}\pi\epsilon\eta^{3/2}B_1^2V_0^{1/2}\sin^2\frac{\psi}{2} \\ &= 5.81\times10^6\, B_1^2V_0^{1/2}\sin^2\frac{\psi}{2}\ \text{amperes}. \end{aligned} \tag{15}$$

III. Energy and Velocity Considerations

The electrostatic potential in the beam is a function of the angle θ only. For small θ we may use the approximation that

$$E_\theta \simeq \frac{q\theta}{2\epsilon r}\quad(\theta\ \text{small}),$$

which gives

$$V \simeq V_0 - \frac{q\theta^2}{4\epsilon}\quad(\theta\ \text{small}). \tag{16}$$

If the electrons were emitted from a cathode at zero potential, their kinetic energies must correspond to the space potential V, as expressed by the equation

$$r^2\dot{\theta}^2 + \dot{r}^2 + (r\sin\theta\dot{\phi})^2 = 2\eta V.$$

Substitution from (4), (5), (6), (14) and (16) yields

$$2\eta V_0 + \frac{\sin^2\theta\eta^2B_1^2}{4\cos^4\frac{\theta}{2}} \simeq 2\eta\left(V_0 + \frac{\eta B_1^2\theta^2}{8}\right),$$

which approaches an identity for small θ.

IV. Boundary Conditions

For the electrostatic field we have postulated a cone-shaped conducting shell surrounding the beam. For such a boundary the electrostatic fields will be oriented as shown in Fig. 2(b), following page.

The magnetic-field configuration is also shown in Fig. 2(a). Both equipotentials and flux lines conform to the surfaces of paraboloids of revolution, which have a common focus with the electron stream. There should be no difficulty in simulating the required field with large-sized paraboloidal pole pieces.

This type of electron flow must originate from a cathode which is shielded from the magnetic field, otherwise the required angular velocity cannot be obtained. The transition zone between the field-free region and region of prescribed field may have important effects on establishment of proper velocity distribution.

Fig. 3 shows an arrangement which may be capable of producing this type of flow. A conventional Pierce[1] type of point-focused gun is enclosed by a magnetic shield

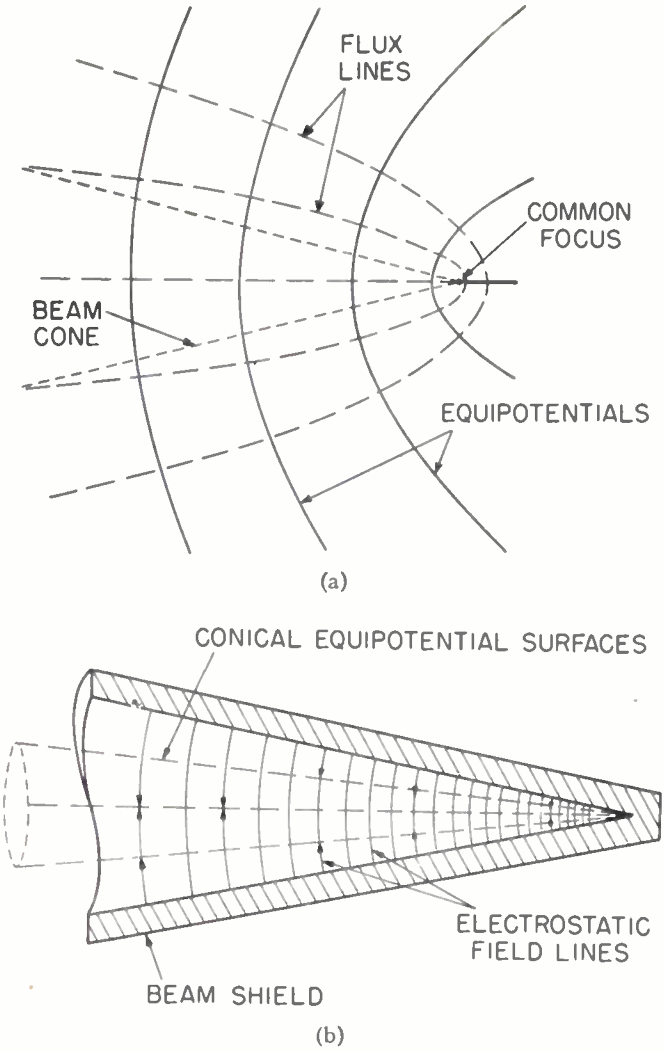

Fig. 2—(a) Paraboloidal magnetic field required for conical flow. (b) Electrostatic field from space charge for the case of a conical conducting boundary.

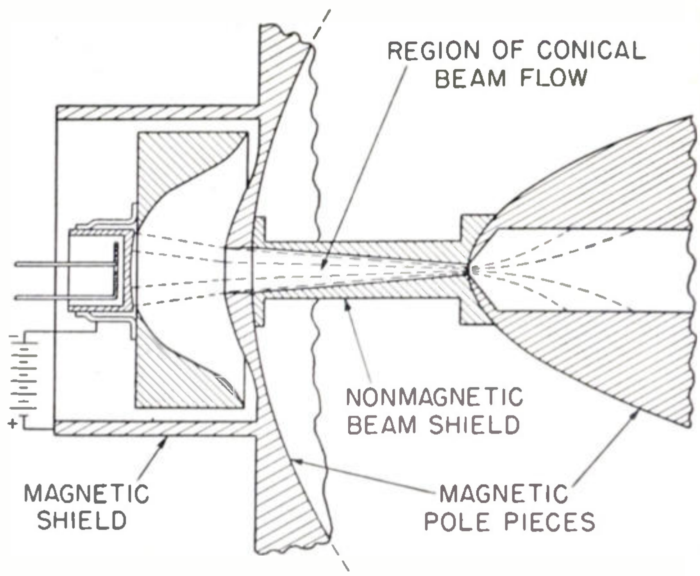

Fig. 3—Configuration of electrodes and magnetic-pole pieces for producing conical flow (not drawn to scale).

so arranged that the beam is injected through an aperture into the region of paraboloidal field. Upon passing through the aperture, the local transverse components of field will give the beam a twist of exactly the right amount, as specified by Busch's theorem. If the magnetic field were to build up suddenly in a very short length, then the only effect of the transition region would be that of providing beam rotation. Actually, the zone must have a finite length so that there will be some change in the angle of convergence. This effect can be minimized by making the aperture as small as possible without intercepting portions of the beam. Low current density will also help in this regard. Within the transition zone the beam will tend to spread because the space-charge forces are not completely balanced out. The amount of spread within this zone will be less than that which would be caused by the space-charge forces alone. It should be noted that the anode aperture in the Pierce gun causes beam spreading also because of local electrostatic fields at the aperture. It has been assumed in the above that this effect has already been taken into account.

Correction

W. E. Mathews, author of the paper, "Traveling-Wave Amplification by Means of Coupled Transmission Lines," which appeared on pages 1044–1051 of the September, 1951 issue of the PROCEEDINGS OF THE I.R.E., has brought the following corrections to the attention to the editors:

On page 1044, in the second column and 32nd line, it should read $\sqrt{\mu\sigma_2}$ instead of $\pi\sqrt{\mu\sigma_2}$.

On page 1048, the symbol μ should be inserted to the left of the equal sign in equation (47).

Traveling-Wave Tube Noise Figure*

D. A. WATKINS†, ASSOCIATE, IRE

Summary—The reduction of shot noise by space charge at high frequencies in a parallel-plane diode was predicted by Rack.[1] Neglecting space charge and circuit loss, Pierce[2] has employed Rack's method in estimating the noise figure of the traveling-wave tube. In the present paper, use is made of the Hahn-Ramo[3,4] space-charge waves together with Pierce's theory to show that the noise convection current has maxima and minima along the stream. Cutler and Quate[5] have described an experiment in which these space-charge waves of noise were observed experimentally. The present analysis shows that there is an optimum location of the traveling-wave tube circuit entrance with respect to the space-charge waves for minimum noise figure. The magnitude of this minimum and the optimum position are presented graphically as functions of space charge and circuit loss. It is then shown that passing the electron stream through a short nonresonant gap which suddenly accelerates the electrons causes a further reduction in the tube noise figure if the gap is placed at one of the noise-convection current minima between the electron gun and the circuit entrance. It is also possible to use two properly placed voltage jumps for noise-figure reduction. An experimental tube of the latter type is described which verifies the theory. The data obtained from this tube agree reasonably well with the theoretical predictions.

Introduction

PIERCE[2] has estimated the noise figure of the traveling-wave amplifier by using the method which Rack[1] applied to the parallel-plane diode. Rack's method uses the Llewellyn-Peterson[6] equations to calculate the noise voltage of a space-charge limited parallel-plane diode at high frequencies. This calculation involves replacing the actual multivalued velocity at the potential minimum by a single-valued velocity having the same mean-square fluctuations. That such a procedure leads to usable results at high frequencies is somewhat surprising, but an experiment reported by Cutler and Quate[5] and other experiments carried out by the author at Stanford University show that the theory predicts observed data at frequencies as high as 3,000 to 4,000 mc. It is the purpose of the present paper to show the effect of space charge and circuit loss upon the traveling-wave tube noise figure calculated by this method, and to describe some new methods by which low figures in traveling-wave tubes may be obtained.

Noise Space-Charge Waves

Consider a traveling-wave tube consisting of a Pierce electron gun[7] followed by a region containing various electrodes whose configuration is as yet unspecified, followed in turn by the traveling-wave circuit. Just preceding the circuit, a short drift region operated at the circuit dc voltage is assumed to exist. The following symbols in mks units will be used.

a = radius of a hollow cylindrical drift tube.
b = Pierce's traveling-wave tube electron-speed parameter.[2]
b = radius of a solid cylindrical beam in Fig. 6, only.
d = Pierce's loss parameter.[2]
Δf = frequency interval or bandwidth.
$j = (-1)^{1/2}$.
m = electronic mass.
q = ac rms convection current (with various subscripts defined in the text).
t = time coordinate.
u = dc beam velocity (with various subscripts defined in the text).
v = ac rms velocity (with various subscripts defined in the text).
v_m = maximum ac rms velocity of a space-charge wave.
x_n = real part of δ_n $n = 1, 2, 3$.
y_n = imaginary part of δ_n $n = 1, 2, 3$.
z = axial coordinate.
C = Pierce's gain parameter.[2]
F = noise figure.
I_D = dc beam current density.
I_0 = dc beam current.
K = Boltzmann's constant.
Q = Pierce's space-charge parameter.[2]
T = circuit temperature.
T_c = cathode temperature.
V = dc beam voltage (with various subscripts defined in the text).
β_e = electronic wave number $= \omega/u_0$.
δ = effective plasma wave number $= \omega_q/u_0$.
δ = Pierce's unknown incremental propagation constant[2] in (7) and (8), only.

* Decimal classification: R339.2. Original manuscript received by the Institute, February 14, 1951; revised manuscript received, July 25, 1951.
This paper is based on a dissertation submitted by the author to Stanford University. Reference is made to this dissertation for complete details.
† Electron-Tube Laboratory, Hughes Aircraft Co., Culver City, Calif.
[1] A. J. Rack, "Effect of space charge and transit time on the shot noise in diodes," *Bell Sys. Tech. Jour.*, vol. 17, pp. 592–619; October, 1938.
[2] J. R. Pierce, "Traveling-Wave Tubes," D. Van Nostrand Co., Inc., New York, N. Y.; 1950.
[3] W. C. Hahn, "Small signal theory of velocity-modulated electron beams," *Gen. Elec. Rev.*, vol. 42, pp. 258–270; June, 1939.
[4] S. Ramo, "The electronic-wave theory of velocity-modulation tubes," PROC. I.R.E., vol. 27, pp. 757–763; December, 1939.
[5] C. C. Cutler and C. F. Quate, "Experimental verification of space charge and transit time reduction of noise in electron beams," *Phys. Rev.*, vol. 80, pp. 875–878; December 15, 1950.
[6] F. B. Llewellyn and L. C. Peterson, "Vacuum-tube networks," PROC. I.R.E., vol. 32, pp. 144–166; March, 1944.
[7] J. R. Pierce, "Theory and Design of Electron Beams," D. Van Nostrand Co., Inc., New York, N. Y., Chap. X; 1949.

δ_n = Pierce's incremental propagation constants[2] $n=1, 2, 3$.
ϵ_0 = dielectric constant of vacuum.
η = electronic charge-to-mass ratio.
θ = gun transit angle.
ϕ = distance measured in a drift region in space-charge radians.
ω = radian frequency of interest.
ω_p = radian plasma frequency in a beam of infinite cross-section.
ω_q = radian effective plasma frequency in a beam of finite cross section.

Following the method of Pierce,[8] but including the space-charge term which he omits, the noise figure of the traveling-wave amplifier with high gain can be written

$$F = 1 + \frac{I_0}{2\eta CKT\Delta f}\left|(\delta_2 + \delta_3)v + \frac{u_0 C}{jI_0}(\delta_2\delta_3 - 4QC)q\right|^2. \quad (1)$$

The q and v are the noise convection current and velocity in the electron beam at the circuit entrance. The notation is the same as Pierce's,[2] with the exception that the ac quantities are root-mean-square rather than peak.

It is now postulated that the noise convection current and velocity can be represented in the drift region preceding the circuit entrance by a space-charge standing wave[3,4] as follows:

$$\begin{aligned} v &= v_m \cos \delta z \exp j(\omega t - \omega z/u_0) \\ q &= -jv_m \frac{\omega I_0}{\omega_q u_0} \sin \delta z \exp j(\omega t - \omega z/u_0). \end{aligned} \quad (2)$$

Such a representation will be valid as long as the ac convection current and ac velocity at the entrance to drift region are 90 degrees out of phase in time. Such a relationship exists at the electron-gun anode and will be preserved through the intervening region as long as the stream does not pass through resonant gaps or near wave-carrying circuits. If the 90-degree relationship is destroyed, perfect standing waves, as given by (2), will not be set up in the drift region, and a slightly more complicated representation must be employed.

If the ac convection current and velocity in (1) are replaced by those given by (2), the result is

$$F = 1 + \frac{I_0 v_m^2}{2\eta CKT\Delta f}\left|(\delta_2 + \delta_3)\cos\delta z - (\delta_2\delta_3 - 4QC)\frac{1}{(4QC)^{1/2}}\sin\delta z\right|^2. \quad (3)$$

The quantity, r, is now defined by

$$r = \frac{v_m^2}{v_a^2}, \quad (4)$$

where v_a^2 is the spectrum of the mean-square fluctuation in the average velocity of the electron stream at the space-charge potential minimum in the electron gun. This quantity is given by Rack[1] as follows:

$$v_a^2 = (4 - \pi)\eta \frac{KT_c}{I_0}\Delta f. \quad (5)$$

The values taken on by r will depend upon the operations performed on the beam between the electron gun and the circuit drift region. Using (4) and (5) in the noise-figure expression (3) leads to

$$F = 1 + \tfrac{1}{2}(4 - \pi)\frac{T_c}{T}\frac{r}{C}\left|(\delta_2 + \delta_3)\cos\delta z - (\delta_2\delta_3 - 4QC)\frac{1}{(4QC)^{1/2}}\sin\delta z\right|^2. \quad (6)$$

The quantity

$$\left|(\delta_2 + \delta_3)\cos\delta z - (\delta_2\delta_3 - 4QC)\frac{1}{(4QC)^{1/2}}\sin\delta z\right|^2$$

is a function of the position of the circuit entrance along the space-charge wave given by δz, of the incremental propagation constants, δ_2 and δ_3, and of the degree of space charge given by QC. The incremental propagation constants are, in turn, functions of electron speed, circuit loss, and QC. They are the three solutions of Equation (7.14) of footnote reference 2, which contains a typographical error and is correctly written in Pierce's notation as follows:

$$\delta^2 = \frac{1}{(-b + jd + j\delta)} - 4QC. \quad (7)$$

Writing

$$\delta = x + jy \quad (8)$$

and equating the real and imaginary parts of (7) leads to the following simultaneous equations whose three solutions are the incremental attenuation and phase constants of the three forward waves.

$$\begin{aligned} y^3 + by^2 - y(3x^2 + 2dx + 4QC) - 4QCb - bx^2 - 1 &= 0 \\ x^3 + dx^2 - x(3y^2 + 2by - 4QC) + 4QCd - dy^2 &= 0. \end{aligned} \quad (9)$$

The solution to (9), which has a positive value of x, is labeled x_1 and y_1. These are the incremental attenuation and phase constants for the increasing wave. Equation (9) has been solved numerically for various values of QC and d under the condition that b has the value for which x_1 is a maximum. This means physically that the circuit dc voltage is adjusted for maximum rate-of-increase of the increasing wave for each value of space charge and loss. Most traveling-wave tubes are operated under this condition. With this restriction, we define

$$f(QC, d, \delta z) = \Big|(\delta_2 + \delta_3)\cos\delta z$$

[8] Footnote Reference 2, Chaps. IX and X.

$$-\left(\delta_2\delta_3 - 4QC\right)\frac{1}{(4QC)^{1/2}}\sin\delta z\,\Big|^2. \qquad (10)$$

Considered as a function of δz, $f(QC, d, \delta z)$ has the form of a constant plus a sinusoid repeating every space-charge half wavelength. This is shown in Fig. 1.

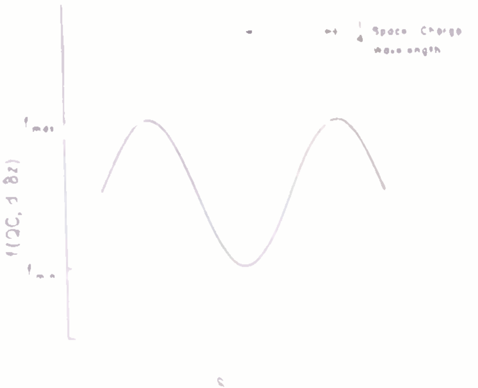

Fig. 1—The traveling-wave tube noise figure is found to be a periodic function of the position of the circuit entrance along the electron stream. Here is shown the form of $f(QC, d, \delta z)$ as a function of δz. The noise figure is proportional to this function.

It has maximum and minimum values which are functions of QC and d. Because the coefficients of the trigonometric functions are complex, $f(QC, d, \delta z)$ has no zeros for real δz. The position of a minimum along δz is also a function of QC and d. A plot of the minimum

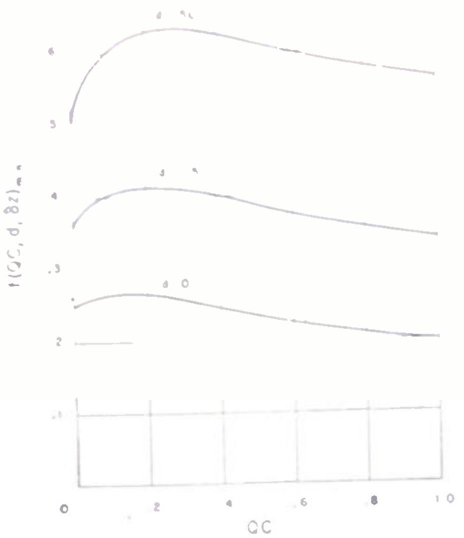

Fig. 2—If the circuit entrance is placed at one of the optimum positions along the electron stream, the noise figure will be a minimum and $f(QC, d, \delta z)$ will have its minimum value. This minimum value is a function of QC, the space-charge parameter, and d, the circuit loss parameter. Its value is shown versus QC for three values of d.

value of the function is given in Fig. 2 versus QC for several values of d. The curves suggest that best noise figures are obtained with low values of the loss parameter d. At 3,000 mc., values of d as low as 0.12 have been obtained for a C of 0.02 with copper-coated helices. There appears to be considerable reduction of the minimum for large values of QC; but since values of QC above unity are extremely difficult to obtain, this does not seem a practical method of reducing noise figure.

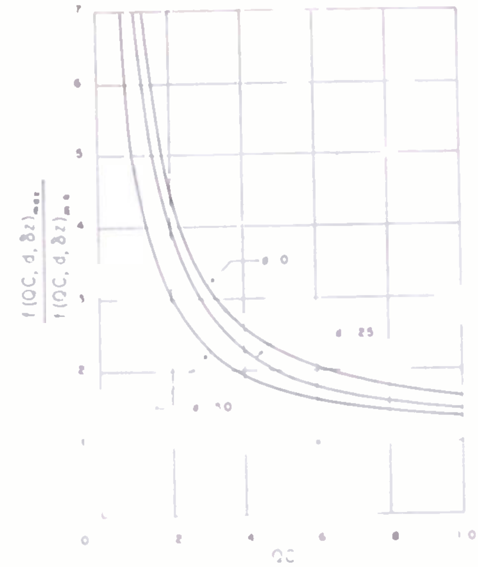

Fig. 3—The ratio of the worst noise figure to the best noise figure of a given traveling wave tube with its circuit entrance beginning at the worst and the best positions, respectively, is shown here as a function of space-charge and loss. The ratio of the maximum to minimum value of the noise-figure function versus QC is given for three values of d. This ratio was verified experimentally at $QC=0.46$ and $d=0.37$ with a sliding helix tube.

The ratio of the maximum to the minimum value of $f(QC, d, \delta z)$ is given in Fig. 3 versus QC for various values of d. This set of curves measures the increase in the noise figure resulting from starting the circuit at

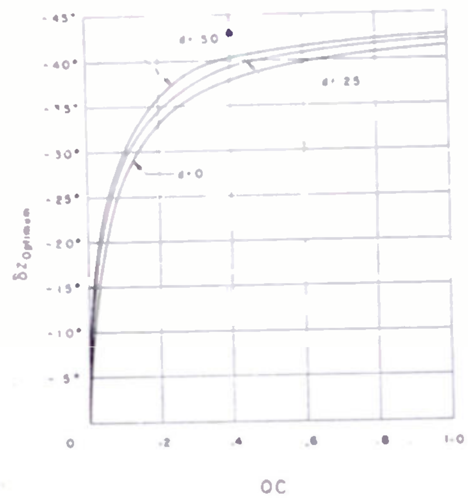

Fig. 4—The optimum position of a traveling-wave tube circuit entrance with respect to the space-charge standing waves of noise in an electron stream is a function of space-charge and circuit loss. Shown here is the location of the optimum position in space-charge wave degrees versus QC for three values of d.

the worst position along the stream. For example, at $QC=0.1$ and $d=0.25$, the ratio is 7, which is an increase in noise figure of 8.5 db over that obtained at the optimum position.

Fig. 4 shows where the circuit entrance should be placed so that the minimum value of the function is obtained. This position is measured in space-charge wave degrees from the point of maximum noise velocity. There is another optimum position located every 180 degrees of space-charge wavelength along the drift tube.

Evaluation of r

The value of r in (6) must be calculated for each configuration used between the electron gun and the circuit drift region. Of the infinite number of possibilities, only those configurations will be considered here which define a constant or suddenly discontinuous dc potential along the axis of the beam. This restriction is applied because such configurations can be handled easily mathematically. The constant potential regions, or drift regions, will support space-charge waves, and the discontinuities between them can be handled by simple kinematics.

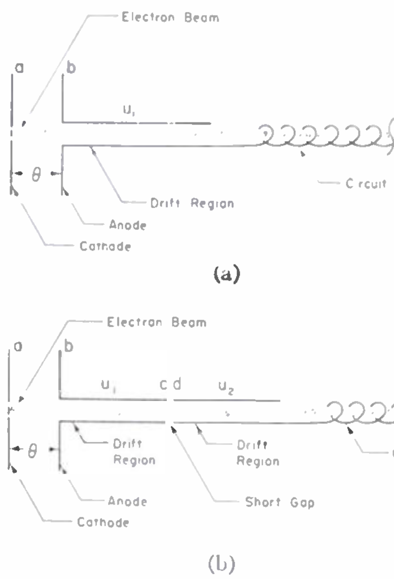

Fig. 5—The noise figure of traveling-wave tubes is proportional to a parameter r, which depends upon the operations performed upon the electron stream between the electron gun and the circuit drift region. Shown are two of the configurations which are analyzed. The second arrangement is the single dc velocity jump tube which has resulted in considerable noise-figure improvement. The first is the traveling-wave tube analyzed by Pierce.

Consider, first, the configuration analyzed by Pierce,[2] as shown schematically in Fig. 5(a). Here the anode is followed by the circuit drift region at the same dc potential. The application of the Llewellyn equations[6] to the electron gun yields, for the noise quantities at the gun anode (b-plane),

$$q_b = -j\frac{I_0}{u_b}\theta v_a$$
$$v_b = -v_a. \tag{11}$$

Taking these as the initial conditions for the excitation of a set of the space-charge standing waves given by (2) and dropping the exp $j(\omega t-\omega z/u_0)$ leads to

$$-v_a = v_m \cos \delta z$$
$$j\theta\frac{I_0}{u_0}v_a = \frac{\omega}{\omega_q}v_m j\frac{I_0}{u_0}\sin \delta z. \tag{12}$$

These may be solved for $(v_m/v_a)^2$, which is the definition of r. This leads to

$$r = 1 + \left(\frac{\omega_q\theta}{\omega}\right)^2. \tag{13}$$

The effective plasma frequency ω_q is related to the infinite beam plasma frequency ω_p by a reduction factor which is less than unity. This reduction factor is a function of frequency, beam radius, and beam velocity. The value of the reduction factor is plotted in Fig. 6

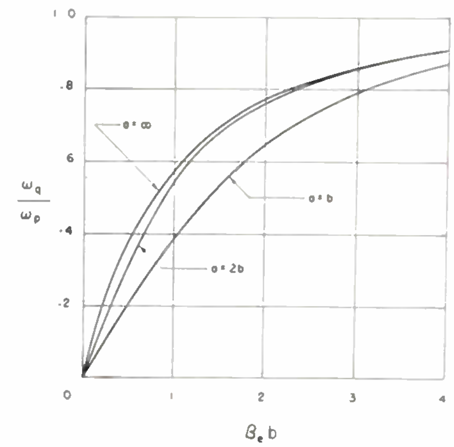

Fig. 6—Space-charge waves in drifting electron streams behave differently in beams of finite diameter from those in beams of infinite cross section. The effect of the finiteness of the beam can be described in terms of a reduction factor which is a function of beam radius b, drift tube radius a, frequency ω, and dc beam velocity u_0. Here $\beta_e = \omega/u_0$. The reduction factor is written as the ratio of an effective plasma frequency ω_q and an actual plasma frequency ω_p, where $\omega_p = (\eta I_D/\epsilon u_0)^{1/2}$.

for various values of drift-tube radius a and beam radius b. The curves of Fig. 6 were calculated by assuming values of a/b and $\beta_e b$ and finding the solution to the transcendental matching equation (Equation (25) of footnote reference 4) by numerical means. Physically, ω_q/u_0 is the effective debunching wave number of the velocity-modulation theory, while ω_p/u_0 is the debunching wave number which would exist if the stream were of infinite cross section with the same dc current density and dc velocity. The infinite beam plasma frequency ω_p is given by

$$\omega_p = \left(\frac{\eta I_D}{\epsilon_0 u_0}\right)^{1/2}. \tag{14}$$

Equation (13) may then be written

$$r = 1 + \frac{\eta I_D\theta^2}{\epsilon_0 u_0 \omega^2}\left(\frac{\omega_q}{\omega_p}\right)^2. \tag{15}$$

For a space-charge limited diode,

$$\frac{\eta I_D}{\epsilon_0 u_b}\left(\frac{\theta}{\omega}\right)^2 = 2^6. \tag{16}$$

Since $u_0 = u_b$,

$$r = 1 + 2\left(\frac{\omega_q}{\omega_p}\right)^2 \tag{17}$$

for this configuration. The noise figure becomes

$$F = 1 + \tfrac{1}{2}(4-\pi)\frac{T_c}{T}\,\frac{1+2\left(\frac{\omega_q}{\omega_p}\right)^2}{C} f(QC, d, \delta z). \tag{18}$$

This is equivalent to the result obtained by Pierce[2] for $QC = (\omega_q/\omega_p) = d = 0$.

The second electrode arrangement to be considered is that shown in Fig. 5(b). Following the gun anode, there is a drift tube at the anode voltage, followed in turn by a drift tube at the circuit voltage. Between them is a short, nonresonant gap. In the first drift tube, there will be a space-charge wave given by

$$\begin{aligned} v_1 &= v_{m1}\cos\phi_1 \\ q_1 &= -jv_{m1}\frac{\omega}{\omega_{q1}}\frac{I_0}{u_1}\sin\phi_1, \end{aligned} \tag{19}$$

and in the second drift tube, a space-charge wave given by

$$\begin{aligned} v_2 &= v_{m2}\cos\phi_2 \\ q_2 &= -jv_{m2}\frac{\omega}{\omega_{q2}}\frac{I_0}{u_2}\sin\phi_2. \end{aligned} \tag{20}$$

The subscripts 1 and 2 distinguish between quantities in the first and second drift regions, and the δz used in (2) has been replaced by ϕ_1 and ϕ_2, respectively. At the gap cd the ac quantities will be related by

$$\begin{aligned} q_d &= q_c \\ v_d &= (u_1/u_2)v_c \end{aligned} \tag{21}$$

from simple kinematics.[9]

Inserting (18) and (19) into (20) leads to

$$\begin{aligned} -jv_{m2}\frac{\omega}{\omega_{q2}}\frac{I_0}{u_2}\sin\phi_2 &= -jv_{m1}\frac{\omega}{\omega_{q1}}\frac{I_0}{u_1}\sin\phi_1 \\ v_{m2}\cos\phi_2 &= (u_1/u_2)v_{m1}\cos\phi_1. \end{aligned} \tag{22}$$

These are two equations relating v_{m2} to v_{m1} and relating ϕ_2 to ϕ_1. These relationships are

[9] Application of the Llewellyn equations to a short gap leads to identical results. The only restriction seems to be that the gap length must be short compared with a space-charge quarter wavelength at the lower of the two drift voltages.

$$\begin{aligned} \left(\frac{v_{m2}}{v_{m1}}\right)^2 &= \frac{V_1}{V_2}\cos^2\phi_1 + \left(\frac{V_2}{V_1}\right)^{1/2}\left(\frac{\omega_{q2}/\omega_{p2}}{\omega_{q1}/\omega_{p1}}\right)^2\sin^2\phi_1 \\ \tan\phi_2 &= \left(\frac{V_2}{V_1}\right)^{3/4}\left[\frac{\frac{\omega_{q2}}{\omega_{p2}}}{\frac{\omega_{q1}}{\omega_{p1}}}\right]\tan\phi_1. \end{aligned} \tag{23}$$

If the first drift tube is of such length that the gap cd occurs at an ac velocity maximum ($\phi_1 = 0$),

$$\left(\frac{v_{m2}}{v_{m1}}\right)^2 = \frac{V_1}{V_2}, \tag{24}$$

with this restriction

$$r = \left[1 + 2\left(\frac{\omega_{q1}}{\omega_{p1}}\right)^2\right]\frac{V_1}{V_2}. \tag{25}$$

The noise figure becomes

$$F = 1 + \tfrac{1}{2}(4-\pi)\frac{T_c}{T}\,\frac{\left[1+2\left(\frac{\omega_{q1}}{\omega_{p1}}\right)^2\right]V_1}{CV_2} f(QC, d, \delta z). \tag{26}$$

This is interesting because it suggests a method of materially reducing the noise figure of a traveling-wave amplifier by using a low anode voltage and a high circuit voltage with a dc-velocity jump properly placed between them.

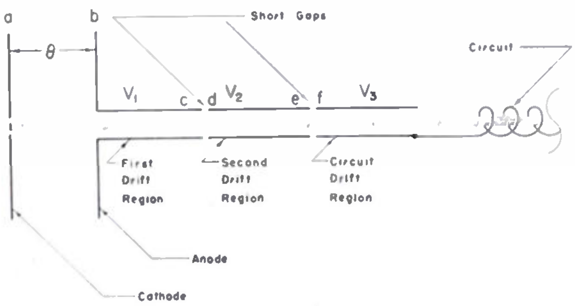

Fig. 7—The noise-reducing configuration shown is the double-velocity jump type. Here the beam is first decelerated and then accelerated so as to reduce the noise content of the electron stream before it is allowed to enter the traveling-wave tube circuit.

Another configuration is that shown schematically in Fig. 7. Here it is intended that the anode drift tube be operated at a fairly high voltage, the next drift tube at a low voltage, and the circuit drift tube at a high voltage. The first velocity jump cd is placed at a noise current maximum ($\phi_1 = 90°$), and the second jump ef at a noise velocity maximum ($\phi_2 = 0°$). For this case

$$r = \left[1 + 2\left(\frac{\omega_{q1}}{\omega_{p1}}\right)^2\right]\left(\frac{V_2}{V_1}\right)^{1/2}\left[\frac{\dfrac{\omega_{q2}}{\omega_{p2}}}{\dfrac{\omega_{q1}}{\omega_{p1}}}\right]^2 \frac{V_2}{V_3}. \tag{27}$$

The advantage of this scheme over the preceding one is that it is possible to obtain low noise figures without having to use a low anode voltage and a high circuit voltage. In addition, it has more flexibility because of the possibility of adjusting V_2 without changing any of the other parameters. The mechanism of this noise reduction is essentially the reverse of the mechanism employed for signal amplification in the space-charge wave amplifier described earlier.[10]

Experimental Tubes

The predicted variation of the noise figure as a function of the position of the circuit entrance has been verified at 3,000 mc in a tube with a sliding helix. The calculated ratio of maximum to minimum was 1.9 read from Fig. 3. The measured value was very nearly 2. The calculated space-charge wavelength agreed with the measured length within about 12 per cent. The location of a minimum was within 6 per cent in space-charge wavelengths of that predicted by the theory.

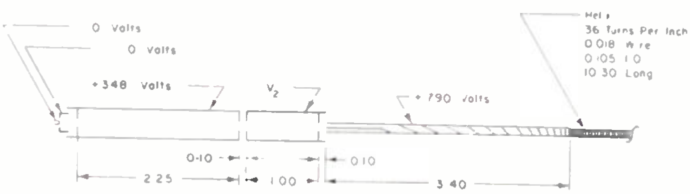

Fig. 8—Tube No. 112. Beam current 0.60 ma. Dimensions in inches. These are the important dimensions and operating conditions of an experimental low-noise tube for which the theoretical and experimental noise figures are compared. This tube employed the spiral-type rf input and the double-velocity jump noise-reduction configuration.

Using the noise-reducing principles described here, a number of low noise amplifiers have been built for 3,000 mc. One of the most interesting is the tube shown in Fig. 8. This tube is of the double jump type shown schematically in Fig. 7 The variation of the noise figure as a function of the voltage V_2 is shown in Fig. 9. The theoretical curve was calculated, using (6) and (23) and Figs. 2, 3, 4, and 6. A cathode temperature of 1,020-degree K and a circuit temperature of 290-degree K were used in the calculation. The discrepancy in the location of corresponding maxima and minima could be corrected by assuming a smaller beam diameter for the calculated curve. This tube did not give a particularly low noise figure because of the unavoidable length of the distance from the second jump to the circuit entrance occupied by the spiral match. Another tube, using similar noise-reducing electrodes but having an antenna and short cylinder for input matching, had a similar behavior, but gave a noise figure of 11 db with a gain of 18 db at 3,000 mc. Tubes employing the configuration of Fig. 5(b) gave noise figures of 10 db.

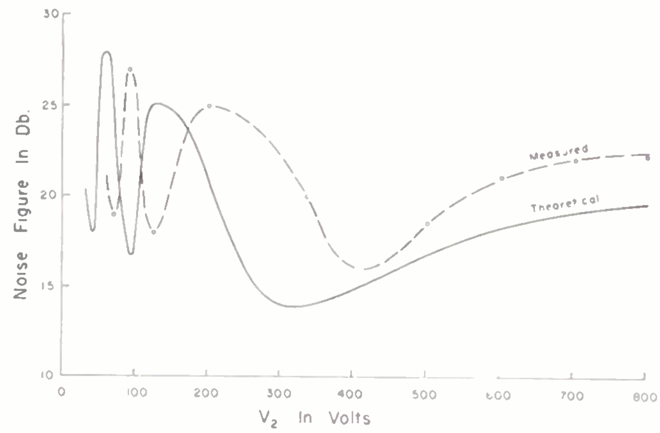

Fig. 9—For the tube of Fig. 8 it is possible to calculate the noise figure as a function of the dc voltage applied to the second drift space using the curves and equations given in the text. This is shown as the solid line. The broken line is the measured noise figure as a function of that voltage. In calculating the theoretical curve, it was necessary to assume a value of beam diameter. This was taken as 0.057 inch. If the beam diameter were assigned a somewhat smaller value, the minima and maxima of the theoretical curve would be shifted to the right and would correspond more closely to those of the experimental curve. Thus, the fact that one curve has a maximum where the other has a minimum is not significant, but the agreement in the form of the curves shows that the theory has validity.

Conclusion

Pierce's estimate of the noise figure, when extended to include the effects of space-charge and loss, has been found to be reasonably accurate in predicting noise figures of experimental tubes. The schemes for reducing stream noise content have proved successful in practical tubes and suggest a general approach to the problem of noise reduction in beam-type amplifiers.

Acknowledgment

The author wishes to acknowledge his indebtedness to L. M. Field for his many suggestions and his encouragement during this investigation. The curves were calculated by H. D. Cohen and G. W. Tautfest, the experimental tubes were built by A. F. Carpenter and R. F. Stewart, and the drawings were prepared by E. D. Frazer. The work was supported by the Office of Naval Research, the Army Signal Corps, and the Air Force.

[10] L. M. Field, P. K. Tien, and D. A. Watkins, "Amplification by acceleration and deceleration of a single-velocity stream," Proc. I.R.E., vol. 39, p. 194; February, 1951.

A Broadside Dielectric Antenna*

GEORGE E. MUELLER†, SENIOR MEMBER, IRE

Summary—**An antenna is described which makes use of the properties of a nonuniform dielectric transmission line to produce a broadside directive pattern. A simple array theory is developed which serves to predict the major features of the radiation patterns, thus providing the means for the engineering design of such antennas.**

I. INTRODUCTION

A DIELECTRIC transmission line may be made to act as a broadside antenna by permitting only those components of the energy to be radiated which are in phase with some reference voltage. This is analogous to the "loaded wire" antenna[1] of longer wavelengths. In the broadside dielectric antenna, the properties of dielectric waveguides are utilized to confine the out-of-phase energy to the transmission line while enhancing and controlling the radiation of the in-phase energy. One form of the antenna[2] is shown in Fig. 1. It is a nonuniform dielectric transmission line consisting of disks of high dielectric constant supported on a polystyrene rod.

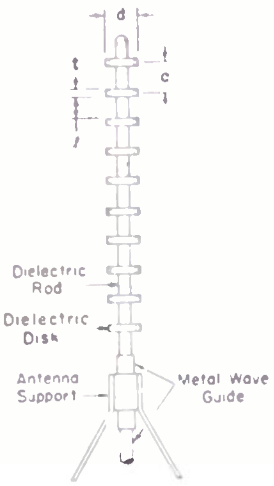

Fig. 1—Broadside dielectric antenna.

The operation of this antenna is most easily explained by analogy with the radiation patterns obtained from arrays of isotropic radiators. Essentially, this amounts to replacing the actual antenna with an array of isotropic radiators, the amplitude and phase distribution being determined qualitatively from the known properties of dielectric transmission lines.

II. DIELECTRIC TRANSMISSION LINES[3–5]

The properties of the uniform dielectric waveguide may be summarized as follows: (1) The phase velocity is a function of the dielectric constant and of the rod diameter. The phase velocity of the dominant mode (which corresponds to the TE_{11} mode in a cylindrical metal guide) varies between the velocity of light in free space when the effective rod diameter ($D\sqrt{\epsilon}$) is small, and the velocity of light in a medium of the same dielectric constant when the rod is large. (2) The guided energy is divided between the dielectric and the surrounding medium. The energy outside the guide increases as the effective diameter decreases, and vice versa. These relations are illustrated in Figs. 2 and 3.[6]

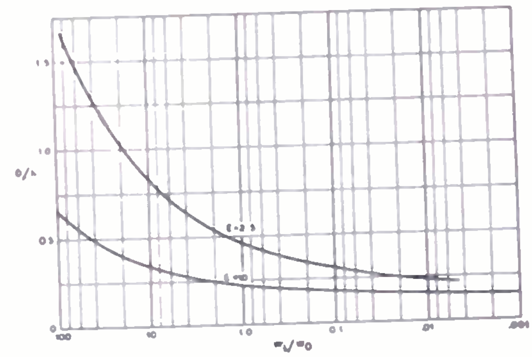

Fig. 2—Ratio of power inside W_i to power outside W_o for a cylindrical dielectric wire.

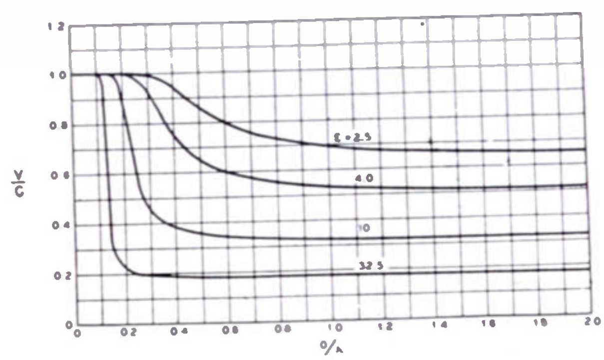

Fig. 3—Normalized phase velocity for a cylindrical dielectric wire.

* Decimal classification: R329. Original manuscript received by the Institute, October 6, 1950; revised manuscript received, April 23, 1951.

The work described in this paper was begun at the Bell Telephone Laboratories in 1943, and has been carried on sporadically over the intervening years. Most of the results quoted here were obtained in the past year as the result of work conducted in the Department of Electrical Engineering, The Ohio State University Research Foundation, under Contract W 36-039 sc38168, with The Signal Corps Engineering Laboratories, Fort Monmouth, N. J.

† The Ohio State University, Columbus, Ohio.

[1] J. E. Stratton, "Electromagnetic Theory," McGraw-Hill Book Co., Inc., New York, N. Y.; 1941.

[2] G. C. Southworth, Patent 12,206,923; 1947.

[3] D. Hondros and P. Debye, "Elektromagnetische Wellen an dielektrischen Drahten," *Ann. der. Phys.*, vol. 32, pp. 465–476; 1910.

[4] G. C. Southworth, "Hyperfrequency wave guides—general considerations," *Bell Sys. Tech. Jour.*, vol. 15, pp. 284–309; 1936.

[5] S. Schelkunoff, "Electromagnetic Waves," D. Van Nostrand and Co., Inc., New York, N. Y.; 1943.

[6] These figures are taken from G. E. Mueller and W. A. Tyrrell, "Polyrod antennas," *Bell Sys. Tech. Jour.*, vol. 26, pp. 837–851; 1947.

It is noteworthy that, except for those waves having circular symmetry, the guided waves are hybrid; that is, they have longitudinal components of both E and H. Also, for the dominant mode, there is no cutoff frequency; theoretically, a direct current will be guided by the dielectric. However, the amount of energy within the dielectric falls off very rapidly as the rod becomes less than a half-wavelength in effective diameter.

The above relations are true for guides of uniform cross section, in which case there is no radiation. But at a discontinuity, such as in one of the disks in Fig. 1, only part of the enérgy continues along the guide, and this at a velocity determined by the effective diameter of the new transmission line. A second part is reflected and travels back to the source, and a third part is radiated. At each successive discontinuity, this same division of energy takes place until all the energy has been radiated. This phenomenon is too complicated for exact analysis at present, but qualitative conclusions may be drawn. In the nonuniform transmission line, the amount of energy radiated because of a discontinuity should be proportional to the energy outside of the dielectric. In addition, it will depend on the magnitude of the discontinuity.

Thus, by proper selection of the effective diameters of the rod and disk and of the length of path in each, it is possible to control to a large extent the amplitude and phase of the radiated energy.

III. Broadside Antenna Array Theory

Consider a linear array of equiamplitude isotropic

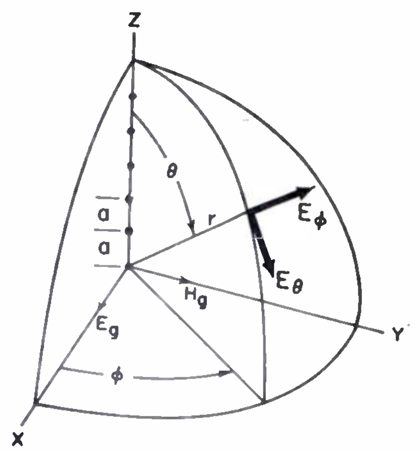

Fig. 4—The broadside array and its co-ordinates.

radiators which are spaced uniformly along the z axis as in Fig. 4. The radiation pattern is given by[7,8]

$$R = \frac{\sin n\pi(a \cos \theta + b)}{n \sin \pi(a \cos \theta + b)}, \tag{1}$$

wherein $R(\theta)$ is the relative field strength, $E_p(\theta)/E_0$

$E_p(\theta)$ = electric field at radius r
E_0 = maximum field strength at radius r
θ = as shown in Fig. 4
n = the number of radiating elements
$a\lambda$ = the spacing between radiators
$2\pi b$ = the phase shift between adjacent radiators in radians.

In order to take account of the directive properties of the individual radiators, this must be multiplied by a factor expressing their directivities.

The gain[9] of the uniformly excited broadside array is

$$g = 4\rho \tag{2}$$

in which ρ is the effective length of the antenna in wavelengths.

The width of the major lobe is given by

$$\theta_0 \approx \frac{B}{\rho} \tag{3}$$

as may readily be calculated from (1). The constant B depends on the energy distribution and on the definition of beam width. For width in degrees between half-power points, B is about 55 degrees.

For antennas more than a few wavelengths long, a universal curve may be drawn, giving the directional pattern of the major lobe and first minor lobe of the broadside antenna in terms of the angle θ/ρ. This is an approximation amounting to the replacement of sin x by x near $x=0$. It should be noted that in this region the angle of maximum radiation in radians is given by

$$\theta_m \approx \frac{\pi}{2} - \frac{b}{a}, \tag{4}$$

and is independent of the length of the array. This universal broadside directivity curve is plotted in Fig. 5.

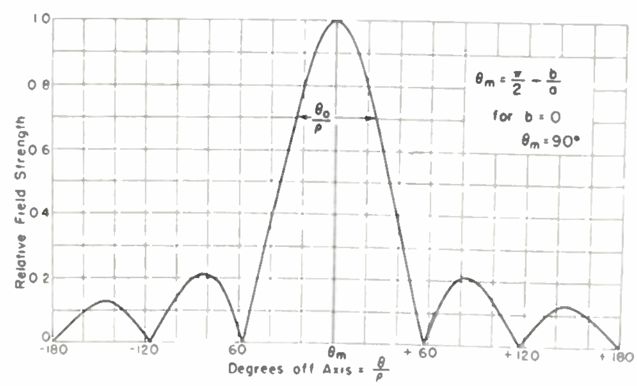

Fig. 5—Universal directive pattern for broadside antennas.

It is well known that the effect of tapering the amplitude of the radiators along an array, so that the ends radiate less energy than the center, is to broaden the major lobe and reduce the amplitude of the minor lobes. A non-uniform variation in the phase shift between adjacent elements along an array has much the same effect on the radiation pattern, as is evident from purely physical considerations.

[7] G. C. Southworth, "Factors affecting the gain of directive antennas," Proc. I.R.E., vol. 18, pp. 1502–1536; September, 1930.
[8] R. N. Foster, "Directive diagrams of antenna arrays," *Bell Sys. Tech. Jour.*, vol. 5, p. 292; 1926.

[9] See page 347 of footnote reference 5.

IV. The Broadside Dielectric Antenna

The operation of the broadside dielectric antenna may be explained on the basis of an analogy with array theory. The justification for this analogy is the correlation of the radiation patterns predicted with those obtained experimentally. This approach provides no knowledge of the fields in the vicinity of the dielectric, nor of their behavior in the nonuniform guide. This could be obtained only by solving Maxwell's equations subject to the boundary conditions imposed by the guide. However, it does provide the basis for design when coupled with certain empirically derived constants for the nonuniform dielectric transmission line.

The loaded dielectric transmission line of Fig. 1 acts as a broadside antenna since the energy is radiated from the sections of polystyrene rod between the disks while the out-of-phase energy traveling through the disks is constrained, because of the high dielectric constant and larger diameter, to stay within the disks. Then, when the disks and the radiating sections are each a half-guide wavelength long, the energy radiated from every section is in phase, the condition for broadside radiation. It should be noted that there are many physical arrangements which can suppress the out-of-phase radiation and lead to broadside antennas. For instance, metal sleeves, alternate sections of dielectric of the same diameter but differing dielectric constant, and so on, suggest themselves. The disks used here were chosen because of their convenience and flexibility.

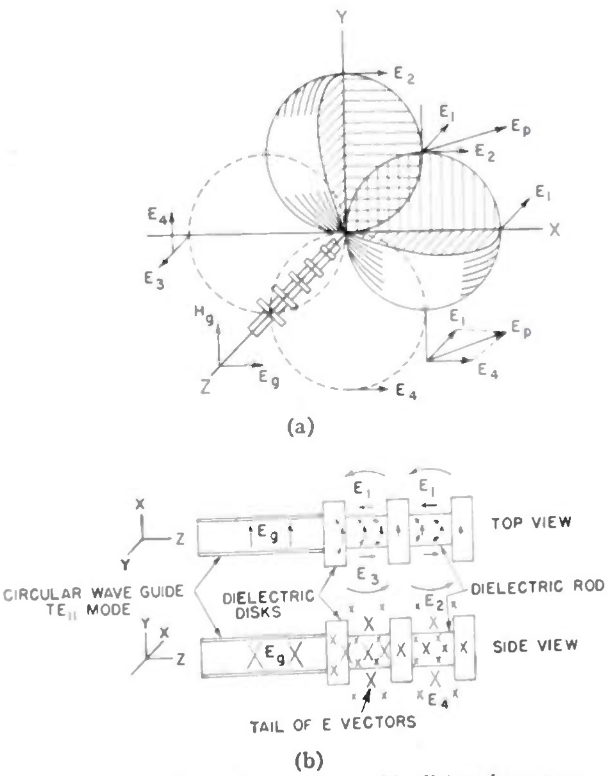

Fig. 6—The radiation from a broadside dielectric antenna.

A three-dimensional radiation pattern of a typical broadside antenna is sketched in Fig. 6. Note that the electric field in the xz plane is parallel to the array axis, while that in the yz plane is perpendicular thereto. This field pattern is one that would be produced by an array of crossed electric and magnetic dipoles which are perpendicular to the axis of the array and are fed in phase. In all cases discussed in this section, the antennas have been excited with the TE_{11} mode from a dielectric-filled metal guide which has been abruptly terminated, the dielectric continuing on as the radiator. In Fig. 6(b) an attempt has been made to show the behavior of the electric field as it leaves the dielectric disks and is radiated. The radiation pattern in the plane perpendicular to the array axis will be, therefore, similar to that obtained from a clover-leaf antenna, but the polarization will vary in this plane from horizontal at $\phi = 0$, to an angle of 45 degrees at $\phi = 45$ degrees, to vertical at $\phi = 90$ degrees, and so on.

The earliest experiments were made on disk antennas such as that of Fig. 1. These and all later experiments were made at 1.25 cm. A typical set of patterns obtained for a number of different disk separations is shown in Fig. 7. In this and succeeding patterns, dimensions are given in terms of free-space wavelength. The patterns are definitely broadside, and the direction of the major lobe varies with disk spacing as the theory predicts; but the minor lobes are larger and the major lobes are ragged. Much of the distortion seems to be due to interbead reflections.

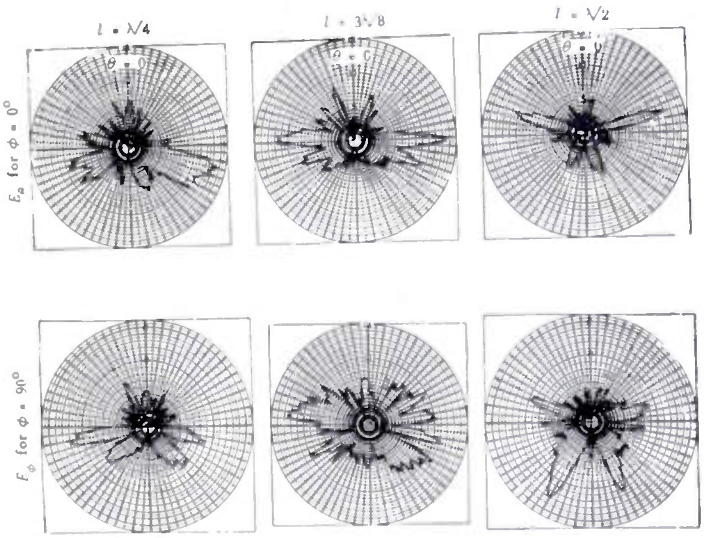

Fig. 7—Radiation patterns of 5 λ/4 diameter dielectric disks λ/4 thick for various disk spacings.

A very considerable improvement in the radiation pattern is achieved by tapering the disk diameter as in Fig. 8. The effect of this tapering is to reduce the dis-

Fig. 8—Tapered disk antenna.

continuity to the wave traveling on the dielectric wire, and thus to decrease the radiation from those sections near the feed. In this way, a more uniform distribution of radiated energy is achieved. Although the reduction in disk diameter does increase the energy outside the disks, Fig. 2 shows this energy to be small even for the smallest disks, and thus to a first approximation, the radiation from the disk may be neglected.

A set of patterns for various disk spacings is shown in Fig. 9 for radiation in the yz plane. An approximate pattern for the radiation perpendicular to the array axis (the xy plane) is also shown. Although there are actually seven disks, there are only six radiating elements; the first disk serves mainly as a matching transformer to launch the wave onto the dielectric transmission line.

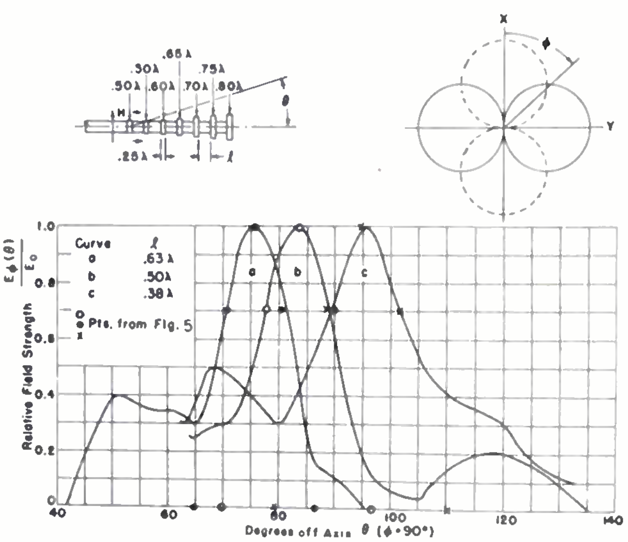

Fig. 9—Radiation pattern of six-element broadside dielectric antenna.

The patterns shown in Figs. 9, 10, and 11 were made using a rotating mount and an automatic recorder.[10] In general, the minor lobe amplitude is only 6 to 9 db down for the short antennas and 10 to 15 db down for the longer antennas. By careful selection of disks, it is possible to reduce these amplitudes considerably for a given spacing, usually at the cost of higher minor lobes for other spacings. This is illustrated by the polar patterns of the 18-element antenna shown in Fig. 10.

Superposed on the experimental curves are points obtained by substituting the proper values of a and b into (3) and (4), or taken from the universal directive curve of Fig. 5. The agreement of angle and width at the half-power points is quite good, but the location of the nulls and the amplitude of the minor lobes are off.

The patterns in Fig. 11 are the radiation patterns for an 18-element array. As expected, the major lobes are narrower. The calculated points show continued agreement of experiment with the simple theory. Thus the directivity is proportional to the array length, at least over the range from 3 to 18 wavelengths. The limit of this proportionality is not at present known, but it is dependent on the dielectric losses.

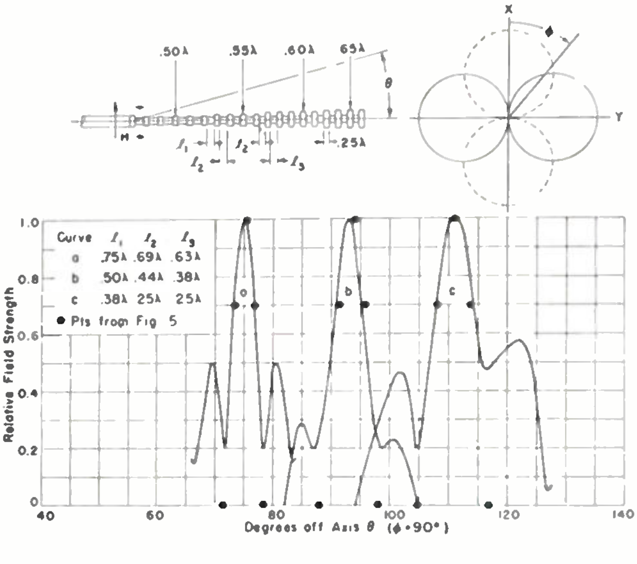

Fig. 11—Radiation patterns for broadside dielectric antennas of 18 elements. Patterns for E_ϕ with $\phi=90°$.

Figs. 9, 10, and 11 show that broadside dielectric antennas of reasonable directivity can be constructed, that it is possible to vary the angle of the major lobe with respect to the array axis by changing the spacing between disks, and that surprisingly good predictions of shape and form of radiation pattern can be made.

V. Design of Broadside Dielectric Antennas

The qualitative prediction of the direction and beam width of the radiation by (1) may be made the basis for the engineering design of these antennas. For this it is

[10] Automatic pattern measuring apparatus developed by the Antenna Laboratory, The Ohio State University, was used for all measurements.

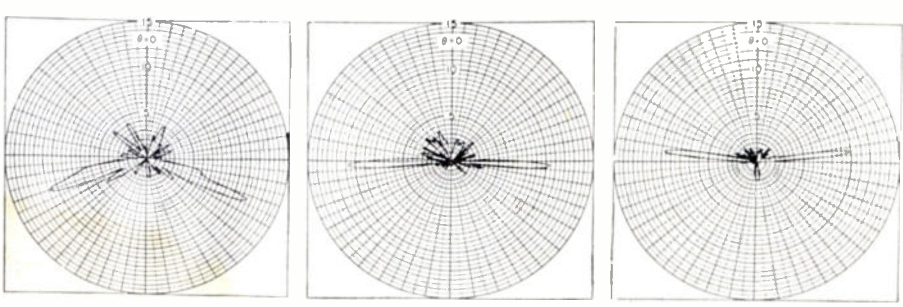

Fig. 10—Polar directive patterns of the 18-element broadside dielectric antenna of Fig. 11.

necessary to know the approximate phase velocity in the dielectric sections and the approximate energy distribution. The phase velocity fixes the value of b in (1) and may be determined from the properties of dielectric transmission lines. The disks, which were made of a mixture of lead chloride and polystyrene, have a dielectric constant of 8. The effective dielectric constant of the section of dielectric waveguide made up of the disk and its supporting polystyrene rod must, therefore, lie between $\epsilon_{rod} = 2.6$ and $\epsilon_{disk} = 8$. A value of 5, the average of the refractive indices, correlates well with experiment when the rod is about $\lambda/2$ in diameter. These values, in a uniform transmission line, would give a guide wavelength 0.45 times the free-space wavelength λ in the loaded section of the antenna, and 0.93 λ in the radiating section. For the uniform line, over half of the energy would be outside the guide in the radiating sections, while only a small fraction would be outside the guide in the disk sections. While these values are little more than educated guesses, they may be used as a first approximation in calculating the field patterns.

Equation (1) may be improved by taking account of the directive patterns of the radiating sections, which are given by

$$R = \left| \frac{\sin \pi(l \cos \theta - m)}{\pi(l \cos \theta - m)} \right|, \tag{5}$$

where $l\lambda$ is the length of the segment. $2\pi m$ is the phase shift along the segment in radians. This equation is the same as that for an end-fire dielectric antenna. It arises because the radiating sections have an appreciable length.

The directive pattern of a disk antenna should be approximately given by the product of (1) and (5) or

$$R = \left| \frac{\sin n\pi(a \cos \theta + b)}{\pi \sin \pi(a \cos \theta + b)} \quad \frac{\sin \pi(l \cos \theta - m)}{\pi(l \cos \theta - m)} \right|, \tag{6}$$

wherein the various quantities are as shown in Fig. 1. The patterns calculated from this assume equal energy radiation from all sections of the array.

On examining experimentally the effect of varying the thickness of the disks, it was found that the 0.25-λ thick disks have smaller minor lobes than either the thinner or thicker disks. In particular, there is a large (3 or 4 db down) end-fire lobe with the thin disks, due to a net radiated component from the traveling wave in the dielectric wire. This is to be contrasted with the standing wave which produces the broadside pattern, and these two may be regarded as two separate modes radiated independently of each other.

In these antennas the disks are all of the same thickness; and for the shorter antennas the spacing between disks is uniform. For the 12- and 18-element arrays, the disks near the feed were smaller in diameter and the phase velocity was higher. Consequently, it was necessary either to increase the spacing between disks near the feed, or to increase the thickness of the disks. The amount of increase required is readily determined from Fig. 3, remembering that the phase shift per section of the array should be constant. This tapered spacing is shown in Fig. 11. The effect of other than optimum spacing is to broaden the major lobe and to reduce the amplitude of the minor lobes. Thus, it is similar to tapering the amplitude of the radiation along the array.

The effects of a change in disk diameter are found primarily in the minor lobe structure, as might be expected. The largest effects are observed in changing the first few disks, while the end disks have little effect. Appropriate diameters for the disks have been determined empirically. The diameters used are noted on the figures.

The interrelation between the disk diameter and the magnitude of the radiated energy is clearly shown in Figs. 9 and 11. In the six-element array of Fig. 9, the diameter of the disks increases rapidly as the distance from the feed increases. This is necessary in order that the major part of the energy be radiated by the time the wave reaches the end of the antenna. On the other hand, in the 18-element array, quite small disks are used near the feed and the increase in diameter is very slow. In this way, the energy radiated per unit length of antenna is reduced, and a relatively uniform distribution along the entire antenna is obtained.

Finally, it may be of interest to mention two other forms for these antennas. In the first, the polystyrene supporting rod is replaced by one of pure rubber. By stretching this rod, a continuous variation in disk spacing is obtained, with a corresponding continuous variation in the angle of radiation. In the second, the energy is fed in the center of the antenna, producing a center-fed array with about twice the maximum length of the end-fed antenna, and the possibility of some minor lobe cancellation.

Brief experiments indicate that these forms of the antenna operate as the foregoing theory predicts.

VI. Conclusions

The dielectric antenna using loading disks has been demonstrated to be a practical broadside radiator for lengths from three to 18 wavelengths and longer. The major characteristics of its radiation pattern may be predicted from a simple array theory, which, in turn, permits the engineering design of such antennas.

The work detailed herein does not represent a completed development of such antennas for practical applications. It shows only that antennas of this general design are feasible.

VII. Acknowledgment

The work described above would not have been possible without the aid and co-operation of the author's colleagues at Holmdel, N. J., one of the Bell Telephone Laboratories, and at the Antenna Research Laboratories of the Department of Electrical Engineering at The Ohio State University, Columbus, Ohio.

Correlation of the Faraday and Kerr Magneto-Optical Effects in Transmission-Line Terms*

C. H. LUHRS†, MEMBER, IRE

Summary—**The subject effects follow immediately from the assumption of the inequality of the two sets of Maxwell's material constants, one set for right-handed circularly polarized waves and the other for left-handed circularly polarized waves. The Faraday magneto-optical effect is derived from phase considerations, and the Kerr magneto-optical effect is derived from impedance considerations.**

I. Introduction

IT IS OUR purpose here to establish explicitly direct relation of the subject effects, and to predict the co-existence of related effects in quantitative terms. The discovery[1] by Michael Faraday in 1845 of the rotation of the plane of polarization of light while propagating through various substances in the presence of a longitudinal magnetic field was followed rather closely by the discovery by Kerr[2] of the rotation of the plane of polarization of light upon reflection from the surface of a magnet.

The basic connection between the two phenomena was soon realized by Fitzgerald and set down by him in very clear fashion in a paper[3] published in 1876.

Others[4] have, after the date of Fitzgerald's deductions, accepted various Kerr magneto-optical effect explanations, either directly stating or implying the necessity of, assuming a mechanism of reflection in the process of which light partially enters the medium, suffering direct Faraday rotation all the while, i.e., during the period of "partial entrance."

II. The Basic Assumptions

A study of the literature suggests that the following list of statements can be taken without reserve as a starting point in the development of a useful and correct theory.

1. The statement of the Faraday magneto-optical effect.
2. The statement of the Kerr magneto-optical effect.
3. Explanation, of the Faraday effect in terms of the difference between the velocities of left-handed circularly polarized waves (lhcpw) and right-handed circularly polarized waves (rhcpw).[5-9]
4. Fitzgerald's philosophy.[3]
5. The fact that, in view of statements 1–4, a greater reduction to fundamentals can be achieved by accepting the implication of the inequality of the two sets of Maxwell's material constants.

(a) $$\epsilon_L,\ \mu_L,$$

and

(b) $$\epsilon_R,\ \mu_R,$$

where

ϵ_L = complex permittivity for left-handed circularly polarized waves (lhcpw)
ϵ_R = complex permittivity for right-handed circularly polarized waves (rhcpw)
μ_L = complex permeability for lhcpw
μ_R = complex permeability for rhcpw.

III. Derivation of the Basic Formulas

Looking in the direction of propagation, the division of electromagnetic waves into two types, A. lhcpw and B. rhcpw, is very basic, and the respective voltage of propagation are

$$E_L = E_L' e^{-\alpha_L z} e^{j(\omega t - \beta_L z)} \tag{1}$$

$$E_R = E_R' e^{-\alpha_R z} e^{-j(\omega t - \beta_R z)}, \tag{2}$$

where

ω = angular frequency $2\pi f$
t = time
α = attenuation constant
β = phase constant
z = distance along direction of propagation.

Subscripts L and R, where appearing, refer to left-handed and right-handed values for the corresponding circularly polarized waves.

The total voltage

$$E_T = E_L + E_R, \tag{3}$$

the terms of the right-handed member of which can, of

* Decimal classification: 535×538. Original manuscript received by the Institute, November 22, 1950; revised manuscript received, April 25, 1951.

† 979 Grace Terrace, Teaneck, N. J.

[1] M. Faraday, "Experimental Researches," London University; London, England, vol. 3, pp. 1–26; 1855.

[2] J. Kerr, "On rotation of the plane of polarization by reflection from the pole of a magnet," *Phil. Mag.*, 5th ser., vol. 3, pp. 321–343; May, 1877. Also, "On reflection of polarized light from the equatorial surface of a magnet," *Phil. Mag.*, 5th ser., pp. 161–177; March, 1878.

[3] G. F. Fitzgerald, "On the rotation of the plane of polarization of light by reflection from the pole of a magnet," *Proc. Roy. Soc. A*, vol. 25, pp. 447–450; December, 1876.

[4] A. Kundt, "On the electromagnetic rotation of the plane of polarization of light by means of iron, cobalt, and nickel," *Phil. Mag.*, Ser. 5, vol. 18, pp. 308–327; October, 1884.

[5] A. J. Fresnel, "Collected Papers," Henri de Senavmont, Paris, France, vol. 1, p. 743; 1823.

[6] A. Righi, "Sulla velocita della luce neo corpi trasparenti magnetizzati," *Nuov. Cim.*, vol. 3, pp. 212–234; November, 1878.

[7] H. Becquerel, "Sur la propagation mégale de la lumière polarisée circulairement, dans les corps soumis à l'action du magnetisme, suivant le sens de l'aimantation et le sens des vibrations lumineuses," *Compt. Rend.*, vol. 88, pp. 334–336; February, 1879. Also "Sur une interpretation applicable au phènoméne de Faraday et au phènoméne de Zeeman," *Compt. Rend.*, vol. 125, pp. 679–685; November, 1897.

[8] D. B. Brace, "The observation of the resolution of light into its circular components in the Faraday effect," *Phil. Mag.*, 6th ser., vol. 1, pp. 464–475; April, 1901.

[9] J. Mills, "On the velocity of light in a magnetic field," *Phys. Rev.*, vol. 18, pp. 64–69; February, 1901.

course, be expanded and regrouped at any time. Thus, first, for simplicity, writing (3) as

$$E_T = E'\left[e^{j(\omega t-\beta_L z)} + e^{-j(\omega t-\beta_R z)}\right], \tag{4}$$

implying that loss is neglected and that $E_L' = E_R'$, $E_L' + E_R' = E'$

$$\begin{aligned} E_T &= E' \cos(\omega t - B_L z) + E' \cos(\omega t - B_R z) \\ &\quad + E'j \sin(\omega t - B_L z) - j\,E' \sin(\omega t - B_R z) \\ &= E'2 \cos\left(\omega t - \frac{\beta_L + \beta_R}{2}\cdot z\right) \cos\left(\frac{\beta_R - \beta_L}{2}\cdot z\right), \qquad (5) \\ &\quad + E'j \cos\left(\omega t - \frac{\beta_L + \beta_R}{2}\cdot z\right) \sin\left(\frac{\beta_R - \beta_L}{2}\cdot z\right) \end{aligned}$$

in which the first term is E_x and the second term is E_y of E_T, the angle of which with respect to the x axis, (Fig. 1) is $\delta_5 = \beta_R - \beta_L/2$, the angle of rotation discovered by Michael Faraday.

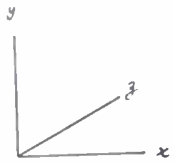

Fig. 1—Co-ordination.

Now consider other aspects of propagation in a system such as that of Fig. 2. In this, M represents a slab of material possessing an impedance for lhcpw $Z_L = R_L + jX_L$ and an impedance for rhcpw $Z_R = R_R + jX_R$ residing in what will be here taken as an ordinary

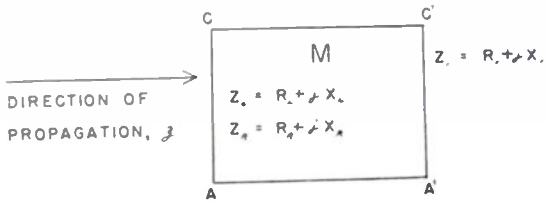

Fig. 2—Slab of material of impedances Z_L and Z_R residing in medium of impedance Z_1.

medium, such as vacua characterized by a single impedance $Z_1 = R_1 + jX_1$. The complex impedances are determined by the complex dielectric constants and complex permeabilities and by the geometry of the guiding surfaces, if any.

Then, for waves given by forms (3) and (4), incident at the first boundary AC, the reflection coefficients are

$$\begin{aligned} r_L &= |r_L| \underline{/\phi_L'} = \frac{Z_L - Z_1}{Z_L + Z_1} \\ &= \frac{(R_L - R_1) + j(X_L - X_1)}{(R_L + R_1) + j(X_L + X_1)} \end{aligned} \tag{6}$$

$$\begin{aligned} r_R &= |r_R| \underline{/\phi_R'} = \frac{Z_R - Z_1}{Z_R + Z_1} \\ &= \frac{(R_R - R_1) + j(X_R - X_1)}{(R_R + R_1) + j(X_R + X_1)} \end{aligned} \tag{7}$$

$$\phi_L' = \tan^{-1} 2\cdot\frac{R_1 X_L - R_L X_1}{R_L^2 - R_1^2 + X_L^2 - X_1^2} \tag{8}$$

$$\phi_R' = \tan^{-1} 2\cdot\frac{R_1 X_R - R_R X_1}{R_R^2 - R_1^2 + X_R^2 - X_1^2}. \tag{9}$$

Likewise, the transmission coefficients are

$$\begin{aligned} t_L &= |t_L| \underline{/\phi_L''} = \frac{2Z_L}{Z_L + Z_1} \\ &= 2\cdot\frac{R_L + jX_L}{(R_L + R_1) + j(X_L + X_1)} \end{aligned} \tag{10}$$

$$\begin{aligned} t_R &= |t_R| \underline{/\phi_R''} = \frac{2Z_R}{Z_R + Z_1} \\ &= 2\cdot\frac{R_R + jX_R}{(R_R + R_1) + j(X_R + X_1)} \end{aligned} \tag{11}$$

$$\phi_L'' = \tan^{-1}\frac{R_1 X_L - R_L X_1}{R_L(R_L + R_1) + X_L(X_L + X_1)} \tag{10A}$$

$$\phi_R'' = \tan^{-1}\frac{R_1 X_R - R_R X_1}{R_R(R_R + R_1) + X_R(X_R + X_1)}. \tag{10B}$$

Now, the reflected voltages $\underline{E}_R$ and $\underline{E}_L$ corresponding to the incident voltages E_R and E_L are, making use of the above relations,

$$\underline{E}_L = E' \cos(\omega t + \beta_1 z + \phi_L') \tag{12}$$

$$\underline{E}_R = E' \cos(\omega t + \beta_1 z + \phi_R') \tag{13}$$

$$\underline{E}_x = 2E' \cos\left(\omega t + \beta_1 z + \frac{\phi_L + \phi_R}{2}\right) \cos\frac{\phi_R - \phi_L}{2} \tag{14}$$

$$\underline{E}_y = 2E' \cos\left(\omega t + \beta_1 z + \frac{\phi_L + \phi_R}{2}\right) \sin\frac{\phi_L - \phi_R}{2}, \tag{15}$$

and the angle of the compounded vector $\underline{E}_T$, where $\underline{E}_T = \underline{E}_L + \underline{E}_R$, is

$$\delta_1 = \tfrac{1}{2}(\phi_L' - \phi_R'), \tag{16}$$

Kerr's angle of rotation of polarization by reflection from a magnetized surface.

Likewise, continuing, the transmitted voltages in the medium M of Fig. 2 are, using E'' in place of E' in recognition of the change in amplitude which has occurred at the boundary,

$$\underline{E}_L = \cos(\omega t + \phi_L'' + \beta_L z) - j \sin(\omega t + \phi_L'' + \beta_L z) \tag{17}$$

$$\underline{E}_R = \cos(\omega t + \phi_R'' + \beta_R z) - j \sin(\omega t + \phi_R'' + \beta_R z) \tag{18}$$

$$\underline{E}_x = \cos(\omega t + \phi_R'') + \cos(\omega t + \phi_L'') \tag{19}$$

$$\underline{E}_y = \sin(\omega t + \phi_L'') - \sin(\omega t + \phi_R''), \tag{20}$$

where "z" is omitted for phase considerations at the boundary, and the angle of the compounded vector $\underline{E}_T$, where $\underline{E}_T = \underline{E}_L + \underline{E}_R$, is

$$\delta_2 = \tfrac{1}{2}(\phi_L'' - \phi_R''). \tag{21}$$

We can also predict rotations of polarization upon incidence at, and transmission through, the second boundary $A'C'$ (Fig. 2). In like fashion, these "exit Kerr angles," δ_3 and δ_4, can be shown to be the negative of the corresponding "entrance Kerr angles" δ_1 and δ_2. In short,

$$\delta_1 = -\delta_3 = 1/2(\phi_L' - \phi_R') \tag{22}$$

$$\delta_2 = -\delta_4 = 1/2(\phi_L'' - \phi_R'') \tag{23}$$

$$\delta_5 = 1/2(\beta_R - \beta_L)\cdot z. \tag{24}$$

IV. CONCLUSION

Summarizing, this treatment establishes

1. A quantitative description of the Kerr magneto-optical effect.

2. The existence of five angles of rotation of polarization in the complete passage of electromagnetic radiation through a magneto optically active material:

δ_1, upon reflection from the first interface
δ_2, upon transmission across the first interface
δ_3, upon reflection from the second interface
δ_4, upon transmission across the second interface
δ_5, during propagation in the active medium
δ_5 and δ_1 being, respectively, the angles of Faraday and Kerr.

3. The dependence of δ_1, δ_2, δ_3, and δ_4 upon the material constants of the media immediately adjacent to the entering and exit surfaces of the active material.

A Method for Calculating the Current Distribution of Tschebyscheff Arrays*

DOMENICK BARBIERE†

Summary—**Dolph has derived an optimum current distribution for equispaced broadside arrays based upon the properties of the Tschebyscheff polynomials.[1] Design curves are given for arrays of 8, 12, 16, 20, and 24 elements. The equations to be computed are bulky, however, so that the numerical calculations become cumbersome for arrays of more than 24 elements. In this paper, the equations of Dolph's method are considerably simplified by algebraic means with no loss in exactness. The final current expressions are given in a closed, exact form. It is also shown that the expressions for the current elements may be easily tabulated. A table for a 24-element array is constructed as an example which may readily be extended to arrays of any number of elements.**

DISCUSSION

A BRIEF REVIEW of Dolph's derivation will first be given. It is shown that the "Tschebyscheff current distribution" may be calculated after either the side-lobe level or the position of the first null is specified. The "Tschebyscheff pattern" resulting from this current distribution is optimum in the sense that (a) if the side-lobe level is specified, the beamwidth of the resultant pattern can be proved a minimum, or (b) if the beamwidth is specified, the side-lobe level will be a minimum. A detailed calculation of the pattern is unnecessary since the character of the pattern, in particular the side-lobe and null positions, is completely specified from the well-known properties of the Tschebyscheff polynomials. In a later paper, Riblet[2] extended Dolph's method to remove some of its limitations.

It is well known that the radiation pattern of a linear equispaced broadside symmetric array of point sources is proportional to

$$|E_{2N-1}(\theta)| = \left|\sum_{k=1}^{N} I_k \cos\left[\frac{2k-1}{2}\left(\frac{2\pi d}{\lambda}\right)\sin\theta\right]\right| \tag{1}$$

$$|E_{2N}(\theta)| = \left|\sum_{k=0}^{N} I_k \cos\left[k\left(\frac{2\pi d}{\lambda}\right)\sin\theta\right]\right|, \tag{1'}$$

where (1) and (1′) apply to an even number ($2N$) and an odd number ($2N+1$) of elements, respectively. The variable θ denotes the angle between the direction of the field to the distant point P and the normal to the array, d is the element spacing, and I_k represents the current in the kth element from the center of the array. The above equations are valid only if all the currents are in phase along the array. An extension of the method for out of phase currents is given by Riblet.[2]

The odd and even cases were developed simultaneously by Dolph. However, the equations for both cases are fundamentally similar, differing essentially in the matter of superscripts and subscripts. In the section of this paper reviewing Dolph's material, therefore, the even case only will be discussed.

Introduction of the new variable

$$u = \frac{\pi d \sin\theta}{\lambda}$$

simplifies (1) to

$$F_{2N-1}(u) = \sum_{k=1}^{N} I_k \cos(2k-1)u, \tag{2}$$

where, henceforth, only the absolute values of all pattern expressions will be considered so that the absolute value signs may be omitted.

A term of the form $\cos nu$ may be expanded into a polynomial in powers of $\cos u$ whenever n is an integer. More exactly, it can be verified that

* Decimal classification: R325.11×R242. Original manuscript received by the Institute, July 24, 1950; revised manuscript received, April 30, 1951.

† Formerly, the Glenn L. Martin Company, Baltimore, Md.; now, Radiation Laboratory, Johns Hopkins University, Baltimore, Md.

[1] C. L. Dolph, "A current distribution which optimizes the relationship between beam-width and side-lobe level," PROC. I.R.E., vol. 34, pp. 335–348; June, 1946.

[2] H. J. Riblet and C. L. Dolph, Discussion on "A current distribution for broadside arrays which optimizes the relationship between beam-width and side-lobe level," PROC. I.R.E., vol. 35, pp. 489–492; May, 1947.

$$\cos(2k-1)u = \sum_{q=1}^{k} A_{2q-1}^{2k-1} x^{2q-1}, \tag{3}$$

where

$$A_{2q-1}^{2k-1} = (-1)^{k-q} \sum_{p=k-q}^{k} \binom{p}{p-k+q}\binom{2k-1}{2p}$$

$$x = \cos u \text{ and } \binom{n}{m} = \frac{n!}{m!(n-m)!}.$$

When (3) is substituted into (2) and the summation signs rearranged, the pattern equation, $F_{2N-1}(u)$, takes the polynomial form

$$G_{2N-1}(x) = \sum_{q=1}^{N}\sum_{k=q}^{N} I_k A_{2q-1}^{2k-1} x^{2q-1}, \tag{4}$$

where x is restricted to $|x| = |\cos u| \leq 1$.

It will now be shown that with suitable values of the currents (I_k) the antenna pattern described by the polynomial (4) may be made to coincide with the pattern of an appropriate Tschebyscheff polynomial, which in turn possesses all of the previously mentioned optimum properties. The nonnormalized Tschebyscheff polynomials are defined by

$$T_n(z) = \cos(n \arccos z); \quad |z| \leq 1, \tag{5}$$

where n is an integer. Clearly, the maxima and nulls of (5) are given by

$$|T_n(z)| = 1 \quad \text{for} \quad z = \cos\frac{k\pi}{n}; \; k = 0, 1, 2, \cdots, n \tag{6}$$

$$T_n(z) = 0 \quad \text{for} \quad z = \cos(2k-1)\frac{\pi}{2n};$$
$$k = 1, 2, \cdots, n.$$

$T_n(z)$ is also of the form $\cos n\phi$, where $\phi = \arccos z$ and n is an integer. Therefore, it may be converted into a polynomial in powers of $\cos\phi = \cos(\arccos z) = z$. Expansion of $T_{2N-1}(z)$ using (3) yields

$$T_{2N-1}(z) = \cos[(2N-1)\arccos z]$$
$$= \sum_{q=1}^{N} A_{2q-1}^{2N-1} z^{2q-1}. \tag{7}$$

Forms (5) and (7) of the Tschebyscheff polynomial are equivalent. Whenever $T_n(z)$ is expressed in the finite polynomial form (7), the limits of z may be extended to $\pm\infty$. In the region $|z| \leq 1$ forms (5) and (7) yield the same results, with (5) simpler for computational purposes. However, for $|z| \geq 1$, the polynomial form only is valid. Equations (7) and (4) are similar in form, except that while $|x| = |\cos u| \leq 1$ in (4), the limits of z above are $\pm\infty$. Nevertheless, the two polynomials may be made to correspond exactly by restricting the variable in (7) to $z \leq z_0$, where z_0 is an arbitrary parameter, and setting $x = \cos u = z/z_0$.

Equation (7) may now be written

$$T_{2N-1}(z_0 x) = \sum_{q=1}^{N} A_{2q-1}^{2N-1} z_0^{2q-1} x^{2q-1}, \tag{8}$$

where $|x| \leq 1$. Equations (8), representing the Tschebyscheff polynomial limited to the region within $\pm z_0$, and (4), representing the antenna pattern, are now in the same form. Corresponding coefficients may be equated and solved for the currents. Thus

$$\sum_{k=q}^{N} I_k A_{2q-1}^{2k-1} = A_{2q-1}^{2N-1} z_0^{2q-1}; \quad q = 1, 2, \cdots, N, \tag{9}$$

whence

$$I_q = \frac{1}{A_{2q-1}^{2q-1}}\left\{A_{2q-1}^{2N-1} z_0^{2q-1} - \sum_{k=q+1}^{N} I_k A_{2q-1}^{2k-1}\right\}. \tag{10}$$

If the I's are computed from (10), the resultant field pattern given by (4) will agree with the Tschebyscheff pattern shown in (8). The side-lobes and nulls of the antenna pattern will coincide with the maxima and minima of the Tschebyscheff pattern given by (6) and will occur in the region $|z_0 x| \leq 1$. In the region $1 \leq |z_0 x| \leq z_0$, the Tschebyscheff polynomial rises very steeply. This portion will represent the main lobes whose shape may be deduced from the polynomial form of $T_n(z_0 x)$. It was proven rigorously by Dolph that the Tschebyscheff pattern yields a minimum beamwidth when the side-lobe levels are known and a minimum side-lobe level when the beamwidth is specified.

The adjustable parameter z_0 may be calculated when either the side-lobe level or the beamwidth (position of the first null) is given. In the first case, z_0 must satisfy the equation $T_{2N-1}(z_0) = r$, where $r/1$ is the specified main-beam to side-lobe ratio. Since $r > 1$, z_0 must be evaluated from the polynomial form of $T_{2N-1}(z_0)$. However, Dolph[2] derived a simpler formula for computing z_0 from still another form of the Tschebyscheff polynomial. The final result is

$$z_0 = \tfrac{1}{2}\left\{(r + \sqrt{r^2-1})^{1/(2N-1)} + (r - \sqrt{r^2-1})^{1/(2N-1)}\right\}. \tag{11}$$

From (6), the nulls of $T_{2N-1}(z_0 x)$ are at

$$z_0 x = \cos\left(\frac{2k-1}{2}\,\frac{\pi}{2N-1}\right),$$

whence

$$z_0 x_1^0 = \cos\frac{\pi}{2(2N-1)}$$

defines the position of the first null. When θ_0 is specified as the angular position of the first null, z_0 may be deduced from the relations

$$z_0 = \frac{1}{x_1^0}\cos\frac{\pi}{2(2N-1)};$$

$$x_1^0 = \cos u_1^0 = \cos\left(\frac{\pi d}{\lambda}\sin\theta_0\right).$$

It is hoped the short synopsis of Dolph's material presented above is sufficient so the remainder of this paper may be understood. For a more detailed account of the method, the reader is referred to the original sources.

It is evident that the numerical work involved in calculating the current distribution from (10) and z_0 from (11) can become extremely tedious as the number of elements increases. In the discussion that follows, a simple method of computing the I's is derived whereby the currents will be given immediately in simple terms of z_0. Also, a very rapid method for computing z_0 will be given.

We may equate (2) to (8) so that

$$\sum_{k=1}^{N} I_k \cos(2k-1)u = \sum_{q=1}^{N} A_{2q-1}^{2N-1} z_0^{2q-1} (\cos u)^{2q-1} \quad (12)$$

$$\sum_{k=0}^{N} I_k \cos(2ku) = \sum_{q=0}^{N} A_{2q}^{2N} z_0^{2q} (\cos u)^{2q}, \quad (12')$$

where the odd case has been reintroduced. The left sides of the above equations may be treated as parts of a Fourier series. Thus, if both sides of (12) and (12′) are multiplied by $\cos(2k-1)u$ and $\cos(2k)u$, respectively, and integrated from 0 to 2π, there remains only

$$\pi I_k = \sum_{q=1}^{N} A_{2q-1}^{2N-1} z_0^{2q-1} \int_0^{2\pi} \cos^{2q-1} u \cos(2k-1) u du \quad (13)$$

$$\pi I_k = \sum_{q=0}^{N} A_{2q}^{2N} Z_0^{2q} \int_0^{2\pi} \cos^{2q} u \cos(2ku) du. \quad (13')$$

The integrals above are of the form

$$\int_0^{2\pi} \cos^m x \cos nx dx,$$

where m and n are arbitrary integers. Using formulas 360 and 267 of Pierce's tables, it can be seen that

$$\int_0^{2\pi} \cos^m x \cos nx dx$$
$$= 2\pi \left\{ \left(\frac{m}{m+n}\right)\left(\frac{m-1}{m+n-2}\right) \cdots \right.$$
$$\left. \left(\frac{m-n+1}{m-n+2}\right)\left(\frac{m-n-1}{m-n}\right) \cdots \left(\tfrac{1}{2}\right) \right\}, \quad (14)$$

with the restriction that $m \geqq n$ and $m-n$ be even. When $n > m$ or $m-n$ is odd, the integral is equal to zero. Setting $m=2q-1$, $n=2k-1$ for (12) and $m=2q$, $n=2k$ for (12′) yields for the currents

$$I_k = \sum_{q=k}^{N} A_{2q-1}^{2N-1} z_0^{2q-1} \left\{ 2\left(\frac{2q-1}{2q+2k-2}\right)\left(\frac{2q-2}{2q+2k-4}\right) \cdots \right.$$
$$\left. \left(\frac{2q-2k+1}{2q-2k+2}\right)\left(\frac{2q-2k-1}{2q-2k}\right) \cdots \left(\tfrac{1}{2}\right) \right\} \quad (15)$$

$$I_k = \sum_{q=k}^{N} A_{2q}^{2N} z_0^{2q} \left\{ 2\left(\frac{2q}{2q+2k}\right)\left(\frac{2q-1}{2q+2k-2}\right) \cdots \right.$$
$$\left. \left(\frac{2q-2k+1}{2q-2k+2}\right)\left(\frac{2q-2k-1}{2q-2k}\right) \cdots \left(\tfrac{1}{2}\right) \right\}, \quad (15')$$

where $m \geqq n (q \geqq k)$.

If the numerator of the bracketed expression in (15) is multiplied by $(2q-2k)(2q-2k-2) \cdots 2 = (q-k)!2^{q-k}$, it then becomes equal to $2(2q-1)!$ Thus, the numerator in question may be written as $(2q-1)!/(q-k)!2^{q-k-1}$. The denominator of this expression may be written as $1/(q+k-1)!2^{q+k-1}$. The substitution of the above into (15) and the application of a similar manipulation to the bracketed expression of (15′) yields

$$I_k = \sum_{q=k}^{N} A_{2q-1}^{2N-1} z_0^{2q-1} \frac{(2q-1)!}{(q-k)!(q+k-1)!2^{2q-2}} \quad (16)$$

$$I_k = \sum_{q=k}^{N} A_{2q}^{2N} z_0^{2q} \frac{(2q)!}{(q-k)!(q+k)!2^{2q-1}}, \quad (16')$$

where (16) is for an even number ($2N$) elements and (16′) for an odd number ($2N+1$) elements.

Further simplification is still possible by incorporating the A's, or Tschebyscheff coefficients (see (7)), into the factorial expression. The Tschebyscheff polynomial is actually a particular form of Gauss's hypergeometric series and may be written[3]

$$T_n(x) = 2^{2n-1}\left\{ x^n - \frac{n}{1!2^2} x^{n-2} + \frac{(n)(n-3)}{2!2^4} x^{n-4} - \frac{(n)(n-4)(n-5)}{3!2^6} x^{n-6} + \cdots \right\}. \quad (17)$$

With some manipulation, it can be seen that $T_n(x)$ may also be written in the alternate form

$$T_n(x) = \sum_{m=0,1}^{n} (-1)^{(n-m)/2} 2^{2n-1} \left\{ \frac{n\left(m + \frac{n-m}{2} - 1\right)!}{\left(\frac{n-m}{2}\right)! m! 2^{n-m}} x^m \right\}, \quad (18)$$

where $m = n, n-2, n-4 \cdots 0$, or 1. By comparing (18) with (7), the Tschebyscheff coefficients become

$$A_{2q-1}^{2N-1} = (-1)^{N-q} 2^{2N-2} \frac{(2N-1)(q+N-2)!}{(N-q)!(2q-1)!2^{2N-2q}} \quad (19)$$

$$A_{2q}^{2N} = (-1)^{N-q} 2^{2N-1} \frac{(2N)(q+N-1)!}{(N-q)!(2q)!\,2^{2N-2q}}. \quad (19')$$

Introducing the results (19) and (19′) into (16) and (16′) yields finally

$$I_k = \sum_{q=k}^{N} (-1)^{N-q} z_0^{2q-1} \frac{(2N-1)(q+N-2)!}{(q-k)!(q+k-1)!(N-q)!} \quad (20)$$

$$I_k = \sum_{q=k}^{N} (-1)^{N-q} z_0^{2q} \frac{(2N)(q+N-1)!}{(q-k)!(q+k)!(N-q)!}, \quad (20')$$

where (20) and (20′) apply to $2N$ and $2N+1$ element arrays, respectively.

Equations (20) and (20′) are most readily solved by

[3] H. Margenau and G. Murphy, "Mathematics of Physics and Chemistry," Van Nostrand and Co., Inc., New York, N. Y., p. 74; 1943. This equation is given incorrectly in the earlier editions of the book.

constructing a table of coefficients wherein the I_k's form the rows and the z_0's the columns. See Table I for 24 elements. The 24-element case was solved by Dolph, and is introduced here as a check on the new method of attack. The results agree perfectly with those of Dolph, and yet were obtained with only a few hours of computation. The table shows that once the upper left-hand corner is constructed by substituting for q, N, and k the remainder of the table may be readily extended from sequence considerations.

The tables also lend themselves to quick checks for errors. The sums across the rows, which are actually the current values for $z_0=1$, should equal zero for all the currents except the final one, I_N. Thus, for the even case,

$$\sum_{k=1}^{N} I_k(z_0)\cos(2k-1)u = T_{2N-1}(z_0x).$$

But, when $z_0=1$, $T_{2N-1}(z_0x)=\cos[(2N-1)\arccos x]=\cos(2N-1)u$. Thus, $I_k=0$, except for $k=N$ where $I_N=1$. Also, the sum down each column should equal the coefficient of the corresponding term of the Tschebyscheff polynomial. When $x=\cos u=1$, $\cos(2k-1)u=1$ for all k so that $\sum I_k(z_0)=T_{2N-1}(z_0)$ from the above.

TABLE I

CURRENT DISTRIBUTION FOR A 24-ELEMENT ARRAY YIELDING A TSCHEBYSHEFF PATTERN

	$q=12(+z_0^{23})$	$q=11(-z_0^{21})$	$q=10(+z_0^{19})$	$q=9(-z_0^{17})$	$q=8(+z_0^{15})$	$q=7(-z_0^{13})$	$q=6(+z_0^{11})$	$q=5(-z_0^{9})$	$q=4(+z_0^{7})$	$q=3(-z_0^{5})$	$q=2(+z_0^{3})$	$q=1(-z_0)$
I_1	$\frac{(23)22!}{12!11!0!}$ 1352078	$\frac{(23)21!}{11!10!1!}$ 8112468	$\frac{(23)20!}{10!9!2!}$ 21246940	$\frac{(23)19!}{9!8!3!}$ 31870410	$\frac{(23)18!}{8!7!4!}$ 30193020	$\frac{(23)17!}{7!6!5!}$ 18786768	$\frac{(23)16!}{6!5!6!}$ 7735728	$\frac{(23)15!}{5!4!7!}$ 2072070	$\frac{(23)14!}{4!3!8!}$ 345345	$\frac{(23)13!}{3!2!9!}$ 32890	$\frac{(23)12!}{2!1!10!}$ 1518	$\frac{(23)11!}{1!0!11!}$ 23
I_2	$\frac{(23)22!}{13!10!0!}$ 1144066	$\frac{(23)21!}{12!9!1!}$ 6760390	$\frac{(23)20!}{11!8!2!}$ 17383860	$\frac{(23)19!}{10!7!3!}$ 25496328	$\frac{(23)18!}{9!6!4!}$ 23483460	$\frac{(23)17!}{8!5!5!}$ 14090076	$\frac{(23)16!}{7!4!6!}$ 5525520	$\frac{(23)15!}{6!3!7!}$ 1381380	$\frac{(23)14!}{5!2!8!}$ 207207	$\frac{(23)13!}{4!1!9!}$ 16445	$\frac{(23)12!}{3!0!10!}$ 506	
I_3	$\frac{(23)22!}{14!9!0!}$ 817190	$\frac{(23)21!}{13!8!1!}$ 4680270	$\frac{(23)20!}{12!7!2!}$ 11589240	$\frac{(23)19!}{11!6!3!}$ 16224936	$\frac{(23)18!}{10!5!4!}$ 14090076	$\frac{(23)17!}{9!4!5!}$ 7827820	$\frac{(23)16!}{8!3!6!}$ 2762760	$\frac{(23)15!}{7!2!7!}$ 592020	$\frac{(23)14!}{6!1!8!}$ 69069	$\frac{(23)13!}{5!0!9!}$ 3289		
I_4	$\frac{(23)22!}{15!8!0!}$ 490314	$\frac{(23)21!}{14!7!1!}$ 2674440	$\frac{(23)20!}{13!6!2!}$ 6240360	$\frac{(23)19!}{12!5!3!}$ 8112468	$\frac{(23)18!}{11!4!4!}$ 6404580	$\frac{(23)17!}{10!3!5!}$ 3131128	$\frac{(23)16!}{9!2!6!}$ 920920	$\frac{(23)15!}{8!1!7!}$ 148005	$\frac{(23)14!}{7!0!8!}$ 9867			
I_5	$\frac{(23)22!}{16!7!0!}$ 245157	$\frac{(23)21!}{15!6!1!}$ 1248072	$\frac{(23)20!}{14!5!2!}$ 2674440	$\frac{(23)19!}{13!4!3!}$ 3120180	$\frac{(23)18!}{12!3!4!}$ 2134860	$\frac{(23)17!}{11!2!5!}$ 853944	$\frac{(23)16!}{10!1!6!}$ 184184	$\frac{(23)15!}{9!0!7!}$ 16445				
I_6	$\frac{(23)22!}{17!6!0!}$ 100947	$\frac{(23)21!}{16!5!1!}$ 468027	$\frac{(23)20!}{15!4!2!}$ 891480	$\frac{(23)19!}{14!3!3!}$ 891480	$\frac{(23)18!}{13!2!4!}$ 492660	$\frac{(23)17!}{12!1!5!}$ 142324	$\frac{(23)16!}{11!0!6!}$ 16744					
I_7	$\frac{(23)22!}{18!5!0!}$ 33649	$\frac{(23)21!}{17!4!1!}$ 137655	$\frac{(23)20!}{16!3!2!}$ 222870	$\frac{(23)19!}{15!2!3!}$ 178296	$\frac{(23)18!}{14!1!4!}$ 70380	$\frac{(23)17!}{13!0!5!}$ 10948						
I_8	$\frac{(23)22!}{19!4!0!}$ 8855	$\frac{(23)21!}{18!3!1!}$ 30590	$\frac{(23)20!}{17!2!2!}$ 39330	$\frac{(23)19!}{16!1!3!}$ 22287	$\frac{(23)18!}{15!0!4!}$ 4692							
I_9	$\frac{(23)22!}{20!3!0!}$ 1771	$\frac{(23)21!}{19!2!1!}$ 4830	$\frac{(23)20!}{18!1!2!}$ 4370	$\frac{(23)19!}{17!0!3!}$ 1311								
I_{10}	$\frac{(23)22!}{21!2!0!}$ 253	$\frac{(23)21!}{20!1!1!}$ 483	$\frac{(23)20!}{19!0!2!}$ 230									
I_{11}	$\frac{(23)22!}{22!1!0!}$ 23	$\frac{(23)21!}{21!0!1!}$ 23										
I_{12}	$\frac{(23)22!}{23!0!0!}$ 1											
$T_{23}(z_0)$	4194304	24117248	60293120	85917696	76873728	44843008	17145856	4209920	631488	52624	2024	23

$$I_k=\sum_{q=k}^{N}(-1)^{N-q}z_0^{2q-1}\frac{(2N-1)(q+N-2)!}{(q+k-1)!(q-k)!(N-q)!}$$

$N=12$

Sum across a row $=0$ except for I_{12}

Sum down a column $=$ corresponding Tschebysheff coefficient

Note: When q is odd, the column is negative.

The currents are now given as a function of the parameter, z_0. z_0 may be calculated from $T_{2N-1}(z_0)=r$ using (11). However, it will now be shown that z_0 may be computed from a much simpler formula. Heretofore, $T_n(z)$ was given by cos (n arccos z) in the region $|z| \leqq 1$, and it was noted that $T_n(z)$ could not exceed 1 there. When the limits of z were extended to $\pm\infty$, the polynomial form or the closed form (11) had to be employed, particularly when solving the equation $T_{2N-1}(z_0)=r$ for $r>1$. However, it is possible to modify the simple cosine form of $T_n(z)$ so that it will apply to the region $|z| \geqq 1$.

From (5), $T_n(z)=\cos(n \text{ arccos } z)=r$, but here $r>1$. For the cosine of an argument to exceed one, the argument must be imaginary. Therefore, let cos $inu=r$ and $iu=\text{arccos } z$. The above is equivalent to setting cosh $nu=r$ and $u=\text{arccosh } z$. Thus, for values of $|z| \geqq 1$, $T_n(z)$ may be written $T_n(z)=\cosh(n \text{ arccosh } z)$. The equation $\cosh[(2N-1) \text{ arccosh } z_0]=r$ is simply solved for z_0 to give

$$z_0 = \cosh\left(\frac{\text{arccosh } r}{2N-1}\right), \tag{21}$$

whence z_0 may readily be obtained from the mathematical tables.

As further proof of the above, it will be shown that the form cosh (n arccosh z) leads to the same polynomial in z as does cos (n arccos z). Whence it can be concluded that the cosh formula represents the Tschebyscheff polynomial, but in a different region. It was noted above that cos $n\theta$ may be expanded into a polynomial in $x=\cos\theta$. This fact may be derived from $(\cos n\theta+i \sin n\theta)=(\cos\theta+i\sin\theta)^n$. Expanding the terms on the right and equating real and imaginary terms yields

$$\cos n\theta = \cos^n\theta - \binom{n}{2}\cos^{n-2}\theta\sin^2\theta + \binom{n}{4}\cos^{n-4}\theta\sin^4\theta\cdots, \tag{22}$$

where

$$\binom{n}{k} = \frac{n!}{k!(n-k)!}.$$

If $\sin^2\theta$ is replaced by $(1-\cos^2\theta)$, it is apparent that cos $n\theta$ will emerge as a polynomial in powers of cos θ.

The expansion of cosh $n\theta$ may be effected in a somewhat similar manner. Since $\cosh n\theta+\sinh n\theta=e^{n\theta}=(e^\theta)^n=(\cosh\theta+\sinh\theta)^n$ and $\cosh n\theta-\sinh n\theta=e^{-n\theta}=(e^{-\theta})^n=(\cosh\theta-\sinh\theta)^n$, we may solve for cosh $n\theta$ and expand so that

$$\cosh n\theta = \cosh^{n\theta} + \binom{n}{2}\cosh^{n-2}\theta\sinh^2\theta + \binom{n}{4}\cos^{n-4}\theta\sinh^4\theta\cdots. \tag{23}$$

If $\sinh^2\theta$ is replaced by $-(1-\cosh^2\theta)$, (23) will have exactly the same coefficients as (22).

As an afterthought, it may be of interest to note that the above might be more simply established by reasoning that if $\cos n\theta=P(\cos\theta)$ where P denotes some polynomial one may also write $\cos in\theta=P(\cos i\theta)$ whence $\cosh n\theta=P(\cosh\theta)$.

It is now established that cosh $n\theta$ leads to exactly the same polynomial in powers of cosh θ as does cos $n\theta$ in powers of cos θ. From this it follows that cosh(n arccosh z) may be expanded into a polynomial in cosh (arccosh z) $=z$ and will yield the same Tschebyscheff polynomial as the expansion of cos (n arccos z). Thus, the two formulas represent the same polynomial, except that the cosine form is applicable in the region $z \leqq 1$ and the cosh formula is applicable in the region $z \geqq 1$. The complete Tschebyscheff polynomial may now be written

$$\begin{aligned} T_n(z) &= \cos(n \text{ arccos } z); \quad z \leqq 1 \\ T_n(z) &= \cosh(n \text{ arccosh } z); \quad z \geqq 1. \end{aligned} \tag{24}$$

As a check, the equation $T_{23}(z_0)=r$ for the 24-element case was solved for several values of r by formulas (11) and (21). The z_0's resulting from the two methods were exactly the same.

Acknowledgment

The author wishes to express his thanks to the Glenn L. Martin Company at Baltimore, Maryland for supervising the project and to Dr. D. D. King and H. M. Watts of the Radiation Laboratory of Johns Hopkins University for proofreading and giving many helpful suggestions.

Correction

N. W. Mather, author of the paper, "An Analysis of Triple-Tuned Coupled Circuits," which appeared on pages 813–822 of the July, 1950 issue of the Proceedings of the I.R.E., has brought the following error to the attention of the editors:

The contour values given in Fig. 8 are incorrect. The values indicated should all be halved and should agree with the tabulation in Table I.

Directional Antenna Arrays of Elements Circularly Disposed About a Cylindrical Reflector*

ROGER F. HARRINGTON†, STUDENT, IRE, AND WILBUR R. LEPAGE‡, SENIOR MEMBER, IRE

Summary—**The general solution for the field pattern of a circular array is adapted to include the effect of a concentric reflecting cylinder. Two solutions are presented, one giving the field as a Fourier series, and the other as an infinite series of Bessel functions. The results are general, being applicable to any array dimensions and for arbitrary distribution of excitation. The solution is idealized to the extent of assuming a continuous current sheet, rather than discrete elements, and an infinitely long cylindrical reflector.**

Introduction

Antenna arrays having circular symmetry are useful in applications requiring a directional pattern with electrical control of the beam direction. Equations for the field patterns of circularly disposed elements without a reflector have been developed.[1] The present paper is an extension to include the effect of a concentric reflecting cylinder. General equations are given which are valid for either vertical or horizontal polarization, and the case for vertical polarization is developed in some detail. The vertical direction is parallel to the z axis of Fig. 1. The array is considered in a transmitting condition, and the effect of the reflector is introduced by ascribing a field pattern to each mathematical element of current. This pattern is a function of the curvature of the reflector, the separation between the element and the reflector, and the polarization.

Practical application of the analysis is limited to those cases for which a continuous distribution of current can be substituted for a system of discrete elements. This is not a serious limitation, because it can be shown that the actual field pattern has undesirable side lobes, when the element spacing is so great that the continuous current distribution is not a good approximation. The maximum allowable spacing between elements depends somewhat on the current distribution. If the distribution is uniform, it can be shown that the maximum allowable element spacing is about a half wavelength. If the distribution is not uniform, a closer spacing must be used, the closeness depending on the variation of the current.

Two forms of the general solution are presented. One is a Fourier series in ϕ, and the other is a series of Bessel functions of ϕ with trigonometric multipliers. In both cases θ appears in the coefficients. The Fourier series solution is useful when the array is small, and the Bessel function solution is preferable for large arrays. All distances are given in radian-length measure ($2\pi/\lambda$ times the actual length).

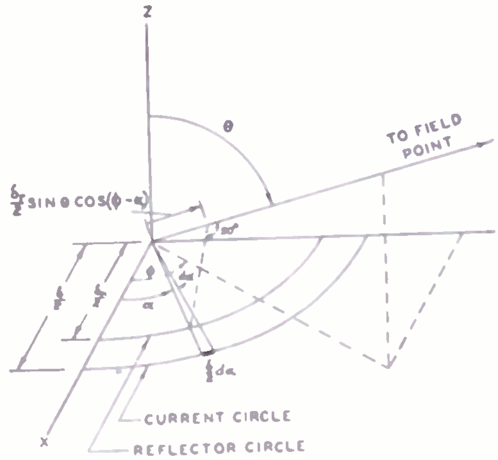

Fig. 1—Geometry of array with circular symmetry.

Fourier Series Solution

Let $\overline{R}_e(\phi-\alpha, \theta)$ be the field pattern of a current element at angular position α, with the center of the array used as the datum for phase-angle measurement.[2] The current distribution is represented by the complex function $\overline{I}(\alpha)$. Its amplitude is measured in amperes per radian length. The total field at a distant point is proportional to

$$\overline{E}(\phi, \theta) = \frac{\delta}{2\pi}\int_0^{2\pi} \overline{R}_e(\phi - \alpha, \theta)\overline{I}(\alpha)d\alpha. \tag{1}$$

The multiplying factor $1/\pi$ is chosen for convenience. Each of the functions of the integrand is expressible as a Fourier series;

$$\overline{R}_e(\phi - \alpha, \theta) = \sum_{n=-\infty}^{\infty} \overline{G}_n(\theta)e^{jn(\phi-\alpha)}, \tag{2}$$

$$\overline{I}(\alpha) = \sum_{k=-\infty}^{\infty} \overline{C}_k e^{jk\alpha}. \tag{3}$$

Symmetry dictates that $\overline{R}_e$ is an even function of $\phi-\alpha$, and for most practical situations $\overline{I}$ will be an even function of α. These conditions ensure that $\overline{G}_{-n}=\overline{G}_n$, and $\overline{C}_{-k}=\overline{C}_k$. A substitution of (2) and (3) into (1), followed by integration, gives

$$\overline{E}(\phi, \theta) = \delta\sum_{n=0}^{\infty} \epsilon_n\overline{G}_n(\theta)\overline{C}_n \cos n\phi, \tag{4}$$

* Decimal classification: R325.11. Original manuscript received by the Institute, October 6, 1950; revised manuscript received, May 10, 1951.

† Formerly, Syracuse University, Syracuse, N. Y.; now, Ohio State University, Columbus, Ohio.

‡ Syracuse University, Syracuse, N. Y.

[1] W. R. LePage, C. S. Roys, and S. Seely, "Radiation from circular current sheets," Proc. I.R.E., vol. 38, p. 1069; September, 1950.

[2] A bar above a symbol implies that it is a complex quantity.

where ϵ_n is Neuman's number. This is the most general form of the solution.

Suppose the current distribution is

$$\overline{I}(\alpha) = \overline{A}\,(\alpha)e^{-j\frac{\delta r}{2}\sin\theta_0\cos\alpha}. \tag{5}$$

This is a convenient form for the current because it is approximately the beam-cophasal excitation if $\overline{A}$ is real, as may be seen by referring to the section on single-element patterns. The function $\overline{A}(\alpha)$ can be expressed as the Fourier series

$$\overline{A}(\alpha) = \sum_{v=-\infty}^{\infty} \overline{D}_v e^{jv\alpha}. \tag{6}$$

The usual formulas for determining the coefficients of (3) are applied to the combination of (5) and (6), with the added condition that $\overline{A}(\alpha)$ is symmetrical about the point $\alpha=0$. Manipulation yields

$$\overline{C}_n = \frac{1}{2}\sum_{s=0}^{\infty} \epsilon_s j^{-s}(\overline{D}_{n-s} + \overline{D}_{n+s})J_s\left(\frac{\delta r}{2}\sin\theta_0\right), \tag{7}$$

in which J_s is the Bessel function of the first kind.

Equation (7) may be incorporated into (4) to give a solution in terms of properties of $\overline{A}(\alpha)$, rather than $\overline{I}(\alpha)$. This is convenient for the approximate beam-cophasal case, in which case $\overline{A}(\alpha)$ is real.

Bessel-Trigonometric Solution

Another form for the general solution is obtained by writing

$$\overline{R}_c(\phi-\alpha,\theta) = R(\phi-\alpha,\theta)e^{j\xi(\phi-\alpha,\theta)}. \tag{8}$$

In the section on single-element patterns it is shown that

$$\xi(\phi-\alpha,\theta) = \frac{\delta_r}{2}\sin\theta\cos(\phi-\alpha)$$

to a good approximation. The amplitude function is written as the Fourier series

$$R(\phi-\alpha,\theta) = \sum_{n=-\infty}^{\infty} B_n(\theta)e^{jn(\phi-\alpha)}. \tag{9}$$

The B coefficients are all real, and $B_{-n}=B_n$ because R is an even function and real.

When (5), (6), (8), and (9) are combined and substituted into (1), the result is

$$\overline{E}(\phi,\theta) = \delta\sum_{v,n=-\infty}^{\infty} j^v\overline{D}_{v+n}B_n(\theta)e^{j(v\Delta+n\phi)}J_v(\delta_r f), \tag{10}$$

where

$$f = \tfrac{1}{2}\sqrt{\sin^2\theta + \sin^2\theta_0 - 2\sin\theta_0\sin\theta\cos\phi}, \tag{11}$$

$$\Delta = \tan^{-1}\frac{\sin\theta\sin\phi}{\sin\theta\cos\phi - \sin\theta_0}. \tag{12}$$

The details of this development are given in the literature.[1]

In the surface $\theta=\theta_0$, the formulas for f and Δ reduce to: $f=\sin\theta_0\sin(\phi/2)$ and $\Delta=(\phi+\pi)/2$; allowing (10) to become

$$\overline{E}(\phi,\theta_0) = \sum_{v=0}^{\infty}\epsilon_v j^v\left[\sum_{n=-\infty}^{\infty} D_{v+n}B_n(\theta_0)\cos\left(v\frac{\pi}{2} + \frac{2n+v}{2}\phi\right)\right]J_v\left(\delta_r\sin\theta_0\sin\frac{\phi}{2}\right). \tag{13}$$

Equations (4) and (10) are alternate expressions for the field pattern. A comparison of their relative usability is dependent upon the following discussion of the single-element patterns.

Single-Element Patterns for Vertical Polarization

Expressions for the field patterns of a current element near a conducting cylinder are given in a paper by Carter.[3] For a short element parallel to the cylinder it is found that

$$\overline{G}_n(\theta) = j^{n+1}\sin\theta\,\frac{J_n\left(\frac{\delta_r}{2}\sin\theta\right)Y_n\left(\frac{\delta}{2}\sin\theta\right) - J_n\left(\frac{\delta}{2}\sin\theta\right)Y_n\left(\frac{\delta_r}{2}\sin\theta\right)}{J_n\left(\frac{\delta_r}{2}\sin\theta\right) - jY_n\left(\frac{\delta_r}{2}\sin\theta\right)}, \tag{14}$$

where Y_n is the nth-order Bessel function of the second kind. This is applicable for all θ if the cylinder is infinitely long; otherwise it should be used with caution when θ deviates appreciably from 90°.

For arrays of large diameter, it may be permissible to use an approximate single-element pattern obtained by replacing the cylinder by an infinite plane, tangent to the cylinder at the point nearest the element. Using the center of the array for the phase datum, the pattern of a short element parallel to the z axis is

[3] P. S. Carter, "Antenna arrays around cylinders," Proc. I.R.E., vol. 31, p. 671; December, 1943.

$$\overline{R}_c = \begin{cases} \sin\theta \sin\left[l \sin\theta \cos(\phi-\alpha)\right] e^{-j(\delta_r/2)\sin\theta\cos(\phi-\alpha)}, & |\phi-\alpha| \leqq \dfrac{\pi}{2}, \\ 0, & |\phi-\alpha| > \dfrac{\pi}{2}, \end{cases} \tag{15}$$

where l is the element-reflector separation. The function $\sin\left[l \sin\theta \cos(\phi-\alpha)\right]$ is a standard form for which the Fourier series may be written directly.[4] The series thus obtained represents (15), only if $|\phi-\alpha| \leqq \pi/2$, but it can be converted to a series which is valid for the entire range of $|\phi-\alpha|$, by applying the integral expressions for the Fourier coefficients. The results are:

$$B_n(\theta) = \begin{cases} j^{n-1} \dfrac{\sin\theta}{2} J_n(l \sin\theta), & n \text{ odd}, \\ j^n \dfrac{2\sin\theta}{\pi} \displaystyle\sum_{\substack{s=1 \\ s=\text{odd}}}^{\infty} \frac{s}{(s-n)(s+n)} J_s(l\sin\theta), & n \text{ even}. \end{cases} \tag{16}$$

For any $\overline{R}_c$ function for which the phase-angle part is the same as in (15), the $\overline{G}$ coefficients can be expressed in terms of the B coefficients, or vice versa. In similarity with the development of (7) it is found that

$$\overline{G}_n = \frac{1}{2}\sum_{r=0}^{\infty} \epsilon_r j^r (B_{r-n} + B_{r+n}) J_r\left(\frac{\delta_r}{2}\sin\theta\right), \tag{17}$$

and

$$B_n = \frac{1}{2}\sum_{r=0}^{\infty} \epsilon_r j^{-r} (\overline{G}_{r-n} + \overline{G}_{r+n}) J_r\left(\frac{\delta_r}{2}\sin\theta\right). \tag{18}$$

Comparison of the Solutions for Vertical Polarization

It is instructive to compare the two solutions in the light of their applicability for computation. The Fourier series form is perhaps the simpler, because each term is simply a trigonometric function of ϕ. However, the preference depends to a great extent on the array diameter.

First consider (10), finding an estimate of the necessary range of v. In practical cases $\overline{A}$ and R are slowly varying functions, and so their series will converge rather rapidly. Let $|\overline{D}_n|$ and B_n be negligible for $n > N_d$ and N_b, respectively. Fig. 2 illustrates how an estimate of the range of v can be obtained. An upper bound of a coefficient in (10) is proportional to the area of the product of the two distribution functions. From the diagram, it can be seen that this area is negligible when $v > (N_d + N_b)$.

For each value of v the number of terms due to the summation over n is the amount of overlap of the two distribution graphs. As v becomes smaller the range of n increases up to $2N_s+1$, where N_s is the smaller of N_d and N_b. If N_m is the larger of N_d and N_b, there will be $N_m - N_s$ values of v for which n has the maximum range $(2N_s+1)$. Therefore, letting P be the number of terms in (10),

$$P \approx 1 + 2 + \cdots + (2N_s + 1) + (N_m - N_s)(2N_s + 1)$$
$$= (2N_s + 1)(N_m + 1). \tag{19}$$

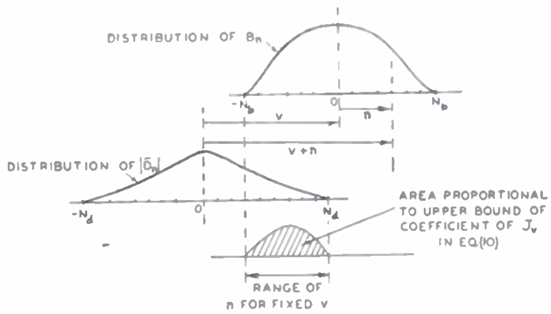

Fig. 2—Diagram for estimating the number of terms in equation (10).

The convergence of (4) depends on the convergences of the series for $\overline{I}$ and $\overline{R}_c$. Estimates of these rates of convergence can be obtained by using (5) and (15) as typical examples. Each can be broken up into the product of a series for the magnitude function, which has already been considered, and the series for the exponential part. For simplicity, consider the case $\theta=\theta_0=90°$. The exponential part is the same for both functions and is expressible by a known series,[3] the kth coefficient being $J_k(\delta_r/2)$.

An estimate of the number of significant terms is obtained by recalling that $J_k(x)$ becomes quite negligible when k is greater than $x+4$. Therefore, in each case the series for the exponential factor contains approximately $(\delta_r/2)+4$ terms.

The above series is multiplied by the series for either $\overline{A}$ or R which have, respectively, N_d and N_b significant terms. The approximate numbers of terms in the series for $\overline{I}$ and $\overline{R}_c$ are then $(\delta_r/2)+4+N_d$ and $(\delta_r/2)+4+N_b$, respectively. The smaller of these is the required estimate of the number of significant terms in (4). Thus,

$$\text{number of terms in (4)} \approx \frac{\delta_r}{2} + 4 + N_s. \tag{20}$$

When N_s+4 is small compared with $\delta_r/2$, the number of terms is approximately proportional to the array diameter. For very small diameters N_s may be a function of δ_r, but this possibility may be omitted in this approximate analysis.

[4] G. N. Watson, "Theory of Bessel Functions," Second ed., Cambridge University Press, Cambridge, Mass., p. 22; 1945.

From (19) and (20), it is possible to see that (4) may be preferable for small arrays, while (10) may be preferable for large arrays. If $N_s = N_m = N$, the transition occurs when

$$\delta_r = 4N^2 + 4N - 6. \tag{21}$$

For practical cases N may be rather small, perhaps as low as 3. This value of N gives $\delta_r = 42$ (approximately 7 wavelengths diameter) as the largest array for which it would be profitable to use (4).

Beamwidth for Vertical Polarization

Beamwidth is not very sensitive to minor details of variation of the R and $\overline{A}$ functions. Therefore, a reasonable estimate of beamwidth may be obtained by assuming convenient typical forms for R and $\overline{A}$. A simple result is obtained by taking

$$R(\phi - \alpha, \theta_0) = \begin{cases} \cos(\phi - \alpha), & 0 \leqq |\phi - \alpha| \leqq \dfrac{\pi}{2}, \\ 0, & \dfrac{\pi}{2} < |\phi - \alpha| \leqq \pi, \end{cases} \tag{22}$$

$$A(\alpha) = \begin{cases} \cos\alpha, & 0 \leqq |\alpha| \leqq \dfrac{\pi}{2}, \\ 0, & \dfrac{\pi}{2} < |\alpha| \leqq \pi. \end{cases} \tag{23}$$

Equation (22) is a fair approximation for the normalized magnitude function of (15), when the element-to-reflector spacing is less than a quarter wavelength. Equation (23) is a reasonable tapering of the excitation toward the sides. For this case routine manipulations give the field function

$$\begin{aligned} E(\phi, \theta_0) = {} & \left(1 + \frac{\pi^2}{8}\cos\phi + \frac{2}{9}\cos 2\phi + \cdots\right) J_0\left(\delta_r \sin\theta_0 \sin\frac{\phi}{2}\right) \\ & + \left(\frac{\pi^2}{8} + \frac{4}{3}\cos\phi - \frac{4}{45}\cos 3\phi + \cdots\right) J_2\left(\delta_r \sin\theta_0 \sin\frac{\phi}{2}\right) \\ & + \left(\frac{2}{9} - \frac{2}{15}\cos 2\phi + \cdots\right) J_4\left(\delta_r \sin\theta_0 \sin\frac{\phi}{2}\right) \\ & + \left(\frac{4}{45} - \frac{4}{45}\cos 3\phi + \cdots\right) J_6\left(\delta_r \sin\theta_0 \sin\frac{\phi}{2}\right). \end{aligned} \tag{24}$$

A multiplying factor is omitted from (24).

For consideration of beamwidth, ϕ can be restricted to the main lobe, allowing a much simpler expression to be used. For the main lobe, the range of ϕ is such that $\delta_r \sin\theta_0 \sin\phi/2 < 2.40$. Reference to tabulated values of Bessel functions shows that the J_4 and J_6 terms may be dropped for this restricted range. Furthermore, in the range of $|\phi|$ up to 20° the coefficient of J_0 varies less than 5 per cent, and the coefficient of J_2 varies less than 2 per cent. When $\phi = 0$, these two coefficients are nearly the same and therefore, omitting multiplying factors, the equation of the main lobe is approximately

$$E(\phi, \theta_0) = J_0\left(\delta_r \sin\theta_0 \sin\frac{\phi}{2}\right) + J_2\left(\delta_r \sin\theta_0 \sin\frac{\phi}{2}\right), \tag{25}$$

if the array is large enough to make the width of the beam less than 40°. From a tabulation of Bessel functions, it is found that the half power point occurs when $\delta_r \sin\theta_0 \sin\phi/2 = 1.61$, so that

$$\text{beamwidth} \approx 4 \sin^{-1} \frac{1.61}{\delta_r \sin\theta_0}. \tag{26}$$

Vertical Patterns for Vertical Polarization

Equations (4) and (10) provide vertical pattern information, if either R or $\overline{R}_c$ is known as a function of θ. However, if (15) is used as an approximation for $\overline{R}_c$, it is preferable to go directly to (1) for the vertical pattern of the beam. If the element excitation is restricted to the range $|\alpha| \leqq \pi/2$, each term of the integrand reduces to a Bessel function, when the integration is performed. The result is

$$\begin{aligned} \overline{E}(0, \theta) = {} & \frac{\delta}{2}\sin\theta \sum_{k=0}^{\infty} \epsilon_k j^{k-1} \overline{D}_k \left\{ J_k\left[\left(\frac{\delta_r}{2} + l\right)\sin\theta - \frac{\delta_r}{2}\sin\theta_0\right] \right. \\ & \left. - J_k\left[\left(\frac{\delta_r}{2} - l\right)\sin\theta - \frac{\delta_r}{2}\sin\theta_0\right]\right\}. \end{aligned} \tag{27}$$

It is to be emphasized that this is not a reliable approximation when the axial length of the reflecting cylinder is small, or when the diameter is small.

Acknowledgment

Grateful acknowledgment is made to the Watson Laboratories Air Materiel Command, Rome, New York, for their generous sponsorship of the research activity from which this paper was derived.

Radio-Wave Propagation at Oblique Incidence Including the Lorentz Polarization Term*

JOHN M. KELSO†

Summary—The application of the Lorentz theory of dispersion to some problems in the theory of the propagation of radio waves incident obliquely on a plane ionosphere is considered. The true height of reflection, ray path, reflection coefficient, range in the ionosphere, and group path in the ionosphere are studied without introducing the effect of the earth. For both a plane- and curved-earth geometry, the following quantities are determined: ground range, group path, reflection coefficient as a function of the ground range, and the maximum usable frequency.

The following restrictions apply to the material presented: (1) all limitations on the Chapman distribution hold; (2) the earth's magnetic field is neglected; (3) the angular operating frequency is assumed to be greater than the collisional frequency wherever appreciable absorption occurs; (4) the absorption per vacuum wavelength is assumed to be small; and (5) ray theory is used.

Introduction

A PREVIOUS PAPER[1] considered the effect of the Lorentz polarization term on the verticalrincidence absorption of a radio wave in a deviating ionosphere layer. The purpose of the present work is to extend this treatment to the case of waves incident obliquely on a plane ionosphere. The material in the present instance, as well as the vertical-incidence paper, is based on approximations given by Hacke.[2]

Hacke determined a double-parabola approximation to the well-known Chapman distribution[3] of electron density as a function of height, as well as a single-parabola approximation to the height variation of the product of electron density times the collision frequency. These approximations were used by Hacke to compute the true and group heights of reflection, as well as the reflection coefficient, at vertical incidence using the Sellmeyer theory of dispersion. Hacke and Kelso[4] later extended this treatment to the case of waves incident obliquely on a plane ionosphere, obtaining the true and apparent heights of reflection, the ray paths, the reflection coefficient, and the range in the ionosphere, all using the Sellmeyer theory of dispersion.

* Decimal classification: R112.624. Original manuscript received by the Institute, October 5, 1950; revised manuscript received, March 5, 1951.

† Ionosphere Research Laboratory, The Pennsylvania State College, State College, Pa.

[1] J. M. Kelso, "The effect of the Lorentz polarization term on the vertical incidence absorption in a deviating ionosphere layer," Proc. I.R.E., vol. 39, pp. 412–419; April, 1951.

[2] J. E. Hacke, Jr., "An approach to the approximate solution of the ionosphere absorption problem," Proc. I.R.E., vol. 36, pp. 724–728; June, 1948.

[3] S. Chapman, "The absorption and dissociative or ionizing effect of monochromatic radiation in an atmosphere on a rotating earth," *Proc. Phys. Soc.* (London), vol. 43, pp. 26–45; January, 1931.

[4] J. E. Hacke, Jr., and J. M. Kelso, "An approximate solution to the problem of path and absorption of a radio wave in a deviating ionosphere layer," Proc. I.R.E., vol. 36, pp. 1477–1482; December, 1948.

It is the purpose of this paper to consider the above quantities, using the Lorentz theory of dispersion. In addition, we consider analytically the ground range, the reflection coefficient as a function of ground range, and the group path assuming the earth to be first plane and then curved. The maximum-usable-frequency factor is studied graphically for both types of geometry of the earth.

A number of restrictions must be considered in the application of the material given here: (1) since the approximations are based on the Chapman distribution,[3] all of the limitations on the use of that distribution apply; (2) the earth's magnetic field is neglected; (3) the angular operating frequency is assumed to be very much greater than the collisional frequency where appreciable absorption takes place; (4) the absorption per vacuum wavelength is assumed to be small; and (5) ray theory is used. These restrictions should hold fairly well for the ordinary ray in quasi-transverse propagation via the E layer, for frequencies above about one megacycle.

Summary of Introductory Work

Chapman[3] showed that the electron density as a function of height in a Chapman region is given by

$$N = N_m Ch(x), \tag{1}$$

where

$$Ch(x) = \exp \tfrac{1}{2}(1 - x - \exp\{-x\})$$
$$x = (h - h_m)/H - l_n \sec x, \tag{2}$$

in which

N = the electron density
N_m = the maximum value of the electron density in the layer
H = the scale height of the atmosphere in the region where the ionization is produced
h_m = the height at which N is a maximum when $\chi = 0$
h = the height at which the ionization is being considered
χ = the sun's angular distance from the zenith.

Hacke[2] approximated (2) by two parabolas shown in Fig. 1: $P_1(x)$, used for the region contained between the level of maximum ionization and the height, $x_1 = -1.3170$, of the lower inflection point of (2); and $P_2(x)$, used for the region between this latter level and the level $x_2 = -2.7811$. The quantity x_2 is the value of x for which the second parabola, $P_2(x)$, becomes zero. Thus, x_2 defines the term "bottom of the layer" as used in the remaining parts of this work. The region $x_1<x<0$ where $P_1(x)$ is used is called the "upper region"; and the region $x_2<x<x_1$ where $P_2(x)$ is used is called the "lower region." The two approximations are

$$P_1(x) = 1 - \frac{x^2}{T^2}, \qquad x_1 < x < 0 \tag{3}$$

$$P_2(x) = A^2(x - x_2)^2, \qquad x_2 < x < x_1, \tag{4}$$

where $T=1.848$ and $A=0.4792$ are parameters adjusted to fit (2).

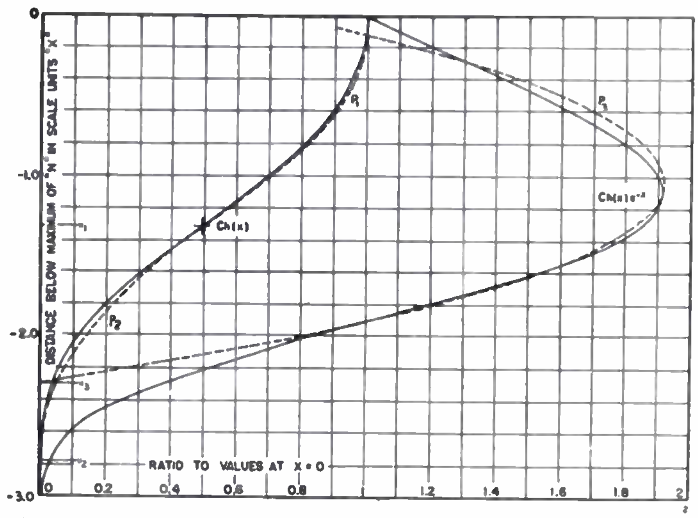

Fig. 1—Ratio of ion density and its product with collision frequency to the values at $x=0$ as functions of height in scale units below point of maximum ion density. Solid curves, Chapman distributions; dashed curves, parabolic approximations.

It is sometimes useful, when working in the lower region, to change from the co-ordinate x to the co-ordinate y, given by

$$y = x - x_2 = 2.7811 + x. \tag{5}$$

Making this substitution, we may rewrite (4) as

$$P_2(y) = A^2y^2, \qquad 0 < y < 1.4641, \tag{4a}$$

where $y_1=1.4641$, $y_2=0$. In the y co-ordinates, the subscripts are used for the same function as the corresponding subscripts in the x co-ordinate system.

The product $Ch(x)e^{-x}$ (proportional to the product of electron density times the collisional frequency, ν) is approximated by the parabola

$$P_3(x) = a_0 + a_1x + a_2x^2, \qquad x_3 < x < 0, \tag{6}$$

where $a_0=0.7055$, $a_1=-2.382$, and $a_2=-1.1696$ are parameters used in the curve fitting, and $x_3=-2.299$ is the negative root of $P_3(x)=0$. When the y co-ordinate system is used, this becomes

$$P_3(y) = b_0 + b_1y + b_2y^2,$$
$$y_3 = 0.4821 < y < 2.7811; \tag{6a}$$

with $b_0=-1.7162$, $b_1=4.1236$, and $b_2=-1.1696$.

For values of $x<x_3$, the parabola $P_3(x)$ is negative, and thus the product of electron density times collisional frequency is meaningless in our approximation for such values of x. Consequently, integrations of quantities containing $P_3(x)$ will have as a lower limit the value $x=x_3$, rather than $x=x_2$, the latter value representing the bottom of the layer. As a result of this, the theory will show some possible reflections for which the absorption is given as zero. This anomaly occurs, however, only for values of the frequency such that the angular frequency of the signal is no longer greater than the E-region collisional frequency, and hence, for which the present theory is not valid.

The ratios $N/N_m=Ch(x)$ and $N\nu/(N_m\nu_m)=Ch(x)e^{-x}$ (where ν_m is the value of the collisional frequency, ν, at the level $x=0$) are plotted as functions of x in Fig. 1. The parabolic approximations $P_1(x)$, $P_2(x)$, and $P_3(x)$ are indicated on the same figure as dashed curves.

When the Lorentz theory of dispersion is used and the previously noted restrictions are applied to the Appleton-Hartree dispersion equation,[5,6] the expression for the index of refraction is[1]

$$\mu^2 = \frac{1 - Ch(x)/R^2}{1 + \frac{1}{2}Ch(x)/R^2}, \tag{7}$$

and the absorption coefficient is given as

$$k = \frac{3}{2}\,\frac{K_mCh(x)e^{-x}}{\mu R^2[1 + \frac{1}{2}Ch(x)/R^2]^2}, \tag{8}$$

where

μ = the index of refraction
k = the absorption coefficient per unit path length
R = the ratio of the operating frequency to the vertical incidence critical frequency
$K_m=\nu_m/2c$.

Quantities Involving the Ionosphere Only

As a first step, we consider some quantities which depend only on the ionosphere, and not on the earth. In two later sections we will then introduce the geometry of the earth, first as a plane parallel to the ionosphere, and then as a sphere. The quantities which depend on the ionosphere only are the true height of reflection, ray path, reflection coefficient, group path, and the range, all in the ionosphere. Fig. 2 shows a diagram of the ray trajectory in the plane ionosphere, and serves to define the symbols used.

A. True Height of Reflection

As is well known, the condition for reflection at oblique incidence in a plane ionosphere is given by

$$\mu^2(x_0) = \sin^2\theta_0, \tag{9}$$

where $\mu(x_0)$ is the index of refraction at the point x_0, at which the wave is reflected and θ_0 is the angle of inci-

[5] E. V. Appleton, "Wireless studies of the ionosphere," *Jour. IEE* (London), vol. 71, pp. 642–650; October, 1932.
[6] D. R. Hartree, "The propagation of electromagnetic waves in a stratified medium," *Proc. Camb. Phil. Soc.*, vol. 25, pp. 97–120; January, 1929.

dence of the signal on the ionosphere. Writing μ^2 from (7) and approximating $Ch(x)$ by $P_1(x)$ and $P_2(x)$ in their appropriate regions, we get

$$x_0 = x_2 + \frac{R\cos\theta_0}{A}\sqrt{\frac{1}{1+\frac{1}{2}\sin^2\theta_0}}, \qquad x_2 < x_0 < x_1$$
$$x_0 = -T\sqrt{1-\frac{R^2\cos\theta_0}{1+\frac{1}{2}\sin^2\theta_0}}, \qquad x_1 < x_0 < 0. \tag{10}$$

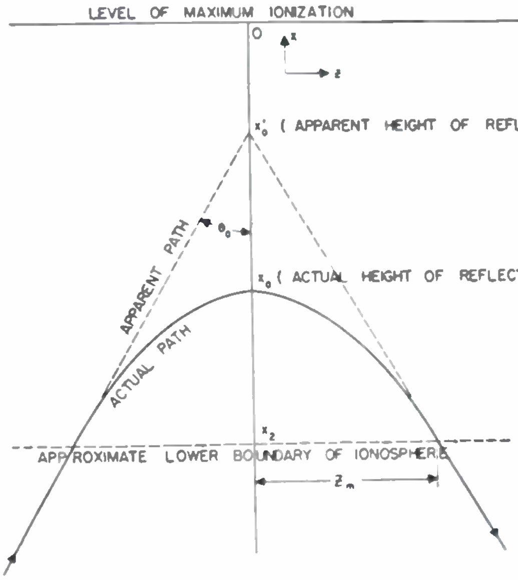

Fig. 2—Diagram illustrating ray path of radio wave through plane ionosphere.

Hacke and Kelso[4] have shown that the corresponding expressions obtained by use of the Sellmeyer dispersion theory are

$$x_0 = x_2 + \frac{R\cos\theta_0}{A}, \qquad x_2 < x_0 < x_1$$
$$x_0 = -T\sqrt{1-R^2\cos^2\theta_0}, \qquad x_1 < x_0 < 0.$$

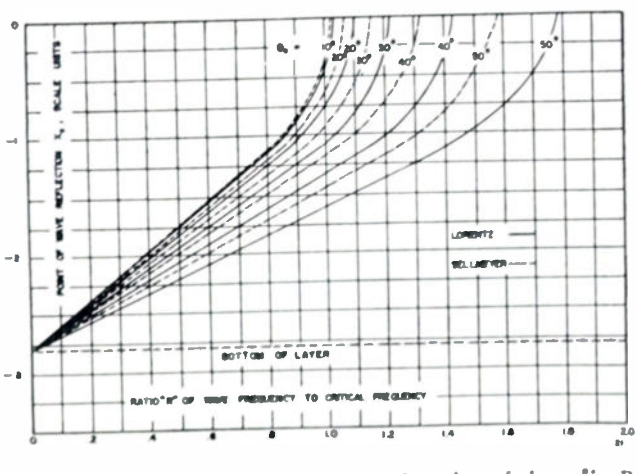

Fig. 3—True height of reflection x_0 as a function of the ratio R of wave frequency to vertical incidence critical frequency, with the angle of incidence θ_0 as a parameter.

In the Sellmeyer case, the quantity x_0 can be expressed as a function of the single variable, $R\cos\theta_0$. However, as can be seen from (10), in the Lorentz case we must give values to R and θ_0 separately. Thus, in Fig. 3 we plot x_0 for both the Lorentz and Sellmeyer theories as a function of R for the parametric values of the angle of incidence $\theta_0 = 10°, 20°, 30°, 40°, 50°$. In Fig. 4 we plot, for both theories, x_0 as a function of θ_0 with the values of the parameter $R = 1, 2, 3, 4, 5$. In both figures the Sellmeyer results are shown dotted.

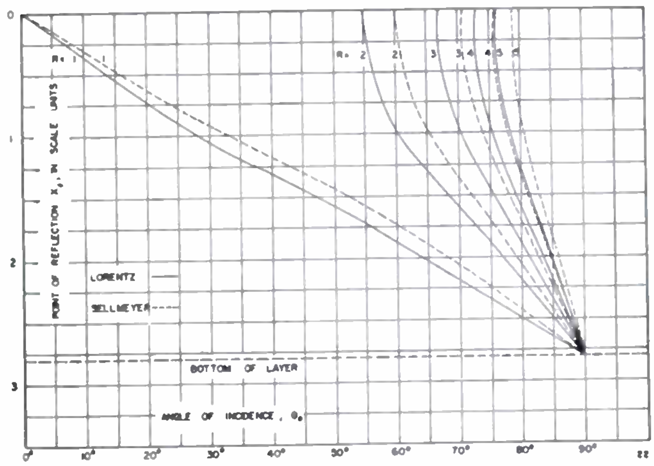

Fig. 4—True height of reflection x_0 as a function of the angle of incidence θ_0 with R as a parameter.

B. Ray Path

In this section we calculate the actual trajectory of the ray through the ionosphere. At a point P, the index of refraction is related by Snell's law to the angle that the ray makes with the vertical at P, θ, and to the angle of incidence on the ionosphere as

$$\frac{\sin\theta_0}{\sin\theta} = \mu. \tag{11}$$

From this equation,

$$\frac{dz}{dx} = \tan\theta = \frac{\sin\theta_0}{\sqrt{\mu^2-\sin^2\theta_0}}, \tag{12}$$

where dz is the horizontal displacement and dx is the vertical displacement, both in scale units. If we substitute for μ^2 from (7), we obtain

$$dz = \sin\theta_0 dx\sqrt{\frac{R^2+\frac{1}{2}Ch(x)}{R^2\cos^2\theta_0-(1+\frac{1}{2}\sin^2\theta_0)Ch(x)}}. \tag{13}$$

We again replace $Ch(x)$ by the parabolic approximations $P_1(x)$ and $P_2(x)$. We then must treat three cases:

(i) behavior in the upper region, $x_1<x<0$, when the ray penetrates to that region;

(ii) behavior in the lower region, $x_2<x<x_1$, when the ray is reflected in the upper region;

(iii) behavior in the lower region, $x_2<x<x_1$, when the ray is reflected in that region.

In Case (i), the approximation $P_1(x)$ is used in place of $Ch(x)$, and dz becomes

$$dz=\frac{\sin\theta_0 dx}{\sqrt{2+\sin^2\theta_0}}\sqrt{\frac{(T^2+2T^2R^2)-x^2}{\dfrac{T^2R^2\cos\theta_0-(1+\frac{1}{2}\sin^2\theta_0)}{(1+\frac{1}{2}\sin^2\theta_0)}+x^2}}.$$

Integrating from x_1 to x,

$$Z_1=\frac{T\sqrt{1+2R^2}\sin\theta_0}{k\sqrt{2+\sin^2\theta_0}}\left[F(\psi,k)-E(\psi,k)\right]_{\psi}^{\psi_1},$$

where $E(\psi, k)$ and $F(\psi, k)$ are elliptic integrals, and

$$k=a/\sqrt{a^2+b^2}$$

$$\psi=\cos^{-1}(x/a), \qquad \psi_{0,1}=\cos^{-1}(x_{0,1}/a)$$

$$a^2=T^2(1+2R^2)$$

$$b^2=\frac{T^2R^2\cos^2\theta_0-T^2(1+\frac{1}{2}\sin^2\theta_0)}{(1+\frac{1}{2}\sin^2\theta_0)}.$$

We now make the transformation given by

$$Z_1(x)=Z(x_0)-Z(x),$$

in order to place the origin of the horizontal co-ordinates directly below the point of reflection. Then

$$Z_1(x)=\frac{T\sqrt{1+2R^2}\sin\theta_0}{k\sqrt{2+\sin^2\theta_0}}\left[F(\psi,k)-E(\psi,k)\right]_{\psi}^{\psi_0}. \quad (14)$$

In Cases (ii) and (iii), where we wish to determine the paths in the lower region, $x_2<x<x_1$, we use the parabola $P_2(y)$ in place of $Ch(x)$, and obtain

$$dz=\frac{\sin\theta_0 dy}{\sqrt{2+\sin^2\theta_0}}\sqrt{\frac{2(R^2/A^2)+y^2}{\dfrac{R^2\cos^2\theta_0}{A^2(1+\frac{1}{2}\sin\theta_0)}-y^2}}.$$

Integrating from 0 to y,

$$Z=\frac{\sqrt{\alpha^2+\beta^2}\sin\theta_0}{\sqrt{2+\sin^2\theta_0}}\left[E(\phi,K)\right]_{\phi}^{\pi/2},$$

where

$$\phi=\cos^{-1}\left(\frac{x-x_2}{\beta}\right)$$

$$K=\sqrt{\beta^2/(\alpha^2+\beta^2)}$$

$$\alpha^2=2R^2/A^2$$

$$\beta^2=[(R^2/A^2)\cos^2\theta_0]/(1+\tfrac{1}{2}\sin^2\theta_0).$$

In Case (ii), when reflection occurs in the upper region, we transform to the co-ordinates $Z_2(y)$, defined by

$$Z_2(y)=Z(x_1)-Z(y),$$

and obtain

$$Z_2(y)=\frac{\sqrt{\alpha^2+\beta^2}\sin\theta_0}{\sqrt{2+\sin^2\theta_0}}\left[E(\phi,K)\right]_{\phi}^{\phi_1}+\frac{\sqrt{2}R\sin\theta_0}{Ak\sqrt{2+\sin^2\theta_0}}\left[F(\psi,k)-E(\psi,k)\right]_{\psi_0}^{\psi_1}, \quad (15)$$

where

$$\phi_{0,1}=\cos^{-1}\left(\frac{x_{0,1}-x_2}{\beta}\right).$$

In Case (iii), when reflection occurs in the lower region, we again wish to make the reflection point the origin of the horizontal co-ordinates. Making the transformation,

$$Z_3(y)=Z(y_0)-Z(y),$$

we get

$$Z_3(y)=\frac{\sqrt{\alpha^2+\beta^2}\sin\theta_0}{\sqrt{2+\sin^2\theta_0}}\left[E(\phi,K)\right]_{\phi}^{\phi_0}, \quad (16)$$

where α, β, K, and ϕ are defined above.

Fig. 5 shows two ray paths, both for $R=2.0$, one for $\theta_0=59°\ 9'\ 16''$ and the other for $\theta_0=73°\ 11'\ 0''$, which give reflection in the upper region at a height of 2.5 scale units from the bottom of the layer, and reflection in the lower region at 1.0 scale units from the bottom of the layer, respectively.

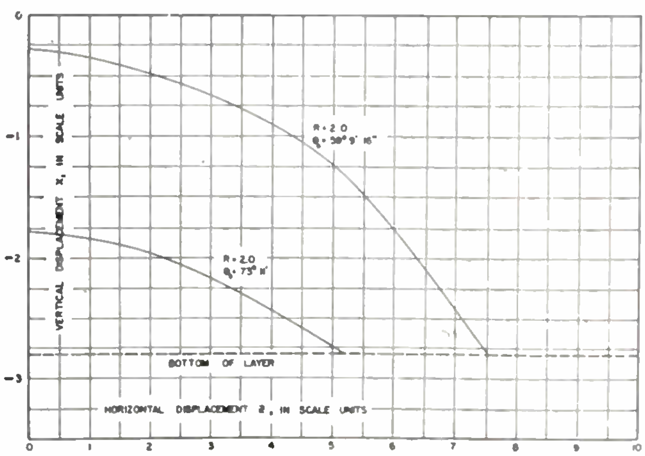

Fig. 5—Ray paths in a plane ionosphere with R and θ_0 as parameters. Lorentz theory of dispersion.

C. Reflection Coefficient

The reflection coefficient ρ gives the ratio of the reflected intensity to the incident intensity, and is defined by the equation

$$\rho=\exp\left(-2\int kds\right), \quad (17)$$

where ds is the differential of path length, k is the absorption coefficient defined in (8), and the integral is to be taken from the bottom of the layer to the reflection point. Now

$$ds = H\sqrt{dx^2 + dz^2},$$

and, using the expression for dz given with the discussion of ray paths, we obtain

$$ds = \frac{H\mu\, dx}{\sqrt{\mu^2 - \sin^2\theta_0}}.$$

Obtaining k from (8), the natural logarithm of the reflection coefficient, $\ln \rho$, becomes

$$\ln \rho = -12HK_mR^2 \int \frac{Ch(x)e^{-x}dx}{[2R^2 + Ch(x)]^2\sqrt{\mu^2 - \sin^2\theta_0}}. \tag{18}$$

Again we have three cases to consider. These are defined in the same manner as in the ray path calculations.

In Case (i), the wave is reflected in the upper region, and the quantity $Ch(x)$ is approximated by $P_1(x)$, while the quantity $Ch(x)e^{-x}$ is approximated by $P_3(x)$. Writing μ^2 from (7) and making these substitutions,

$$\ln \rho = \frac{\sqrt{72}\, HK_mR^2T^4}{\sqrt{1 + \frac{1}{2}\sin^2\theta_0}} \int_{x_1}^{x_0} \frac{(a_0 + a_1x + a_2x^2)dx}{\sqrt{\{T^2(2R^2+1) - x^2\}^2\left\{\dfrac{T^2R^2\cos^2\theta_0 - T^2(1 + \frac{1}{2}\sin^2\theta_0)}{1 + \frac{1}{2}\sin^2\theta_0} + x^2\right\}}}.$$

Then,

$$\begin{aligned}
\ln \rho_1 = {} & \frac{\sqrt{8}\, HK_mTa_0\sqrt{1 + \frac{1}{2}\sin^2\theta_0}}{\sqrt{2R^2 + 1}}\left[F(\psi, 1/k) - E(\psi, 1/k) - \frac{\sqrt{1 - 1/k^2\sin^2\psi}}{\tan\psi}\right]_{\psi_1}^{\psi_0} \\
& + \sqrt{8}\, HK_mT^2a_1\sqrt{1 + \tfrac{1}{2}\sin^2\theta_0}\left[\frac{1}{\tan\psi}\right]_{\psi_0}^{\psi_1} \\
& + \sqrt{8}\, HK_mT^3a_2\sqrt{(2R^2+1)(1 + \tfrac{1}{2}\sin^2\theta_0)}\left[\left\{1 - \frac{3R^2}{(2R^2+1)(1 + \frac{1}{2}\sin^2\theta_0)}\right\}F(\psi, 1/k)\right. \\
& \left. - E(\psi, 1/k) - \frac{\sqrt{1 - 1/k^2\sin^2\psi}}{\tan\psi}\right]_{\psi_1}^{\psi_0},
\end{aligned} \tag{19}$$

where

$$\psi = \sin^{-1}\left(k \sin\left[\cos^{-1}\frac{x}{\alpha}\right]\right)$$

$$k^2 = \alpha^2/(\alpha^2 + \beta^2)$$

$$\alpha^2 = T^2(2R^2 + 1)$$

$$\beta^2 = \{T^2R^2\cos^2\theta_0 - T^2(1 + \tfrac{1}{2}\sin^2\theta_0)\}/(1 + \tfrac{1}{2}\sin^2\theta_0).$$

In Case (ii) we consider the behavior of the wave in the lower region when reflection occurs in the upper region. We introduce the co-ordinate $y = 2.7811 + x$, and approximate $Ch(x)$ by $P_2(y)$, and $Ch(x)e^{-x}$ by $P_3(y)$. Then $\ln \rho_2$ becomes

$$\ln \rho_2 = -\sqrt{72}\, HK_mR^2 \int_{y_2}^{y_1} \frac{(b_0 + b_1y + b_2y^2)dy}{\sqrt{\{2R^2 + A^2y^2\}^2\{R^2\cos^2\theta_0 - (1 + \frac{1}{2}\sin^2\theta_0)A^2y^2\}}}.$$

Integrating, we get,

$$\ln \rho_2 = -\frac{HK_m}{A}\left[\frac{\sqrt{6}\, b_0}{R}E(\psi, k) + \frac{2b_1\cos\theta_0\cos\psi}{A} - \frac{\sqrt{24}\, b_2R}{A^2}(F(\psi, k) - E(\psi, k))\right]_{\psi_2}^{\psi_1}, \tag{20}$$

where

$$k = \frac{1}{\sqrt{3}}\cos\theta_0$$

$$\psi_{0,1,3} = \sin^{-1}\left[\frac{1}{k}\sin\left(\tan^{-1}\frac{Ay_{0,1,3}}{\sqrt{2}\, R}\right)\right].$$

When the reflection occurs in the upper region, the complete reflection coefficient is given by

$$\ln \rho = \ln \rho_1 + \ln \rho_2. \tag{21}$$

In Case (iii), where the reflection occurs in the lower region, we obtain the same result as in Case (ii), except that the integration is taken from y_3 to y_0 instead of from y_3 to y_1. Making this change in (20), $\ln \rho_3$ becomes

$$\ln \rho_3 = -\frac{HK_m}{A}\left[\frac{\sqrt{6}\, b_0}{R}E(\psi, k) + \frac{2b_1\cos\theta_0\cos\psi}{A} - \frac{\sqrt{24}\, Rb_2}{A^2}(F(\psi, k) - E(\psi, k))\right]_{\psi_3}^{\psi_0}. \tag{22}$$

In Fig. 6 (p. 92) the quantity $(-\ln \rho)/(HK_m)$ is plotted as a function of θ_0 for values of the parameter $R = 1, 2,$

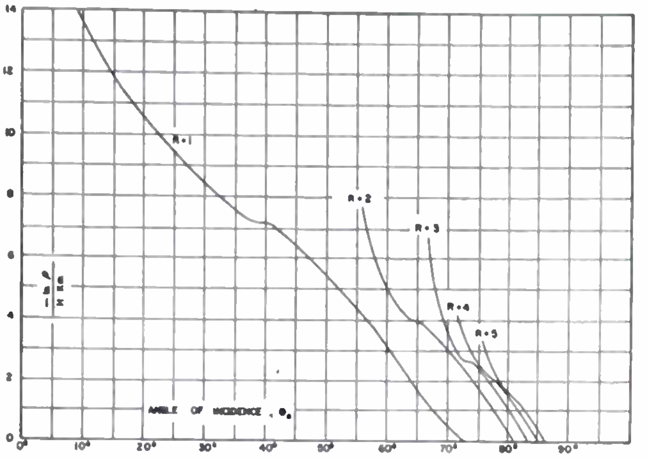

Fig. 6—$(-\ln \rho)/(HK_m)$ as a function of angle of incidence θ_0 with R as a parameter. Plane ionosphere; Lorentz theory of dispersion.

$$P_1 = \frac{2H}{\sqrt{2+\sin^2\theta_0}} \int_{x_1}^{x_0} \frac{[T^2(R^2-1)+x^2]dx}{\sqrt{\{T^2(2R^2+1)-x^2\}\left\{T^2\dfrac{(2R^2\cos^2\theta_0-2-\sin^2\theta_0)}{2+\sin^2\theta_0}+x^2\right\}}}.$$

3, 4, 5. The comparison of this result with the Sellmeyer result given by Hacke and Kelso[4] will be made when the effect of the earth has been included in the calculations by plotting $(-\ln \rho)/K_m$ as a function of the ground range for the two dispersion theories.

D. Group Path in the Ionosphere

In computing the group path at vertical incidence using the Lorentz theory,[1] it was noted that this could not be done in as simple a manner as in the Sellmeyer case. At oblique incidence, this difficulty is even more apparent, for the theorem of Breit and Tuve[7] does not apply when the Lorentz dispersion theory is used. Consequently, it is not sufficient to get the group path from the sides of the isosceles triangle formed by the extension of the path from the ground to the ionosphere. Furthermore, the relation $P' = \int ds/\mu$, used in the Sellmeyer theory, is a special case of the more general equations relating phase path P, and group path P',

$$P' = P + R(dP/dR) \tag{23}$$

$$P = \int \mu ds. \tag{24}$$

Substituting the Lorentz form of (24) into (23), we do not obtain the simplified form used for the Sellmeyer theory. Instead, it is necessary to determine the phase path P, and then to compute P' from (23).

In calculating the phase path, we consider, as usual, the three cases defined in the ray path calculations, and denote the values of P and P' by appropriate numerical subscripts.

In Case (i), we wish the phase path in the upper region when reflection occurs there. We approximate $Ch(x)$ by the parabola $P_1(x)$, and then P_1 becomes

Integrating,

$$\begin{aligned} P_1 = {} & \frac{-2HT(R^2-1)}{\sqrt{2+\sin^2\theta_0}\sqrt{2R^2+1}} [F(\phi, k)]_{\phi_1}^{\pi/2} \\ & - \frac{2HT\sqrt{2R^2+1}}{\sqrt{2+\sin^2\theta_0}} [E(\phi, k)]_{\phi_1}^{\pi/2}, \end{aligned} \tag{25}$$

where

$$\begin{aligned} k^2 &= 6R^2/(2R^2+1)(2+\sin^2\theta_0) \\ \phi_1 &= \sin^{-1}\sqrt{(b^2-x_1^2)/(b^2-c^2)} \\ b^2 &= T^2(2R^2+1) \\ c^2 &= -T^2(2R^2\cos^2\theta_0-2-\sin^2\theta_0)/(2+\sin^2\theta_0). \end{aligned} \tag{26}$$

We now differentiate (25) with respect to R, remembering that both ϕ_1 and k are functions of R, and substitute the results into (23). Then P_1' is given by

$$\begin{aligned} P_1' = {} & \frac{-2HT}{\sqrt{2+\sin^2\theta_0}\sqrt{2R^2+1}} \left\{(2R^2-1)[F(\phi, k)]_{\phi_1}^{\pi/2} + \left\{\frac{(8R^4+8R^2+2)+(R^2-1)/(1-R^2)}{(2R^2+1)}\right\} [E(\phi, k)]_{\phi_1}^{\pi/2} \right. \\ & - \left[\frac{2T^2R^2\left\{(x_1^2-c^2) - \dfrac{\cos^2\theta_0}{(2+\sin^2\theta_0)}(b^2-x_1^2)\right\}}{(b^2-c^2)\sqrt{b^2-x_1^2}\sqrt{x_1^2-c^2}}\right] \left(\frac{3R^2-(2R^2+1)k^2\sin^2\phi_1}{\sqrt{1-k^2\sin^2\phi_1}}\right) \\ & \left. - \frac{(1-R^2)k^2\sin\phi_1\cos\phi_1}{(2R^2+1)(1-k^2)\sqrt{1-k^2\sin^2\phi_1}}\right\}, \quad x_1 < x_0 < 0. \end{aligned} \tag{27}$$

In Case (ii) and (iii), we wish the phase path in the lower region, where $Ch(x)$ is to be replaced by the parabola $P_2(y)$. Then

[7] G. Breit, and M. Tuve, "A test of the existence of the conducting layers," *Phys. Rev.*, vol. 28, pp. 554–573; September, 1926.

$$P_{2,3} = \frac{\sqrt{2}H}{\sqrt{1+\frac{1}{2}\sin^2\theta_0}} \int_0^{y_{1,0}} \frac{(R^2/A^2 - y^2)dy}{\sqrt{\frac{2R^2}{A^2}+y^2}\sqrt{\frac{R^2/A^2\cos^2\theta_0}{1+\frac{1}{2}\sin^2\theta_0} - y^2}}.$$

Making several changes of variable, the above equation reduces to

$$P_{2,3} = \sqrt{\frac{2}{3}}\frac{HR}{A}\int_0^{\phi_{1,0}} \frac{d\phi}{\sqrt{1-k^2\sin^2\phi}} - \frac{2}{3}\sqrt{\frac{2}{3}}\frac{RH}{A}\cos^2\theta_0 \int_0^{\phi_{1,0}} \frac{\sin^2\phi d\phi}{(1-k^2\sin^2\phi)^{3/2}}, \quad (28)$$

where

$$k^2 = 1/3\cos^2\theta_0$$

$$\phi_{0,1} = \sin^{-1}\left(\frac{\sqrt{3}}{\cos\theta_0}\sin\left[\tan^{-1}\frac{Ay_{0,1}}{\sqrt{2}R}\right]\right). \quad (29)$$

The two integrals in (28) are standard elliptic integral combinations whose values are given in terms of elliptic integrals of the first and second kind in combination with ordinary trigonometric and algebraic functions. For the purpose of obtaining P' by use of (23), it is simpler to retain these in their integral form.

We now wish to evaluate P' using the relation in (23).

In Case (iii), which we discuss before Case (ii), ϕ_0 and k are functions of θ_0 only, so that the integrals are independent of R. Carrying out the differentiation, and using (23),

$$P_3' = 2\sqrt{\frac{2}{3}}\frac{RH}{A}F(\phi_0, k) - 4\sqrt{\frac{2}{3}}\frac{RH}{A}\frac{\cos^2\theta_0}{(3-\cos^2\theta_0)}\left[F(\phi_0, k) - \frac{F(\phi_0, k) - E(\phi_0, k)}{k^2} - \frac{\sin\phi_0\cos\phi_0}{\sqrt{1-k^2\sin^2\phi_0}}\right],$$

$$x_2 < x_0 < x_1. \quad (30)$$

In Case (ii), the quantity ϕ_1 is a function of R, and so the differentiation of (28) must include the derivative of ϕ_1 with respect to R. After considerable manipulation, we obtain P_2'.

where

$$\psi_1 = \tan^{-1}\frac{Ay_1}{\sqrt{2}R}$$

and k and ϕ_1 are defined in (29).

In order to obtain the complete group path when the wave is reflected in the upper region, we must add the results of (27) and (31).

Numerical results will be given for the group path when the geometry of the earth is considered in the following sections.

A simple comparison of these oblique-incidence results shows that the theorem of Breit and Tuve[7] does not apply here. (It is not meant to imply that anyone has suggested that this theorem should apply; the orginal derivation of the theorem was made on the basis of the Sellmeyer theory of dispersion and a plane ionosphere.)

Effect of a Plane Earth

We now consider the effect of the earth's geometry by first assuming the earth to be plane and parallel to the plane ionosphere used above. The ionosphere is taken to be a distance h_0 above the earth. The quantity h_0 is measured in kilometers, and is called "the height of the bottom of the layer."

A. Ground Range

The ground range is obtained by letting $y = y_2$ in the expressions for the ray path in (15) and (16). Twice this quantity, then, gives the range in the ionosphere. To this quantity we add the range along the ground corresponding to the portion of the path from the ground to the ionosphere, i.e., we add $2h_0\tan\theta_0$. Thus, the range D is given by

$$D = \frac{2H\sqrt{\alpha^2+\beta^2}\sin\theta_0}{\sqrt{2+\sin^2\theta_0}}\left[E(\phi, k)\right]_{\phi_2}^{\phi_1} + \frac{2\sqrt{2}HR\sin\theta_0}{Ak\sqrt{2+\sin^2\theta_0}}\left[F(\psi, k) - E(\psi, k)\right]_{\psi_0}^{\psi_1}$$

$$P_2' = \sqrt{\frac{2}{3}}\frac{RH}{A}\left[2F(\phi, k) - \frac{4\cos^2\theta_0}{(3-\cos^2\theta_0)}\left\{F(\phi, k) - \frac{F(\phi_1, k) - E(\phi_1, k)}{k^2} - \frac{\sin\phi_1\cos\phi_1}{\sqrt{1-k^2\sin^2\phi_1}}\right\} - \frac{\sqrt{3}\cos\psi_1\tan\psi_1}{\cos\theta_0[1+\tan^2\psi_1]\sqrt{1-\frac{3}{\cos^2\theta_0}\sin\psi_1}}\left\{\frac{1}{\sqrt{1-k^2\sin^2\phi_1}} - \frac{2}{3}\frac{\cos^2\theta_0\sin^2\phi_1}{(1-k^2\sin^2\phi_1)^{3/2}}\right\}\right],$$

$$x_2 < x < x_1 < x_0 < 0, \quad (31)$$

$$+ 2h_0 \tan\theta_0, \quad x_1 < x_0 < 0;$$

$$D = \frac{2H\sqrt{\alpha^2+\beta^2}\sin\theta_0}{\sqrt{2+\sin^2\theta_0}}\left[E(\phi, K)\right]_{\phi_2}^{\phi_0} \tag{32}$$

$$+ 2h_0 \tan\theta_0, \quad x_2 < x_0 < x_1,$$

where α, β, K, k, ψ, and ϕ have been defined in the section on ray paths.

The ground range D in kilometers is plotted as a function of the angle of incidence θ_0 in Fig. 7 for $R=1, 2, 3, 4, 5$. In this, and all of the succeeding calculations, it is assumed that the scale height H is 10 km, and that the height of the bottom of the layer h_0 has the value 90 km. These are reasonable values for the E layer under "normal" conditions.

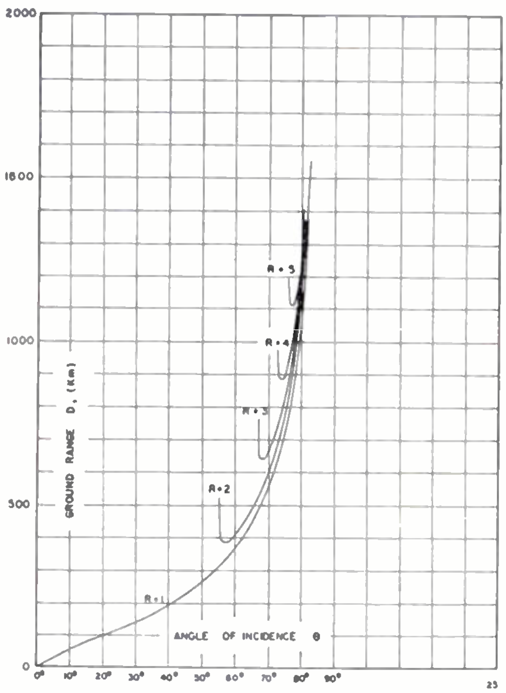

Fig. 7—Ground range D as a function of the angle of incidence θ_0 with R as a parameter. Lorentz theory of dispersion; plane-ionosphere and plane-earth geometry. $H=10$ km, $h_0=90$ km.

In a similar manner, the ground range has been obtained from the range in the ionosphere as given by Hacke and Kelso[4] for the Sellmeyer theory. Fig. 8 shows curves for this case corresponding to those for the Lorentz case in Fig. 7.

B. Group Path

The group path in the ionosphere itself has been given in (27), (30), and (31). To this we must add twice the distance from the transmitter to the point of incidence on the layer, given by 2 $h_0/\cos\theta_0$. For the Sellmeyer dispersion theory, the theorem of Breit and Tuve[7] gives $P'=D/\sin\theta_0$. A curve of P' versus R for the Lorentz theory and for a ground range of 1,500 km is given in Fig. 9, along with a dotted curve for the same case using the Sellmeyer theory of dispersion.

The Lorentz curve is not as complete as the Sellmeyer curve, in that the upper part of the curve is very short. This does not mean that the curve does not go off to infinity at the critical frequency as in the Sellmeyer case, but rather that it was not possible to perform the numerical calculations in this region. When the reflection height approaches the level of maximum ionization, it becomes necessary to evaluate the elliptic integral $F(\phi, k)$ for $\phi=90°$ and $\sin^{-1} k$ between 89° and 90°.

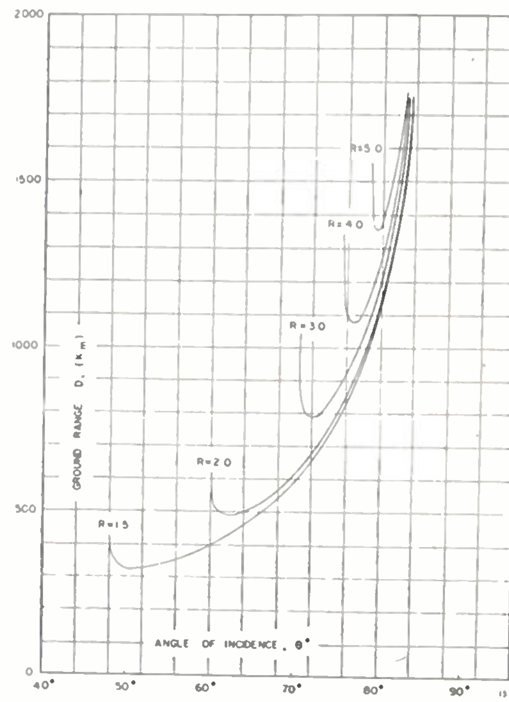

Fig. 8—Ground range D as a function of the angle of incidence θ_0. Sellmeyer theory of dispersion; plane-earth and plane-ionosphere. $H=10$ km, $h_0=90$ km.

The best table of elliptic integrals available for this work[8] does not permit the evaluation of such values, for it would be necessary to interpolate between 5.43490 and infinity. This loss of a portion of the curve is not sufficiently serious to warrant a special effort to evaluate the elliptic integral beyond this interval since the

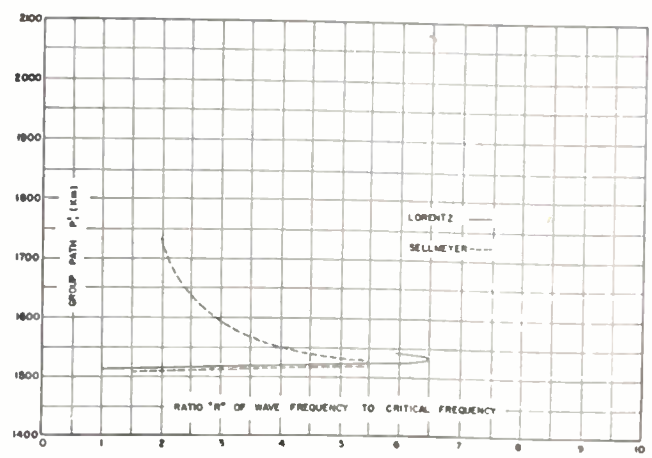

Fig. 9—Group path P' as a function of the ratio R of wave frequency to vertical-incidence critical frequency for a ground range of 1,500 km. $H=10$ km, $h_0=90$ km.

[8] L. Potin, "Tormules et Tables Numeriques," Gauthier-Villars et Cie. Paris, France; 1925.

attenuation is very high for such waves and this part of the curve is not ordinarily observed experimentally.

C. Reflection Coefficient as a Function of Ground Range

If we assume that the scale height H has the value 10 km and that the height of the bottom of the layer h_0 has the value 90 km, we may use the curves of ground range as a function of the angle of incidence in Fig. 7, and the curves of $(-\ln \rho)/(HK_m)$ as a function of the angle of incidence in Fig. 6 to plot in Fig. 10 the quantity $(-\ln \rho)/K_m$ as a function of ground range for

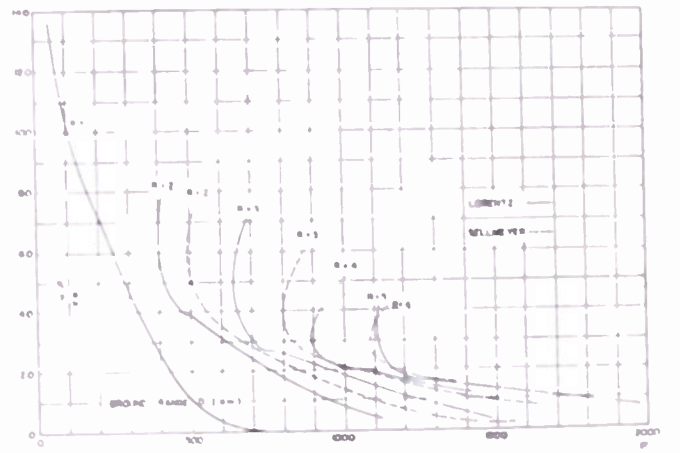

Fig. 10—$(-\ln \rho)/(K_m)$ as a function of ground range D with R as a parameter. Plane-ionosphere, plane-earth. $H = 10$ km, $h_0 = 90$ km.

$R = 1, 2, 3, 4, 5$. Corresponding curves for the Sellmeyer theory are shown dotted. These latter curves were obtained from Fig. 8, and from the curve[4] of $(-R \ln \rho)$ (HTK_m) as a function of $R \cos \theta_0$ in Fig. 11.

One must be quite careful in attempting to make comparisons on the basis of Fig. 10. It should be noted that the scale height and height of the bottom of the layer have the same values for the two theories. In using the ordinary[9] method for the determination of these two quantities, the same experimental results would lead to different calculated values for H and h_0 according to which dispersion theory was used for the calculations. Thus, using Fig. 10 for a comparison of the Lorentz versus the Sellmeyer theory of dispersion would be equivalent to assuming that h_0 and H had been determined by some means independent of the two dispersion theories.

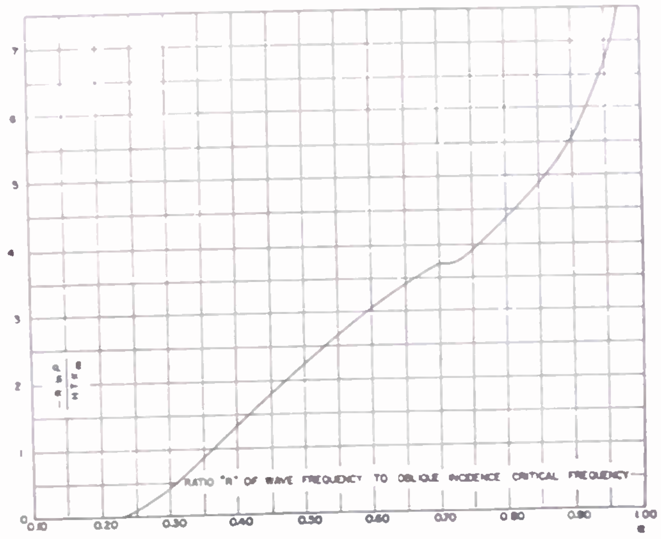

Fig. 11—Absorption as a function of $R \cos \theta_0$. The quantity is $(-R \ln \rho)/(HTK_m)$. Sellmeyer theory of dispersion.

[9] E. V. Appleton and W. J. G. Beynon, "The application of ionospheric data to radio-communication problems: Part 1," *Proc. Phys. Soc.* (London), vol. 52, pp. 518–533; July, 1940.

D. Maximum Usable Frequency

Observing the curves of range as a function of the angle of incidence in Figs. 7 and 8, it is seen that, for each value of $R > 1$, there is some range D_s, such that for $D < D_s$ there is no angle of incidence for which the signal has the range D. This value D_s is called the "skip distance" for a given R. Conversely, the value of R, written R_{mut}, is called the "maximum-usable-frequency" factor for the given range. The maximum usable frequency $f_{mut} = R_{mut}$ times the vertical incidence critical frequency is the greatest frequency that can be used for transmission over the given range.

Appleton and Beynon[9] determined the position of this minimum for the single-parabola approximation and the Sellmeyer theory of dispersion by differentiating the expression for range with respect to the angle of incidence. Beynon[10] extended this to the inclusion of the Lorentz polarization term, but still with the single-parabola approximation. When this procedure is applied to the double-parabola approximation with the Sellmeyer dispersion theory, one obtains for the angle of incidence at which this minimum occurs

$$\Theta_{mut} = \cos^{-1} \sqrt{\frac{W' + 2h_0}{W' - P}},$$

where

$$W' = Q + 2HT^2R'^2 x_1/\sqrt{x_1^2 - x_0^2}$$

$$P' = \frac{2R'H}{A} \sin^{-1}\left[\frac{A(x_1 - x_2)}{R'}\right] - 2HR'T \ln \left\{\frac{x_0}{x_1 + \sqrt{x_1^2 - x_0^2}}\right\}$$

$$Q = 2H(x_1 - x_2)/\sqrt{1 - A^2(x_1 - x_2)^2/R'^2}$$

$$R' = R \cos \theta_0.$$

A glance at the expression for the ground range using the Lorentz theory of dispersion in (32) shows that this method of solution would be extremely complicated in the present case, if, indeed, it would be possible at all. Consequently, the information given here for the R_{mut} as a function of range has been obtained graphically from the range versus angle of incidence curves in Fig. 7.

The quantity R_{mut} is plotted as a function of the ground range in Fig. 12. On this figure, the notation used is: *PI-PE* indicates plane ionosphere and plane earth; *PI-CE* indicates plane ionosphere and curved

[10] W. J. G. Beynon, "Oblique radio transmission in the ionosphere and the Lorentz polarization term," *Proc. Phys. Soc.* (London), vol. 59, pp. 97–107; January, 1947.

earth. The corresponding Sellmeyer results are shown dotted. It is seen that the differences between the two dispersion theories become quite appreciable at long ranges, and Beynon[10] has reported that measurements of the maximum usable frequency at a range of 700 km have confirmed the applicability of the Sellmeyer theory of dispersion on the basis of the single-parabola approximation.

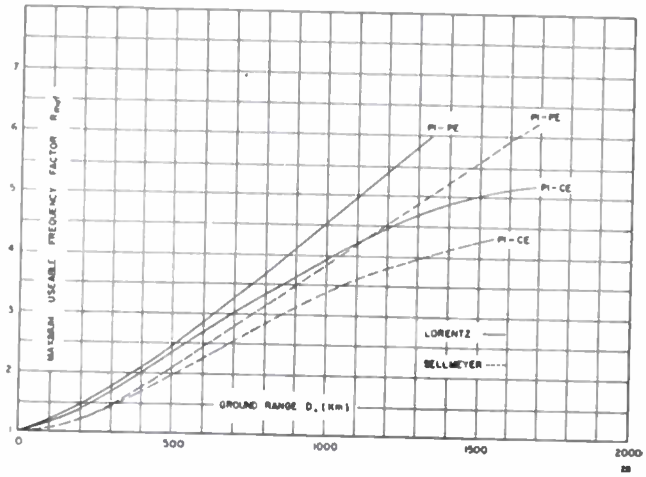

Fig. 12—Maximum-usable-frequency factor R_{muf} as a function of the ground range D. For plane-ionosphere and plane- and curved-earth geometries. $H = 10$ km, $h_0 = 90$ km.

Effect of a Curved Earth

We now repeat the work of the previous section, but assume that the earth is spherical and such that the ionosphere is at the same height h_0, as in the previous section; however the height is to be measured as a radial distance along a line from the center of the earth to the point of wave reflection. The geometry used is shown in Fig. 13.

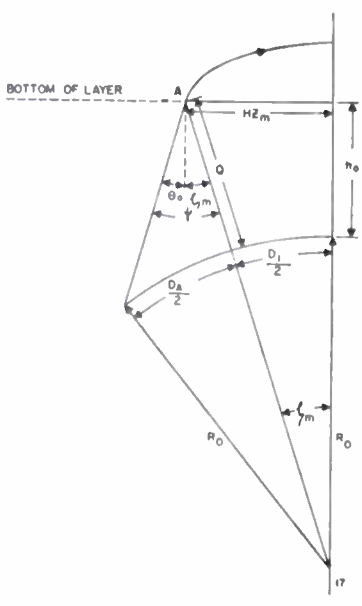

Fig. 13—Diagram showing ray trajectory of a plane-ionosphere and curved-earth geometry.

A. Ground Range

In Fig. 13, HZ_m is the half range in the ionosphere, and is obtained from (15) and (16) by letting $y=0$. ζ_m is the angle intercepted at the center of the earth by radial lines to the point of incidence and to the reflection point. If R_0 is the radius of the earth and h_0 the distance from the ground to the ionosphere immediately below the reflection point, then $\zeta_m = \tan^{-1}[HZ_m/(R_0+h_0)]$. If $\frac{1}{2}D_I$ is the range along the curved earth corresponding to HZ_m, then $\frac{1}{2}D_I = R_0\zeta_m$, where ζ_m is in radians. From the figure, it is seen that the angle $\psi = \theta_0 + \zeta_m$, and Q is

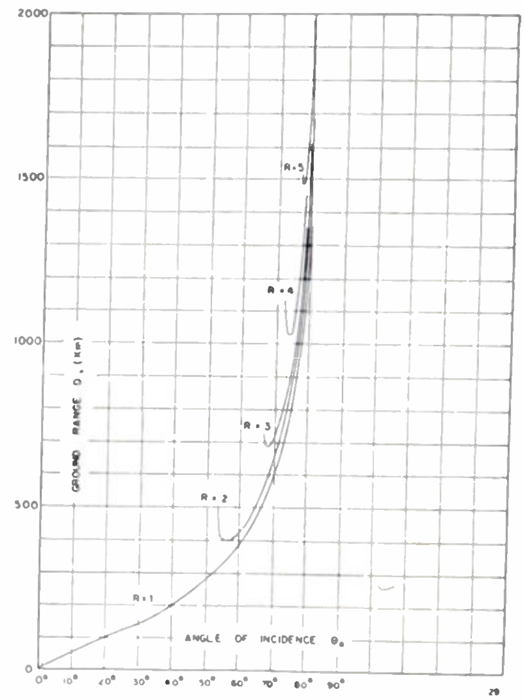

Fig. 14.—Ground range D, as a function of the angle of incidence θ_0 with R as a parameter. Lorentz theory of dispersion; plane-ionosphere and curved-earth geometry. $H = 10$ km, $h_0 = 90$ km.

the radial distance from the point of incidence to the ground. Smith[11] has shown that the ground range corresponding to the part of the path from the ground to the ionosphere can be approximated by

$$\tfrac{1}{2}D_A = R_0 \cot\psi - R_0\sqrt{\cot^2\psi - 2Q/R_0}. \qquad (34)$$

Now $OA = HZ_m/\sin\zeta_m$, and $Q = OA - R_0$, so that all the quantities in the expression for $\frac{1}{2}D_A$ have been determined. The total ground range of the signal is then given by

$$D = D_I + D_A. \qquad (35)$$

The quantity D is plotted as a function of θ_0, for $R=1, 2, 3, 4, 5$ in Fig. 14, assuming $h_0 = 90$ km and $H = 10$ km. The corresponding result for the Sellmeyer theory of dispersion is shown in Fig. 15 (following page).

B. Group Path

If the theorem of Breit and Tuve[7] applied in the present case, the group path would be given by the length of the sides of an isosceles triangle formed by the transmitter, the apparent point of reflection, and

[11] N. Smith, "The relation of radio sky-wave transmission to ionosphere measurements," Proc. I.R.E., vol. 27, pp. 332–348; May, 1939.

the receiver. Simple geometry gives this quantity as

$$2R_0 \sin(\tfrac{1}{2}D/R_0)/\sin\theta_0.$$

From this result, we subtract the length of this path in the ionosphere itself, and add the group path in the ionosphere as given by (27), (30), and (31).

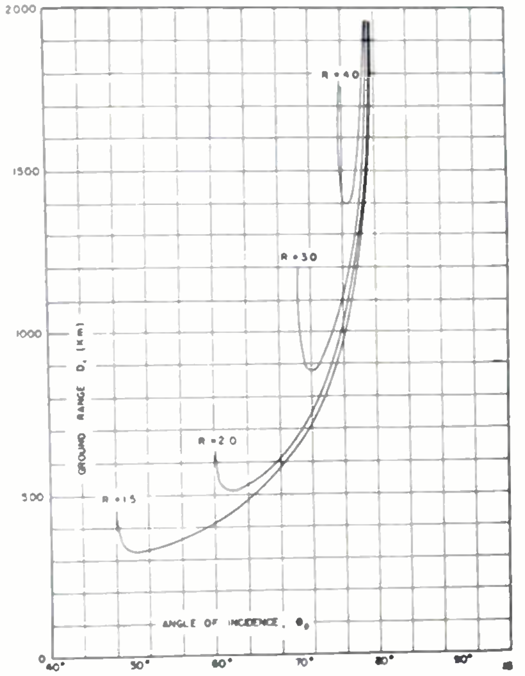

Fig. 15—Ground range D as a function of angle of incidence θ_0 with R as a parameter. For the Sellmeyer theory of dispersion, and plane-ionosphere and curved-earth geometry. $H=10$ km and $h_0=90$ km.

Using the procedure outlined above, a curve of P' as a function of R is plotted in Fig. 16 for a range of 1,500 km. The corresponding curve for the Sellmeyer theory is shown dotted.

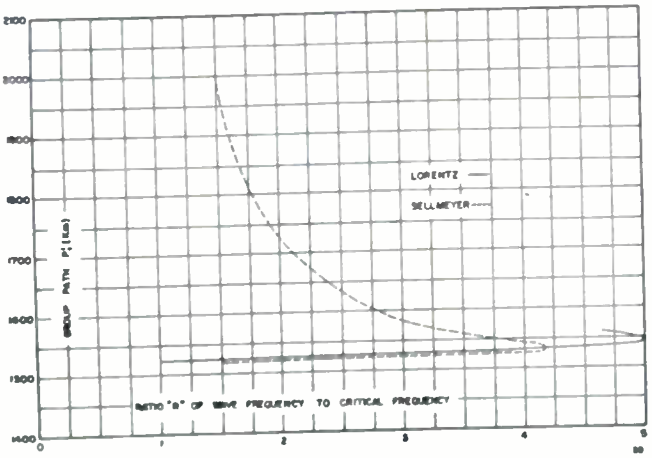

Fig. 16—Group path P' as a function of the ratio R of wave frequency to vertical incidence critical frequency, for a ground range, $D=1{,}500$ km. Plane-ionosphere, curved-earth. $H=10$ km, $h_0=90$ km.

C. *Reflection Coefficient as a Function of Ground Range*

Using the range versus angle of incidence curves in Fig. 14 and the curves of $(-\ln\rho)/(HK_m)$ from Fig. 6, we obtain the curves in Fig. 17 giving $(-\ln\rho)/K_m$ as a function of the ground range for $R=1, 2, 3, 4, 5$, for a curved earth and plane-ionosphere geometry and the Lorentz theory of dispersion. The corresponding curves for the Sellmeyer theory are shown dotted. In both cases $H=10$ km and $h_0=90$ km, so that the remarks made in the plane earth case regarding the comparisons of the results for the two dispersion theories apply here equally well.

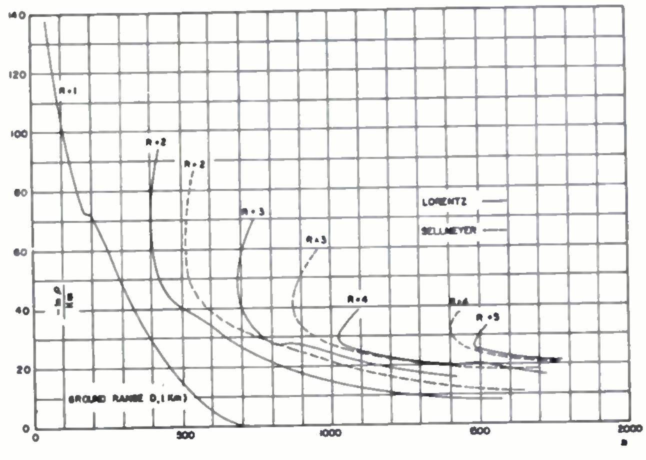

Fig. 17—$(-\ln\rho)/(K_m)$ as a function of ground range D with R as a parameter. Plane-ionosphere, curved-earth. $H=10$ km, $h_0=90$ km.

D. *Maximum Usable Frequency*

In this case, the same objections as in the plane ionosphere case are raised against an attempt to obtain an analytic solution for the maximum usable frequency. Thus, for both the Lorentz and Sellmeyer theories of dispersion, the results for R_{muf} versus range are obtained from the range versus angle of incidence curves in the manner discussed previously. These results are shown in Fig. 12 along with the plane earth curves.

Conclusions

The application of the Lorentz theory of dispersion to some problems in the theory of the propagation of radio waves incident obliquely on a plane ionosphere has been considered. The true height of reflection, ray paths, reflection coefficient, range in the ionosphere, and group path in the ionosphere are considered without including the earth. For both a plane and a curved earth the following quantities are studied; ground range, group path, reflection coefficient as a function of ground range, and maximum usable frequency. All of this work is done under the restrictions noted in the introduction.

Acknowledgments

The authors wishes to thank A. H. Waynick of The Pennsylvania State College, under whose supervision and direction this work was performed.

The material is taken (in a slightly altered form) from a dissertation submitted in partial fulfillment of requirements for a Ph.D. in physics at The Pennsylvania State College.

This work has been supported in part by Contract No. AF19(122)-44 with the U. S. Air Force, through sponsorship of the Geophysical Research Directorate, Air Materiel Command.

Contributors to Proceedings of the I.R.E.

Albert A. Auerbach (A'48) was born on November 19, 1918, in New York, N. Y. He received the B.A. degree in chemistry in 1939 and the M.A. degree in physics in 1941, both from Temple University. The following year, he taught mathematics at the same school.

A. A. AUERBACH

During World War II Mr. Auerbach was a Project Officer for the Army Air Force's Board. He worked primarily with large ground radar early warning installations. In 1946 he was discharged with the rank of Captain.

From 1946 through 1947 he was employed in the advanced development section of RCA, and was engaged in the design of transmitting equipment, in particular, the Teleran transmitter.

In 1947 he joined the staff of the Eckert-Mauchly Computer Corp., and worked until April, 1951 on the design development and test of arithmetic equipment associated with the Binac, Univac, and other devices.

He received the degree of M.S. in electrical engineering at the Moore School, University of Pennsylvania, in 1950.

For a short time Mr. Auerbach was associated with Remington Rand, Inc., where he worked on the development of devices in the business-machine field. He has recently rejoined the staff of the Eckert-Mauchly Computer Corp.

❖

W. R. G. Baker is vice-president of the General Electric Company, Electronics Park, Syracuse, N. Y. and a leader in the development of radio and television. A graduate of Union College with three degress, Dr. Baker joined General Electric's Research Laboratory in 1917.

W. R. G. BAKER

His first work on radio included the development and testing of radio apparatus for aircraft, submarines, captive balloons, torpedo boats, destroyers, and battleships. Dr. Baker was later made designing engineer.

In 1942 this responsibility was enlarged to include the design of all radio products, and in 1926, he was given complete charge of development, design, and production. He supervised the design of pioneer broadcasting stations WGY in Schenectady, KOA in Denver, and KGO in Oakland, and the Schenectady radio developmental laboratory. The latter aided in maintaining communications with both Byrd Antarctic expeditions.

On the formation of the RCA-Victor Corporation in 1929, Dr. Baker went to Camden, N. J. to head the radio-engineering activities of the new organization. He was in charge of production and later vice-president of engineering and manufacturing.

In 1935 General Electric resumed its radio-receiver activities at Bridgeport, Conn., and Dr. Baker renewed his connections with the company. He was named managing engineer in 1936, a post he held until May, 1939, when he was promoted to the position of manager of the company's radio and television department.

In October, 1941, Dr. Baker was elected a vice-president. His department was subsequently redesignated the Electronics Department, now one of the nine GE operating departments and producer of radio, radar, television, and similar equipment in the rapidly expanding electronics industry.

The present Electronics Park of the General Electric Company of Syracuse, N. Y. is one of the largest centers of activity in this field. It is the realization of an ambition which Dr. Baker has long carried in his mind. For this the nation is indebted to him.

Under Dr. Baker's direction as chairman of the National Television System Committee, the standards for monochrome telecasting were developed, recommended, and adopted by the FCC. As Director of Engineering for the Radio-Television Manufacturers Association, he is actively engaged in co-ordinating the work of the industry on color television. He is also chairman of NTSC, which has been expanded to develop standards for color television.

Under his supervision as chairman of the Radio Technical Planning Board, recommendations for frequency allocations of all broadcasting services were formulated.

Dr. Baker became a Member of the Institute in 1919 and a Fellow in 1928. He was president in 1947, a director in 1940 and 1946-1951, and treasurer in 1951. Dr. Baker was Standards Co-ordinator during 1948–1950.

❖

Domenick Barbiere was born in Brooklyn, N. Y., on August 10, 1924. He received the A.B. and M.S. degrees in 1945 and 1948, respectively, both in physics, from New York University. During the summers of 1947 and 1948 he was engaged in theoretical research on gas discharges at the Westinghouse Research Laboratories, in Pittsburgh, Pa.

D. BARBIERE

From December, 1948 to August, 1950, Mr. Barbiere was employed by the Glenn L. Martin Co., Baltimore, Md., for design and development work in the fields of servomechanisms and antennas. Since August, 1950, he has been engaged in electronic research and design at the Radiation Laboratory of Johns Hopkins University, Baltimore, Md. He is a member of Sigma Xi and the American Physical Society.

Cullen M. Crain (S'42–M'49) was born at Goodnight, Texas, in 1920. He received the B.S. degree in electrical engineering from the University of Texas in 1942. After a year with the Philco Radio and Television Corporation in Philadelphia, Pa., he returned to the University of Texas as an instructor in the electrical engineering department.

C. M. CRAIN

From 1944 to 1946 Mr. Crain was on active duty in the United States Naval Reserve, attached to the Bureau of Ordnance, where he worked in the mine program, and to the office of Research and Inventions, where he worked on the development of radar bombing trainers.

Since 1946 Mr. Crain has been associated with the University of Texas, where he received the M.S. degree in electrical engineering in 1947. He is at present an assistant professor in the electrical engineering department, and a radio engineer with the electrical engineering research laboratory.

Mr. Crain is a member of Tau Beta Pi, Eta Kappa Nu, and Sigma Xi.

❖

J. P. Eckert, Jr. (S'41–A'47) was born on April 9, 1919, in Philadelphia, Pa. In 1937 he entered the Moore School of Electrical Engineering of the University of Pennsylvania. He received the B.S. degree in electrical engineering in 1941, and the following year taught engineering, science, and management defense training at the Moore School.

J. P. ECKERT, JR.

In June, 1943 Mr. Eckert received the M.S. degree in electrical engineering from the Moore School, after which time he became chief engineer for the ENIAC project. In 1945 Mr. Eckert was concerned with the design and construction of the EDVAC, the successor to the ENIAC. In the summer of 1946 he taught a course on electronic computing devices at the Moore School.

The following fall Mr. Eckert and Dr. John W. Mauchly formed a partnership, known as the Electronic Control Co., for the purpose of designing and building large-scale, all-electronic, high-speed digital computing devices. This partnership was incorporated in December, 1947 as the Eckert-Mauchly Computer Corp. As chief engineer, Mr. Eckert was responsible for the design and construction of the Binac, an all-electronic computer, and the Univac, a large-scale electronic digital computer designed to handle both numeric and alpha-

Contributors to Proceedings of the I.R.E.

betic data. He now holds the position of vice president and director of engineering.

On October 19, 1949, Mr. Eckert and Dr. Mauchly were awarded the Howard N. Potts Medal by the Franklin Institute.

❖

Eduard A. Gerber (A'50) was born in Fuerth, Bavaria, Germany, on April 3, 1907. He received the Dipl. Phys. degree in 1930, and the Dr. Ing. degree in 1934, both from the Munich Technical University. In 1935 he joined the scientific staff of the Carl Zeiss Works, Jena, Germany, and was in charge of the research and development work on piezoelectric crystals. Before he arrived in this country, he was one of the co-authors of the volumes on "Physics of Solids," of the *FIAT Review* of German Science, published by the Military Government for Germany.

E. A. Gerber

Dr. Gerber is now a consultant of the Signal Corps Engineering Laboratories, Fort Monmouth, N. J. He is a member of the IRE Committee on Piezoelectric Crystals.

❖

J. R. Gerhardt was born in Omaha, Neb., on April 29, 1918. He received the B.S. in engineering science in 1940 from the Illinois Institute of Technology. Entering the Air Force in 1941, he was graduated from the New York University meteorology course for weather officers in 1943. Following a period of special training in radio and radar propagation, he was engaged for several years on special Air Force projects involving the forecasting and analysis of the meteorological parameters affecting radar propagation. Assignments were with the Radiation Laboratory, MIT, the AAF Board at Orlando, Fla., and with the OCSiGO on their radio relay projects in California and Florida.

J. R. Gerhardt

Since 1946, Mr. Gerhardt has been associated with the electrical engineering research laboratory of the University of Texas, formerly as chief meteorologist and currently as assistant director. This laboratory is engaged in research in the field of radio wave propagation and micrometeorology. He is a member of Phi Lambda Upsilon, Sigma Xi, The American Meteorological Society, The American Geophysical Union, and the New York Academy of Sciences.

Harry J. Gray, Jr., (S'45–A'46) was born in St. Louis, Mo., on June 24, 1924. He entered Lehigh University in 1941, and after two years was ordered to the University of Pennsylvania under the Navy V-12 program, where he received the degree of B.S. in electrical engineering in 1944. After commissioning as an ensign, he studied Navy radio and radar at Bowdoin College and the Massachusetts Institute of Technology, later serving in the Pacific until 1946. He received the M.S. degree in 1947 from the University of Pennsylvania, where he has been engaged since 1947 in teaching electromagnetic field theory, further work on digital computers, and graduate study in electrical engineering.

H. J. Gray, Jr.

Mr. Gray is a member of Tau Beta Pi, Eta Kappa Nu, and is an associate of Sigma Xi.

❖

Roger F. Harrington was born in Buffalo, New York, on December 24, 1925. He received the B.E.E. degree in 1948, and the M.E.E. in 1950, both from Syracuse University.

From 1945 to 1946 he served as an instructor at the Naval Radio Material School, at Dearborne, Michigan. From 1948 to 1950 Mr. Harrington was employed as an instructor and research assistant at Syracuse University. While at Syracuse, he worked under contract with the Watson Laboratories, AAF, investigating the properties of radio direction finding systems.

R. F. Harrington

At present, Mr. Harrington is serving as a research fellow in the electrical engineering department at Ohio State University, Columbus, Ohio, while studying for his Ph.D. degree.

Mr. Harrington is a member of Tau Beta Pi, and the Society of Sigma Xi.

❖

M. E. Hines (S'46–A'47–M'50) was born on November 30, 1918, in Bellingham, Wash. He attended the California Institute of Technology, where he received the B.S. degree in applied physics in 1940 and where, as a member of the Air Force Weather Service, he received the B.S. degree in meteorology in 1941. After World War II he returned to the Institute and received the M.S. degree in electrical engineering in 1946.

At the California Institute of Technology Mr. Hines worked on the determination of the dielectric constants of gases at microwave frequencies. Since 1946 he has been engaged in the development of traveling-wave tubes and close-spaced triodes for use as microwave amplifiers at the Bell Telephone Laboratories in Murray Hill, N. J.

M. E. Hines

Mr. Hines is a member of the IRE subcommittee on small high-vacuum tubes and the task group on traveling-wave tubes.

❖

Craig C. Johnson was born in San Marcos, Texas, on February 27, 1924. He entered the University of Texas in 1941 and graduated in 1948 with a B.S. degree in mechanical engineering, in the interim having spent three years, 1943 through 1945, as an Air Force pilot.

After graduation Mr. Johnson joined the Defense Research Laboratory at the University of Texas as a research engineer engaged in guided missile work for the United States Navy. Since June, 1951 he has been employed as a research engineer at the North American Aerophysics Laboratory in Downey, Calif.

Craig C. Johnson

While at college Mr. Johnson was a student member of the American Society of Mechanical Engineers. He is a member of Phi Eta Sigma, Pi Tau Sigma, and Tau Beta Pi. In 1947 he was awarded a Westinghouse Achievement Scholarship.

❖

John M. Kelso was born in Punxsutawney, Pa., on March 12, 1922. He received the A.B. degree in physics from Gettysburg College in 1943, and the M.S. degree from the Pennsylvania State College in 1945. In 1949 he received the Ph.D. degree from the latter institution, having done a thesis on ionospheric radio propagation.

From 1943 to 1948 Dr. Kelso was associated with the physics department at the Pennsylvania State College. Two years of this time were

John M. Kelso

Contributors to Proceedings of the I.R.E.

spent in teaching physics, and the remainder were spent with the Wind Tunnel Laboratory and the Electromagnetic Propagation Laboratory.

Since 1948 Dr. Kelso has been employed by the Radio Propagation Laboratory of the Pennsylvania State College, where he now holds the rank of assistant professor of engineering research. He is a member of the American Physical Society, Sigma Xi, Sigma Pi Sigma, and Pi Mu Epsilon.

❖

Wilbur R. LePage (SM'46) was born in Kearney, New Jersey, on November 16, 1911. He received the E.E. degree at Cornell University, Ithaca, New York, in 1933, and the M.S. degree at Cornell in 1941. He was a teacher in electrical engineering at the University of Rochester from 1933 to 1938. Mr. LePage also taught one term at Cornell in 1941.

Wilbur R. LePage

Mr. LePage worked in the advanced development division of RCA for part of 1941, and in 1942 went to the radiation laboratory of Johns Hopkins University, where he participated in the proximity fuse program during the war. While with RCA, Mr. LePage did part-time teaching for John's Hopkins University and for Purdue University.

In 1946 Mr. LePage went to the Stromberg Carlson Company as a senior research engineer. Since 1947 he has been at Syracuse University, Syracuse, N. Y., where he is now professor of electrical engineering. Mr. LePage has also been doing antenna research for the Air Forces.

❖

C. H. Luhrs (A'45–M'50) was born at West New York, N. J., on January 3, 1912. He studied at the Cooper Union Night School of Engineering, in New York City, and the Polytechnic Institute of Brooklyn.

C. H. Luhrs

Mr. Luhrs has served successively as student assistant at the Bell Telephone Laboratories, Inc., junior observer at the National Geophysical Company, assistant project engineer at the Sperry Gyroscope Company, staff member of the General Precision Laboratory, and is presently engaged in the development and production of high-frequency electrical components at the C. H. Luhrs and Company, in Hackensack, N. J.

Roy A. Martin (S'45–A'46–M'49) was born in Coffee County, Tenn., on March 8, 1920. He received the B.S. degree in 1942 and the M.S. degree in 1951, both in electrical engineering, from the Georgia Institute of Technology.

Roy A. Martin

Mr. Martin entered the armed forces in 1942 and served two years as station commander and technical officer at various radar stations in Ecuador and the Republic of Panama. Upon return to the United States he was in charge of Radar Countermeasures training, first at the Aircraft Warning Unit Training Center, Drew Field, Florida, and later at the Western Signal Aviation Unit Training Center, Camp Pinedale, California. While at Camp Pinedale he also served as RCM liaison officer to Hdg. 4th AF and the 11th Naval District.

In 1946, Mr. Martin joined the applied engineering group of the Western Union Telegraph Company as a radio engineer and worked for a short time on microwave relay systems. In the same year he became a member of the research faculty at the Georgia Institute of Technology, where he has worked on problems such as microwave propagation, electronic-control applications, electro static separation, and dielectric heating.

At present Mr. Martin is engaged in the development of precision-frequency measuring and standardization equipment.

❖

George E. Mueller (S'39–A'42–SM'46) was born in St. Louis, Mo., on July 16, 1918. He received the B.S. degree in electrical engineering from the Missouri School of Mines and Metallurgy in 1939, the M.S. degree in engineering from Purdue University in 1940, and the Ph.D. degree in physics from the Ohio State University in 1951. From 1940 through 1946 he was a member of the technical staff of the Bell Telephone Laboratories, engaged in television and radio research. Since 1946 Dr. Mueller has been an assistant professor in the Electrical Engineering Department at the Ohio State University.

George E. Mueller

Dr. Mueller is a member of the American Physical Society, Tau Beta Pi, Sigma Xi, Eta Kappa Nu, and Sigma Pi Sigma.

❖

Arnold P. G. Peterson (S'34–A'38–SM'46) was born in De Kalb, Illinois, on August 7, 1914. He received the Bachelor of Engineering degree from the University of Toledo in 1934, and the degrees of S.M. in 1937, and Sc.D. in 1941, from the Massachusetts Institute of Technology.

A. P. G. Peterson

From 1936 to 1940 he was a Research Assistant in the Electrical Engineering Department of MIT, working on ultra-high-frequency oscillators and measurements on a co-operative program with the General Radio Company. Since 1940 he has been an engineer at the General Radio Company, working on the development of electronic measuring instruments and associated apparatus.

Dr. Peterson is a member of Sigma Xi, the Acoustical Society of America, the American Physical Society, the American Association for the Advancement of Science, the American Institute of Electrical Engineers, and the American Geophysical Union.

❖

James W. Sauber (M'51) was born in Youngstown, Ohio, on May 7, 1925. He attended Allegheny College and Lehigh University, and received the B.S. degree in 1946. For the following year he was employed as a test engineer by the General Electric Company. From 1947 to 1951 he was an instructor and assistant professor in electrical engineering at the University of Tennessee, and simultaneously took graduate studies for which the M.S. degree was received in 1950.

James W. Sauber

Mr. Sauber is now on the staff of Ballantine Laboratories, Inc., Boonton, N. J. He is a member of Phi Beta Kappa, Tau Beta Pi, and Eta Kappa Nu.

❖

Robert F. Shaw (S'35-A'43-M'45-SM'47) was born at Warsaw, Ohio, on July 10, 1915. He received the A.B. degree in physics from Princeton University in 1937, after which he did graduate work in electrical engineering at the Moore School of the University of Pennsylvania.

Robert F. Shaw

Mr. Shaw taught radio theory for the U. S. Navy in 1942 and 1943, and in the latter year he returned to the Moore School as a research engineer connected with

Contributors to Proceedings of the I.R.E.

the development of the ENIAC (electronic numerical integrator and computer). He remained there until completion of the project, and carried out preliminary logical design work on the EDVAC (electronic discrete variable computer).

In 1946 Mr. Shaw joined the staff of the Electronic Computer Project at the Institute for Advanced Study, and later that year became a member of the staff of the Electronic Control Co., now known as the Eckert-Mauchly Computer Corp., where his work was concerned mainly with logical design of computers and associated equipment. Since July, 1951 he has been engaged in similar work with the Electronic Computer Corp.

Mr. Shaw is a member of the American Mathematical Society, the American Association for the Advancement of Science, the Association for Computing Machinery, the Franklin Institute, and Sigma Xi.

❖

Donald B. Sinclair (J'30–A'33–M'38–SM'43–F'44) was born at Winnipeg, Manitoba, Canada, on May 23, 1910. He attended the University of Manitoba from 1926 to 1929, later transferring to the Massachusetts Institute of Technology, where he received the S.B. degree in 1931, the S.M. in 1932, and the Sc.D. in 1935.

D. B. Sinclair

Dr. Sinclair was a research assistant at MIT from 1932 to 1935, and a research associate from 1935 to 1936, working mainly on high-frequency measurements. In 1936 he joined the staff of the General Radio Company as an engineer. There he worked chiefly on the general development and design of measuring instruments, with emphasis on high-frequency measuring equipment. He was appointed assistant chief engineer of the General Radio Company in 1944, and chief engineer in 1949.

Dr. Sinclair is a fellow of the American Institute of Electrical Engineers, a member of Sigma Xi, and a member of the American Association for the Advancement of Science.

❖

John L. Stewart (S'48–A'50) was born in Pasadena, Calif., on April 19, 1925. He received the B.S. and M.S degrees in electrical engineering from Stanford University in 1948 and 1949, respectively. From 1943 to 1945 he served as a combat aerial navigator in the U. S. 8th Air Force.

John L. Stewart

From 1949 to 1951 Mr. Stewart was employed by the California Institute of Technology Jet Propulsion Laboratory as a research engineer, doing research and development work on radar, analog computers, and other equipment. During the summer of 1951, he worked in system analysis, Hughes Aircraft Co., Culver City, Calif., and is now doing graduate work at Stanford University.

Mr. Stewart is a member of Tau Beta Pi and Sigma Xi.

❖

Robert D. Teasdale (S'44–A'46–M'49) was born in Mt. Lebanon, Pa., in 1924. From 1942 to 1944 he served in the U. S. Army. He received the B.S. degree in electrical engineering from Carnegie Institute of Technology, where he was a George Westinghouse scholar. He received the M.S. degree in 1947 and the Ph.D. degree in 1949, both in electrical engineering, from the Illinois Institute of Technology. He has recently earned the LL.B. degree at night school.

R. D. Teasdale

In 1947 and 1948 Dr. Teasdale was a Gerard Swope fellow, and in 1948 and 1949 he held an RCA Fellowship in Electronics.

During 1945 Dr. Teasdale was on a training program with the Westinghouse Electric Corporation in East Pittsburgh, Baltimore, and Bloomfield. In 1947 he worked briefly with the High-Frequency Division of the Engineering Consulting Laboratories of the General Electric Company in Schenectady, N. Y. He has done some part-time work for the Engineering Experiment Station of Georgia.

At present Dr. Teasdale is an associate professor of electrical engineering at the Georgia Institute of Technology, where he specializes in transient circuit analysis and electromagnetic theory.

Dr. Teasdale is a member of the American Institute of Electrical Engineers, Tau Beta Pi, Eta Kappa Nu, and Sigma Xi, and is a registered professional engineer in electrical engineering.

❖

J. Torkel Wallmark (A'48) was born in Stockholm, Sweden, on June 4, 1919. He received Civilingenjorsexamen in electrical engineering at the Royal Institute of Technology in Stockholm, in 1944; and Teknologie Licentiatexamen in 1947.

J. T. Wallmark

From 1944 to 1945 he worked as a tube designer with the A.B. Standard Radiofabrik, and from 1945 to 1947, he was with the Royal Institute of Technology, in Stockholm, Sweden, as a research engineer. In 1947 Mr. Wallmark was granted a fellowship by the American Scandinavian Foundation and spent a year with the RCA Laboratories, Princeton, N. J. At present, Mr. Wallmark is back at the Royal Institute of Technology in Sweden.

❖

Dean A. Watkins (A'47–M'48–S'49–A'51) was born in Omaha, Neb., on October 23, 1922. He specialized in electrical engineering, receiving the B.S. degree from Iowa State College in 1944, the M.S. degree from California Institute of Technology in 1947, and the Ph.D. degree from Stanford University in 1951. He was a Gerard Swope Fellow from 1950 to 1951 at the latter institution.

Dean A. Watkins

In World War II, Dr. Watkins served in the Army Engineers in the European and Pacific theaters. He was employed by the Collins Radio Company from 1947 to 1948 and at the Los Alamos Scientific Laboratory from 1948 to 1949. He is now engaged in microwave-tube research in the Electron Tube Laboratory of the Hughes Aircraft Company.

Dr. Watkins is a member of the American Physical Society, Sigma Xi, Tau Beta Pi, and Eta Kappa Nu.

❖

James R. Weiner (S'41–A'47) was born in Chicago, Ill., on February 3, 1920. He received the B.S. degree in engineering physics from the University of Illinois. He did graduate work at the Polytechnic Institute of Brooklyn, from which he received the M.S. degree in electrical engineering in 1946, and has done further graduate work at Harvard and M.I.T.

James R. Weiner

From 1942 to 1945 Mr. Weiner was employed by the RCA Manufacturing Co. and RCA Laboratories as a research engineer, in which capacity he worked on a variety of projects, including optical systems, secrecy systems, communications equipment, and television equipment.

In 1945 Mr. Weiner was employed by the Columbia Broadcasting System as a group leader in charge of test equipment in the television laboratories. From this time until the end of World War II, he worked on radar countermeasures and radar relay systems. He was then made assistant group leader in charge of television studio equipment, and was concerned with the development and test of high-definition color-television equipment.

Contributors to Proceedings of the I.R.E.

Mr. Weiner became affiliated with the Raytheon Manufacturing Co. in 1946. His work was concerned with the design of guidance and control equipment for missiles. Shortly after being placed in charge of the systems analysis group, he was asked to form and supervise a digital computer equipment section. He has been active in this field since that time.

Since 1948 Mr. Weiner has been employed by the Eckert-Mauchly Computer Corp. He joined the company as general consultant, and shortly thereafter was given the position of chief electronic engineer. He has recently been named chief engineer, and as such is responsible for all phases of engineering work.

Mr. Weiner served as chairman of the IRE Technical Committee on Electronic Computers. He has served on other IRE committees, and is presently a member of the Circuits Committee, the Electronic Computers Committee, and the Papers Review Committee. Mr. Weiner is also a member of Sigma Xi, Tau Beta Pi, Sigma Tau, and various professional societies.

Raymond M. Wilmotte was born in Paris, France, on August 13, 1901. He took first class honors in Mechanical Science (Engineering) at Cambridge University, England, in 1920 when he received the M.A. degree.

Until 1929 he was engaged at the National Physical Laboratory in research on radio measurements, direction finding, wave propagation, and theory and design of antennas.

R. M. Wilmotte

In 1929 Mr. Wilmotte came to the United States and worked until 1931 at Boonton Aircraft Corporation on research and development on aircraft equipment, including antennas and blind landing system. He opened a consulting practice in 1931 on being requested by Commander Craven to solve the problem of a client of his, Station WFLA, which interfered with Station WTMJ. This led him to design, install, and test the first directional antenna used for this purpose. He has appeared in patent cases and before the Federal Communications Commission. During the war he carried out design and development contracts for the Signal Corps, the Navy, and NDRC. At the request of the latter he established a small manufacturing facility for specialized production where one of the projects was the modification of radar units to meet the Japanese Kamikaze menace. For this work he was awarded the Bureau of Ordnance Development Award.

Mr. Wilmotte invented the antifading broadcast antenna recently used in Germany. Recently he has demonstrated the possibility of receiving a weak FM signal in the presence of a strong one in the same frequency band. He was one of the original members of the "Ad Hoc" Committee of the Federal Communications Commission.

Louis D. Wilson (M'46) was born in Philadelphia, Pa., on December 17, 1917. In 1941 he received the B.A. degree and in 1942 the M.A. degree, both in physics from Temple University.

Louis D. Wilson

From 1942 to 1944 Mr. Wilson was a teaching fellow in physics at the Massachusetts Institute of Technology. From 1944 to 1945 he joined the M.I.T. staff as an instructor in electrical engineering. He became a research engineer at the Massachusetts Institute of Technology Servomechanisms Laboratory in 1945, where he remained until 1947. During this period of his career he worked on the electrical design of the Whirl-wind computer, and was in charge of the development of arithmetic circuits.

From 1947 to the present, Mr. Wilson has been employed by the Eckert-Mauchly Computer Corp., during which time he has worked on the logical design of the Binac computer, on the circuit design for the Binac and Univac computers, and also on the development of special input-output devices for use with the Univac computer system. Recently he was named Project Engineer responsible for development of input-output devices.

Correspondence

Note on "Correlation Functions and Power Spectra in Variable Networks"*

In his recent article[1] Zadeh introduced a method for handling the linear variable network through the concept of the correlation function of the network system function. By a small extension of Zadeh's work a simple theorem may be obtained for the correlation function of a system function in which the variables are separable. For such a linear time-varying network it is shown below that the correlation function of the system function is the product of two correlation functions, one being the correlation function of the time-dependent portion of the system function and the other being the correlation function of the frequency-dependent portion of the system function. The utility of this extension lies in its application to problems of gating and clamping.

Zadeh defines the correlation function $\psi_H(\tau;\omega)$ of the system function $H(j\omega;t)$ of a stationary variable network by

$$\psi_H(\tau;\omega) = \lim_{T\to\infty}\frac{1}{T}\int_0^T H(j\omega;t)H(-j\omega;t+\tau)dt$$
$$= \overline{H(j\omega;t)H(-j\omega;t+\tau)}.$$

Let the variables in the system function be separable, then

$$H(j\omega;t) = \Omega(j\omega)T(t)$$

and

$$\begin{aligned}\psi_H(\tau;\omega) &= \overline{\Omega(j\omega)T(t)\Omega(-j\omega)T(t+\tau)}\\ &= \Omega(j\omega)\Omega(-j\omega)\overline{T(t)T(t+\tau)}\\ &= |\Omega(j\omega)|^2\overline{T(t)T(t+\tau)}.\end{aligned}$$

Now $|\Omega(j\omega)|^2$ is the correlation function of the system function of a fixed network, a relation established by Zadeh in the article (Equation 28). In the case of the network for which the variables of the system function are separable, it is the correlation function of the nontime-varying portion of the system function. Thus we may write

$$|\Omega(j\omega)|^2 = \psi_B(\omega).$$

The term $T(t)T(t+\tau)$ is simply the correlation function of the time-varying portion of the system function, and may be written

$$\overline{T(t)T(t+\tau)} = \psi_H(\tau).$$

Consequently, the complete correlation function of the network system function is

$$\psi_H(\tau;\omega) = \psi_H(\omega)\psi_H(\tau).$$

In other words, if the variables in the system function are separable, the variables are also separable in the correlation function of the system function, the latter correlation function being the product of the correlation function of the time-dependent portion of the system function and the frequency-dependent portion of the system function.

In addition to its utility in problems of an on-off nature, the above theorem may have application to other classes of problems. It would seem, therefore, that the determination of the types of networks in which the variables are separable would prove a worthwhile study.

Bernard D. Steinberg
Research Division
Philco Corp.
Philadelphia, Pa.

* Received by the Institute, August 14, 1951.

[1] L. A. Zadeh, "Correlation functions and power spectra in variable networks," Proc. I.R.E., vol. 38, pp. 1342–1345; November, 1950.

General Input-Output Relations for Linear Networks*

The analysis and synthesis of signal transmission systems is usually carried out in the frequency domain by using the Laplace or Fourier transformation technique This involves the resolution of signals into exponential components by means of the basic relation

$$u(t) = \frac{1}{2\pi j}\int_C e^{st}U(s)ds, \tag{1}$$

where $u(t)$ is a signal, $e^{st}/2\pi j$ represents the component signals, $U(s)$ is the Laplace transform of $u(t)$, and C is the Bromwich-Wagner contour.

A more general technique, which is briefly outlined below, is based on the resolution of signals into a set of "elementary" or component signals $k(t;\lambda)$ of some suitable type by means of the relation

$$u(t) = \int_C k(t;\lambda)U(\lambda)d\lambda, \tag{2}$$

where λ plays the same role as s in (1); $U(\lambda)$ is called the spectral function of $u(t)$ relative to $k(t;\lambda)$, and C is a contour in the λ-plane (generally a straight line parallel to either the imaginary or real axis). It is assumed that the kernel $k(t;\lambda)$ has an inverse $k^{-1}(\lambda;t)$ such that

$$\int_C k(t;\lambda)k^{-1}(\lambda;t')d\lambda = \delta(t-t'), \tag{3}$$

where $\delta(t-t')$ is a unit impulse function. In terms of $k^{-1}(\lambda;t)$, the spectral function $U(\lambda)$ may be written

$$U(\lambda) = \int_{-\infty}^{\infty} k^{-1}(\lambda;t)u(t)dt. \tag{4}$$

Suppose that $u(t)$ is the input to a linear network N (fixed or variable) and $v(t)$ is the response of N (at rest) to $u(t)$. Let $K(t;\lambda)$ be the response of N to $k(t;\lambda)$, both regarded as functions of time involving λ as a parameter. The function $K(t;\lambda)$ will be called a *characteristic* function of N since it provides a complete characterization of the relation between the input and output of N. It will be observed that such descriptive functions as the impulsive response, unit-step response, and system function are special cases of $K(t;\lambda)$ corresponding, respectively, to the unit impulse, unit step, and exponential types of component signals.

In terms of $K(t;\lambda)$, the response of N to a specified input $u(t)$ is given by

$$v(t) = \int_C K(t;\lambda)U(\lambda)d\lambda. \tag{5}$$

The familiar relation

$$v(t) = \int_{-\infty}^{\infty} W(t,\xi)u(\xi)d\xi,\ (\lambda = \xi), \tag{6}$$

where $W(t,\xi)$ is the impulsive response of N, as well as the relation

$$v(t) = \frac{1}{2\pi j}\int_{\sigma-j\infty}^{\sigma+j\infty} H(s;t)U(s)e^{st}ds,\ (\lambda = s), \tag{7}$$

where $H(s;t)$ is the system function and $U(s)$ is the Laplace transform of $u(t)$, are special cases of (5). It will be noted that in (7) the component signals are of the form $e^{st}/2\pi j$ and the corresponding characteristic function is $H(s,t)e^{st}/2\pi j$.

A very important concept which heretofore has been used chiefly in connection with fixed networks is that of an *ideal filter*. Such a filter may be defined as a network N which passes without distortion (or delay) all component signals in which the parameter λ belongs to a set A on C and rejects all those in which λ (on C) does not belong to A. It is readily found that the impulsive response of an ideal filter is given by

$$W(t,\xi) = \int_A k(t;\lambda)k^{-1}(\lambda;\xi)d\lambda, \tag{8}$$

where the integral is taken over the set A. In general, $W(t,\xi)$ is not physically realizable, but one can approximate to $W(t-\beta,\xi)$, where β is a sufficiently large constant, by a physical filter.

In geometrical terms, the operation performed by an ideal filter corresponds to an oblique projection of the signal space Σ (in which $u(t)$ is a vector) on a linear subspace of Σ. Since projection is an idempotent operation, and vice-versa, one can alternatively define an ideal filter in the following manner: *A linear filter N is an ideal filter if it is idempotent, that is, if it is equivalent to a tandem combination of two filters, each of which is identical with N.* Ideal filters, linear and nonlinear, play an important role in a generalized theory of filtration of signals.[1,2,3]

The general approach outlined here may be called the "λ-domain" approach since the role of λ is the same as that of frequency in the case of the frequency domain approach. It should be remarked that some of the relations given above are commonly employed in quantum mechanics, although in a somewhat different form and for different purposes.

L. A Zadeh
Department of Electrical Engineering
Columbia University
New York 27, N. Y.

* Received by the Institute, July 17, 1951.

[1] L. A. Zadeh, "Theory of filtering of signals in a λ domain," *Bull. Amer. Math. Soc.*, vol. 57, p. 278; July, 1951. Presented New York Meeting of the American Mathematical Society, April 27, 1951.

[2] L. A. Zadeh, "A general theory of linear signal transmission systems" (to be published in *Jour. Frank. Inst.*)

[3] L. A. Zadeh and K. S. Miller, "Generalized ideal filters" (to be published in *Jour. Appl. Phys.*)

Institute News and Radio Notes

Technical Committee Notes

The Standards Committee, under the Chairmanship of A. G. Jensen, met on November 8, 1951. Chairman Jensen reviewed the discussion of the Administrative Committee meeting held prior to the main committee meeting. The Pulse Definitions, prepared by the Pulse and Task Group, under the Chairmanship of C. J. Hirsch, were approved for submission to the IRE Executive Committee. The Standards Committee approved the change in the title of the **Committee on Electron Tubes and Solid State Devices** to the Committee on Electron Devices. This change will also be submitted to the IRE Executive Committee for approval. At the October 11, meeting of the Standards Committee it was agreed that revised scopes of all the Technical Committees should be submitted to the Standards Committee, so that they might be brought into uniform style and approved collectively.

Under the Chairmanship of J. L. Dalke, **the Industrial Electronics Committee** meeting was held on September 27, 1951. The scope of this committee was discussed with relationship to the work of other committees, particularly the **Committee on Measurements and Instrumentation.** Co-ordination of these two committees is being considered.

The **Committee of Radio Transmitters** met on October 11, 1951, Chairman M. R. Briggs presiding. The activities of the various Subcommittees were discussed with detailed reports given by the chairmen of the subcommittees.

On October 5, 1951, the **Facsimile Committee** met under the Chairmanship of R. J. Wise. Material prepared for the Annual Review committee was turned over to J. H. Hackenberg who is the representative for this committee. The Facsimile Committee is planning to review the definitions and test standards. The committee discussed inclusion of pseudofacsimile in the definitions, the methods of measuring numerous facsimile characteristics, the acceptable limits for the various characteristics, and whether performance standards should be recommended.

A need for standardization in the field of video recording was discussed at the **Video Techniques Committee** meeting, held on October 4, 1951, under the chairmanship of W. J. Poch. A. J. Barackct, Chairman of Subcommittee 23.3, reported that the work in progress in this subcommittee included the measurement of geometric distortion, pickup tube interlacing, transfer characteristics, the rate of change of frequency of synchronizing signals, and the measurement of dc insertion systems. A report of the work in progress in Subcommittee 23.4 was given by Chairman J. L. Jones; the most important phase being the measurement of frequency and transfer response.

At a meeting of the **Modulation Systems Committee,** held on October 26, 1951, under the Chairmanship of W. G. Tuller, the committee decided to submit a change in its title and scope to the IRE Executive Committee for their approval.

The **Navigation Aids Committee** met on October 29, 1951, under the Chairmanship of P. C. Sandretto, who reported to the Committee on the status of the subcommittees. Chairman Sandretto stated that there are two active subcommittees, 12.2, "Standards of Direction-Finder Measurements," and 12.3, "Measurement for Navigation Systems," which was organized under the Chairmanship of Harry Davis. The Subcommittee on Direction-Finder Measurement is now working on its final report which will be sent to the main committee for consideration. Chairman Sandretto said that as soon as work has been completed on the definitions now under review, the committee would be prepared to review the report of Subcommittee 12.2.

Program Committee Members

Pictured above is the program committee for the meeting on land mobile communications sponsored by the IRE Professional Group on Vehicular Communications, held in Chicago, on October 25–26, 1951. (from left to right) Bert Zarky, W. J. Weisz, J. M. Clark, Elmer V. Carlson K. V. Glentzer, R. V. Dondanville, and E. S. Goebel.

Professional Group Notes

On November 7, 1951, the **IRE Board of Directors** approved an amendment to the IRE Bylaw, 70-F, which now states that all members of the IRE, are eligible for membership in the IRE Professional Groups, including Student Members. This new ruling is effective immediately.

The IRE Professional Groups on Broadcast and Television Receivers, Broadcast Transmission Systems, and **Instrumentation** have recently voted for assessments to cover costs of printing publications. Assessment notices will go forward to the entire membership of each of these groups.

Two papers selected by the **IRE Professional Group on Airborne Electronics** for publication as monographs are, "Systems Consideration in Aircraft Antennas Design," by J. V. N. Granger, and, "The Electrical Characteristics of Shaker Systems Used for Vibration Testing of Equipment," by R. C. Lewis and D. J. Fritch. This Group is also planning to hold a membership drive during the IAS National Convention which is being held the last week in January, 1952.

The IRE Professional Group on Circuit Theory Papers Committee held a meeting on November 9, 1951, to discuss plans for a Transistor Circuitry Symposium to be held during the 1952 IRE National Convention.

The Administrative Committee of the **IRE Professional Group on Electronic Computers** held a meeting during the IRE-AIEE Computer Conference in Philadelphia, on December 10, 11, and 12, 1951.

The IRE-AIEE Conference on Induction and Dielectric Heating, in February, 1952, is to be co-sponsored by the **IRE Professional Group on Industrial Electronics.**

The IRE Professional Group on Radio Telemetry and Remote Control is planning a special technical conference on Telemetering for the latter part of May or early June, 1952. The conference will be held in cooperation with the AIEE.

Under the Chairmanship of Winslow Palmer, the program committee of the IRE **Professional Group on Information Theory** held a meeting on November 14 and 27. Plans were discussed at the time for a meeting on Information Theory to be held in 1952, tentatively decided on as a three or four day session in September. Mischa Schwartz has been appointed to represent the Group on the Technical Program Com-

Institute News and Radio Notes

mittee for the 1952 IRE National Convention and will make plans for a Symposium on Information Theory to be held during the Convention.

Canvassing of the IRE Sections throughout the country is being carried out by the **IRE Professional Group on Audio** with the aim of increasing the activity of the Group on a Section level. To date, approximately 40 replies have been received and work is proceeding to establish Group Chapters where interest has been evidenced. At the National Electronics Conference in Chicago, the Group co-operated in presenting a program of four papers in a technical session on Audio. The papers were received with much interest. Plans are under way to include reviews of books pertinent to the Audio field in future issues of the Audio Group NEWSLETTER.

PROFESSIONAL GROUP BANQUET

Among those seated at the head table of the banquet given by the IRE Professional Group on Vehicular Communications, in Chicago, were (from left to right), Mr. and Mrs. G. M. Brown, New York Central Railway; E. M. Webster, FCC Commissioner; and Austin Bailey, Group Chairman.

NOTICE TO PROCEEDINGS AUTHORS AND READERS

The volume of material submitted for consideration for publication in the PROCEEDINGS OF THE I.R.E. has, in recent years, exceeded the available space. As a result, it has been found necessary in the past to reject in some cases lengthy descriptive or mathematical papers of some value.

In the future, in order that this material might be made available to interested readers, the manuscripts of such papers will be deposited (with the author's consent) with the American Documentation Institute in Washington, D. C. Abstracts of these papers will then be published in the PROCEEDINGS, accompanied in each case by a footnote advising readers of the availability, identification means, and cost of microfilm or photocopies of the full-length papers.

AEC FELLOWSHIPS OPEN

The Oak Ridge Institute of Nuclear Studies is now receiving applications for Atomic Energy Commission Graduate Fellowships for specialized training in radiological physics for the 1952–1953 school year.

The fellowships are awarded at either the University of Rochester, in co-operation with Brookhaven National Laboratory, or the Vanderbilt University, in co-operation with the Oak Ridge National Laboratory. The final three months of the fellowships will be spent at the national laboratory.

Applicants must hold an undergraduate degree, preferably with a major in physics, chemistry, or engineering, and a minor in mathematics, biophysics, or similar fields. Fellows must be citizens of the United States and must receive security clearance in accordance with existing laws.

The annual basic stipend is $1,500, with an additional allowance for dependents making a maximum stipend of $2,500. University tuition and fees will be paid by the Oak Ridge Institute of Nuclear Studies.

Application blanks and further information may be obtained from the heads of science and engineering departments of colleges and universities or from the University Relations Division, Oak Ridge Institute of Nuclear Studies, P.O. Box 117, Oak Ridge, Tenn. Applications must be in the hands of the Oak Ridge Institute by March 1, 1952.

ETA KAPPA NU AWARD ANNOUNCED

Eta Kappa Nu will present its annual Outstanding Young Electrical Engineer Award at a dinner to be held on January 21, 1952, at the Henry Hudson Hotel, New York, N. Y.

Winner of the award is Louis G. Gitzendanner, General Electric Co., Schenectady, N. Y. Honorable mention went to Burton R. Lester (S'41–A'43–M'47), General Electric Co., Syracuse, N. Y., and Robert L. Trent (M'45), Bell Telephone Laboratories, Murray Hill, N. J.

FORTESCUE FELLOWSHIPS OFFERED

Funds have been made available for one or more Charles LeGeyt Fortescue fellowships for 1952–1953. The awards are made to postgraduate students in the field of electrical engineering who have received their baccalaureate degree from a duly recognized technical school in the United States or Canada. The awards range from $1000 to $1500 per annum depending upon the decisions of the committee in charge. Application forms can be obtained from the deans or chairmen of the department of electrical engineering of the various engineering schools. Additional copies of the application forms can be procured from H. H. Henline, Secretary of the AIEE, 33 West 39 Street, New York, N. Y. Applications must be received not later than February 15, 1952.

Calendar of COMING EVENTS

IAS-IRE-ION-RTCA Conference on Electronics in Aviation, IAS 20th National Convention, Astor Hotel, New York, N. Y., January 28–31

1952 IRE National Convention, Waldorf-Astoria Hotel and Grand Central Palace, New York, N. Y., March 3–6

Radio Component Show, London, England, April 7–9

Radio and Television Show, Manchester, England, April 23–May 3

IRE Cincinnati Section Spring Technical Conference, Cincinnati Engineering Societies Building, Cincinnati, Ohio, April 19

IEE Television Convention, London, England, April 28–May 3

IRE-AIEE-RTMA Symposium on Progress in Quality Electronic Components, Washington, D. C., May 5–7

IRE New England Radio Engineering Meeting, Copley Plaza Hotel, Boston, Mass., May 10

IRE National Conference on Airborne Electronics, Hotel Biltmore, Dayton, Ohio, May 12–14

4th Southwestern IRE Conference and Radio Engineering Show, Rice Hotel, Houston, Tex., May 16–17

Radio Parts and Electronic Equipment Show, Conrad Hilton Hotel, Chicago, Ill., May 19–22

1952 IRE Western Convention, Municipal Auditorium, Long Beach, Calif., August 27–29

National Electronics Conference, Chicago, Ill., September 29–October 1

IRE-RTMA Radio Fall Meeting, Syracuse, N. Y., October 27–29

INDIA RADIO AND ELECTRONICS EXHIBITION POSTPONED

The International Radio and Electronics Exhibition, formerly scheduled for February 9–29, 1952, in Bombay, India, has been postponed until November 9–29, 1952. The exhibition will be sponsored by the Radio and Electronics Society of India, an organization recently formed by the All India Radio Merchant's Association, whose aim is to create and promote popular interest in the science and application of radio and electronics.

Postponement of the exhibition was caused by the failure of the monsoon in India and a drastic cut in the water and electricity supply. Previously scheduled plans will be carried out for the November date.

IRE-URSI Fall Meeting*

CORNELL UNIVERSITY, ITHACA, N. Y.—OCTOBER 8-10, 1951

SUMMARIES OF TECHNICAL PAPERS

1. CURRENT STATUS OF RESEARCH AND DEVELOPMENT ON TRAVELING-WAVE TUBES

J. R. Pierce
(Bell Telephone Laboratories, Murray Hill, N. J.)

Considerable advances have been made in the understanding of the behavior of traveling-wave tubes, and especially with regard to the focusing, of electron streams, the generation of noise, and the behavior at high levels. Experimental work shows that it is possible to obtain almost complete transmission of a beam of electrons through the tube, that noise figures of better than 10 db can be attained, and that efficiencies higher than 25 per cent can be attained.

2. SOME CHARACTERISTICS OF TROPOSPHERIC SCATTERING

A. H. LaGrone
(University of Texas, Austin, Texas)

Three problems are considered which are important in determining the effect of scattering on distance radio fields.

The first problem is the attenuation of radio signals caused by scattering. The total power scattered per unit macroscopic element of volume relative to the power incident on the volume is determined. The second problem is a volume integration to determine the total scattered signal reaching a receiver point. An equation is developed in terms of the propagation parameters which will give this total signal. The third problem is that of cross polarization in the scattered wave. Equations are developed for determining the scattered signal received on dipoles oriented at right angles to each other.

3. THE WORLD CHAIN OF SOLAR RADIO OBSERVATORIES

A. H. Shapley
(Central Radio Propagation Laboratory, Washington, D. C.)

A program for continuous radio observation of the sun is emerging under the encouragement of the URSI and the International Astronomical Union. As techniques improve and observing schedules become longer, it will be possible to measure more nearly continuously the hour-to-hour variations in solar radiation at about 200 and about 3,000 mc. The observations from ten stations are compared and combined for selected periods in the spring of 1951 to illustrate the potential utility of a world chain of solar radio observatories.

* Co-sponsored by the IRE Professional Group on Antennas and Propagation and the USA National Committee of URSI.

4. CURRENT STATUS OF TRANSISTOR RESEARCH AND DEVELOPMENT

J. A. Morton
(Bell Telephone Laboratories, Murray Hill, N. J.)

A discussion of the limitations of transistors as an electronic circuit element is given. The following was discussed:

(1) The reproducibility of units was poor—units intended to be alike were not interchangeable in circuits. (2) The reliability was poor—in an uncomfortably large fraction of units made, the characteristics changed suddenly and inexplicably. (3) The "designability" was poor—it was difficult to make devices to the wide range of desirable characteristics needed in modern communications functions.

The paper describes the progress which has been made in reducing these limitations and extending the range of performance and usefulness of transistors in communications systems.

5. VALIDITY OF THE SUBSTITUTION PRINCIPLE IN BOLOMETER POWER MEASUREMENTS

Max Sucher and H. J. Carlin
(Microwave Research Institute, Brooklyn, N. Y.)

The accuracy of bolometric techniques for high-frequency power measurements depends chiefly on the validity of substituting low frequency for rf power. Under certain conditions this substitution technique introduces large errors. This paper demonstrates that very thin Wollaston wire bolometers, mounted in air, are free of this type of error even when the rf power distribution along the wire is extremely nonuniform. It is concluded that bolometers whose thermal losses are essentially convective may safely be used as absolute microwave power meters.

6. USE OF SAMPLING THEOREMS IN MEETING ANTENNA SPECIFICATIONS

W. L. Murdock
(General Electric Company, Syracuse, N. Y.)

It is known that the transient response to the step function of a filter with cut off α is determined by its values at times spaced π/α apart. Mathematically, this means that if a function $(F(\omega))$ vanishes outside a finite region $(|\omega| < \alpha)$, then its Fourier transform is determined by its values at a sequence of points $(Z = Z_0 + K\pi/\alpha)$. It is shown that this idea may be applied to double Fourier transforms and to Bessel transforms. These two cases are used to impose far-field specifications on a rectangular or round-antenna aperture by setting the value of the far field at a set of points thereby determining the far field and the aperture illumination so that the specifications are satisfied.

7. MEASUREMENT AND DEVELOPMENT OF HIGH FREQUENCY RESISTORS

C. Wellard and S. R. Parker
(International Resistance Company, Philadelphia, Pa.)

In order to measure the high-frequency properties of resistors, special equipment has been developed. This equipment permits the measurement of the parallel resistance and capacitance of resistors from 300 ohms to one megohm in the frequency range from 2 to 400 megacycles per second. The heart of the equipment is a coaxial cavity tuned to the frequency of interest. The measuring technique essentially consists of noting the change in the tuning and the Q of the cavity with and without the unknown resistor connected.

A good resistor at high frequencies should have low-shunt capacity, a high percentage of Rac/Rdc, and be able to dissipate the required power.

8. MICROWAVE BRIDGE FOR RECORDING OF A TIME-VARYING COMPLEX PROPAGATION CONSTANT

D. L. Fye and H. H. Grimm
(Naval Research Laboratory, Washington, D. C.)

A system is proposed employing a balanced null detector, which solves the problem encountered in continuous time recording of complex propagation characteristics. The direct application of this system is restricted to microwaves traveling through a medium whose physical state is varying slowly with time.

Employment of the two-path instantaneously recording bridge requires the measurement of an initial maximum and minimum, and the knowledge of the change in this maximum and minimum when the unknown propagation path is disturbed by a change in the medium or the insertion of a new medium in a portion of the unknown propagation path. The vector equations of the system and their solution are presented.

9. THE ROLE OF PARTIAL REFLECTIONS IN TROPOSPHERIC PROPAGATION BEYOND THE HORIZON

Joseph Feinstein
(Central Radio Propagation Laboratory, Washington, D. C.)

The continuous partial reflections, which must occur as a consequence of the gradient of refractive index present in the atmosphere, are evaluated on a hybrid-ray and wave theory. It is found that the inhomogeneity associated with the standard atmosphere is sufficient to account for the anomalous field strengths found far beyond the horizon. The wave length, distance, and angular dependences associated with this reflected energy are examined and compared with observation. The extent to which the approximate methods employed may be justified on a rigorous wave basis is indicated. The mathematics of the conventional-mode treatment is examined with a view toward ascertaining the reason for its neglect of this field contribution.

10. INTERNAL REFLECTION IN THE TROPOSPHERE AND PROPAGATION BEYOND THE HORIZON

T. J. Carroll
(Central Radio Propagation Laboratory, Washington, D. C.)

Bremmer has emphasized that the WKB approximation neglects the continuous reflections which must in principle be present when electromagnetic waves are propagated through a stratified medium. It appears that the unexpectedly high observed field strengths from high power vhf and microwave transmitters can be explained by "internal reflection" from the troposphere with a standard linear decrease of index-of-refraction with height. Beyond the horizon, the ratio of the internally reflected field to the free-space field turns out to be proportional to $\lambda^{1/3}D^{-2/3}|dn/dh|$, where D is the distance between horizon points, λ the wavelength, and $|dn/dh|$, the vertical index gradient. The numerical results appear consistent with certain observations both at microwave and at vhf frequencies.

11. FIELD STRENGTHS RECORDED ON ADJACENT FM CHANNELS AT 93 MEGACYCLES OVER DISTANCES FROM 40 TO 159 MILES

G. S. Wickizer and A. M. Braaten
(Radio Corporation of America, Riverhead, L. I., N. Y.)

Field strengths of KF2XCC (Alpine, N. J.) and WBZ-FM, (Boston, Mass.) have been recorded for more than a year at two locations on Long Island. Statistical analysis of data for the evening hours reveals a broad seasonal trend toward higher intensities in the summer, with larger overall variation on the longer transmission paths. Based on analysis of one summer month, refraction effects appeared to vary independently in the two directions. The ratio of field strength between the near and distant transmitters, analyzed with respect to time, was found to approach a normal probability distribution at Riverhead, N. J., and a Rayleigh distribution at Hauppauge, N. J.

12. THE EFFECT OF UNIFORM LAYERS ON THE PROPAGATION OF RADIO WAVES

L. J. Anderson and J. B. Smyth
(Navy Electronics Laboratory, San Diego, Calif.)

This study utilizes field strength data at 52, 100, and 550 mc., taken on an over-water nonoptical path 90 miles long. It is shown that the best correlations of field strength with layer height are obtained when uniform layers are used. For layer heights below 1,500 feet, fields calculated assuming reflection from smooth layers show good agreement with experiment. It appears that small undulations of higher layers affect the 550-mc fields more than the lower frequencies. Calculations assuming a sinusoidal undulation are in good agreement with observations.

13. REFRACTION OF RADIO WAVES IN ARBITRARY ATMOSPHERE-RAYTRACING PICTURE

M. S. Wong
(Wright-Patterson Air Force Base, Dayton, Ohio)

A development following Hartree, etc., is carried out of raytracing using a REAC differential analyzer. Ray families, are obtained for an atmosphere with a single n-profile (index-of-refraction versus altitude curve), and for an atmosphere with three n-profiles over the region of interest. The n-profiles used were measured up to a 10,000-foot altitude. The variation in radio-field strength, with separation between airplanes as measured in a recent air-to-air propagation flight, is correlated with a variation of ray density based on index-of-refraction data, taken during the flight.

14. THE DIELECTRIC PROPERTIES OF ICE AND SNOW AT 3.2 CENTIMETERS AS RELATED TO THE REFLECTION COEFFICIENT OF SNOW-COVERED SURFACES

W. A. Cumming
(National Research Council, Ottawa, Canada)

A study has been made of the reflecting properties of snow- and ice-covered surfaces at a wavelength of 3.2 centimeters.

Using waveguide techniques, curves have been obtained of snow permittivity as a function of density, and snow and ice loss tangent as functions of temperature, density, and crystalline structure. The permittivity of ice was found to be 3.15.

The loss tangent of ice, found to vary considerably with temperature, has a value of 27×10^{-4} at 0°C, and a value of 6×10^{-4} at -20°C.

The reflection coefficients, measured on an outdoor range, were found to be dependent on snow temperature, and the effects of multiple reflections were not as great as had been anticipated.

15. THE NRL FIFTY-FOOT MICROWAVE TELESCOPE

F. T. Haddock
(Naval Research Laboratory, Washington, D. C.)

Construction has been completed on the fifty-foot diameter solid paraboloidal reflector useful at wavelengths from a few meters to a centimeter. The attainable antenna gain is over a million. The reflector is mounted on alt-azimuth axes. An electromechanical axis converter makes it possible to automatically track in celestial co-ordinates. It is planned, to use the reflector at wavelengths of 0.85, 3.15, and 9.4 cm for the measurement of extraterrestrial radiation, and at 3 cm for moon radar experiments. The methods of evaluating the antenna performance by measuring the shape of the surface, gain, beam pattern, and the feed pattern, are discussed.

16. RADIATION FROM HYPERFINE LEVELS OF INTERSTELLAR HYDROGEN

H. I. Ewen and E. M. Purcell
(Harvard University, Cambridge, Mass.)

The hyperfine transition in the ground state of atomic hydrogen ($\nu H = 1420.405$ mc/sec) has been detected in galactic radiation. Measurements were made at a declination of $-5°$ with a calculated antenna beam width of approximately 12° between half power points. The line as measured in the vicinity of the galactic center appears in emission with a temperature difference of $40° \pm 5$°C with respect to the radiation field, and with a width of approximately 80 kc. The line shows a doppler shift which is in reasonable agreement with the earth's orbital motion and the motion of the solar system. Evidence that the source is extended is provided by the variation of doppler shift during the time of observation.

17. SOLAR BURSTS AND COHERENT ELECTRON MOTIONS

R. E. Williamson
(David Dunlap Observatory and Cornell University Radio Astronomy Project, Ithaca, N. Y.)

The motions of electrons near a sheet of protons are considered as a possible cause of solar bursts. If the polarizing force is suddenly removed, restoring forces will initiate coherent electron oscillations at the plasma frequency. For conditions in the sun's outer atmosphere, it is found that diffusion and collision damping are negligible. Electromagnetic forces will destroy large-scale coherence, so that the motion is broken up into a large number of cells, each internally coherent, but of random phase. Radiation damping is very great; the total energy of the electrons will be dissipated in one cycle.

It is found that (a) an area 10^4 km² will suffice for the energy observed in a large burst, and (b) a strong frequency dependence in the observed direction is predicted.

18. SPACE CHARGE WAVE AMPLIFICATION IN PLASMAS OF NONUNIFORM DENSITY

H. K. Sen
(Central Radio Propagation Laboratory, Washington, D. C.)

Space-charge wave amplification in interacting beams of moving electrons has been observed under laboratory conditions. The necessity of a sharp density gradient for amplification by multi-stream charge interaction is examined.

An exponential density gradient has been assumed, and an expression derived for the corresponding dispersion equation. Application of the dispersion equation to a static plasma of nonuniform density shows that amplification is possible only for wave-propagation in the direction of decreasing density. A numerical evaluation shows that for the density gradient at the borders of prominence material, amplification as high as 10^6 could be reached in a centimetric path. The analysis indicates that sharp gradients are not necessary for wave amplification by interacting beams.

19. MOVING PROMINENCES AND SOLAR NOISE

H. K. Sen
(Central Radio Propagation Laboratory, Washington, D. C.)

A more detailed examination of Ryle's controversy about solar radio noise is made. The dispersion equation as a function of the velocity of the prominence and the temperatures and densities of the prominence and the corona, is derived. For the conditions met with in the solar atmosphere, the prominence has to move at least as fast as the thermal motion of the coronal electrons (6,700 km). Fairly large amplifications are available under these circumstances. This velocity is much greater than that of prominence material (500 km).

20. SOLAR NOISE STORMS AND PLASMA OSCILLATIONS

H. K. Sen
(Central Radio Propagation Laboratory, Washington, D. C.)

The plasma oscillations in a system of electrons gyrating round a static magnetic field is discussed. The analysis does not indicate gaps in the frequency spectrum at multiples of the gyrofrequency. It shows the instability of oscillations in frequency bands round multiples of the gyrofrequency. A numerical application to spot magnetic fields at coronal distances indicates sufficient amplification to make plausible the theory of the origin of solar "noise storms" in plasma oscillations of electrons gyrating round the magnetic field of sunspots.

To explain the phenomenon of "noise storms" Landav's operational method is considered.

21. THE ROLE OF PLASMA OSCILLATIONS IN SOLAR RADIO NOISE BURSTS

J. Feinstein
(Central Radio Propagation Laboratory, Washington, D. C.)

The interaction of moving charged streams gives rise to bands of amplification which lie in the radio frequency region for the charge densities present in the solar corona. It has been demonstrated that wave growth remains possible in the presence of thermal velocities greater than the injected beam velocity; the frequency band over which amplification may occur becomes quite narrow under these circumstances. It is shown that the rapid growth rates associated with the longitudinal modes give rise to a coupling with the transverse modes associated with a radiation field. An approximate treatment of this coupling, based on consideration of the growing plasma wave as an excited antenna, indicates that large energy conversions are possible.

22. ON THE QUESTION OF THE MAGNITUDE OF THE LUNAR VARIATION IN RADIO FIELD STRENGTH

T. N. Gautier, M. B. Harrington, and R. W. Knecht
(Central Radio Propagation Laboratory, Washington, D. C.)

Eight years of continuous recordings of the field strength of station WLW, and nine years of recordings of station W8XAL, both located near Cincinnati, Ohio, were examined for a lunar variation. The recordings were made at Washington, D. C., approximately 600 kilometers away. The transmitted frequencies were 700 and 6,080 kilocycles per second, respectively. Night-time values of hourly median field strength were used for WLW. Midday values were used for W8XAL. In neither case was the amplitude of the lunar semidiurnal harmonic greater than the probable error of 0.3 db.

23. RADIO WAVE PROPAGATION OVER LONG DISTANCES AT 100 KC

R. H. Woodward and Oscar Goldberg
(Rome Air Development Center, Rome, N. Y.)

A description of the program on long distance propagation at 100 kc sponsored by the Rome Air Development Center, is given. The work consists mainly of:

(a) Determination of the presence or absence of a useful signal at various distances from a transmitting point at a specified received bandwidth.
(b) Determination of the characteristics of the received signal and its components at the various distances.

24. THE LOWER *E* AND *D* REGIONS OF THE IONOSPHERE AS DEDUCED FROM LONG WAVE MEASUREMENTS[1]

J. J. Gibbons, H. J. Nearhoof, R. J. Nertney, and A. H. Waynick
(Pennsylvania State College, State College, Pa.)

A diurnal and seasonal model representing the *E* and *D* regions of the ionosphere above State College, Pennsylvania is presented.

Approximately 150 kc wave solutions including coupling are obtained for this model. It is shown that the effect of the coupling is to cause a wave traversing a coupling region to excite a new wave propagated in the direction of propagation of the incident wave and also a back-scattered wave propagated in the reverse direction. The back-scattered wave will appear as a reflected wave originating in the coupling region. The forward-scattered wave due to the downgoing wave from the upper "reflection" level also must be considered in calculating the polarization of ionospherically reflected waves. The experimental results to be expected from this model are compared in detail with our 150 kc polarization, absorption, and height results. The predicted experimental results are compared qualitatively with the actual experimental results at several other frequencies.

[1] The research reported in this paper has been sponsored by the Geophysical Research Division of the Air Force Cambridge Research Center under Contract AF19(122)-44.

25. THE EFFECT OF SPORADIC *E* ON TELEVISION RECEPTION

E. K. Smith
(Central Radio Propagation Laboratory, Washington, D. C.)

A study of 456 reports of high- and low-band television reception greater than 200 miles shows both ionosphere and troposphere propagation. The distribution of reports with distance indicates that those with transmission paths between 200 and 500 miles are tropospherically propagated, whereas those between 500 and 1,500 miles are propagated by single-hop reflection from the sporadic *E* region of the ionosphere.

26. THE FEBRUARY, 1952 ECLIPSE OF THE SUN

J. P. Hagen, and F. T. Haddock
(Naval Research Laboratory, Washington, D. C.)
W. O. Roberts
(High Altitude Observatory, Climax, Colo.)

The Naval Research Laboratory is attempting to clarify the problem of the temperature gradients in the atmosphere of the sun. Radio and optical studies give divergent results; the radio data indicate a relatively cool chromosphere with a steep gradient to a hot corona, the optical data, on the other hand, give evidence of material being at temperatures of about 30,000° Kelvin deep in the chromosphere. Simultaneous observations of the eclipse at 8.5 mm, 10 cm, and at optical wavelengths, are to be made. A description of the radio and optical equipment is given.

27. RADIO MEASUREMENTS PLANNED FOR THE NEXT TOTAL SOLAR ECLIPSE

F. T. Haddock and J. P. Hagen
(Naval Research Laboratory, Washington, D. C.)

On February 25, 1952, the sun will be totally eclipsed by the moon for three minures. NRL is planning an expedition to Khartoum, Anglo-Egyptian Sudan, to determine the distribution of radio emission over the solar disk. Radio emission measurements will be made at 0.85 and 9.4 cm wavelength. The antenna and radiometer systems will be described. The expected variations of received energy during the eclipse on the basis of several models of the undisturbed solar atmosphere, and the effect of localized sources of enhanced radiation generally associated with sunspots, will be discussed.

28. RADIO ASTRONOMY AT CORNELL UNIVERSITY

C. R. Burrows
(Cornell University, Ithaca, N. Y.)

Cornell University and the Office of Naval Research have been jointly sponsoring research work in the field of Radio Astronomy being conducted at Ithaca, New York, since November, 1946. Cornell University, under the sponsorship of the Research and Development Command of the Air Force, has established a Radio Astronomy Observatory at Sacramento Peak near Almogordo, New Mexico.

Solar observations are being made on frequencies of 50, 200, 1,420, and 3,200 mc. Galactic observations have been confined to measurements on 200 mc. The solar measurements made at Sacramento Peak are being co-ordinated with optical measurements being made concurrently by Harvard University.

29. OBSERVATION OF ACTIVE REGIONS OF THE SUN BY RADIO INTERFEROMETER AND SPECTROHELIOGRAPH

H. W. Dodson
(McMath-Hulbert Observatory, Ann Arbor, Mich.)
Lief Owren
(Cornell University, Ithaca, N. Y.)

Simultaneous 200 mc radio interferometer and radio-telescope observations at the Radio Astronomy Observatory, of Cornell University, during upper transit of the sun make possible determination of the region of the sun's disk where bursts and enhanced base level originate. The equipment and measurement procedures are described.

The positions of the source of the 200 mc radio emissions determined for 13 cases have been compared with optical observations recorded or compiled at the McMath-Hulbert Observatory of the University of Michigan. The positions agree with active regions on the sun. In two cases the regions included flares associated with radio outbursts.

30. AN APPLICATION AT 50 MC OF A THEORY OF RADIO FREQUENCY RADIATION FROM THE QUIET SUN

R. E. Williamson
(David Dunlap Observatory)
E. E. Reinhart
(Cornell University, Ithaca, N. Y.)

The corona of the quiet sun is represented as a magnetic-field-free, constant temperature, spherically symmetric region of fully ionized hydrogen gas, whose electron density varies according to the formula of Baumbach, as corrected by Van de Hulst and Allen. The ray theory of the propagation of radio-frequency radiation through such a solar atmosphere is then examined critically, and the appropriate equations and methods of calculation are developed to compute the ray trajectories of those rays which can reach the earth, and also the values of opacity along them. It is concluded that at 50 mc: (1) The effects of varying index of refraction cannot be negelected. (2) Radiation from the quiet sun arises wholly from the corona. (3) There is no limb brightening.

31. SOLAR RADIATION AT A WAVELENTGH OF 3.15 CM

F. T. Haddock
(Naval Research Laboratory, Washington, D. C.)

Spot measurements of solar radiation at 3.15 cm wavelength on 285 days during 1947–1949, continuous recordings during 163 days in 1950, and for several months in 1951, are discussed. The variation of this solar radiation is compared with other evidences of solar activity. Only a few outbursts of emission were noted during 1947–1949, because of the small amount of observing time. Since January, 1950, a few dozen bursts have been recorded. Several of these were greater than ten times the intensity of the quiet sun value. The occurrence and structure of bursts are compared with bursts at other frequencies, solar flares, etc.

32. OUTBURSTS OF SOLAR RADIATION OBSERVED AT 8.5 MM WAVELENGTH

J. P. Hagen and N. Hepburn
(Naval Research Laboratory, Washington, D. C.)

Bursts of solar radiation at 8.5 mm wavelength have recently been observed. The first observation was on May 8, 1951, at the time of a solar flare observed on the limb of the sun. Subsequent observations confirm the existence of the bursts and reveal information concerning the character of the bursts at 8 mm as contrasted with bursts observed at nearly the same time at longer wavelengths.

33. A NEW TECHNIQUE IN RADAR RECEIVER PERFORMANCE MEASUREMENT

J. H. Vogelman
(Rome Air Development Center, Rome, N. Y.)

A microwave impulse generator, which produces a uniform output amplitude from the very-low frequencies to above 30 kmc, has been developed for radar receiver testing. This impulse generator is essentially an open-circuited air-dielectric transmission line which is charged to a given potential and then discharged into a finite impedance. The output of this impulse generator when fed through a receiver can be precisely determined as a function of the charging voltage in terms of decibels above theoretical noise. Three basic methods of measurement will be provided, one utilizing the *A* scope presentation of the radar system, and the other two utilizing meter indicators.

34. A SLOPE METHOD OF MEASURING PULSE-NOISE SPECTRA

J. R. Burnett, G. R. Cooper, and R. H. George
(Purdue University, Lafayette, Ind.)

The slope of the response of the measurement equipment to a step function is the basis of a method for measuring frequency spectra of pulse-type noise generators.

The measuring equipment is a frequency selective system such as is used in bandwidth measurements of frequency spectra. It is shown that the frequency spectrum at the selective frequency of the measuring equipment is given by the product of the height of the noise response times the signal generator output, all divided by the product of the charging voltage times the maximum slope of the step function response. A means of obtaining the necessary step function is given. Experimental results are shown which substantiate the theory.

35. STUDIES OF NOISE FROM MICROWAVE OSCILLATORS

Winston Gottschalk
(Raytheon Manufacturing Company, Waltham, Mass.)

As a first problem in a comprehensive program of noise study, the characteristics of a magnetron oscillator are investigated theoretically. A companion program is also outlined dealing with the basic requirements and design of apparatus needed in the experimental portions of the program. A preliminary discussion of certain fundamental aspects of noise is included from the point of view of the modern theory of random processes. Models of a microwave generator, based on experimental observations, are being constructed and investigated. A review of the experimental studies is included along with a critical discussion of the more difficult experimental and theoretical features of the program.

36. HIGH-*Q* MEASURMENTS IN THE 1000-MEGACYCLE RANGE

A. Horvath
(Federal Telecommunications Laboratories, Nutley, N. J.)

The problem of measuring the unloaded *Q* of various cavities is one that requires several precautions quite often neglected when only one or two answers are required over rather long intervals. If the unloaded *Q* is high, the errors in measurements may be as large as plus or minus 50 per cent from the true value. In this paper, several procedures are given from which an appropriate choice may be made, depending on the *Q* to be measured. The errors in results appear to be in the order of plus or minus 4 per cent.

37. ON THE PRESENTATION OF MICROWAVE CIRCUITS BY LUMPED ELEMENTS

Georg Goubau
(Signal Corps Engineering Laboratories, Fort Monmouth, N. J.)

Microwave circuits are usually represented by equivalent circuits of lumped elements in order to make them accessible to the familiar network analysis. The values of the lumped elements representing a cavity, depend on the type of equivalent circuit used. Those equivalent circuits are preferable in which the values of the lumped elements depend only on the dimensions of the part of the microwave circuit which they represent, and not on the ensemble.

The fundamentals of this theory are outlined, and tables of the quantities in the corresponding lumped circuit representation of cavities, waveguides, and coupling elements are presented.

38. THE EFFECT OF LAMINAR FLOW ON THE DURATION OF METEOR ECHOES

T. N. Gautier
(Central Radio Propagation Laboratory, Washington, D. C.)

An analysis is made of the effect of simple laminar flow acting together with diffusion upon the duration of radar echoes from meteoric ionization. Under appropriate conditions laminar flow may increase the duration by as much as a factor of four. Variations of flow gradient with altitude might produce "stratified" echoes such as have been observed. The dependence of duration upon the square of the radio wavelength predicted by ordinary diffusion theory is modified if laminar flow is considered.

39. THE POLARIZATION CHARACTERISTICS OF METEORIC ECHOES

A. Manning and M. E. Van Valkenberg
(Stanford University, Stanford, Calif.)

The relative amplitudes of the two characteristic waves at a frequency of 23.1 mc returned from meteoric ionization columns, is studied by means of an experiment involving the use of helical transmitting and receiving antennas. Circular polarization is generated at the sender.

The long-duration fading meteors commonly retain the linear polarized behavior for much of their duration, while the rapidly decaying echoes quickly demonstrate circularity. The polarization behavior suggests the existence of greater ionization densities than usually assumed, and does not appear to be explainable in terms of previously existing theories.

40. METEORIC ECHO MEASUREMENT OF IONOSPHERIC DRIFT AND TURBULENCE

L. A. Manning and A. M. Peterson
(Stanford University, Stanford, Calif.)

The Doppler frequency shift imparted to a wave which is returned from a fully formed meteoric ionization column is a measure of the velocity component of the trail in the direction towards the observer. Statistical considerations show that the accuracy obtained in determining average drift velocity ordinarily corresponds to an error of about 420/(number of meteors) 1/2 kilometers per hour. Study of Doppler shift versus meteoric elevation angle can be used to determine the root-mean-square horizontal and vertical components of turbulent velocity. The method suggests means for finding the detailed structure of the wind at heights from 80 to 120 kilometers. Evidence pointing to the existence of a complex stratified region is presented.

41. SYSTEMATIC IONOSPHERIC WINDS

Reynold Greenstone
(Central Radio Propagation Laboratory, Washington, D. C.)

A study of fading patterns of radio waves reflected by the ionosphere has led to the determination of horizontal drifts in the ionosphere. Equipment has been operated at 2.3 mc at the National Bureau of Standards since March, 1949. The wind direction exhibits diurnal characteristics which change with the seasons. Apparent wind speeds may range up to 300 m/sec, but are predominantly in the range from 50 to 100 m/sec. Marked changes in the character of the winds are associated with the transition from *E-F*-region reflections. Good agreement is found between wind directions and speeds observed at Washington, D. C., and those observed at Cambridge, England.

42. EXPERIMENTAL DETERMINATION OF RATES OF DECAY OF METEORIC ECHOES AS FUNCTIONS OF WAVE FREQUENCY AND HEIGHT

V. C. Pineo
(Central Radio Propagation Laboratory, Washington, D. C.)

Radar-type reflections from ionized meteor trails are used to determine the rates of decay of meteoric echoes as functions of wave frequency and height. Experimental data showing the relative rates of decay observed at 27 mc, 41 mc, and 54 mc, and the rate of decay at 27 mc as a function of height, are presented. The possibility of determining diffusion coefficients from these data is discussed.

43. TECHNIQUES IN METEOR IONIZATION STUDIES AT 23 MEGACYCLES

O. G. Villard, Jr., and A. M. Peterson
(Stanford University, Stanford, Calif.)

Experimental measurement of the time variation of phase, amplitude, and polarization of 23.1-megacycle meteor echoes is compared with the reported results of workers using other frequencies. Pulse-Doppler apparatus used in making these measurements is described, and sample records shown. Direction and height-finding equipment needed for wind measurements are discussed, together with ancillary circuitry such as Doppler frequency multipliers and vector displays.

IRE People

Walter J. Seeley (A'22–SM'46), Professor and Head of the Electrical Engineering Department of Duke University, was recently appoined chairman of the student development committee of the Engineer's Council for Professional Development on which he also represents the AIEE. The committee is charged with co-ordinating and administering those relations between engineering schools, engineering societies, and industry which will promote the professional development of student engineers. As research and development director for the college of engineering at Duke University, he will have charge of co-ordinating research activities within the college and with other organizations.

Professor Seeley was born on November 30, 1894, in Hazelton, Pa. He studied electrical engineering at the Brooklyn Polytechnic Institute where he received the E.E. degree in 1917. In 1924 he received the M.S. degree from the University of Pennsylvania. He was appointed to the faculty of the University of Pennsylvania in 1920, specializing in measurements and vacuum tubes, and later joined the staff of Duke University.

Professor Seeley has been active as the IRE Representative at Duke University in 1942–1948, and 1949–1951. He has also served on the IRE Education Committee.

⁘

Harrison Johnston (A'51) has been appointed manager of the product engineering division of the Ampex Electric Corporation in Red Wood City, Calif. Prior to this appointment Mr. Johnston was associated with the General Electric Corporation for 12 years where he became that company's sales manager of the laboratory products section, and later transferred to their San Francisco office.

Harrison Johnston

A native of Missouri, Mr. Johnston graduated from Princeton University in 1939 with the B.S.E. degree. He has won recognition for his lectures and writings on special electrical and electronic apparatus. Mr. Johnston is a member of the American Institute of Electrical Engineers.

IRE People

Rear-Admiral Stanley F. Patten, (M'50–SM'50) U.S.N. (Ret.), has been elected Vice-President of the Allen B. Du Mont Laboratories, Inc., it was announced recently by Dr. Allen B. Du Mont, President. Admiral Patten has been with the Du Mont organization as assistant to the president since July, 1947. He also has been the director of mobilization planning for the government department of the Du Mont Laboratories.

Stanley F. Patten

Admiral Patten, a native of New York, was born in May, 1896. After completing a course at the Marconi School of Instruction, he became a radio operator with the Marconi Radio Telegraph Company in 1914, and in 1915, he was a radio electrician at the New York State Nautical Schoolship at Newport. Admiral Patten served in the United States Navy from 1917–1947, as a line officer, specializing in electronics and communications. In 1925-1927, he completed post graduate work at the United States Naval Academy and Yale University. During World War I, he served in the North Atlantic and European waters, and during World War II, he served as assistant head of the Radio Division, Bureau of Ships, from 1940–1943. In May, 1943 he was ordered to command the U.S.S. *Rocky Mount*, which served as flagship for the amphibious forces in the Pacific during the Marshall and Mariannas Islands invasions.

He participated in the Kwajalein, Saipan, and Leyte Gulf campaigns, retiring from active duty with the Navy in January, 1947. His last assignment before retirement was that of District Communications officer of the 13th Naval District at Seattle, Wash.

❖

Alexander A. Kiriloff (M'50) has recently been appointed research engineer in charge of research and development of microwaves, vhf, and electronic test equipment, at the Sherron Electronic Company, Brooklyn, N. Y.

A. A. Kiriloff

Born in Tomsk, Russia, Mr. Kiriloff emigrated to France in 1922. He studied at the Ecole Superieure d'Électricité, Radio Section, in Paris, and received the radio engineer degree in 1926. For 25 years he worked in several French companies in the interests of microwaves, vhf, and electronics, and in 1936 he was invited to the United States as consulting research engineer by the V. S. Johnson Laboratories in Chicago, where he remained for 3 years. During 1947–1949, Mr. Kiriloff was a professor at the French Polytechnical Industrial Institute, returning to this country in 1949.

Mr. Kiriloff holds several patents on radio and electronic devices and is the author of several radio electronic books and articles in French technical and scientific periodicals. He is a member of the Société Française des Radioelectriciens and the Société Française de Physique.

❖

F. T. Budelman (A'41) has been named president of the newly formed Budelman Radio Corporation at Stamford, Conn. Previously, Mr Budelman was associated for many years with the Link Radio Corporation in which he was active in the development of FM communication equipment for land-mobile services and for important military applications such as multi-channel radio relay systems.

F. T. Budelman

A native of Newark, N. J., Mr. Budelman studied electrical engineering at Cornell University where he received the E.E. degree in 1931. Mr. Budelman is also a member of the American Institute of Electrical Engineers.

❖

Bernard Hecht (M'45) has been appointed general manager of the Starrett Television Corporation, New York, N. Y., it was recently announced. He will direct and co-ordinate all phases of management of that concern, with special emphasis on quality control for government operations.

Bernard Hecht

Mr. Hecht received his B.E.E. degree from the School of Technology, City College of New York, and later received the M.S. degree from the University of Pennsylvania. At the outbreak of World War II, he was a civilian officer in charge of radio inspection for the Signal Corps, and in 1943 he was selected to represent the U. S. Army-Navy Specification Program for electronic components, embracing the standardization of tubes, resistors, capacitors, and transformers. Serving in the army, Mr. Hecht was relieved of his military status when he was assigned to aid in the reconversion to peacetime production of the plant operation of the International Resistance Company in Philadelphia.

Mr. Hecht is the vice-chairman of the IRE Professional group on Quality Control, and a senior founder member of the American Society for Quality Control.

❖

Maurice Harp (A'49) has joined the engineering staff of the Lenkurt Electric Company, San Carlos, Calif. His function will be that of applications engineer for the development of FM and single-side-band space-carrier equipment.

Maurice Harp

A native of California, Mr. Harp has been the chief engineer of the Globe Wireless Company, and a flight radio officer with Pan American Airways. During the war he was with the Army's Trans-Pacific Communications System. Prior to his present appointment, Mr. Harp was chief engineer in the Heintz and Kaufman Equipment Division of the Robert Dollar Company. He is radio amateur, W6KJG.

❖

A. V. Platter (A'49), an engineer of the International Business Machines Corporation, died recently in Poughkeepsie, N. Y. His death was the result of his service in the Armed Forces of World War II.

Mr. Platter, a native of Altus, Okla., was born on November 10, 1920, and received the B.E.E. degree at the Lawrence Institute of Technology in June, 1941. He also studied electronics and advanced mathematics at the University of Maryland. He joined the IBM Corporation in Detroit, Mich., and in 1947 he became a technical engineer in the electron and tube development and production section of IBM in Poughkeepsie. From 1943–1946, Mr. Platter served with the United States Navy in the Development and Underwater Ordnance and V-T Fuze Program, at the Naval Ordnance Laboratory, Washington, D. C.

Mr. Platter was the Secretary-Treasurer of the IRE Mid-Hudson Subsection, and was active in the formation of this Subsection.

Books

Electric Transmission Lines by Hugh Hildreth Skilling

Published (1951) by McGraw-Hill Book Company, Inc., 330 West 42 Street, New York 18, N. Y. 414 pages +8-page index +14-page appendix +xiii pages. 172 figures. 9×6. $6.50.

Hugh Hildreth Skilling is Professor of Electrical Engineering at Stanford University, Stanford, Calif.

This new volume, the outgrowth of a plan of presentation developed through ten years of teaching, is an excellent and thoroughly up-to-date textbook written especially for undergraduate students of electrical and electronic engineering. Free from inconsistencies and unnecessary repetitions of subject matter, and, with its information reasonably complete, the book is ideally suited to home study. Although it is elementary and not intended to train specialists, its unified treatment of theory and application, which is sufficient to the extent needed by electrical engineers, should appeal to practicing engineers.

It is assumed that the reader is familiar with ordinary circuit theory involving lumped constants and that he has a knowledge of differential and integral calculus. The book can be read consecutively, but later chapters are sufficiently independent of certain preceding chapters so that they may be read separately. The first eight chapters present the theory of circuits with distributed constants; the next five chapters apply this theory successively to telephone lines, filters, power lines, radio-frequency lines, and waveguides. The last chapter treats transient-traveling waves.

The first five chapters cover basic theory, and are essential for all that follows. Chapters 6 and 7 deal with line constants, namely, inductance, capacitance, resistance, (including a treatment of skin effect), and insulation loss. Chapter 8 on artificial line concepts is essential to chapters 9 and 11 on telephone and power lines. Chapter 10 on filters is preferably preceded by Chapter 9. A table of collected formulas of transmission lines, which is on the inside of the front cover, is convenient, as is the table on the relations of trigonometric and hyperbolic functions found on the inside of the back cover.

H. S. Black
Bell Telephone Laboratories
Murray Hill, N. J.

Communication Networks and Lines by Walter J. Cramer

Published (1951) by Harper & Brothers Publishers, 49 East 33 Street, New York 33, N. Y. 329 pages +5-page index +19-page appendix +x pages. 9¼×6. $6.00.

The author is Professor of Communication Engineering, Head of the Department of Electrical Engineering, University of Maine, Orono, Me.

The publisher's jacket of this book says, "This is a comprehensive and unusually thorough mathematical treatment of its subject." Indeed it is this, but almost to the point where it has made virtue a fault. The book is actually a collection of detailed design formulas with instructions on how to use them. One will also find here the detailed circuit equations for an anti-side tone telephone subset. However, one will not find a proof of the Superposition Theorem. (One is referred, therefore, to Guilleman.)

This is useful for those who want a handy reference on the design of wave filters for given attenuation (although very little attention is given to phase characteristics), or transmission lines of the standard telephone types. The jacket also states, "Designed as a basic text for the communications option," and this reviewer questions as to how much time can be found in a crowded curriculum for one to spend so much time with this phase.

The book is useful for those having sufficient interest in this narrow field, and accepting the general thesis that such a text as this is needed, then it can be said that the job is very well done. The exposition is clear, the various designs are well illustrated by many practical examples, the book is well ordered, and remarkably free from typographical errors.

Knox McIlwain
Hazeltine Electronics Corp.
58-25 Little Neck Pkwy.
Little Neck, N. Y.

Guide to Broadcasting Stations, Sixth Edition

Published (1951) by Dorset House, Stamford Street, London, S.E.1, Eng. 94 pages. 5¼×4¼. Price, 2s. 0d. Postage 2d.

Despite the efforts of international bodies and representations from individual governments, the congestion in the long-wave-medium-wave broadcasting bands in Europe is eased but very little. There are nearly 200 stations working on unauthorized frequencies. Operating details of these stations and of the 350 or more authorized transmitters are included in this book, together with details of over 1400 short-wave broadcasting stations operating in 117 countries. The stations are listed both geographically and in order of frequency, and the data have been checked against the frequency measurements made at the B.B.C. receiving station at Tatsfield.

The list giving operating details of nearly 50 vhf broadcasting stations in Europe gives some indication of the growth of this form of broadcasting since the publication of the last edition which listed eleven. Details of 14 European television transmitters and a number of consol and standard frequency stations are also included.

The contents include: Long- and medium-wave European stations, with frequencies, wavelengths, and powers; A geographical list of long- and medium-wave European stations, with frequencies; Short-wave stations of the world, with frequencies, wavelengths, powers, and call signs; A geographical list of short-wave stations, with frequencies; European television stations; Consol and standard frequency stations; Meter-wave European stations; British amateur transmitting frequencies international allocation of call signs; Standard time; and Wavelength and frequency conversion, formulas and tables.

Magnetic Materials by F. Brailsford

Published (1951) by John Wiley & Sons, Inc., 440 Fourth Avenue, New York 16, N. Y. 150 pages +6-page index +ix pages. 86 figures. 4½×6¾. $1.50.

F. Brailsford is with the Research Department, Metropolitan-Vickers Electrical Company Ltd., Manchester, Eng.

This pocket-size monograph has been prepared with the objective of giving the advanced student, the research worker, and those concerned with the technological applications of magnetic materials, a comprehensive outline of the present state of knowledge on magnetic materials. With a rather elementary introduction, chapters follow on ferromagnetism, properties and theory of single crystals, factors affecting magnetic properties, iron and silicon-iron alloys, nickel-iron and other alloys, and permanent magnet materials. References to original works are given with each chapter.

The subject of ferromagnetism and magnetic materials has grown important in the light of the recent research and engineering requirements, although too complex for adequate treatment in general text books for electrical and electronic engineers, metallurgists, and physicists, who should have at least a basic understanding of the problems involved and the present state of the development. The reviewers agree that the author has given a most interesting and lucid account of the theory of ferromagnetism and of the factors affecting magnetic properties, particularly with regard to silicon-iron and nickel-iron alloys. It seems unfortunate, however, that, since this is a second edition of a 1948 printing, the author did not expand the text slightly and include topics of such theoretical and technical importance as fine powder permanent magnets, grain-oriented nickel-iron, and ferrite materials, all of which are conspicuously absent in the text as well as in the literature references.

Beyond the criticisms mentioned, the reviewers consider the book an interesting addition to the library of anyone concerned with the subject, and to those who may like to carry pocket-size, spare time literature.

Harold A. Zahl
Eberhard Both
Signal Corps Engineering Laboratories
Fort Monmouth, N. J.

Sections and Subsections*

Chairman		Secretary
R. L. Burtner Goodyear Aircraft Corp. 1210 Massillon Rd. Akron, Ohio	Akron (4)	R. M. Byrne 316 Melbourne Ave. Akron 3, Ohio
E. S. Lammers, Jr. Westinghouse Electric Corp. Box 4808 Atlanta 2, Ga.	Atlanta (6)	D. B. Buchanan 5130 Powers Ferry Rd., N.W. Atlanta, Ga.
D. G. Little 408 Old Orchard Rd. Baltimore 29, Md.	Baltimore (3)	G. R. White Bendix Radio Div. Towson 4, Md.
E. D. Coburn Box 793 Nederland, Texas	Beaumont-Port Arthur (6)	C. B. Trevey 2555 Pierce St. Beaumont, Texas
L. E. Packard Technology Instrument Corp. 1058 Main St. Waltham 54, Mass.	Boston (1)	Beverly Dudley The Technology Review Mass. Inst. of Tech. Cambridge 39, Mass.
G. J. Andrews Fernandez Spiro 286 Acassuso, F.C.N.G.B.M. Buenos Aires, Argentina, S.A.	Buenos Aires	I. C. Grant San Martin 379 Buenos Aires, Argentina, S.A.
R. E. Frazier R.D. 1. Center St. East Aurora, N. Y.	Buffalo-Niagara (4)	W. K. Squires 115 St. John's Ave. Kenmore 23, N. Y.
V. R. Hudek 137 29 St. Drive S.E. Cedar Rapids, Iowa	Cedar Rapids (5)	R. M. Mitchell 357 Garden St., S.E. Cedar Rapids, Iowa
Leroy Clardy Research Labs. Swift & Co. U.S. Yards Chicago 9, Ill.	Chicago (5)	A. A. Gerlach 4020 Overhill Ave. Chicago 34, Ill.
Calvin Bopp 1114 Maycliff Pl. Cincinnati 30, Ohio	Cincinnati (5)	R. A. Maher 1329 Arlington St. Cincinnati 25, Ohio
T. B. Friedman 1900 E. 30 St. Cleveland 14, Ohio	Cleveland (4)	A. L. Hammerschmidt 111 Westbridge Dr. Berea, Ohio
D. C. Cleckner 1376 Aberdeen Ave. Columbus 3, Ohio	Columbus (4)	J. H. Jaeger Ohio Bell Telephone Co. 42 E. Gay St. Columbus 15, Ohio
L. E. Williams Dept. of Elec. Eng. University of Connecticut Storrs, Conn.	Connecticut Valley (1)	H. E. Rohloff The Southern New England Tel. Co. 227 Church St. New Haven, Conn.
E. A. Hegar 802 Telephone Bldg. Dallas 2, Texas	Dallas-Fort Worth (6)	J. K. Godbey Magnolia Pet. Co. Field Research Lab. Box 900 Dallas 9, Texas
Joseph General 1116 Lexington Ave. Dayton 7, Ohio	Dayton (5)	A. H. Petit 444 E. Peach Orchard Ave. Dayton 9, Ohio
E. A. Post 3037 Dexter Ave. Denver 7, Colo.	Denver (5)	S. A. Harvey Signal Officer Fitzsimmons Army Hospital Denver, Colo.
Otto A. Tennant 1408 Walnut St. Des Moines, Iowa	Des Moines-Ames (5)	A. D. Parrott 1515—45 Des Moines 11, Iowa
K. R. Schmeisser 13117 La Salle Blvd. Detroit 6, Mich.	Detroit (4)	F. W. Chapman 1756 Graefield Rd. Birmingham, Mich.
W. R. Rolf 364 E. 5th St. Emporium, Pa.	Emporium (4)	L. R. Maguire 4 E. 6 St. Emporium, Pa.
J. F. Sears 1736 Washington Ave. Evansville 14, Ind.	Evansville-Owensboro (5)	F. A. Gehres 2232 E. Powell Evansville 14, Ind.
J. F. Conway, Jr. 4610 Plaza Dr. Fort Wayne, Ind.	Fort Wayne (5)	L. F. Mayle The Magnavox Co. Fort Wayne 4, Ind.
J. S. Turner 3422 Alani Dr. Honolulu, T.H.	Territory of Hawaii (7)	S. H. Lewbel P.O. Box 3564 Honolulu, T.H.
S. A. Martin, Jr. Box 2180, Rm. 209 Houston 1, Texas	Houston (6)	H. T. Wheeler 802 N. Avenue "A" Bellaire, Texas
F. O. Meadows 1449 N. Emerson Indianapolis, Ind.	Indianapolis (5)	R. T. Van Niman 4441 Indianola Ave. Indianapolis 5, Ind.
J. H. Gregory 200-A Ellis China Lake, Calif.	Inyokern (7)	W. E. Vore 420-A Nimitz Ave. China Lake, Calif.
C. L. Foster 1901 W. 73 Terrace Kansas City 5, Mo.	Kansas City (5)	Mrs. G. L. Curtis Radio Industries, Inc. 1307 Central Ave. Kansas City 2, Kan.
G. R. Hosker c/o Richards-Wilcox Canadian Ltd. London, Ont., Canada	London, Ontario (8)	Glenn Robitaille 19 McKinnon Place London, Ont., Canada
J. J. Fiske 128 W. Las Flores Ave. Arcadia, Calif.	Los Angeles (7)	Ellis King 3171 Federal Ave. Los Angeles 34, Calif.
R. B. McGregor 2100 Confederate Pl. Louisville, Ky.	Louisville (5)	M. I. Schwalbe Nichols Veterans Hospital Louisville 2, Ky.
P. H. Craig 1042 Catalonia Ave. Coral Gables, Fla.	Miami (6)	F. B. Lucas 5340 Davis Rd., S.W. South Miami 43, Fla.
W. H. Elliot 4747 N. Larkin St. Milwaukee 11, Wis.	Milwaukee (5)	D. A. Weller c/o WISN 540 N. Plankinton Ave. Milwaukee 1, Wis.
N. R. Olding Canadian Broadcasting Corp. Box 6000 Montreal, P.Q., Canada	Montreal, Quebec (8)	R. W. Cooke Canadian Marconi Co. 2442 Trenton Rd. Montreal, P. Q., Canada
B. J. Bittner 3110—42 Pl., Sandia Base Albuquerque, N. M.	New Mexico (7)	G. A. Arnot, Jr. 401 N. 6 St. Albuquerque, N. M.
J. H. Mulligan, Jr. 14 Mitchell Pl. East Orange, N. J.	New York (2)	H. S. Moncton Sylvania Elec. Prods. Inc. Bayside, L. I., N. Y.
C. E. Hastings 117 Hampton Rd. Hampton, Va.	North Carolina-Virginia (3)	P. F. Hedrick 2472 Maplewood Ave. Winston-Salem 7, N. C.
C. L. Farrar 927 Chautauqua Norman, Okla.	Oklahoma City (6)	O. A. Nash c/o C.A.A., AC-60 Box 1082 Oklahoma City, Okla.
F. W. Norris 3303 Woods Ave. Lincoln, Neb.	Omaha-Lincoln (5)	C. W. Rook Dept. of Elec. Eng. University of Nebraska Lincoln 8, Neb.
W. R. Wilson c/o Royal Canadian Mounted Police Ottawa, Ont., Canada	Ottawa, Ontario (8)	D. V. Carroll Box 527 Ottawa, Ont., Canada
L. M. Rodgers 400 Wellesley Rd. Philadelphia 19, Pa.	Philadelphia (3)	J. G. Brainerd Moore School of Elec. Eng. Univ. of Pennsylvania Philadelphia 4, Pa.
G. C. Rich Box 737 Scottsdale, Ariz.	Phoenix (7)	A. M. Creighton, Jr. 2221 E. Osborn Rd. Phoenix, Ariz.
W. P. Caywood, Jr. 23 Sandy Creek Rd. Pittsburgh 21, Pa.	Pittsburgh (4)	V. G. Shaw 17 Franklin Rd. Pittsburgh 35, Pa.
L. C. White 3236 N. E. 63 Ave. Portland 13, Ore.	Portland (7)	G. C. Ellison 11310 S. E. Market St. Portland 16, Ore.
W. H. Bliss 300 Western Way Princeton, N. J.	Princeton (3)	J. S. Donal, Jr. RCA Labs. Princeton, N. J.
J. A. Rodgers Huntington Hills Rochester 9, N. Y.	Rochester (4)	J. C. O'Brien 283 Malden St. Rochester 13, N. Y.
W. F. Koch 1340-33 St. Sacramento 16, Calif.	Sacramento (7)	H. C. Slater 1945 Bidwell Way Sacramento 18, Calif.
H. G. Wise 1705 N. 48 St. East St. Louis, Ill.	St. Louis (5)	E. F. O'Hare 8325 Delcrest Dr. University City 24, Mo.
L. S. Cole 696 E. 4 North St. Logan, Utah	Salt Lake City (7)	E. C. Madsen 739 Scott Ave. Salt Lake City 6, Utah

* Numerals in parentheses following Section designate Region number.

Sections and Subsections

Chairman		Secretary
W. J. Hamm St. Mary's University San Antonio 7, Texas	San Antonio (6)	Paul Tarrodaychik 215 Christine Dr. San Antonio 10, Texas
J. P. Day 3565 Ingraham St. San Diego 9, Calif.	San Diego (7)	I. L. McNally 2714 Azalea Dr. San Diego 6, Calif.
A. R. Ogilvie 505 Darrell Rd. Hillsborough Burlingame, Calif.	San Francisco (7)	W. E. Noller 1229 Josephine St. Berkeley 3, Calif.
E. S. Sampson 1402 Union St. Schenectady 8, N. Y.	Schenectady (2)	D. E. Norgaard 1908 Townsend Rd. Schenectady 9, N. Y.
J. E. Hogg General Electric Co. 710 2 Ave. Seattle 11, Wash.	Seattle (7)	H. M. Swarm Dept. Elec. Eng. Univ. of Washington Seattle 5, Wash.
D. C. Pinkerton 312 Cherry Rd. Syracuse 9, N. Y.	Syracuse (4)	Samuel Seely College Applied Science Syracuse University Syrcause 10, N. Y.
H. N. Rowe Rowe Industries 1702 Wayne St. Toledo 9, Ohio	Toledo (4)	R. G. Larson 2647 Scottwood Ave. Toledo 10, Ohio
George Sinclair Dept. of Elec. Eng. Univ. of Toronto Toronto, Ont., Canada	Toronto, Ontario (8)	J. R. Bain Dominion Sound Equip., Ltd. 386 Victoria St. Toronto, Ont., Canada
Daniel Silverman Stanolind Oil & Gas Co., Research Library Box 591 Tulsa 2, Okla.	Tulsa (6)	C. E. Buffum Box 591 Tulsa 2, Okla.
A. A. Cohen Eng. Research Assoc. 1902 W. Minnehaha Ave. St. Paul 4, Minn.	Twin Cities (5)	O. W. Muckenhirn Dept. of Elec. Eng. University of Minnesota Minneapolis 14, Minn.
G. C. Chandler 846 Howe St. Vancouver, B. C., Canada	Vancouver (8)	D. D. Carpenter 1689 W. 29 Ave. Vancouver, B. C., Canada
P. De Forrest McKeel 9203 Sligo Creek Pkwy. Silver Spring, Md.	Washington (3)	H. P. Meisinger Hull Rd. & Old Court-house Rd. Route 3 Vienna, Va.
F. H. Scheer College Park Lewisburg, Pa.	Williamsport (4)	B. H. Bueffel, Jr. Dept. of Elec. Eng. Bucknell University Lewisburg, Pa.
D. G. Harmon Dept. of Elec. Eng. Texas Tech. College Lubbock, Texas	Amarillo-Lubbock (6) (Dallas-Ft. Worth Subsection)	R. B. Spear 510 E. Hill St. Brownfield, Texas
L. H. Stantz 168 Moeller St. Binghamton, N. Y.	Binghamton (4) (Syracuse Subsection)	E. L. Pittsley Reynolds Rd. R. D. 1 Johnson City, N. Y.
W. R. Smith Dept. of Elec. Eng. Pennsylvania State College State College, Pa.	Centre County (4) (Emporium Subsection)	H. F. Wischnia Dept. of Elec. Eng. Pennsylvania State College State College, Pa.
J. H. Pickett Aerovox Canada Ltd. 1551 Barton St., E. Hamilton, Ont., Canada	Hamilton (8) (Toronto Subsection)	G. F. Beaumont 1932 King St. E. Hamilton, Ont., Canada
E. E. Spitzer c/o RCA Victor Div. Radio Corp. of America Lancaster, Pa.	Lancaster (3) (Philadelphia Subsection)	Werner Rueggeberg Research Lab. Armstrong Cork Co. Lancaster, Pa.
H. E. Webber Sperry Gyroscope Co. Lake Success, L. I., N. Y.	Long Island (2) (New York Subsection)	J. F. Craib R. D. 1 Hicksville, L. I., N. Y.
A. L. Samuel Electronics Labs. I.B.M. Corp. Plant 2, Dept. 532 Poughkeepsie, N. Y.	Mid-Hudson (2) (New York Subsection)	
B. V. Blom 38 Lafayette St. Rumson, N. J.	Monmouth (2) (New York Subsection)	H. S. Bennett 31 Cedar Ave., Apt. 23 Long Branch, N. J.
J. F. Morrison Bell Telephone Labs. Whippany, N. J.	Northern N. J. (2) (New York Subsection)	P. S. Christaldi Box 145 Clifton, N. J.
J. M. Pettit Dept. of Elec. Eng. Stanford Univ. Stanford, Calif.	Palo Alto (7) (San Francisco Subsection)	H. M. Stearns 99 Washington St. San Carlos, Calif.
R. I. Cole Griffiss AFB Rome, N. Y.	Rome (4) (Syracuse Subsection)	G. E. Merer 112 Ringdahl Court Mohawk Gardens Rome, N. Y.
George Weiler 1429 E. Monroe South Bend, Ind.	South Bend (5) (Chicago) Subsection)	A. R. O'Neil Apt. 302 6712 Lake St. Falls Church, Va.
R. M. Wainwright Dept. of Elec. Eng. University of Illinois Urbana, Ill.	Urbana (5) (Chicago Subsection)	M. H. Crothers Dept. of Elec. Eng. University of Illinois Urbana, Ill.
	Winnipeg (8) (Toronto Subsection)	W. F. Souch Canadian Marconi Co. 149 Portage Ave., E. Winnipeg, Canada

Professional Groups

	Chairman
Airborne Electronics	John E. Keto Wright Field Dayton, Ohio
Antennas and Propagation	George Sinclair Dept. of Elec. Eng. University of Toronto Toronto, Ont. Canada
Audio	B. B. Bauer Shure Brothers, Inc. 225 W. Huron St. Chicago 10, Ill.
Broadcast and Television Receivers	D. D. Israel Emerson Radio & Phonograph Co. 111 8 Ave. New York 11, N. Y.
Broadcast Transmission Systems	Lewis Winner *TeleVision Engineering* 52 Vanderbilt Ave. New York 17, N. Y.
Circuit Theory	J. G. Brainerd University of Pennsylvania Philadelphia, Pa.
Electron Devices	George D. O'Neill Sylvania Electric Products Co. Bayside, L. I., N. Y.
Electronic Computers	M. M. Astrahan I.B.M. Plant no. 2 Poughkeepsie, N. Y.
Engineering Management	Ralph I. Cole Griffiss Air Force Base Rome, N. Y.
Industrial Electronics	Eugene Mittelmann 549 West Washington Blvd. Chicago 6, Ill.
Information Theory	Nathan Marchand Sylvania Electric Products Inc. Bayside, L. I., N. Y.
Instrumentation	Ernst Weber Polytechnic Institute of Brooklyn Brooklyn, N. Y.
Nuclear Science	Dr. L. R. Hafstad Atomic Energy Comm. Rm. 132, 1901 Constitution Ave. Washington, D. C.
Quality Control	R. F. Rollman Allen B. DuMont Laboratories 1000 Main Ave. Clifton, N. J.
Radio Telemetry and Remote Control	W. J. Mayo-Wells The Johns Hopkins University Silver Spring, Md.
Vehicular Communications	Austin Bailey American Telephone and Telegraph Co. 195 Broadway New York, N. Y.

Abstracts and References

Compiled by the Radio Research Organization of the Department of Scientific and Industrial Research, London, England, and Published by Arrangement with That Department and the *Wireless Engineer*, London, England

NOTE: The Institute of Radio Engineers does not have available copies of the publications mentioned in these pages, nor does it have reprints of the articles abstracted. Correspondence regarding these articles and requests for their procurement should be addressed to the individual publications, not to the IRE.

The number in heavy type at the upper left of each Abstract is its Universal Decimal Classification number and is not to be confused with the Decimal Classification used by the United States National Bureau of Standards. The number in heavy type at the top right is the serial number of the Abstract. DC numbers marked with a dagger (†) must be regarded as provisional.

The Annual Index to these Abstracts and References, covering those published in the PROC. I.R.E. from February, 1950, through January, 1951, may be obtained for 2s.8d. postage included from the *Wireless Engineer*, Dorset House, Stamford St., London S.E., England. This index includes a list of the journals abstracted together with the addresses of their publishers.

ACOUSTICS AND AUDIO FREQUENCIES

534.321.9 **2885**

Heavy-Duty Quartz Ultrasonic Generator—H. H. Rust. (*Naturwiss.*, vol. 38, pp. 235–236; May, 1951.) Quartz plates, with electrodes consisting of grids of parallel thin copper wires, were found to stand up to heavy duty better than types with metal-plate electrodes.

534.321.9 **2886**

Research and Analysis relating to Ultrasonics in Everyday Life—P. Chavasse and R. Lehmann. (*Ann. Télécommun.*, vol. 6, pp. 98–101; April, 1951.) Difficulties in the analysis of sonic and ultrasonic vibrations are discussed, and the heterodyne frequency analyzer noted in 936 of 1950 (Pimonov) is briefly described. Examples of the occurrence of ultrasonic vibrations in nature and in industry are given.

534.41.087.252 **2887**

Musical Stroboscopes and Strobographs—V. Gavreau. (*Ann. Télécommun.*, vol. 6, pp. 117–121; May, 1951.) Description of the principle and uses of stroboscopes designed for testing musical instruments and for analyzing sounds. A series of endless ribbons, graduated to correspond, respectively, with the notes of the musical scale, are driven at fixed frequency by a drum, and illuminated by a neon lamp controlled by the output from a microphone. In the recording type of instrument, a transparent stroboscopic plate is fixed in front of a constant-speed film.

534.613 **2888**

Radiation Pressure in Acoustics—J. Mercier. (*Compt. Rend. Acad. Sci.*, (Paris), vol. 232, pp. 2181–2183; June 11, 1951.) Radiation pressure is evaluated in general terms by considering the propagation of energy along the wave. It is found to be given by the time rate of change of quantity of movement, which is equal to the density of energy of the waves in contact with the obstacle.

534.75 **2889**

The Cerebral Mechanisms of the Binaural Functions. Summation and Lateral Location—H. Piéron. (*Ann. Télécommun.*, vol 6, pp. 102–109; April, 1951.) Criticism of a paper by Fletcher (2398 of 1938). Oversimplification of theory is alleged, leading to results directly contradicting accepted physiological facts of binaural hearing. Fletcher's loudness curve is regarded as invalid.

534.84 **2890**

Sound Reproduction in Halls and Open Spaces—F. Bergtold. (*Fernmeldetech. Z.*, vol. 4, pp. 112–116; March, 1951.) General discussion of the arrangement of loudspeakers to give pleasing reproduction, taking into account size and shape of the hall, attenuation of higher frequencies, distortion and noise at the sound source, and reverberation. The methods of beamed and diffuse sound projection are compared from both technical and economic viewpoints.

534.86:534.322.1 **2891**

The Effect of Sound Intensity Level on Judgment of 'Tonal Range' and 'Volume Level'—S. E. Stuntz. (*Audio Eng.*, vol. 35, pp. 17–19, 26; June, 1951.) A discussion of factors affecting the conclusions drawn from listener preference tests.

621.3.018.78† **2892**

The Influence of High-Order Products in Nonlinear Distortion—D. E. L. Shorter. (*Electronic Eng.*, (London), vol. 22, pp. 152–153; April, 1950.) Subjective assessments of nonlinear distortion in a transmitting system are compared with the objective results obtained by using the rms total harmonic distortion figures, and with those obtained by taking special account of high order harmonics. The influence of high order harmonics on reproduction is out of proportion to their energy content, and some system of weighting is advocated.

621.3.018.78† **2893**

The Influence of High-Order Products in Nonlinear Distortion—M. V. Callendar: D. E. L. Shorter. (*Electronic Eng.*, vol. 22, p. 443; October, 1950.) Comment on 2892 above, and author's reply.

621.3.018.78† **2894**

The Influence of High-Order Products on Nonlinear Distortion—D. B. Corbyn: D. E. L. Shorter. (*Electronic Eng.*, vol. 23, p. 35; January, 1951.) Further comment on 2892 above, and author's reply.

621.395.62:621.317.3 **2895**

Objective Measurements on Telephone Earpieces—H. Meister. (*Tech. Mitt. schweiz. Telegr.-Teleph. Verw.*, vol. 29, pp. 220–222; June, 1951. In German and French.) Methods adopted by the Swiss telephone authority for measuring frequency response and volume characteristics, are discussed briefly (see also 2896 below). Good agreement was found between the results of these objective tests and those obtained by subjective methods used earlier.

621.395.62:621.317.79 **2896**

Apparatus for Testing Telephone Earpieces—R. Kallen. (*Tech. Mitt. schweiz. Telegr.-Teleph. Verw.*, vol. 29, pp. 222–228; June 1, 1951. In German and French.) Detailed description of the apparatus referred to in 2895 above. The frequency of the testing voltage is varied logarithmically from 4 kc to 400 cps in ½ second. The output from the earpiece is picked up by an artificial ear consisting of a capacitor microphone with a pressure chamber whose acoustic impedance corresponds to that of the ear. The amplified voltage from this is rectified, and the output, varying as the square root of the input, is examined by means of an integrating circuit and voltmeter, or displayed on a cro screen.

621.395.623.7 **2897**

Cabinets for High-Quality Direct Radiator Loudspeakers—H. F. Olson. (*Radio and Telev. News*, vol. 45, pp. 53–56, . . . 86; May, 1951.) An experimental examination of the various factors which influence the performance of a loudspeaker mounted in a completely closed cabinet.

621.395.623.7 **2898**

The Fidelity of Transient Reproduction by Loudspeakers—J. C. Hentsch. (*Tech. Mitt. schweiz. Telegr.-Teleph. Verw.*, vol. 29, pp. 201–211; June 1, 1951. In French.) The response of the human ear to transient sounds, and the effect of binaural hearing are discussed. A method of obtaining and analyzing the mean frequency-response curve of a loudspeaker, allowing for subjective effects, is outlined. This curve suffices to determine the quality of reproduction of transients. Oscillographic examination of the actual deformations caused by the reproducer is not a reliable means. A method for eliminating loudspeaker interference effects is described.

621.395.623.7 **2899**

Explosion-Proof Loudspeaker—S. J. White. (*Tele-Tech.*, vol. 10, pp. 46–47, 86; May, 1951.) The driver unit is enclosed in a cast housing attached to the horn structure, and between them is a barrier with an effective porosity which is a function of air particle velocity. Sudden internal or external blast is resisted, but normal audio transmission is permitted.

621.395.625.3 **2900**

Broadcast Tape Speed Control—D. R. Andrews. (*Electronics*, vol. 24, pp. 120–123; July, 1951.) To ensure that the duration of a half hour program played back from a magnetic tape record is constant to within 1 second, timing marks are printed on the back of the tape and scanned by a photoelectric arrangement to provide a reference signal.

621.395.625.3:778.5 2901
Special Techniques in Magnetic Recording for Motion Picture Production—G. Lewin. (*Jour. Soc. Mot. Pic. & Telev. Eng.*, vol. 56, pp. 653–663; June, 1951.)

621.396.645.029,3:621.385.3/.4 2902
A Comparison of Triodes and Beam-Tetrodes as Power Output Valves in Audio Amplifiers—Bruckmann, Carey, and Fuller. (*See* 2959.)

681.85 2903
Recording Styli, the Burnishing Facet, and a Process for Resharpening—C. F. Strandberg. (*Elec. Eng.*, vol. 70, pp. 447–450; May, 1951.) A method of resharpening sapphire, stellite, and steel styli without regrinding, involves immersion in a NaOH cleansing solution.

534.84 2904
Die wissenschaftlichen Grundlagen der Raumakustik: Band 3—Wellentheoretische Raumakustik [Book Review]—L. Cremer. Publishers: S. Hirzel Verlag, Leipzig, Germany, 1950, 355 pp., 21.50 DM. (*Z. Ver. Dtsch. Ing.*, vol. 93, p. 623; June 21, 1951.) Written primarily for physicists, this volume deals with the systematic development and investigation of sound-absorbing arrangements by means of wave theory.

ANTENNAS AND TRANSMISSION LINES

621.315.21:621.395.97 2905
Cables for Sound Distribution—R. C. Mildner. (*Elec. Radio Trading*, vol. 23, pp. 77–81; May, 1951.) A practical review, primarily for the installation engineer, of the types of cable available, and the factors to be considered in designing and installing a distribution system.

621.316.683 2906
High-Frequency Connectors—H. Nitsche. (*Fernmeldetech. Z.*, vol. 4, pp. 97–102; March, 1951.) An account of the design and characteristics of "Dezifix"-type connectors developed for coaxial cable coupling at frequencies up to 3 kmc. The two halves of the connector are identical, and are secured by a square-threaded cap.

621.392 2907
A Variable-Length Radio-Frequency Transmission-Line Section—K. R. McAlister. (*Jour. Sci. Instr.*, vol. 28, pp. 142–143; May, 1951.) Description of a coaxial line lengthener having constant characteristic impedance (50 ohms) throughout its length. It is not frequency selective, and its reflection coefficient is $\not> 5$ per cent.

621.392+621.315.212].018.44 2908
Reduction of Skin-Effect Losses by the Use of Laminated Conductors—A. M. Clogston (Proc. I.R.E., vol. 39, pp. 767–782; July, 1951. *Bell Sys. Tech. Jour.*, vol. 30, pp. 491–529; July, 1951.) Skin-effect losses can be reduced in transmission lines by using conductors composed of insulated laminations, and adjusting the velocity of wave transmission. Theory for such laminated lines is presented for the case of planar systems with infinitesimally thin laminae, and with laminae of finite thickness. A transmission line completely filled with laminated material is considered. An analysis is given of the modes of transmission in a laminated line, and of the problem of terminating such a line.

621.392.22:517.512.2 2909
Fourier Transforms in the Theory of Inhomogeneous Transmission Lines—F. Bolinder. (*Kungl. Tekn. Högsk. Handl.* (Stockholm), no. 48, 84 pp.; 1951. In English.) In comparison with other theoretical methods, the Fourier-integral method appears to give the best approximate solution for inhomogeneous lines. The analogy with antenna and pulse theories, and the method applied to various types of nonuniform lines with constant or varying propagation velocity, are discussed. A fundamental law governing the problem of "broad banding" is indicated. See also 562 of April.

621.392.26† 2910
Metal Waveguides with Parallelogram Cross-Section—R. Malvano. (*Nuovo Cim.*, vol. 6, pp. 265–273; July 2, 1949.) Formulas are derived for the TM and TE modes. Possible applications of this waveguide are indicated.

621.392.26†:538.61 2911
Magneto-optics of an Electron Gas with Guided Microwaves—L. Goldstein, M. Lampert, and J. Heney. (*Phys. Rev.*, vol. 82, pp. 956–957; June 15, 1951.) Frequencies between 4.6 and 5.5 kmc were used with a circular guide in an axial magnetic field, the plasma from a pulsed dc gas discharge being used as the dielectric. Large angles of rotation of the electric field were observed, and resonance occurred near the gyromagnetic frequency. The results are explained in terms of the decomposition of the "linear" wave into "anomalous" and "normal" circularly polarized waves.

621.392.26†:621.392.52 2912
Corrugated-Waveguide Band-Pass Filters—J. C. Greene. (*Electronics*, vol. 24, pp. 117–119; July, 1951.) Design principles and experimental results are presented. The high-pass properties of a waveguide are combined with the low-pass properties of a corrugated surface inserted into the waveguide, giving a sharp transition between pass and attenuation bands. A single corrugated element replaces several elements used in conventional designs.

621.392.26†:621.396.6.002.2 2913
Microwave Components: Precision Casting vs Electroforming—A. A. Feldmann. (*Materials & Methods*, vol. 34, pp. 70–72; July, 1951.) Description of methods used in the manufacture of waveguide elements.

621.392.5 2914
Delay Lines—J. Moline. (*Radio Franç.*, nos. 3 and 4, pp. 16–19 and 5–8; March and April, 1951.) Phenomena of propagation in transmission lines are explained, and the construction and various uses of artificial delay lines are described.

621.392.54 2915
Long-Line Attenuation Equalization—K. M. Garven. (*Commun. Rev.*, vol. 2, pp. 53–62; June, 1950.) A convenient formula is worked out for the insertion loss of a network, the conventional interaction term being avoided. The general formula for the over-all insertion loss of a succession of four-terminal networks connected in tandem, is derived and applied to consideration of equalization requirements in a long line.

621.396.67 2916
Practical Calculation of Modern Broadcast Transmitting Aerials in the Medium Wave-Band—K. Fischer. (*Electrotech. u. Maschinenb.*, vol. 68, pp. 153–157 and 183–187; March 15, and April 1, 1951.) Discussion of (a) graphical determination of impedance and mutual coupling of antenna elements; (b) the influence of a capacitive roof on a mast radiator; (c) the method of calculating the radiation diagram of vertical arrays, and means of obtaining a directional characteristic. Supplementary to paper noted in 38 of 1950.

621.396.67:517.6 2917
Method of calculating Integrals of the Form $J_{CS} = \int_0^\infty \frac{\cos k\sqrt{\lambda^2+\alpha^2}}{\sqrt{\lambda^2+\alpha^2}} \sin p\lambda\, d\lambda$. G. Soule-Nan and J. Peltier. (*Compt. Rend. Acad. Sci.*, (Paris) vol. 232, pp. 2076–2078; June 4, 1951). The integrals discussed occur in calculations of the current distribution in antennas.

621.396.67:621.397.6 2918
Engineering a Super-gain TV Antenna—M. E. Hiehle. (*TV Eng.* vol. 2, pp. 16–18, 28; May, 1951.) Omnidirectional antennas with power gains $\geqq 10$ relative to a dipole, and radiating almost entirely in the horizontal plane, raise special problems in respect of reception close to the antenna and the effect of tower sway. Methods of overcoming these effects and of filling up "holes" in the coverage area are outlined.

621.396.67:621.397.6 2919
Practical Considerations in the Use of Television Super-turnstile and Super-gain Antennas—II. E. Gihring. (*RCA Rev.*, vol. 12, pp. 159–176; June, 1951.) Some general considerations concerning vertical directivity, horizontal polar diagram, bandwidth, and the use of common antennas for sound and vision transmission, are presented. The Empire State antenna system, in which four "super-gain" antennas connected to separate television transmitters in the building below are stacked vertically on one mast, is discussed in detail.

621.396.67.029.64 2920
Horizontally Polarized Omnidirectional Antenna—C. Brasse, Jr., and R. Thomas. (*Electronics*, vol. 24, pp. 86–87; July, 1951.) Three cophased horizontal loops mounted on a rigid coaxial line are used to provide a radiation pattern with an azimuth ratio <3db in the 10-cm band. The array is enclosed in a hollow plexiglas ball for pressurizing. The vertical pattern has half-power points at 45°, giving a gain over a half-wave dipole of 2db.

621.396.677 2921
Dielectric Aerials with Shaped Radiation Patterns—D. G. Kiely. (*Wireless Eng.*, vol. 28, pp. 177–178; June, 1951.) An empirical technique is described for designing a solid-dielectric radiator for operation at a wavelength of 3.2 cm with a beam width of 240° to 6-db points. The method is applicable to antennas with other patterns.

621.396.677 2922
Slot Antenna Developments—D. R. Rhodes. (*Radio and Telev. News, Radio Electronic Eng. Suppl.* vol. 16, pp. 3A–5A, 31A, and 7–9, . . 30; May and June, 1951.) A comprehensive, nonmathematical discussion, with a bibliography of 13 items.

621.396.677 2923
The Effects of Anisotropy in a Three-Dimensional Array of Conducting Disks—G. Estrin. (Proc. I.R.E., vol. 39, pp. 821–826; July, 1951.) The microwave delay-lens medium considered has both magnetic and electric anisotropy. To determine its refractive properties for obliquely incident waves, the field equations are subjected to a transformation making them applicable to a magnetically isotropic medium. The classical solutions from optics are then available. An inverse transformation is applied to give the "ray velocity surfaces" in the original medium.

621.396.677 2924
Microwave Lenses—K. S. Kelleher: J. Brown and S. S. D. Jones. (*Electronic Eng.* vol. 23, pp. 236–237; June, 1951.) Discussion on 36 of February.

621.392 2925
Transmission Lines and Filter Networks [Book Review]—J. Karakash. Publishers: Mac-

millan, New York, N. Y., 1950, 413 pp., $6.00. (*Electronics*, vol. 24, pp. 152, 278; April, 1951.) Elementary theory applicable from audio frequencies to the microwave range.

CIRCUITS AND CIRCUIT ELEMENTS

621.3.011.2 2926
Impedance and the Laplace Transform—I. E. Ward. (*Wireless Eng.*, vol. 28, pp. 192–194; June, 1951.) An examination of the meaning of the term "impedance" in the presence of transients, using the Argand diagram to simplify the presentation. The transient and steady-state responses of a linear system initially at rest, are determined as special cases of the general theory.

621.3.015.7 2927
Sinusoid-Pulse and Pulse-Sinusoid Transformations—J. Moline. (*Radio Franç.*, no. 2, pp. 9–12; February, 1951.) The subject is discussed in general terms, and various circuit techniques are described for deriving waveforms of the one type from the other.

621.314.2 2928
Transformation Ratio and Leakage Distribution in Transformers with more than two Windings—P. Wittich. (*Electrotech. u. Maschinb.*, vol. 68, pp. 157–159; March 15, 1951.) Expressions are derived for the value of the turns ratio corresponding to equal distribution of leakage loss in terms of the no-load characteristics of the individual windings.

621.314.2 2929
The Design and Performance of Double-Tuned Transformers in Tandem: An Application of Landon's Theorem—R. G. Kitchenn. (*Jour. Brit. IRE*, vol. 11, pp. 227–232; June, 1951.) Theory is given for a simple type of band-pass filter in which the insertion loss in the pass band and that in the attenuated band are less than the values obtained using two similar double-tuned transformers isolated by a tube, for the same bandwidth. The performance of an eight-channel filter unit is described.

621.314.2 2930
Multi-Winding Transformers—R. Willheim. (*Elec. Times*, vol. 119, pp. 991–994; June 14, 1951.) The equivalent circuit of a multi-winding transformer is reduced to a T-type filter. The main application is to power transformers.

621.314.2+621.318.42].003.1 2931
Minimum-Cost Transformers and Chokes: Part 2—Various Alternative Solutions: the Economic Life of a Transformer—H. C. Hamaker and T. Hehenkamp. (*Philips Res. Rep.*, vol. 6, pp. 105–134; April, 1951.) Continuation of 1853 of September, dealing with two further classes of designs, viz., (a) those giving minimum cost, and (b) those giving minimum losses, for prescribed values of the power and of the product of peak magnetic-flux density and effective current strength. The three classes of designs are compared. The problem is considered of designing a transformer such that its cost, plus the cost of the electrical energy dissipated as heat during its life, is a minimum.

621.314.3† 2932
Response of Saturable Reactor with Resistive Load—H. F. Storm. (*Elec. Eng.*, vol. 70, p. 442; May, 1951.) Digest of a paper presented at the AIEE Winter General Meeting in New York, January, 1951, and to be published in *Trans. Amer. I.E.E.*, vol. 70; 1951. The analysis considers a reactor with a core material having a rectangular magnetization curve, operating in the proportional region. The variation of the load current with change of control voltage, supply voltage, and load resistance, is exponential with a single time constant.

621.317.35:517.512 2933
Decomposition of a Signal into Components in Cos²—J. Ville. (*Câbles & Trans.* (Paris), vol. 5, pp. 126–135; April, 1951.) A mathematical analysis showing how a signal including only components of frequencies lower than a given value f, can be resolved into a series of elementary signals expressed in terms of cos², all having the same frequency f, but having different amplitudes and time origin. The time interval between two successive half-maximum tubes of each elementary signal is equal to $\frac{1}{2}f$, and the time separation between the peaks of two successive component signals is also equal to $\frac{1}{2}f$.

621.318.4(083.74) 2934
Standardized Magnetic Circuits of the French P.T.T. Administration—P. Andrieux. (*Câbles & Trans.* (Paris), vol. 5, pp. 101–109; April, 1951.) A review of standards and specifications relating to inductors. Dimensions of magnetic circuits and properties of materials used are summarized in tables. The performance of various types is described, with illustrative graphs.

621.318.572 2935
Modern Designs of Electronic Switches—H. Boucke and H. Lennartz. (*Radio Mentor*, vol. 17, pp. 129–133; March, 1951.) Circuit diagrams and descriptions are given of switching circuits for multiplex transmission on a single channel, and for displaying a number of phenomena on a cro. Methods include the phase-shift, multiple-frequency, and step-voltage techniques. A diode circuit for switching the AM signal on a carrier, and its application in the determination of voltage distribution along an uhf transmission line, are outlined.

621.318.572 2936
Speed-Controlled Switch—H. W. Kretsch and F. J. Walker. (*Electronics*, vol. 24, pp. 112–113; July, 1951.) The output of a standard ac tachometer operates through a frequency-sensitive circuit to actuate the switch when a predetermined speed is attained.

621.318.572 2937
A Three State Flip-Flop—K. C. Johnson, A. D. Booth, and J. Ringrose. (*Electronic Eng.*, vol. 23, p. 237; June, 1951.) Discussion on 2367 of November.

621.319.4(083.74) 2938
The Stability of Mica Standards of Capacitance—G. H. Rayner and L. H. Ford. (*Jour. Sci. Instr.*, vol. 28, pp. 168–171; June, 1951.) "The stability of the National Physical Laboratory substandard mica capacitors since their manufacture in 1932 is described, with special attention to the period of 1944–1950."

621.392 2939
The Theory of Biconjugate Networks—L. J. Cutrona. (Proc. I.R.E., vol. 39, pp. 827–832; July, 1951.) The properties of such networks are: (a) of the six possible transfer impedances only three are independent, one being infinite; (b) the magnitudes of the reflection coefficients at each resistance are equal; (c) the phase angles of the transfer impedances are not independent, but must satisfy certain relations. One form of waveguide network, the $7\lambda_g/2$ hybrid circle, is analyzed in detail, and the driving-point and transfer impedances are computed and plotted.

621.392 2940
Synthesis of Passive RC Networks with Gains Greater than Unity—H. Epstein. (Proc. I.R.E., vol. 39, pp. 833–835; July, 1951.) Known methods of synthesis are used for designing three-terminal networks having unity voltage gain at zero frequency, and voltage gain greater than unity over a prescribed frequency band. Two examples illustrate the method.

621.392:512.831 2941
The Formation of Positive Definite Matrices—M. Parodi. (*Compt. Rend. Acad. Sci.* (Paris), vol. 232, pp. 2390–2392; June 25, 1951.) A new method is presented for determining the upper limit for small variations to which the elements of a matrix may be subjected in order that the matrix shall remain positive definite. The method is useful for determining the upper limit to the real parts of the roots of the equations for the natural frequencies of a network.

621.392:517.544.2 2942
Estimation of Probable Error in the Solution of a Finite-Difference Equation Approximating Dirichlet's Problem for Laplace's Equation in Electrical Networks—M. P. Shura-Bura. (*Compt. Rend. Acad. Sci.* URSS, vol. 78, pp. 21–24; May 1, 1951. In Russian.)

621.392.5 2943
A Note on a Bridged-T Network—P. G. Sulzer. (Proc. I.R.E., vol. 39, pp. 819–821; July, 1951.) A bridged-T network described by Honnell (2368 of 1940) for measurement of rf resistance is analyzed and shown to be suitable for use as frequency-determining element of a resistance-tuned oscillator.

621.392.5:621.3.015.3 2944
Solution of Transients in Active Four-Terminal Networks—H. Epstein. (*Jour. Frank. Inst.*, vol. 251, pp. 607–616; June, 1951.) The advantages of using matrix and operational methods together for the solution of this problem are illustrated by applying the method to the example of a grounded-grid amplifier followed by a cathode follower with a pulse input.

621.392.5:621.396.611.3 2945
Resonant Circuits coupled by a Passive Four-Pole that may violate the Reciprocity Relation—B. D. H. Tellegen and E. Klauss. (*Philips Res. Rep.*, vol. 6, pp. 86–95; April, 1951.) A theoretical treatment having particular reference to the use of coupled tuned circuits as interstage networks in amplifiers. The circuit conditions for maximum transfer between input current and output voltage, for a given shape of resonance curve, are considered. These conditions do not coincide with those applying to circuits coupled by a passive quadripole satisfying the reciprocity relation.

621.392.52 2946
Filter Design Simplified—B. Sheffield. (*Audio Eng.* vol. 35, pp. 26, . . 58; May, 1951.) The method previously outlined (2127 of October) is extended to the design of band-pass and band-stop filters and filter-type dividing networks.

621.396.6 2947
Component Miniaturization Techniques—R. G. Peters. (*TV Eng.*, vol. 2, pp. 12–13, 29; June, 1951.) A summary of the properties of materials used in miniature capacitors and resistors.

621.396.6.002.2 2948
Mechanized Production and Unitized Construction—R. G. Peters. (*TV Eng.*, vol. 2, pp. 18–20; April, 1951.) General discussion of techniques developed for increasing and cheapening production of electronic equipment.

621.396.6.002.2 2949
Auto-Sembly of Miniature Military Equipment—S. F. Danko and S. J. Lanzalotti. (*Electronics*, vol. 24, pp. 94–98; July, 1951.) Wiring is printed on an insulating base most conveniently by the etching of copper-faced laminates. Holes are punched to take component leads, and all joints are made simultaneously using the one-shot solder-dip technique.

621.396.6.002.2 2950
Production Planning speeds Military Or-

ders—J. D. F. (*Electronics*, vol. 24, pp. 82–85; July, 1951.) Mass production methods, practised by a U.S. manufacturer of electronic equipment, are described. Special attention is focused on the organization of the wiring.

621.396.611.1 2951

Mathieu's Nonlinear Oscillator—N. Minorsky. (*Compt. Rend. Acad. Sci.* (Paris), vol. 232, pp. 2179–2180; June 11, 1951.) By applying the calculus of perturbations to Mathieu's nonlinear differential equation of the form $\ddot{x}+[1+\epsilon(A-Cx^2)\cos 2t]x=0$, it is shown that, to a first approximation, a stable periodic solution exists if A and C have the same sign.

621.396.611.21 2952

Piezoelectric Crystals in Flexural Vibration—H. Keller. (*Wireless Eng.*, vol. 28, pp. 179–186; June, 1951.) "The values of the equivalent circuit elements of several flexural vibrating piezoelectric crystals, slabs, double-T-shaped plates, and double strips, are calculated from the effective stiffness and mass, and the electromechanical coupling."

621.396.611.4 2953

On the Theory of Electromagnetic Waves in Resonant Cavities—H. B. G. Casimir. (*Philips Res. Rep.*, vol. 6, pp. 162–182; June, 1951.) The formal analogy between the modes of oscillation of a cavity, the modes of oscillation of a network, and the oscillation of a simple LC circuit is emphasized. Perturbation theory is used to investigate a number of examples, including the determination of the hf properties of magnetic materials, and the coupling of cavities by a hole in a partition. The zero-point energy of empty space is discussed.

621.396.611.4 2954

A Resonator for Metre and Decimetre Waves—M. Magat and M. Bruma. (*Compt. Rend. Acad. Sci.* (Paris), vol. 232, pp. 2413–2415; June 25, 1951.) A piston-type resonator has a tube of dielectric introduced between the inner and outer metal cylinders to provide a capacitance in parallel with that due to the plane ends. The arrangement permits tuning without instability.

621.396.615 2955

RC Tuned Oscillators—P. Kundu. (*Jour. Brit. IRE*, vol. 11, pp. 233–241; June, 1951.) A frequency-selective feedback network is used to obtain sinusoidal oscillations of good waveform, with frequencies from a few cycles to a few megacycles. The loop gain is not affected by frequency, and the frequency can be controlled by varying a single element of the network. The same system can also be used as a selective amplifier or as a rejection filter, by controlling the amount of reaction in the regenerative loop.

621.396.645 2956

Relations between Amplitudes of Harmonics and Intermodulation Frequencies in the Output from a Non-linear Amplifier or Mixer—M. V. Callendar and S. Matthews. (*Electronic Eng.*, vol. 23, pp. 230–232; June, 1951.) The output from an amplifier (or mixer) is calculated for an input of two superposed sine waves of different frequencies, for an assumed nonlinear amplifier characteristic free from discontinuities. The coefficients of all the terms in the output are tabulated.

621.396.645:621.385.3:546.289 2957

Some Circuit Properties and Applications of *n-p-n* Transistors—R. L. Wallace, Jr., and W. J. Pietenpol. (Proc. I.R.E., vol. 39, pp. 753–767; July, 1951. *Bell Sys. Tech. Jour.*, vol. 30, pp. 530–563; July, 1951.) Preliminary studies of circuit performance show that the *n-p-n* transistor is a stable, high-gain, quiet amplifier of practical interest. The performance of a few early experimental units is analyzed; details are given of the physical appearance and construction, static characteristics, and variation of properties with operating point. General considerations and formulas are presented for the grounded-base stage, the grounded-emitter amplifier, and the grounded-collector stage. Collector cutoff in these stages, frequency response, and noise, are examined.

621.396.645:621.385.3:546.289 2958

Application of Germanium Triodes for the Amplification of Low- and Medium-Frequency Currents—H. Salow. (*Fernmeldetech. Z.*, vol. 4, pp. 103–106; March, 1951.) The value of power gain obtainable in a transistor circuit is derived from the impedance matrix of the quadripole represented by the resistance characteristics of the crystal, which are determined experimentally. Some performance figures for an experimental lf amplifier are given.

621.396.645.029.3:621.385.3/.4 2959

A Comparison of Triodes and Beam-Tetrodes as Power Output Valves in Audio Amplifiers—D. Bruckmann, W. S. Carey, and D. J. Fuller. (*Trans. S. Afr. Inst. Elec. Eng.*, vol. 42, pp. 65–66; February, 1951.) Further discussion of paper noted in 1123 of June.

621.396.822 2960

Limiting the Noise Spectrum in Oscillatory Circuits—W. Böer. (*Ann. Phys.* (Lpz.), vol. 8, pp. 87–92; July 31, 1950.) Continuation of an investigation by Feldtkeller (1714 of 1937). The noise in an oscillatory circuit is calculated as a function of the bandwidth of a succeeding amplifier. Noise voltage decreases with increasing circuit damping, and increases with increasing relative bandwidth. Operation with least possible input damping is not necessarily advantageous in every case. The optimum ratio of C to L is discussed for special cases.

621.392 2961

Transmission Lines and Filter Networks [Book Review]—Karakash. (*See* 2925.)

GENERAL PHYSICS

534.23+538.566 2962

Kirchhoff's Formula, its Vector Analogue, and Other Field Equivalence Theorems—S. A. Schelkunoff. (*Commun. Pure Appl. Math.*, vol. 4, pp. 43–59; June, 1951.) A detailed physical and mathematical discussion of the problem of calculating the fields associated with acoustic or electromagnetic horn radiators. Four field-equivalence theorems are proved for each case. The relations between these theorems and Kirchhoff's formula and its vector analogue are discussed. Permissible and nonpermissible methods of approximation are distinguished. The method of successive approximation cannot be applied to calculations based on Kirchhoff's formula, all the approximate forms being exactly identical. The conditions under which Kirchhoff's formula is consistent with Maxwell's equations are examined.

534.26+535.42+534.24+535.312 2963

Diffraction and Reflection of Pulses by Wedges and Corners—J. B. Keller and A. Blank. (*Commun. Pure Appl. Math.*, vol. 4, pp. 75–94; June, 1951.) Exact explicit solutions of the equations for two- and three-dimensional diffraction of pulses by wedges and corners, are obtained by using Busemann's conical-flow method and Luneberg's results on the propagation of discontinuities. The solutions for waves with arbitrary dependence of amplitude on time may be found by using Duhamel's theorem.

535.214.6+538.6 2964

Photophoresis, Magnetophotophoresis, Magneto-Chemical Effect—J. v. Harlem. (*Physikalische Blätter*, vol. 7, no. 3, pp. 110–113; 1951.) Review of investigations of these effects, particularly those made by Ehrenhaft, and their interpretation.

535.338.32 2965

A Study of Nuclear and Electronic Magnetic Resonance—K. K. Darrow. (*Elec. Eng.*, vol. 70, pp. 401–404; May, 1951.) Survey of the history of the discovery and measurement of magnetic resonance in solids, liquids, and gases. A simple outline of the theory of the phenomenon is given, and its importance in the study of nuclear magnetic moments, crystal structure, and relaxation times, is mentioned. A practical application is the measurement of magnetic field strengths.

535.42:538.56 2966

Diffraction of Electromagnetic Waves by a Plane Wire Grating—J. Shmoys. (*Jour. Opt. Soc. Amer.*, vol. 41, pp. 324–328; May, 1951.) "The problem of diffraction by a finite grating consisting of perfectly conducting wires of arbitrary cross section, is formulated in terms of characteristic plane waves corresponding to the various order spectra defined in optics. Scattering matrix elements are expressed as stationary functionals of current distribution on the grating wires, for the incident wave falling at right angles to the grating elements, and polarized either parallel or perpendicular to them. These are evaluated for the thin wire grating and parallel polarization."

537.122:537.217 2967

The Electrical Flywheel and Electron Inertia—P. Selényi. (*Z. Phys.*, vol. 130, pp. 124–128; May 28, 1951.)

537.226.1 2968

The Dielectric Properties of Various Solid Crystalline Proteins, Amino Acids and Peptides—S. T. Bayley. (*Trans. Faraday Soc.*, vol. 47, pp. 509–517; May, 1951.) Details are given of experimental methods for determining the dielectric properties of organic powders at frequencies ranging from 300 to 4×10^9 cps, over the temperature range $-100°$ to 0°C.

537.226.1 2969

The Dielectric Properties of Adsorbed Water Layers on Inorganic Crystals—S. T. Bayley. (*Trans. Faraday Soc.*, vol. 47, pp. 518–522; May, 1951.) Adsorbed water causes peaks at about $-30°$C in the variation with temperature of the dielectric constant and power factor of a number of inorganic crystal powders.

537.311.5:517.311.5 2970

The Discharge of a Series of Equal Condensers having Arbitrary Resistances connected in Parallel—H. Bremmer. (*Philips Res. Rep.*, vol. 6, pp. 81–85; April, 1951.) The flow of current through a ballistic galvanometer, through which the capacitors are discharged, is calculated by means of the operational calculus. The discussion is relevant to van Geel and Scholte's work on the electrical properties of Al_2O_3 layers (see 3022 below).

537.523.5 2971

A Technique for Arc Initiation—H. Edels. (*Brit. Jour. Appl. Phys.*, vol. 2, pp. 171–174; June, 1951.) Discussion of a method in which fixed electrodes and an auxiliary spark discharge are used.

537.525:621.385.13 2972

Rapid Determination of Gas Discharge Constants from Probe Data—L. Malter and W. M. Webster. (*RCA Rev.*, vol. 12, pp. 191–210; June, 1951) A series of nomograms for determination of plasma density, wall potential, etc. An analysis of the space-charge conditions is appended.

537.525.4 2973

Influence of Cathode Surface Layers on Minimum Sparking Potential of Air and Hydrogen—F. L. Jones and D. E. Davies. (*Proc. Phys. Soc.*, vol. 64, pp. 397–404; May 1, 1951.)

537.525.6:538.56 2974
Current Fluctuations in the Direct-Current Gas Discharge Plasma—P. Parzen and L. Goldstein. (*Phys. Rev.*, vol. 82, pp. 724–726; June 1, 1951.) The noise power from the gas discharge plasma, which is ascribed to the electron current fluctuations due to collisions with atoms or ions, is recognized to be the sum of two parts. One is determined by the thermal velocities (characterized by the electron temperature) and the other by the average direct current.

537.525.6:538.56]537.122 2975
A Collective Description of Electron Interactions: Part 1.—Magnetic Interactions—D. Bohm and D. Pines. (*Phys. Rev.*, vol. 82, pp. 625–634; June 1, 1951.) The "collective" description of the behavior of electrons in a plasma is developed for presenting the long-range correlations in electron positions brought about by their mutual interaction. "The transition from the usual single particle description to the collective description of the electron motion in terms of organized oscillations, is obtained by a suitable canonical transformation. The complete hamiltonian for a collection of charges interacting with the transverse electromagnetic field, is re-expressed as a sum of three terms. One involves the collective field co-ordinates, and expresses the degree of excitation of organized oscillations. The others represent the kinetic energy of the electrons and the residual particle interaction, which is not describable in terms of the organized oscillations, and corresponds to a screened interparticle force of short range. Both a classical and a quantum-mechanical treatment are given, and the criteria for the validity of the collective description are discussed."

537.71 2976
Fundamental and Derived Magnitudes—R. W. Pohl. (*Naturwiss.*, vol. 38, pp. 247–248; June, 1951.) A short discussion the object of which is to clear up existing confusion concerning the definitions of physical magnitudes.

538.221 2977
Antiferromagnetism—R. Street. (*Sci. Progr.* vol. 39, pp. 258–281; April, 1951.) The behavior of ferrimagnetic and antiferromagnetic materials is discussed, and an account is given of recent research.

538.311:621.318.423:513.647.1 2978
General Expression for the Electromagnetic Field of a Helix—É. Roubine. (*Compt. Rend. Acad. Sci.* (Paris), vol. 232, pp. 2297–2298; June 18, 1951.) Expressions previously derived (2691 of December) are applied to the case of an infinitely thin wire considered as the limit, when the width tends to zero, of an infinitely thin helically wound ribbon.

538.566:537.562 2979
Derivation of the Dispersion Equation for Alfvén's Magneto-hydrodynamic Waves from Bailey's Electromagneto-ionic Theory—J. W. Dungey. (*Nature* (London), vol. 167, pp. 1029–1030; June 23, 1951.) An analysis is presented which relates the work of Alfvén (2777 of 1950) and his collaborators to that of Bailey (2785 of 1949). As well as giving the dispersion of the waves, Bailey's theory may be useful for studying turbulence in an ionized gas in a magnetic field by means of Fourier components.

538.61:621.392.26† 2980
Magneto-optics of an Electron Gas with Guided Microwaves—Goldstein, Lampert, and Heney. (*See* 2911).

537/.538 2981
Électricité [Book Review]—Y. Rocard. Publishers: Masson and Cie., Paris, France, 1800 Fr. (paper), 2200 Fr. (bound). (*Engineering* (London), vol. 171, p. 585; May 18, 1951.) A treatise based on a course of lectures given at the Sorbonne in 1941–1942, but including later material, e.g., double-stream amplifier tubes, up to 1949. A chapter on the transmission of radio waves is included.

539 2982
Theory of Electrons [Book Review]—L. Rosenfeld. Publishers: North-Holland Publishing Co., Amsterdam, Netherlands, 1951, 120 pp., 7.50 florins. (*Nature* (London), vol. 167, p. 1044; June 30, 1951.) A discussion of the fundamental principles relating the macroscopic electrical and magnetic properties of matter to the behavior of individual atoms and molecules.

GEOPHYSICAL AND EXTRATERRESTRIAL PHENOMENA

523.72:550.38 2983
Correlation of Geomagnetic Activity with [passage of] Centres of Solar Activity distinguished according to their Radio Properties—J. F. Denisse, J. L. Steinberg, and S. Zisler. (*Compt. Rend. Acad. Sci.* (Paris), vol. 232, pp. 2290–2292; June 18, 1951.) Based on observations recorded at Meudon since 1948, on a frequency of 158 mc, centers of solar activity are classed as radio-emissive or otherwise according to an index depending both on the mean level of radio intensity and on the extent of fluctuations. Graphs of mean-intensity/time for the two types are compared with graphs of magnetic-intensity/time. A peak of magnetic intensity occurs at one to two days after the radio peak corresponding to the passage of the radio-emissive center across the sun's central meridian, whereas a trough of magnetic intensity occurs two to three days after the passage of the nonradio-emissive center.

523.72:621.396.822 2984
A Study on the Solar Noise at 3300 Mc/s—M. Oda and T. Takakura. (*Jour. Phys. Soc.* (Japan), vol. 6, p. 202; May/June, 1951.) A preliminary note. Observations from April to October, 1950, indicate that intensity of noise is approximately proportional to the whole-disk sunspot number. The apparent period of fluctuation averages about 20 minutes, and is independent of the intensity. Also, the mean fluctuation of the intensity is approximately proportional to the square root of the intensity. These conclusions are briefly discussed.

523.72:621.396.822 2985
The *F*-Radiation of the Sun—O. Burkard. (*Acta Phys. austriaca*, vol. 1, pp. 98–102; May, 1947.) Use is made of the critical frequencies of the ionosphere F_2 layer to calculate the magnitude of a parameter, which is a measure of the particular component of the solar radiation producing the ionization of the F_2 layer. The mean monthly values of this radiation at Kochel (near Munich) over the period 1940–1944 are given. There is a 97 per cent correlation between these figures derived from ionosphere observations, and the optically estimated character figures for the *Ca*-flocculi.

523.72:621.396.822 2986
Source Points of Radio Noise Bursts associated with Solar Flares—M. A. Ellison. (*Nature* (London,) vol. 167, pp. 941–942; June 9, 1951.) It has been shown that the solar sources of enhanced radio noise at meter wavelengths observed at times of intense solar flares, may travel some hundreds of thousand kilometers outwards from the photosphere in a period of a few minutes. Visible disturbances have been found to move in a similar way, suggesting that the visible and radio phenomena are closely related.

523.72:621.396.822 2987
Distribution of Radiation across the Solar Disk at a Frequency of 81.5 Mc/s—K. E. Machin. (*Nature* (London), vol. 167, pp. 889–891; June 2, 1951.) The distribution was measured by studying the variations in the received noise as the sun crossed the interference pattern of several coupled, widely-spaced antenna systems. A technique was developed which allowed for the fluctuating noise from sunspots. Results are compared with values predicted according to Smerd's theory (344 of March).

523.745:550.385 2988
Geomagnetic Effects of Solar Flares—D. H. McIntosh. (*Nature* (London), vol. 167, p. 985; June 16, 1951.) Observations at Lerwick and Eskdalemuir of the vertical component of the earth's magnetic field during flares, are interpreted as indicating substantial differences between the space distribution of the ionospheric currents producing the geomagnetic effects of flares and those producing the normal daily magnetic variations. See also 1910 of 1950 (Newton).

523.841.2:538.12 2989
Cosmic Radiation and Cosmic Magnetic Fields: Part 2—Origin of Cosmic Magnetic Fields—L. Biermann and A. Schlüter. (*Phys. Rev.*, vol. 82, pp. 863–868; June 15, 1951.) The equations governing the behavior of a wholly or partly ionized gas moving in the presence of a magnetic field are given. Modifications are necessary when the conducting medium is turbulent. The results are considered in relation to the fields in our galaxy. Part 1: 2990 below.

523.854:621.396.822]+537.591 2990
Cosmic Radiation and Cosmic Magnetic Fields: Part 1—Origin and Propagation of Cosmic Rays in our Galaxy—A. Unsöld. (*Phys. Rev.*, vol. 82, pp. 857–863; June 15, 1951.) The rf radiation of the galaxy is shown to be analogous not to the "quiet," but to the "disturbed" radiation from the sun, which is probably produced by plasma oscillations. It originates in stars for which the relation between rf radiation and cosmic rays is similar to that observed for the sun by Forbush and Ehmert. The propagation of cosmic radiation in the galaxy is discussed in relation to the observed directional isotropy of cosmic rays. Other theories of cosmic rays are discussed critically. Part 2: 2989 above.

537.591 2991
Variations and Origin of Cosmic Radiation—A. Dauvillier. (*Cahiers de Phys.*, nos. 35/36, 78 pp.; January/March, 1951.) Study of periodic variations based on past observations, and a discussion of explanatory theories.

537.591:551.594.5 2992
Correlation of Auroras with Increased Cosmic Ray Intensities (November 19, 1949)—N. C. Gerson. (*Nature* (London), vol. 167, pp. 894–895; June 2, 1951.) A summary of the visual, cosmic-ray, and radio phenomena observed during a solar disturbance. It is concluded that the cosmic-ray particles were charged, and that the auroras may have been caused by charged particles of lower energy.

550.385+551.594.5 2993
The Theory of Magnetic Storms and Auroras—H. Alfvén: D. F. Martyn. (*Nature*, (London,) vol. 167, pp. 984–985; June 16, 1951.) Critical comment on 1374 of July, and author's reply.

550.385+551.594.5:621.396.11 2994
Aurora and Magnetic Storms—R. K. Moore. (*QST*, vol. 35, pp. 14–19, 110; June, 1951.) Discussion of the nature of ionospheric disturbances and their effects on radio communication.

551.510.535 2995
Formation of Ionized Layers: Effect of Temperature—P. Lejay and D. Lepechinsky.

(*Compt. Rend. Acad. Sci.* (Paris), vol. 232, pp. 2058–2061; June 4, 1951.) Chapman's theory of photo-ionization of a gas of density decreasing exponentially with increasing height, assumes a constant temperature. A simple analysis shows that when the mean temperature rises, the level of the maximum ionization layer also rises, while the maximum ionization intensity I_0 decreases. Families of curves showing the variation of relative height with I/I_0 are given for three different values of mean temperature. For a given height and zenithal angle, the ionization intensity is very sensitive to temperature variation. The thickness of the ionized layer increases with temperature rise. Variations of the characteristics of the F layer with season and with time of day, predicted from the foregoing results, are in agreement with observations. The theory affords an explanation of the ionization intensity minimum observed around midday, particularly in summer.

551.510.535 2996

The Ionosphere during the Partial Eclipe of the Sun on 28th April 1949—D. Stranz. (*Z. Naturf.*, vol. 5a, pp. 172–173; March, 1950.) Observations made at Gothenburg, Lindau, and Tromsö are reported. Increases of the hourly F-layer critical frequencies, as compared with the median monthly values, were observed at all three stations, the deviation at Gothenburg amounting to 4 mc at the maximum phase of the eclipse. Possible physical explanations are discussed briefly. The increase in charge density may be due to lowering of the temperature.

551.510.535 2997

Anomalous Ionospheric Soundings observed during the Voyage of the 'Commandant Charcot' to Adélie Land—M. Barré and K. Rawer. (*Rev. Sci.* (Paris), vol. 88, pp. 147–154; July/September, 1950.) An account of observations taken between Hobart and Adélie Land, from December 20, 1949, to February 20, 1950. In general, ionospheric conditions were quiet throughout the period, except for a violent ionospheric storm in the first week of February, and sudden short disturbances of the Mögel-Dellinger type. Soundings were made with standard gear of the Service de Prévision Ionosphérique Militaire. Anomalous results are classified under eight heads, referring to the form of the curves obtained by reflection in the normal layers, the occurrence of E_s layers of various characteristics, and other effects. They were observed mainly during quiet periods, tending to disappear during periods of high absorption. They disappeared completely during the storm of February 1 to 6, 1950. They appear to result from the heterogeneity and turbulence of the ionosphere in the Antarctic, caused by the incidence of corpuscular radiation. But so called "vertical" soundings are unreliable in the vicinity of the magnetic pole, particularly in the case of the ordinary ray, and there is as yet no completely satisfactory explanation. See also 112 of February.

551.510.535 2998

Abnormal E-Region Ionization—N. C. Gerson. (*Canad. Jour. Phys.*, vol. 29, pp. 251–261; May, 1951.) The movement and extent of sporadic-E clouds over North America were determined by oblique-incidence radio observations. On June 13, 1949, two E_s centers were observed. The first developed rapidly until it included an area of over 10^6 km². The second was much smaller. The velocity of the center of mass of the first area was about SE 100 km per hour, and of the second, SSE 270 km per hour. Drift velocities in the ionosphere obtained by other investigators are of about this order of magnitude.

551.510.535+551.5]:523.7 2999

Geophysical and Meteorological Changes in the Period January-April 1949—W. J. G. Beynon and G. M. Brown. (*Nature* (London), vol. 167, pp. 1012–1014; June 23, 1951.) Abnormally great cyclical variations in the ground pressure and E- and F-region ionization densities over southern England were found during the period January to April, 1949. These were closely connected with solar and magnetic activity. A summary of similar phenomena reported elsewhere is included.

551.510.535:621.396.11 3000

Approximate Expressions for the Refractive Index of an Ionized Medium Acted upon by the Earth's Magnetic Field—Argence. (*See* 3094.)

551.578.11 3001

A Balloon-Borne Instrument for Telemetering Raindrop-Size Distribution and Rainwater Content of Cloud—B. F. Cooper. (*Aust. Jour. Appl. Sci.*, vol. 2, pp. 43–55; March, 1951.) Each drop impinges on a microphone, and the resulting impulse modulates a transmitter. The amplitudes of the impulses are analyzed and the distribution of drop size determined. Total rainwater content is measured simultaneously in a similar system by catching drops in a funnel before they reach the microphone. This ensures that small drops which do not produce an impulse, are taken into account. Experimental soundings are described.

LOCATION AND AIDS TO NAVIGATION

621.396.9 3002

Resolution in Radar Systems—J. Freedman (PROC. I.R.E., vol. 39, pp. 813–818; July, 1951.) The resolution is shown to be related to antenna beam width, and hence to size of aperture. The limitations on the improvement of resolution are presented from two aspects; firstly, from considerations associated with attempts to build a super-gain antenna; and secondly, from considerations of filter equalization techniques. In practice, no appreciable improvement is obtainable with either of these methods.

621.396.9:523.5 3003

A Radio Echo Apparatus for the Delineation of Meteor Radiants—A. Aspinall, J. A. Clegg, and G. S. Hawkins. (*Phil. Mag.*, vol. 42, pp. 504–514; May, 1951.) A description of apparatus for the continuous recording of 72-mc radio echoes from meteor ionization, using Yagi arrays directed on two bearings differing 50°. Returned pulses are displayed on an intensity-modulated trace, calibrated in echo range. From the times of observation of maximum ranges on the two antenna systems, the co-ordinates of active meteor radiants may be obtained. Typical results obtained on the Geminid showers of 1949 and 1950 are illustrated. An examination is made of the accuracy and resolving power of the equipment, and radiants are classified according to their echo properties.

621.396.9:621.396.621 3004

A Simple Logarithmic Receiver—Croney. (*See* 3096.)

621.396.933 3005

Air Navigational Aids—B. Clarke. (*Wireless World*, vol. 57, pp. 329–331; August, 1951.) A brief survey of the systems in current use. Those mentioned are (a) long-range: loran and consol; (b) medium-range: American radio range (300–400 kc), Gee, Decca, and V.O.R.; (c) local: British S.B.A. and American S.C.S-51 landing beam systems, G.C.A. (or P.A.R.) and S.R.E; (d) miscellaneous: mf beacons, cloud and collision-warning radar, altimeters, and D.M.E.

621.396.933 3006

Experimental Results of Continuous-Wave Navigation Systems—F. S. Howell. (PROC. I.R.E., vol. 39, p. 841; July, 1951.) Operational tests on Raydist equipment showed that reradiation and two-path transmission effects might cause erroneous position measurements in a system depending on cw phase-angle measurements. Two simple precautions against such errors are recommended.

621.396.933 3007

Prevention of Echo Interference in Double-Pulse Coded Interrogator-Responder Systems—R. S. Styles. (*Aust. Jour. Appl. Sci.*, vol. 2, pp. 26–42; March, 1951). A method of echo suppression is proposed based on an instantaneous agc system having a recovery time-constant of 30 μs. This effectively suppresses the echoes following the main pulses, while passing the pulses themselves. Tests made near Sydney with prototype equipment are described.

621.396.933 3008

Ultrasonics in the Loran Trainer—P. D. Stahl. (*Audio Eng.*, vol. 35, pp. 13–14, 53, and 14–16; May and June, 1951.) A device is described for the classroom training of navigators. An outline is given of the actual loran system operating at about 2 mc. To scale down a large ground area, an ultrasonic frequency of 175 kc is used in the model, the transmitting stations being represented by oil-damped crystal transducers. Details of the transmitter channel, including the method of simulating sky-wave splitting, are given.

621.396.933 3009

Air Safety Measures at the Intercontinental Airport of Zürich-Kloten—A. Fischer. (*Tech. Mitt. schweiz. Telegr.-Teleph Verw.*, vol. 29, pp. 86–92; March 1, 1951. In German.) An account of the approach and I.L.S. facilities available.

621.396.933:621.96.621.089.6 3010

A New Method of Testing the Mark V Decca Navigator Receiver in High Noise Levels—Hewitt. (*See* 3062.)

621.396.9 3011

Principles and Practice of Radar [Book Review]—H. E. Penrose and R. S. H. Boulding. Publishers: Newnes, London, England, 3rd edn, 1950, 708 pp., 42s. (*Electronic Eng.*, vol. 23, p. 241; June, 1951.) "In order to make the third edition as up-to-date as possible, the authors have fully considered microwaves and the particular problems met with at these wavelengths."

MATERIALS AND SUBSIDIARY TECHNIQUES

533.583:621.385.1 3012

Efficiency and Mechanism of Barium Getters at Low Pressures—S. Wagener. (*Brit. Jour. Appl. Phys.*, vol. 2, pp. 132–138; May, 1951.) The gettering rates of Ba getters for O, N, H, CO, CO_2, and water vapor are measured in the pressure range 5×10^{-8}; to 5×10^{-5} mm Hg. Values for the decay in gettering rate during use of the getter are given. The gettering effect at these low pressures is almost entirely the result of the take-up of atoms or metastable molecules produced by the impact of electrons on the stable gas molecules, ions playing a negligibly small part. The influence of the position of the getter is investigated.

537.311.33 3013

Rectifying Effect in Thin, Asymmetrically Illuminated Semiconductor Layers—G. Wlérick. (*Compt. Rend. Acad. Sci.* (Paris), vol. 232, pp. 2199–2201; June 11, 1951.) Amirkhanoff investigated asymmetrical condution in semiconductors in the vicinity of electrodes, which was due to geometrical, chemical, and thermal causes (2601 of 1946). The present work is a study of conduction in a semiconductor/metal two-contact system, with one contact illuminated and the other unilluminated. The semiconductor is a thin layer of CdS on a glass base, and the contacts are gold. The asymmetrical illumination is found to reduce the thickness of the semiconductor/metal barrier while increasing the contact difference of potential. An internal barrier arises at the boundary of the illuminated area. This, together with the contacts, causes the rectification.

537.311.33 3014

The Parameters of Simple Excess Semiconductors—P. T. Landsberg, R. W. Mackay, and A. D. McRonald. (*Proc. Phys. Soc.*, vol. 64, pp. 476–480; May 1, 1951.) Curves are given for the concentration of conduction electrons, the reduced Fermi level, and the concentration of available impurity-bound electrons, as functions of absolute temperature.

537.311.33 3015

The Combination of Resistivities in Semiconductors—V. A. Johnson and K. Lark-Horovitz. (*Phys. Rev.*, vol. 82, pp. 977–978; June 15, 1951.) Confirms Jones's analysis (1357 of July) of the resistivity and Hall coefficient of a semiconductor in which scattering is due to both lattice ions and impurity ions. Experimental evidence suggests that other types of scattering may also be significant.

537.311.3 3016

Temperature Dependence of the Energy Gap in Semiconductors—H. Y. Fan. (*Phys. Rev.*, vol. 82, pp. 900–905; June 15, 1951.) Lattice vibrations in semiconductors are assumed to produce a shift of the energy levels, resulting in variation of the energy gap with temperature. The quantitative results predicted according to the theory are compared with those given by earlier theories.

538.221 3017

Coercive Field of Ferro-Nickel Powders: Influence of Compression and Heat Treatment—L. Weil. (*Jour. Phys. Radium*, vol. 12, pp. 520–526; April, 1951.) Experimental study of the variation of the coercive field at temperatures between +300° and −193°C as a function of the agglomeration structure. Without heat treatment, the field conforms to Néel's theory (3151 of 1947). After heat treatment, the value of the field decreases as the measurement temperature is increased. This is ascribed to displacement of the Bloch walls formed by certain grains in contact.

538.221 3018

The Saturation Magneto-Resistance of Ferromagnetic Alloys—R. Parker. (*Proc. Phys. Soc.*, vol. 64, pp. 447–452; May 1, 1951.) It is suggested that the magnetoresistance coefficient of a ferromagnetic alloy is composed of two terms, one associated with the temperature-dependent, the other with the temperature-independent contribution to the electrical resistivity. An equation based on this hypothesis is in good agreement with the experimental results for silicon-iron alloys. The validity of the equation for other alloys is discussed.

538.221 3019

Investigation of Magnetic Properties of Well Ordered Alloys of the Co/Mn System—F. Gal'perin. (*Compt. Rend. Acad. Sci.* (URSS), vol. 77, pp. 1011–1014; April 21, 1951. In Russian.)

538.652:[546.74:548.55 3020

A Phenomenological Derivation of the First- and Second-Order Magnetostriction and Morphic Effects for a Nickel Crystal—W. P. Mason. (*Phys. Rev.*, vol. 82, pp. 715–723; June 1, 1951.) Report of a phenomenological investigation of the stress, strain, and magnetic relations for single Ni crystals, undertaken to account for experimental results obtained by McSkimin (2844 of 1950) showing that the saturation elastic constants of a single Ni crystal vary with direction of magnetization.

546.289:539.23 3021

The Electrical Properties of Thin Germanium Layers—J. M. Dunoyer. (*Jour. Phys. Radium*, vol. 12, pp. 602–606; May, 1951.) Layers about 1μ thick, obtained by evaporation in vacuo, were of two kinds: (a) amorphous layers having resistances of the order of a megohm at ambient temperature, and (b) crystalline layers of resistance not greater than a few tens of ohms. In both cases, rectified power is very small. Type (a) is obtained with the support at a temperature <270°C during deposition, type (b) above about 370°C. Composite layers consisting of an amorphous layer superimposed on a crystalline one gave greater rectified power, but results varied very widely from one sample to another.

546.623-31:621.3.011.4/.5:621.319.45 3022

Capacitance and Dielectric Losses of a Layer of Oxide deposited on Aluminum by Anodic Oxidation—W. C. van Geel and J. W. A. Scholte. (*Philips Res. Rep.*, vol. 6, pp. 54–74; February, 1951. In French.) Based on bridge measurements at frequencies up to 30 kc of the capacitance and dielectric loss, and on ballistic measurements of capacitance, a circuit equivalent for the structure of an oxide layer on Al is proposed. This consists of a number of parallel-RC circuits in series, the capacitances having the same value in each element, while the resistances increase steadily through the layer. An explanation in terms of an electrochemical process is advanced.

548.0:537 3023

Dielectric Properties of Sodium and Potassium Niobates—B. T. Matthias and J. P. Remeika. (*Phys. Rev.*, vol. 82, pp. 727–729; June 1, 1951.) Both substances are ferroelectric. The temperatures at which they undergo crystallographic changes, and the corresponding changes in dielectric constant and loss tangent, are reported. Dielectric-hysteresis loops, and values of saturation polarization for $KNbO_3$ at points in the temperature range 220°C to 472°C, are given.

548.0:549.514.51 3024

Growth of Large Quartz Crystals—C. S. Brown, R. C. Kell, L. A. Thomas, N. Wooster, and W. A. Wooster. (*Nature* (London), vol. 167, pp. 940–941; June 9, 1951.) Details are given of an experimental temperature-gradient process. Values of some physical properties of the synthesized crystals were compared with those for natural Brazilian crystals. No difference was observed.

620.193.82 3025

Effect of Fungus Growth on the Tensile Strength of Pressure-Sensitive Electrical Insulating Tapes—S. Berk and L. Teitell. (*ASTM Bull.*, no. 174, pp. 67–71; May, 1951.)

621.314.63 3026

Application of the Image-Force Model to the Theory of Contact Rectification and of Rectifier Breakdown—E. Billig. (*Proc. Roy. Soc. A*, vol. 207, pp. 156–181; June 22, 1951.) The basic assumptions of the current-diffusion theory of rectification are examined. A curved potential barrier at the rectifying junction is assumed to explain the behavior with high inverse voltages. The theory is applied to the case of the Se plate rectifier, and is shown to give results in good agreement with experiment. Useful rectifying junctions can only be made up from materials combining a reasonably high barrier with a fairly low electronic conductivity of the semiconductor.

621.315.615.011.5 3027

The Dielectric Dispersion of Dioxan-Water Mixtures—J. B. Hasted, G. H. Haggis, and P. Hutton. (*Trans. Faraday Soc.*, vol. 47, pp. 577–580; June, 1951.) Measurements are reported of the properties of dioxan-water mixtures, up to 45 per cent dioxan, at wavelengths of 9.22 and 1.26 cm. The single relaxation time of water is raised from 0.83 to 1.43×10^{-11} second when 45 per cent dioxan is added, while the static dielectric constant falls linearly, giving a molar decrement of −7.7. Energy of activation of relaxation is 20 per cent lower than that of pure water.

621.359.3 3028

Applying Coatings by Electrophoresis—S. A. Troelstra. (*Philips Tech. Rev.*, vol. 12, pp. 293–303; April, 1951.) The mechanism of electrophoresis (transportation by an electric field of a particle in a colloidal solution or in suspension) is explained and analyzed. The process differs from electroplating in that insulating substances can be deposited. Stability of suspensions, formation of double layers, and theoretical rate of buildup are analyzed, and the effect of added electrolyte and pitting due to liberated gases are considered. The coating on the electrode resembles sediment deposited by gravity. The process is used in the manufacture of tube filaments and cathodes.

621.793.1 3029

Evaporation in Vacuo by Direct Bombardment using an Electron Gun—J. Brochard, P. Giacomo, P. Jacquinot, and S. Roizen. (*Jour. Phys. Radium*, vol. 12, p. 632; May, 1951.) The method avoids attack on the support by the substance to be evaporated. A slight modification enables nonconducting substances, e.g., silicon and refractory oxides, to be treated.

621.924 3030

Making Small Spheres—W. L. Bond. (*Rev. Sci. Instr.*, vol. 22, p. 344–345; May, 1951.) A "spinning" method is described, which is capable of producing in a few minutes, spheres of diameter 0.100 to 0.004 inch, of Ge, EDT, nickel ferrite, etc.

666.1:621.317.374 3031

Some Experiments and Theories on the Power Factor of Glasses as a Function of their Composition: Part 2—J. M. Stevels. (*Philips Res. Rep.*, vol. 6, pp. 34–53; February, 1951.) Presentation and discussion of information about the structure of glass, obtained from dielectric-constant and power-factor measurements of glasses with graded compositions, at a frequency of 1.5 mc. Part 1: 3075 of 1950.

666.1.037:539.319 3032

A Theory of Stresses in Glass Butt Seals—H. Rawson. (*Brit. Jour. Appl. Phys.*, vol. 2, pp. 151–156; June, 1951.) A series of equations are derived for the calculation of stresses between materials of different expansion coefficients in butt-type and graded seals. Stress determinations made by the photoelastic method are in good agreement with theoretical values.

669.245:621.385.032.216 3033

Nickel Alloys for Oxide-Coated Cathodes—A. M. Bounds and T. H. Briggs. (Proc. I.R.E., vol. 39, pp. 788–799; July, 1951.) The metallurgy of Ni and the methods of manufacturing cathodes are reviewed. Four tube parameters are defined, viz., rate of free Ba evolution, rate of activation, rate of sublimation, and interface impedance. The influence of the Ni-alloy composition of these parameters is examined. Suggestions are made for developing cathode materials to meet the severer demands likely to be imposed in future.

MATHEMATICS

517.37:538.566 3034

Extension of Weyl's Integral for Harmonic Spherical Waves to Arbitrary Wave Shapes—H. Poritsky. (*Commun. Pure Appl. Math.*, vol. 4, pp. 33–42; June, 1951.) Analysis relevant to the propagation of radio waves generated by a dipole near a flat earth is presented.

517.564.4 3035
Vector Wave Functions—E. D. Spence and C. P. Wells. (*Commun. Pure Appl. Math.*, vol. 4, pp. 95–104; June, 1951.) A discussion of the problem of finding spheroidal solutions of the vector wave equation. The solutions cannot be orthogonal, and hence it appears preferable to use the orthogonal set of scalar solutions. This also involves serious difficulties. The boundary conditions for spheroidal cavities and radiators are complex, since the TE and TM modes do not separate as in the spherical or cylindrical cases. Solutions are only practicable in the case of azimuthal symmetry, i.e., for circularly symmetrical fields. Other methods of dealing with the problem are discussed briefly.

517.93 3036
Note on Levinson's Existence Theorem for Forced Periodic Solutions of a Second Order Differential Equation—C. E. Langenhop. (*Jour. Math. Phys.*, vol. 30, pp. 36–39; April, 1951.) Comment on paper noted in 2069 of 1944.

681.142:621.3 3037
Applications of a Mechanical Differential Analyzer to Electrical Engineering—E. Janssen and D. Lebell. (*Elec. Eng.*, vol. 70, pp. 432–435; May, 1951.) The basic components of a differential analyzer and their mathematical functions are discussed, and application to magnetic amplifiers, pulse transformers, and particle trajectories in accelerators is described.

501 3038
Mathematical Engineering Analysis [Book Review]—R. Oldenburger. Publishers: Macmillan, New York, N. Y., 1950, 414 pp., $6.00. (Proc. I.R.E., vol. 39, p. 849; July, 1951.) "A large portion of the field of mathematical physics is covered. . . ."

517.942.82:621.3 3039
Laplace Transformation Theory and Engineering Applications [Book Review]—W. Tyrrell. Publishers: Prentice-Hall, New York, N. Y., 1950, 230 pp., $3.75. (*Jour. Frank. Inst.*, vol. 251, p. 555; May, 1951.) A presentation in a form "readily useful to the average engineer." Applications dealt with include partial differential equations, difference equations, and closed-loop systems.

MEASUREMENTS AND TEST GEAR

538.3:532.5 3040
Further Development of Fluid Mappers—A. D. Moore. (*Elec. Eng.*, vol. 70, pp. 396–401; May, 1951.) Essential text of paper published in *Trans. Amer. IEE*, vol. 69, part II, pp. 1615–1624; 1950. The development of various types of field simulators (*see* 154 of 1950) is described, and their limitations are discussed.

621.317+621.317.083.7]:621.39.001.11 3041
An 'Informational' Theory of Measurement and Telemetry—J. Loeb. (*Ann. Télécommun.*, vol. 6, pp. 90–97; April, 1951.) The features of similarity between telecommunication systems and measurement systems are recognized, and the latter are examined in the light of Shannon's information theory. The quantity of information actually obtained concerning the physical dimension measured, governed by a known probability law, is compared with the potentialities of the apparatus used, and definitions of matching and efficiency are established. Various aspects and applications of the theory are discussed, in particular its use in assessing the fitness of equipment to perform its designed function.

621.317.3 3042
A Method of Measurement of Reactance and Impedance with the Double Voltage Divider—W. Weinitschke. (*Fernmeldetech. Z.*, vol. 4, pp. 117–121; March, 1951.) Zinke's method (1075 of 1948) is modified to eliminate the need of standard reactors.

621.317.3:621.396.822 3043
Direct-Reading Noise-Factor Measuring System—R. W. Peter (*RCA Rev.*, vol. 12, pp. 269–281; June, 1951.) The concept of noise factor of a receiver and methods for its measurement are discussed. A direct-reading arrangement for the centimeter-wave band is described in which a pulse gas-discharge-tube source is used in conjunction with a cro display of rectified receiver output. AGC is provided to hold the receiver output constant; the output with the noise source off then becomes a measure of noise factor.

621.317.313 3044
Works Instruments for Measurement of High-Frequency Current—H. Wechsung. (*Elektrotech. Z.*, vol. 72, pp. 255–257; May 1, 1951.) The widespread use of hf techniques in industry necessitates provision of robust hf measuring instruments. Thermocouple types for currents of 0.5 to 6 A, and current-transformer types for higher values of current, are described.

621.317.335.3† 3045
R.F. Dielectric Standards—(*Tech. Bull. Nat. Bur. Stand.*, vol. 35, pp. 77–78; June, 1951.) A short account of the measurement service provided by the National Bureau of Standards on dielectric materials in the frequency range 10 kc to 600 mc. Bridge or resonance methods are used; at frequencies above 100 mc, cavity-type resonators are particularly suitable. For frequencies below 50 mc, a circuit has been developed including a stable linear negative resistance to balance out the resistance of the rest of the system, and thus provide a high value of Q (up to 10^6).

621.317.335.3.029.63†:621.315.615 3046
A Method of determining the Dielectric Constant and Dielectric Loss of Liquids in the Decimetre Waveband—O. Huber (*Naturwiss.*, vol. 38, pp. 281–282; June, 1951.) When measurements are made at frequencies over 200 mc using a coaxial-line probe method, the maxima and minima exhibited by the voltage and current curves may be rather flat. This drawback is removed by making use not only of the wavelength reduction due to the introduction of the test substance into the line, but also of the capacitive impedance variation at high-voltage points along the line. The probe is kept fixed, while the liquid level is varied.

621.317.335.3.029.64†:546.217 3047
The Permittivity of Air at a Wavelength of Ten Centimeters—J. V. Hughes and W. Lavrench. (Proc. I.R.E., vol. 39, p. 839; July, 1951.) Experimental results confirming those found by Phillips (2827 of 1950) are reported. An outline is given of the method used.

621.317.336.029.64 3048
Inductive Probe for Microwave Measurement Lines and Proximity-Field-Strength Meters—F. Tischer. (*Kungl. tekn. Högsk. Handl.*, (Stockholm), no. 45, 18 pp.; 1951. In German, with English summary.) The performance of a slotted-line standing-wave detector can be improved by using an inductive probe in the form of a wire loop. The loop must be symmetrical with respect to a plane perpendicular to the axis of the slotted line. If it is a pure inductance, its dimensions do not affect the results. If it contains a capacitive element, the dimensions of the loop should be small compared with the wavelength. To compensate for the capacitive element, part of the loop is screened by a short curl of wire attached to one side and at the end of the probe. The theory of this type of probe is developed, and results of measurements are presented. See also 3093 of 1950.

621.317.351:621.396.621.54 3049
Indicator and Measurement Apparatus with Frequency-Sweep Oscillator or Generator—W. Kroebel (*Fernmeldetech. Z.*, vol. 4, pp. 70–76 and 106–111; February and March, 1951.) Relations derived from an experimental and theoretical study of optimum superheterodyne-receiver IF bandwidth, connecting this with intermediate frequency, required frequency band, and local-oscillator (wobbulator) frequencies, are applied in the design of hf spectrometers. Methods of effecting the local frequency variation and applications of the instruments are discussed. See also 406 of 1950.

621.317.361.029.3 3050
A Method for Precision Measurement of Frequency in the A.F. Range—J. C. Hentsch. (*Tech. Mitt. schweiz. Telegr.-Teleph Verw.*, vol. 29, pp. 121–126; April 1, 1951. In French and German.) The signal under test is applied to the vertical deflection plates of a cro operated with a sawtooth timebase synchronized with a standard frequency. A number b of separate waveforms appear simultaneously on the screen. A table is provided from which the signal frequency can be found as a fraction of the standard frequency, using the observed value of b.

621.317.723:621.385 3051
Electrometer Valve Balanced Circuits with Special Reference to the Ferranti BM4A—H. A. Hughes. (*Electronic Eng.* vol. 23, pp. 217–221; June, 1951.) A review with particular reference to the Barth and Caldwell circuits, which are analyzed. The electrometer tube characteristics impose restrictions on the value of supply voltage necessary to balance the circuit.

621.317.725 3052
Square-Law Rectifier Voltmeter—T. Roddam. (*Wireless World*, vol. 57, pp. 316–319; August, 1951.) Development of a bridge circuit giving a satisfactory square-law response over an input range of 0.1 to 3 v, and comprising a combination of resistors and Ge-crystal rectifiers.

621.317.737† 3053
Dielectric Measurements with Two Magic Tees on Shorted Wave Guides—H. G. Beljers and W. J. van de Lindt. (*Philips Res. Rep.*, vol. 6, pp. 96–104; April, 1951.) Using a "magic Tee" as a bridge, a dielectric measurement can be carried out with greater accuracy than by the conventional method with a standing-wave detector. Some details of the construction of the apparatus and the method of measurement are given.

621.317.755 3054
Millimicrosecond Oscillography—Y. P. Yu, H. E. Kallmann, and P. S. Christaldi. (*Electronics*, vol. 24, pp. 106–111; July, 1951.) Equipment for viewing and recording pulses as short as 0.5 mμs is described. Distributed amplifiers are used, with gains as great as 5,000 developing an undistorted output of 130 v. To avoid jitter, vacuum rather than gas-filled tubes are used for the sweep generators, which have speeds up to 400 inches/μs, with departure from linearity $\not>$5 per cent. See also *Proc. Nat. Electronics Conference*, (Chicago), vol. 6, pp. 360–372; 1950.

621.317.755:621.385.832 3055
A Storage Oscilloscope—L. E. Flory, J. E. Dilley, W. S. Pike, and R. W. Smith. (*RCA Rev.*, vol. 12, pp. 220–229; June, 1951.) An instrument for the observation of transients without use of photography. Transients are written on the screen of a Graphechon storage tube whose sweep time may be as low as 0.15 μs, and the signal obtained by reading at slow speed is used to produce a visible image on a cathode ray tube.

621.317.757 3056
A Spectrometer for Radiotelegraphy—A. Tchernicheff. (*Ann. Télécommun.*, vol. 6, pp. 110–116; April, 1951.) A heterodyne wave

analyzer for determining to within 1 per cent the component frequencies of radiotelegraph signals emitted at a rate of ≥50 bauds. A quartz-controlled frequency of 170 kc is passed to a frequency changer giving an output at 70 kc ±3 kc. This is applied to a quartz filter having a pass band of 12 cps, permitting the resolution of spectral components spaced not less than 25 cps. This is followed by a constant-impedance attenuator and a resistance-coupled feedback amplifier, feeding the measurement diode through a high-pass filter cutting off at 1 kc. A generator for producing pulses of controllable shape is described. Various results obtained are illustrated.

621.317.763 3057

Compagnie Industrielle des Téléphones Wave Analyser—J. Sels and A. de Leudeville. (*Câbles & Trans.* (Paris), vol. 5, pp. 110–118, April, 1951.) The M 20 heterodyne-type analyzer, covering the range 1 to 100 kc. Output is proportional to the logarithm of the input voltage for values of the latter ranging from 1 to 10,000 μv or from 10 to 100,000 μv, corresponding to a variation in level of 80 db. Frequency control is by a variable capacitor which may be driven by an electric motor, permitting automatic recording of output/frequency curves.

621.317.772 3058

Measuring Vector Relationships—Y. P. Yu. (*Electronics*, vol. 24, pp. 124–127; July, 1951.) Equipment is described by means of which imaginary and real components of an unknown voltage are indicated directly in terms of a reference voltage, over a frequency range 8 cps to 500 mc. Phase differences between two voltages can also be measured.

621.317.794 3059

A Bolometer with Short Time-Lag—M. Czerny, W. Kofink, and W. Lippert. (*Ann. Phys.*, (Lpz.), vol. 8, pp. 65–86; July 31, 1950.) Account of the development of bolometers comprising a very thin layer of Bi evaporated onto a celluloid film.

621.385.2:621.396.822 3060

Methods to Extend the Frequency Range of Untuned Diode Noise Generators—H. Johnson. (*RCA Rev.*, vol. 12, pp. 251–257, June, 1951.) The use of an inductance in series with the load resistance of the diode noise generator, by compensating for the effects of diode capacitance at high frequencies, substantially doubles the usable frequency range. An additional twofold extension is made possible by the use of a symmetrical diode arrangement as a balanced generator.

621.396.615.17 3061

Square-Wave Generator using Gated-Beam Tube—L. E. Garner, Jr. (*Electronics*, vol. 24, pp. 128–129; July, 1951.) A generator operating at discrete repetition rates between 50 and 500,000 pulses per second comprises an anode-coupled symmetrical multivibrator (12AU7), followed by a gated-beam clipper (6BN6), wide-band amplifier, and cathode follower. The rise-time at 500 kc is <0.07 μs.

621.396.621.089.6:621.396.933 3062

A New Method of Testing the Mark V Decca Navigator Receiver in High Noise Levels—F. J. Hewitt. (*Trans. S. Afr. Inst. Elec. Eng.*, vol. 42, pp. 111–125; March, 1951.) Measurements were made to evaluate the serviceability of the equipment at various atmospheric noise levels and aircraft speeds. Aircraft motion and lane-identification were simulated by special circuits. The observations of lane slip and of failure of lane-identification were compared with noise figures recorded simultaneously. The required signal-to-noise ratios for effective working were assessed, the importance of aircraft speed and direction being emphasized. Using available noise data, the numbers of days of unserviceability per annum under various conditions are tabulated.

621.396.645 3063

A New, Instantaneously Logarithmic Wide-Band Amplifier—G. Epprecht. (*Tech. Mitt. schweiz. Telegr.-Teleph Verw.*, vol. 29, pp. 161–167; May 1, 1951. In German.) In principle, the logarithmic characteristic is obtained by the use of nonlinear circuit elements, not by gain control. An approximation is produced by a suitable arrangement of linear elements. Special circuits are described for overcoming the drawbacks of diode insensitivity at low input levels, and amplifier saturation with large inputs. The degree of approximation to a truly logarithmic law is calculated, and the influence of the various parameters is discussed. A prototype amplifier is described, giving logarithmic response over the frequency range 0.5 kc to 2.5 mc.

621.317.083.7 3064

Registrierinstrumente (Recording Instruments) [Book Review]—A. Palm. Publishers: Springer, Berlin/Göttingen/Heidelberg, Germany, 1950, 220 pp., 19.50 DM. (*Naturwiss.*, vol. 38, p. 239, May, 1951.) Gives valuable information about the principles of construction and the field of application of recording instruments, considering mainly those with typical and interesting features, and those in common use.

621.317.3/.7 3065

Radio Laboratory Handbook [Book Review]—M. G. Scroggie. Publishers: Iliffe and Sons, London, England, 5th edn, 1950, 430 pp., 15s. (*Electronic Eng.*, vol. 23, p. 241; June, 1951.) "The fifth edition has been revised and new material added, in particular, the more recent developments in tube oscillator design."

621.317.725 3066

Vacuum-Tube Voltmeters [Book Review]—J. F. Rider. Publishers: J. F. Rider, New York, N. Y., 2nd edn, 422 pp., $4.50 (*Electronics*, vol. 24, pp. 254, 256; July, 1951.) "This second edition brings the first (1941) edition up to date . . . It is difficult to think of a single aspect of this particular instrument that has been neglected."

OTHER APPLICATIONS OF RADIO AND ELECTRONICS

536.53:537.312.6:621.315.592† 3067

The Design of Thermistor Thermometers with Linear Calibration—W. R. Beakley. (*Jour. Sci. Instr.*, vol. 28, pp. 176–179, June, 1951.)

537.312.6:621.315.592† 3068

Thermistors as used in Ultrasonic Interferometry—O. Lindström. (*Research*, (London), vol. 4, pp. 238–239; May, 1951.) The high sensitivity of the thermistor as a power-indicating device makes it possible to work at low ultrasonic intensities while using rugged measuring devices.

537.533 3069

The Generation of Intense Electron Flashes—W. Schaffs. (*Z. Naturf.*, vol. 5a, pp. 132–136; March, 1950.) A capacitor and spark gap are connected in series across the anode-cathode path of an evacuated tube. When the capacitor discharges, electrons are pulled out of the cold cathode through the cylindrical anode, and pass out through a Lenard window. The electron flashes thus produced can be applied in the same way as X-ray flashes. Mean current strengths of some amperes and durations $<10^{-7}$ seconds have been obtained.

551.501.9 3070

An Air-Launched Automatic Weather Station—(*Tech. Bull. Nat. Bur. Stand.*, vol. 35, pp. 61–63; May, 1951.) This unit falls by parachute to the ground, where its antenna is erected by explosive charges. Separate mechanisms responsive to pressure, temperature, and humidity, cause variations in associated resistors which govern the pulse rate of a radio transmitter in the unit.

620.179.16 3071

Practical Testing of Materials by Ultrasonic Means—H. Krautkrämer and J. Krautkrämer. (*Z. Ver. Dtsch. Ing.*, vol. 93, pp. 349–362; May 1, 1951.) Brief review of modern methods, description of a German pulse-type equipment, and practical details of its operation in detecting flaws in castings, forgings, welds, etc.

620.179.16 3072

Improvements in the Design of Ultrasonic Lamination Detection Equipment—H. R. Clayton and R. S. Young. (*Jour. Sci. Instr.*, vol. 28, pp. 129–132; May, 1951.) To reduce standing-wave effects in the ultrasonic examination of Al blanks and sheet, the transmitting crystal is energised over a wide band of frequencies. Defective areas of diameter <½ inch have been detected, and the contours of a lamination can be traced with satisfactory accuracy.

621.317.087.5 3073

Recording of Very-High-Speed Phenomena—J. Granier. (*Tech. Mod.* (Paris), vol. 43, pp. 213–221; April, 1951.) Electronic methods for recording phenomena of duration <1 ms are described.

621.317.335.3†:547 3074

The Construction of a Hertzian Oscillator and its Application to Organic Analysis—H. A. Sack and B. Sack. (*Jour. Rech. Centre Nat. Rech. Sci.*, vol. 3, pp. 325–331; 1950, 1951.) The liquid specimen to be analysed is contained in a quartz test tube forming the dielectric of a capacitor which determines the wavelength of the vhf oscillator. The grid current of the oscillator provides a measure of the electrical constants of the specimen by comparison with the results obtained with known specimens.

621.317.755.087.4 3075

The Electrical Recording of Diagrams with a Calibrated System of Coordinates—B. G. Dammers, P. D. van der Knaap, and A. G. W. Uitjens. (*Philips Tech. Rev.*, vol. 12, pp. 283–292; April, 1951.) Description of apparatus for displaying families of curves, such as tube characteristics, on a cro, together with the relevant co-ordinate system. The vertical reference lines, the test function, and the horizontal reference lines, are traced in sequence at an overall repetition frequency of 25 per second.

621.318.572:535.33 3076

Suppression of Certain Parts in Spark Spectra by Electronic Time Switching—H. M. Crosswhite, D. W. Steinhaus, and G. H. Dieke. (*Jour. Opt. Soc. Amer.*, vol. 41, pp. 299–302; May, 1951.) Description of a device which renders a photocell sensitive only at desired intervals of a spark cycle. Use of the arrangement for spectrochemical analysis is discussed.

621.365.54† 3077

Induction Heating Installation for Motor-Car Components—(*Machinery*, (London), vol. 79, pp. 69–71; July 12, 1951.) An 8-kw equipment with automatic controls for hardening or annealing small metal parts is described.

621.365.54† 3078

A High-Temperature Vacuum Induction Furnace—H. T. Smyth, R. H. Meinken, and L. G. Wisnyi. (*Jour. Amer. Ceram. Soc.*, vol. 34, pp. 161–163; May, 1951.) Heat is developed by induction in an Mo or Ta tube. Power is supplied from an hf tube generator of 10 kw. The apparatus was developed for measuring physical properties at temperatures >2,000°C.

621.38.001.8:539.17 3079
Practical Aspects of Radioactivity Instruments: Part 1—Construction—W. C. Elmore, H. Kallman, and C. E. Mandeville. (*Nucleonics*, vol. 8, pp. S3-S12; June, 1951.) Technique of wiring, selection of components, and mechanical construction of electronic equipment is discussed. G-M tubes, photomultipliers, and ionization chambers are considered particularly.

621.383.001.8:535.61-15:778.37 3080
Use of Image Phototube as a High-Speed Camera Shutter—A. W. Hogan. (*Jour. Soc. Mot. Pic. & Telev. Eng.*, vol. 56, pp. 635-641; June, 1951.) See 2250 of October.

621.385.833 3081
Calculation of Electronoptical Image Formation for Three Typical Powerful Magnetic Lenses; Relation with the Usual Lens Equation—W. Glaser and F. Lenz. (*Ann. Phys.*, (Lpz.), vol. 9, pp. 19-28; March 15, 1951.)

621.385.833 3082
The General Properties of Low-Power Electron Lenses. A First Approximation—F. Bertein. (*Jour. Phys. Radium*, vol. 12, pp. 595-601; May, 1951.) Analysis is given for electrostatic lenses, space charge being neglected. The average convergence has a uniform value over the whole aperture and depends, for electrons of given energy, only on the original field. The focal length is determined for the cases of an infinite slit, a cylindrically symmetrical lens, and an elliptic aperture. Magnetic lenses are analyzed by the same method.

621.385.833 3083
Apparatus for Electron-Optical Demonstrations—C. Fert. (*Compt. Rend. Acad. Sci.*, (Paris), vol. 232, pp. 2085-2087; June 4, 1951.) A simple, multi-purpose, cathode ray tube apparatus is described, permitting demonstration to an audience of fundamental experiments such as the formation of images, the deflection of electrons, etc.

621.387.4† 3084
Temperature Effect in Counters and Radio Valves—A. Daudin and J. Daudin. (*Jour. Phys. Radium*, vol. 12, p. 564; April, 1951.) A current of cool air circulating around a 6J5 tube operating below its rated voltage in a cosmic-ray counter circuit, caused a reduction of 70 per cent in recorded coincidences.

621.387.424† 3085
Geiger-Müller Photo-Counter with Ferro-Nickel Cathode for Ultraviolet Rays—J. Labeyrie. (*Jour. Phys. Radium*, vol. 12, pp. 569-570; April, 1951.) Description of the design and performance of a stable counter highly sensitive to ultraviolet radiation of wavelengths between 2,000 and 3,000 Å.

621.387.464† 3086
Delayed Coincidence Circuit for Scintillation Counters—A. Lundry. (*Rev. Sci. Instr.*, vol. 22, pp. 324-327; May ,1951.) Pulses from the photomultipliers used as detectors are amplified in distributed amplifiers and applied to a Ge-diode-bridge coincidence circuit.

621.387.464† 3087
Nuclear Scintillation Counters—J. B. Birks. (*Jour. Brit. IRE*, vol. 11, pp. 209-220; discussion, pp. 221-223; June, 1951.) Physical processes affecting the design of these counters are discussed, with particular reference to the choice of suitable phosphors and photomultipliers. Advantages of scintillation counters over conventional gas-ionization counters are illustrated.

PROPAGATION OF WAVES

538.566 3088
The W.K.B. Approximation as the First Term of a Geometric-Optical Series—H. Bremmer. (*Commun. Pure Appl. Math.*, vol. 4, pp. 105-115; June, 1951.) The propagation of waves in an inhomogeneous medium is analyzed in a manner which stresses the effects of successive scattering reflections in the medium. The W.K.B. approximation is then seen to be the first term of an infinite series, and to correspond to an analysis of primary scattering only. Simple relations between the higher-order terms are obtained, and the limitations of the W.K.B. approximation discussed. The resultant reflection coefficient of an inhomogeneous medium is calculated for a single case.

538.566 3089
Remarks concerning Wave Propagation in Stratified Media—S. A. Schelkunoff. (*Commun. Pure Appl. Math.*, vol. 4, pp. 117-128; June, 1951.) The reflection coefficients for a stratified medium are considered physically and mathematically. The dependence of the coefficient on layer thickness and shape is discussed fully. Factors causing variations of the reflection coefficient with frequency are examined. For a wave incident on an inhomogeneous layer, no meaning can be attached to the term "reflection coefficient." Propagation is controlled by the higher-order derivatives of the variation of reflection parameters with distance in the layer, e.g., an Epstein layer gives a particular variation of reflection coefficient with thickness not found for other types of layer.

621.396.11 3090
Polarization of the Z-Trace—J. E. Hogarth. (*Nature*, (London), vol. 167, p. 943; June 9, 1951.) An experiment carried out at Fort Chimo (58.1°N, 68.3°W) on September 30, 1950, showed the polarization of the Z trace (third critical frequency) to be ordinary. This is compatible with the theory that the Z trace is the longitudinal ordinary reflection, made possible at off-longitudinal directions by the effect of collision [see 1471 of July (Scott)].

621.396.11 3091
Measurements of the Direction of Arrival of Short Radio Waves Reflected at the Ionosphere—E. N. Bramley and W. Ross. (*Proc. Roy. Soc. A*, vol. 207, pp. 251-267; June 22, 1951.) Report of observations made mainly on first-order F-layer reflections in normal day-time conditions, both over an oblique path corresponding to a range of 700 km, and at nearly vertical incidence. A phase-comparison method was used, with pulse signals, over the frequency range 4 to 15 mc. A typical echo shows both rapid (second-to-second) fluctuations in direction, and slow changes having a quasi-period of up to more than 30 minutes, indicating the occurrence of large-scale random tilts in the ionosphere of an rms magnitude about 1.5 to 2°, and extending horizontally over at least some tens of kilometers.

621.396.11:535 3092
Remarks on the Optics of Radio Waves—O. Halpern. (*Phys. Rev.*, vol. 82, pp. 971-972; June 15, 1951.) Optical theory is extended to show that any metallic layer is a good reflector for radio waves as long as the rf conductivity is not too different from the dc value.

621.396.11:[550.385+551.594.5 3093
Aurora and Magnetic Storms—R. K. Moore. (*QST*, vol. 35, pp. 14-19, 110; June, 1951.) Discussion of the nature of ionospheric disturbances and their effects on radio communication.

621.396.11:551.510.535 3094
Approximate Expressions for the Refractive Index of an Ionized Medium acted upon by the Earth's Magnetic Field—É. Argence. (*Compt. Rend. Acad. Sci.*, (Paris), vol. 232, pp. 2080-2082; June 4, 1951.) Approximate formulas are derived based on Poeverlein's graphical determination of the paths of em waves refracted by the ionosphere (718 and 2875 of 1950) and taking the earth's magnetic field into account.

621.396.11.029.62/.63 3095
Coverage on 45 to 450 Mcs—K. Bullington. (*FM-TV*, vol. 11, pp. 21-24, 36; May, 1951.) See 1496 of 1950.

RECEPTION

621.396.621:621.396.9 3096
A Simple Logarithmic Receiver—J. Croney. (Proc. I.R.E., vol. 39, pp. 807-813; July, 1951.) A description is given of a successive-detection logarithmic amplifier and of a simplified circuit producing either logarithmic or linear amplification by operation of a single switch. A method of calculating the shape of the output/input curve is described, the measured curves for three logarithmic receivers of this simplified type are shown, and the relevant circuit values specified. The advantages of the logarithmic receiver for radar work are indicated.

621.396.621.029.51/.53 3097
A Subminiature Low-Frequency Radio Receiver—(*Tech. Bull. Nat. Bur. Stand.*, vol. 35, pp. 68-70; May, 1951.) Description of a radio range receiver tunable from 190 to 550 kc, and using printed circuits in seven subassemblies, details of which are given. The entire unit is hermetically sealed.

621.396.622:621.396.822 3098
The Rectification and Observation of Signals in the presence of Noise—R. E. Burgess. (*Phil. Mag.*, vol. 42, pp. 475-503; May, 1951.) The rectification of random narrow-band noise in the presence of a cw or modulated signal is analyzed. The detector considered is of the type providing a rectified voltage which is a function of the instantaneous amplitude of the input wave. The smoothing present in the detector circuit is such that the hf components of the applied wave are removed, but the lf variations of its envelope are faithfully transmitted. The mean (or dc) component of the rectified voltage and its rms fluctuation about that mean (or lf noise output) are calculated as a function of the input signal-to-noise ratio, and particular attention is paid to linear and square-law detectors. The output signal-to-noise ratio for an AM signal input, and for the audible-beat reception of a cw signal, are calculated. The spectrum of the lf noise output from a detector supplied with random noise is closely similar for linear and square-law detectors. The discrimination of a weak signal in noise is not critically dependent upon the law of the detector, and in particular the difference for a linear and a square-law detector is negligible. The effect of receiver bandwidth, meter time-constant, and integration time, in improving the discernment of a weak signal, is considered.

621.396.397].82 3099
Standards on Radio Receivers: Open Field Method of Measurement of Spurious Radiation from Frequency Modulation and Television Broadcast Receivers, 1951—(Proc. I.R.E., vol. 39, pp. 803-806; July, 1951.) Reprints of this Standard, 51 IRE 17 S1, may be purchased while available from the Institute of Radio Engineers, 1 East 79 Street, New York 21, N. Y., at $0.50 per copy.

621.396.82:621.396.41 3100
Interference In Multi-Channel Circuits—L. Lewin (*Elec. Commun.*, (London), vol. 28, pp. 142-155; June, 1951.) Reprint of 986 of May.

621.396.822 3101
The Effect of Circuit Losses on Noise Factor—D. McDonnell. (*Jour. Brit. IRE*, vol. 11, pp. 224-226; June, 1951.) The optimum input conditions for minimum noise factor in a

neutralized triode input stage are considered, and theoretically derived curves are given of the variations in noise factors with input circuit losses.

621.396.823 3102

Corona Problems on 400-kV Lines: Part 2—Radio Interference from Corona Effect on Conductors—N. B. Bogdanova and A. M. Lifshits. (*Bull. Acad. Sci.* (URSS), no. 4, pp. 497–505; April, 1951. In Russian.)

621.396.828:354.42/.44 3103

The High-Frequency Statutes [in Germany]—H. Pressler. (*Fernmeldetech. Z.*, vol. 4, pp. 123–129; March, 1951.) Report and discussion on present regulations governing the use of hf equipment.

621.396.621 3104

Receiver Circuitry and Operation [Book Review]—A. A. Ghirardi and J. R. Johnson. Publishers: Rinehart Books Inc., New York, N. Y., 1951, 669 pp., $6.00. (*Electronics*, vol. 24, pp. 258, 260; July, 1951.) "Here is basic coverage of the circuits most often encountered in modern television, AM radio, and FM radio receivers, written for the technician and student who seeks to bring his education up to date."

STATIONS AND COMMUNICATION SYSTEMS

621.39.001.11 3105

A Note on Autocorrelation and Entropy—P. Elias. (Proc. I.R.E., vol. 39, p. 839; July, 1951.) A simple relation between the information content per symbol of a message and its auto-correlation function is presented.

621.39.001.11:621.317.35 3106

Random Signals with Limited Spectra—J. Oswald. (*Câbles & Trans.* (Paris), vol. 5, pp. 158–177; April, 1951.) A theoretical study emphasizing the principal mathematical properties of such signals and showing how these define the nature of the signals. The theory is applied to the particular cases of single-sideband modulation multiplex time-division and pulse-code systems. See also 210 of February.

621.394.3 3107

Tape Relay—S. A. Westwood. (*Proc. IRE* (Australia), vol. 12, pp. 131–141; May, 1951.) Describes modern practice in the automatic handling of material at the transmitting and receiving stations of a printing telegraph system. Relevant radio technique is discussed briefly.

621.396.41 3108

Four/Two-Channel Time-Division Multiplex Telegraph System for Long-Distance Radio Circuits—W. C. Peterman and A. Minc. (*Elec. Commun.* (London), vol. 28, pp. 127–141; June, 1951.) Description, with circuit diagrams, of equipment and operation of a frequency-shift system.

621.396.61/.62 3109

Miniature Walkie-Talkie—(*Wireless World*, vol. 57, pp. 323–324; August, 1951.) Description of Pye equipment type PTC 120, operating on two spot frequencies (crystal-controlled) in the band 60 to 100 mc. Dimensions are $9\frac{1}{2}$ inches$\times 6\frac{1}{2}$ inches$\times 3\frac{1}{4}$ inches, and weight is $8\frac{1}{2}$ pounds complete. Only six tubes plus Ge crystal and quartz crystals are used. The transmitter rf power output is 0.1 w.

621.396.61/.62 3110

A Civil Defense Portable—E. P. Tilton. (*QST*, vol. 35, pp. 35–38, . . 120; May, 1951.) A transmitter-receiver for operation on 50 mc, comprising a transmitter having a single-tube rf section with an audio pentode as modulator, and a simple superregenerative receiver with one audio stage. It is operated by three batteries, 1.4-v, 90-v, and 6-v, and weighs 4 pounds.

621.396.619.16 3111

Pulse Generation and Shaping at Microwave Frequencies—W. A. Klute. (*Bell Lab. Rec.*, vol. 29, pp. 216–220; May, 1951.) A system for the generation of pulses of the on-or-off type, suitable for pcm, at a repetition frequency of 18.432 mc and in four adjacent bands with 30-mc spacing. The carrier frequency is about 4 kmc. A method of pulse generation, based on the variation with beam voltage of the gain of a traveling-wave tube, is used.

621.396.664 3112

A New Television Studio Audio Console—R. W. Byloff. (*RCA Rev.*, vol. 12, pp. 211–219; June, 1951.) Features of the apparatus, which is designed for compactness and flexibility in operation, include twelve-channel mixing, removable vision-monitoring unit, etc.

621.396.67:621.396.65 3113

Application of Polarity Diplexing to Microwave Relay Systems—C. A. Rosencrans. (*TV Eng.*, vol. 2, pp. 14, 27; June, 1951.) A practical diplexing system uses horizontal and vertical polarization, respectively, for two signals transmitted along the same path. A small frequency shift is introduced to minimize depolarization interference.

621.396.712 3114

Broadcast Station Construction Practices—Q. G. Cumeralto. (*Tele-Tech*, vol. 10, pp. 34–36, 89; June, 1951.) A very general survey of factors to be considered in siting and designing a radio station.

621.396.73:621.396.11.029.64 3115

Mobile Equipment for the Study of Centimetre-Wave Propagation—J. Maillard, J. Voge, and P. Chavance. (*Ann. Télécommun.*, vol. 6, pp. 131–144; May, 1951.) Propagation theory is applied in the design of the equipment, in respect of transmitter power, receiver noise factor, and bandwidth. Chief features of the apparatus are the afc system and the transmission of information regarding the instantaneous level of the emitted signal. This is achieved by modulating the frequency of the radiated signal to a depth corresponding to the power transmitted. The pulse detector circuit receiving this information also feeds a cro for examination of pulse shape. A "peak detector" circuit records the level of the received pulse. The transmission-level recording channel may be modified for simultaneous reception of two transmissions on different close frequencies.

621.396.931 3116

Radiotelephony for Communication with Vehicles—P. Häni. (*Tech. Mitt. schweiz. Telegr.-Teleph Verw.*, vol. 29, pp. 168–177; May 1, 1951. In German.) Description of FM equipment at the fixed station and in the subscriber's vehicle in the system operating in Zürich. Calling from the normal telephone network is fully automatic. Subscription rate is 18 Swiss francs per month, plus the cost of the mobile equipment. Unattended relay stations extend the range beyond 25 km for police services, etc. See also 2350 of 1950 (Kappeler).

621.396.931 3117

Crowded-Band Mobile Equipment—H. H. Davids and T. J. Foster. (*Electronics*, vol. 24, pp. 102–105; July, 1951.) A transmitter-receiver system for the 148–174-mc band is described. The receiver uses triple-tuned IF transformers to reduce adjacent-channel interference, and controlled rf gain to reduce intermodulation interference. Results of field tests are given.

621.396.97 3118

The Development of Broadcasting in the Union of South Africa—H. O. Collett. (*Trans. S. Afr. Inst. Elec. Eng.*, vol. 42, pp. 175–187; May, 1951.) An historical survey of the service. Developments in transmitters, studios, manufacturing facilities, and the use of recording are traced. Probable future developments include the linking of the transmitters by telephone lines.

SUBSIDIARY APPARATUS

621.314.63 3119

Developments in Metal Rectifiers—G. E. B. White. (*Elec. Times*, vol. 119, pp. 901–904; May 31, 1951.) Review of characteristics of copper-oxide and selenium rectifiers manufactured by the Westinghouse Brake and Signal Co. Ltd.

621.352/.353 3120

Modern Batteries and Their Use in Telecommunications (Miniature Batteries)—J. Pernik. (*Ann. Télécommun.*, vol. 6, pp. 122–126; May, 1951.) Discussion of experimental developments in the design and manufacture of light-weight cells. The replacement of Zn by Mg, and the use of methylamine electrolytes in the Leclanché-type cell are considered. Construction and characteristics of mercuric oxide- and silver-chloride cells are reviewed.

621.352 3121

Developments in Dry Batteries and Associated Electronic Equipment—P. H. Adams. (*Proc. IRE* (Australia), vol. 12, pp. 167–178; June, 1951.) Developments in dry batteries are described, and the design of receivers, hearing aids, photoflash equipment, and radiosonde equipment is examined in relation to battery requirements.

TELEVISION AND PHOTOTELEGRAPHY

621.396/.397].82 3122

Standards on Radio Receivers: Open Field Method of Measurement of Spurious Radiation from Frequency Modulation and Television Broadcast Receivers, 1951—(*See* 3099.)

621.397 3123

Picture Telegraphy by Wire—V. Castell. (*Tech. Mitt. schweiz. Telegr.-Teleph Verw.*, vol. 29, pp. 236–239; June 1, 1951. In German.) Description of the terminal apparatus in Zürich for black-and-white phototelegraphy. The picture is scanned in 684 lines across a 13 cm$\times$8 cm frame at 7,850 pulses per second. The motor driving the revolving drum is tuning-fork controlled. Synchronization is by tone wheel and stroboscope.

621.397.26 3124

A Diversity Receiving System for Radio Frequency Carrier Shift Radiophoto Signals—J. B. Atwood. (*RCA Rev.*, vol. 12, pp. 177–190; June, 1951.) As compared with the FM subcarrier system, the radio-frequency carrier shift (rfcs) system shows improvement in signal-to-noise ratio, and reduction of interference due to the narrower bandwidth which can be used in the receiver. Further definite improvement was obtained with rfcs using the space diversity system described. The diversity receiving arrangement, used with two single sideband receivers, also effected an improvement in reception by the FM-subcarrier system.

621.397.26 3125

Strato-vision in Swiss Territory?—W. Kuentz. (*Tech. Mitt. schweiz. Telegr.-Teleph-Verw.*, vol. 29, pp. 126–131; April 1, 1951.) In French and German.) Maps of Swiss districts are reproduced showing the areas in which television reception should be possible from an airborne transmitter 10 km above Berne.

621.397.26 3126

Television-Link Sound Diplexer—L. Staschover and H. G. Miller. (*Elec. Commun.*, vol. 28, pp. 108–109; June, 1951.) A 5-mc subcarrier, modulated in frequency by the sound program, is combined with the video frequencies (bandwidth 4.5 mc) and then passed to the link transmitter. The sound frequencies in the demodulated output from the link receiver are separated from the vision frequencies by a filter, amplified, limited, and demodulated in a balanced discriminator. The final af output is 18 db above 1 mw into balanced or unbalanced impedances of 50, 150, and 600 ohms.

621.397.26:621.396.615.142.2:621.396.621.53 3127

Application of the Klystron Mixer to Frequency Changing in Television Relays—V. Learned. (*Ann. Télécommun.*, vol. 6, pp. 127–130; May, 1951.) French version of 256 of February.

621.397.26:621.397.81 3128

Polycasting—R. M. Wilmotte. (Proc. I.R.E., vol. 39, pp. 740–752; July, 1951.) A theoretical study is made of the service obtainable in the vhf and uhf bands by broadcasting a program from a number of low-powered stations instead of from a single high-powered one to cover a continuous area. Estimates of service, evaluated statistically and taking into account ghosts and signal intensity required to overcome noise, are given together with a tentative allocation of stations in two typical areas of the United States.

621.397.5 3129

Experimental Television Transmissions in North-West Germany—W. Nestel. (*Elektrotech. Z.*, vol. 72, pp. 346–348; June 1, 1951.) The development of television in Germany is surveyed, and a short explanation of the principles of television transmission are given. The advantages and disadvantages of the three different line standards are discussed, and the reasons for choosing the 625-line system indicated. The preparations for public transmissions are described.

621.397.5:535.62 3130

The Present Status of Color Television—(*Proc. IRE* (Australia), vol. 12, pp. 109–115 and 141–150; April and May, 1951.) Reprint. See 249 of February.

621.397.5:535.62 3131

Spectrum Utilization in Color Television—R. B. Dome (*Gen. Elec. Rev.*, vol. 54, pp. 18–22; June, 1951.) Comparison of various time- and frequency-division multiplexing techniques from the point of view of securing the most efficient use of available transmission channels.

621.397.5:535.88:791 3132

A Comprehensive Proposal for a Closed-Loop Theater Television System—R. L. Garman and R. W. Lee (*Jour. Soc. Mot. Pic. & Telev. Eng.*, vol. 56, pp. 473–483; discussion, pp. 483–486; May, 1951.) The system described permits selection of programs at will from its own studio or from outside sources. To obtain picture quality comparable with that of the commercial cinema, it is proposed to adopt a standard of 675 lines double interlaced at a frame frequency of 24 per second.

621.397.5(083.74) 3133

The C.C.I.R. 625-Line Television Standards—H. Laett. (*Tech. Mitt. schweiz. Telegr.-Teleph Verw.*, vol. 29, pp. 81–86 and 132–136; March 1, and April 1, 1951. In German and French.) Full text and explanatory comment.

621.397.6 3134

Automatic TV Sync Lock—L. M. Leeds. (*Electronics*, vol. 24, pp. 99–101; July, 1951.) See also 2294 of October (Roe).

621.397.6:[778.5+621.395.625.6 3135

New Video Recording Camera—F. N. Gillette and R. A. White. (*Jour. Soc. Mot. Pic. & Telev. Eng.*, vol. 56, pp. 672–679; June, 1951.) The problem of television recording is discussed, and a camera using 16-mm film and recording both vision and sound, is described. The film is ready for projection within 60 seconds of the television reception.

261.397.61 3136

Continuous Film Scanner for TV—D. G. F. (*Electronics*, vol. 24, pp. 114–116; July, 1951.) Equipment under development at the Bell Telephone Laboratories is described. A mirror-drum projector is used, with two electronic servo-controls to compensate for jitter and flicker. The arrangement permits flying-spot scanning of a 24-frames per second film at 60 fields per second.

621.397.611.2 3137

On the Mechanism of High-Velocity Target Stabilization and the Mode of Operation of Television-Camera Tubes of the Image-Iconoscope Type—P. Schagen. (*Philips Res. Rep.*, vol. 6, pp. 135–153; April, 1951.) Hypotheses are advanced, and from them equations are derived, for the variation of target-element potential with time, and for the signal voltage. The theory indicates that improvement of picture quality should result from increase of secondary-emission coefficient and capacitance of target. This is confirmed by experiments.

621.397.62 3138

The Cosine Deflection Yoke—J. Pell. (*TV Eng.*, vol. 2, pp. 10–11, 27; June, 1951.) A uniform deflecting field producing no distortion of the cathode ray tube spot, is obtained by using a coil wound so that the number of turns varies as the cosine of the angle between the deflection direction and the radius to the particular point of the winding. Residual barrel, or pincushion distortion due to geometrical factors, can be corrected by means of small permanent magnets.

621.397.62 3139

High-Efficiency Horizontal-Deflection System and High-Voltage Supply—J. Henry. (*Radio franç.*, no. 2, pp. 1–8; February, 1951.) Efficiency of generation of the sawtooth scanning voltage, and of high-voltage supply in television reception, is improved by the use of a line autotransformer, with ferroxcube core, and of regeneration. See also 3674 of 1947 and 1783 of 1950 (Schade).

621.397.62 3140

40 Faults Occurring in Television—(*Télév. Franç.*, no. 69, pp. 19–26; April, 1951.) A chart listing the major faults likely to occur in a television receiver, illustrated by diagrams of the display produced.

621.397.62:535.88 3141

High-Definition Projection Receiver—R. Gondry. (*Télévision*, no. 13, pp. 105–110; May, 1951.) Full constructional details are given of a receiver using the "Télécran" optical system, permitting variation of the distance between objective and screen from 40 cm to 250 cm, with picture size varying from 19.5×26 cm to 90×120 cm.

621.397.62:621.396.822 3142

Expediting TV Receiver Noise Calculations—D. A. Miller and E. A. Slusser. (*TV Eng.*, vol. 2, pp. 12, 13, 35; April, 1951.) Abacs are presented for calculation of thermal noise, equivalent noise input, etc.

621.397.7 3143

Kirk O'Shotts Television Transmitting Station—*Engineer* (London), vol. 191, p. 863; June 29, 1951; *Engineering* (London), vol. 171, p. 793; June 29, 1951. Some details are given of the high-power station under construction near Glasgow, on a site 900 feet above sea level. The vision transmitter is to have a power output of 50 kw, with an operating frequency of 56.75 mc. The frequency of the sound transmitter will be 53.25 mc.

621.397.828 3144

Suppression of Harmonics in Radio Transmitters—G. T. Royden. (*Elec. Commun.*, (London), vol. 28, pp. 112–120; June, 1951.) A Π-network filter in the transmitter output circuit, with screening of the transmitter and its supply leads, should give sufficient general suppression for a transmitter in an isolated position. For greater suppression, a double-Π network with a common shunt capacitance should be used. Particular harmonics may be attenuated by simple single filters or by quarter-wavelength open-ended stubs connected directly to the transmitter output terminals.

TRANSMISSION

621.316.726.078.3:621.396.615 3145

A Simple Crystal Discriminator for F.M. Oscillator Stabilization—J. Ruston. (Proc. I.R.E., vol. 39, pp. 783–788; July, 1951.) Detailed description of a single-crystal discriminator designed for use in a television sound transmitter.

621.396.615.142.2:621.396.621.53:621.397.26 3146

Application of the Klystron Mixer to Frequency Changing in Television Relays—V. Learned. (*Ann. Télécommun.*, vol. 6, pp. 127–130; May, 1951.) French version of 256 of February.

621.396.619.2 3147

Transistor Frequency Modulator Circuit—L. L. Koros and R. F. Schwartz. (*Electronics*, vol. 24, pp. 130–132, 134; July, 1951.) Design and circuit details are given and performance tests reported. The simplicity and power economy consequent on the use of the transistor are stressed. The wide variation of internal collector impedance on application of audio voltages to the emitter is used to vary the resonance frequency of the tank circuit in a conventional oscillator. Modulation characteristics and distortion are shown in graphs.

621.397.828 3148

Suppression of Harmonics in Radio Transmitters—Royden (*See* 3144).

TUBES AND THERMIONICS

535.215.4 3149

Photoconductivity in the Elements—T. S. Moss. (*Proc. Phys. Soc.*, vol. 64, pp. 590–591; June 1, 1951.) The photoconducting elements are nonmetallic and have a refractive index > 2. They are: Te, P, I, As, B, Se (red), S, C (diamond), Si, and Ge. The activation energies determined from photoconductivity measurements agree closely with those from resistance/temperature measurements. Refractive index is related to the photoconductive threshold wavelength. For Ge, Si, and diamond, a quantitative relation holds, namely En^4=constant (E is activation energy, n is refractive index). See also 1273 of June.

537.533.8 3150

Secondary Electron Emission from Ni, Mo, MgO and Glass—G. Blankenfeld. (*Ann. Phys.* (Lpz.), vol. 9, pp. 48–56; March 15, 1951.) The variation with temperature of the secondary emission of Ni, Mo, MgO, and glass is investigated, by an experimental method briefly described, for various values of primary energy. For Ni and Mo, the temperature variation is zero; for glass, it is very small. For MgO, the secondary emission decreases as temperature rises. The results are discussed in the light of Hackenberg's theory (see *Ann. Phys.*, (Lpz.), vol. 6, no. 2, p. 404; 1948).

537.581 3151

Electron Emission from Metal Surfaces as an After Effect of Mechanical Working, or Glow Discharge—O. Haxel, F. G. Houtermans, and K. Seegar. (*Z. Phys.*, vol. 130, pp. 109–123; May 28, 1951.)

537.583 3152

The Origin of Bombardment-Enhanced Thermionic Emission—J. B. Johnson. (*Phys. Rev.*, vol. 83, pp. 49–53; July 1, 1951.) "Measurements on bombardment-enhanced thermionic emission from oxide cathodes show that

(a) the effect is not related to normal fading and recovery of thermionic emission; (b) the emitted electrons have energies in the thermal range rather than in the secondary range. Calculations indicate that the electron bombardment releases more than enough internal secondaries to account for the effect as increased thermionic emission. A more comprehensive theory is needed for explaining why the observed effect is not even larger."

621.314.63 3153
Height of the Potential Barrier in Contact Rectifiers and Its Change with Temperature—E. Billig and M. S. Ridout. (*Nature* (London), vol. 167, pp. 1028–1029; June 23, 1951.) Preliminary investigations on Ge, Si, and Se rectifier cells, and on Se photocells, are reported. Current was measured with voltages from 0.2 to 50 mv applied in both the forward and reverse directions, and the temperature dependence of the zero-voltage resistance was observed. Deviation of the results from the values given by the theoretical expression, relating zero-voltage resistance to barrier height, is ascribed to a lowering of the latter at temperatures below 300°K.

621.383:546.289 3154
Germanium Trigger Photocells—F. A. Stahl. (*Elec. Eng.*, vol. 70, pp. 518–520; June, 1951.) 1951 AIEE Winter General Meeting paper. The occurrence of *n*-type and *p*-type Ge in the same crystal can give rise to trigger action upon excitation by infra-red radiation. The operating mechanism of the composite contact is explained. When used in on-off devices, the on current is high enough to develop useful power in low resistances.

621.383.27† 3155
The Time Dependence of the Sensitivity of Photomultiplier Tubes—M. Hillert. (*Brit. Jour. Appl. Phys.*, vol. 2, pp. 164–167; June, 1951.) An experimental investigation of fatigue and recovery effects in photomultipliers under typical operating conditions, particularly the change of sensitivity following a sudden change in illumination. An empirical formula is derived to express this effect, which is traced to phenomena occurring at the dynodes rather than at the photocathode. An electrical model representing their behavior is outlined.

621.383.4:546.816.221 3156
The Characteristics of Long Period Photo-Effects in Lead Sulphide—R. P. Chasmar and A. F. Gibson. (*Proc. Phys. Soc.*, vol. 64, pp. 595–602; July 1, 1951.) A photoconductive effect having a decay time of several hours has been observed in specially prepared layers of lead sulphide when maintained at low temperatures. These effects are characteristic of layers that have been treated in a certain manner with sulphur or with oxygen. No first-order differences are found between the properties of the layers containing O and those containing S. A physical explanation of the effect is advanced.

621.383.4:546.816.221 3157
The Sensitivity and Response Time of Lead Sulphide Photoconductive Cells—A. F. Gibson. (*Proc. Phys. Soc.*, vol. 64, pp. 603–615; July 1, 1951.) Measurements were made with a view to establishing a theoretical model for photoconductors of this type. Variations of response time and sensitivity with temperature, background illumination, applied electric field, and other parameters, were investigated. The results give qualitative support to a theory postulating the existence of space-charge barriers at intercrystalline contacts, the height of these barriers being reduced on illumination.

621.383.42 3158
Investigation of the Influence of Photocurrent and External Resistance on the Spectral Sensitivity of Selenium Photocells—I. Wolf. (*Ann. Phys.* (Lpz.), vol. 8, pp. 30–40; July 31, 1950.) Two methods are discussed for measuring spectral sensitivity, viz., (a) using an illuminating source with uniform energy spectrum, and (b) with the photocurrent maintained constant. The spectral sensitivity varies in the former case with the intensity of the illumination; in the latter case, with the value of the photocurrent, and in both cases with the value of the external resistance connected. A physical explanation is advanced.

621.384.5:621.316.722 3159
Variations in Extinction Voltages of Glow-Discharge Voltage-Regulator Tubes—F. A. Benson (*Jour. Sci. Instr.*, vol. 28, p. 186; June, 1951.) "The extinction voltages of a large number of tubes covering fifteen different types have been recorded. The effect of life on extinction voltage has also been determined."

621.384.5:621.396.662 3160
The Development of Tuning-Indicator Valves for Broadcast Receivers—F. Malsch. (*Radio Mentor*, vol. 17, pp. 124–129; March, 1951.) Review of development leading to the design of the EM71, a small loktal-base magic-eye tube giving a single wide-angle shadow sector. The cathode is offset from the axis of the tube, and the beam deflection is produced by a rod nearly parallel to the cathode, together with a symmetrically placed pair of auxiliary angle plate electrodes held at target potential.

621.385 3161
New Vacuum Tube Materials—A. P. Haase and F. B. Fehr. (*Tele-Tech*, vol. 10, pp. 30–32 and 33–35; June and July, 1951.) Processing steps applied to terratex, a mica substitute, to render it suitable for use in tubes, are described, and properties of the material are compared with those of natural micas. Developments in the use of Al-clad Fe as a substitute for Ni are also reported.

621.385:621.397.62 3162
Characteristics of the New Transcontinental Series of Television Valves—J. Moline. (*Radio franç.*, nos. 2 and 4, pp. 16 and 22–24; February and April, 1951.) Details of a set of nine tubes for use in television receivers.

621.385:681.142 3163
Systematization of Tube Surveillance in Large Scale Computers—H. W. Spence. (*Elec. Eng.*, vol. 70, pp. 605–608; July, 1951.) 1951 AIEE Winter General Meeting paper. When failure occurs in the ENIAC AC computer, all tubes in the faulty circuit are replaced; the old tubes are tested, and results are logged on a card index. Results of the analysis of the data are presented, showing the average life of the various types. Details of the methods of testing and of the functions of the tubes in the circuits are given.

621.385.012 3164
Electron Tube Ratings at Very High Altitudes—R. J. Bibbero. (*Tele-Tech*, vol. 10, pp. 42–44; May, 1951.) A discussion of the effects of altitude on envelope temperature, and the extent to which anode dissipation must be derated to prevent excessive heating and reduction of tube life. Measurements are described, and typical graphs included for specific tube types.

621.385.029.64+621.396.622.6 3165
Valves and Crystals for Ultra-high Frequencies—(*Radio franç.*, no. 4, pp. 14–18; April, 1951.) Productions of the Compagnie Française Thomson-Houston are described, with their working characteristics. These include: the magnetron RHM 1232, giving a pulsed output of the order of 40 kw at 3 cm wavelength; the reflex klystron RHK 6332, for the same band; and Si-crystal mixers and detectors for the 3-cm and 10-cm bands.

621.385.029.64 3166
Electron Beams and Electro-magnetic Waves—R. Warnecke, O. Döhler, and W. Kleen. (*Wireless Eng.*, vol. 28, pp. 167–176; June, 1951.) A generalised theory of interaction, restricted to the case of small signals and applicable to the behavior of an electron beam in the drift space of a velocity-modulated tube, to the traveling-wave tube, including its operation at high current density, and to the properties of the electron-wave tube. Comparison is made with the theories of other workers.

621.385.029.64:537.533.72 3167
Space-Charge Effects in H. F. Modulated Electron Streams—J. Labus. (*Ann. Phys.*, (Lpz.), vol. 9, pp. 6–18; March, 15, 1951.) Dynamic space-charge effects, which arise in an initially neutral plasma as a result of the inability of the heavy ions to oscillate at high frequencies, have an adverse influence on the phase focusing of a beam. Static (i.e., time-invariable) electronic space charge, on the other hand, is advantageous in that it increases transit time. A differential equation for the electron velocity is developed in which the coefficients are independent of position for vanishingly small values of static space charge. Starting from this static condition, a solution is derived in terms of a disturbing parameter defined by the ratio of the space charge to the electronic charge. The closer the condition of a pure electron stream is approached, the smaller is the defocusing action of the dynamic space-charge effect compared with the static.

621.385.032.216 3168
Life of Valves with Oxide-Coated Cathodes—C. C. Eaglesfield. (*Elec. Commun.* (London), vol. 28, pp. 95–102; June, 1951.) Tube-emission characteristics deteriorate because of the formation of a resistive barrier between the cathode core and the oxide coating. This gradually builds up to a normalised resistance value of about 40 Ω, and then stays constant. The possibility of reducing the effects of this resistance by suitable circuit design is discussed briefly.

621.385.032.216:546.841-3 3169
Thoria as a Cathode Emitter—W. E. Danforth. (*Jour. Frank. Inst.*, vol. 251, pp. 515–520; May, 1951.) The characteristics which render thoria in some cases more suitable as a cathode material than Ba/Sr oxides, are examined. Pulsed emission currents up to 4 a/cm^2 at 1,600°C and 15 a/cm^2 at 1,800°C, can be obtained. The decay of emission with time is much slower than with Ba/Sr oxides, the time constants being of the order of 0.1 second. The maximum dc emission, i.e., the equilibrium emission after decay, is between 1 and 5 a/cm^2. In pulsed applications, the life of a thoria-coated cathode is determined by its evaporation rate. At 1,800°C the coating disappears at the rate of about 1 mil thickness in 300 hours.

621.385.15.012.6:537.525.92 3170
High-Speed Ten Volt Effect—R. M. Matheson and L. S. Nergaard. (*RCA Rev.*, vol. 12, pp. 258–268; June, 1951.) The I/V curve for diodes with oxide-coated cathodes has been observed to depart from the Langmuir $\frac{3}{2}$-power law for anode voltages greater than 10 v. Experiments indicate that the departure is due to secondary emission of electrons from a layer of BaO formed on the anode.

621.385.2 3171
Potential and Gradient Distributions in Parallel Plane Diodes at Currents below Space-Charge-Limited Values—W. M. Brubaker. (*Phys. Rev.*, vol. 83, pp. 268–270; July 15, 1951.) Solutions for the equations of electron motion in a plane diode, taking space charge into account, are derived in terms of four dimensionless parameters related, respectively, to current density, potential, distance from cathode, and potential gradient at cathode. For one particular distance, the gradient is independent of the current density.

621.385.2 3172

Determination of the Point Representing the Saturation of a Diode on an Experimental log $I=f(\sqrt{F})$ Curve—H. Bonifas. (*Compt. Rend. Acad. Sci.* (Paris), vol. 232, pp. 2082–2084; June 4, 1951.) Quantum-theory considerations are applied to an examination of the field conditions at the surface of a thermionic cathode, assuming a Maxwellian distribution of emission velocities, and a formula is derived relating the anode and cathode fields (F and H_0, respectively) and the current (I). At saturation current, the resultant field at the cathode surface is zero, log I passing through a maximum or an inflection point with horizontal tangent. Confirmatory experiments have been made with cathodes of various types, and a "universal" value of the order of 10 kv/cm is found for H_0, while the "radius of action of the surface atom" is estimated at 3.8×10^{-8} cm.

621.385.2 3173

Microwave Diode Conductance in the Exponential Region of the Characteristic—G. Diemer. (*Philips Res. Rep.*, vol. 6, pp. 211–223; June, 1951.) A transit-time theory is developed, assuming a linear retarding field and ignoring electron interaction. For diodes with close anode-cathode spacing, the value of the conductance over the exponential part of the characteristic, for anode voltages between -2v and -1v, may considerably exceed the total-emission conductance even in the microwave band. Application of the theory to earlier measurements on closely spaced diodes reduces the existing discrepancy between theoretical and experimental results.

621.385.2 3174

Space-Charge Distribution, Characteristic and Current Fluctuations in "Double Diodes"—R. Fürth. (*Proc. Phys. Soc.*, vol. 64, pp. 404–412; May 1, 1951.) "The distribution of space charge and potential in thermionic tubes with two hot electrodes ("double diodes") is derived by the method of statistical mechanics for plane parallel electrodes, first for tubes in true thermodynamic equilibrium, and then, approximately, for tubes with applied external voltage or with electrodes at slightly different temperatures. The dependence of current on voltage in the first case (characteristic), and on temperature difference in the second case, is calculated. Finally, a general expression for the current fluctuations ("noise") in double diodes is given and discussed. The application of this formula to other types of conductors is also indicated."

621.385.2.01:621.396.822 3175

Theory and Experiments on Electrical Fluctuations and Damping of Double-Cathode Valves—K. S. Knol and G. Diemer. (*Philips Res. Rep.*, vol. 6, p. 14; February, 1951.) Correction to papers abstracted in 791 of 1950 and 507 of March.

621.385.3:537.212 3176

The Penetration Factor and the Potential Field of a Planar Triode—P. H. J. A. Kleijnen. (*Philips Res. Rep.*, vol. 6, pp. 15–33; February, 1951.) A calculation of the penetration factor is given which is valid for all values of grid-wire diameter and anode-grid spacing. This calculation being too complicated for general practical use, the numerical evaluation is given for a large number of electrode configurations. The results are compared with those obtained from previously derived formulas.

621.385.3:546.289 3177

p-n Junction Transistors—W. Shockley, M. Sparks, and G. K. Teal. (*Phys. Rev.*, vol. 83, pp. 151–162; July 1, 1951.) "The effects of diffusion of electrons through a thin p-type layer of germanium have been studied in specimens consisting of two n-type regions with the p-type region interposed. It is found that potentials applied to one n-type region are transmitted by diffusing electrons through the p-type layer, although the latter is grounded through an ohmic contact. When one of the p-n junctions is biased to saturation, power gain can be obtained through the device. Used as "n-p-n transistors" these units will operate on currents as low as 10 μa and voltages as low as 0.1 v, have power gains of 50 db, and noise figures of about 10 db at 1,000 cps. Their current voltage characteristics are in good agreement with the diffusion theory."

621.385.3.029.63 3178

A 1.5 kW 500-Mc/s Grounded-Grid Triode—C. E. Fay, D. A. S. Hale, and R. J. Kircher. (Proc. I.R.E., vol. 39, pp. 800–803; July, 1951.) The triode described is of planar design, operated at an anode voltage of 3kv, and water-cooled. Copper is used as the grid material to reduce its thermionic emission. The apparent efficiency at 500 mc, with an output of 1.5 kw, is 55 per cent, and the power gain is 6.5.

621.385.5.011.2 3179

The Internal Resistance of a Pentode—J. L. H. Jonker. (*Philips Res. Rep.*, vol. 6, pp. 1–13; February, 1951.) Analysis of R_i, defined as $\partial V_a/\partial I_a$ with the grid potentials fixed. For output pentodes, the electrostatic influence of the anode potential on the cathode current produces the main contribution. In hf pentodes, the most important effect is that of the electrons collected by the screen grid after being reflected by either the suppressor grid or the anode. Comparison of the theoretical and measured values of R_i for EF6, EF50, EL3, EL50, and AF7 tubes shows rough agreement. The possible reasons for discrepancy are discussed.

621.385.832 3180

Switch and Storage Tubes—L S. Allard and R. T. Hill. (*Wireless Eng.*, vol. 28, pp. 187–191; June, 1951.) Brief descriptions are given of a number of tubes, including an indication of the type of service for which they are suitable, methods of construction, and performance. Precautions necessary to eliminate spurious signals in the case of storage tubes with fluorescent screens are discussed.

621.385.832:621.3.087 3181

The Recording Storage Tube—R. C. Hergenrother and B. C. Gardner. (Proc. I.R.E., vol. 39, p. 806; July, 1951.) Correction to paper noted in 2942 of 1950.

621.385.832:621.397.6 3182

Graphechon Writing Characteristics—A. H. Benner and L. M. Seeberger. (*RCA Rev.*, vol. 12, pp. 230–250; June, 1951.) The results of an experimental investigation are presented. Graphs are given for calculating the performance of graphechons as storage devices for radar ppi displays. By integrating successive radar pulses, improvement of signal-to-noise ratio can be obtained.

621.385.832:621.397.621.2 3183

Improved Electron-Gun Ion Traps—C. S. Szegho and T. S. Noskowicz. (*Tele-Tech*, vol. 10, pp. 45–47; June, 1951.) The design is based on parallel displacement of the anode axis from the cathode-grid axis. Negative ions and electrons are equally deflected by the electrostatic field caused by this displacement. Subsequent magnetic deflection separates the ions from the electrons, the latter being guided through a small aperture in the anode. The design ensures good spot roundness. Correct axial displacement in assembly is facilitated by using a fluorescent coating on the outside of the anode.

621.396.615.141.2 3184

Low-Voltage Tunable X-Band Magnetron Development—G. A. Espersen and B. Arfin. (*Tele-Tech.*, vol. 10, pp. 50–51, 84 and 30–31, 70; June and July, 1951.) Description of the Type PAX3 magnetron. The tuning range is 9.300 to 9.320 kmc, peak power output is 50w minimum, weight <2.5 pounds. Frequency is stable to within ±3 mc over a temperature range of 80°C.

621.396.615.141.2 3185

The Magnetron in the Cut-Off State; Transition from Cylindrical to Planar Case—J. L. Delcroix. (*Compt. Rend. Acad. Sci.*, (Paris), vol. 232, pp. 2298–2300; June 18, 1951.) The planar magnetron has been treated elsewhere as the limiting case of the cylindrical magnetron when the radii of cutoff surface (b) and cathode (a) tend to equality, but this holds only if a tends simultaneously to ∞. A critical value of b/a exists for which the Brillouin and bidromic states become identical. The distribution of the space charge for the bidromic case with b/a nearly equal to the critical value is discussed, and a correct method for effecting the transition from the cylindrical to the planar case is presented.

621.396.615.141.2 3186

An Experimental Investigation of the Electron Orbits in a Magnetron—R. Svensson. (Proc. I.R.E., vol. 39, p. 838; July, 1951.) An experimental tube for investigating non-oscillating magnetrons is described. Photographs of the traces observed on a fluorescent screen are consistent with electron orbits of cycloidal character. Modifications for use with an oscillating magnetron are suggested.

621.396.615.142.2:537.291:537.525.92 3187

The Influence of Space Charge on the Phase Focusing of Electron Beams—F. Borgnis: J. Labus. (*Z. Naturf.*, vol. 5a, pp. 175–176; March, 1950.) Comment on paper noted in 3568 of 1948 (Labus) and author's reply.

MISCELLANEOUS

014.5:05 Electronics 3188

Electronics Cumulative Index, 1930–1939—(*Electronics, Annual Buyers' Guide Issue*, vol. 24, pp. C1-C36; June, 1951.) Alphabetical subject and author indexes are given for all articles in *Electronics* during the first ten years of publication. It is planned to publish similar indexes for the period 1940 to 1949 in the 1952 Buyers' Guide Issue.

058.7 3189

Alphabetical Listings of All Components, Complete Units and Allied Products used in Electronic Equipment for All Purposes—(*Electronics, Annual Buyers' Guide Issue*, vol. 24, pp. D1–D168; June, 1951.) Lists are given of the products of more than 2,500 American manufacturers. A trade-name index and a list of distributors are also included.

621.3 3190

Electricity at the 35th Swiss Industries Fair at Basle—(*Bull. schweiz. elektrotech. Ver.*, vol. 42, pp. 162–198; March 24, 1951.) Illustrated review of equipment shown, including power units, regulators, meters, etc.

621.396.029.6 3191

Grundlagen der Hochstfrequenztechnik (Principles of Very-High-Frequency Engineering) [Book Review]—F. W. Gundlach. Publishers: Springer Verfag, Berlin/Göttingen /Heidelberg, and J. F. Bergmann, München, Germany, 1950, 499 pp., 48 DM. (*Z. Ver. Dtsch. Ing.*, vol. 93, p. 456; June 1, 1951.) A comprehensive work of the greatest value for engineers and others. Knowledge of the theory of electrodynamics is assumed.

ABSTRACTS AND REFERENCES INDEX

The Index to the Abstracts and References published throughout the year is in course of preparation and will, it is hoped, be available in February, price 2s. 8d. (including postage). As supplies are limited our Publishers ask us to stress the need for early application for copies. Included with the Index is a selected list of journals scanned for abstracting, with publishers' addresses.